AD A104399

FOREIGN TECHNOLOGY DIVISION

BASIC AERODYNAMICS OF COMBUSTION CHAMBERS

by

Ning Huang
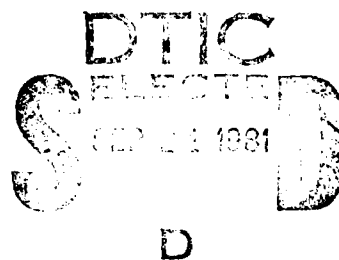
DISCLAIMER NOTICE

THIS DOCUMENT IS BEST QUALITY
PRACTICABLE. THE COPY FURNISHED
TO DTIC CONTAINED A SIGNIFICANT
NUMBER OF PAGES WHICH DO NOT
REPRODUCE LEGIBLY.

EDITED TRANSLATION

DTIC
ELECT
SEP 2 1 1981

D

TABLE OF CONTENTS

SHORT INTRODUCTION TO CONTENTS

Both in China and abroad, in thermal physics and engineering circles, the trend in the design of new types of combustion chambers is to combine the use of aerodynamics, the science of heat transfer and heat transfering materials and the theory of the science of combustion with experimental testing carried out by using the technology available for precise, high speed, automatic measurements; the theoretical knowledge available and the data which can be obtained are then combined to improve the quality of physical and mathematical models of the flow fields in question; programs for the calculations are arranged, and computers are used to figure out flow field characteristics and, at the same time, collaborate the test results.

This book analyses the air flow structures and flow field characteristics of the combustion chambers of jet engines from the point of view of aerodynamics; it introduces basic concepts and basic equations, and it places emphasis on theory and experimentation describing vortex flow fields and turbulence jets; this is to form a preparatory foundation for the numerical calculation of combustion chamber flow fields.

There are sixteen chapters all together in this book, and it could be usefully studied by senior students or research personnel specializing in thermal physics engineering and dynamics at major technical academies and schools; it can also be usefully studied by scientific and technical personnel in fields related to combustion.

CHAPTER 1   INTRODUCTION

Section 1   Capability Targets for Combustion Chambers of Turbine Jet Engines

Combustion chambers are the "ovens" of turbine jet engines, called "turbine jets" for short. With air flow, fuel injection and ignition, one gets combustion which throws out heat energy and increases air flow. High pressure, high temperature gases flow through the turbine wheels, and the expansion of these gases inside the jet tubes creates power. If there is no air flow, there is no combustion, and the "turbine jet" cannot maintain its functioning cycle. If combustion is bad, then, the capabilities of turbine jets cannot be good.

Aircraft fly in different climates, at different altitudes and different speeds. The technological requirements for the combustion chambers of turbine jets must be particularly strict. It is required that, within the "flight envelope", engines not be extinguished, that combustion be fast, stable, even and good. Beyond this, it is also required that there be few combustion chamber failures, that chamber life is long and that the chambers are small in volume and light in weight. The quality of combustion produced by various combustion chambers are called "capability targets."

A fighter aircraft flies above an isothermic layer, and, because it has developed a flame out malfunction, the compressor turbines turn in vain. In such a circumstance, the combustion chamber intake pressure can drop to $p_2 \leqslant$ 0.3 (N/cm^2); temperature can drop to $t_2 \cong -30^{o}(C)$; and, flow speed can rise as high as $\overline{u}_2 \cong 100$ (m/s). The only thing to do is to dive to a lower altitude or temporarily change over to gasoline; moreover, one must inject oxygen, and, only then, can the engine be reignited. The altitude at which an extinguished engine can be reignited is called "ignition altitude"; it is generally between 8000 and 12000 m. Ignition altitudes are safe altitudes.

By using the volume of flow Q (m^3/s) to eliminate the combustion chamber volume V (m^3), one can obtain the air flow "stop over period" $t_s^{\sim} = 6-8$ (ms). In this period of time, the air intake volume G must be apportioned to various areas, the jet fuel must be atomized, vaporized, mixed, heat must be released by chemical reaction, the air mixture must be reburned, the temperature must be lowered, etc; and all these processes must take place in a timely manner because, only then, can continuous, stable combustion be sustained.

Combustion is the violent collision of molecules of oxygen with molecules of fuel in such a way as to destroy the structure of the fuel molecules and form molecules of a new compound. Under conditions of high temperature and pressure, molecules have many opportunities to collide and many opportunities to reform; the chemical reaction time $t_k \leqslant 1$ (ms). As far as speed of combustion is concerned, it is primarily decided by the speeds of air flow distribution and mixing. Aerodynamic nozzles and vapor tubes cause liquid fuel to atomize ahead of schedule, which causes vapor and shortens the mixing preparation time within the combustion chamber. One can say, "Even mixing means fast burning." Within a combustion chamber, how many kilocalories of heat energy can be produced by each square meter of volume, for each hour, for each atmosphere of pressure is called "heat emission strength" or I. The I value for turbine jet combustion chambers is $(2 \sim 5) \times 10^7$ ($kcal/m^3 \cdot hr \cdot atm$); the same value for a normal boiler is $I \cong 5 \times 10^5$ ($kcal/m^3 \cdot hr \cdot atm$); so, the combustion chamber is about 100 times hotter. Given a fixed value of I, it is possible to estimate the volume of the combustion chamber involved.

According to the quantitative equilibrium equations for the chemical reactions, every kg of kerosene will burn its precisely required quantity of air $L_0 \cong 14.7$. The actual ratio between air flow quantity G and L_0 is called the gas remainder coefficient $\bar{a}$. When a turbine jet is cruising at high altitudes, the amount of air entering the chamber G can be right around 120 times the amount of fuel being injected G_f; under maximum conditions it will be around 50 times G_f. That is to say that the whole variation range for the gas remainder coefficient a is wide, i.e. $3.5 \leqslant a \leqslant 8$. In actuality, when local values of $a > 2$, it is very difficult to ignite the fuel. Therefore, no matter what kind of operational configuration a turbine jet is in, it is necessary to take pains to maintain the local value of the gas remainder coefficient in the main combustion area of the combustion chamber within the range $0.5 \leqslant a \leqslant 1$ in order to prevent flame out. The average intake air flow speed for combustion chambers can be in the range of $u_1 \cong 30\text{-}100$ (m/s). Stability of combustion is evidenced by such things as tolerance of a wide range of lean and rich mixtures, low temperature, low pressure, high air speed, while still maintaining flame stability and vigor without deviation or flame out.

As far as the use of high capability ignition gear for the forcing of ignition is concerned, when such equipment is used to start aircraft in cold weather, it is particularly important to be sure that the throttle is not pushed too fast increasing speed too violently. Because of the fact that when rotation speed is low, kerosene atomization, vaporizing and mixing are not yet completely prepared for, it is not possible to achieve stable combustion in the main combustion area. However, if forced ignition is not stopped, the fire can flow down and reach the

2

exhaust port of the combustion chamber or even the turbine wheels before it really starts to burn; this condition raises the temperature but does not increase the rotation speed of the turbine; this can lead to the destruction of the turbine fan blades by the heat. This is called a "heat stoppage" malfunction.

There are three important indicators of good combustion:

(1) Overall combustion efficiency η and Local Combustion Efficiency η.

Make H= the fuel heat value, $\bar{j}=1/\bar{a}L_0$= the fuel to air ratio; let the total heat content of the gases when they are at the exhaust port of the combustion chamber and have already been burned $= i_3^*$; and, let the total heat content of air at the intake port $= i_2^*$. If one takes each kilogram of air as the basis, then

$$\text{overall combustion efficiency } \eta = \frac{(1 + \bar{j})i_3^* - i_1^*}{\bar{j}H} \%$$

We already know $\bar{a}$; we measure the average overall temperature of the intake and exhaust gas flow $\bar{T}_1^*$ and $\bar{T}_3^*$; and, we can figure η by checking a gas heat engineering properties chart or by getting i_3^* and i_2^*. At the present time, $\eta \geqslant 99\%$ for the main combustion chambers of turbine jets. This is a numerical value for this characteristic, which is obtained through static engine testing. In flight η will be lower.

In the interior of the combustion chamber, measurements of local fuel concentrations in different parts of the chamber $= C_f$ (kg/m^3). The initial fuel concentration before combustion is taken to equal C_{f_o} (kg/m^3); and, the fuel consumption ratio $\phi = C_f/C_{f_o}$. Before combustion, $\phi = 1$; after combustion, it equals 0.

Local combustion efficiency $\eta = (1 - \phi)\%$; the local rates of chemical reaction

$$W = -\frac{d}{d\tau}(\eta C_{f_o}) = -C_{f_o}\frac{d\phi}{d\tau} \quad [\text{kg/m}^3 \cdot \text{s}].$$

Local rates of combustion η follow the course of the flow and gradually rises until it reaches the overall combustion efficiency η .

(2) δ, the "unevenness" level of the exhaust port temperature field of combustion chambers.

3

Because the flow speed distribution inside combustion chambers is uneven, and the distribution of fuel concentration is uneven, therefore, there is no way for the exhaust port temperature distribution to be even. In order to assure the strength level of the turbine fan blades, strict limits must be placed on the "uneveness" of radial and circumferential temperature distributions in the air flow coming out the exhaust port:

Define $\delta =$ <u>Highest overall exhaust port temp-Avg overall exhaust temp</u>
Avg overall exhaust port temp-Avg overall intake temp

$$= \quad \frac{T_m^* - \bar{T}_3^*}{\bar{T}_3^* - \bar{T}_1^*} \leqslant 25\%.$$

If one can raise the average, overall exhaust port temperature for combustion chambers, $\bar{T}_3^*$ and reduce the "uneveness", δ ; then, it is certain that one can raise the capabilities of turbine jets. If $\overrightarrow{T_3}$ can be raised so that $\bar{T}_3^* \cong 2000K$, then, low temperature mixing is not required and neither is assisted combustion.

(3) Wall temperature distributions of flame tubes.

The material in the thin panels of flame tubes have a limited ability to resist high temperatures. If the temperature distribution on a wall surface is not even, and the surfaces are subjected to aerodynamic and mechanical vibrations, causing stress concentrations along the edges of openings in the panels, it is very easy to have fatigue, creasing damage, cracking and complete failure. Pieces of failed material can then flow with the air current down into the engine where they can damage the turbine fan blades, and this can lead to a whole range of accidents! At present, localized hot spots in the walls of flame tubes should not exceed $850^{\circ}C$, and the average temperature throughout the walls is $\leqslant 600^{\circ}C$. In order to prevent overheating of the flame tubes, first, combustion must be stable, that is, the flames must not expand, wobble or consume the inside of the tubes. Secondly, air film cooling or "sweat cooling" must be used to protect the inside walls. The air films which stick to the inside walls of the tubes very seldom take part in the combustion, and are not a main force in the operation of the engine; therefore, every effort must be made to reduce the amount of air film cooling; the amount of air used for this purpose should not exceed 25%.

The lack of carbon accumulation in jet tubes and around jet mouths, the lack of exhaust smoke, minimal quantities of the poisonous gases CO and NO in exhaust,

4

a minimal amount of combustion noise — all these things are also are indicators of "good burning." The Peoples Laws concerning these matters set strict limits on exhaust smoke, CO and NO content of exhaust and noise.

If one is to achieve fast combustion, stable combustion and good combustion, then, the construction of combustion chambers — speaking from an aerodynamic point of view — poses many obstacles and limitations. For example, compressors, swirl atomizers, stabilizers, evaporization tubes or jet nozzles, as well as current direction baffles, shunting panel mixing apertures and narrow cracks can all be considered as obstacles; forcing air currents to reduce speed, to suddenly intensify, to turn, to rotate, to divide, to blast and to mix can all be considered as limitations. These "obstacles" and "limiations" cause air flow speed distribution to be extremely uneven; this produces turbulence and vortices. The viscosity shear forces between layers of air and the friction between the air flow and the solid surfaces of the engine will both tend to reduce the total pressure ΔP^*. The total pressure P^* represents the size of the total amount of mechanical energy in the air flow; that is to say, the amount of work that the expansion of the air flow is capable of doing. There is an overall pressure loss of 1% in front of the tail jet nozzle, and the thrust of the turbine jet is reduced by something more than 1%. Drops in air flow pressure which occur as a result of energy expended in order to overcome blockages are called "flow blockage losses." Even if one has a flat, smooth, straight tube with no surface friction and no vortical turbulance, it only takes an increase in the heat of combustion, and such an increase will necessarily increase the speed of the air flow and decrease the pressure. This phenomenon is called "heat blockage loss." It can be clearly seen from all this that the basic contradiction in the design of combustion chambers is that in order to improve combustion capabilities one must introduce many flow blockages and heat blockages. The general pressure ratio between the exhaust nozzle and the intake nozzle of a combustion chamber is called the "general pressure repletion coefficient" σ. For combustion chambers of the same form and dimensions, it is obvious that the higher σ is the better. In general, σ should be $\geq$ 0.94.

A "thermal expansion strength", I, which has a high value is a reflection of a combustion chamber which has a small volume. The design of a turbine jet must make rational use of limited space. The process of development goes from single or simple tubes to interconnected tubes and, finally, to the tubular combustion cavities themselves. Recently, the trend has been toward the use of shortened

cavities, double cavities and sub-divided cavities in the construction of combustion chambers.

Shortening the length of combustion chambers not only reduces the volume of the chamber and lightens its weight, it is also capable of reducing the amount of air required for air film cooling, which allows the absolute maximum amount of the air entering the chamber to take part in mixing and combustion; shortening the span between the turbine wheels and the compressors increases rigidity along the main axis as well as critical rotation speed.

This method for shortening the length of combustion chambers involves shortening the chamber entry compressor or the use of a "sudden compression form" gas entry; these types of chamber entries take advantage of vortex reflux and shorten flame length; they also increase the maximum permissible temperature in front of the turbines, $\overline{T}_3^*$, and increase combustion efficiency η; therefore, it is possible to shorten or eliminate areas of supplementary fuel feed and lowered temperature; with such a design it is possible to adjust combustion to different operational configurations and eliminate exhaust gas passages.

Because their heat emission strength is high, their operating conditions diverse and their technical requirements stringent, the general overhaul life of turbine jet combustion chambers is much shorter than that of naval ship boilers or surface ovens. The general overhaul life for the combustion chambers of fighter aircraft is approximately 200-500 hours. The general overhaul life of the combustion chambers of civilian aircraft can exceed 1000 hours. All the technical requirements for a combustion chamber cannot be satisfied at the same time. For example, fast burning and long life, good combustion and small losses are contradictory requirements. One must set the main capability targets for a combustion chamber according to its intended application.

2. Flow Distribution in Combustion Chambers of Turbine Jet Engines

Fig 1.1 is a cross section diagram of the cavity of a connecting-tube type combustion chamber. The compressors send air flow G (kg/s) through the cavity's pressure intensification apparatus where it slows down and is pressured into the combustion chamber entrance with an average flow speed of $\overline{u}_2$ (m/s), a density of ρ_H (kg/m^3), an average overall pressure of $\overline{P}_1^*$ (N/cm^2) and an average overall temperature of $\overline{T}_2^*$ (K). Distributions for the entering air flow G in certain predetermined configurations are as follows:

6

(1) The amount of gas flowing from the eddy current gear into the main combustion area, G_1, accounts for approximately 8-10%. the exhaust at the end of the eddy current apparatus is fitted with flow guide baffles which have numerous holes in them; this is to prevent the accumulation of carbon. The blades of the eddy current devices force the air flow to rotate; this creates the vortical reflux area (see Chapter 6 for a detailed treatment of this subject).

(2) The gas volume, G_2, which flows into the main combustion area from the gas mixture apertures and the main fuel apertures accounts for approximately 16-20%. These two constituents of the gas volume $(G_1 + G_2)$ and the amount of jet fuel which is mixed in in appropriate proportions together form a local gas remainder coefficient $\alpha \approx 1.0$. A rich mixture in the main combustion area with $\alpha < 1.0$, is advantageous for starting combustion and for the stability of high altitude combustion; however, the local combustion efficiency η is too low, and a relatively long supplementary combustion area is required. A lean mixture in the main combustion area with $\alpha \geq 1$ has advantages which are the exact opposite of those of a rich mixture.

The gas volume distribution and $\bar{P}^*$ and $\bar{T}^*$ of the gases entering the flame tube of the connected tube combustion chamber in Fig 1.1 change along the course of the flow.

(3) The gas volume, G_3, which comes from the supplementary fuel apertures and enters and enters the supplementary combustion area accounts for approximately 20-25%. If the main combustion area has a rich mixture to begin with, theoretically, the mutual interaction and mixing of $(G_1 + G_2 + G_3)$ and G_f should cause the local gas remainder coefficient at the exit of the supplementary combustion area to reach $\alpha \cong 2$ with local combustion efficiency reaching $\eta \geq 98\%$.

(4) The gas volume, G_4, which is entering the cooling area from the large cooling aperture added to the gas volume used in air film cooling, G_5, accounts for approximately 45-55%. If one can raise the overall temperature, $\bar{T}_3^*$, which is permissible for entrance into the turbines from $1200^\circ K$ to $1600^\circ K$, then, it is possible to reduce the amount of gas necessary for cooling, G_4. If one can shorten the combustion chamber, lessening the amount of wall surface necessary in cooling, then, it is possible to reduce the amount of gas used in the air film, G_5. Not only can this raise the thermal emission strength, I, it can also greatly lower fuel consumption, sfc, (the number of kg of fuel consumed per hour for each kg of thrust).

In Fig 1.1 one can see that, in the area in front of the main fuel

aperture, that is, in the main combustion area, the drop in overall pressure and the rise in overall temperature are both very fast. This explains why both the mixing and combustion of air and fuel are very violent.
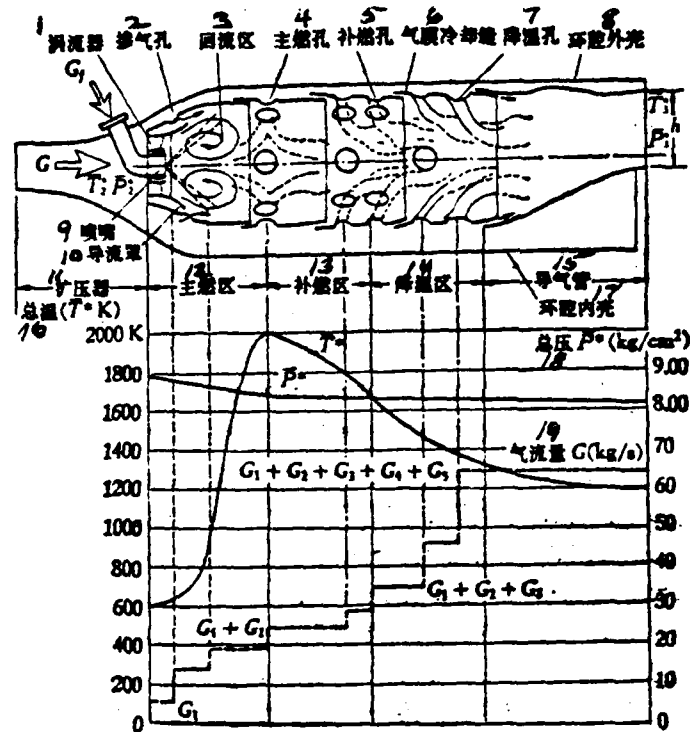
Fig 1.1

1. Eddy Current Apparatus 2. Gas Mixture Aperture 3. Reflux Area 4. Main Fuel Aperture 5. Supplementary Fuel Aperture 6. Air Film Cooling Crack 7. Cooling Aperture 8. Outer Cavity Skin 9. Jet Nozzle or Mouth 10. Flow Guide Baffle 11. Pressure Intensification Apparatus 12. Main Combustion Area 13. Supplementary Combustion Area 14. Cooling Area 15. Gas Guide Tube 16. Overall Temperature 17. Inner Cavity Skin 18. Overall Pressure 19. Gas Flow Momentum

Sec 3 Flow Field Structure in Combustion Chambers of Turbine Jet Engines

At any given instant, the form of the distribution of the air flow speed vector, V, pressure strength, p, fuel concentration, c_f, and overall temperature, T^*, within a limited space is called the "flow field structure" of the combustion chamber, or

"speed field", "pressure strength field", "concentration field" and "temperature field." Through the use of high speed cameras or pulse laser integrated information photography, it is possible to photograph a certain cross section of the "air flow structure" in a limited space. If several cross sections are photographed, it becomes possible to analyse the "flow field structure" of the space.

Fuel mist vaporization, speed of diffusion mixing and concentration of diffusion and mixing are all determined by local flow speeds. Therefore, the "speed field " determines the "concentration field." Molecular collisions and the speed and amount of thermal emission from combustion are all determined by local temperatures, pressures and fuel concentrations. Therefore, the "concentration field" determines the "temperature field." Looking at it from this point of view, the speed field of the main combustion area determines the temperature field of the exhaust port of flame tubes. If the exhaust port temperature distribution does not measure up to standards, then, it is necessary to improve the "flow field structure" of the main combustion area. If holes or secondary seams open later in the middle section of flame tubes, it has no great effect.

Air flow is movement by a "collective of molecules" or a "micro-mass of gas." Flow speed is the speed of the center of mass of the "micro-mass of gas" also called the "material point particle." Even if the collective flow speed, $V=0$, if one could bore into the microcosm of the "micro-mass of gas, one would see large numbers of gas molecules each haphazardly ricocheting and colliding with each other at different speeds, U, and from different directions. If one looks at the sunshine which penetrates into a dark room through a crack in a window, one can see smoke and dust rolling and bouncing back and forth in the column of light; splash a few drops of perfume here and there, and one can smell it throughout a whole room; both these observations are manifestations of "molecular motion." Under conditions of standard temperature and pressure, every 22.4 liters of gas contain $N_o = 6.023 \times 10^{23}$ molecules. Say the volume of the "micro-mass of gas" is 1 cm^3, it still contains $N \approx 2.7 \times 10^{19}$ molecules. According to the theory of molecular motion, temperature, T, expresses the level of intensity of the linear motion of molecules, or it represents the statistical average of the kinetic energies of the molecules $(1/2)m\overline{U}^2$; it has nothing to do with the volume of the "micro-mass of gas." Pressure is an expression of the size of the strength of the molecular collisions which occur on each unit of surface area of the inner wall of the "micro-mass of gas; it is related to the molecular number and the number of collisions. When a given number or molecules absorbs thermal energy, its movement is violent, its

9

average kinetic energy is large; its temperature is high; the space between one molecule and another is widened; the volume occupied by the micro-mass of gas is increased, or, one could say, its density is diminished. Therefore, if the number of molecular collisions recieved by each surface area unit of the inner wall of the micro-mass of gas is reduced, then, the pressure will be diminished.

What has been said above can explain why the air flow through a clean, unobstructed tube must be speeded up as soon as heat is added to the system and the volume of the micro-mass of gas expands if the air flow is to maintain the same speed it has through an unobstructed tube. A drop in pressure in the air flow produces a "temperature blockage."

It can also explain why it is difficult to start ignition and combustion under conditions of low temperature and pressure. Because oxygen molecules and molecules of fuel are few in number, their motion is slow, and their collisions are not violent enough, opportunities for their combining are few.

We recognize the fact that "flow fields" are formed by continuous micro-masses of gas without gaps of spaces. Even the smallest micro-masses of gas are much larger than the dimensions of a single molecule. Therefore, they are called continuous media or macrocosms and are not considered in terms of molecular motion.

The influence of the circumferential pressure which is recieved by the micro-masses of gas can cause deformations. When the density, ρ, also changes in line with these deformations, it is called the "compressibity" of the gas. All gases are compressible. However, when the air flow Mach number is $M \leqslant 0.20$ or the flow speed $V \leqslant 60$ (m/s), compressibility is not noticable, and one can treat gases under these conditions as non-compressible fluids, that is, with density, ρ, approximately equal to a constant.

Imagine that there is a fixed, rectangular coordinate system superimposed over the flow field. The coordinates for the material point particle, i, of a certain micro-mass of gas are (x,y,z); the components of speed vector, V, along x, y and z are u, v and w. Using x, y and z as well as time, τ, as independent variables, it is possible to write functional equations for the flow structure by using standard values for the variables p, T and ρ of the micro-mass of gas along with the components of the vector quantity, V. The equations are as follows:

$$p = p(x, y, z, \tau) \qquad u = u(x, y, z, \tau)$$
$$T = T(x, y, z, \tau) \qquad v = v(x, y, z, \tau)$$
$$\rho = \rho(x, y, z, \tau) \qquad w = w(x, y, z, \tau)$$

If one uses experimentation or theoretical methods to provide precise values
for the functional equations above, one has a grasp of "flow fields." If the con-
dition parameters, p, T and ρ, as well as the flow speed vector components u, v,
and w do not vary with changes in time, τ, then:

$$\frac{\partial p}{\partial \tau}, \frac{\partial T}{\partial \tau}, \frac{\partial \rho}{\partial \tau}, \frac{\partial u}{\partial \tau}, \frac{\partial v}{\partial \tau}, \frac{\partial w}{\partial \tau}$$

are all equal to zero, and this is called a "steady flow field." Only when one has
appropriate values for flight altitude, H, flight Mach number, M, rotation speed, s,
air intake, G, and jet fuel quantity, G_f, so that they are stable and unchanging,
without fluctuations, and there is stable combustion, can one consider there to be
a stable flow field within and outside the flame tubes.

When condition parameters and flow speed vary with changes in one coordinate,
this is called a single-element stable flow field; when condition parameters and
flow speed vary with changes in two coordinates, this is called a two-element stable
flow field; and, when condition parameters and flow speed vary with changes in
three coordinates, this is called a three-element stable flow field.

Suppose there were no viscosity shear forces between micro-masses of gas;
then, during movements of the micro-masses of gas there would only be deformation
displacement; there would be no rotational movement; this is called "non-rot-
ational displacement, that is, it depends only on the "pressure gradient" to pro-
duce flow speed. If one takes the material particle points for the micro-masses
of gas in a stable flow field and connects them together to form a line, this line
is called the "flow line." The special characteristics of "flow lines" are as
follows: the speed vector, V, of material particle points correspond everywhere
to the flow lines; two flow lines cannot cross each other; there is no cross
flow speed, therefore, micro-masses of gas cannot cut across flow lines; the dif-
fusion and exchange of momentum, mass and energy between flow line and flow line
must depend on molecular motion; the rarity or density of the intervals between
flow lines represents the amount of flow passing through each unit cross section
perpendicular to the lines of flow, that is to say, the size of the "density of
flow", $\rho V'$.

In a two-element stable flow field produced in a wind tunnel, it is possible to
observe a smoke-marked flow line curling around an obstacle. Except for the "tail
flow" area, the shape of the flow line and the interval between it and other flow

lines remain almost stable and unchanging.

In a flow field without a rotational value, draw a set of closed lines. From the various points on these lines, extend several boundary flow lines to form a boundary wall called a "flow tube." Obviously, the gases flowing inside and outside the flow tube cannot penetrate its sides. This principle is constantly utilized in the designing of the gas flow passages of turbine jets, that is to say, the "boundary flow lines" of the sides of the flow tube are taken to represent the shape of the inside walls of the passages involved. For example, the pressure intensification apparatus, etc., on the intake of the combustion chambers of turbine jet engines on test firing beds.

In reality, there are viscosity shear forces between micro-masses of gas. During the movement of micro-masses of gas, there are not only deformation displacements, but also rotations and pulsations. "Spirals" are nothing but the violent rotation of micro-masses of gas, also called "vortical masses." Two times the angular velocity of rotation of the "vortical masses", 2ω, is called "curl." Flow fields in which large and small vortical masses roll over and over each other and pulsate are called "turbulence flow fields." "Turbulence flow fields" are unstable flow fields, therefore, it is not possible to draw out regular flow lines. However, following the statical averaging methods of "molecular motion theory", if one does not follow the progress of individual "vortical masses", but only observes the "average time" parameter for large numbers of "vortical masses" as they flow past specific points in a turbulence flow field, it becomes possible to obtain what is called an "average time parameter." The instantaneous parameter = the average time parameter + the pulsation parameter. Symbolically speaking, if one adds a horizontal line to represent an average time value and a comma shape in the upper right to denote a pulsation value, then, it is possible to write:

$$\rho = \bar{\rho} + \rho' \qquad u = \bar{u} + u'$$

$$T = \bar{T} + T' \qquad v = \bar{v} + v'$$

$$\rho = \bar{\rho} + \rho' \qquad w = \bar{w} + w'$$

In the laboratory, it is possible to explore flow fields using regular instrument pickups like pitot tubes, thermo-couples, etc. ; because the pick-ups have large inertias, the measurements from them are only of average pressures, $\bar{p}$, during a given time, of average temperatures, $\bar{T}$, during a given time, and of average flow

12

speed, $\overline{V}_o$, during a given time; for pulsation parameters, it is possible to use pick-ups with small inertias in order to measure the "pulsation wave shape". Speaking in terms of these average time parameters, "turbulence flow fields" can also have average time stable states and average time flow lines.

The special characteristics of the tumbling and pulsating of vortical masses in turbulence flow fields are as follows: the diffusion and exchange of mass, momentum and energy between vortical masses is particularly fast—from ten times to several hundred times faster than the exchange and diffusion accounted for by "molecular motion." The use of eddy current apparatus and stabilizing apparatus in combustion chambers is nothing but an attempt to utilize the particularly high speeds of mixing and diffusion which exist in turbulence flow fields in order to shorten combustion time and shorten flame length.

Sec 4 Jet Forms in Combustion Chambers of Turbine Jet Engines

It does not matter what type of structure a combustion chamber has; its air flow distribution and flow field structure must be able to satisfy the following conditions: mixing of fuel and air must be even; ignition must be fast; combustion must be stable; flames must be short; and the combustion chamber must put out exhaust gases within a certain limited range of evenly high temperatures. To meet these conditions one must utilize the differential between the inside and outside static pressures of flame tubes or the impulse pressure of intake gases as they flow through the eddy current apparatus, large apertures, small apertures, cracks, ducts, jet nozzles, etc and enter into the jet flow in order to control the flow field structure. A jet is a current which passes through a jet nozzle from one space into another space. This second space is filled with either stationary or moving gases. This current may have the same composition and temperature as the gases around it, or it may be composed of different elements at a different temperature; however, on all surfaces at which the boundaries of the jet contact the surrounding environment, the static pressures are the same. Depending on the form of the jet nozzle and the current, jets in combustion chambers can be divided as follows:

- Flat mouth, two-element jets, as in long, narrow intermixings of gases
- Round aperture, three-element jets, as found in the cooling apertures of the main combustion area
- Ring mouth, spiral jets, as found in the eddy current apparatus

- Narrow crack, half-jets that hug wall surfaces, as found in cooling gas films
- Vapor cones shot out by the small apertures of straight fuel spray nozzles
- Hollow vapor cones shot out by the ring nozzles of centrifugal jets
- Fuel and air, dual-state rotational jets shot out by pneumatic jet nozzles
- Dual-state jets put out by vaporization tubes, which, then, collide with sheild plates to form radial jets and vortices.

When cracks form in the walls of the tubes formed along the flow lines, fan-shaped jets are spewed out across the main direction of flow and are washed away by the main flow to form a curtain of gas; the reflux area behind this gas curtain is able to stabilize flames and is called an aerodynamic stabilizer.

All the various types of flame stabilizers used in afterburners are blunt obstacles and form reflux areas in their wakes. These wakes and jet fields have analogous locations.
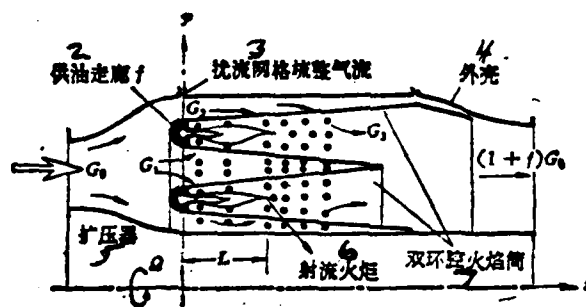
Fig 1.2

1. Combustion Chamber with Double-cavity Flame Tube and Parallel Flow Difusion Plume
2. Fuel Feed Passageway f 3. Disturbed Flow Lattice Smooths Out and Rectifies Air Flow 4. Outer Skin 5. Pressure Intensification Apparatus 6. Jet Plume 7. Double-Cavity Flame Tube

Two jets can flow parallel to each other; they can flow across each other in a perpendicular way; they can simply intersect each other, or, they can directly collide. In areas in which neighboring jets come into contact with each other, there

14

are sudden changes in flow speed; this produces shear layers (mixing layers).

Figure 1.2 shows a combustion chamber with parallel flow jets within a double cavity flame tube with a turbulence flow diffusion plume. Along the circumference of the fuel feed passageways there are two sets of numerous fuel jet nozzles which put out numerous vapor cones. The air intake, G_o, divides to become three layers; the first layer is air for the main combustion area, G_1; the second layer is the air for the supplementary combustion area, G_2, and the third layer is the air that goes to cooling, G_3; in turn, this air is supplied to the double-cavity flame tubes through small holes in the walls. The jets from the small holes and the main current together form a cross current curved jet. The fuel vapor evaporates and is diffused into the surrounding cross currents; the surrounding air disperses in the directions of the cross currents of the vapor cones; upon ignition, these become blowtorch-like plumes with length = L. The flow structure is simple; however, when the combustion chamber is relatively long, it becomes rather clumsy.

Figure 1.3 shows the flow field structure for the cavity of a flame tube with a fuel dispersion plate. The air intake, G_o, divides itself into three currents. One current of air, G_1, follows the spiral flow lines from the time they advance on the air plate and bore through the holes with the three fish-scale flaps into the forward portion of the flame tube cavity; these lines then mate up with the vortical flow which is induced by the fuel dispersion plate. A second current of air, G_2, passes through the hollow nozzle guide vane and, from there, enters the four round holes at the end of the gas cone where it is blown into the forward portion of the flame tube. The jets from these holes merge, push together and expand the radius of the vortex, R_v. Mixed and cooled, the third current of air, G_3, enters the rear portion of the cavity by following the rectangular air mix cowling which is arranged around the girth of the flame tube. Because the vortex induces an attractive force, the jet, G_3, which enters the cowling, is sub-divided again into two currents; one current is drawn forward into the vortex, and one current is drawn backward almost to the root of the nozzle guide vane. The jets from the three fish-scale holes in the forward gas plate flow smoothly, change direction and merge to become an intense spiral jet, appropriate for use by the eddy current apparatus. The jets from the four round apertures in the after gas plate merge to become jets with a fixed direction; these jets mate up with vortices to form ignition sources and to function as flame stabilizers. The cross currents that enter from the rectangular cowling divide to form branch jets; they pass through the flames and aid the functions of mixing and cooling. The half jets that enter from the air film cooling cracks

15

and stick to the walls protect the flame tube and the side walls of the after gas cone. The aerodynamic structure of this type of combustion chamber is relatively complex, and combustion in an undesigned state is difficult to stabilize; however, with a compact design, the length to radius ratio of combustion chambers can be made relatively small, and their weights can be made light.

One can study the flow fields of jets independently, from the points of view of nozzle size, shape and location.

Sec 5   Test Production Methods for Combustion Chambers of Turbine Jets

(1) Component Testing Methods:

With reference to the structure of various types of combustion chambers, we coordinated selection plans with other components. According to the various principal dimensions in the estimates of the unified, stable flow field required by operational conditions, we combined our experiences and made decisions for the design of test production originals of components. Large numbers of tests were run on components on test stands and in high altitude chambers. We made improvements to the design over and over again, and we tested over and over again until the capabilities of the combustion chamber measured up to the required standards, then, we reassembled the whole mechanism in order to make tests to see that the components mated together properly. In recent years, turbo-fans have already developed to the point where air flow quantities, $G \geqslant 400$; in the case of turbine jets, $G \geqslant 100$ (kg/s); overall combustion chamber intake pressures, $\overline{P}_2^* \cong 30$ atmospheres, and temperatures, $\overline{T}_2^* \cong 900K$. The use of components in original dimensions for making tests requires very large sources of air flow and pre-heating equipment as well as instrumentation for detection, testing and recording as well as the processing of data.

(2) Simulation Testing Methods:

In employing simulation testing methods, first, set out the set of partial differential equations which apply to the flow field of the combustion chamber in question. According to "equivalence theory", that is, the idea that, if the original form of a flow field and its simulated form are geometrically equivalent, if the flow conditions of the two are equivalent, and if both their motive forces and their heat

16

图1.3 电油盘环型火焰筒
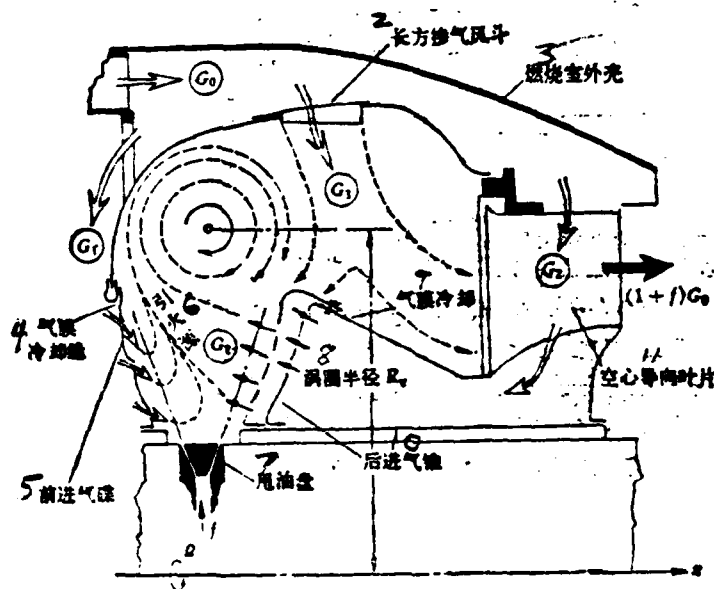
Fig 1.3

1. Fuel Dispersion Plate Annular Cavity Flame Tube 2. Rectangular Gas Mix Cowling
3. Outer Skin of Combustion Chamber 4. Air Film Cooling Crack 5. Forward Gas
Plate 6. Ignition Source 7. Fuel Dispersion Plate 8. Vortex Radius, R_v 9. Air
Film Cooling 10. After Gas Cone 11. Hollow Nozzle Guide Vane

states are equivalent, then, several "principles of equivalence" can be derived from
the differential equations. For example, the Reynolds number, $Re = VL/\nu$; the Mach
number, $M = V/a$; the special Prandtl number, $Pr = c\mu/\lambda$; the spiral density

number $Sc = \nu/D$, etc. V = flow speed; L = passage diameter; a = the speed
of sound; c = isostatic specific heat; λ = rate of thermal conductivity; μ = dyn-
amic viscosity; ν = kinetic viscosity, D = coefficient of diffusion. Whether one
makes a reduced scale model of the flow fields in question or cuts out a sector of
the original, on the test bed during experimentation, the simulations of the orig-
inal operational configuaration maintained the "principles of equivalence" through-
out. The scale of this type of test equipment is relatively small; the number of

17

repetitions of experiments required is also somewhat reduced. It is also possible to
use these simulation techniques to study some striking phenomenon. For example:

-Flow simulation testing of gas mixture bubbles. It is possible to observe the
configuration of the turbulent flow on the inside and the outside of transparent
models in order to aid in the analysis of the geometrical configuration and air flow
distribution of combustion chambers so as to determine whether they are satisfac-
tory or not.

-The injection of helium gas into the vortical reflux area. Simulations with
vapor fuels diffuse the mixing process. When one extracts a sample of the gases
involved and analyses them using a chromatagraph, it is possible to determine the
distribution of concentration.

The "principles of equivalence" of combustion flow fields can reach more than
ten in number. During testing it is not possible to simulate an perfect equivalent
of the operational configuration and flow field structure of the original form.
Therefore, the results of simulation testing have limitations. For example: when
one extracts a flame tube from a cannular combustion chamber and conducts combustion
tests with it in a laboratory air channel, one discovers that the ignition range,
the combustion efficiency, the overall pressure losses and the exhaust nozzle temp-
erature field all fit expectations and satisfy requirements. D = the diameter of
the flame tube. Maintaining the principles of equivalence, the following must be true.

$$K = \frac{G}{P_T^{*1.75} T_T^* D^3}$$

When this is compared with the capabilities as measured with the original combustion
chamber complete and on a test bed, one finds that the reality is not necessarily
satisfactory. The standard value of K is arrived at from the rate of chemical reac-
tion and the gas mass stop-over period; it does not take into consideration the "flow
field structures" of the intake, the interior and the external surroundings of the
flame tube. The flow field structures and turbulent flow configurations for the
interior and exterior of the flame tube are dissimilar as to the values obtained in
the laboratory air channel and those obtained when the complete chamber was on a
test bed; the air flow distributions were also dissimilar.

(3) Numerical Calculation Methods:

Physical modeling: The flow fields of combustion chambers are relatively com-
plex. The reasons for this include the fact that gases are compressible, that they

18

have viscosity, that flow fields have turbulence flow vortical bodies which diffuse and exchange mass, momentum and energy, that they have chemical reactions which change a variety of the constituents of the gases involved, that they have different size fuel droplets which vaporize in the flow and change the local concentrations; the gases involved exchange heat by radiation and convection with the walls of the flame tube; moreover, this is a three-element stable flow field. It is very difficult to sort out the equations for the mutually interacting influences of all the physical and chemical processes going on. Therefore, it is necessary, on the basis of the structural form of the combustion chamber, its operational configuration, its initial conditions and boundary conditions, to divide up the flow field and treat its various pieces differently. Axisymetric flow fields can be simplified into a two-element flow field on a meridian surface. Using average time parameters, it is possible to determine that it is a stable flow field when averaged over time. When one uses vaporization tubes or vapor fuels, it is possible to leave out of consideration the influence of fuel droplet vaporization. Assuming that combustion is the mixing together of two types of gases, it is possible to reduce the number of types of gases involved. Assuming a turbulent flow state model, it is possible to initially determine the coefficient of diffusion for mass, momentum and energy. The object of physical modeling is to highlight important contradictions, to extract the regularities governing changes, and, finally, to analyse the flow field structure of the combustion chamber in question.

Mathematical modeling: Based on the independent variables chosen for physical modeling (coordinates x, y, z ; time, τ) and the dependent variables ϕ (flow speed, concentration, temperature, pressure, etc) as well as on the principles of the conservation of mass, momentum and energy, if one uses the equations of Newtonian viscosity shear stresses, the equations of Fei Ke for the diffusion of matter and the equations of Fu Li-ye for rates of thermal conductance, it is possible to work out the continuity equations, certain averaged time equations as well as energy equations, and so on. These equations constitute a set of non-linear, second degree, non-homogeneous partial differential equations. Except under special circumstances, this set of partial differential equations is very difficult to figure out from a theoretical point of view.

Difference equations: The set of partial differential equations discussed above represents a set of related equations in which dependent variables, ϕ, follow, in some manner, independent changes which are introduced sep$a$rately into an independent variable. If one divides flow fields up into logical sections

in the form of a fine grid pattern, then, this grid pattern will have on it many "nodes." The values for the dependent variables, ϕ, as well as the derived first and second degree functions of the stresses involved will be different. Using the distance between two neighboring nodes, which is called the "step length," one replaces dx, dy, dz and $d\tau$ with Δx, Δy, Δz and Δr in the set of equations;

dy, dz, $d\tau$; $d\phi/dx$, $d^2\phi/dx^2$ likewise can be computed. In this way one one changes the original set of differential equations into a set of "limited difference" "algebraic equations" which can also be called a set of "difference equations.

Computer programing: Using computer language, take the operational procedure for solving sets of differential equations, and use it to write the program; then, put in the computer. If one has made the model of the flow field correctly and written the program correctly, then, in ten seconds to several minutes, the computer will give you a print-out of the structure of the flow field.

Chapter 2 Combustion Chamber Entry Diffusers

Sec 1 Diffuser Performance Requirements

As far as the subsonic portions of the entry passages of turbine jets are concerned, both the area in front of the entry to the main combustion chamber and the area in front of the entry to the after burner combustion chamber must have a diffuser to reduce speed and increase pressure. As far as the diffuser for the main combustion chamber is concerned, the requirements are as follows:

(1) It must take the air flow speed coming out of the compressors, i.e., $\bar{u}_1 = 120\text{-}200$ (m/s), $M_1 = 0.4\text{-}0.6$, and reduce them until the values in front of the entry to the combustion chamber are $\bar{u}_2 = 30\text{-}60$ (m/s), $M_2 = 0.1\text{-}0.2$; at the same time, the diffuser must increase the static pressure of the air flow so that $p_2 > p_1$. This will insure that the main combustion area allows for easy ignition and stable combustion.

(2) The overall pressure recovery coefficient of the diffusers, $\sigma = \bar{p}_2^* / \bar{p}_1^*$ is at its maximum which is the same as saying that the overall pressure loss, $\Delta \bar{p}^*$, must be minimized.

(3) In order to prevent boundary layer separation on the inner walls, the exhaust flow speed distribution must be made as uniform as possible in order to guard against a shift toward a pulsating gas flow which will interfere with the distribution of the amount of flow and the flow field structure in the flame tubes under different types of operational configurations.

Sec 2 Total Pressure Losses in Diffusers

There are two reasons for a loss of overall pressure during the process of diffusion: boundary layer separation and surface friction. Fig 2.1 (a) is a chart of the flow lines in a diffuser passage shaped like a conic section; Fig. 2.1 (b) shows local boundary layer separations which have given rise to spiral turbulence. Because of the viscosity of the gas, the speed of the flow line s-x, which sticks close to the surface of the wall, has the value, u = 0. The flow speed of the flow line, n, along the wall gets larger the closer it comes to the main flow until, when it reaches the place where the thickness of the boundary layer is δ, the flow speed has already approached the flow speed of the main

flow, $u = 0.99\tilde{U}$. Within the boundary layer, the laminar speeds, u, along n are distributed according to fixed laws. There is a direct ratio ($\partial u/\partial n$) between the stress caused by the viscous friction between two layers of gas which are flowing at different rates of speed, τ, and the gradient of the changes in flow speed which exists between two such layers:

$$\tau = \mu \frac{\partial u}{\partial n} \quad [N/m^2] \qquad (2.1)$$

μ is the "dynamic viscosity" of a gas. The engineering unit is $(kg \cdot s/m^2)$; the physical unit is $(N \cdot s/m^2)$. $(\mu/\rho) = \nu$, and this is called "kinetic viscosity"; the unit for this quantity is (m^2/s). Gases are the exact opposite of liquids in the respect that increases in the viscosity of a gas follow increases in the temperature of the gas. For example, between $20^{\circ}C$ and $100^{\circ}C$, the value of μ for water drops from 1.03×10^{-4} to $0.28 \times 10^{-4} (kg \cdot s/m^2)$; in the same temperature range, the value of μ for air actually increases from 1.8×10^{-6} to 2.22×10^{-6} $(kg \cdot s/m^2)$.

In the diffusion passage, gas can only flow by overcoming the pressure boost gradient ($\partial p/\partial x$). The mass of the micro-masses of gas must have sufficient momentum, mu, to overcome the viscous drag, $f = \pi Dl \cdot \tau$; only then can it flow. D = the internal diameter of the tube; l = the length of the tube. In the boundary layers, the closer one gets to the surface of the walls the lower are the values for the flow speed, u. Imagine, in Fig 2.1 (b), that, when the
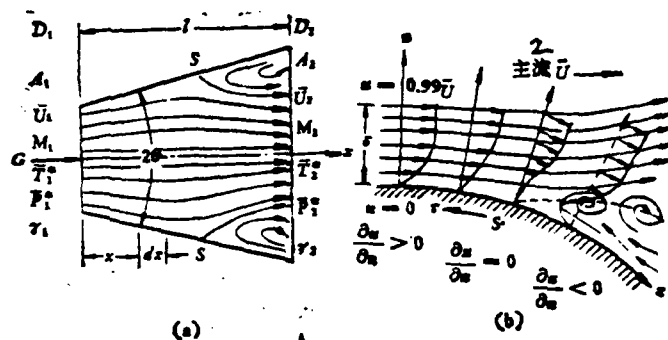

图2.1 扩压通道及附面层分离

Fig 2.1

1. Diffusion Passage and Boundary Layer Separation 2. Main Flow

static pressure is sufficiently high, and the flow speed gradient ($\partial u/\partial n$) reaches the place where it equals 0; then, the layer of gas that sticks to the wall will be unable to flow, and it will begin to separate from the surface of the wall at

point s. It is not permissible that there should be a vacuum between the separated flow and the surface of the wall. Because of this, the gas which flows down against the current and fills in the vacuum creates a negative flow speed gradient along flow line, $n_i = (\partial u/\partial n)_i$. The counter-current is erroded and overcome by the separated air current and turned so that it flows with the main current, creating a vortical turbulence flow. This vortical air mass spirals at high speed consuming energy. Because of this there is a loss in overall pressure:

$$(\Delta \bar{P}^*)_i = \psi \frac{\rho}{2} \bar{u}_1^2 \left(1 - \frac{\bar{u}_2}{\bar{u}_1}\right)^2,$$

ρ does not change, so

$$(\Delta \bar{P}^*)_i = \psi \frac{\rho}{2} \bar{u}_1^2 \left(1 - \frac{A_1}{A_2}\right)^2 \qquad (2.2)$$

ψ is called the "coefficient of expansion" and is related to the angle of expansion 2θ. Concerning equal cross sections of a straight tube, where $A_1 = A_2$, there is no expansion; $2\theta = 0$; there is no reduction in speed or increase in pressure; there is no separation; $\psi = 0$. If $2\theta = 180°$, suddenly there is expansion; suddenly there is reduction in speed and separation; $\psi = 1$. Fig 2.2 draws out the curve described by the values of ψ, the coefficient of expansion, as they vary with changes in the angle of expansion, 2θ; these values reflect conditions in a conic section-type diffuser. When $2\theta = 60°$, ψ can be 1.2. This is due to the fact that there is separation of the boundary layers all along the walls of the diffusion passage; moreover, this is accompanied by periodic pulsations; in this situation the overall pressure is still large compared to losses from sudden diffusion. After the angle of expansion, 2θ, reaches the point where it is $\geqslant 40°$, it is better not to use a straight tube for sudden diffusion and the reduction of speed; however, the use of such a tube does lessen the losses due to separation.

When the air flow overcomes the friction drag of the inside walls of the diffuser, f, there is an accompanying loss of overall pressure, $(\Delta P^*)_f$. The losses in overall pressure from friction drag are defined by the following equation

$$(\Delta P^*)_f = \xi_f \frac{l}{D} \frac{\rho \bar{u}_1^2}{2}, D = \frac{D_1 + D_2}{2}; \qquad (2.3)$$

ξ_f is called the "coefficient of friction drag;" it is a function of the degree of roughness of the wall surfaces and the Reynolds number of the intake as defined by the equation below

$$Re = \frac{a_1 D_1}{\nu}$$

$2300 < Re < 10^5,$ $\qquad \xi_f = 0.3164\, Re^{-0.25}$ $\qquad$ (2.4)

$Re \geqslant 10^5$ 以后, $\qquad \xi_f = 0.0032 + 0.221 Re^{-0.237}$ $\qquad$ (2.5)

Experimentation proves that, when the inside walls are smooth, $Re > 10^5$, $\xi_f \approx 0.004$ and there is almost no change.
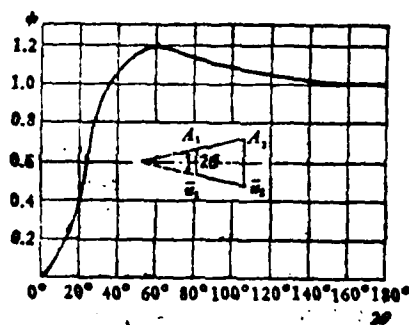

图2.2 锥筒扩压器"扩张系数"ψ变化曲线

Fig 2.2

1. Curve Defined by Changes in the "Coefficient of Expansion", ψ, for a Conic Section-type Diffuser

There are two types of overall pressure losses that must be figured together when dealing with diffusers; they are defined by the following equations:

$$\Delta \bar{P}^* = (\Delta P^*)_f + (\Delta P^*)_t = P_1^*(1 - \sigma).$$ $\qquad$ (2.6)

24

Sec 3 Coefficient of Total Diffuser Pressure Losses

It is possible to use different values of the angle of expansion, 2θ, in conducting wind tunnel–type experiments. In such experiments, the area to be studied is divided into parts and roving measurements are taken of the total pressures at various points on the cross sections of the intake and exhaust; on the basis of the distribution of the amount of flow $\rho u \, dA$ or momentum $\rho u^2 dA$, it is possible to obtain the weighted average total pressures $\overline{P}_1^*$ and $\overline{P}_2^*$, that is to say, it is possible to determine a precise value for total pressure loss, $\Delta \overline{P}^* = \overline{P}_1^* - \overline{P}_2^*$; therefore, it is possible to precisely determine the total pressure recovery coefficient, σ. Aerodynamic calculations habitually take the total pressure loss $\Delta \overline{P}^*$ to be several times the impact head or kinetic pressure of the intake, $q = \dfrac{1}{2} \rho_1 u_1^2$; this is

called   the coefficient of total pressure loss (or, flow drag coefficient) ξ; using the speed of sound, $a^2 = kp/\rho$, it is possible to write:

$$\rho = k\frac{p_1}{a^2}, \quad \xi = \frac{\Delta \overline{P}^*}{q} = \frac{\Delta \overline{P}^*}{\frac{1}{2}\rho u_1^2} = \frac{\Delta \overline{P}^*}{\frac{k}{2}p_1 M_1^2}$$

$$= \frac{(1-\sigma)}{\frac{k}{2} M_1^2\left(\frac{p_1}{\overline{P}_1}\right)}, \tag{2.7}$$

$$\sigma = 1 - \xi \frac{k}{2} M_1^2 \left(1 + \frac{k-1}{2} M_1^2\right)^{\frac{-k}{k-1}}$$

$$\cong 1 - \xi \frac{k M_1^2}{2}\left(1 - \frac{k}{2} M_1^2\right), \tag{2.8}$$

If one makes $a^* = 18.3\sqrt{T_1^*}$,   or uses coefficients of speed

$$\lambda_1 = \frac{u_1}{a^*}, \quad \sigma \cong 1 - \frac{k}{k+1} \xi \lambda_1^2, \tag{2.9}$$

it is possible to measure the ratio between the static pressure and the total pressure in the intake, $\pi(\lambda_1)$, and determine λ_1 or M_1. We already knew σ, so we can simply substitute it into the calculation. Not even considering the diffuser,

it is possible, using the values we already know for M_1 and 2θ to consult Fig 2.3(a) and obtain the coefficient of total pressure loss, ξ, for an incompressible gas flow. If one is considering the cross section of a rectangular diffuser, use Fig 2.3 (c); adjusted for the influence of compressibility, $\xi = \xi_0 K$.

(a) 锥形扩压器 ξ_0 随 M_1 及 2θ 变化

(b) 矩形扩压器

(c) 锥形扩压器
($\xi = \xi_0 K$, $K = $ 修正系数)
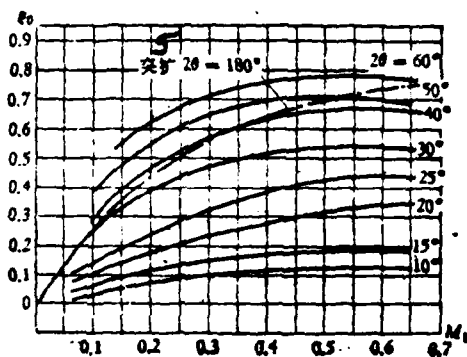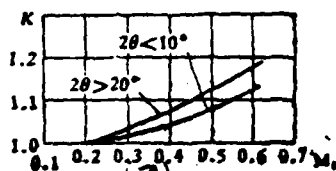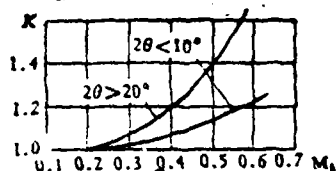
Fig 2.3

1. ξ_0 for a Conic Section-type Diffuser as it Varies With Changes in M_1 and 2θ

2. Rectangular Diffuser 3. Conic Section-type Diffuser 4. Correction Factor

5. Sudden Diffusion

In the case of a ring cavity diffuser, it is first necessary to make substitutions, so that it can be treated as an equivalent conic section-type diffuser; only then can one apply equation 2.2 or use Fig 2.3. If one has chosen a "turbine jet" design plan, one has already estimated the dimensions of the outline of the engine, and one already knows the exterior diameters, $\bar{D}_1$ and $\bar{D}_2$, for the intake and exhaust

of the ring cavity diffuser as well as their interior diameters, $\bar{d}_1$ and $\bar{d}_2$, and length $l_{:}$ then,

- The area of the intake of the ring cavity is $A_1 = \frac{\pi}{4}(\bar{D}_1^2 - \bar{d}_1^2)$,

- The length of the circumference is $L_1 = \pi(\bar{D}_1 + \bar{d}_1)$;

- The area of the exhaust of the ring cavity is $A_2 = \frac{\pi}{4}(\bar{D}_2^2 - \bar{d}_2^2)$,

- The length of the circumference is $L_2 = \pi(\bar{D}_2 + \bar{d}_2)$;

- The intake diameter of the equivalent conic section-type diffuser is $D_1 = \frac{4A_1}{L_1}$,

- The exhaust diameter is $D_2 = \frac{4A_2}{L_2}$;

- The angle of expansion for the equivalent conic section is

$$\operatorname{tg}\theta = \frac{D_2 - D_1}{2l} = \frac{r_2 - r_1}{l}. \quad (2.10)$$

Sec 4. Design Methods for Interior Walls of Diffusers

The shorter is the length l of the diffuser the better it is. When one figures out the angle of expansion, 2θ , by substituing in equation (2.10), it turns out to be quite large. In order to prevent boundary layer separation and to reduce losses in overall pressure, one must always employ the principle of "equal pressure gradients" in the design of the shape of the interior walls of diffusers. The design procedure is as follows:

(1) Data which is already known: intake area, A_1;   quantity of gas flow, G;   overall temperature, $\bar{T}_1^*$;   overall pressure, $\bar{P}_1^*$;   Mach number, M_1, or speed coefficient, λ_1;   area expansion ratio, A_2/A_1;   and length, l.

(2) Figure out D_1 and D_2, and figure out the angle of expansion, 2θ., using equation (2.10).

(3) Consult Fig 2.3 (a) and (c) on the basis of the values of M_1 and 2θ , and

27

(3) (cont'd) after the introduction of appropriate corrections, the coefficient of total pressure loss, $\xi = \xi_0 K$.

(4) Using equation (2.?) or (2.9), first calculate the coefficient of total pressure recovery, σ and $\overrightarrow{P_2^*} = \sigma \overrightarrow{P_1^*}$.

(5) According to the continuity equation of flow amount:

$$G = 0.396 \frac{\overline{P_1^*} A_1 q(\lambda_1)}{\sqrt{\overline{T_1^*}}} = 0.396 \frac{\sigma A_2 q(\lambda_2) \overline{P_1^*}}{\sqrt{\overline{T_1^*}}} \ [kg/s]$$

(2.11)

Because this is an adiabatic aerodynamic process, the overall temperature along the air channel does not change, that is, $\overrightarrow{T_1^*} = \overrightarrow{T_x^*} = \overrightarrow{T_2^*}$; therefore:

$$q(\lambda_2) = q(\lambda_1) \frac{A_1}{\sigma A_2},$$

To get a precise value for $q(\lambda_2)$, check out the charts and get values for λ_2 and σ_2). (2.12)

Based on the values obtained for $\pi(\lambda_1)$ and $\pi(\lambda_2)$:

- Intake static pressure is $\quad p_1 = \overline{P_1^*}\pi(\lambda_1)$ (2.13)

- Exhaust static pressure is $\quad p_2 = \overline{P_2^*}\pi(\lambda_2)$ (2.14)

- The static pressure at x is $\quad p_x = \overline{P_x^*}\pi(\lambda_x)$ (2.15)

Determine the length, l , of the diffuser along the horizontal or x coordinate by using the scale. First, assume that the total pressure, $\overrightarrow{P_{\sigma_x}^*}$, falls from $\overline{1}$ along a straight line, x. (Fig 2.4) Calculating in this way, any possible one might deviate on the low side can be overcome later by corrections. Draw out the equal pressure gradient

$$\frac{dp}{dx} = \frac{\Delta p}{\Delta x} = \frac{p_2 - p_1}{l} = \beta = \text{constant straight line} \quad p_x = \beta x + p_1.. \quad (2.16)$$

Since we already know the air flow quantity, G, make use of the aero-

dynamic functions:

$$\frac{q(\lambda_z)}{z(\lambda_z)} = y(\lambda_z), \quad G = 0.396 \frac{p_z A_z y(\lambda_z)}{\sqrt{\overline{T_1^*}}}, \quad A_z = \pi r_z^2,$$

$$p_z \pi r_z^2 y(\lambda_z) = \frac{G\sqrt{\overline{T_1^*}}}{0.396}, \quad \overset{or}{\text{或}} \quad r_z^2 = \frac{C}{p_z y(\lambda_z)},$$

$$C = \frac{G\sqrt{\overline{T_1^*}}}{0.396 \pi} = \text{constant} \qquad (2.17)$$

(10) From Fig 2.4 one can get values for $\overline{P_x^*}$ and p_x; in order to obtain $x'(\lambda_x)$, get values for λ_x and $y(\lambda_x)$, substitute them into equation (2.17), and figure out r_x and the cross section, $A_x = \pi r_x^2$. .

(11) On the basis of this value of r_x, figure out $\mathrm{tg}\,\theta_x = \frac{r_x - r_1}{x}$,

then, using $2\theta_x$ and M_1, go back to Fig 2.3 (a) and (c) and get ξ_z.

(12) Using equations (2.8) or (2.9), find the value of σ_x and see if it corresponds with the value of σ_x postulated on Fig 2.4.

(13) If it does not correspond, then, one can adjust the value of σ_x as shown on Fig 2.4 and redo the calculations.

(14) Take l and divide it into several sections using an interval Δx to define the sections; take the M_x value for the forward section of the exhaust and use it as the M_1 value for the lower section of the intake; on the basis of this procedure, figure out the various values of r_x, that is to say, draw out the equal pressure gradient which defines the profile line of the interior wall of the diffuser.

(15) In order to guarantee the smoothness of the air flow, one ought to use a smoothly curving, continuous line to connect the exhaust of the diffuser with the interior and exterior shells of the combustion chamber, as shown by the broken line in Fig 2.4. In order to improve the technical characteristics, it is best to use a segmented, rounded arc in order to piece together the line which defines the form of the interior wall. When one considers the "displacement thickness" of the boundary layers, it becomes appropriate to enlarge somewhat the cross section of the exhaust, A_2.
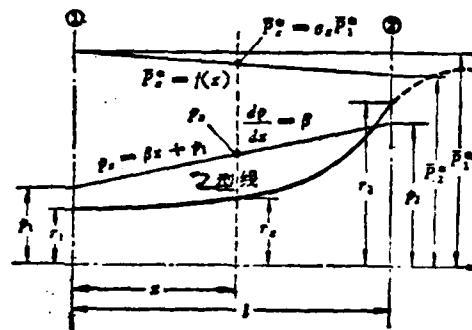
图2.4 等压梯度内壁型线画法

Fig 2.4

1. Method for Drawing Out the Form Line of the Interior Wall Defined by the Equal Pressure Gradient 2. Form Line

Sec 5 Influences of Diversion Sub-surfaces on Cavity Diffusers and Combustion

(1) Because of the limitations on space, the length, l , of ring cavity diffusers is very short; the equivalent angle of expansion, $2\theta \geqslant 40^{\circ}$; therefore, the boundary layers on the interior walls will certainly experience separation, and there will be formed vortical turbulence flow; because of this, the total pressure losses, $\Delta \overline{P_4^*}$ are very large. Even if the system is in a state of stable operation, the axial flow (or centrifugal) compressors, due to the power added by the blades, cause the flow speed distributions in the intake of ring cavity diffusers to be extremely uneven in both a radial and a circumferential direction. On top of this, after the turbulence flow caused by boundary layer separation inside the diffuser has its effect, the distributions of total pressure and quantity of flow in the exhaust will be even more uneven. This will influence the air intake of flame tubes in a way which is distributed according to predetermined proportions as well as influencing the internal flow field structure of the flame tubes; because of this, it will also influence combustion characteristics.

If one chooses an "appropriate location" on the inside walls of a diffuser and cuts a ring-shaped trough, then, bores several air holes in it, connecting them to a vacuum pump or to a telescoping jet apparatus in the tailpipe, then, it is

30

possible to draw off sensitive boundary layers and prevent separation and the formation of spiral flow patterns, thus improving the exhaust flow speed distribution (Fig 2.5).

The width of the ring-shaped trough for drawing off the gases is 0.25 (cm), and its depth if 0.63 (cm);

图2.5 短环扩压器抽走附面层实验方案图
（① 进口流道径向分布；② 扩压器环腔外壁；③ 扩压器环腔内壁；
④ 外壁环形槽及抽气孔；⑤ 内壁环形槽及抽气孔；⑥ 气态燃料供
应管；⑦ 支撑架；⑧ 外圈 48 个涡流罐；⑨ 中圈 40个 涡流罐；
⑩内圈 32 个涡流罐；⑪ 短环腔火焰筒外壁；⑫ 短环腔火焰筒内
壁；⑬ 16 根抽气管，外壁；⑭ 16 根软管，内壁抽气）

Fig 2.5

1. Diagram of a Plan for an Experiment in Drawing Off Boundary Layers in a Short Ring Cavity Diffuser 2. Amount of Air Extracted Through the Outside Wall 3. Amount of Air Extracted Through the Inside Wall 4. Radial Distribution of Intake Flow Speed 5. Outside Wall of the Ring Cavity of the Diffuser 6. Inside Wall of the Ring Cavity of the Diffuser 7. Ring-shaped Trough and Suction Holes on the Outside Wall 8. Ring-shaped Trough and Suction Holes on the Inside Wall 9. Feed Line for Fuel in Gaseous State 10. Brace Assembly 11. The Outboard Set of 48 Vortical Flow Canisters 12. The Middle Set of 40 Vortical Flow Cannisters 13. The Inboard Set of 32 Vortical Cannisters 14. Exterior Wall of Short Ring Cavity Flame Tube 15. Interior Wall of Short Ring Cavity Flame Tube 16. 16 Gas Suction Tubes, Outside Wall 17. 16 Flexible Hoses on the Inside Wall for Gas Suction

On the interior walls, each trough has drilled in it 440 ϕ 2.4 gas suction holes; the gas suction area $\doteq$ 39.4 (cm^2); the volume of gas drawn off, X_i = 1.25% of the intake volume; on the exterior walls, each trough has drilled in it 480 ϕ 2.4 gas suction holes; the gas suction area $\doteq$ 43 (cm^2); the amount of gas drawn off, X_o = 1.1-3% of the intake volume, and the total amount of gas drawn off, X = 2.35 - 4.25% of the intake volume.

For the forward ring cavity of the intake of a diffuser, the exterior wall diameter is ϕ_o, and the interior wall diameter is ϕ_i; the largest diameter of the combustion chamber is D_m = 106 (cm), and the overall length , L = 51 (cm). In this case

$$L/D_m \cong \frac{1}{2};$$

The 120 vortical flow cannisters are arranged in three concentric rings— the outside, middle and inside. In order to eliminate the influence of the vaporization of liquid fuel, during experimentation, a natural gas containing 93.5% methane was used as fuel. This natural fuel was distributed among the various ducts and fed into the vortical flow cannisters; there was ignition and combustion, and the exhaust from the vortical flow cannisters became the main combustion area for the "spiral flames." The secondary combustion area and cooling area were both greatly shortened.

The angle of expansion of the exterior wall of the diffuser, θ_o = 25°; the angle of expansion of the interior wall, $\overline{\theta_i}$ = 15°; and, they are not symmetrical with respect to the center line of the ring cavity. Because the area of contact between the outer ring cavity and the air flow is large, the viscous flow drag is large, the flow speed is low, and, therefore, when simulating high altitude flight at low speed, the major part of the intake quantity, G, passes through the inner ring cavity and does not pass through the vortical flow cannisters. In this way it is possible to create a rich fuel mixture in the main combustion area and widen the flameout thresholds. The parameters obtained from combustion testing to simulate "cruising" and " high altitude flameout thresholds" are presented below:

模拟状态	进气压力 P_2^* [kg/cm^2]	进气温度 T_2^* [K]	进气量 G[kg/s]	参考流速 θ_2[m/s]	"油气"比 $f = \frac{G_f}{(1-X)G}$
巡航	2.13	589	19.5	30	0.015
高空熄火	1.05	300	19.5	15—30	0.015

1. State Being Simulated 2. Cruising 3. High Altitude Flameout 4. Total Intake Pressure 5. Overall Intake Temperature 6. Quantity of Intake 7. Reference Flow Speed 8. Fuel-to-Air Ratio

(2) The Measurement of Parameters and the Calculation of Capability Targets

Ring Cavity Diffuser Intake: We already know the area of the intake, A_1, the quantity of intake, G, and we can measure the total pressure, $\overline{P}_1^*$, the static pressure, p_1, and the overall temperature, $\overline{T}_1^*$; we can then, on the basis of functional equations for aerodynamic quantities of flow, figure out λ_1. According to critical sonic equations, $a^* = 18.3 \cdot \sqrt{\overline{T}_1^*}$, so we can figure out a^* or the sonic a. Because of this, it is possible to deduce the average intake flow speed $\overline{u}_1 = \lambda_2 a^*$ (m/s). In these experiments, $M_1 = 0.2 \sim 0.5$.

Ring Cavity Diffuser Exhaust: We already know the area of the exhaust, $A_2 = 2260$ (cm^2). We have measured the total pressure, $\overline{P}_2^*$, and the overall temperature, $\overline{T}_2^* = \overline{T}_1^*$; on the basis of continuous flow equations, it is possible to obtain values for $q(\lambda_1)$; we can get the value of λ_1 from the chart and deduce the average exhaust flow speed $\overline{u}_2 = \lambda_2 a^*$ (m/s). In these experiments $M_2 = 0.05 \sim 0.15$.

Ring Cavity Combustion Chamber Exhaust: Using a suction-type (platinum – platinum + 13% rhodium) mobile, supported thermocouple to take sample measurements at scattered points, it is possible to obtain the overall temperature, $\overline{T}_3^*$, of the exhaust on the basis of the flow distribution weighted average. Using the same type of scattered readings, it is possible to obtain a weighted average for the total exhaust pressure, $\overline{P}_3^*$. On the basis of the amount of fuel supplied, G_f, and the amount of intake, G, minus the amount of gas that is drawn off in the form of boundary layers, X%, it is possible to figure out the fuel to air ratio for the whole combustion chamber, $f = G_f/(1 - X) G$.

We already know f (or $\frac{\alpha}{\alpha L_o}$), $\overline{T}_2$ and $\overline{T}_3^*$; by checking a table or graph, we can get the average specific heat, $\overline{c}_p$.

We already know the value for the amount of heat contained in each kg of gaseous fuel, H_u, and, based on the relationship $fH_u = \overline{c}_p(\overline{T}_3^* - \overline{T}_1^*)$ it is possible to determine the "ideal overall temperature", $\overline{T}_{13}^*$ (K), for the combustion chamber exhaust. In this experiment, the average overall temperature of the exhaust, $\overline{T}_3^* = 1230$ (K).

Through manipulation of the movable support apparatus, it is possible to take scattered readings in the exhaust which reflect the radial and circumferential overall temperature distributions, r and θ; $T_3^* = f(r)$ and $T_3^* = f(r\theta)$; it is also

33

possible to record the highest temperature, T_{3m}^* (K).

The calculations below then become possible:,

—Combustion Efficiency

$$\eta = \frac{\overline{T}_3^* - \overline{T}_2^*}{\overline{T}_{i_1}^* - \overline{T}_2^*} \times 100\%$$

—Overall Temperature Field Form Coefficient

$$\delta = \frac{T_{3m}^* - \overline{T}_2^*}{\overline{T}_3^* - \overline{T}_2^*} > 1$$

(3) Results of Experimentation and Discussion

The influence of the drawing off of boundary layers through suction on combustion efficiency, η, is shown in Fig 2.6. In this illustration, the average overall temperature of the combustion chamber intake, $\overline{T}_2^* = 300$ (K), simulating a condition approaching the threshold of high altitude flameout. When there is no suction, X = 0% as compared with $X_o = 3\%$ for the gas sucked through the exterior wall: when the overall intake pressure, $\overline{P}_2^* \cong 2$ (kg/cm^2), the combustion efficiency, $\overline{\eta}$, when there is suction as compared to when there is no suction, rises from 68% to 100%; when $\overline{P}_2^*$ is reduced to 1.35 (kg/cm^2), the absence of suction causes a flameout, and $\overline{\eta} = 0$;
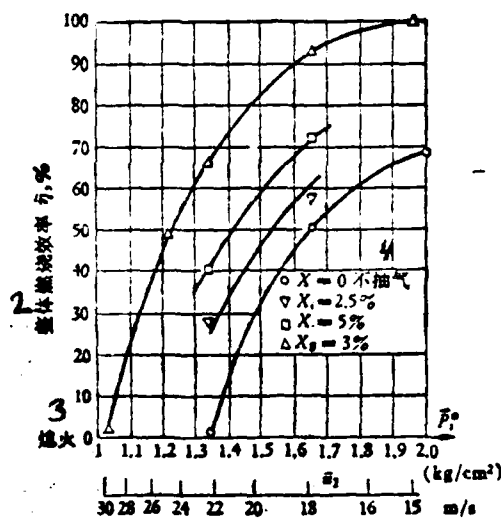

图2.6 抽气量 X% 对 $\overline{\eta}$ 的影响

Fig 2.6

1. Influence of the Amount of Suction, X%, on $\overline{\eta}$ 2. Overall Combustion Efficiency, $\overline{\eta}$, %

3. Flameout   4. No Suction

34

however, with suction, combustion efficiency can still reach 66%. With suction, one can make further reductions and still not get flameout until $\overline{P}_2^* \cong 1.05$ (kg/cm^2) and $\overline{u}_2 \cong 30$ (m/s). This proves that if the amount of outer wall suction, X%, in asymmetrical diffusers is chosen correctly, then, it is possible to postpone high altitude flameout and expand the stability boundaries for lean mixtures. If only gas sucked through the interior wall, $X_i = 2.5\%$, there is only a small improvement in combustion efficiency. If there is suction through the interior and exterior walls at the same time, and $x_i + x_o = X = 5\%$, there is an improvement; however, the results are not as good as when only suction through the exterior wall is involved. The reason for this is that the angle of expansion for the exterior wall is large; the angle of expansion for the interior wall is small; even if there is no suction, and X = 0%, there is already separation along the exterior wall of the ring cavity flow path; the radial flow speed distribution is already faster than the interior wall flow speed, and its volume of flow is greater. The small amount of suction through the interior wall cannot change the situation as a whole; however, a diminution in suction through the exterior wall can most certainly eliminate separation and cause the flow speed distribution to reach toward uniformity; because of this fact, there is an improvement in the intake conditions for the three rings of vortical flow cannisters and in the distribution of local air-to-fuel ratios. Combustion efficiency, η, is raised, and stability is improved.

The lay-out of the arrangement of the three rings of vortical flow cannisters should also conform itself to the exhaust flow field of the ring cavity diffuser. The distance between the inner ring of vortical flow cannisters and the inner wall as well as the distance between the middle ring and inner ring of vortical flow cannisters should both be somewhat larger than the distance between the middle ring and the outside ring or the outside ring and the outside wall. When there is no suction, this causes the middle ring of vortical flow cannisters to do everything possible to prevent a shortage of air.

The radial distribution of overall temperature in the exhaust of the combustion chamber follows changes in the amount of suction, X%. (Fig 2.7) When in a state designed to simulate "cruising", the average overall temperature, $\overline{T}_3^*$, of the exhaust of the combustion chamber equals 1230°K, the average overall temperature of the intake, $\overline{T}_2^* = 589$ (K), and the overall "fuel-to-air ratio", f = 0.015.

If one refers to Fig 2.7 (a), the amount of gas drawn off from ∇ of the interior wall, $X_i = 1.25\%$; if one eliminates the boundary layer separation from the interior wall, then, the flow along the interior wall is unimpeded, and the amount of the flow is increased; because of this, the amount of flow along the exterior wall

35

is reduced. As a result, the peak exhaust temperature value moves out toward the tips of the blades. The field pattern coefficient, δ, goes from a value of 1.47 when there is no suction through an increase to a value of 1.75. This is because, when there is no suction, the middle ring of vortical flow cannisters is already short on air, and the local fuel-to-air ratio deviates toward the "rich" side; besides that, the amount of air flow which supplies the middle ring and comes from the suction through the interior wall is even less. Above the radius of the middle ring, the air flow temperature shows a deviation on the high side; below the radius of the middle ring, it shows a deviation on the low side; there-fore, the efficiency of combustion, η, contrary to expectations, drops to 39% from the 96% which is its value when there is no suction.

When the suction $\triangle$ of the outer wall, $X_o = 1.1\%$, the result is the exact opposite. The peak temperature value for the exhaust, $\overline{T}_{3m}^{*}$, moves toward the base of the blades. The temperature at the base of the blades is raised approximately $\cdots$°C as compared to when there is no suction, and the temperature at the tip of the blades is reduced approximately 284°C. The major portion of the air intake supplies the area above the middle ring of vortical flow cannisters, in order to improve the combustion situation. The field pattern coefficient, δ, still equals 1.75; however, the efficiency of combustion, η, is raised to 98.5%.

Refering to Fig 2.7 (b), suction on both sides causes the peak temperature values for the exhaust to appear in the area of the ring cavity about half way up its h/eight. When there is no suction, the center ring of vortical flow cannisters will already be short of air; if the suction starts up on both sides at the same time, the middle ring will be even shorter on air; therefore, the temperature of the middle belt of the exhaust will tend toward the high side.

The effect that suction on both sides has on combustion efficiency, η, is not good, and the field pattern coefficient, δ, also shows harmful changes. The reason for this is that this type of suction causes the distribution of air flow to the three rings of vortical flow cannisters to be uneven, differences in concentration to be large, and the whole efficiency of combustion, η, to drop. Besides this, suction on both sides causes the main flow to be very sensitive, suffer somewhat from the effects of pulse interference, and immediate changes in the distributions of the amount of flow and flow speed cause instability in combustion.

The overall amount of suction, $X\%$, as it affects the total pressure losses $(1-\sigma^{*})$ in the intake and exhaust of the combustion chamber is shown in Fig 2.8. The total pressure of the diffuser exhaust, $\overline{P}_2^{*} = 2.13$ (kg/cm^2); the overall temp-

erature, $\overline{T}_2^* = 590$ (K);   the Mach number of the diffuser intake, $M_1 = 0.28$;   and,
the Reynolds number, $Re = 1.9 \times 10^5 \sim 3.3 \times 10^5$.   In a cruising configuration, experiments that have been carried out have led to the conclusion that: suction can
prevent or control boundary layer separation, reduce total pressure losses, and
improve combustion characteristics; *however,* the positioning of the suction and
the amount of the suction must be appropriate.
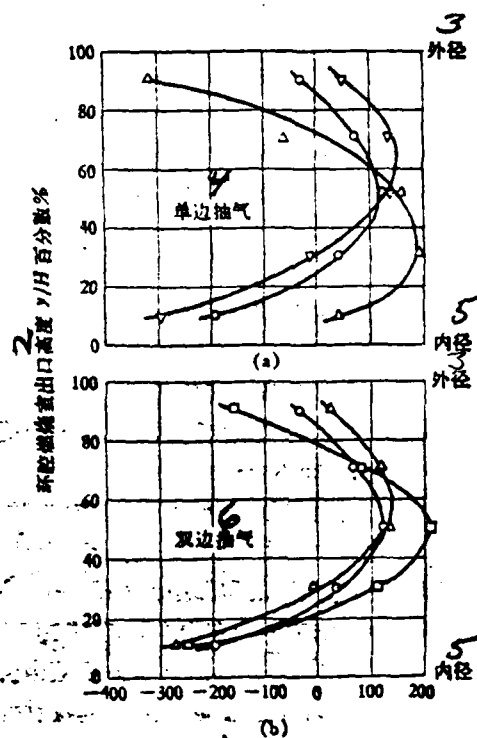
图 2.7   与出口平均温度的偏差 $(T_3^* - \overline{T}_3^*)$ [℃]
[图2.7   (a) 单边抽气影响: ○ 不抽气 $X = 0\%$; ▽ 内壁抽
气 $X_i = 1.25\%$; △外壁抽气$X_o = 1.1\%$; ○ $\delta = 1.47$, $\bar{\eta} = $
96%; ▽ $\delta = 1.75$, $\bar{\eta} = 89\%$; △ $\delta = 1.75$, $\bar{\eta} = 98.5\%$.
图2.7(b) 双边抽气影响: △ $X_i = 0.95\%$, $X_o = 1.2\%$; □
$X_i = 1.96\%$, $X_o = 3.14\%$; ○ 不抽气, $\delta = 1.47$, $\bar{\eta} = 96\%$;
△ $X = 2.15\%$, $\delta = 1.63$, $\bar{\eta} = 90\%$; □ $X = 5.1\%$, $\delta = $
1.89, $\bar{\eta} = 93.8\%$. $H = $ 环腔燃烧室出口径向高度, $0 < y < H$,
$y = $ 径向距离]

Fig 2.7

1.   Deviation From the Average Temperature of Exhaust   2.   y/H % of the Exhaust Height
of Ring Cavity Combustion Chamber   3.   Outside Diameter   4.   Unilateral Suction.
5.   Inside Diameter   6. Suction on Both Sides   7.   Figure   8. Influence of Unilateral
Suction   9. No Suction 10. Inner Wall Suction   11. Outer Wall Suction   12. Influence
of Suction on Both Sides   13. Radial Exhaust Height of Ring Cavity Combustion Chamber
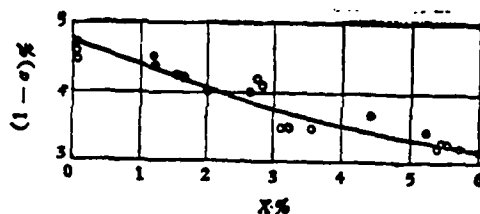14. Radial Distance   37

図 2.8 总抽气量对燃烧室总压损失的影响
(○ 冷吹风测得数据: ● 有燃烧, $f = 0.015$; 总压损失:
$\Delta P^* = P_1^* - P_2^* = P_1^*(1 - \sigma))$

Fig 2.8

1. The Influence of the Total Amount of Suction on the Total Pressure Losses in the Combustion Chamber 2. Data obtained from Air Flow Tests Without Ignition 3. With Combustion 4. Total Pressure Losses

Sec 6 Special Characteristics of Sub-surfaces

(1) Boundary layers, as they flow along the walls, can divided into laminar flow and turbulent flow. Because there are vortical masses in the turbulent flow which cut across the flow and diffuse, exchanging energy and momentum, turbulent flow boundary layers are usually somewhat thicker than laminar flow boundary layers; these turbulent flow boundary layers can withstand relatively higher pressure gradients without exhibiting separation.

(2) The laminar flow boundary layers get thicker as they flow along their course. For example, if a laminar flow boundary layer is flowing along a flat surface from the forward edge to a place 1000 (mm) down the flow, its thickness at the end of the run, $\delta \approx$ 5 (mm). If it receives pulsating interference from the main flow, a laminar boundary layer can turn into a turbulent flow boundary layer and increase its flow drag.

(3) In the main flow, the flow speed in the normal direction is distributed evenly; the cross current speed gradient, $\partial U/\partial y \approx 0$; therefore, the viscous friction stress, τ , can be ignored; however, in the boundary layers, changes in flow speed are great; the flow speed gradient $\partial u/\partial y$ along direction y cannot be ignored; because of this, one must consider the stresses caused by viscous friction; however, when flow speeds are relatively slow, one can ignore compressibility, that is to say, $\rho \approx$ a constant.

(4) The static pressure of the main flow, p , as it exists along the normal

38

line y, passes through the boundary layer and straight on to the surface of the wall; because of this, the rate of pressure change, $\partial p/\partial x$, along the x coordinate is the same in the boundary layer and the main flow.

(5) As far as the two-level boundary layer displacement thickness, δ^*, is concerned, if one locates a certain point A on a wall surface, then, the boundary layer thickness at point A = δ (Fig 2.9).

Suppose the flow speed of the main flow in direction x at a point outside the boundary layer which corresponds to point A = U, then, the flow speed inside the boundary layer, u, along normal line y, changes from u = 0 to u = U. However, if there is no viscous friction drag, then, there is no boundary layer, and, necessarily, flow speed, u, along direction x of thickness δ should not be reduced, but should always be equal to U. Suppose one drops a perpendicular to the surface of the illustration with a length = 1 (of some unit of length). Then, suppose one sets things up so that the distribution function, u, along y, is equal to $f(y)$. In such a case,
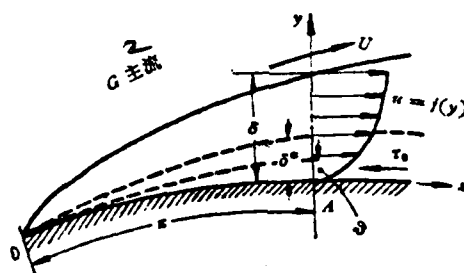

图2.9 二元曲面附面层

Fig 2.9

1. A Two-Element Boundary Layer Along a Curved Surface 2. Main Flow

if one has to contend with both viscosity and boundary layers, then, there is a mass flow rate of $\delta \times 1$ every second, and

$$\dot{m} = \int_0^\delta \rho u \, dy, \qquad (2.18)$$

if one discounts viscosity and boundary layers, then, there is a mass flow rate of $\delta \times 1$, and

$$\dot{m}_t = \int_0^\delta \rho U \, dy;$$

therefore, because there is viscosity, μ', the actual rate of mass flow through δ every second is diminished so that $\Delta \dot{m} = \dot{m}_i - \dot{m}$;

$$\Delta \dot{m} = \int_0^\delta \rho U \, dy - \int_0^\delta \rho u \, dy = \int_0^\delta \rho(U - u) \, dy$$

$$= \frac{\Delta G}{g} = \rho U \delta^*; \tag{2.19}$$

That is to say that, because there is viscosity, and the wall surface produces friction stress, τ_0, it is as though the wall surface has squeezed inward a certain distance, δ^*, causing the passageway to become narrower. Because of this fact, the actual amount of air flow, as compared to a circumstance when there is no viscous friction drag, is reduced to an amount, ΔG. Therefore, δ^* is called the "displacement thickness." On the basis of equation (2.19), one can say that

$$\text{displacement thickness, } \delta^* = \frac{1}{U} \int_0^\delta (U - u) \, dy = \int_0^\delta \left(1 - \frac{u}{U}\right) dy \tag{2.20}$$

In order to get the integral for equation 2.20, one must know the laws which govern the flow speed distribution inside the boundary layer, $u = f(y)$, as well as the thickness, δ, of the boundary layer. If one is concerned with a turbulent flow boundary layer, it is possible to use the "averaged time parameters" $\overline{U}$ and $\overline{u}$, etc. and still be able to obtain the average time displacement thickness, δ^*, on the basis of equation (2.20).

(6) Two-Element Boundary Layer Momentum Thickness, ϑ

Refering to Fig 2.9, the amount of movement through δ along direction x each second is represented by $M = \int_0^\delta \rho u^2 \, dy$.

Even if one supposes that there is no viscosity, there is still an actual $\dot{m}$ passing through δ in direction x, and this amount of motion, $M_i = U\dot{m}$; therefore, because there is viscosity, the amount of movement or momentum lost when $\dot{m}$ passes through δ is described by the following:

$$\Delta M = M_i - M = \overline{U} \int_0^\delta \rho u \, dy - \int_0^\delta \rho u^2 \, dy$$

$$= \int_0^\delta \rho u(U - u) \, dy = \rho U \vartheta; \tag{2.21}$$

ϑ increases in thickness along x, and the amount of movement involved loses thickness

$$\vartheta = \int_0^\delta \frac{u}{U}\left(1 - \frac{u}{U}\right) dy, \quad U^2\vartheta = \int_0^\delta u(U - u)dy; \quad (2.22)$$

That is to say, because of viscosity, flow speed distribution within a boundary layer decreases from the boundary, δ, with its value U to the value of u on the wall surface which is $u = 0$; although the rates of mass flow, $\dot{m}$, through $\delta \times 1$ are all the same, it is as though the wall surface squeezes in a distance ϑ toward the main flow; due to this fact, the actual air flow loses an amount of momentum, ΔM, as compared to an air flow with no viscosity. $\delta > \delta^* > \vartheta$, $\delta^*/\vartheta = H > 1$, is called the "speed pattern template."

Sec 7   Integral Equations for Momentum of Dual Turbulance Sub-surfaces

If one supposes that he is dealing with a non-steady state, two element, non-compressible turbulence boundary layer (Fig 2.10), perpendicular to the surface of the illustration with a dimension = 1 (of some unit of thickness); then the thickness of the boundary layer, δ, varies with changes in x. τ_0 = the viscous friction stress of the wall surface (N/m^2).

First one draws out a differentiation control area ABCD. At a given instant, t, the flow speed of a certain point in the boundary layer, $u = u(x, y, t)$, and the differentiated volume within the control area = dxdy · 1.

The mass flowing in from side AB is

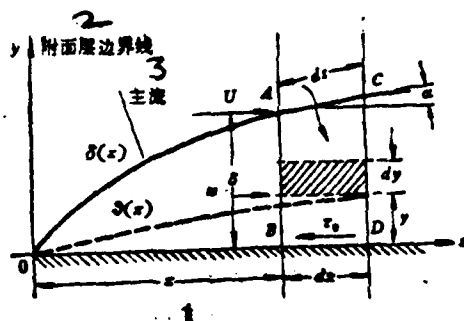$$m(x, t) = dt \int_0^\delta \rho u dy,$$

图2.10　附面层积分方程示意图(考大)

Fig 2.10

1. Diagram of Integral Equations for Boundary Layer (Enlarged)   2. Boundary Layer Limit
3. Main Flow

The mass flowing in from side CD is

$$m(x + dx, t) = m + \frac{\partial m}{\partial x} dx = dt \int_0^s \rho u \, dy$$
$$+ \left(dt \frac{\partial}{\partial x} \int_0^s \rho u \, dy \right) dx \; ;$$

The difference between the masses entering from side AB and CD is

$$m(x + dx, t) - m(x, t) = dt \, dx \frac{\partial}{\partial x} \int_0^s \rho u \, dy;$$

The wall surface is non-permeable; therefore, it is necessary for the air flow

$$\left(dt \, dx \frac{\partial}{\partial x} \int_0^s \rho u \, dy \right)$$ to come in from side AC and refill the control area.

The momentum of the air that flows in through side AC $= U \left(dt \, dx \frac{\partial}{\partial x} \int_0^s \rho u \, dy \right)$,

The momentum of the air that flows in through side AB $= \int_0^s \rho u^2 \, dy = M$,

The momentum of the air that flows in through side BD $= 0$.

The momentum of the air that flows in through side CD $= M + \frac{\partial M}{\partial x} dx$

$$= \int_0^s \rho u^2 \, dy \, dt + dx \, dt \frac{\partial}{\partial x} \int_0^s \rho u^2 \, dy.$$

Therefore, the momentum of flow from ABCD along direction x $= dt \, dx \frac{\partial}{\partial x} \int_0^s \rho u^2 \, dy$

$$- U \, dt \, dx \frac{\partial}{\partial x} \int_0^s \rho u \, dy. \tag{2.23}$$

Concerning changes in the momentum along x, if t = time t, the diffential momentum of the control area $dxdy \cdot 1 = \rho dxdy \cdot u$; t = time t+dt, and the momentum of the differential $dxdy \cdot 1$

42

$$= \rho \left(u + \frac{\partial u}{\partial t} \cdot dt \right) dx dy \cdot 1.$$

The increase in the amount of momentum along direction x which occurs within the time interval dt inside the differentiated volume

$$= dx dy dt \rho \frac{\partial u}{\partial t},$$

The increase in the amount of momentum in direction x which occurs within the time interval dt inside the control area ABCD

$$= \rho dx dt \int_0^{\delta} \frac{\partial u}{\partial t} \, dy . \qquad (2.24)$$

The rate of change of momentum along direction x per second should be equation (2.39) + (2.40) once again divided by the time interval dt, that is to say,

$$\frac{dM}{dt} = \rho dx \int_0^{\delta} \frac{\partial u}{\partial t} dy + \rho dx \left(\frac{\partial}{\partial x} \int_0^{\delta} u^2 dy - U \frac{\partial}{\partial x} \int_0^{\delta} u dy \right) \qquad (2.25)$$

If one ignores gravity, then, the external forces exerted on surface AB $= + p\delta$, (values in the direction of the air flow have a positive sign);

The external forces exerted on surface CD $= - \left(p + \frac{\partial p}{\partial x} dx \right) (\delta + d\delta)$

$$\cong - p\delta - \delta dx \frac{\partial p}{\partial x} - p d\delta,$$

The external forces exerted on surface BD $= - \tau_0 dx \cdot 1$ (the viscous friction drag of the wall surface);

As far as the contact between the surface AC and the main flow goes, if one ignores the viscosity, μ, then, the force of friction $= 0$.

If one assumes the average pressure received by surface AC to be p, then, the force exerted on surface AC $= pds \cdot 1$; the projection of pds in direction x $=$

$(pds) \cdot \frac{d\delta}{ds} = p d\delta.$ $d\delta/ds \cong \operatorname{tg} \alpha$

(Fig 2.10). Therefore, the total of all

43

the external forces exerted on ABCD in direction x is:

$$\Sigma F = p\delta - p\delta - \delta dx \frac{\partial p}{\partial x} - pd\delta - \tau_0 dx + pd\delta$$

$$= -\delta dx \frac{\partial p}{\partial x} - \tau_0 dx \quad [N] \qquad (2.26)$$

According to the principles of Newtonian momentum, if equation (2.41) is set equal to (2.42), one gets the differential equation of momentum for non-stable state, two element turbulence flow boundary layers:

$$\rho \int_0^\delta \frac{\partial u}{\partial t} dy + \frac{\partial}{\partial x} \int_0^\delta \rho u^2 dy - U \frac{\partial}{\partial x} \int_0^\delta \rho u dy$$

$$= -\delta \frac{\partial p}{\partial x} - \tau_0 \quad [N/m^2] \qquad (2.27)$$

From this equation one can infer four unknown quantities relating to boundary layer flow at an instant, δ : the flow speed, u, in direction x; friction stress on the wall surface, τ_0; the flow speed, U, on the boundary lines of the main flow and the principles which connect it with pressure, p. The independent variables are the instant of time, t, and the coordinates x and y.

Sec 8 Analysis of Stable State Dual Incompressible Turbulence Sub-surfaces

(1) Method of Analysis

It is for the lack of only four unknown quantities that we cannot solve the equation (2.27). By the skillful use of "averaged time" parameters, such as $U = \overline{U} + U'$, $u = \overline{u} + u'$ etc., it is possible to use non-steady states in the role of steady states in order to analyse air flows, that is $\partial \overline{u}_{//}\partial t = 0$. The main flow can function in the role of non-viscous "positional flow" or "potential flow" in order to handle the analysis. If one already knows the parameters, $\overrightarrow{P_1^*}$, $\overrightarrow{T_1^*}$, $\overline{p_1}$ and $\overline{M_1}$ for the shape of the diffuser passage and the intake flow, then, it is possible to figure out, on the basis of the "potential flow" the values of $\overline{U}$ and $\partial \overline{p}/\partial x$ for the main flow. This quantity, $\partial \overline{p}/\partial x$, is also the pressure gradient for the boundary layer in the direction, x (See Sec 6(4)). Within the boundary layer, it is possible to think of the density, ρ, as being unchanging, that is to say, to ignore any compressibility that might be involved (See Sec 6(3)). As far as the friction stress, τ_0, of the wall surface is concerned, it is not possible to figure this quantity by using once again equation (2.1) from this chapter. Because of the fact that, within the boundary

44

layer, there is no striated, non-turbulent, laminar flow, but, on the contrary, vortical masses tumbling over one another and pulsating, the value of the viscous friction drag involved is very greatly increased. Due to this fact, it is only possible to induce experimental data in order to obtain an empirical formula for figuring τ_0.

(2) "Speed Pattern Template" Equations for Turbulence Boundary Layers

When one is considering a steady-state, non-compressible flow, then, in equation (2.27), $\frac{\partial u}{\partial t} = 0$, and ρ = a constant; because of these facts

$$\rho \frac{d}{dx} \int_0^\delta u^2 dy - \rho U \frac{d}{dx} \int_0^\delta u dy = -\delta \frac{dp}{dx} - \tau_0$$

(2.28)

(The main flow, U, and δ are unrelated)

If the two functional products are differentiated over x:

$$\frac{d}{dx}\left[U \cdot \int_0^\delta u dy \right] = \frac{dU}{dx} \int_0^\delta u dy + U \frac{d}{dx} \int_0^\delta u dy, \quad \text{(a)}$$

Considering the main flow, the Bernoulli equation can be differentiated to become:

$$-\frac{dp}{dx} = \rho U \frac{dU}{dx}, \quad \text{(b)}$$

U is simply a function of x; it is not related to y; therefore,

$$U\delta = U \int_0^\delta dy = \int_0^\delta U dy, \quad \text{(c)}$$

If one take (a) and (b) and substitutes them into equation (2.28), it is possible to get the following:

$$\rho \frac{d}{dx} \int_0^\delta u^2 dy - \rho \frac{d}{dx}\left[U \cdot \int_0^\delta u dy \right] + \rho \frac{dU}{dx} \int_0^\delta u dy$$
$$- \rho U \frac{dU}{dx} \delta = -\tau_0 \quad \text{(d)}$$

Using (c) and (d)

$$\rho \frac{dU}{dx} \int_0^\delta (U - u) dy + \rho \frac{d}{dx} \int_0^\delta u(U - u) dy = \tau_0 \quad \text{(2.29)}$$

Using the displacement thickness, δ^*, and the momentum thickness, ϑ, (See Sec 6(5) and (6) of this book), equation 2.29 becomes:

$$\rho U \frac{dU}{dx} \delta^* + \rho \frac{d}{dx} (U^2 \vartheta) = \tau_0$$

This can be rewritten as follows:

45

$$\frac{d\vartheta}{dx} + \frac{\vartheta}{U}(2+H)\frac{dU}{dx} = \frac{\tau_0}{\rho U^2}, \text{ where } H = \frac{\delta^*}{\vartheta} > 1,$$

$$(2.30)$$

(3) Estimation of the Boundary Layer Thickness on a Smooth Surface with No
Increase in Pressure as Based on Empirical Formulae

The different boundary layer thicknesses, which all have different meanings,
δ, δ^* and ϑ, as well as the friction stress of the wall surfaces, τ_0, are all functions of x. On the basis of wind experiments with tubing and flat surfaces, within the boundary layer , the distribution of flow speed, u, along normal line, y, is u equal to $f(y)$, which can be represented by the empirical formula presented below: the empirical formula for flow speed distribution is

$$\frac{u}{U} = \left(\frac{y}{\delta}\right)^{\frac{1}{n}}, \quad n = 2, 3, 5, 6, 7 \qquad (2.31)$$

The empirical formula for friction stress is

$$\frac{\tau_0}{\rho U^2} = 0.0225\left(\frac{\nu}{U\delta}\right)^{\frac{1}{4}}, \quad \nu = \text{kinetic viscosity}, n = 7; (2.32)$$

If, in the main flow, the static pressure, P, in direction x does not change, and, if one sets n = 7 in equation (2.31) and, then, substitues this into equations (2.20) and (2.22); after integration, it is possible to arrive separately at values for the displacement thickness, $\delta^* = \frac{1}{8}\delta$, and for the momentum thickness $\vartheta = \frac{7}{72}\delta$. (2.33).

Assuming a smooth wall, from the forward edge to the lower reaches of the flow at a point, x, within the boundary layer, because of the necessity to overcome the viscous drag, f, before there will be a loss of momentum each second,

$$f = \rho\int_0^\delta u(U-u)dy,$$

; however,

$$\tau_0 = \frac{df}{dx \cdot 1};$$

therefore, the friction stress on the wall at a point, x,

$$\tau_0 = \rho\frac{d}{dx}\int_0^\delta u(U-u)\,dy,$$

46

Using (2.22)

$$\tau_0 = \frac{df}{dx} = \rho U^2 \frac{d\vartheta}{dx};$$ (2.34)

Comparing equations (2.32) and (2.34),

$$\frac{\tau_0}{\rho U^2} = \frac{d\vartheta}{dx} = \frac{7}{72}\frac{d\delta}{dx} = 0.0255\left(\frac{\nu}{U\delta}\right)^{\frac{1}{4}}$$ (2.35)

Utilizing the boundary conditions: Let $x = 0$, $\delta = 0$ (Fig 2.10) using the integral equation (2.35) we get the following values for a flat surface:

-Boundary layer thickness

$$\delta = 0.37\, x^{\frac{4}{5}}\left(\frac{U}{\nu}\right)^{-\frac{1}{5}}$$ (2.36)

-Displacement thickness

$$\delta^* = 0.046\, x^{\frac{4}{5}}\left(\frac{U}{\nu}\right)^{-\frac{1}{5}}$$ (2.37)

-Momentum thickness

$$\vartheta = 0.036\, x^{\frac{4}{5}}\left(\frac{U}{\nu}\right)^{-\frac{1}{5}}$$ (2.38)

It is possible to figure δ^* on the basis of equation (2.37) for axisymetric flow fields in passages with equal cross sections and , consequently, possible to appropriately expand the cross section of the exhaust.

(4) Ascertaining the Conditions for Separation of Turbulence Boundary Layers

Concerning the drop in speed and increase in pressure which one finds in an expansion passage, there is a positive pressure gradient dp/dx , and one cannot use $\frac{1}{n} = \frac{1}{7}$ as the exponent of the empirical formula for the distribution of flow speed in turbulence flow boundary layers.

Assume that the flow speed within a boundary layer equals $u(\vartheta)$ at a place where the momentum thickness is ϑ, and assume that the total pressure at that place is $P^*(\vartheta)$. Ignoring compressibility, the total pressure of the main flow, P^*, and its kinetic pressure are, respectively: $P^* = p + \frac{1}{2}\rho U^2,$

$$q = \frac{1}{2}\rho U^2$$ (2.39)

The total pressure, $P^*(\vartheta)$ at a place ϑ within a boundary layer $< P^*$,

$$P^*(\vartheta) = p + \frac{1}{2}\rho u^2(\vartheta)$$

47

Because viscous friction at a place ϑ causes losses in the total pressure,

$$\Delta P^* = P^* - P^*(\vartheta) = \frac{1}{2}\rho U^2\left[1 - \frac{u^2(\vartheta)}{U^2}\right] = q\eta, \qquad (2.40)$$

In the equation above, the coefficient of speed pattern losses in total pressure, $n = 1 - \frac{u^2(\vartheta)}{U^2}$ is a function of H.

Making deductions from experimental data, one arrives at the speed pattern template, H and its relationship to η, as presented in Fig 2.11.

$$\eta = 1 - \left[\frac{H-1}{H(H+1)}\right]^{(H-1)} \qquad (2.41)$$

The speed pattern template $H = \dfrac{\delta^*}{\vartheta} \geq 1.$
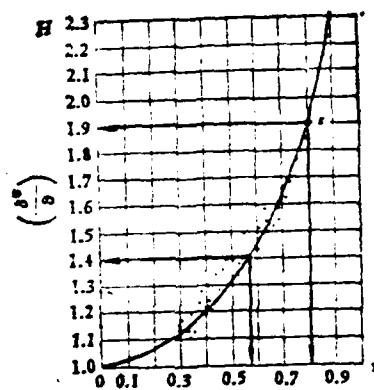
Fig 2.11

The Curve Defining the Relationship Between the Speed Pattern Template, H, and η

When $H = 1.9$, and $\eta = 0.8$, a turbulent boundary layer begins to separate.

(5) Figuring the Position of Separation Point, s

The Reynolds number at the place ϑ, $Re(\vartheta) = \dfrac{U\vartheta}{\nu} = 6 \times 10^2 \sim 5 \times 10^3$;

The viscous friction stresses on the wall surface are as follows:

$$\frac{\tau_0}{\rho U^2}Re^{\frac{1}{4}}(\vartheta) = \zeta \approx 0.0128, \text{ or } \frac{\tau_0}{\rho U^2} = \zeta\left(\frac{U\vartheta}{\nu}\right)^{-\frac{1}{4}} \quad (2.42)$$

If one substitutes equation (2.42) into equation (2.30) one gets the following:

$$\frac{d\vartheta}{dx} + (2+H)\frac{\vartheta}{U}\frac{dU}{dx} = \zeta\left(\frac{U\vartheta}{\nu}\right)^{-\frac{1}{4}}$$

48

$$\left(\frac{U\vartheta}{\nu}\right)^{\frac{1}{4}}\frac{d\vartheta}{dx} + \left(\frac{U\vartheta}{\nu}\right)^{\frac{1}{4}}(2+H)\frac{\vartheta}{U}\frac{dU}{dx} = \zeta \quad (2.43)$$

According to the principles governing potential flows which have no viscosity, and on the basis of the parameters, $\overrightarrow{P_1^*}$, $\overrightarrow{T_1^*}$, p_1, and M_1 for diffuser passageway configuration and intake air flow, one can first figure out the laws which govern the way in which the speed of the main flow, U and $\frac{dU}{dx}$ vary with changes in x.

If one temporarily supposes the speed pattern template, H = a constant, and the kinetic viscosity, ν = a constant; then, suppose there is a complex parameter,

$Q = \nu^{-\frac{1}{4}}U^{\frac{5}{4}(2+H)}\vartheta^{\frac{5}{4}}$, which varies with changes in x. $\quad (2.44)$

$$\frac{dQ}{dx} = \frac{5}{4}U^{\frac{5}{4}(2+H)-\frac{1}{4}}\left[\left(\frac{U\vartheta}{\nu}\right)^{\frac{1}{4}}\frac{d\vartheta}{dx}\right.$$
$$\left. + \left(\frac{U\vartheta}{\nu}\right)^{\frac{1}{4}}(2+H)\frac{\vartheta}{U}\frac{dU}{dx}\right] \quad (2.45)$$

If one makes $m = \frac{5}{4}(2+H) - \frac{1}{4}$, a comparison with equation (2.43) reveals that

$$\frac{dQ}{dx} = \frac{5}{4}\zeta U^m, \quad Q = \int_{x_1}^{x}\frac{5}{4}\zeta U^m dx + C \quad (2.46)$$

However, from equation (2.44),

$$Q = \nu^{-\frac{1}{4}}\vartheta^{\frac{5}{4}}U^{\frac{1}{4}}U^{\frac{5}{4}(2+H)-\frac{1}{4}}\vartheta = \left(\frac{U\vartheta}{\nu}\right)^{\frac{1}{4}}\vartheta U^m \quad (2.47)$$

If one compares equations (2.46) and (2.47) and consults Fig 2.12, he will see that

$$\vartheta\left(\frac{U\vartheta}{\nu}\right)^{\frac{1}{4}} = \frac{\frac{5}{4}\zeta}{U^m}\left[\int_{x_1}^{x}U^m dx + C\right] \quad (2.48)$$

Taking $\zeta = 0.0128$, and $H = \frac{7}{5} = 1.4$, then, $m = 4$; it is then possible to get the formula for the relationship between ϑ and x as ϑ varies with changes in x: x = the distance along the wall surface, and

$$\vartheta\left(\frac{U\vartheta}{\nu}\right)^{\frac{1}{4}} = \frac{0.016}{U^4}\left[\int_{x_1}^{x}U^4 dx + C\right] \quad (2.49)$$

Suppose that we already know that, for the diffuser intake, $x = x_1$ and $U = U_1$; moreover, suppose that, according to equation (2.38), we figure out the momentum thickness, ϑ_1, of the boundary layer at a place, A_1, in the intake, and, then, it is

49

possible to get a precise value for the integral constant, C, of equation (2.49) as shown below:

$$\vartheta_1 \left(\frac{U_1 \vartheta_1}{\nu} \right)^{\frac{1}{4}} = \frac{0.016C}{U_1^4}, \qquad C = \frac{U_1^{(4+\frac{1}{4})} \vartheta_1^{(1+\frac{1}{4})}}{0.016\nu^{\frac{1}{4}}}, \quad (2.50)$$

From equation (2.38)

$$\vartheta_1 = 0.036 x_1^{\frac{4}{5}} \left(\frac{\nu}{U_1} \right)^{\frac{1}{5}}, \quad \vartheta_1^{\frac{1}{4}} = \left[(0.036)^{\frac{1}{4}} x_1 \left(\frac{\nu}{U_1} \right)^{\frac{1}{4}} \right]$$

$$(2.51)$$

Then we substitute equation (2.51) into equation (2.50), we get

$$C = \frac{(0.036)^{1.25}}{0.016} x_1 U_1^4 = \frac{0.0158}{0.016} x_1 U_1^4 \cong x_1 U_1^4 \quad (2.52)$$

Fig 2.12 is a detail from the inner intake wall of the ring cavity diffuser shown in Fig 2.5. Oy represents a cross section of the final stage of the exhaust of the compressor; x_1 is the length of the cylindrical passageway which has cross sections identical with the first one; ① is a cross section of the diffuser intake. We already know the value of $x_1 U_1^4$, and, knowing this, equation (2.49) represents the equation for figuring the increase in the momentum thickness, ϑ, from x_1 to the separation point, s_2, in the direction x. If one choses a test value for the distance, x_s, and for the corresponding value of U for the main flow, then, it is possible to figure out a corresponding ϑ, from equation (2.49).

Besides this, through the use of dimensional analysis it is possible to obtain the result given below:

$$\frac{\vartheta}{q} \frac{d\bar{P}^*(\vartheta)}{dx} = A\eta - B, \quad \left[q = \frac{1}{2} \rho U^2 \right], \quad (2.53)$$
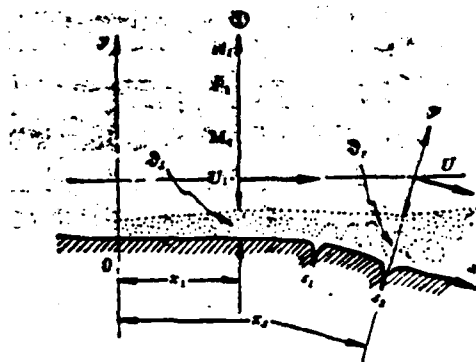

Fig 2.12

Figuring the Position of the Separation Point, s

The main flow has no viscosity and no loss in total pressure; therefore, $\overline{P}^*$ equals a constant. When the differential equation, (2.40):

$$\frac{d\overline{P}^*(\vartheta)}{dx} = -\frac{d(q\eta)}{dx}$$ is substituted into equation (2.53), one gets:

$$\vartheta \frac{d(q\eta)}{dx} + A(q\eta) = Bq \qquad (2.54)$$

Eliminating the various $(1/2)\,\rho$ quantities in equation (2.54), one gets:

$$\vartheta \frac{d(U^2\eta)}{dx} + A(U^2\eta) = BU^2 \qquad (2.55)$$

In the equation above, the constant, $A = 0.00894$; $B = 0.00461$; and, $\frac{B}{A} \cong 0.516$. If the speed pattern total pressure coefficient, $\eta > 0.516$, then, the right side of equation (2.53) will be positive overall. That is to say, the mechanical potential energy which is received by the layer of air flow that has a thickness, ϑ, from contact with the outside layers is greater than the mechanical potential energy which is transferred to the wall surface. Or, one could also say that it is smaller than ϑ', and that the air flow that hugs the wall surface does not furnish enough momemtum to higher layers of air flow, and they lose their energy for forward movement; therefore, the onset of separation occurs.

If one takes the value of ϑ, which is arrived at empirically and substitutes it into equation (2.55), one can solve for η; check to see whether or not $\eta = 0.6 \sim$ 0.8, or, one can check Fig 2.11 to see whether or not $H = 1.4 \sim 1.9$. If these values are within this range, then, the x_s which you have figured is indeed the coordinate for the point of separation, s_1 and s_2. One should locate the positions on the wall surface for the coordinates of s_1 and s_2, open a seam and drill a hole there for the drawing off of gas.

(6) A Quick Way of Determining the Position of the Boundary Layer Separation Point, s

Making reference to Fig 2.1 (b), due to the reduction in speed and the increase in pressure, the pressure gradient dp/dx, of the main flow in the direction of flow is too steep; it enters the boundary layer and, within the layer, it causes the curve, $u(n)$, for the distribution of flow speed along the normal direction to run right along the wall, and, consequently, its slope, $(du/dy) = 0$; the stress of friction drag for the wall surface, $\tau = 0$, or, the curvature $((\partial^2 u/\partial n^2))$ quickly changes to a negative value; the place where this occurs is the position of the point of separation, s.

The place in the intake of the diffuser, which has the lowest static pressure,

51

p_1, is the place where the speed of the main flow, $\overline{U}_1$, has its highest value.

Assuming that, outside the bottom layer of the laminar flow, the values for the total pressure, $\overrightarrow{P}$, along the direction of flow, are all equal, then, from the intake to the exhaust, the speed of the main flow, $\overline{U}$, decreases in value in a linear fashion.

By definition, the coefficient of static pressure is as follows:

$$C_p = \frac{(p - p_1)}{\frac{1}{2}\rho\overline{U}_1^2} = 1 - \frac{\overline{U}^2}{\overline{U}_1^2}, \quad C_p > 0, \quad (2.50)'$$

The coordinates for the cross section of the intake and the point of separation are, respectively, x_1 and x_s (Fig 2.12). If one figures out C_p and (dC_p/d_x) according to the laws governing a linear reduction in speed, then, they ought to agree with the empirical formula below:

$$(x_s - x_1)^2 C_p \left(\frac{dC_p}{dx}\right)^2 \cong 0.0104 = \text{a constant} \quad (2.51)'$$

The softer and slower is the decrease in the speed of the main flow, $\overline{U}$, the more does the point of separation, s, move down the path of the flow.

Sec 9   Diffuser Experiments Concerning Sudden Diffusion

(1) Sec 2 of this chapter pointed out the fact that after the angle of expansion of the diffuser, $2\theta > 40°$, the losses in total pressure were even larger than the sudden diffusion losses. If one eliminated the effects of suction in controling boundary layers, then, the periodic separation of boundary layers gives rise to a pulsating flow, and combustion is not stable. The purpose of putting an "elephant trunk" or a "fish mouth" at the forward end of a flame tube is to do everything possible to cause the core of the main flow entering the tube to flow evenly. Conventional ring cavity diffusers not only occupy a long space, but they also can only respond appropriately to the intake flow fields and distributions of flow of predetermined configurations. Operating speed changes; flight configurations change; the intake flow fields for diffusers and the internal and external ring cavity flow distributions of the type M_o/M_i all change. Conventional diffusers cannot respond appropriately to these types of changes; due to this fact, the characteristics of combustion take a turn for the worse. Sudden diffusion, on the other hand, can respond appropriately to flow field changes.

(2) The Purpose and Methods of Model Testing of Sudden Diffusion Diffusers in Short Ring Combustion Chambers

In the intake of the ring cavity of combustion chambers, if one uses small, short, ring-shaped "pre-diffusers" in conjunction with the compressor, then, the angle of expansion, 2θ, will not exceed 18° (Fig 2.13). These "prediffusers" extend into the combustion chamber ring cavity and suddenly expand to form turbulent and disorderly flow fields; moreover, around the circumference of the exhaust, they separate to form a pair of large spirals (actually, these are two large, concentric vortical rings symmetical around the center line of the turbine jet). If the shapes of the internal and external shells of the ring cavity are appropriate, it is possible to maintain these two vortical rings in a steady and unmoving condition; due to this fact, the amount of intake flow into the eddy current apparatus and the amount of intake flow into the interior and exterior ring cavities, M_i and M_o, can maintain a very steady distribution. Even though sudden diffusion flow fields are disorderly, they can lessen aerodynamic interference in the upper reaches of the flow path and retard surging.

In these experiments, we followed the corresponding dimensions of actual objects in the making of models and in changes: the ratio of the amounts of flow in the interior and exterior ring cavities, M_o/M_i, the distance, D, from the forward portion of the ring cavity flame tube to the exhaust of the prediffuser, and the prediffuser angle of expansion, 2θ, in test bed air flow experiments without ignition, all determine the intake flow speed distribution at A_1 and the coefficient of total pressure loss

$$\xi = \frac{\bar{P}_1^* - \bar{P}_3^*}{\frac{1}{2}\rho_1 \overline{W}_1^2}$$

(weighted average of scattered readings on the momentum)

The static pressure recovery coefficient

$$C_p = \frac{\bar{P}_1 - \bar{P}_{1,1}}{\frac{1}{2}\rho_1 \overline{W}_1^2}$$

(arithmetical reaveraging of readings for the static pressure on the interior and exterior walls)

For a representation to scale of the dimensions of the model, see Fig 2.13 (for numerical values, see the table given below).

The ratio, D/h_1, between the distance from the exhaust of the "prediffuser" to the top of the flame tube and the height of the ring cavity passageway changes from 0.9 to 2.5; $2\theta = 6^\circ$, 14° and 17°; the distribution of the amount of flow, $M_o/M_i =$

$0.5 \sim 2.0$. Measurements were taken of the distribution of total pressure and the static pressure on the interior and exterior walls for the three cross sections ①, ② and ③. Once measurements were taken of the intake volume, G_1, and the intake Mach number, $M_1 \cong 0.26$, then, on the basis of h_1, it is possible to figure the Reynolds number, $Re_1 = \frac{h_1 \overline{W}_1}{\nu} \cong 1 \times 10^5$.

$\frac{l}{h_1}$	$\frac{d_1}{d_0}$	$\frac{2h_1}{d_m}$	$\frac{d_{l_0}}{d_m}$	$\frac{d_{l_0}}{d_m}$	$\frac{d_{ll}}{d_{ai}}$	$\frac{2H_f}{d_m}$
0.944	0.911	0.094	1.245	0.928	1.160	0.49

$\frac{H_f}{H_a}$	$\frac{L}{H_f}$	$\frac{A_{aa}}{A_{ai}}$	$\frac{A_{aa}}{A_1}$	$\frac{A_{ai}}{A_1}$	$\frac{A_{aa} + A_{ai}}{A_1}$
0.707	1.50	1.773	1.353	0.773	2.135

In the final sections of actual compressors there are flow guides and a string of wake vortices; because of these, the distributions of circumferential and radial total pressures, $\overline{P}_1^*$, which are caused in ring-shaped passages, as well as the distributions of flow speed, W_1, and density, ρ_1, are all very uneven; due to this fact, the total pressure losses are increased. Because the influence which a string of wake vortices has on a flow field is uneven, it is possible to define three types of flow form parameters. During these tests, in measurements made of the intake, A_1, these three types of parameters could be distinguished by their cross section occlusion ratios

$$B_1 = \frac{1}{A_1} \iint \left[1 - \frac{\rho_1 W_1}{(\rho_1 W_1)_m} \right] dA_1 = 0.282$$

The momentum flow form parameter

$$\beta_1 = \frac{1}{A_1} \iint \frac{\rho_1}{\overline{\rho}_1} \left(\frac{W_1}{\overline{W}_1} \right)^2 dA_1 = 1.12$$

The kinetic energy flow form parameter

$$\alpha_1 = \frac{1}{A_1} \iint \frac{\rho_1}{\overline{\rho}_1} \left(\frac{W_1}{\overline{W}_1} \right)^3 dA_1 = 1.06.$$

(3) Results of Experimentation and Discussion (For conventinal ring cavity diffusers, $\bar{\zeta} \cong 0.3 \sim 0.4$)

Fig 2.14 is the curve for the distribution of radial flow speed in the diffuser intake, A_1, as obtained by the plotting of measurements. Due to the influences of flow guide wakes and secondary flows, in vicinities where the inner shell and outer shell radiae, $r-r_i/h_1 = 0$ and $r-r_i/h_1 = 1.0$, the flow speed is very low and $W_1/\overline{W} < 1.0$. When wakes were involved the eveness of the speed form distribution was not as

good as when there were no wakes; because of this fact, the total pressure losses
in the diffuser were increased. A string of wake vortices is a layer of air in
which viscosity shear stresses are concentrated. After this layer of air enters the
"prediffuser", the vortical masses are attenuated and dispersed, stirring up
boundary layer separation counter-currents, and disrupting the functioning of the
diffuser in the areas of reducing speed and increasing pressure.

Experiments revealed that the presence or absence of flow guides in the final
stages of the compressor had a great influence on the intake diffuser of the com-
bustion chamber.

	无尾波	有尾波
B_1	0.107	0.282
a_1	1.086	1.120
β_1	1.039	1.060
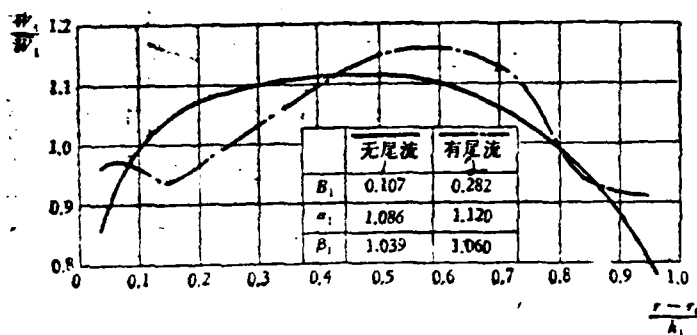
图2.14 进口速型

Fig 2.14

Intake Speed Pattern ──── No Wakes ─── With Wakes

Fig 2.15 shows how the total pressure loss coefficient, ξ , varies with changes
in different flow amount ratios, M_o/M_i, and distances, (D/h_1). If one is considering
the influence of the absence of wakes, then, the lowest values of ξ occur under con-
ditions in which $(D/h_o) \cong 1.0$ and $M_o/M_i \cong 1.3 \sim 1.4$. When there are wakes present,
the lowest values of ξ occur under conditions when $(D/h_1) \approx 1.25$, and $(M_o/M_i) = 1.0 \sim$
1.1. When there are no flow guides present, the most advantageous dimensions and the
most advantageous distribution for the amounts of flow are as follows: $2\theta = 15^\circ$,
$(D/h_1) = 1.25$, $(M_o/M_i) = 1.2$.

Fig 2.16 shows how the static pressure recovery coefficient, C_p, varies with
changes in (D/h_1) and (M_o/M_i). C_p in the diagram is the ratio between the speed
reduction and pressure increase of the prediffuser and the quantity $\frac{1}{2}\rho_1\overline{W}_1^2$.

C_{p1} is the static pressure recovery coefficient from cross section ① to cross section
⑧. When there are no wakes, and $(D/h_1) > 1.6$ while $(M_o/M_i) = 1.25$, the decrease in
speed and the increase in pressure occur almost entirely in the "prediffuser." At
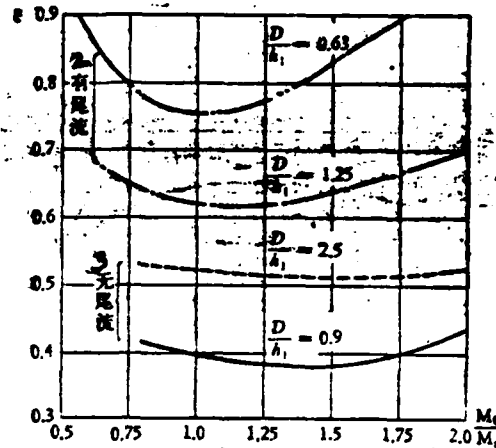the same time, on the other hand, the air flow which divides between the inner and

55

图2.15 外环腔与内环腔流量比 (2θ = 17°)

Fig 2.15

The Ratio of the Amounts of Flow in the Interior and Exterior Ring Cavities (2θ = 17°) 2. With Wakes , Without Wakes
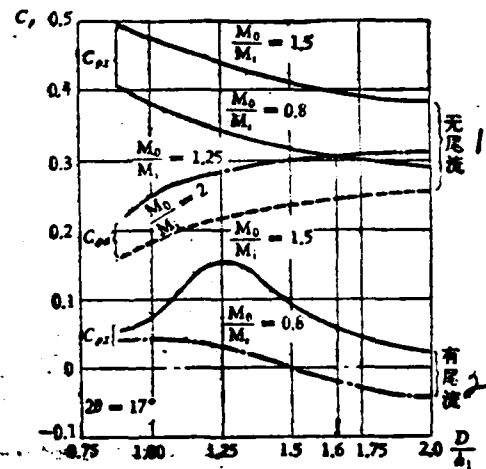

图2.16 静压恢复系数 C_p 随 D/h_1 及 M_0/M_1 变化

Fig 2.16

The Static Pressure Recovery Coefficient Varies with Changes in D/h_1 and M_0/M_i
1 Without Wakes 2 With Wakes

outer ring cavities actually drops in static pressure, which is shown by the relationship, $C_{p_2} < C_{p_1}$. This explains why it is not appropriate for D to be too long. Besides this, if D is too short, C_{p_4} is also reduced. Such a structure is also troublesome.

Sec 1   Tracer Point Dispersion Rays

In an air flow it is possible to mix in a fixed concentration of particles, such as dust pollutants, vaporized oil droplets or to intentionally mix in some vaporized silica oil. These tracer particles receive the illumination of laser light and become many "secondary point sources of light" putting out diffusion rays in all directions. When gurgling water is interspersed with grains of sand, and these grains are hit by the glorious rays of sunlight, then, one can see the flash of golden light; this is nothing but the reflection of diffusion rays from the grains of sand. A peculiar characteristic of these diffusion or scattering rays is the fact that, along the path of the incoming light rays, the part of the diffusion or scattering ray which is reflected back along this path is about 100 times stronger than the part of the diffusion ray that goes on in the original direction. The random movements of extremely small particles (i.e., particles with diameters of $d \leqslant 0.1\mu$)   (Brown motion) are analogous to molecular motion; however, compared with the turbulent pulsating flow speed, flow speed, u', the "extent of the motion" is negligible. Although minute particles can accurately follow the directions of lines of flow, the diffusion rays from them are too weak and are not very good to use. Relatively larger particles ($d \geqslant 1.0\mu$,), because of their large inertia, can exhibit "speed differentials" during violent increases or decreases in the speed of flow. Because of this, the use of the diffusion rays from large particles in order to measure flow speeds can produce errors. Therefore, it is necessary for the dimensions of the tracer particles to be such that $0.1\mu < d \leqslant 1.0$ μ ; moreover, the corresponding concentrations of the particles and the air flow should not exceed 1:2000. In this way, the error in the measurement of speed can be kept smaller than 1%.

Sec 2 Double Bundle Parallel Laser Method for Measuring Average Flow Speeds

Fig 3.1 shows a flow field which has been measured by a double bundle parallel laser emanation. The signals from the light rays scattered back by the tracer particles is received by two photoelectiric multiplier tubes and sent back to an oscilloscope timer or a multiple path sampling oscilloscope which handle the data. The laser light source is a continuous optical excitation tube using ions of helium, neon or argon and with a power rating of approximately 100 mW. On the pre-

focal plane of lens, L_1, there is arranged a double refraction crystal; this crystal takes the laser light source and divides it into two bundles of polarized light (See the enlargement of detail A in Fig 3.1). These sheaves of polarized light pass through the rear focus plane of the lens, L_1, and become two parallel bundles of laser light, 1 and 2; these two bundles then shine through the set of lenses, L_2, and onto the area of the flow field being measured, area B. From the enlargement of detail B, one can see that when the two parallel bundles of laser light are focused on the vertical cross section of the flow field being measured they form two "light passages", 1 and 2; the distance between two of these passages $= \Delta s$. Each of the light passages is like a ribbon which is wide at the two ends and narrow in the middle. The thickness at the narrowest point is only $5\sim10\mu$. This can concentrate the strength of the incoming light on a very small area, and increase the sensitivity level of the measurements being taken. If one is considering a single particle, when one takes the average speed, $\bar{u}$; at which it goes through the two light passages, such a particle will produce, in turn, two diffusion or scattering ray pulses. These two scattered ray pulses , ① and ②, are gathered by lens, L_3, reflected and concentrated by a perforated plane mirror, and, after passing through a microscope, become two bundles of amplified light. The purpose of the amplification is to make it possible, through the careful adjustment of the two light apertures, to cut down as much as possible the interference caused by reflections from the background will behind the flow field being measured and, thereby, to increase the "signal-to-noise ratio." The two bundles of light that come through the apertures form two separate optical signals, one for each hole and are accepted or received respectively by photoelectric tubes ② and ③. When the converted electrical signals are displayed on an oscilliscope equipped with a memory capability, it records the duration, Δs , in which the tracer particles pass through the two light apertures. If we assume that $\Delta s = 2\mu$ seconds, we already know the $\Delta s = 0.5mm$, and, consequently, the average time flow speed of the particles being measured is:

$$\bar{u} = \frac{\Delta s}{\Delta s} = \frac{0.5 \times 10^{-3}}{2 \times 10^{-6}} = 250 \ [m/s]. \qquad (3.1)$$

With new types of electronic instrumentation, it is possible to get a clear resolution even on signals with values of $\Delta s \cong 1$, millimicrosecond (10^{-9} sec). If there is a need for it, it is also possible to make fine adjustments in the light path so as to widen the interval between light apertures, Δs . Because of these methods, it is possible to measure super-sonic flow speeds of several thousand meters per second without the degree of error rising above 0.5%.

Before one can employ these methods, one must first know the direction of the
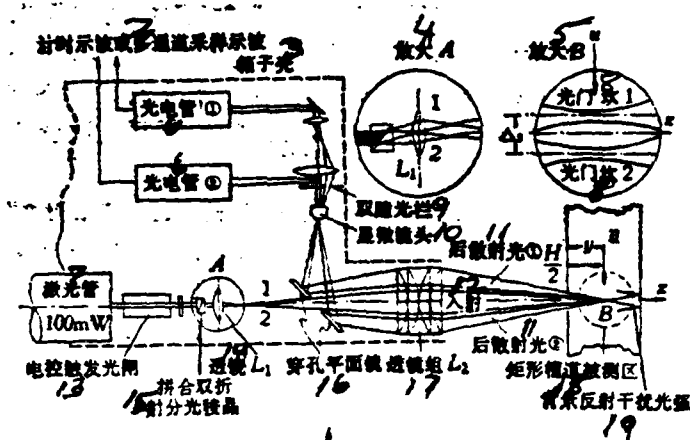
图3.1 双束平行散光散射测速仪原理方案

Fig 3.1

1. A Schematic Diagram for a Double Bundle Parallel Laser Scattered Ray Instrument for the Measuring of Flow Speeds 2. Time Display Oscilliscope or a Multiple Path Sampling Oscilliscope 3. Shell of the box 4. Detail A 5. Detail B 6. Photoelectric tube 7. Laser Tube 8. Light Aperture 9. A Two-hole Light Barrier 10. Microscope 11. Rays Scattered Back 12. Light Rays Entering the Flow Field to be Measured 13. Electrically Controlled Contact Optical Emmision Gate 14. Lens, L_1 15. Complex Double Refractive Divider Lens 16. Perforated Plane Mirror 17. Lens Set, L_2 18. Rectangular Trough-shaped Area Being Measured 19. Reflected Optical Interference from the Background

averaged time flow speed, u_ϕ If one rotates the double refraction divider lens and adjusts the plane of the "light apertures" so that it is parallel to the direction of flow, $\bar{u}$, then, the "light apertures" are perpendicular to u. If one wishes to measure a two-element flow field, one can take into consideration the averaged time flow speed vector, $\bar{v}$, in the direction of the additional coordinate and turn the azimuth of the "light apertures" 90°. However, this method is unable to measure the flow speed, $\bar{w}$, along the axis, z, of the light rays coming in.

Sec 3 Measuring Turbulence Strength

As far as turbulent air flow is concerned, because of the fact that the size and direction of an instantaneous flow speed, u, pulsate over time, it is necessary to surround a point which is to be measured and, at first, simply measure large amounts of data; only after this is done is it possible determine the statistical

59

average flow speed, $\bar{u}$, and the pulsating flow speed, u', that is to say, $u = \bar{u} + u'$; the root-mean-square pulsation flow speed $= \sqrt{\overline{u'^2}}$. In order to utilize mathematical and statistical methods for the analysis of turbulence flow pulsations, the best procedure is to take the azimuth angle, a, of the plane of the "light apertures" and change it so as to go around the axis of the light rays, z, in 8 ~ 10 "stops"; during each of the stops, the strength of the scattered rays should be measured about 1,000 times. Concerning the 8,000 ~ 10,000 pieces of pulsation data collected in this way, it is possible to use a "multiple path scanning and sampling oscilliscope" to induce the distribution curve for the "probability density" of photoelectric signals. The horizontal coordinate in Fig 5.2 shows the time, Δt , required for particles to go through the two "light apertures"; the vertical coordinate indicates the probability density, ϕ, for each of the various photoelectric pulse signals. Different values of azimuth angle, a, all have different datum lines; however, when measuring each of the values of a, the number of particles entering into the area being measured is always the same.

When an averaged time flow speed, $\bar{u}$, coincides with $a = 0°$, the light scattered from particles as they flow down the path of the flow and from the two "light apertures" is at its brightest; at such times, the probability density, ϕ, of photoelectric pulse signals is also at its largest. After the azimuth angle, a, is increased, the strength of the light scattered back at the two "light apertures" is quickly diminished, and the probability density, ϕ, of photoelectric pulse signals is reduced. After $a \geq 1.5°$, then, signals almost disappear. If one changes a back in the opposite direction, he gets similar results. The peak of the distribution curve of the probability density, ϕ, represents the instantaneous flow speed, u. The width of the curve at the base line represents the maximum amplitude range of flow speed pulsation. It can be seen that the probability density, ϕ, of photoelectric pulsation signals from rays scattered by particles is a function of the azimuth angle, a, and the time, t, and it closely resembles the curve for a Gaussian distribution. If one holds a constant, then,

$$\phi(t) = \frac{1}{\sigma\sqrt{2\pi}} exp\left[-\frac{(t-a)^2}{2\sigma^2}\right], \qquad (3.2)$$

a = the mathematical expectation, and σ^2 = the variance. By using mathematical and statistical methods of analysis on the distribution curve of probability densities, it is possible to figure out the direction and magnitude of the averaged time flow speed, $\bar{u}$, as well as the turbulence flow strength, $\sqrt{\overline{u'^2}}/U$, both parallel or perpendicular to $\bar{u}$. U is the largest flow speed along the center line of the
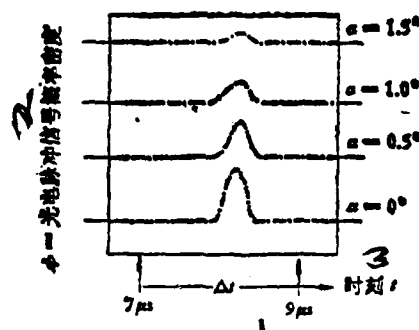
60

图3.2 不同 α 概率密度分布曲线

Fig 3.2

1. The Distribution Curve of Probability Densities for Different Values of α
2. Photoelectric Pulse Signal Probability Density 3. Time

trough. Depending on the density of the tracer particles which are added to the air flow, it requires from 3 ~ 4 seconds to do 8,000 ~ 10,000 sample measurements which includes the time needed to construct the distribution curve for the probability densities involved. Because of this, when making measurements, it is required that general stability be maintained in the air flow; only in this way can reliable data be measured. Fig 3.3 shows the flow speed distribution measured in the rectangular trough as well as the results for turbulence flow strength. The horizontal coordinate represents the ratio of cross current depth, $y = \frac{y}{H}$, H = the width of the trough. The origin point, O, is the surface of the wall. The depth ratio is 1 on the center line of the trough. If one uses the measurements resulting from the "double bundle parallel laser" method and the use of a "hot wire wind speed meter" and makes a comparison of them, there are almost no areas of disagreement. The same thing is found if one compares the Reynolds numbers of the flow fields.

In Fig 3.4, the "electrical control contact optical emission gate" installed in front of the laser tube — or Pockel's cell, as it is called — is installed there for the purpose of timing and localizing the exposures which are used to investigate the flow field in the troughs of the turning blades; it can also be used to investigate two-element spiral combustion flow fields. It is possible to install circuit breakers on a turbine wheel in order to indicate the position of the blades or to install "heat sensitive resistances" on key components of spiral flow combustion chambers. When there is no external electric field, "light gate crystal bodies" interupt the laser source. When the timing and location circuit breaker on the turbine wheel or the "heat sensitive resistances" in a spiral combustion chamber send
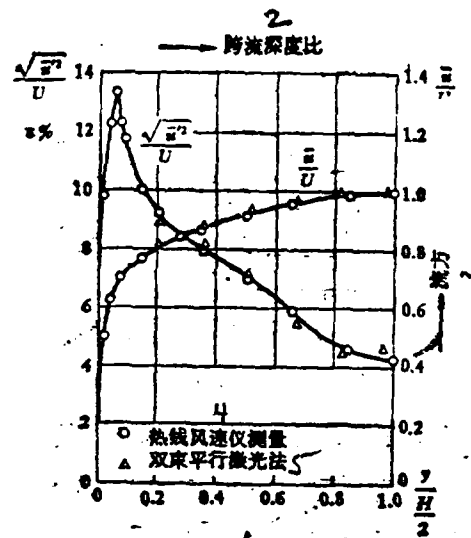
61

图3.3 流速分布及紊流强度测量

Fig 3.3

1. Flow Speed Distribution and Turbulence Flow Strength Measurements 2. Cross Current Depth Ratio 3. Direction of Flow 4. Hot Wire Wind Speed Guage Measurements 5. Double Bundle Parallel Laser Method

out a signal, triggering the light gate, there is immediately released a large, strong bundle of pulse laser light, which illuminates the troughs of the blades or a certain point in the spiral flames. An electrically triggered light gate (a Bao Keer box) is linked to the shutter of a high speed camera. The exposure time can be as short as 10 μsec. The area on which the illumination is concentrated is very small, and the exposure time is short; therefore, what is actually illuminated is almost an instantaneously stable flow form.

Sec. 4 Principles of the Laser Doppler Frequency Deviation Method for Measuring Flow Speed

Different colors of light have different wavelengths, λ, and different frequencies, f. Laser light is light that is almost of one wavelength, one frequency and one color. For example, the wavelength of helium and neon gas lasers in a vacuum is $\lambda = 6,328$ Å (1 Å $= 10^{-8}$ cm); this is red light. No matter what color light may be, in a vacuum, the speed of that light is always $c_0 = 3 \times 10^{10}$ (cm/s). Therefore, the oscillation frequency of helium and neon laser light with a wavelength of $6,328$ Å is $f_0 = c_0 / \lambda_0 \cong 5 \times 10^{14}$ (Hz). The speed of propagation of light waves in a medium is somewhat slower than their speed of propagation in a vacuum, $c < c_0$; $c_0/c = \lambda_0/\lambda = n > 1$ is the characteristic of refracted light in a medium called the index of refraction, n. Under conditions of standard temperature and pressure ($0°$C, 1 atmosphere of pressure) the index of refraction of air, $n \cong 1.0003$.

The stationary laser tube shoots out a   bundle of light which is divided into two   bundles by the light dividing lens; after this has happened, these bundles are focused by lenses and shot onto the tracer particles, P in the two-element flow field (Fig 3.4). The direction of the strong incoming light, I_i, is represented by the unit vector, $\hat{n}_i$. The direction of the optical power, I_s, which is scattered forward from the particles, P, is expressed by the unit vector, $\hat{n}_s$. The frequency of the incoming light $= f_i$, and the wavelength of the incoming light $= \lambda_i$. The frequency of the scattered light $= f_s$, and the wavelength of the scattered light $= \lambda_s$. $f_i \lambda_i = c$, $f_s \lambda_s = c$.

Because of the Doppler effect, it is as though the waves of the incoming light leave a point, P, with a relative speed $c - \mathbf{u} \cdot \hat{n}_i = c - u \cos \theta$. By the same token, it is as though the scattered waves of light leave a point, P, at a relative speed of $c - \mathbf{u} \cdot \hat{n}_s = c - u \cos \phi$.

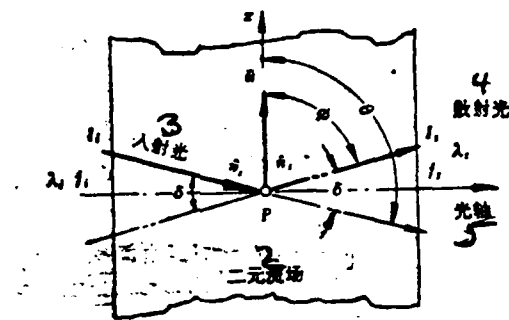Therefore, the Doppler effect relative frequency

63

图3.4 双束激光聚焦向量

Fig 3.4

1. Focus Vectors of Double Sheaf laser Light 2. Two-element Flow Field 3. Incoming Light 4. Scattered Light 5. Axis of Light

$$f_i = \frac{c - \bar{u} \cdot \hat{n}_i}{\lambda_i} = \frac{c - \bar{u} \cdot \hat{n}_s}{\lambda_s} \qquad (3.3)$$

or

$$\frac{\lambda_i}{\lambda_s} = \frac{f_s}{f_i} = \frac{c - \bar{u} \cdot \hat{n}_i}{c - \bar{u} \cdot \hat{n}_s} \qquad (3.4)$$

The capabilities of the instrumentation are as follows: range of possible speed measurements. 3m/s - 300m/s; upper limit frequency of fluid pulsations = 120 kHz; maximum turbulence flow strength, $\varepsilon \leqslant 70\%$; simulation of voltage output is proportional to flow speed, $\bar{u}$; accuracy is in the range of $\pm 1\%$.

The laser Doppler frequency deviation

$$f_D = f_s - f_i = f_i\left[\frac{f_s}{f_i} - 1\right] = f_i\left[\frac{\lambda_i}{\lambda_s} - 1\right], \quad (3.5)$$

If one substitutes equation (3.4) into equation (3.5), one can obtain

$$f_D = \frac{f_i\bar{u}}{c}\left[\frac{\hat{n}_s - \hat{n}_i}{1 - \frac{\bar{u}}{c} \cdot \hat{n}_s}\right], \qquad (3.6)$$

As far as the incoming waves of light are concerned, the propagation frequency in a vacuum as well as in a physical medium does not change; only the wavelength and the speed change; therefore

$$f_i = f_0 = \frac{c_0}{\lambda_0} = \frac{cn}{\lambda_0}, \quad \frac{f_i}{c} = \frac{n}{\lambda_0} \qquad (3.7)$$

Because of the fact that, if one compares the flow speed, $\bar{u}$, which is being measured, to the speed of light, $c \approx 3 \times 10^5 (km/s)$, it is possible to ignore the quantity, $\bar{u}/c$,
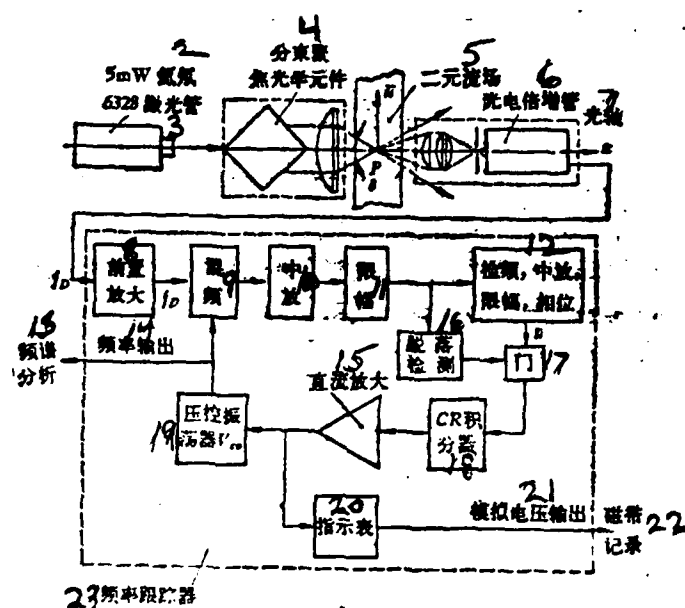
64

图3.5 激光多普勒双束系焦测速仪示意

Fig 3.5

1. A Schematic Diagram for an Instrument for Measuring Flow Speed Through the Use of Laser Light Doppler Double bundle Focusing 2. Helium and Neon 3. Laser Tube 4. Optical Element for the Separation and Focusing of bundles 5. Two- element Flow Field 6. Photoelectric Multiplier Tube 7. Axis of Light 8. Preamplification 9. Mixer 10. Middle Amplifier 11. Limiter 12. Frequency Monitor, Middle Amplification, Limiter, Phase 13. Frequency Spectrum Analysis 14. Frequency Output 15. DC Amplification 16. Drop Measurement 17. Gate 18. CR Integraph 19. Voltage Controlled Oscillator, Vco 20. Dial Guage 21. Voltage Output Analog 22. Magnetic Recording 23. Frequency Tracking Device

on the basis of which, equation (3.6) can be simplified to

$$f_D = \frac{\pi U}{\lambda_0} \cdot (\hat{n}_s - \hat{n}_i) \cong \frac{U}{\lambda_0}(\cos\phi - \cos\theta) \quad (3.8)$$

Because the index of refraction of air, 'n ≅ 1, it is possible to see, from Fig 3.4, that $\phi + \theta = \pi, \theta - \overline{\phi} = \delta$. Using trigonometric identities, equation (3.8) then becomes

$$f_D \cong \frac{U}{\lambda_0}\left[-2\sin\frac{(\phi+\theta)}{2}\sin\frac{(\phi-\theta)}{2}\right]$$

$$= \frac{2U}{\lambda_0}\sin\frac{\delta}{2} \text{ [Hz]} \quad (3.9)$$

δ is the "scattering angle" which takes for its base line the direction of the incoming light and is determined by the design of the light path of the instrument used.

The laser wavelength, $\lambda_i = 6,328\ \overset{\circ}{A} = 6,328\times10^{-10}$ m. Therefore, it is only necessary to use the instrument in Fig 3.5 to measure the Doppler frequency variation, f_D, of a point, P, that is to say that it is possible to figure the local flow speed, $\bar{u}$, on the basis of equation (3.9). If one changes the position of the focal point, P, of the double bundle laser, then, it is possible to shed some light on the flow speed distribution. In order to increase the degree of sensitivity, select for use a scattering angle $5^{\circ} \leqslant \delta \leqslant 20^{\circ}$, $\phi + \dfrac{\delta}{2} = 90^{\circ}$.

Sec 5 Pulse Laser Photography of Interference Band Spectra

(1) Integrated Information Photographic Negatives from Double Pulse Laser Photography of Flow Fields (Fig 5.6)

The ruby pulse laser equipment, LQ, has a "Q adjustment switch" (it is also possible to use an acetone and chlorophyll Kerr box as a substitute for this.) This switch is similar to the "electrically triggered light gate" mentioned in a previous section. The purpose of this is to allow electromagnetic waves within the ruby rod to resonate, amplify and store energy which, when it has reached a sufficiently high level, can trigger the Q switch, instantaneously shooting out a large, strong pulse of laser light. The pulse width is approximately 20 millimicroseconds (10^{-9} sec), and the energy of the pulse is greater than 400 millijoules. Pulses with this kind of strength are capable of "freezing" transient phenomena, suppressing the effects of light radiated by flames and making photographs possible.

The purpose of using the "light filter form selection device", FP, is to filter out the "boundary frequencies" of the oscillating laser light and to only allow electromagnetic oscillating single form waves with wave lengths $\approx 6943\ \overset{\circ}{A}$ to pass through. In this way, it is possible to guarantee that the two sheaves of laser light which are separated by the light separation plates, BS, are still of the same frequency. The first bundle is the illuminating light, I_1; it passes through the lens, L_1, expanding the cross section of the light bundle; M_2 and P_1 reflect the light rays so that they become parallel; after they illuminate the flame flow field, TS, they are projected onto the integrated information photographic negative, HP. The second bundle is the reference light, I_2; this passes through M_1, M_2 and L_2 and is projected onto the integrated information photographic negative, HP. The two laser bundles, I_1 and I_2, come in contact and intersect each other in front of HP, forming the "light wave interference area", SP; this area is projected onto the surface of HP and forms a series of light and dark interference streaks.
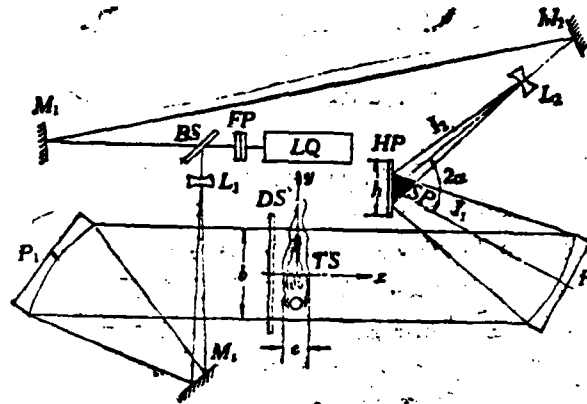
图3.6 脉冲激光拍摄火焰流场全息照片

M_1, M_2, M_3 全反射镜　　L_1, L_2 扩束透镜　　HP 全息底片
LQ 脉冲激光 6943Å　　P_1, P_2 抛物面镜　　I_1, I_2 探测及参考光束
FP 法白，滤光选频器　　DS 漫射屏　　　2a 双光束夹角
BS 半透明分光片　　　　TS 被测火焰流场　　SP 光波干涉空域

Fig 3.6

1. Pulse Laser Photography Flame Flow Field Integrated Information Negative 2. Plane Reflection Lenses 3. Concave Transparent Lenses 4. Integrated Information Photographic Negative 5. Pulse Laser 6. Parabolic Lenses 7. Illumination and Reference Light Bundles 8. White Light Filter Form Selection Instrument 9. Diffused Reflection Screen 10. Double Light Bundle Included Angle 11. Translucent Spectral Comparator 12. The Measured Flame Flow Field 13. Light Wave Interference Area

According to the azimuth of HP, movements forward and back as well as fine adjustments can be accomplished by turning lens, L_2; in order to facilitate adjustment, the "light course" of the reference light, I_2, from BS to HP does not have a large phase deviation as compared to the "light course" or "light path" of the illumination light, I_1; the basic difference in light paths, $(l_2 - l_1)$ is approximately within a few centimeters; the included angle between I_1 and I_2, 2a, is kept quite small, as much as it is possible to do so $(2a \leqslant 8^\circ)$; moreover, the normal line HP divides the angle 2a equally. In this way, the interference streaks being put out are relatively clearer, and the separation interval between streaks, s, is relatively wide.

(2) Measurement Procedure

The first light exposure triggered from switch Q. There are no flames in the flow field (in a two-dimensional flow field, there is no air flow whether there is a pattern to the flow field or not). Distributions of density and temperature are

67

basic conditions which cannot be interfered with. Concerning the illumination and reference light sheaves, because of the fact that the basic difference between the paths of the two lights (l_1-l_2) does exist, there are recorded on the integrated information photographic negative a set of "background interference streaks"; the interval between these streaks or lines = s.

The second light exposure triggered by switch Q. There are flames in the field of view (or boundary layer separation, shock waves, expansion waves, etc), and these interfer with the flow field. Because the density distribution changes, the distribution of the index of refraction, n, within the flow field also changes. The illumination light bundle,I_1, is influenced by the index of refraction of the new distributions, and this influence is exerted in opposition to the new difference in light paths (l_2-l_1) of the reference light bundle,I_2. Due to this fact, there is produced a set of "deformation interference streaks" which overlap on top of the "background interference streaks." Along the x or y coordinates, the deformation streaks of certain specific points have a positional displacement, Δs, as compared to the background streaks. It is necessary for $\Delta s > s$; only under such conditions are there produced complete and clear interference streak spectra. The time interval used to control the two pulses of light exposure, $\Delta t \leqslant 2$ seconds.

On the integrated information photographic negative, the positional displacement, Δs, which corresponds to a designated point ① is equal to $N \cdot s$; the corresponding point ① in the flow field is interferred with by the corresponding changes, $\Delta_{l\rho}$, in the various local densities. This value, Δs, arises at the beginning and the end of the time interval, Δt, between the two light exposures; the overlapping streaks which result are called the "time differential for integrated information displays." Because Δs is related to changes in s, even if the background interference streaks have basically distorted forms, it does not make any difference. This simply lowers the requirements for the optical components and simplifies the measurements.

(3) Principles of Light Wave Interference

Assuming that, after rectification, the laser light is a pure plane polarized light with a wavelength of $\lambda = 6943$ Å, then, concerning the propagation of these light rays, it is possible to write simple wave motion equations:
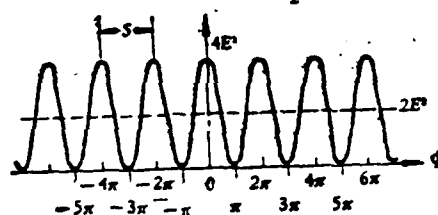
The point displacement of the measurement light sheaf

$$y_i = E_1 \sin(2\pi/t + \phi_i) = E_1 \sin \frac{2\pi}{\lambda}(ct + l_i),$$

$$(3.10)$$

68

(a)
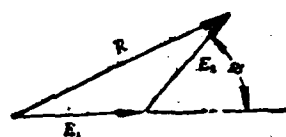
(a) 向量图

$$I = 4E_0^2 \cos^2 \frac{\phi}{2}$$

(b)

(b) 干涉条纹光强分布

图3.7 同频同振幅两束相干光

Fig 3.7

1. Two Bundles of Mutually Interfering Light With the Same Frequency and the Same Amplitude 2. Vector Diagram 3. Interference Streak Light Strength Distribution

68a

The point displacement of the reference light <u>bundle</u>

$$y_2 = E_2 \sin(2\pi f t + \phi_2) = E_2 \sin \frac{2\pi}{\lambda}(ct + l_2), \quad (3.11)$$

E_1, E_2 = the amplitude and the frequency respectively

$$f = \frac{c}{\lambda}, \quad \phi_1 = \frac{2\pi}{\lambda}l_1 \quad \text{and} \quad \phi_2 = \frac{2\pi}{\lambda}l_2 = \begin{array}{l}\text{original phase}\\ \text{angle}\end{array}$$

The integrated information photographic negative, HP, receives the total light strength from the intersecting light waves from the two bundles, I (W/cm^2), and they are in direct proportion with the combined amplitudes of the light waves of the two bundles, R^2. Using the addition of vectors method:

$$R^2 = E_1^2 + E_2^2 + 2E_1 E_2 \cos(\phi_2 - \phi_1) \qquad (3.12)$$

Assuming that the amplitudes of the illumination bundle and the reference bundle are both equal so that $E_1 = E_2 = E$, then, the total light strength

$$I = R^2 = 2E^2[1 + \cos(\phi_2 - \phi_1)]$$
$$= 4E^2 \cos^2\left[\frac{1}{2}(\phi_2 - \phi_1)\right] = 4E^2 \cos^2 \frac{\phi}{2} \qquad (3.13)$$

The relative phase differential of the two bundles

$$\phi = (\phi_2 - \phi_1) = \frac{2\pi}{\lambda}(l_2 - l_1) \qquad (3.14)$$

The relationship, $k = \frac{2\pi}{\lambda}$, is called the "wave number", that is to say, in every 2π cm along the axis of the light there are this certain number of waves; this quantity also represents the frequency, f. It is worthwhile to remember and bear in mind the significance and meaning of equation (3.14), i.e. "When two bundles of light with the same frequencies intersect, the phase differential of their mutual interference is equal to the wave number times the light path differential".From equation (3.13), it can be seen that the strength of the total light, I, must depend on this "phase shift differential" ϕ. Fig 3.7 (a) shows the combined amplitude vector, R, of two bundles of light waves as well as the corresponding phase differential, ϕ; (b) shows the total light strength, I, and how it varies with changes in the phase shift, ϕ. When the phase differential, $\phi = 0$, 2π, 4π, ..., $2N\pi$, I = 4 E^2, and one sees appearing patterns of bright stripes. When the phase differential, $\phi = \pi$, 3π, 5π, ..., $(2N + 1)\pi$, and I = 0, then, one sees dark stripes appearing. When N = 0, 1, 2, 3, ... and so on in whole numbers, these are called "interference stages" or an "interference series." From the spectral plate, BS, to HP, the quantity $(l_2 - l_1)$ is different for different points; ϕ is also different; due

to this fact, HP shows the appearance of light and dark stripes.

Sec 6 Analysis of Interference Band Spectra and the Figuring of Temperature

The integrated information photographic negative, HP, which is taken of combustion flow fields during two-pulse laser photography, records complete information on the light path differentials and light strength distributions within the field of view both when there are flames present and when there are none. After the development of these photographic negatives it is necessary to recapture the positions which correspond to those which existed at the time of the original photograph; if one uses a continuous laser light (such as helium and neon at 6328 Å) and uses a lens to project the light onto a light sensitive photographic negative or photographic paper, one finds appearing again the original interference situation; only in this way is it possible to obtain the interference stripe spectra in Fig 3.8.

Assuming that one already knows the background temperature, T_o, in the field of vision during the first light exposure, and, assuming one also already knows the pressure, p_o, the density, ρ_o, and the index of refraction, n_o, and, further assuming that one already knows that the thickness of the flames in direction z is e = 20 (mm), then, on the basis of physical optics:

$$\frac{n_0 - 1}{\rho_0} = \frac{n - 1}{\rho} = \text{constant } K, \quad \underset{\text{if}}{n - 1 = \delta,}$$

$$\underset{\text{then}}{\frac{\delta_0}{\rho_0}} = \frac{\delta}{\rho} = K \qquad (3.15)$$

Changes in the gaseous index of refraction, Δn, and changes in density, $\Delta \rho$, are related in the following way:

$$\Delta n = n_0 - n = \delta_0 - \delta = K\Delta\rho \qquad (3.16)$$

Concerning the two-pulse light exposure of a given point ①corresponding to the flow field, the deformation patterns of light and dark stripes are related to erroneous background values

$$N = \frac{\int_0^e n_0 dz - \int_0^e n dz}{\lambda} = \frac{(n_0 - n)e}{\lambda} = \frac{\Delta s}{s}, \qquad (3.17)$$

$$\underset{\text{therefore}}{N\lambda = K\Delta\rho \cdot e} \qquad (3.18)$$

If one assumes that, through the entire process of combustion, the flow field pressure, p, remains a constant, then, according to the gas state equation, $p = \rho g \cdot RT$, it should be true that

$$\frac{\rho}{\rho_0} = \frac{T_0}{T} = \frac{\delta}{\delta_0}, \quad \text{or} \quad \frac{\rho'}{\rho_0} = \frac{\rho_0 - \Delta\rho}{\rho_0} = 1 - \frac{\Delta\rho}{\rho_0},$$

$$\frac{T}{T_0} = \frac{1}{1 - \frac{\Delta\rho}{\rho_0}} \qquad (3.19)$$

$$\frac{\text{Temperature of the illumination point}}{\text{when there is combustion}} = \frac{T}{T_0} = \frac{1}{1 - \frac{N\lambda}{\delta_0 c}},$$
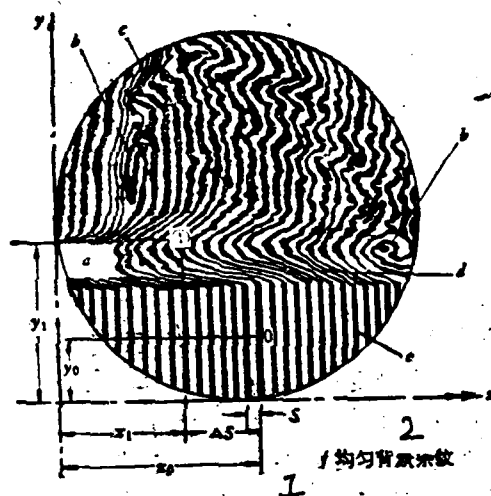
no combustion

图3.8 燃烧流场的干涉条纹谱

Fig 3.8

1. Interference Stripe Spectra of Combustion Flow Field ∴. f is an even or uniform background stripe pattern

$$N = \frac{\Delta s}{s}; \qquad (3.20)$$

We already know that under standard temperature and pressure conditions ($T_s = 273K$, $p_s = 1.033$ kg/cm^2) the refractive index of air, $n_s = 1.0003$; therefore, $\delta_s = 3 \times 10^{-4}$. If one assumes that the background temperature, $T_0 = 293(K)$, then, $p_0 = p_s$. Due to the fact that δ and T have a relationship with each other that is defined by a hyperbolic curve, one can substitute
$$\delta_0 = \delta_s \times \frac{273}{293} = 2.8 \times 10^{-4}$$

In Fig 3.8, the illuminated point ① and the background base point 0 (x_0, y_0) are deformed along the x axis, and the erroneous values for the background strips

71

$$\frac{\Delta s}{s} = N = 6, \quad \lambda = 6943\,\text{Å} = 0.6943 \times 10^{-3}\,[\text{mm}].$$

$$\frac{N\lambda}{\delta_0 c} = \frac{6 \times 0.6943 \times 10^{-3}}{2.8 \times 10^{-4} \times 20} = \frac{4.166}{5.6} = 0.744$$

By substitution in equation (3.20), one can figure out the temperature of the illuminated point ①

$$T_1 = \frac{T_0}{1 - 0.744} = \frac{293}{0.256} = 1144\,[\text{K}].$$

Using the set of conditions in which different values of y = a constant value of the x coordinate, one can figure out enough temperatures to make it possible to precisely determine the temperature distribution of the combustion flow field.

When one carries out the actual analysis involved, it is possible to use a microdensitometer to clear up the spectral patterns of the interference and substitute these into manual successive point calculations. At the present time, the use of this instrument still only gives one the capability to measure the density and temperature distributions of two dimensional flow fields. It is also possible to make multiple photographs of several cross sections and then put them together to form a three-dimensional or cubic diagram.

Chapter 4 Basic Equations of Flow Fields

Sec 1 Characteristics and Concepts of Flow Fields

The space filled by a flowing body or fluid is called a flow field. After
selecting the coordinate system to be used, one already knows that the intake of
the field and the boundary conditions do not vary with time, and the peculiar
characteristic of stable flow fields is that flow speed pressure, pressure, density
(or concentration) and temperature all have fixed patterns of distribution within
the scope of the flow field and their values do not vary with time; these distribu-
tions are also called speed fields, pressure fields, density (or concentration)
fields, and temperature fields. During the performance of tests on whole combus-
tion chamber designs or parts of those designs, whether it is with ignition or
only in the form of an air flow test, by the use of tiny transmitters or laser light
test techniques connected to mutiple path data collection and processing machines
(PDI) equipped with a printer or an optical display, it is possible to measure the
form of the distribution of flow speed, density, pressure and temperature. This
capability has great reference value for the work of determining and improving the
capabilities and structures of combustion chambers. On the basis of a theoretical
analysis of flow fields, the process of figuring out the characteristics of flow
fields can enter into a relationship of mutual corroboration with the results of
tests done on different forms and shapes of combustion chambers, and this can form
the basis for the test production of new shapes and types of combustion chambers.
This makes it possible to save equipment, manpower, resources and time as compared
to "dimension adequacy, high-altitude flight simulation, and combustion chamber
component test" procedures.

Flow fields analysed from the perspective of fluid mechanics are partial
abstractions of real flow fields. For example, when one is analyzing the flow field
of a diffuser, one uses a value of $u = 0.99\ \overline{U}$ as the boundary line of flow which
is used to divide the main flow field from the boundary layer flow field. In the
case of a jet exhaust, it is possible to separate the core flow field, which has
an even flow speed, from boundary layer flow fields, which are characterized by
turbulent shear forces. In such main flows or core flows is   possible for one
to ignore viscosity and only consider compressibility, and such flow fields are
call aviscous, avortical   or potential flow fields. In boundary layers, if it
is possible to ignore compressibility and only consider viscosity, then, this
type of flow field is called an incompressible flow field.

73

Many designs of combustion chamber are axially symmetrical. In the flame tubes of single tube and cannular types of combustion chambers, the mid-lines of these tubes can be taken to be the axes of symmetry of the flow fields in the flame tubes. The axis of symmetry of ring cavity combustion chambers is the centerline of the jet engine. If the air flow parameters are all the same at equal distances out from the axes of symmetry, that is around the circumference of a circle with the axis of symmetry as its center and the distance in question as the radius, then, this is called an axisymmetric flow field. A vertical cross section running through the radius and axis of symmetry of the flow fields involved is called the meridian plane. Each meridian plane in a flow field structure is similar. Therefore, axisymmetric, three-dimensional flow fields can be simplified into two-dimensional flow fields for purposes of handling. Even if a flow field is not axisymmetric, it is only necessary for the mechanical structure to be axisymmetric in order for it to be possible to take the flow field and "cut it up" into several planes of rotation and meridian planes, which can be analysed as two-dimensional flow fields, and then put back together into an image of a three-dimensional flow field. The blade cascade in the plane of the blade wheel mechanism uses precisely these planes of rotation to cut up all the blades and open them up to form plane flow fields. The eddy current apparatus of combustion chambers has spiral flow blades, and these can also be cut up to form a plane blade cascade. To talk for a moment about the forward section of flame tubes, the ring-shaped spiral jet which comes from the eddy current apparatus, can be thought of as a three-dimensional spiral flow field in which a vortex is added to a jet. Each gas distribution hole puts out one jet. The cold air jets that enter through the holes where the gases from the main combustion and cooling areas mix together are blown away and bent and broken up by the hot gases from the main air flow within the flame tubes; this creates a three-dimensional flow field where the hot and cold air flows mix together.

Moving on to a more generalized discussion of combustion chambers, if there is a vertical turbulence flow present in a combustion chamber, then, one cannot ignore viscosity any longer; if there are changes in density, then, one can no longer ignore compressibility; if there is a temperature gradient, then, one can no longer ignore heat transfer; if there is combustion, then, one cannot ignore changes in the constitution of the gases involved. Even if there is no combustion, a cold air flow test in the interior of a combustion chamber creates a three-dimensional, viscous, compressible flow field. In order to simplify calculations, every effort should be made, on the basis of the structural peculiarities of the combustion

74

chamber involved, to divide up the three-dimensional flow field into several local-ized, two-dimensional flow fields. Speaking of combustion in general, the larger the number of types of gases it mixes together, the more complicated are the analy-tical computations associated with it.

Sec 2 Flow Field Gradients

Among the parameters associated with flow fields, there are some which are simply numerical quantities of size and have no direction attached to them, for example, temperature, T, concentration, c (density, ρ), pressure, p, energy, E, and so on. The space in which non-directional parameters are distributed is called a quantitative field. There are some parameters, however, which have not only mag-nitude, but also, a directional quality to them, for example, speed, **V**, acceler-ation, **a**, momentum, **mV**, and force, **F**, etc. The space in which directional param-eters are distributed is called a vector field. The flow field of a combustion chamber is not only a quantitative field, but also a vector field. On a map, if one takes sea level as a base, and represents the height of mountains and the depth of waters by the use of contour lines, then, along a given normal line, a place in which the contour lines are close together means a very steep sloped wall, where the gradient is large. Heat transfer is a flow of heat from high temperature to area of low temperature, and this heat flow is represented by **q** ($kcal/m^2.s$); any given substance diffuses from places where its concentration is heavy to places where its concentration is sparse, and this diffusion is represented by **f** ($kg/m^2.s$); gases tend to flow from areas in which the pressure is high to areas in which the pressure is low, and this density flow is represented by ρ**V** ($kg/m^2.s$); all the quantities mentioned here are vector quantities. In a flow field under examination, it is pos-sible to draw out a contour map for total pressure, total temperature, concentration, and speed for the flow field by using several point values for the respective quan-tities within the flow field in question. When these curves are projected onto a coordinate plane, they become nothing more than isothermal lines, lines of equal pressure, etc. , etc.

In the case of a stable flow field, it is possible to get the distribution fun-ction for total pressure, overall temperature, and concentration within the space of the flow field, and these functions are called potential functions $\phi = \phi$ (x,y,z). ϕ = a constant, and it is called the equal potential surface. Concerning the pot-ential function, ϕ, its rate of change along a normal line, n, or its directional

75

derivative is called the "gradient" of 'ϕ', grad ϕ.

$$\text{grad}\phi = \nabla\phi = \left(i\frac{\partial}{\partial x} + j\frac{\partial}{\partial y} + k\frac{\partial}{\partial z} \right)\phi$$

$$= i\frac{\partial\phi}{\partial x} + j\frac{\partial\phi}{\partial y} + k\frac{\partial\phi}{\partial z} \qquad (4.1)$$

i, j, and k are respectively the unit vectors for the positive lengths along x, y, and z. The inverted triangle

$$\nabla = \left(i\frac{\partial}{\partial x} + j\frac{\partial}{\partial y} + k\frac{\partial}{\partial z} \right)$$

and it is the vector differential of the orthogonal coordinate system or the operator of the directional derivative. The symbol, ∇, in and of itself, is a vector; therefore, the gradient, $\nabla\phi$ is a vector, which has three components, one each along the x, y, and z axes. By using the concept of the gradient, it is possible to derive several formulae reflecting basic principles. For example, in the investigation of the heat flow that travels outward through the equipotential surface as well as the investigation of the question of the diffusion density flow of physical substances, etc. :

If one assumes that $\phi = T$, then, the heat flow

$$q = -\lambda\nabla T = -\lambda\left(i\frac{\partial T}{\partial x} + j\frac{\partial T}{\partial y} + k\frac{\partial T}{\partial z} \right) \quad [\text{kcal}/\text{m}^2 \cdot s]$$

$$(4.2)$$

λ is the rate of thermal conductance (kcal/m^2. s . E). The heat flow, q, and the temperature gradient are related quantities. The negative sign expresses the transfer of heat from areas of high temperature to areas of low temperature as well as the reversed direction of the gradient. If one makes $\phi = c$, the diffused density flow

$$f = -D\nabla c = -D\left(i\frac{\partial c}{\partial x} + j\frac{\partial c}{\partial y} + k\frac{\partial c}{\partial z} \right) \quad [\text{kg}/\text{m}^2 \cdot s]$$

$$(4.3)$$

D is the diffussion coefficient (m^2/s), and c is the concentration (kg/m^3). The diffusion density flow, f, and the concentration gradient are related quantities, and they are related by the Fei Ke equation just as the heat flow and the temperature gradient were related by the Fu Li Ye equations. The negative sign expresses the mutual opposition of the direction of diffusion and the direction of the gradient. If one sets $\phi =$ to the speed value, then, the density flow

$$\rho V = -\rho\nabla\phi = -\rho\left(i\frac{\partial\phi}{\partial x} + j\frac{\partial\phi}{\partial y} + k\frac{\partial\phi}{\partial z} \right) \quad [\text{kg}/\text{m}^2 \cdot s]$$

$$(4.4)$$

76

The gradient of the speed values, $\nabla\phi$, equals the flow speed vector, $\mathbf{V}$, and the directions of $\mathbf{V}$ and the direction of the gradient are opposite.

Sec 3 Practice in Multiplication of Vector Quantities

(1) Supposing that the included angle between two vectors, a and b, is θ, so that $0 \leqslant \theta \leqslant \pi$.   Then, the scalar product of a and b (the point product) is a magnitude $a \cdot b = ab \cos \theta$.

$$\theta = 90°, \mathbf{a} \cdot \mathbf{b} = 0; \theta = 0°, \mathbf{a} \cdot \mathbf{b} = ab. \quad (4.5)$$

Concerning the magnitudes of identities

$$i \cdot i = j \cdot j = k \cdot k = 1, \quad i \cdot j = j \cdot k = k \cdot i = 0. \quad (4.6)$$

(2) The "vector product" of two vectors, a and b, (also called the cross product) $\mathbf{a} \times \mathbf{b} = \mathbf{c}$ which is a third magnitude, c perpendicular to the plane of a and b. If θ is the included angle between $\mathbf{a}$ and $\mathbf{b}$, so that $0 \leqslant \theta \leqslant \pi$.

The magnitude of $\mathbf{c}$ is $\mathbf{c} = \mathbf{a} \times \mathbf{b} = |a| \cdot |b| \sin \theta$ (4.7)   = the surface area of a quadralateral.

The direction of c is determined by the use of a rule called the left-hand convention, that is, one takes the thumb of one's left hand and wraps his thumb and hand so that the thumb of the left hand points in the direction of c and that the other four figures wrap around that direction at an angle $\theta < \pi$ and coincident with b. Or, one could think of it as looking up the vector, c, as though it were an arrow; in such a case, a turns around the arrow in a counterclockwise direction at an angle, $\theta < \pi$ and coincident with b. According to this rule, if the cross products of a and b are reversed in order, then, the direction of the third vector, c, is turned around, that is.

$$\mathbf{b} \times \mathbf{a} = |b| \cdot |a| \sin (-\theta) = -\mathbf{c} = -(\mathbf{a} \times \mathbf{b}). \quad (4.8)$$

If we talk about the three "unit vectors" i, j, and k for a moment, then, we come up with the following relationships

$$i \times i = j \times j = k \times k = 0; \quad (4.9)$$
$$i \times j = k, \; j \times k = i, \; k \times i = j; \; j \times i = -k,$$
$$k \times j = -i, \; i \times k = -j. \quad (4.10)$$

(3) "The dot cross product " of three vectors, $\mathbf{a} \cdot (\mathbf{b} \times \mathbf{c})$ is the volume of an equilateral parallelipiped, $\mathbf{a}, \mathbf{b}, \mathbf{c}$. Since $(\mathbf{b} \times \mathbf{c})$ represents the lower surface area, and $\mathbf{a}$ represents the slope height. The included angle between $\mathbf{a}$ and $(\mathbf{b} \times \mathbf{c})$ $= \theta$. $\mathbf{a} \cdot (\mathbf{b} \times \mathbf{c}) = |a| \cos \theta \cdot |\mathbf{b} \times \mathbf{c}|$. , and within this expression $|a| \cos \theta = h$ is an altitude perpendicular to the base surface area; if, in equation (4.11) there are the three vectors $\mathbf{a} = ia_1 + ja_2 + ka_3,$ $\mathbf{b} = ib_1 + jb_2 + kb_3,$ $\mathbf{c} = ic_1 + jc_2 + kc_3$, then, it is possible to use determinants to express the dot cross products of the three vectors

$$\mathbf{a} \cdot (\mathbf{b} \times \mathbf{c}) = \begin{vmatrix} a_1 & a_2 & a_3 \\ b_1 & b_2 & b_3 \\ c_1 & c_2 & c_3 \end{vmatrix},$$ (4.12)

Due to the fact that the "dot products" of the three vectors represent volumes, if

$\mathbf{a} \cdot (\mathbf{b} \times \mathbf{c}) = 0$, then, the volume equals 0, and the three vectors, $\mathbf{a}, \mathbf{b},$ and $\mathbf{c}$, must lie within the same plane. The reverse of this is also true.

(4) The Continued Cross Product of Three Vectors

$$\mathbf{a} \times (\mathbf{b} \times \mathbf{c}) = (\mathbf{a} \cdot \mathbf{c})\mathbf{b} - (\mathbf{a} \cdot \mathbf{b})\mathbf{c}$$ (4.13)

The cross product of two vectors, $\mathbf{b} \times \mathbf{c} = \mathbf{d}$, is a third vector, $\mathbf{d}$, which is perpendicular to the plane of the original two vectors, $\mathbf{b}$, and $\mathbf{c}$. $\mathbf{a} \times (\mathbf{b} \times \mathbf{c}) = \mathbf{a} \times \mathbf{d} = \mathbf{e}.$ $\mathbf{e}$ is perpendicular to the plane of vectors $\mathbf{a}$, and $\mathbf{d}$, and is still a vector.

Sec 4 Continuous Equations and "Dispersion" of Flow Fields

Imagine the use of a thin transparent film of air, which is also called a "control surface", S , and closely adheres to the inner walls of flame tubes as well as intakes and exhausts and coats them (Fig 4.1). The space within the thin membrane, S, is called the "control volume", V_s. There is matter, momentum, energy, etc, continuously passing through V_s from the surface, S, and flowing in and out of the flame tube. On the surface, S, a designated point, P, has running through it the normal line n, and the unit vector, $\mathbf{n}$, along the normal line, n. Around the point, P, there are deliniated a differential surface, dS, as well as a differential volume, ΔV_s. If one sets the included angle between $\mathbf{n}$ and the flow speed vector of outward scattering equal to θ at a point, P, then, $\mathbf{V} \cdot \mathbf{n} = V \cos \theta$ which is perpendicular to the outward flow speed, dS. If one establishes that the direction along external normal line, n is figured to be positive, then, the matter, momentum and energy, etc., which are flowing out are figured to be positive values, and the inward flow, V_s, is con-

78

sidered as having a negative sign. The volume, Q, which is dispersed outward every second from the control surface is $\mathbf{V} \cdot \mathbf{n}$, is the integral along the entire surface, S, and is called "scattering magnitude":

$$Q = \oint^s \mathbf{V} \cdot \mathbf{n} dS \quad [\text{m}^3/\text{s}] \qquad (4.14)$$

The "divergence" of the speed vector field

$$\text{div } \mathbf{V} = \nabla \mathbf{V} = \lim_{\Delta V_s \to 0} \left[\frac{Q}{\Delta V_s} \right] = \lim_{\Delta V_s \to 0} \left[\frac{\oint^s \mathbf{V} \cdot \mathbf{n} dS}{\Delta V_s} \right] \qquad (4.15)$$

therefore, the divergence is equal to the volume scattered out from the control surface, S, every second, from each unit of control volume; the unit for this quantity is $(\text{m}^3/\text{s} \cdot \text{m}^3)$. When ΔV_s, tends toward a trace amount, dV_s, it is possible to obtain from equation (4.15) the relationship

$$Q = \oint^s \mathbf{V} \cdot \mathbf{n} dS = \oint^{V_s} \nabla \mathbf{V} dV, \quad [\text{m}^3/\text{s}] \qquad (4.16)$$
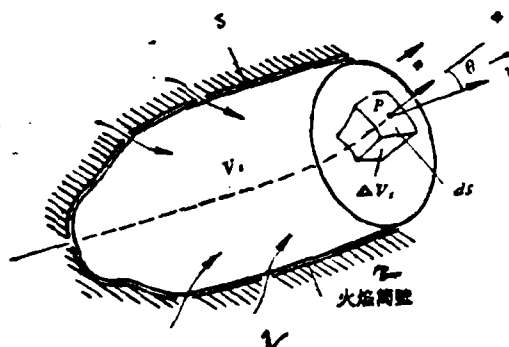

图4.1 控制体积 V_s, 控制表面 S

Fig 4.1

1. Control Volume, V_s, and, Control Surface, S 2. Walls of the flame tube

The equation above takes $\mathbf{V} \cdot \mathbf{n}$, the double integral along the surface, S, and turns it into the divergence, $\nabla \mathbf{V}$ on the basis of the triple integral of the volume, V_s. In fluid mechanics, this is Gauss's theorem.

The divergence, $\nabla \mathbf{V}$, is the dot product of two vectors, and is a magnitude. Using equation (4.6)

$$\text{div } \mathbf{V} = \nabla \mathbf{V} = \left(i \frac{\partial}{\partial x} + j \frac{\partial}{\partial y} + k \frac{\partial}{\partial z} \right) \cdot (iu + jv + kw)$$
$$= \frac{\partial u}{\partial x} + \frac{\partial v}{\partial y} + \frac{\partial w}{\partial z} \quad [1/\text{s}] \qquad (4.17)$$

Imagine that the micro-masses of gas in Fig 4.1 have a ΔV_s value that is appropriate to elastic solids; in this case, the three partial derivatives on the right

79

side of equation (4.17) represent the rates of change of the "tensile strain" along the x, y, and z axes or the "linear deformation rate".

Take the symbol ξ to represent density, ρ [kg/m³], density flow, ρV (kg/m²·s) or total enthalmic density ρi^* (kcal/m³), $i^* =$ (kcal/kg); with these ideas, then, it is possible to generalize the concept of "magnitude of divergence": i.e.

—the amount of matter, momentum or energy which is scattered out from the control surface per second

$$= \oint^s \xi V \cdot n dS \qquad (4.18)$$

—within a control body (for matter, momentum or energy) the rate of transformation per second

$$= \oint^{V_s} \frac{\partial \xi}{\partial t} dV_s \qquad (4.19)$$

—if one takes $\xi = \rho$, then, the matter scattering magnitude (or material rate of outward flow)

$$= \oint^s \rho V \cdot n dS \quad \text{[kg/s]} \qquad (4.20)$$

If, within the control body, there is no "point source", (that is to say, a source that gives out matter), then there is also no "point sink" (that is to say, a sink hole into which matter disappears); according to the principle of the conservation of mass, within V_s, it is not possible to simply add mass out of thin air. It is necessary to resupply it from outside (for scattering out resupply, we use a plus sign, and, for resupply of mass we use a negative sign); therefore,

$$\oint^{V_s} \frac{\partial \rho}{\partial t} dV_s = - \oint^s \rho V \cdot n dS \qquad (4.21)$$

Density flow, ρV, is a vector from which, by the use of the concept of "divergence," plus equation (4.16), it is then possible to develop the relationship

$$\oint^{V_s} \frac{\partial \rho}{\partial t} dV_s = - \oint^{V_s} \nabla \cdot \rho V dV_s,$$

or

$$\int^{V_s} \left[\frac{\partial \rho}{\partial t} + \nabla \cdot \rho V \right] dV_s = 0 \qquad (4.22)$$

From the equations above, it necessarily follows that

$$\frac{\partial \rho}{\partial t} + \nabla \cdot \rho V = \frac{\partial \rho}{\partial t} + \rho \nabla \cdot V + V \cdot \nabla \rho = 0 \qquad (4.23)$$

In unstable, compressible flow fields, density is a function of time and coordinates, $\rho = \rho(t, x, y, z)$. If we use the perfect differential method of solution on the basis of the multi-variable functions, then,

$$d\rho = \frac{\partial \rho}{\partial t} dt + \frac{\partial \rho}{\partial x} dx + \frac{\partial \rho}{\partial y} dy + \frac{\partial \rho}{\partial z} dz \qquad (4.24)$$

If one takes the instant, dt, and uses it to divide the various quantities in equation (4.24), because of the fact that

$$\frac{dx}{dt} = u, \quad \frac{dy}{dt} = v, \quad \frac{dz}{dt} = w,$$

therefore,

$$\frac{d\rho}{dt} = \frac{\partial\rho}{\partial t} + \frac{\partial\rho}{\partial x}\frac{dx}{dt} + \frac{\partial\rho}{\partial y}\frac{dy}{dt} + \frac{\partial\rho}{\partial z}\frac{dz}{dt}$$

$$= \frac{\partial\rho}{\partial t} + \frac{\partial\rho}{\partial x}u + \frac{\partial\rho}{\partial y}v + \frac{\partial\rho}{\partial z}w \qquad (4.25)$$

$\nabla\rho$ is the gradient of the numerical field, $\mathbf{V} = iu + jv + kw$, ; according to equation (4.1)

$$\mathbf{V}\cdot\nabla\rho = (iu + jv + kw)\cdot\left(i\frac{\partial\rho}{\partial x} + j\frac{\partial\rho}{\partial y} + k\frac{\partial\rho}{\partial z}\right)$$

$$= \frac{\partial\rho}{\partial x}u + \frac{\partial\rho}{\partial y}v + \frac{\partial\rho}{\partial z}w \qquad (4.26)$$

By comparing equation (4.25) and equation (4.26) it is possible to obtain the following result

$$\frac{d\rho}{dt} = \frac{\partial\rho}{\partial t} + \mathbf{V}\cdot\nabla\rho \qquad (4.27)$$

If one substitutes this expression into equation (4.23) it is possible to obtain the continuity equation for a three-dimensional, unstable, compressible flow field:

$$\frac{d\rho}{dt} + \rho\nabla\cdot\mathbf{V} = 0 \qquad (4.28)$$

If we make use of the divergence, $\nabla\rho\mathbf{V}$, of equation (4.17), then another form of the continuity equation is

$$\frac{\partial\rho}{\partial t} + \nabla\rho\mathbf{V} = \frac{\partial\rho}{\partial t} + \frac{\partial(\rho u)}{\partial x} + \frac{\partial(\rho v)}{\partial y} + \frac{\partial(\rho w)}{\partial z} = 0 \quad (4.29)$$

In the case of an incompressible, stable flow field, $(\partial\rho/\partial t) = 0$, and the divergence, $\nabla\mathbf{V} = 0$. (4.29)

Sec 5 Momentum Equations of Flow Fields

If we use equations (4.18) and (4.19) from a preceding section, and take ξ to be equal to $\rho\mathbf{V}$, then,

—the momentum diffused each second from the control surface, S,

$$-\oint^{s}\rho\mathbf{V}(\mathbf{V}\cdot\mathbf{n})dS \quad [N]$$

—within the control body, V_s, the rate of transformation of momentum per second

$$-\oint^{V_i} \frac{\partial(\rho V)}{\partial t}\, dV, \quad [\text{N}]$$

—the total outside force exerted on the control body

$$F = \oint^{V_i} \frac{\partial(\rho V)}{\partial t}\, dV, + \oint^{S} \rho V(V \cdot n)\, dS \quad [\text{N}], \qquad (4.30)$$

Equation (4.30) is the total outside force exerted on the control body = the total rate of transformation of momentum of the control body.

Outside forces can be divided into two types:

(1) Mass forces. That is to say, it is only because there is mass that external forces can be felt. For example, gravity, ρg , centrifugal force, $mr\omega^2$, inertia, ma , as well as electromagnetic forces, etc. If micro-masses of fluids have no turning motion around a coordinate axis, i.e. $\omega = 0$; then, there is no centrifugal force.

The force of gravity exerted on the control body, $V_s = \oint^{V_i} \rho g\, dV, \quad [\text{N}], \qquad (4.31)$

(2) Surface Forces. These forces include external pulls and pressures on the control surface, S, as well as shear forces which rub along the surface or friction. Assume that each square meter of gas has exerted on it a surface force = R (N/m^2).

The surface forces exerted on the control body, $V_s = \oint^{V_i} R\, dV, \quad [\text{N}] \qquad (4.32)$

Because of this

$$F = \oint^{V_i} \rho g\, dV, + \oint^{V_i} R\, dV, = \oint^{V_i} \frac{\partial(\rho V)}{\partial t}\, dV,$$

$$+ \oint^{S} \rho V(V \cdot n)\, dS \qquad (4.33)$$

According to equation (4.16) $\quad \oint^{S} \rho V(V \cdot n)\, dS = \oint^{V_i} \nabla(\rho V \cdot V)\, dV,$

$$= \oint^{V_i} [\rho V(\nabla V) + (V\nabla)\rho V]\, dV, \qquad (4.34)$$

When equation (4.34) is substituted into equation (4.33) it becomes

$$\oint^{V_i} \left[\frac{\partial(\rho V)}{\partial t} + \rho V(\nabla V) + (V\nabla)\rho V - \rho g - R \right] dV, \qquad (4.35)$$
$$= 0$$

If it is necessary for the integral to be equal to 0, then, it is necessary for the integrated function to be equal to 0; therefore,

$$\frac{\partial(\rho V)}{\partial t} + \rho V(\nabla V) + (V\nabla)\rho V = \rho g + R \quad (\text{N/m}^3] \qquad (4.36)$$

Referring to equation (4.27), if we take (ρV) to stand in place of ρ; then,

$$\frac{d(\rho V)}{dt} = \frac{\partial(\rho V)}{\partial t} + (V\nabla)\rho V \qquad (4.37)$$

However,

$$\frac{d(\rho V)}{dt} = \rho \frac{dV}{dt} + V \frac{d\rho}{dt} \qquad (4.38)$$

82

If we take the relationship between equations (4.37) and (4.38), and substitute it into equation (4.36), then,

$$\rho \frac{d\mathbf{V}}{dt} + \mathbf{V}\left[\frac{d\rho}{dt} + \rho(\nabla\mathbf{V})\right] = \rho g + R \qquad (4.39)$$

According to the continuity equation of equation (4.28), in the equation above, the quantity in the parentheses should be equal to zero. Therefore, we obtain the mass density times the acceleration

$$\rho \frac{d\mathbf{V}}{dt} = \rho g + R \quad [\text{N/m}^3], \qquad (4.40)$$

The perfect integral of $\mathbf{V}$ versus t is the acceleration vector

$$\mathbf{a} = \frac{d\mathbf{V}}{dt} = \frac{\partial\mathbf{V}}{\partial t} + (\mathbf{V}\nabla)\mathbf{V}$$

$$= \text{local acceleration} + \text{shift acceleration}.$$

This is due to the fact that the speed distribution is a function of time and coordinates, $\mathbf{V} = \mathbf{V}(t, x, y, z)$, and, if, according to equation (4.24), we use the perfect differential method equation (4.26), then, it is possible to obtain an equation analogous to equation (4.27). Therefore, equation (4.40) can also be written as the following relationship,

The force exerted on every cubic meter of the control body =

$$= \rho\mathbf{a} = \rho\frac{\partial\mathbf{V}}{\partial t} + \rho(\mathbf{V}\nabla)\mathbf{V}$$

$$= \rho g + R \quad [\text{N/m}^3] \qquad (4.41)$$

What are known as stable flow fields are actually flow fields in which the local acceleration, $\frac{\partial\mathbf{V}}{\partial t} = 0$; moreover, the "shift acceleration" $(\mathbf{V}\nabla)\mathbf{V}$ is still present. Otherwise, the micro-masses of gas would not shift positions, and there would be no flow. The shift acceleration

$$(\mathbf{V}\nabla)\mathbf{V} = (iu + jv + kw) \cdot \left(i\frac{\partial\mathbf{V}}{\partial x} + j\frac{\partial\mathbf{V}}{\partial y} + k\frac{\partial\mathbf{V}}{\partial z}\right)$$

$$= u\frac{\partial\mathbf{V}}{\partial x} + v\frac{\partial\mathbf{V}}{\partial y} + w\frac{\partial\mathbf{V}}{\partial z}, \qquad (4.42)$$

If one takes equation (4.41) and rewrites it as three components along the x, y, and z axes (an orthagonal coordinate Euler equation):

$$\rho\left(\frac{\partial u}{\partial t} + u\frac{\partial u}{\partial x} + v\frac{\partial u}{\partial y} + w\frac{\partial u}{\partial z}\right) = \rho g_x + R_x$$

$$\rho\left(\frac{\partial v}{\partial t} + u\frac{\partial v}{\partial x} + v\frac{\partial v}{\partial y} + w\frac{\partial v}{\partial z}\right) = \rho g_y + R_y \qquad (4.41)'$$

$$\rho\left(\frac{\partial w}{\partial t} + u\frac{\partial w}{\partial x} + v\frac{\partial w}{\partial y} + w\frac{\partial w}{\partial z}\right) = \rho g_z + R_z$$

Sec 6 "Circular Momentum" and "Vorticity" of Flow Fields

Chapter 2 talked about the fact that, in boundary layers, due to the fact that there is viscosity, μ, the normal line y of a given point along the wall surface

83

has a speed distribution $u = f(y)$, and a speed distribution gradient of $(\partial u / \partial y)$. Due to this fact, in the areas between the layers of a laminar flow there are viscous shear forces $\tau = \mu(\partial u / \partial y)[\mathrm{N/m^2}]$.

If, at a place of adhesion to the wall $(\partial u / \partial y) = 0$, $\tau = 0$; then, the flow layer will adhere to the wall because the force acting to blast it off the wall is inadequate, and it cannot flow forward any more, so it will separate. Down stream from the point of separation, s, gases flow upstream against the current in order to fill in the vacuum are ted by the flow layer separation; they, then, roll up or themselves and become eddies (Fig 4.2 (a)). Also concerning boundary layers, after those layers encounter an obstacle, sudden separation occurs along the edge angles, and this also produces separation eddies (Fig 4.2 (b)). If we take two layers of air flow, going in the same direction, and call them u_1 and u_2, and we further stipulate that their speeds are not the same; then, under these conditions, if $\mu = 0$, then, the flow along the boundary between them is smooth; however, if $\mu \neq 0$, then, they pull against each other, exchanging momentum and producing eddy layers (Fig 4.2 (c)). These eddies are micro-masses of gas which are rotating at high speed, giving them an angular velocity vector, ω . Because this vector can be resolved into three component vectors, one for each of the coordinate axses, it is possible to write the following: $\omega = i\omega_x + j\omega_y + k\omega_z$. According to the right hand spiral convention, the direction toward which the threads of a spiral move has a positive sign. This is the same as the directional rule for the cross product of two vectors. Imagine that a turning vortical mass is projected onto the x-y plane in Fig .; in such a case, the separation area, (a), the wake area, (b), and the vortical flow layer, (c), are all vortical flow fields and all have spiral flows around the axis, z. The diameter of the ring flow path of the micro-masses of gas is the length of the circumference, $2\pi r$; the area of the ring flow is $\Delta S = \pi r^2$. Along the path of the ring flow, the length of the differential arc $dl = rd\theta$.

Concerning V, the "ring vector", Γ, around the central axis is equal to $\int^l \mathbf{V} \cdot dl$ which is equal to the linear integral of the closed curve, L defined by the dot product of the arc differential and the shear line speed. To provide an example, it is as though a small donkey were pulling against and rubbing against his corral and every second he rubbed a larger and larger area $(\mathrm{m^2/s})$; this is what is meant by a ring vector.

Assuming we already know the angular velocity, ω_z, and the ring flow radius, r, then, $\mathbf{V} = r\,\omega_z$.

Due to this fact, the ring vector

84
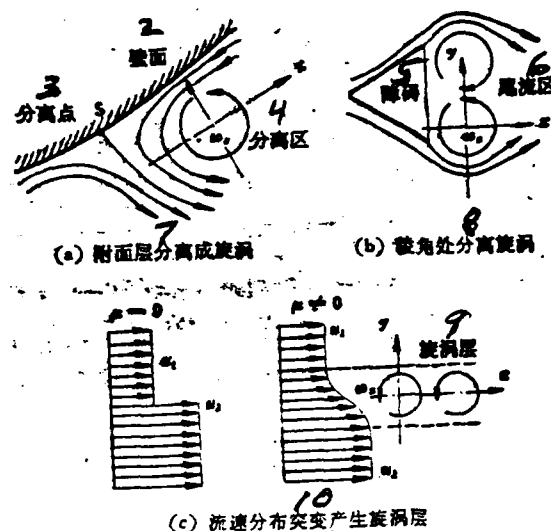
(a) 附面层分离成旋涡   (b) 钝角处分离旋涡

(c) 流速分布突变产生旋涡层

图4.2 粘流分离形成旋涡

Fig 4.2

1. Spirals Formed by Viscous Flow Separation   2. Wall Surface   3. Point of Separation   4. Separation Area   5. Obstacle   6. Tail Flow or Wake Area   7. Boundary Layer Separation Forms Spiral Flow   8. Refraction Angle Separation Spirals   9. Vortical Layer   10. Sudden Changes in Flow Speed Distribution Cause Vortical Layers

$$\Gamma = \oint^L \mathbf{V} \cdot \mathbf{dl} = \int_0^{2\pi} r^2 \omega_z d\theta \qquad (4.42)$$
$$= 2\pi r^2 \omega_z \ [m^2/s],$$

The vorticity of the x-y flow field

$$\xi_z = \frac{\text{环量 } \Gamma}{\text{环流面积 } \Delta S} = \frac{2\pi r^2 \omega_z}{\pi r^2} = 2\omega_z \qquad (4.43)$$

Fig 4.3 (a) shows a spiral turning around the axis, z, as though it were a "solid", with the angular velocity, ω_z. If one assumes the P (x,y) is a fixed point selected on the surface of the "solid", then, from the two similar triangles swept out by the lines in Fig 4.3 (b), it is possible to see that $v:-u:r\omega_z = x:y:r_{,}$. Therefore,

$$\frac{v}{x} = \frac{-u}{y} = \frac{r\omega_z}{r} = \omega_z,$$

Due to this fact $u = -y\omega_z, \quad v = x\omega_z, \quad w = 0.$

The partial derivative:

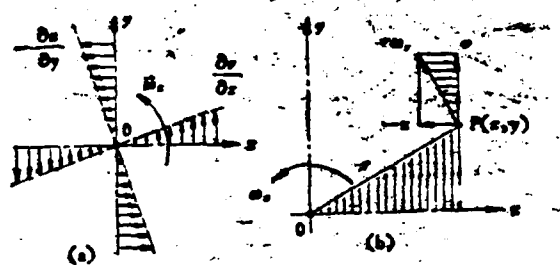$$\frac{\partial v}{\partial x} = \omega_z, \quad -\frac{\partial u}{\partial y} = \omega_z;$$

85

Fig. 4.3 spiral turning around as though it were
a solid.

$$\frac{1}{2}\left(\frac{\partial v}{\partial x} - \frac{\partial u}{\partial y}\right) = \frac{1}{2}\left(\omega_z + \omega_z\right) = \omega_z \qquad (4.44)$$

If equation (4.44) were written as a sentence, it would say, " The vorticity of the flow field, xy, ξ_z, is equal to twice the angular velocity of rotation around axis z, i.e. 2 ω_z." The magnitude of the vorticity is nothing more than the speed of rotation of the vertical masses.

Generalizing this to a three-dimensional vortical flow field. If one supposes the $\mathbf{r} = \mathbf{a}$ "radial vector" put out by a point source, O. If the length of $\mathbf{r}$ does not change and only the directional angle, θ, (longitudinal) and the declination angle, ϕ', (latitudinal) change, then, the end point of the "radial vector", F, traces out, in space, a spherical surface. If the length of $\mathbf{r}$ as well as its direction both change, then, point, F, traces out, in space, a curved surface, S (Fig 4.4). One can take a cross section of the curved surface, S, and generate the closed curve, L. The projection of the flow speed vector, $\mathbf{V}$, of a certain point, F, on L, as it is projected against a tangent to point, P, is $\mathbf{V} \cdot d\mathbf{r}$. At this point $d\mathbf{r} \cong d\mathbf{l}$ and is the differential arc length of the closed curve, L. $\qquad d\mathbf{r} = \mathbf{r}_2 - \mathbf{r}_1$
= the vector difference of the end points of the two "radial vectors" on the tangent L. In conjunction with this, the ring vector, $\mathbf{V}$, around the central axis, O A is governed by the following expressions:

$$\Gamma = \oint^L \mathbf{V} \cdot d\mathbf{r} = \oint^L \mathbf{V} \cdot d\mathbf{l} \quad [m^2/s] \quad (4.45)$$

Concerning the differential area, ΔS, which is cut out of the curved surface, S, $\mathbf{n}$ is the unit vector of the outward normal line of Δ S and forms the angle, α, with O A. By the same token, the vorticity of a three-dimensional vortical flow field = the amount of ring vectors put out by each unit of curved surface

$$\mathrm{curl}\,\mathbf{V} = \xi = \nabla \times \mathbf{V} = \lim_{\Delta S \to 0}\left[\frac{\oint^L \mathbf{V} \cdot d\mathbf{r}}{n\Delta S}\right]\left[\frac{m^2}{s \cdot m^2} = \frac{1}{s}\right]$$

$$(4.46)$$

When $\Delta S \to dS$,

$$\oint^s (\nabla \times \mathbf{V}) \cdot \mathbf{n}dS = \oint^L \mathbf{V} \cdot d\mathbf{r} = \Gamma \qquad (4.47)$$

The equation above takes the linear integral along the path of ring flow, L, and turns it into the duplex integral of the vorticity $(\nabla \times \mathbf{V})$ projected on $\mathbf{n}$ along the curved surface, S. In fluid dynamics, this is called Stokes Law. The "vorticity" of
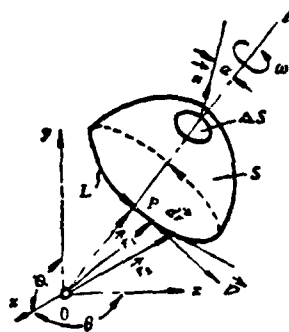
86

图4.4 三元流场旋度

Fig 4.4

1. Vorticity of a Three-Dimensional Flow Field

V is the cross product of two vectors ∇ and V; therefore, it is still a vector. Applying formula (4.10)

$$\xi = \text{curl}V = (\nabla \times V) = \left(i\frac{\partial}{\partial x} + j\frac{\partial}{\partial y} + k\frac{\partial}{\partial z}\right)$$

$$\times (iu + jv + kw) = i\left(\frac{\partial w}{\partial y} - \frac{\partial v}{\partial z}\right)$$

$$+ j\left(\frac{\partial u}{\partial z} - \frac{\partial w}{\partial x}\right) + k\left(\frac{\partial v}{\partial x} - \frac{\partial u}{\partial y}\right)$$

$$= 2(i\omega_x + j\omega_y + k\omega_z) = 2\omega, \qquad (4.48)$$

For the sake of ease of memorization these relationships can be rewritten as the following algebraic matrix

$$\text{curl}V = \nabla \times V = \begin{vmatrix} i & j & k \\ \dfrac{\partial}{\partial x} & \dfrac{\partial}{\partial y} & \dfrac{\partial}{\partial z} \\ u & v & w \end{vmatrix} \left[\frac{m^2}{m^2 \cdot s} = \frac{1}{s}\right], \qquad (4.49)$$

Chapter Two talked about the fact that the flow speed vector, V, is the gradient, $\nabla\phi$, of the "velocity value", ϕ (equation 4.4). According to equation (4.17), it is possible to write the "divergence" of V as $\text{div }V = \nabla \cdot V = \phi$, and the gradient of divergence $= \nabla \cdot \nabla\phi$ in 3d.

$$\text{div} \cdot \text{grad } \phi = \nabla \cdot \nabla\phi = \nabla^2\phi = \frac{\partial^2\phi}{\partial x^2} + \frac{\partial^2\phi}{\partial y^2}$$

$$+ \frac{\partial^2\phi}{\partial z^2} = \Delta\phi \qquad (4.50)$$

The "right-side-up" triangle

$$\Delta = \nabla^2 = \frac{\partial^2}{\partial x^2} + \frac{\partial^2}{\partial y^2} + \frac{\partial^2}{\partial z^2},$$

and is called the orthagonal coordinate Laplacian computational symbol. If one is solving for the "vorticity" of the gradient of ϕ, $\nabla \phi$, then, because of the fact that the square of this vector times itself, $\nabla \times \nabla = 0$; therefore,

$$\text{curl grad } \phi = \nabla \times \nabla \phi = \left(i \frac{\partial}{\partial x} + j \frac{\partial}{\partial y} + k \frac{\partial}{\partial z} \right)$$

$$\times \left(i \frac{\partial \phi}{\partial x} + j \frac{\partial \phi}{\partial y} + k \frac{\partial \phi}{\partial z} \right) = 0 \quad (4.51)$$

The meaning of this is that, if a flow field has a velocity value, ϕ, (in which case, it is called a "value flow field" for short), then, its "vorticity" = 0. According to equations (4.44) and (4.48), this equates to the idea that $\omega = 0$. That is to say that, except for an isolated, special point, within the flow field, there are no spiral masses of gas which have the form of a turning solid. When compared to Fig 1.0, this simply means that there is no viscosity, μ. Therefore, what is meant by "non-viscous flow", "non-vortical flow", "positional flow", and "isenthropic flow" is all the same thing, that is to say, they all mean that, within the flow there is no viscous friction, there are no shear forces, τ, which is to say that there is no loss of power due to vortical turbulence flow with the resulting conversion of such power losses into "heat of friction." Because of this fact, if one does not include boundary layer separation areas, areas of wake behind obstacles, and vortical flow layers, then, it is possible to say that the "main flow area" is a flow field with no rotation vlaue to it. However, attention should be paid to the fact that "spirals" or "vortices" can develop and expand; they can enlarge, break up and decay into turbulence flow which can disrupt the "main flow field." In a combustion chamber, in order to mark out such a "positional flow field", it is necessary to assume that certain conditions are present.

Sec 7 "Deformation Rate Tensors" and "Matrices"

If one chooses a zero point which does not move, then, in a three-dimensional flow field: $\quad V = iu + jv + kw;$ $\quad$; the radial vector

$$r = ix + jy + kz, r \cdot i = x, r \cdot j = y, r \cdot k = z; \quad (4.52)$$

Assume that the velocity vector for the origin point, 0, is $V_0 = 0$; the velocity vectors around the zero point (in its vicinity) $= V$; if we expand V accord-

88

ing to the Taylor series, all that is left is a first degree vector derivative, and, in this case,

$$V = 0 + r \cdot \nabla V = r \cdot D$$

(Take careful note of the fact that ∇V is not the divergence $\nabla \cdot V$) (4.53)

"Deformation tensors"

$$D = \nabla V = i\,\frac{\partial V}{\partial x} + j\,\frac{\partial V}{\partial y} + k\,\frac{\partial V}{\partial z}. \quad (4.54)$$

The three numbers that designate a point in a three-dimensional coordinate system define a vector, r, in that way; the nine numbers designating three vectors define a "tensor", D; equation (4.54) is a combination of three vectors. The component vectors for velocity, u, v, and w, respectively, are partial differentials of x, y, and z, and, altogether, there are nine first order partial derivatives which represent the rate of deformation. If we expand the three vectors of D, we obtain

$$\left.\begin{aligned}
\frac{\partial V}{\partial x} &= i\,\frac{\partial u}{\partial x} + j\,\frac{\partial v}{\partial x} + k\,\frac{\partial w}{\partial x}\\[2pt]
\frac{\partial V}{\partial y} &= i\,\frac{\partial u}{\partial y} + j\,\frac{\partial v}{\partial y} + k\,\frac{\partial w}{\partial y}\\[2pt]
\frac{\partial V}{\partial z} &= i\,\frac{\partial u}{\partial z} + j\,\frac{\partial v}{\partial z} + k\,\frac{\partial w}{\partial z}
\end{aligned}\right\} = D \quad (4.55)$$

If one further takes the right hand sides of the three equations in (4.55) and arranges the nine first order partial derivatives in order in a matrix, then, one obtains the

"Deformation Rate Matrix"
$$\begin{Bmatrix}
\dfrac{\partial u}{\partial x} & \dfrac{\partial v}{\partial x} & \dfrac{\partial w}{\partial x}\\[6pt]
\dfrac{\partial u}{\partial y} & \dfrac{\partial v}{\partial y} & \dfrac{\partial w}{\partial y}\\[6pt]
\dfrac{\partial u}{\partial z} & \dfrac{\partial v}{\partial z} & \dfrac{\partial w}{\partial z}
\end{Bmatrix} \quad (4.56)$$

Sec 8 "Speed Value" ϕ and "Flow Function" ψ

(1) Concerning the speed value, ϕ', if one is speaking of a flow field that has no rotational value to it, then, according to equation (4.44) or equation (4.49), $\omega = 0$; $\nabla \times v = 0$:

$$\left.\begin{aligned}
\omega_x &= \frac{1}{2}\left(\frac{\partial v}{\partial x} - \frac{\partial u}{\partial y}\right) = 0, & \frac{\partial v}{\partial x} &= \frac{\partial u}{\partial y},\\[4pt]
\omega_y &= \frac{1}{2}\left(\frac{\partial u}{\partial z} - \frac{\partial w}{\partial x}\right) = 0, & \frac{\partial u}{\partial z} &= \frac{\partial w}{\partial x},\\[4pt]
\omega_z &= \frac{1}{2}\left(\frac{\partial w}{\partial y} - \frac{\partial v}{\partial z}\right) = 0, & \frac{\partial w}{\partial y} &= \frac{\partial v}{\partial z},
\end{aligned}\right\} \quad (4.57)$$

As far as flow fields are concerned which have no rotational value to them, the speed value function, $\phi = \phi(x, y, z, t)$, when solved for the perfect differential

$$d\phi = \frac{\partial \phi}{\partial x} dx + \frac{\partial \phi}{\partial y} dy + \frac{\partial \phi}{\partial z} dz + \frac{\partial \phi}{\partial t} dt \quad (4.58)$$

According to equation (4.4) from Sec 2, the gradient of ϕ

$$\text{grad } \phi = \nabla \phi = \mathbf{V} = i \frac{\partial \phi}{\partial x} + j \frac{\partial \phi}{\partial y} + k \frac{\partial \phi}{\partial z}$$
$$= iu + jv + kw$$

This sheds light on equation (4.58) and leads to the conclusion that

$$\frac{\partial \phi}{\partial x} = u, \quad \frac{\partial \phi}{\partial y} = v, \quad \frac{\partial \phi}{\partial z} = w; \quad (4.59)$$

In a stable flow field

$$\frac{\partial \phi}{\partial t} = 0, \text{ thus } d\phi = u\,dx + v\,dy + w\,dz \quad (4.60)$$

Because of the fact that the speed distribution $u = f(x, y, z)$, $v = f(x, y, z)$, $w = f(x, y, z)$; therefore, it follows that equation (4.60) is the perfect differential of the speed value, ϕ, and it is possible to get ϕ by integration. Or, to put it the other way around, it is only necessary to know the speed value, ϕ, and it becomes possible, through differentiation, to solve for the three component vectors of speed, u, v, and w, and, thus, to solve for the whole velocity field. Because this is true, flow fields which have no rotational value to them are entirely susceptible to theoretical analysis which makes it possible to calculate their speed distributions.

(2) Flow Function ψ

Sec 1 talked about the fact that, with axially symmetrical flow fields, it is possible to represent them as two-dimensional flow fields either on a meridian plane or on a plane of revolution. The continuity equation for a stable, compressible, two-dimensional, plane flow field is as follows according to equation (4.22)

$$\frac{\partial (\rho u)}{\partial x} + \frac{\partial (\rho v)}{\partial y} = 0, \text{ or } \frac{\partial (\rho u)}{\partial x} = - \frac{\partial (\rho v)}{\partial y};$$

Using an isothermic density, ρ^*, to eliminate various quantities from the equations above

$$\frac{\partial}{\partial x} \left(\frac{\rho u}{\rho^*} \right) = - \frac{\partial}{\partial y} \left(\frac{\rho v}{\rho^*} \right). \quad (4.61)$$

assume $\frac{\partial \psi}{\partial x} = - \frac{\rho}{\rho^*} v, \quad \frac{\partial \psi}{\partial y} = \frac{\rho}{\rho^*} u; \quad \rho^* = \text{constant}$

$$\frac{\partial^2 \psi}{\partial y \partial x} = \frac{\partial}{\partial y} \left(\frac{-\rho v}{\rho^*} \right), \quad \frac{\partial^2 \psi}{\partial x \partial y} = \frac{\partial}{\partial x} \left(\frac{\rho u}{\rho^*} \right),$$

$$(4.62)$$

Consequently, according to equation (4.61)

$$\frac{\partial^2 \psi}{\partial y \partial x} = \frac{\partial^2 \psi}{\partial x \partial y};\qquad (4.63)$$

Solving for the perfect differential of the flow function $\psi = \psi(x, y)$

$$d\psi = \frac{\partial \psi}{\partial x}dx + \frac{\partial \psi}{\partial y}dy.\qquad (4.64)$$

Substituting equation (4.62) into equation (4.64)

$$d\psi = \left(-\frac{\rho}{\rho^*}v\right)dx + \left(\frac{\rho}{\rho^*}u\right)dy\qquad (4.65)$$

Because of the conditions of equation (4.63), it is possible to integrate equation (4.65) and obtain the function ψ. If ψ = a constant ψ_1, ψ_2, ..., then, $d\psi = 0$ or

$$\left(-\frac{\rho}{\rho^*}v\right)dx + \left(\frac{\rho}{\rho^*}u\right)dy = 0,$$

This also leads to

$$-v\,dx + u\,dy = 0;$$

or

$$\frac{u}{dx} = \frac{v}{dy},\quad \frac{dy}{dx} = \frac{v}{u}.\qquad (4.66)$$

Equation (4.66) is called a "flow line equation"; with this equation, it is possible to draw out, on the x-y plane, the flow line $\psi = \psi_1$, ψ_2......; therefore, ψ is called the flow function. Obviously, the direction, v/u, of the speed vector, $\mathbf{V} = \mathbf{i}u + \mathbf{j}v$, is precisely the direction,(dy/dx), of a tangent to a certain point, P, on the flow line; this is precisely the definition of a flow line. Fig 4.5 draws out a flow line spectrum of a two-dimensional, plane flow field. Assume that a perpendicular to the surface of the Fig has a thickness = h. Then, choose an interval distance, ds, between two flow lines, ψ and $d\psi$. If one does these things, then, the flow amount passing through the cross section, hds, = dG. The projection of ds on the y axis = dy, and the projection of ds on the x axis is -dx. From Fig 4.5 one can see that the microflow

$$dG = \rho v(-dx)h + \rho u\,dy\,h \text{ [kg/s]},\qquad (4.67)$$

According to equation (4.65),

$$-\rho v\,dx + \rho u\,dy = \rho^*d\psi,\text{ therefore } dG = h\rho^*d\psi\qquad (4.68)$$

The amount of flow between the two flow lines ψ_1 and ψ_2.

$$\Delta G = G_2 - G_1 = h\rho^* \int_{①}^{②} d\psi = h\rho^*(\psi_2 - \psi_1) \text{ [kg/s]},$$
$$(4.69)$$

The flow function ψ, which corresponds to the flow line which matches the solid surface of the wall is equal to 0. Because of this fact, a certain flow line

'ψ represents the amount of flow in the interval between the given flow line and the surface of the wall, $h\rho_i^* \phi$ (kg/s).

When generalizing the flow function, 'ϕ', it is by no means necessary to assume that there is no rotational value attached to the flow field being considered. Therefore, the function 'ϕ' can also be used in conjunction with flow fields which have rotational values. However, because this is based on a two-dimensional continuity equation, it is limited in its use only to two-dimensional flow fields. The continuity equation for an incompressible, two-dimensional flow field is

Divergence
$$\nabla V = \frac{\partial u}{\partial x} + \frac{\partial v}{\partial y} = 0,$$

Because of this
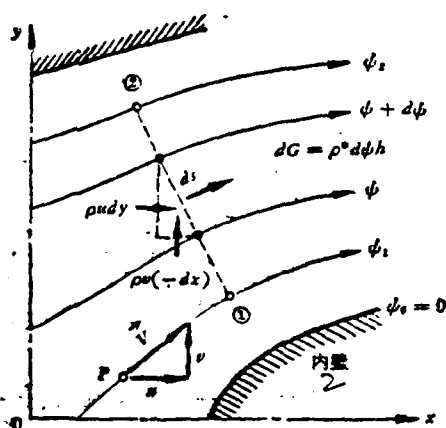$$\frac{\partial \psi}{\partial x} = -v, \quad \frac{\partial \psi}{\partial y} = u \qquad (4.70)$$

图 4.5 二元流场流线谱

Fig 4.5

1. A Flow Line Spectrum for a Two-Dimensional Flow Field   2. Inside Wall

Comparing equation (4.59), it is possible to see that

$$\frac{\partial \phi}{\partial x} = \frac{\partial \psi}{\partial y} = u, \quad \frac{\partial \phi}{\partial y} = -\frac{\partial \psi}{\partial x} = v \qquad (4.71)$$

The gradient for the speed value is

$$\text{grad } \phi = \left(i \frac{\partial}{\partial x} + j \frac{\partial}{\partial y} \right) \phi = i \frac{\partial \phi}{\partial x} + j \frac{\partial \phi}{\partial y} = iu + jv$$

The gradient for the flow function is
$$(4.72)$$

$$\text{grad } \psi = \left(i \frac{\partial}{\partial x} + j \frac{\partial}{\partial y} \right) \psi = i \frac{\partial \psi}{\partial x} + j \frac{\partial \psi}{\partial y}$$
$$= -iv + ju \qquad (4.73)$$

Concerning the scalar product of the gradients of ϕ and ψ, according to equation

92

(4.6) the matrix $ii = jj = 1, ij = ji = 0;$, if this is so,

then, $\text{grad}\phi \cdot \text{grad}\psi = (iu + jv) \cdot (ju - iv) = \overline{iju^2} - iiuv + jjuv - ijv^2 = 0;$;

therefore, grad ϕ and grad ψ are orthogonal gradients, that is to say, the
equipotential lines defined by $\phi = \phi_1, \phi_2\ldots$ and the flow lines $\psi = \psi_1, \psi_2\ldots$
are families of curves which meet each other at right angles, and each four inter-
section points form a square.

Sec 9 "Point Sources" and "Point Sinks"

Let us assume that we have a speed value function $\phi = \dfrac{b}{r}, \; r = (x^2 + y^2 + z^2)^{\frac{1}{2}}$
= the length of the "radial vectors" (4.74). b = a constant. Equipotential sur-
face, $\phi = \phi_1, \phi_2, \ldots,$ that is to say that is equal to the length of the "radial
vectors $r = r_1, r_2\ldots$which describe concentric spherical surfaces with their centers
and origin points at O.

The emission flow speed vector

$$V = \text{grad}\phi = \nabla \cdot \phi = \frac{\partial\phi}{\partial r} = -\frac{b}{r^2}, \quad (4.75)$$

and this is perpendicular to the equipotential surface. $(4.75)'$ The amount of flow
emitted from the origin point, O, is $\qquad G = 4\pi r^2 V\rho = -4\pi b\rho \;\; [kg/s]$

$$(4.76)$$

Equation (4.76) and the radius, r, are unrelated; therefore, the amount of
flow which passes through each spherical surface, G, has the same value in all cases.

If the constant, b, is posititve, then, the flow lines concentrate themselves
toward the center of the spheres and leak out in the amount, G (kg/s); because of
this fact, the O point is called a "point sink." For example, speaking about the
outer ring cavity, the small holes in the walls of flame tubes are all "point sinks".

If the constant, b, has a negative sign, then, the flow lines are emmitted
outward from the center of the spheres and scattered at the rate of G (kg/s). There-
fore, the O point, in this instance, is called a "point source". For example,
the vaporization of the fuel droplets which are sprayed out by centrifugal or strai-
ght jet nozzles.

These concentric sphereical surfaces are all surfaces defined by equal pres-
sure values (Fig 4.6).

If one is dealing with a "point sink", then, the closer one comes to the O
point, the faster the flow speed, V, is going to be, and the lower the pressure,
p, is going to be. In places where $r = 0, \; V \to \infty$. This is actually impossible.
Therefore, the speed value function, $\phi = b/r$ only represents a flow field outside

93

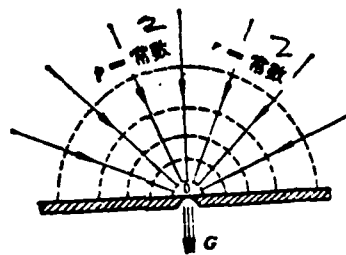a very small spherical surface around the O point.

图4.6 "点潭"$\phi = \dfrac{h}{r}$ 流谱

Fig 4.6

1. Flow Spectrum of a "Point Sink", $\phi = \dfrac{h}{r}$ 2. Constant

Chapter 5 Momentum and Potential Energy Equations for Viscous Flow

Sec 1 Liquid Micro-globular Surface Tension

Imagine a liquid micro-globule in the form of a cube which is separate and standing independently away from a viscous flow field. (Fig 5.1) Using an orthogonal coordinate system in x, y, and z, the volume of the liquid micro-mass, $dV_s = dxdydz$. On each of the six surfaces of the cube-shaped micro mass, it is possible to separate out positive tensile (pressure) forces which act on each face from three different directions; these are $\sigma_x, \sigma_y, \sigma_z$; it is possible to identify friction shear forces which act from six directions --these are $\tau_{xy}, \tau_{yz}, \tau_{zx}, \tau_{xz}, \tau_{yx}, \tau_{zy}$, . Each surface receives the influence of one positive tensile force, σ, and two shear forces, τ. The base coordinate of these shear forces, τ, is determined as follows: the first of the base coordinates indicates along which coordinate axis the direction of the force lies; the second base coordinate to which coordinate axis the plane of operation of the force is perpendicular. For example, τ_{yx} indicates that this force runs along direction y and its plane of operation is perpendicular to the z axis. The total forces which act on the surface of the liquid micro-mass along the direction x

$$\left(\sigma_x + \frac{\partial \sigma_x}{\partial x} dx\right) dydz + (-\sigma_x) dydz + \left(\tau_{xy} + \frac{\partial \tau_{xy}}{\partial y} dy\right)$$

$$\times dxdz - (\tau_{xy}) dxdz + \left(\tau_{xz} + \frac{\partial \tau_{xz}}{\partial z} dz\right) dxdy$$

$$+ (-\tau_{xz}) dxdy = \left(\frac{\partial \sigma_x}{\partial x} + \frac{\partial \tau_{xy}}{\partial y} + \frac{\partial \tau_{xz}}{\partial z}\right) dxdydz \qquad (5.1)$$

By the same token, the total forces which act on the surface in the direction y are

$$\left(\frac{\partial \tau_{yx}}{\partial x} + \frac{\partial \sigma_x}{\partial y} + \frac{\partial \tau_{yz}}{\partial z}\right) dxdydz \qquad (5.2)$$

The total forces which act on the surface in direction z are

$$\left(\frac{\partial \tau_{zx}}{\partial x} + \frac{\partial \tau_{zy}}{\partial y} + \frac{\partial \sigma_z}{\partial z}\right) dxdydz \qquad (5.3)$$

This can be written as the three component forces of the surface tension **R** which is exerted on each unit of volume
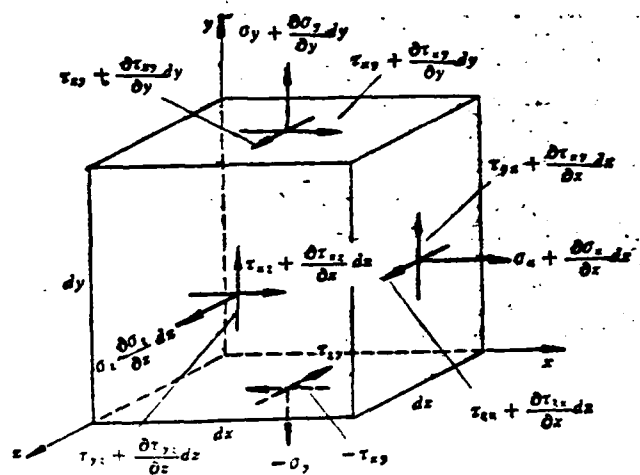
95

Fig. 5.1 micro-globule in the form of a cube, separate and standing away from a viscous flow field.

95a

$$R_x = \frac{\partial \sigma_x}{\partial x} + \frac{\partial \tau_{yx}}{\partial y} + \frac{\partial \tau_{zx}}{\partial z}$$
$$R_y = \frac{\partial \tau_{yx}}{\partial x} + \frac{\partial \sigma_y}{\partial y} + \frac{\partial \tau_{yz}}{\partial z} \Bigg\} \; [N/m^3] \qquad (5.4)$$
$$R_z = \frac{\partial \tau_{zx}}{\partial x} + \frac{\partial \tau_{zy}}{\partial y} + \frac{\partial \sigma_z}{\partial z}$$

$$\mathbf{R} = iR_x + jR_y + kR_z; \qquad (5.5)$$

i, j, and k are unit vectors.

Suppose that the cube-shaped liquid micro-mass in Fig 5.1 is an elastic body and is under static; if this is true, then, the total moment of force around any coordinate axis—x, y, or z— is equal to zero. For example, the moment of force around the z axis is equal to zero, and it is possible to obtain

$$\tau_{yz}\,dy\,dz\,dx = \tau_{zy}\,dx\,dz\,dy, \qquad (5.6)$$

therefore $\tau_{yz} = \tau_{zy}$ (5.7)

According to the same principles, it is possible to obtain

$$\tau_{zx} = \tau_{xz}, \quad \tau_{xy} = \tau_{yx} \qquad (5.8)$$

In this way, the nine forces fall into only six types which determine the three component forces. These three component forces define the total surface forces, **R**, and it is possible to write these in the form of an algebraic matrix; II = the "second order tensor":

$$\mathbf{R} = \nabla \cdot \Pi = \nabla \cdot \left\{ \begin{array}{ccc} \sigma_x & \tau_{xy} & \tau_{xz} \\ \tau_{yx} & \sigma_y & \tau_{yz} \\ \tau_{zx} & \tau_{zy} & \sigma_z \end{array} \right\} \qquad (5.9)$$

Because, in this matrix, the opposite positions in the upper right and lower left correspond to equal magnitudes; therefore, this is called a "symmetrical matrix".

Sec 2   The Relationship Between Surface Tension and the Rate of Deformation

The normal stresses, σ, and the shear forces, τ, cause the liquid micro-mass to deform. According to the conventions of elastic dynamics, the pulling and contracting forces along the normal line of the surface are the "tensile stresses", σ; the compression forces which act against the direction of the normal lines is the "compression force", that is to say, the pressure, -p; therefore, $\sigma = -p$. According to the viscous shear force formula (4.1), if one considers only the shear forces, τ, in the direction, x, then,

$$\tau = \mu(\partial u/\partial y) = \mu \frac{\partial u}{\partial y} [\text{Fig. 5.2 (a)}], \qquad (5.10)$$

Equation (5.10) explains how the shear forces, τ , and the "shear force deformation rate" or "shear force change rate", in a viscous flow, are in direct proportion to each other and that the coefficient of this ratio is the viscosity, μ , (kg/m· s).

When we investigate the projection of the cube-shaped liquid micro-mass on the x-y plane(Fig 5.2 (b) and (c)), we discover that the shear forces, τ, which act on four of the faces pinch and pull the cube out into the shape of a rhombus. The original edge angle, $\pi/2$, reduces the strain angle, $(\tau_1 + \tau_2')$, that is to say that, per second, the "rate of shearing strain" is $\partial\gamma/\partial t = \partial\gamma_1/\partial t + \partial\gamma_2/\partial t$.

• According to equation (5.10), shear forces

$$\tau_{xy} = \tau_{yx} = \tau = \mu\left(\frac{\partial\gamma_1}{\partial t} + \frac{\partial\gamma_2}{\partial t}\right) = \mu\left(\frac{\partial u}{\partial y} + \frac{\partial v}{\partial x}\right),$$

$$(5.11)$$

By the same principle, if one takes a projection of the cube-shaped liquid micro-mass and divides that projection so that it is projected separately onto the planes zy and xz, then, it is possible to obtain

$$\tau_{yz} = \tau_{zy} = \mu\left(\frac{\partial v}{\partial z} + \frac{\partial w}{\partial y}\right) \qquad (5.12)$$

$$\tau_{zx} = \tau_{xz} = \mu\left(\frac{\partial w}{\partial x} + \frac{\partial u}{\partial z}\right). \qquad (5.13)$$
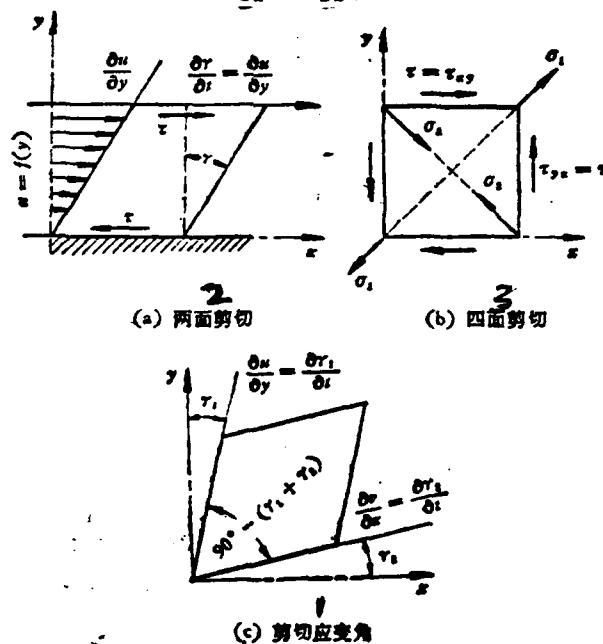

(a) 两面剪切   (b) 四面剪切

(c) 剪切应变角

图 5.2
Fig 5.2

1. Shear Strain Angle 2. Two Plane Shear 3. Four Plane Shear

At the same time that the **quadralateral in Fig 5.2 (b)** is being deformed by shear forces, τ, into the shape of a rhombus, there is produced along a diagonal line a tensile stress, σ_1 and along another diagonal line another tensile stress, σ_2, (Fig 5.3(a)). Within the original square, if one connects the mid-points of the sides, the resulting lines mark out contiguous squares (subdividing lines). This being the case, then, when the original square is changed into the shape of a rhombus, these interior contiguous squares are pushed and pulled into the shape of rectangles.

If one takes the original square and cuts it in half along the diagonal lines (Fig 5.3 (b)), then, according to the equilibrium of forces, it is possible to see that if the force exerted on the slanted side is not tensile stress, σ_1, then, it is certainly compression stress, σ_2. Assume that the length of the sides of the square $= a$, and the depth perpendicular to the surface of the illustration is equal to 1, then, the force equilibrium equations are

$$2a\tau \sin \frac{\pi}{4} - a\sqrt{2}\,\sigma_1 = 0,$$

because

$$\sin \frac{\pi}{4} = \frac{1}{\sqrt{2}}, \ 故 \ \sigma_1 = \tau \qquad (5.14)$$

Concerning the cutting out of triangles along another diagonal line, by the same principles, it is possible to write the force equilibrium equation and prove that $\sigma_2 = -\tau$; due to this fact, $\sigma_1 - \sigma_2 = 2\tau \qquad (5.15)$

Fig 5.3 (c) shows the square, ABCD, changed into the rhombus, A'B'C'D'; the edge angle A is changed from $\pi/2$ to $(\pi/2 - \gamma)$; the diagonal line AC is stretched to the length AC'; the diagonal line BD is shortened to B'D'; moreover, the plane displacement distance, EM' = B B'. It is possible to look at BB' as being a tiny arc length around point A. Because of this fact,

$$BB' = EM' = \overline{AB} \cdot \frac{\gamma}{2} = DD'.$$

EM'M is an isoceles right triangle; therefore,

$$\overline{MM'} = \frac{\overline{EM'}}{\sqrt{2}} = \frac{\overline{AB}}{\sqrt{2}} \cdot \frac{\gamma}{2};$$

Because of the fact that

$$\overline{AM} = \frac{\overline{AC}}{2} = \frac{\overline{AB}\sqrt{2}}{2};$$

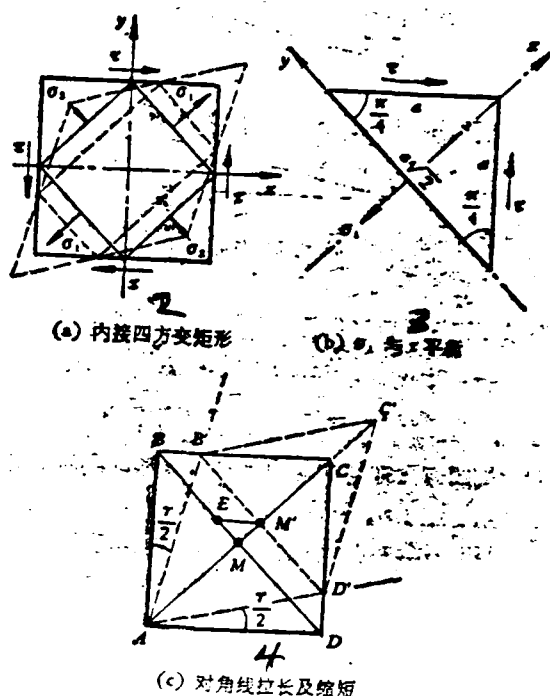therefore, the diagonal line $\overline{AC}$ has a "tensile strain"

(a) 内接四方变矩形　　(b) σ_1 与 x 平行

(c) 对角线拉长及缩短

图 5.3　表面应力 σ, τ 与流体微团变形

Fig 5.3

1. Surface Tensions σ, τ and Deformation of the Liquid Micro-mass 2. Interior Squares Changed to Rectangles 3. σ_1 and τ in Equilibrium 4. Stretching and Shortening of a Diagonal

$$\varepsilon_1 = \frac{\overline{CC'}}{\overline{AC}} = \frac{\overline{MM'}}{\overline{AM}} = \frac{\gamma}{2} \qquad (5.16)$$

By the use of the same principles it is possible to prove that the diagonal $\overline{BD}$ has a "compressive strain" $\varepsilon_2 = -\gamma/2.$ (5.17) ; therefore, the difference between the tensile and compressive strains

$$\varepsilon_1 - \varepsilon_2 = \frac{\gamma}{2} - \left(-\frac{\gamma}{2}\right) = \gamma \qquad (5.18)$$

If one takes the coordinate axis in Fig 5.3 (a) and rotates it $45°$ in a counter-clockwise direction, this causes x and y to respectively converge with the two diagonals of the original square (Fig 5.3 (b); when this happens, $\sigma_1 = \sigma_x, \sigma_2 = \sigma_y$. Going according to equation (5.15), these equalities mean that

$$\sigma_1 - \sigma_2 = \sigma_x - \sigma_y = 2\tau_{xy} = 2\mu \frac{\partial \gamma}{\partial t} = 2\mu \frac{\partial}{\partial t}(\varepsilon_1 - \varepsilon_2)$$

$$(5.19)$$

In all cases, strain on a micro-mass is only present due to fluid motion

$$\epsilon_1 = \frac{u\Delta t}{\Delta x}, \quad \epsilon_2 = \frac{v\Delta t}{\Delta y};$$

therefore,

$$\frac{\partial \epsilon_1}{\partial t} = \frac{\partial u}{\partial x}, \quad \frac{\partial \epsilon_2}{\partial t} = \frac{\partial v}{\partial y}; \qquad (5.19)$$

When these equalities are substituted into equation (5.19), it follows that

$$\sigma_x - \sigma_y = 2\mu\left(\frac{\partial u}{\partial x} - \frac{\partial v}{\partial y}\right),$$

Using the same principles

$$\sigma_x - \sigma_z = 2\mu\left(\frac{\partial u}{\partial x} - \frac{\partial w}{\partial z}\right). \qquad (5.20)$$

The average normal stress on the surface of a liquid micro-mass

$$\sigma = \frac{1}{3}(\sigma_x + \sigma_y + \sigma_z) = -p \quad [N/m^2], \qquad (5.21)$$

If equations (5.20) and (5.21) are added together, then,

$$2\sigma_x - \sigma_y - \sigma_z = 2\mu\left[2\frac{\partial u}{\partial x} - \frac{\partial v}{\partial y} - \frac{\partial w}{\partial z}\right]$$

$$3\sigma_x = (\sigma_x + \sigma_y + \sigma_z) - 2\mu\left[\frac{\partial u}{\partial x} + \frac{\partial v}{\partial y}\right.$$

$$\left. + \frac{\partial w}{\partial z}\right] + 6\mu\frac{\partial u}{\partial x}$$

Making use of equation (5.21)

$$\sigma_x = -p - \frac{2}{3}\mu\left[\frac{\partial u}{\partial x} + \frac{\partial v}{\partial y} + \frac{\partial w}{\partial z}\right] + 2\mu\frac{\partial u}{\partial x} \quad (5.22)$$

By the use of the same principles, it is possible to obtain the following

$$\sigma_y = -p - \frac{2}{3}\mu\left[\frac{\partial u}{\partial x} + \frac{\partial v}{\partial y} + \frac{\partial w}{\partial z}\right] + 2\mu\frac{\partial v}{\partial y} \quad (5.23)$$

$$\sigma_z = -p - \frac{2}{3}\mu\left[\frac{\partial u}{\partial x} + \frac{\partial v}{\partial y} + \frac{\partial w}{\partial z}\right] + 2\mu\frac{\partial w}{\partial z} \quad (5.24)$$

Sec 3 Momentum Equations

Concerning the six equations (5.11) to (5.13) and (5.22) to (5.24), one can take the surface tension tensors in the liquid micro-mass in Fig 5.1, that is to say, the nine stresses in the symmetrical matrix, II, σ_x..., τ_{xy} ... and connect them up with the nine partial flow speed derivatives, $\partial u/\partial x$ ... $\partial u/\partial y$, which come from the stress rate tensor, ∇V. According to the laws of matrices, when the rows

100

and columns of a matrix are interchanged, then, the matrix is called a "transposed matrix." A transposed matrix of a symmetrical matrix is equal to the original matrix. For example, the strain rate matrices that follow

$$\nabla V = \begin{Bmatrix} \dfrac{\partial u}{\partial x} & \dfrac{\partial v}{\partial x} & \dfrac{\partial w}{\partial x} \\ \dfrac{\partial u}{\partial y} & \dfrac{\partial v}{\partial y} & \dfrac{\partial w}{\partial y} \\ \dfrac{\partial u}{\partial z} & \dfrac{\partial v}{\partial z} & \dfrac{\partial w}{\partial z} \end{Bmatrix} \begin{matrix} \text{transposed} \\ \text{matrix} \\ \text{is} \end{matrix} \; V\nabla = \begin{Bmatrix} \dfrac{\partial u}{\partial x} & \dfrac{\partial u}{\partial y} & \dfrac{\partial u}{\partial z} \\ \dfrac{\partial v}{\partial x} & \dfrac{\partial v}{\partial y} & \dfrac{\partial v}{\partial z} \\ \dfrac{\partial w}{\partial x} & \dfrac{\partial w}{\partial y} & \dfrac{\partial w}{\partial z} \end{Bmatrix} \qquad (5.25)$$

By comparing Fig 5.2 (c) and Fig 5.3 (c), one can see that $\gamma_1 = \gamma_2 = \dfrac{\gamma}{2}$,

that is to say,

$$\frac{\partial u}{\partial y} = \frac{\partial v}{\partial x}, \quad \frac{\partial v}{\partial z} = \frac{\partial w}{\partial y}, \quad \frac{\partial w}{\partial x} = \frac{\partial u}{\partial z};$$

Therefore, equation (5.25) is two symmetrical matrices, $\nabla V = V\nabla$ (5.26)

Looking back for a moment to Chapter 4, Sec 4, equations (5.22) to (5.24) contain the "divergence" of speed vectors, V,

$$\nabla V = \left[\frac{\partial u}{\partial x} + \frac{\partial v}{\partial y} + \frac{\partial w}{\partial z} \right] \qquad (5.27)$$

Because of the symmetrical matrix of surface tensions, II, it is possible to write the vector equation

$$\Pi = \mu(\nabla V + V\nabla) - p - \frac{2}{3}\mu\nabla \cdot V \qquad (5.28)$$

According to equations (5.9) and (5.29)

$$R = \nabla \cdot \Pi = \mu\nabla \cdot (\nabla V + V\nabla) - \nabla p$$
$$- \frac{2}{3}\mu\nabla(\nabla \cdot V) \qquad (5.29)$$

Due to the fact that $\mu\nabla \cdot (\nabla V + V\nabla) = \mu\nabla \cdot \nabla V + \mu\nabla\nabla \cdot V$

when one substitutes in the equation above, it, therefore, follows that

$$R = -\nabla p + \frac{1}{3}\mu\nabla(\nabla \cdot V) + \mu\nabla^2 V \qquad (5.30)$$

If we take equation (5.30) and substitute it into the momentum equation from Chapter 4, Sec 5, then one can obtain

$$\rho \frac{dV}{dt} = \rho g + R = \rho g - \nabla p + \frac{1}{3}\mu\nabla(\nabla \cdot V)$$
$$+ \mu\nabla^2 V \quad [N/m^3] \qquad (5.31)$$

If one takes the equations (5.11) to (5.13) and (5.22) to (5.24) and directly sub-

stitutes the stresses from these equations into equation (5.4), then, it is possible
to obtain the three momentum equations that follow:

$$\rho \frac{du}{dt} = \rho g_x - \frac{\partial p}{\partial x} + \frac{\partial}{\partial x}\left[2\mu \frac{\partial u}{\partial x} - \frac{2}{3}\mu\left(\frac{\partial u}{\partial x}\right.\right.$$
$$\left.\left. + \frac{\partial v}{\partial y} + \frac{\partial w}{\partial z}\right)\right] + \frac{\partial}{\partial y}\left[\mu\left(\frac{\partial v}{\partial x} + \frac{\partial u}{\partial y}\right)\right]$$
$$+ \frac{\partial}{\partial z}\left[\mu\left(\frac{\partial w}{\partial x} + \frac{\partial u}{\partial z}\right)\right]$$

$$\rho \frac{dv}{dt} = \rho g_y - \frac{\partial p}{\partial y} + \frac{\partial}{\partial y}\left[2\mu \frac{\partial v}{\partial y} - \frac{2}{3}\mu\left(\frac{\partial u}{\partial x}\right.\right.$$
$$\left.\left. + \frac{\partial v}{\partial y} + \frac{\partial w}{\partial z}\right)\right] + \frac{\partial}{\partial x}\left[\mu\left(\frac{\partial v}{\partial x} + \frac{\partial u}{\partial y}\right)\right]$$
$$+ \frac{\partial}{\partial z}\left[\mu\left(\frac{\partial w}{\partial y} + \frac{\partial v}{\partial z}\right)\right] \qquad\qquad\qquad \Big\} \; (5.32)$$

$$\rho \frac{dw}{dt} = \rho g_z - \frac{\partial p}{\partial z} + \frac{\partial}{\partial z}\left[2\mu \frac{\partial w}{\partial z} - \frac{2}{3}\mu\left(\frac{\partial u}{\partial x}\right.\right.$$
$$\left.\left. + \frac{\partial v}{\partial y} + \frac{\partial w}{\partial z}\right)\right] + \frac{\partial}{\partial x}\left[\mu\left(\frac{\partial w}{\partial x} + \frac{\partial u}{\partial z}\right)\right]$$
$$+ \frac{\partial}{\partial y}\left[\mu\left(\frac{\partial w}{\partial y} + \frac{\partial v}{\partial z}\right)\right]$$

The equations above are a set of momentum equations which pertain to a viscous, com-
pressible flow field in an orthogonal coordinate system; in fluid dynamics, this is
called a set of n-dimensional equations. All these equations have in them a factor
$-2/3\,\mu = \mu'$; this is called secondary viscosity or "volume viscosity."

The perfect differential of this

$$\frac{d}{dt} = \frac{\partial}{\partial t} + u \frac{\partial}{\partial x} + v \frac{\partial}{\partial y} + w \frac{\partial}{\partial z}. \qquad (5.33)$$

Sec 4   Potential Energy Equations for Flow Fields

If one looks at Fig 4.1 in Chapter 4, in the control body, V_s, every unit mass
of liquid contains potential energy $E = \left(U + \frac{1}{2}\mathbf{V}\cdot\mathbf{V}\right)$; $U =$ the internal

energy of each unit mass (the chemical energy contained inside it). $\frac{1}{2}\mathbf{V}\cdot\mathbf{V} =$
the kinetic energy for each unit of mass. Besides these quantities, one can also
take ξ to equal how much mass momentum and energy is contained in each cubic meter;
this quantity is also called "generalized density"; when these symbols stand for
the quantities mentioned, the dispersion amount of ξ, which is put out every second
from the control surface, S,

$$-\oint' \xi V \cdot ndS \qquad (5.34)$$

The rate of increase per second of $\dot{\xi}$ within the control body, V_s

$$=\oint^{V_s} \frac{\partial \xi}{\partial t} dV, \qquad (5.35)$$

In the previous chapter this method has already been used to obtain the continuity equations and momentum equations for a three-dimensional flow field. At present, if we take $\xi_1 = E\rho$, then, within the control body, V_s,

the energy transformation rate $= \oint^{V_s} \frac{\partial(\rho E)}{\partial t} dV, + \oint' \rho$

$$\times E(V \cdot n)dS \quad \left[\frac{N \cdot m}{s}\right] \quad (5.36)$$

According to the principle of the conservation of energy, energy cannot just be produced, neither can it be destroyed for any reason; it can only change form. Therefore, the rate of transformation of energy within the control body, V_s, should be equal to the heat energy being added to V_s every second through its surface contact with the environment plus the power absorbed by V_s every second from external forces.

Sec 2 of the previous chapter introduced the idea that the existence of a temperature gradient produces a heat flow, q, (kcal/m²· s). If we assume that $\xi =$ the thermal energy density (kcal/m³), then, $\xi V = q$. If we substitute this into equation (5.34) and plug it into the negative heat calculation, then, the amount of thermal energy that is received through the external surfaces every second $=$

$$-\oint' q \cdot ndS \quad \left[\frac{N \cdot m}{s}\right], \quad (5.37)$$

The transformation of potential energy per second $= \oint^{V_s} \rho g V dV, \quad \left[\frac{N \cdot m}{s}\right] (5.38)$

Fig (5.4) (a) shows the cube-shaped liquid micro-mass $dxdydz = dV_s$ and the normal forces, σ_x, as well as the shear forces, τ_{xy} which act upon it as projected on the x-y plane. Fig 5.4 (b) shows the shear force, τ_{xy}, acting on the mass and causing a displacement deformation rate $(\partial u/\partial y)dy$, in the direction of the shear; this Fig also shows a normal force, σ_x, which gives rise to a linear deformation rate of $(\partial u/\partial x)dx[m/s]$. If we take one cubic meter as the basic unit, then, the total power, W, which is exerted every second against the liquid micro-mass, dV_s, by external forces is equal to the total power of the tensile forces per second:
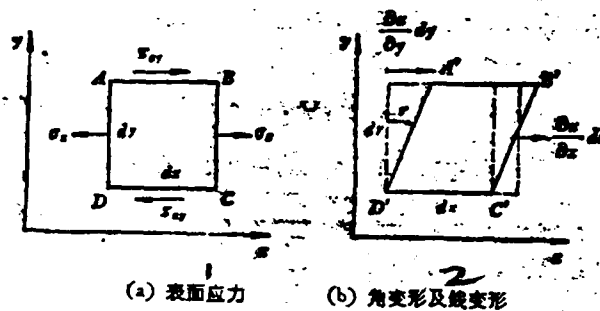
(a) 表面应力   (b) 角变形及线变形

图 5.4

Fig 5.4

1. Surface Tensions 2. Angular Deformation and Linear Deformation

$$W = \sigma_x \frac{\partial u}{\partial x} + \sigma_y \frac{\partial v}{\partial y} + \sigma_z \frac{\partial w}{\partial z} + \tau_{xy} \left(\frac{\partial u}{\partial y} + \frac{\partial v}{\partial x} \right)$$
$$+ \tau_{zx} \left(\frac{\partial w}{\partial x} + \frac{\partial u}{\partial z} \right) + \tau_{yz} \left(\frac{\partial w}{\partial y} + \frac{\partial v}{\partial z} \right) \left[\frac{N \cdot m}{m^3 \cdot s} \right],$$

(5.39)

If we take the stresses from equations (5.11) to (5.13) and (5.22) to (5.24), $\sigma_x \cdots \tau_{xy} \cdots$ and substitute them into equation (5.39), then, it is possible to obtain

$$W = -\nabla \cdot (p\mathbf{V}) + \Phi, \quad \Phi \text{ called "dissipation function"} \quad (5.40)$$

$$\Phi = 2\mu \left[\left(\frac{\partial u}{\partial x} \right)^2 + \left(\frac{\partial v}{\partial y} \right)^2 + \left(\frac{\partial w}{\partial z} \right)^2 \right] - \frac{2}{3} \mu (\nabla \cdot \mathbf{V})^2$$

$$+ \mu \left(\frac{\partial v}{\partial x} + \frac{\partial u}{\partial y} \right)^2 + \mu \left(\frac{\partial w}{\partial x} + \frac{\partial u}{\partial z} \right)^2$$

$$+ \mu \left(\frac{\partial w}{\partial y} + \frac{\partial v}{\partial z} \right)^2 \left[\frac{N \cdot m}{m^3 \cdot s} \right], \quad (5.41)$$

The total power exerted by surface tensions against the control body, $V_s = \oint^{V_s} W \, dV$, (5.42)   Now, according to equation (5.63), one can write out the energy equilibrium equation for the control body, V_s:

$$\oint^{V_s} \frac{\partial (\rho E)}{\partial t} \, dV_s + \oint^{S} (\rho E) \mathbf{V} \cdot \mathbf{n} \, dS$$

$$= -\oint^{S} \mathbf{q} \cdot \mathbf{n} \, dS + \oint^{V_s} \rho g \mathbf{V} \, dV_s + \oint^{V_s} W \, dV_s$$

(5.43)

One ought now to use Gauss's Theorem to transform the double integral along the surface, S, into the triple integral of the control body, V_s,

104

$$\oint' (\rho E)\mathbf{V} \cdot \mathbf{n} dS = \oint^{v'} \nabla \cdot (\rho E)\mathbf{V} dV_{,,} \quad (5.44)$$

$$\oint' \mathbf{q} \cdot \mathbf{n} dS = \oint^{v'} \nabla \cdot \mathbf{q} dV_{,,} \quad \mathbf{q} = -\lambda \nabla T; \quad (5.45)$$

After equations (5.44) and (5.45) are substituted into equation (5.43), then, the integrated functions on the two sides of the equal signs should be equal

$$\frac{\partial(\rho E)}{\partial t} + \nabla \cdot (\rho E)\mathbf{V} = \nabla \cdot (\lambda \nabla T) + \rho g \cdot \mathbf{V}$$

$$- \nabla \cdot (p\mathbf{V}) + \Phi \quad \left[\frac{N \cdot m}{m^3 \cdot s}\right], \quad (5.46)$$

Because of the fact that

$$\frac{\partial}{\partial t}(\rho E) = \rho \frac{\partial E}{\partial t} + E \frac{\partial \rho}{\partial t},$$

$$\nabla \cdot (\rho E)\mathbf{V} = \rho \mathbf{V} \cdot \nabla E + E \mathbf{V} \cdot \nabla \rho + \rho E \nabla \cdot \mathbf{V}$$

By utilizing $E = E(t, x, y, z)$ and $\rho = \rho(t, x, y, z)$ in the form of their perfect differentials, the right side of the equal sign in equation (5.46) can be written as

$$\rho \left(\frac{\partial E}{\partial t} + \mathbf{V} \cdot \nabla E\right) + E\left(\frac{\partial \rho}{\partial t} + \mathbf{V} \cdot \nabla \rho\right) + \rho E \nabla \cdot \mathbf{V}$$

$$= \rho \frac{dE}{dt} + E \frac{d\rho}{dt} + \rho E \nabla \cdot \mathbf{V} = \rho \frac{dE}{dt}$$

$$+ E\left(\frac{d\rho}{dt} + \rho \nabla \cdot \mathbf{V}\right) \quad (5.47)$$

However, in the final analysis, equation (5.47) is nothing but the continuity equation from Chapter 4, Sec 2

$$\left(\frac{d\rho}{dt} + \rho \nabla \cdot \mathbf{V}\right) = 0 \quad (5.48)$$

Therefore, the right side of equation (5.46)

$$\frac{\partial(\rho E)}{\partial t} + \nabla \cdot (\rho E)\mathbf{V} = \rho \frac{dE}{dt}, \quad (5.49)$$

From the definition enthalpy

$$i = U + \frac{p}{\rho}, \quad \frac{di}{dt} = \frac{dU}{dt} + \frac{1}{\rho}\frac{dp}{dt} - \frac{p}{\rho^2}\frac{d\rho}{dt},$$

$$\frac{dU}{dt} = \frac{di}{dt} - \frac{1}{\rho}\frac{dp}{dt} + \frac{p}{\rho^2}\frac{d\rho}{dt} + \left[\frac{p}{\rho^2}(\rho \nabla \cdot \mathbf{V})\right.$$

$$\left. - \frac{p}{\rho^2}(\rho \nabla \cdot \mathbf{V})\right] \quad \text{(Area in curve = no increase or decrease}$$

Still employing the continuity equation (5.48), it is possible to know that

$$\frac{\rho}{\rho^2}\left(\frac{d\rho}{dt} + \rho\overline{\nabla}\cdot\mathbf{V}\right) = 0;$$

Therefore, it is possible to obtain

$$\rho\,\frac{dU}{dt} = \rho\,\frac{di}{dt} - \left(\frac{dp}{dt} + \rho\nabla\cdot\mathbf{V}\right) \quad (5.50)$$

Because

$$E = U + \frac{1}{2}\mathbf{V}\cdot\mathbf{V}, \quad \rho\,\frac{dE}{dt} = \rho\,\frac{dU}{dt} + \rho\,\frac{d}{dt}\left(\frac{1}{2}\mathbf{V}\cdot\mathbf{V}\right)$$

$$(5.51)$$

If one substitutes equation (5.50) into equation (5.51) and then substitutes the new equation into equation (5.46), paying careful attention to the relationship,

$$\nabla\cdot(\rho\mathbf{V}) = \rho\nabla\cdot\mathbf{V} + \mathbf{V}\cdot\nabla\rho \qquad , \text{ then,}$$

$$\rho\,\frac{di}{dt} - \frac{dp}{dt} + \rho\,\frac{d}{dt}\left(\frac{1}{2}\mathbf{V}\cdot\mathbf{V}\right)$$

$$= \nabla\cdot(\lambda\nabla T) + \rho g\mathbf{V} - \mathbf{V}\nabla p + \Phi \qquad (5.52)$$

As far as the relationship, $\mathbf{V}\cdot\mathbf{V} = (iu + jv + kw)\cdot(iu + jv + kw) = u^2 + v^2 + w^2$,

is concerned, by using an orthogonal coordinate system to analyse equation (5.52),
it is possible to obtain the energy equation for a three dimensional, viscous, com-
pressible flow field:

$$\rho\,\frac{di}{dt} - \frac{dp}{dt} + \frac{\rho}{2}\,\frac{d}{dt}(u^2 + v^2 + w^2)$$

$$= \left[\frac{\partial}{\partial x}\left(\lambda\,\frac{\partial T}{\partial x}\right) + \frac{\partial}{\partial y}\left(\lambda\,\frac{\partial T}{\partial y}\right) + \frac{\partial}{\partial z}\left(\lambda\,\frac{\partial T}{\partial z}\right)\right]$$

$$+ \rho(ug_x + vg_y + wg_z) - \left(u\,\frac{\partial p}{\partial x}\right.$$

$$\left. + v\,\frac{\partial p}{\partial y} + w\,\frac{\partial p}{\partial z}\right) + \Phi \qquad (5.53)$$

Φ in the equation above is the dissipation constant (equation (5.41)), that is
to say, it is the power dissipated by friction in each square meter of liquid,

$$\left[\frac{N\cdot m}{m^3\cdot s}\right].$$

Sec 5 Coordinate Transformation (Converted from Amount of Alteration)

Why do we use vectors and tensors? There are three reasons:

(1) Conciseness of Form. Complex functions, equations, and so on, need only

106

one equation or formula in which they can all be summarized.

(2) Ease of calculation. It is possible with vectors and tensors to employ vector algebra, vector differentiation and matrix calculations.

(3) Coordinate flexibility. Vectors and tensors can, according to requirements, be transposed into: orthagonal coordinates, cylindrical coordinates, spherical coordinates or other curvilinear coordinate systems in order to deal appropriately with actual structures and flow fields. The large majority of combustion chamber structures are appropriate for cylindrical coordinate systems or axisymmetric flow fields. This section introduces the method for taking orthagonal coordinates x, y, z and transforming them into cylindrical coordinates r, θ, z.
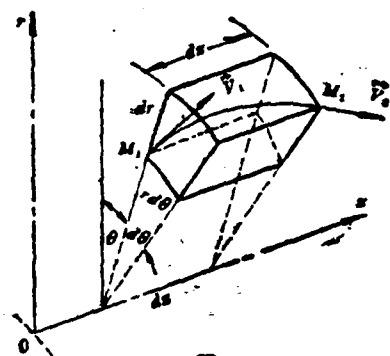
(a) r, θ, z cylindrical coordinate system

(b) r, θ plane

图5.5 r, θ, z 柱坐标系及 r, θ 横削面上投影
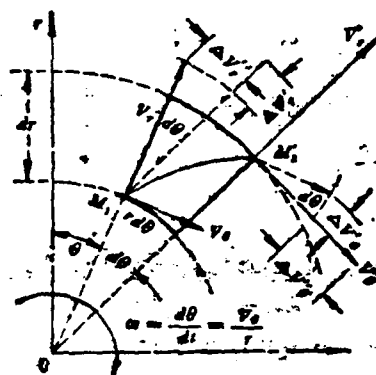
Fig 5.5

1. r, θ, z Cylindrical Coordinate System and a Cross Section Projection in the Plane r, θ

Fig (5.5) (a) shows a fan-shaped control body $dV_s = drrd\theta dz$ generated at an isolated interval in a cylindrical coordinate system r, θ, z in a three- dimensional flow field. This can also represent the control body for a ring shaped com-

107

bustion chamber or an analogous fan-shaped section from a test flow field. Imagine that there are flow lines passing through Fig (5.5) (a) at the points M_1 and M_2 where the edge angle meets the slope of the fan-shaped control body, dV_s. Because of the fact that the coordinate positions of M_1 and M_2 are not the same, the magnitude and directions of the speed vectors V_2 and V_1 are also not the same. Therefore, even if one is dealing with a stable flow field so that $\dfrac{\partial V}{\partial t} = 0$, the local velocities at various points do not change; when the liquid micro-mass, in an interval of time, Δt, flows from M_1 to M_2, it is also possible to have "shift acceleration" $(V \cdot \nabla) V$.

If one defines the unit vectors for the radius, r, the circumference, $r\theta$, and the axis z as e_r, e_θ, e_x, then, according to Chapter 4, Sec 3, we get

$$\left.\begin{array}{l} \cos 0° = 1, \quad e_r \cdot e_r = e_\theta \cdot e_\theta = e_z \cdot e_z = 1 \\ \qquad \text{dot product of parallel vectors} \\[6pt] \cos 90° = 0, \quad e_r \cdot e_\theta = e_\theta \cdot e_z = e_z \cdot e_r = 0 \\ \qquad \text{dot product of perpendicular vectors} \\[6pt] \sin 0° = 0, \quad e_r \times e_r = e_\theta \times e_\theta = e_z \times e_z = 0 \\ \qquad \text{cross product of parallel vectors} \\[6pt] \sin 90° = 1, \quad e_r \times e_\theta = e_\theta \times e_z = e_z \times e_r = 1 \\ \qquad \text{cross product of perpendicular vectors} \end{array}\right\} \quad (5.54)$$

Therefore, the speed vectors in a cylindrical coordinate system

$$V = e_r V_r + e_\theta V_\theta + e_z V_z \qquad (5.55)$$

The acceleration vector

$$a = e_r a_r + e_\theta a_\theta + e_z a_z = \frac{\partial V}{\partial t} + (V \cdot \nabla) V \quad (5.56)$$

Because the horizontal cross section, r, θ, is perpendicular to the z axis, changes in V_θ and V_r do not influence V_x. Therefore, it is possible to take the fan-shaped, six-sided body and project it onto the cross section r, θ, for purposes of analysing the "shift acceleration" $(V \cdot \nabla) V$ from point M_1 to point M_2' (Fig 5.5 (b)).

Take the radial speed distribution of point M_2', V'_r, and move it smoothly to point M_1; then, make a comparison of the magnitude and direction of this vector and V_r. It can be seen that the transition from V_r to V'_r can be divided into two steps:

First, there is a change in direction $d\theta$ with no accompanying change in magnitude; there is an increase in velocity $\Delta V''_r \approx V_\theta d\theta$.

Later, the magnitude of the vector involved does change, and the direction does not change; there is also an increase in speed, $\Delta V'_r$, in this step.

Using the same idea, take the circumferential flow speed distribution, V_θ, for the point M_1 and move it evenly to point M'_2; at this point, compare it with V'_θ in magnitude and direction. If one does this it can be seen that the process of change from V_θ to V'_θ can also be divided into two steps:

First, the direction of $d\theta$ changes without a corresponding change in magnitude; in this step there is also an increase in velocity $-\Delta V'_\theta \approx V_\theta d\theta$.

Later, there is a change in magnitude with no corresponding change in direction; in this step, too, there is an increase in velocity, $\Delta V''_\theta$.

As in (5.5), one can see that the directions of $\Delta V''_r$ and $\Delta V''_\theta$ are the same; both follow the direction of the shear line; however, the radial directions, r, of $\Delta V''_r$ and $\Delta V'_\theta$ are opposite to each other. When M'_2 tends toward the point M_1, and $\Delta t \to 0$, then, it is possible to solve for the extreme limit and obtain the radial direction of acceleration for point M_1

$$a_r = \lim_{\Delta t \to 0} \left[\frac{\Delta V'_r}{\Delta t} - \frac{\Delta V'_\theta}{\Delta t} \right] = \frac{dV_r}{dt} - V_\theta \frac{d\theta}{dt}$$

$$= \frac{dV_r}{dt} - \frac{V_\theta^2}{r}, \qquad (5.57)$$

When one solves for the extreme limit and obtains the circumferential direction of acceleration at a point M_1

$$a_\theta = \lim_{\Delta t \to 0} \left[\frac{\Delta V''_r}{\Delta t} + \frac{\Delta V''_\theta}{\Delta t} \right] = V_r \frac{d\theta}{dt}$$

$$+ \frac{dV_\theta}{dt} = \frac{V_r V_\theta}{r} + \frac{dV_\theta}{dt}, \qquad (5.58)$$

When one solves for the extreme limit and obtains the axial direction of acceleration for the point M_1

$$a_z = \frac{dV_z}{dt}; \qquad (5.59)$$

The three component vectors of velocity are all functions of coordinate and time; if one respectively solves for the perfect differentials, that is to say,

$$V_r = V_r(r, \theta, z, t), \quad \frac{dV_r}{dt} = \frac{\partial V_r}{\partial t} + V_r \frac{\partial V_r}{\partial r}$$

$$+ V_\theta \frac{\partial V_r}{r\partial \theta} + V_z \frac{\partial V_r}{\partial z}, \qquad (5.60)$$

$$V_\theta = V_\theta(r, \theta, z, t), \quad \frac{dV_\theta}{dt} = \frac{\partial V_\theta}{\partial t} + V_r \frac{\partial V_\theta}{\partial r}$$

$$+ V_\theta \frac{\partial V_\theta}{r\partial \theta} + V_z \frac{\partial V_\theta}{\partial z}, \qquad (5.61)$$

$$V_z = V_z(r, \theta, z, t), \quad \frac{dV_z}{dt} = \frac{\partial V_z}{\partial t} + V_r \frac{\partial V_z}{\partial r} \qquad (5.62)$$

$$+ V_\theta \frac{\partial V_z}{r \partial \theta} + V_z \frac{\partial V_z}{\partial z};$$

If one takes equations (5.60) to (5.62) and substitutes them respectively into equations (5.57) to (5.59), then, it is possible to obtain the three directions of acceleration:

Radial Direction

$$a_r = \frac{\partial V_r}{\partial t} + V_r \frac{\partial V_r}{\partial r} + V_\theta \frac{\partial V_r}{r \partial \theta} \qquad (5.63)$$

$$+ V_z \frac{\partial V_r}{\partial z} - \frac{V_\theta^2}{r} \quad [m/s^2]$$

Circumferential Direction

$$a_\theta = \frac{\partial V_\theta}{\partial t} + V_r \frac{\partial V_\theta}{\partial r} + V_\theta \frac{\partial V_\theta}{r \partial \theta} \qquad (5.64)$$

$$+ V_z \frac{\partial V_\theta}{\partial z} + \frac{V_r V_\theta}{r} \quad [m/s^2]$$

Axial Direction

$$a_z = \frac{\partial V_z}{\partial t} + V_r \frac{\partial V_z}{\partial r} + V_\theta \frac{\partial V_z}{r \partial \theta} + V_z \frac{\partial V_z}{\partial z} \quad [m/s^2] \qquad (5.65)$$

The last quantity in equation (5.63) is centripetal acceleration; the last quantity in equation (5.64), $V_r V_\theta / r$, is there because of the fact that there is rotary motion and radial motion going on at the same time, and this produces what is called Ke Shi acceleration.

Looking back on the acceleration vector

$$a = \frac{\partial V}{\partial t} + (V \cdot \nabla)V \quad \text{is only one formula.}$$

The vector differential computational symbol

$$\nabla = i \frac{\partial}{\partial x} + j \frac{\partial}{\partial y} + k \frac{\partial}{\partial z} = e_r \frac{\partial}{\partial r}$$

$$+ e_\theta \frac{\partial}{r \partial \theta} + e_z \frac{\partial}{\partial z}, \qquad (5.66)$$

Equation (5.66) explains the fact that , if one uses a "unit vector", then, it does not make any difference what coordinate system one is dealing with, ∇ is always appropriate to use.

110

The computational symbol for a perfect differential

$$\frac{d}{dt} = \frac{\partial}{\partial t} + (\mathbf{V} \cdot \nabla) = \frac{\partial}{\partial t}$$
$$+ \left(V_r \frac{\partial}{\partial r} + V_\theta \frac{\partial}{r\partial \theta} + V_z \frac{\partial}{\partial z} \right) \quad (5.67)$$

Local acceleration

$$\frac{\partial \mathbf{V}}{\partial t} = \frac{\partial}{\partial t} (e_r V_r + e_\theta V_\theta + e_z V_z) = e_r \frac{\partial V_r}{\partial t}$$
$$+ e_\theta \frac{\partial V_\theta}{\partial t} + e_z \frac{\partial V_z}{\partial t} \quad (5.68)$$

Shift displacement acceleration

$$(\mathbf{V} \cdot \nabla)\mathbf{V} = \left(V_r \frac{\partial}{\partial r} + V_\theta \frac{\partial}{r\partial \theta} + V_z \frac{\partial}{\partial z} \right)$$
$$(e_r V_r + e_\theta V_\theta + e_z V_z) \quad (5.69)$$

According to the analysis in Fig 5.5 (b), e_r and e_θ vary with changes in r and θ. Therefore, when equation (5.69) is expanded, one needs to see $e_r V_r$, $e_\theta V_\theta$ as the product of two functions in order to solve for the perfect differential. After being expanded and set in order in this way, it can be added to equation (5.68), and in this way one can obtain, from equations (5.65) to (5.5), three identical formula for component vectors of acceleration.

If one is dealing with a stable, axially symmetrical flow field in which $\frac{\partial \mathbf{V}}{\partial t} = 0$, then, in all cases where r and z on the meridian plane are the same, the gas flow parameters for the corresponding points are also the same, that is to say that flow speed, $\mathbf{V}$, pressure, p, temperature, T, and so on, also all vary with changes in θ and are merely functions of r and z. all partial differentials of θ

$$\frac{\partial}{r\partial \theta} = 0.$$

If one simplifies the three formulae for acceleration in this stable, axially symmetrical flow field, they become

Radial vector

$$a_r = V_r \frac{\partial V_r}{\partial r} + V_z \frac{\partial V_r}{\partial z} - \frac{V_\theta^2}{r} \quad (5.70)$$

Circumferential vector

$$a_\theta = V_r \frac{\partial V_\theta}{\partial r} + V_z \frac{\partial V_\theta}{\partial z} + \frac{V_r V_\theta}{r} \quad (5.71)$$

Axial vector

$$a_z = V_r \frac{\partial V_z}{\partial r} + V_z \frac{\partial V_z}{\partial z} \quad (5.72)$$

111

If one takes the important equations which were presented in the previous chapter and in this one in terms of an orthagonal coordinate system and transforms them into a cylindrical coordinate system, then,

(1) Gradient

$$\nabla \phi = e_r \frac{\partial \phi}{\partial r} + e_\theta \frac{\partial \phi}{r \partial \theta} + e_z \frac{\partial \phi}{\partial r} \qquad \phi = \text{a function of some value}$$

(5.73)

(2) Divergence

$$\nabla \cdot \mathbf{V} = \frac{1}{r} \frac{\partial (r V_r)}{\partial r} + \frac{1}{r} \frac{\partial V_\theta}{\partial \theta} + \frac{\partial V_z}{\partial z}$$

$$= \frac{\partial V_r}{\partial r} + \frac{V_r}{r} + \frac{1}{r} \frac{\partial V_\theta}{\partial \theta} + \frac{\partial V_z}{\partial z} \qquad (5.74)$$

(3) Vorticity

$$2\omega = \nabla \times \mathbf{V} = e_r \left[\frac{1}{r} \left(\frac{\partial V_z}{\partial \theta} - \frac{\partial r V_\theta}{\partial z} \right) \right]$$

$$+ e_\theta \left[\frac{\partial V_r}{\partial z} - \frac{\partial V_z}{\partial r} \right] + e_z \left[\frac{1}{r} \left(\frac{\partial r V_\theta}{\partial r} - \frac{\partial V_r}{\partial \theta} \right) \right] \quad (5.75)$$

(4) Continuity Equations of Compressible Flow

$$\frac{\partial \rho}{\partial t} + \nabla \cdot (\rho \mathbf{V}) = \frac{\partial \rho}{\partial t} + \frac{1}{r} \frac{\partial (\rho V_r r)}{\partial r}$$

$$+ \frac{1}{r} \frac{\partial (\rho V_\theta)}{\partial \theta} + \frac{\partial (\rho V_z)}{\partial z} = 0 \qquad (5.76)$$

or this can be written

$$\frac{\partial \rho}{\partial t} + \frac{\partial (\rho V_r)}{\partial r} + \frac{(\rho V_r)}{r} + \frac{\partial (\rho V_\theta)}{r \partial \theta} + \frac{\partial (\rho V_z)}{\partial z} = 0$$

(5.76 a)

(5) Employing the accelerations from equations (5.63) to (5.65), one can transfer the three momentum equations of viscous flow (5.53) into a cylindrical coordinate system, and one gets

Radial vector

$$\rho a_r = \rho g_r - \frac{\partial p}{\partial r} + \frac{\partial}{\partial r} \left[\mu \left(2 \frac{\partial V_r}{\partial r} - \frac{2}{3} \nabla \cdot \mathbf{V} \right) \right]$$

$$+ \frac{1}{r} \frac{\partial}{\partial \theta} \left[\mu \left(\frac{1}{r} \frac{\partial V_r}{\partial \theta} + \frac{\partial V_\theta}{\partial r} - \frac{V_\theta}{r} \right) \right]$$

$$+ \frac{\partial}{\partial z} \left[\mu \left(\frac{\partial V_r}{\partial z} + \frac{\partial V_z}{\partial r} \right) \right] + 2 \frac{\mu}{r} \left(\frac{\partial V_r}{\partial r} \right.$$

$$\left. - \frac{1}{r} \frac{\partial V_\theta}{\partial \theta} - \frac{V_r}{r} \right) \text{ [N/m}^3\text{]}, \qquad (5.77)$$

Circumferential vector

112

$$\rho a_\theta = \rho g_\theta - \frac{\partial p}{r\partial \theta} + \frac{1}{r}\left[\mu\left(\frac{2\partial V_\theta}{r\partial \theta} - \frac{2}{3}\nabla\cdot\mathbf{V}\right)\right]$$

$$+ \frac{\partial}{\partial r}\left[\mu\left(\frac{1}{r}\frac{\partial V_r}{\partial \theta} + \frac{\partial V_\theta}{\partial r} - \frac{V_\theta}{r}\right)\right]$$

$$+ \frac{\partial}{\partial z}\left[\mu\left(\frac{\partial V_z}{r\partial \theta} + \frac{\partial V_\theta}{\partial z}\right)\right] + 2\frac{\mu}{r}\left(\frac{2\partial V_r}{r\partial \theta}\right.$$

$$\left. + \frac{\partial V_\theta}{\partial r} - \frac{V_\theta}{r}\right)\,[\text{N/m}^3], \qquad (5.78)$$

Axial vector

$$\rho a_z = \rho g_z - \frac{\partial p}{\partial z} + \frac{\partial}{\partial z}\left[\mu\left(2\frac{\partial V_z}{\partial z} - \frac{2}{3}\nabla\cdot\mathbf{V}\right)\right]$$

$$+ \frac{1}{r}\frac{\partial}{\partial r}\left[\mu r\left(\frac{\partial V_r}{\partial z} + \frac{\partial V_z}{\partial r}\right)\right]$$

$$+ \frac{\partial}{r\partial \theta}\left[\mu\left(\frac{1}{r}\frac{\partial V_z}{\partial \theta} + \frac{\partial V_\theta}{\partial z}\right)\right]\,[\text{N/m}^3].$$

$$(5.79)$$

(6) In considering the dissipation function Φ_c, involved in a transfer to cylindrical coordinates, if one consults equations (5.40) and (5.41):

$$\Phi_c = 2\mu\left[\left(\frac{\partial V_r}{\partial r}\right)^2 + \left(\frac{\partial V_\theta}{r\partial \theta} + \frac{V_r}{r}\right)^2 + \left(\frac{\partial V_z}{\partial z}\right)^2\right]$$

$$+ \mu\left(\frac{\partial V_z}{r\partial \theta} + \frac{\partial V_\theta}{\partial z}\right)^2 + \mu\left(\frac{\partial V_r}{\partial z} + \frac{\partial V_z}{\partial r}\right)^2$$

$$+ \mu\left(\frac{\partial V_r}{r\partial \theta} + \frac{\partial V_\theta}{\partial r} - \frac{V_\theta}{r}\right)^2\left[\frac{\text{N}\cdot\text{m}}{\text{m}^3\cdot\text{s}}\right]; \quad (5.80)$$

(7) If one takes the energy equation of viscous flow (5.53) and transfers it to cylindrical coordinates, then,

$$\rho\frac{di}{dt} - \frac{dp}{dt} + \frac{\rho}{2}\frac{d}{dt}(V_r^2 + V_\theta^2 + V_z^2)$$

$$= \left[\frac{1}{r}\frac{\partial}{\partial r}\left(r\lambda\frac{\partial T}{\partial r}\right) - \frac{1}{r^2}\frac{\partial}{\partial \theta}\left(\lambda\frac{\partial T}{\partial \theta}\right) - \frac{\partial}{\partial z}\left(\lambda\frac{\partial T}{\partial z}\right)\right]$$

$$+ \rho(V_r g_r + V_\theta g_\theta + V_z g_z) - \left(V_r\frac{\partial p}{\partial r}\right.$$

$$\left. + V_\theta\frac{\partial p}{r\partial \theta} + V_z\frac{\partial p}{\partial z}\right) + \Phi_c. \quad \left[\frac{\text{N}\cdot\text{m}}{\text{m}^3\cdot\text{s}}\right] \quad (5.81)$$

(8) The computational symbol for the second degree derived function of a vector $\Delta = \nabla^2$ (also called LaPlace's symbol) is utilized with cylindrical coordinates with the result that

$$\Delta = \nabla^2 = \frac{\partial^2}{\partial r^2} + \frac{1}{r}\frac{\partial}{\partial r} + \frac{1}{r^2}\frac{\partial^2}{\partial \theta^2} + \frac{\partial^2}{\partial z^2} \quad (5.82)$$

If used in a positional function (numerical field) $\phi = \phi(r, \theta, z)$, then

$$\Delta\phi = \nabla^2\phi = \frac{\partial^2\phi}{\partial r^2} + \frac{1}{r}\frac{\partial\phi}{\partial r} + \frac{1}{r^2}\frac{\partial^2\phi}{\partial \theta^2} + \frac{\partial^2\phi}{\partial z^2} \quad (5.83)$$

If used in a vector field, for example $\mathbf{V} = \mathbf{V}(r, \theta, z) = c_r V_r + c_\theta V_\theta + c_z V_z$, then,

$$\Delta\mathbf{V} = \nabla^2\mathbf{V} = c_r \nabla^2 V_r + c_\theta \nabla^2 V_\theta + c_z \nabla^2 V_z \quad (5.84)$$

By the utilization of coordinate transformations and changes in dependent variables as well as by the use of non-dimensional (dimensionless) variables and other methods of this type, it is occasionally possible to take complex flow fields and the rules governing changes in them and simplify these rules and express them in a concise form. Due to this simplification, it also becomes easier to do mathematical calculations concerning these flow fields. Even though the forms of the equations in such cases are changed from head to tail, these equations still follow such natural principles as the conservation of mass, the conservation of momentum and the conservation of energy.

Chapter 6 Spirals and Eddy Current Apparatus

Sec 1 Spiral Phenomena

Swimmers and boatmen all know enough to stay away from whirlpools; they know that the violent spinning flow at the center of a whirlpool is capable of trammeling up a man or a boat and pulling it under. Consider the whirlwind that scours the surface of the land and grabs up dust and leaves and takes them up into its center. On the sea, the water spout of a typhoon is a similar phenomenon. There are examples all over the world: these whirlpools descend from the surface of the water, formed into a vortex of polluted waters. The closer one goes to the center of the vortex, the faster does the water flow revolve. Finally, at the very mouth of the vortex, where the water descends, there is only a hollow center and no water at all, and this center makes noises as it sucks in air as water flows into it.

Cyclonic furnaces and centrifugal dust eliminators all have within them vortical air flows. Centrifugal jet nozzles all supply fuel in the direction of the hole, and in the combustion chamber, this fuel sets up in a vortex and is sprayed out in the form of a hollow cone of spray. Turbine jet 6, turbine jet 7, the exhaust of eddy current devices in these tubes, the intake gases which pass over the vanes in the combustion chamber of a turbine jet 11 —all of these have similar vortical flow fields. This type of vortex is dependent on changes in the potential energy within the fluid (differences in static pressure or differentials of water level) for its operation; because of this it is called a " potential flow vortex." The rotation of potential flow vortices, moreover, is not caused by torque applied from outside. If one ignores losses due to friction, then, for different radii, the moments of momenta of micromasses of liquid should be conserved; therefore, this situation is also called a "free vortex or spiral." The special characteristic of "free vortices" is that "although flow lines are concentric rings, the individual micro-masses of liquid do not in themselves have any rotational movement to them." It is possible, within the round trough of water involved in the production of a "potential or positional flow field vortex", to place a small wooden stopper far from the center of the vortex and to draw a diameter line across the stopper. The floating of the soft wooden stopper along the circumference represents the movement of micro-masses of liquid; however, the direction of the diameter line does not change, that is to say, the soft wooden stopper possesses the general rotation around the center of the vortex, but it does not have a rotation of its own around its own central axis; this is called "avortical" circumferential motion.

If one draws two concentric circles to represent two flow lines of a "free vortex", then, let their separation interval = dr. Choose a micro-mass of liquid ABCD in the midst of the flow around the circumference of the vortex and located between the two flow lines we mentioned earlier (Fig 6.1 (a)). On the radius, r, the shear line velocity = V_θ; on the radius, (r + dr), the shear line velocity is

$$V_\theta + dV_\theta = V_\theta + \frac{\partial V_\theta}{\partial r} dr.$$

Assume a dimension, z = 1, perpendicular to the surface of the figure; if one does this, then, the volume of the micro-mass of liquid = $rd\theta dr$, the mass $m = \rho r d\theta dr$, and the moment of momentum = $mV_\theta r$. Externally added torque, T, is equal to the rate of change over time of the moment of momentum of the micro-mass of liquid or zero. Free vortices most certainly have no externally added torque, T; therefore, if one ignores losses from friction, then,

$$T = m \frac{d}{dt}(V_\theta r) = 0, \text{ or } V_\theta r = \text{a constant K} \qquad (6.1)$$

The circumferential velocity of a free vortex (the shear line or tangential velocity) V_θ forms an inverse proportion with the radius, r, that is to say, the nearer one comes to the center of the vortex, the faster does the circumferential velocity. In the center of the vortex, at a place where r = 0, V_θ should tend toward infinity; this does not correspond to reality. Therefore, equation (6.1) is inappropriate for use under conditions in which r = 0 (See Sec 6 of this chapter).
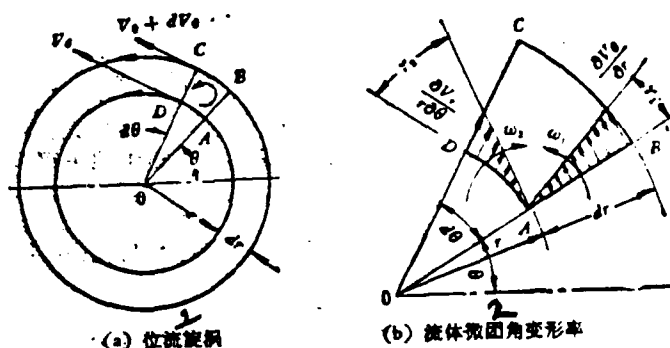

(a) 位流旋涡   (b) 流体微团角变形率

Fig 6.1

1. Positional Flow Vortex   2. Rate of Angular Deformation of Micro-mass of Liquid

According to the definition of a flow line (Chap 4, Sec 8), there is no flow

movement in a direction perpendicular to that of a flow line, that is to say that $V_r = 0$. If one is using a cylindrical coordinate system in r, θ, z, then, the z axis is perpendicular to the surface of the figure, and it is possible, according to the method in Chapter 4, Sec 6, to solve for the circulation, dT, of the differentiated volume ABCD. Because $V_r = 0$,

$$d\Gamma = \left(V_\theta + \frac{\partial V_\theta}{\partial r} dr\right)(r + dr)d\theta - V_\theta r d\theta$$

$$= V_\theta r d\theta + V_\theta dr d\theta + \frac{\partial V_\theta}{\partial r} r dr d\theta +$$

$$\frac{\partial V_\theta}{\partial r} + dr dr d\theta - V_\theta r d\theta = \left(\frac{V_\theta}{r} + \frac{\partial V_\theta}{\partial r}\right) r dr d\theta.$$

ignoring the 3rd degree   amount $\frac{\partial V_\theta}{\partial r} dr dr d\theta$)   (6.2)

From equation (6.1)

$$\frac{V_\theta}{r} = \frac{K}{r^2}, \quad \frac{\partial V_\theta}{\partial r} = -\frac{K}{r^2};$$; if one substitutes this into equation

(6.2), then, it is possible to obtain the circulation for ABCD

$$d\Gamma = \left(\frac{V_\theta}{r} + \frac{\partial V_\theta}{\partial r}\right) r dr d\theta$$

$$= \left(\frac{K}{r^2} - \frac{K}{r^2}\right) r dr d\theta = 0$$

The vorticity around the z axis, $2\omega_z$ = the circulation on each unit of area

$$\frac{d\Gamma}{r d\theta dr} = 0, \text{ therefore } \omega_z = 0. \quad (6.3)$$

Therefore, in the flow field of a free vortex, it is only necessary that the field not contain a center value of zero, and then, the circualtion of the circumferential boundary line for any given differentiated area, $d\Gamma = 0$, or the angular velocity of autorotation $\omega_z = 0$, that is to say that the micro-mass of liquid ABCD has an avertical circumferential motion to it. However, if one looks at the situation of a flow field which includes a vortical center value of 0, then, the radius is r and the circulation on the circumference (also called vortical strength) is

$$\Gamma = \int_0^{2\pi} V_\theta r d\theta = K \int_0^{2\pi} d\theta = 2\pi K = \text{constant} \neq 0 \quad \{m^2/s\} \quad (6.4)$$

Equation (6.4) explains the fact that in flow fields which include vortical centers with values other that zero, for any radius, r, the circulation on the circumference or "vortical strength", Γ, will always be equal. Therefore, the flow fields of

free vortices are also called "equal circulation" or "equal vortical strength" flow fields.

Looking at Fig 6.1 (b): the angular velocity around point A on side AB or the micro-mass of liquid is

$$\omega_1 = \frac{\partial V_\theta}{\partial r} = \frac{\partial \gamma_1}{\partial t},$$

The angular velocity around point A on side AD of the micro-mass of liquid is

$$\omega_2 = \frac{\partial V_r}{r\partial\theta} = \frac{\partial \gamma_2}{\partial t};$$

The average angular velocity around point A is

$$\omega_z = \frac{1}{2}(\omega_1 - \omega_2) = \frac{1}{2r}\left[\frac{\partial r V_\theta}{\partial r} - \frac{\partial V_r}{\partial\theta}\right] \qquad (6.5)$$

which equals the average rate of angular deformation.

If one remembers the formula curl $V = \nabla \times V$ which was found in Chapter 5, Sec 5 and describes the vorticity of a three-dimensional flow field in a cylindrical coordinate system, $V = c_r V_r + c_\theta V_\theta + c_z V_z$, expands into $2\omega = \nabla \times V$:

$$\nabla \times V = \begin{vmatrix} c_r & c_\theta & c_z \\ \frac{\partial}{\partial r} & \frac{\partial}{r\partial\theta} & \frac{\partial}{\partial z} \\ V_r & V_\theta & V_z \end{vmatrix} = \frac{c_r}{r}\left[\frac{\partial V_z}{\partial\theta} - \frac{\partial r V_\theta}{\partial z}\right]$$

or $\omega = c_r\omega_r + c_\theta\omega_\theta + c_z\omega_z$, therefore

$$+ c_\theta\left[\frac{\partial V_r}{\partial z} - \frac{\partial V_z}{\partial r}\right] + \frac{c_z}{r}\left[\frac{\partial_r V_\theta}{\partial r} - \frac{\partial V_r}{\partial\theta}\right] = 2\omega, \qquad \omega_z = \frac{1}{2r}\left[\frac{\partial r V_\theta}{\partial r} - \frac{\partial V_r}{\partial\theta}\right] \quad (6.6)$$

In a two-dimensional positional flow vortex, V_r and V_θ do not vary with changes in z; therefore, all partial derivatives of z are equal to zero. Besides this, $V_z = 0$; therefore, ω_r and ω_θ are both equal to zero. If one is dealing with an avortical potential flow $2\omega' = 0$, then, it is necessary that $2\omega_z = 0$. Equations (6.5) and (6.6) explain the fact that what are called "free vortices" should conform to the condition that the average angular velocity of double the micro-mass of liquid ABCD as well as its vorticity = 0, that is to say that

$$2\omega_z = 0, \left|\frac{\partial(rV_\theta)}{\partial r} - \frac{\partial V_r}{\partial\theta}\right| = 0, \text{ Fig 6.1 (a) of } V_r = 0,$$

$$\text{therefore } \frac{\partial(rV_\theta)}{\partial r} = 0, \text{ or } (rV_\theta) = K \qquad (6.7)$$

The method of analysis of equation (6.7) is different; however, its significance is the same as that of equation (6.1).

Fig 6.2 shows a balanced stable flow state of a micro-mass of liquid, ABCD, between two flow lines, BC and AD, in a two-dimensional free vortex flow field. From equations (6.3) and (6.2), it is possible to obtain the vorticity

$$2\omega_z = \frac{d\Gamma}{rd\theta dr} = \left(\frac{V_\theta}{r} + \frac{\partial V_\theta}{\partial r}\right)' \qquad (6.8)$$
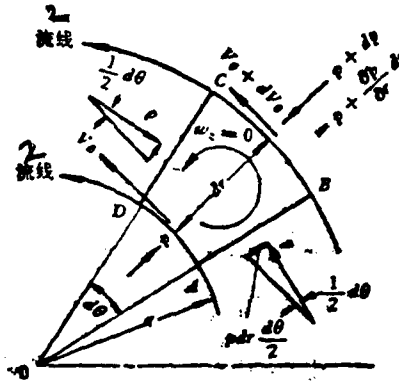
图6.2 液体微团径向平衡

Fig 6.2

1. Radial Equilibrium of Micro-mass of Liquid   2.   Flow Line

The fan-shaped area of the micro-mass of liquid $= rd\theta\, dr$;   the mass, $m = \rho rd\theta\, dr$; the centripetal velocity $= V_\theta /r$, and, ignoring friction and gravity, the only other force involved is surface pressure. We can write out the equilibrium equation of force along a radial direction

$$\left(p + \frac{\partial p}{\partial r}dr\right)(r + dr)d\theta - prd\theta$$

$$- 2\left(pdr\frac{d\theta}{2}\right) = prd\theta dr\frac{V_h^2}{r},$$

After doing some manipulations, and, ignoring the third degree trace quantity

$$\left(\frac{\partial p}{\partial r}drdrd\theta\right)$$

then, we get the relationship $\qquad\qquad \dfrac{\partial p}{\partial r} = \dfrac{\rho V_h^2}{r} \qquad (6.9)$

therefore, if we substitute the equation

119

$$\frac{V_\theta}{r} - \frac{1}{\rho V_\theta}\frac{\partial p}{\partial r}$$

into equation (6.8), then, we can obtain

$$2\omega_z = \frac{1}{\rho V_\theta}\frac{\partial p}{\partial r} + \frac{\partial V_\theta}{\partial r} \qquad (6.10)$$

The total enthalpy along the flow line, $i^* = i + \frac{V_\theta^2}{2}$, has a differential of radius, r,

$$\frac{\partial i^*}{\partial r} = \frac{\partial i}{\partial r} + V_\theta\frac{\partial V_\theta}{\partial r};$$

Besides this, from the differentiated form of the First Law of Thermodynamics, ds = the differentiated increment of heat content

$$Tds = di - \frac{1}{\rho}dp, \text{ or } \frac{\partial i}{\partial r} = T\frac{\partial s}{\partial r}$$
$$+ \frac{1}{\rho}\frac{\partial p}{\partial r} = \frac{\partial i^*}{\partial r} - V_\theta\frac{\partial V_\theta}{\partial r},$$

Due to this fact,

$$\frac{\partial p}{\partial r} = \rho\frac{\partial i^*}{\partial r} - \rho T\frac{\partial s}{\partial r} - \rho V_\theta\frac{\partial V_\theta}{\partial r}, \qquad (6.11)$$

If one takes equation (6.11) and substitutes it into equation (6.10), then, after certain manipulations, it is possible to obtain the vorticity

$$2\omega_z = \frac{1}{V_\theta}\left(\frac{\partial i^*}{\partial r} - T\frac{\partial s}{\partial r}\right) \text{ (Crocco theory (6.12)}$$

From equation (6.12) it can be seen that it is necessary for the total enthalpy i^* and heat content, s, across different flow lines to be equal, and for the total enthalpic gradient $(\partial i^*/\partial r)$ and the heat content gradient $(\partial s/\partial r)$ to be equal to zero, that is to say, an "insulated energy unithermal" flow field, before one can consider this to be an adiabatic potential flow free vortex in which $\omega_z = 0$. This is the equivalent of an ideal condition in which there are no losses due to viscous friction, no heat increment and no heat transfer or differential of total enthalpy. Obviously, if there is heat transfer present or combustion or if there is viscous friction in the boundary layers, then, this does not satisfy the conditions for a free vortex. However, free vortices can act as a standard against which it is possible to measure actual vortices. Free vortices and other flow fields, when added together, can simulate the situation which exists during air flow tests of combustion chambers without ignition.

120

Sec 4   Circumference Spirals

At the center of all vortices or whirlwinds, there is a vortex core with a radius $= R_1$; the rotation of liquid within this vortex core around the center O depends on the rotation of the liquid in individual cases, that is to say, $V_\theta = r\omega$. . This vortical core is also called "forced spiral". The external surroundings of a "forced spiral" is a free vortex or spiral. Concerning the circumferential flow speed of a free spiral, $V_\theta = \frac{K}{r}$, it is possible to say that this speed is one which is induced by the vortical core. On the circumferential edge of the vortical core, R_1, the tangential flow speed, V_m, reaches maximum values, that is to say,

$$V_m = R_1\omega = \frac{K}{R_1}$$

(Referring to Fig 6.3 (a)) The distribution tangential flow speeds, $V_\theta = f(r)$, from the center of the vortex, cut along the radius, r, is as shown in Fig (6.3) (b); the static pressure distribution, $p = f(r)$ is as shown in Fig (6.3) (c); the static temperature distribution $T = f(r)$ is as shown in Fig (6.3) (d). As far as two-dimensional axisymmetrical vortical flow fields are concerned, one need only be concerned with changes in tangential velocity, V_θ, along r; therefore, it is not necessary to use partial differentiation, and equation (6.9) can be written in the form of the ordinary differential equation

$$\frac{dp}{dr} = \rho\frac{V_\theta^2}{r}, \quad dp = \rho\frac{V_\theta^2}{r}dr \quad (6.13)$$

If one assumes $r \geqslant R_1$, then, from the static pressure in the surroundings of a free vortex or spiral $= p_0$, and the static

图6.3 圆周旋涡的 V_θ, p 及 T 沿 r 分布

Fig 6.3
1. Distributions of V_θ p and T along r for a Circumferential Vortex

131

temperature in the same situation $= T_0$; if one substitutes these quantities into the integral equation (6.13) for a certain radius $r \geqslant R_1$ to R_0, then, it is possible to obtain

$$p = p_0 - \int_r^{R_0} \rho \frac{V_\theta^2}{r} dr \qquad (6.14)$$

If one ignores compressibility, makes $\rho = $ a constant, and employs the formula for equal circulation (vortical strength (6.4) $\Gamma = 2\pi r V_\theta$, then

$$\rho \int_r^{R_0} \frac{V_\theta^2}{r} dr = \frac{\rho \Gamma^2}{4\pi^2} \int_r^{R_0} \frac{dr}{r^3} = \frac{\rho \Gamma^2}{8\pi^2 r^2} = \rho \frac{V_\theta^2}{2};$$

therefore,

$$p = p_0 - \rho \frac{V_\theta^2}{2} \qquad (6.15)$$

The static pressure on the boundary of the vortical core, R_1, is

$$p_1 = p_0 - \frac{\rho \Gamma^2}{8\pi^2 R_1^2} = p_0 - \rho \frac{V_m^2}{2} \qquad (6.16)$$

Within the vortical core, because

$$\Gamma = 2\pi K = 2\pi R_1 V_m = 2\pi R_1^2 \omega,$$
$$V_\theta = r\omega = \frac{r\Gamma}{2\pi R_1^2};$$

therefore,

$$\rho \int_r^{R_1} \frac{V_\theta^2}{r} dr = \frac{\rho \Gamma^2}{4\pi^2 R_1^4} \int_r^{R_1} r \, dr = \frac{\rho \Gamma^2 (R_1^2 - r^2)}{8\pi^2 R_1^4},$$

The static pressure within the vortical core

$$p = p_1 - \rho \int_r^{R_1} \frac{V_\theta^2}{r} dr = p_0 - \frac{\rho \Gamma^2 (2R_1^2 - r^2)}{8\pi^2 R_1^4} \quad (6.17)$$

At a place in the heart of the vortex, where $r = 0$, the static pressure is

$$p_c = p_0 - \frac{\rho \Gamma^2}{4\pi^2 R_1^2}, \text{ or } p_0 - p_c = 2(p_0 - p_1) \quad (6.18)$$

Equation (6.17) explains the fact that, within the core of the vortex, if one takes p to be the vertical coordinate and r to be the horizontal coordinate, then, the distribution of the differential of static pressure ($p_0 - p$) is the solid swept out by the parabolic line which passes through the center of the vortex and is axially symmetrical with relation to the z axis. This "low pressure trough" is the cause for the eye of a whirlwind and the collection of dust and the sucking noise caused by air being drawn down into a whirlpool, all of which phenomena we have mentioned before.

The eddy current devices which are installed in the forward section of flame tubes are installed there in order to produce precisely this kind of "low pressure trough" in order to suck in the surrounding gases and the gases down stream and make them flow upstream in order to set up a stable ignition source.

Sec 5   Circular Eddies at the Mouth of Eddy Current Apparatus (Dry Run Without Combustion)

Eddy current devices have vortical flow tubes on them which force the intake gases to become a ring-type vortical jet which shoots into the flame tubes. The tangential flow speeds of these vortical jets, when rotating at high speeds in the plane of a horizontal cross section, form circular vorticies similar to those mentioned in a previous chapter. The "low pressure trough" of these vortices or spirals induces the surrounding gases to flow upstream (a part of the axial flow of vortical jets) and form vortices as shown in Fig 6.4 (a). It is possible to imagine these round vortices as being a closed string of vortices which form round rings from a string of the vortical cores from a limitless number of circular vortices. If we postulate that we already know that the radius of the vortices $= r_o$, then, the circulation of the circular vortex $-\Gamma$. If we also postulate that the axis of symmetry, x, of the vortices meets the direction of the surrounding incoming air in such a way as to have a positive sign, then, we can see the situation portrayed in Fig 6.5 (b). In this instance, we can employ both x, r, θ and x, y, z coordinate systems. From a given point on the circular vortex, P', to another point in the vicinity, P, there is a coordinate vector $\mathbf{R} = i x + j y + k z$; the length of this vector is R. The differentiated arc length at point P', $ds = r_c d\theta$; this corresponds to a differentiated length of a tangent to point P', ds. Therefore, the unit vector of the tangent is $(d\mathbf{s}/ds) = 0i + \cos\theta' j - \sin\theta' k.$. If one takes $\mathbf{R}$ and uses a cylindrical coordinate system to display it, then,

$$\mathbf{R} = i x + j(r \sin\theta - r_o \sin\theta') + k(r\cos\theta - r_o\cos\theta') \tag{6.19}$$

$$R = [x^2 + r^2 + r_o^2 - 2 r r_o \cos(\theta - \theta')]^{\frac{1}{2}} \tag{6.20}$$

$$\mathbf{R} \times \frac{d\mathbf{s}}{ds} = -i [r\cos(\theta - \theta') - r_o]$$
$$+ j x \sin\theta' + k x \cos\theta' \tag{6.21}$$

If we use the Biot-Savart theorem from electrodynamics, then, it is possible to obtain the differentiated arc of the vortex, ds, and the differentiated flow speed vector induced by it at point P $\quad d\mathbf{V} = \frac{\Gamma}{4\pi} \frac{\mathbf{R} \times d\mathbf{s}}{R^3}, (m/s) \tag{6.22}$
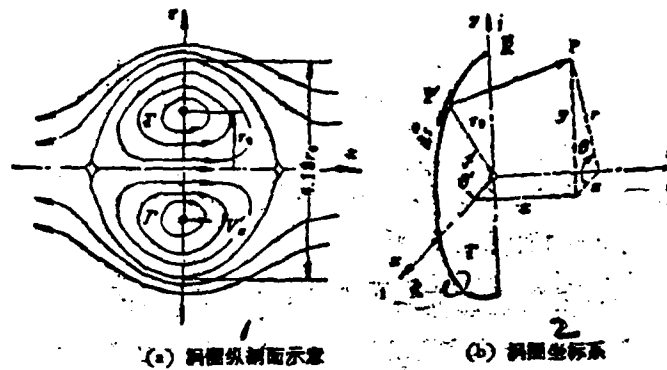
(a) 涡管纵剖面示意   (b) 涡管坐标系
图6.4

Fig 6.4

1. Display of Vertical Cross Section of Vortex   2. Vortex Coordinate System

We can then use the non-dimensional coordinates $\bar{x} = (x/r_0), \bar{r} = (r/r_0)$.
Assuming we use this, concerning the entire vortex $2\pi r_0$, the partial axial velocity,
V_z, which is induced at point P, can be obtained using the circular integration
equation (6.22)

$$V_z = -\frac{\Gamma}{4\pi r_0} \int_0^{2\pi} \frac{\bar{r}\cos(\theta - \theta') - 1}{[\bar{x}^2 + \bar{r}^2 + 1 - 2\bar{r}\cos(\theta - \theta')]^{\frac{3}{2}}} \, d\theta'$$

(6.23)

To make integration easier, take the equation above and change it to be

$$V_z = -\frac{\Gamma}{4\pi r_0} \frac{1}{[\bar{x}^2 + (\bar{r}+1)^2]^{\frac{3}{2}}[\bar{x}^2 + (\bar{r}-1)^2]} I_1$$

In this equation

$$I_1 = \int_0^{2\pi} \bar{r}\cos(\theta - \theta') - 1 \left/ \left\{ 1 - \frac{2\bar{r}[\cos(\theta - \theta') + 1]}{\bar{x}^2 + (\bar{r}+1)^2} \right.\right.$$
$$\times \left.\left[1 + \frac{2\bar{r}[1 - \cos(\theta - \theta')]}{\bar{x}^2 + (\bar{r}-1)^2} \right] \right\}^{\frac{3}{2}} d\theta'$$

In order to simplify the equation, assume that

$$k^2 = \frac{4\bar{r}}{\bar{x}^2 + (\bar{r}+1)^2}, \text{ when } \quad \bar{x} = 0, \bar{r} = 1;$$

Then, the integral equation is

$$I_1 = (1 - k^2) \left\{ \int_0^{2\pi} \frac{\bar{r}\left[2\cos^2\left(\frac{\theta-\theta'}{2}\right) - 1\right]}{\left[1 - k^2\cos^2\left(\frac{\theta-\theta'}{2}\right)\right]^{\frac{3}{2}}} d\theta' \right.$$

124

$$-\int_0^{2\pi} \frac{d\theta'}{\left[1 - k^2\cos^2\left(\frac{\theta - \theta'}{2}\right)\right]^{\frac{1}{2}}}\Bigg\},$$

The various quantities in the equation above can be induced into the form of a standard integral equation for an ellipse

$$K(k) = \int_0^{\frac{\pi}{2}} \frac{1}{(1 - k^2\sin^2\alpha)^{\frac{1}{2}}} \cdot d\alpha$$

$$E(k) = \int_0^{\frac{\pi}{2}} (1 - k^2\sin^2\alpha)^{\frac{1}{2}} \, d\alpha$$

$$D(k) = \int_0^{\frac{\pi}{2}} \frac{\sin^2\alpha}{(1 - k^2\sin^2\alpha)^{\frac{1}{2}}} \, d\alpha = \frac{K - E}{k^2}$$

Consulting the functional table, we obtain

$$\int_0^{\frac{\pi}{2}} \frac{1}{(1 - k^2\sin^2\alpha)^{\frac{3}{2}}} \, d\alpha = \frac{E}{1 - k^2},$$

$$\int_0^{\frac{\pi}{2}} \frac{\sin^2\alpha}{(1 - k^2\sin^2\alpha)^{\frac{3}{2}}} \, d\alpha = \frac{K - D}{1 - k^2};$$

The integral equation I_1 can be expressed as

$$I_1 = 2\bar{r}4(K - D) - 4(\bar{r} + 1)E$$

$$V_z = -\frac{\Gamma}{2\pi r_0} \frac{4\bar{r}(K - D) - 2(\bar{r} + 1)E}{[\bar{z}^2 + (\bar{r} + 1)^2]^{\frac{1}{2}}[\bar{z}^2 + (\bar{r} - 1)^2]},$$

And, finally we obtain

$$V_z = \frac{\Gamma}{2\pi r_0} \frac{1}{[\bar{z}^2 + (\bar{r} + 1)^2]^{\frac{1}{2}}} \left\{ K(k) - \left[1 + \frac{2(\bar{r} - 1)}{\bar{z}^2 + (\bar{r} - 1)^2}\right] E(k) \right\} \text{ [m/s]}. \quad (6.24)$$

r_0 and Γ, which we already know, are functions of $\bar{r}$ and $\bar{x}$. Using $(2\pi r_0/\Gamma)V_z = \bar{V}_z$ the non-dimensional axial velocity component values can be displayed as in Table 6.1.

Concerning the whole vortex, the radial component of velocity induced at point Γ can also be figured according to the procedure utilized above by using the integral of equation (6.??) along the circumference $2\pi r_0$.

$$V_r = \frac{\Gamma}{4\pi r_0} \int_0^{2\pi} \frac{\bar{z}\cos\theta'}{\{\bar{z}^2 + \bar{r}^2 + 1 - 2\bar{r}\cos(\theta - \theta')\}^{\frac{1}{2}}} d\theta'$$

$$= \frac{\Gamma}{4\pi r_0} \frac{\bar{z}}{[\bar{z}^2 + (\bar{r} + 1)^2]^{\frac{1}{2}}[\bar{z}^2 + (\bar{r} - 1)^2]} I_2,$$

z \ r	0	0.2	0.4	0.6	0.8	1.0	1.2	1.4	1.6	1.8	2.0
0	3.142	3.240	3.586	4.432	7.091	—	−3.345	−1.263	−0.666	−0.407	−0.271
0.2	2.962	3.033	3.263	3.695	4.081	1.336	−1.219	−0.887	−0.554	−0.363	−0.250
0.4	2.515	2.534	2.572	2.595	2.115	0.974	−0.061	−0.351	−0.331	−0.260	−0.198
0.6	1.981	1.965	1.899	1.719	1.333	0.756	0.233	−0.048	−0.141	−0.151	−0.135
0.8	1.496	1.469	1.380	1.206	0.934	0.600	0.295	0.089	−0.020	−0.065	−0.077
1.0	1.111	1.086	1.008	0.874	0.690	0.482	0.289	0.142	0.047	−0.006	−0.032
1.2	0.824	0.804	0.746	0.650	0.527	0.390	0.262	0.156	0.080	0.030	0.001
1.4	0.617	0.603	0.560	0.494	0.410	0.318	0.229	0.153	0.093	0.051	0.022
1.6	0.468	0.458	0.428	0.382	0.324	0.260	0.198	0.142	0.096	0.060	0.034
1.8	0.360	0.353	0.332	0.300	0.259	0.215	0.170	0.128	0.093	0.064	0.041
2.0	0.281	0.276	0.261	0.239	0.210	0.178	0.145	0.114	0.087	0.063	0.045

Table 6.1

Axial Velocity Component, $V_z(2\pi r_o/\Gamma)$ Induced at the point $P(R, F)$ in the Vicinity of the Vortex

z \ r	0	0.2	0.4	0.6	0.8	1.0	1.2	1.4	1.6	1.8	2.0
0	0	0	0	0	0	0	0	0	0	0	0
0.2	0	0.183	0.452	1.012	2.547	4.787	2.135	0.746	0.325	0.168	0.096
0.4	0	0.272	0.619	1.137	1.841	2.182	1.586	0.881	0.479	0.275	0.168
0.6	0	0.268	0.565	0.900	1.202	1.287	1.073	0.748	0.484	0.312	0.205
0.8	0	0.220	0.441	0.649	0.801	0.836	0.744	0.584	0.426	0.302	0.213
1.0	0	0.165	0.323	0.458	0.547	0.572	0.530	0.448	0.354	0.270	0.202
1.2	0	0.120	0.231	0.323	0.383	0.403	0.386	0.342	0.287	0.231	0.182
1.4	0	0.086	0.165	0.230	0.273	0.291	0.286	0.266	0.230	0.194	0.160
1.6	0	0.062	0.119	0.166	0.198	0.214	0.215	0.204	0.194	0.161	0.137
1.8	0	0.045	0.087	0.121	0.146	0.160	0.164	0.159	0.148	0.133	0.117
2.0	0	0.033	0.064	0.090	0.109	0.122	0.127	0.125	0.119	0.110	0.099

Table 6.2

Radial Non-dimensional Velocity Component $\left(\dfrac{2\pi r_o}{\Gamma}\right)V_r$ Induced at Point P

$\bar{x}$ \ $\bar{r}$	0	0.2	0.4	0.6	0.8	1.0	1.2	1.4	1.6	1.8	2.0
0	0	0.064	0.268	0.665	1.438	—	1.978	1.448	1.175	0.999	0.873
0.2	0	0.060	0.249	0.596	1.149	1.714	1.613	1.331	1.120	0.968	0.853
0.4	0	0.050	0.204	0.460	0.792	1.075	1.158	1.092	1.986	0.886	0.799
0.6	0	0.040	0.156	0.337	0.552	0.740	0.843	0.861	0.829	0.778	0.724
0.8	0	0.030	0.115	0.245	0.395	0.532	0.628	0.675	0.683	0.667	0.639
1.0	0	0.022	0.085	0.179	0.288	0.398	0.477	0.531	0.558	0.564	0.556
1.2	0	0.016	0.063	0.133	0.215	0.297	0.368	0.421	0.456	0.474	0.479
1.4	0	0.012	0.047	0.100	0.163	0.228	0.288	0.337	0.373	0.397	0.410
1.6	0	0.009	0.036	0.076	0.126	0.178	0.228	0.272	0.307	0.333	0.351
1.8	0	0.007	0.028	0.059	0.098	0.141	0.183	0.222	0.254	0.281	0.301
2.0	0	0.005	0.022	0.047	0.078	0.113	0.148	0.182	0.212	0.237	0.258

$$\left(\frac{2\pi}{\Gamma r_0}\right)\phi$$

In the integral equation

$$I_2 = \int_0^{2\pi} \cos\theta' d\theta' \Big/ \left\{1 - \frac{2\bar{r}[\cos(\theta - \theta') + 1]}{\bar{x}^2 + (\bar{r} + 1)^2}\right\}^{\frac{1}{2}}$$
$$\times \left\{1 + \frac{2\bar{r}[1 - \cos(\theta - \theta')]}{\bar{x}^2 + (\bar{r} - 1)^2}\right\};$$

solving I_2 and manipulates its equivalent so that it becomes a standard integral equation for an ellipse, then, it is possible to obtain

$$V_r = \frac{\Gamma}{2\pi r_0} \frac{2\bar{x}(2K - 2D - E)}{[\bar{x}^2 + (\bar{r} + 1)^2]^{\frac{1}{2}}[\bar{x}^2 + (\bar{r} - 1)^2]},$$

The radial component of velocity

$$V_r = \frac{\Gamma}{2\pi r_0} \frac{-\bar{x}}{[\bar{x}^2 + (\bar{r} + 1)^2]^{\frac{1}{2}}\bar{r}} \left\{K(k)\right.$$
$$\left. - \left[1 + \frac{2\bar{r}}{\bar{x}^2 + (\bar{r} - 1)^2}\right] E(k)\right\} \ [\text{m/s}], \quad (6.25)$$

127

The flow function, ϕ, can be solved for by integration on the basis of the radial component of velocity, V_r, and the axial component of velocity, V_x, as follows:

$$\phi = -r \int_0^x V_r dx + \int_0^r r V_x dr \qquad [m^3/s] \quad (6.26)$$

First, integrate from 0 to x along the axis of symmetry, r = 0; then, at a point, x, integrate from 0 to r along the radius. The integral of the first quantity in the equation above = 0, and the integral of the second quantity is

$$\phi = \frac{\Gamma r_0}{2\pi} \int_0^r \frac{\bar{r}}{[\bar{x}^2(\bar{r}+1)^2]^{\frac{1}{2}}} \Big\{ K(k)$$
$$- \Big[1 + \frac{2(\bar{r}-1)}{\bar{x}^2 + (\bar{r}-1)^2}\Big] E(k) \Big\} d\bar{r} \quad (6.27)$$

If one takes the axis of symmetry, $\bar{x}$ = 0, to be the base flow line, that is to say, if one takes the volume of flow along the axis of symmetry, r = 0, to be ϕ which is equal to 0, then, one can integrate the parts of equation (6.27) and obtain

$$\phi = \frac{\Gamma r_0}{2\pi} [\bar{x}^2 + (\bar{r}+1)^2]^{\frac{1}{2}} \Big[\Big(1 - \frac{k^2}{2}\Big) K(k) - E(k)\Big] [m^3/s]$$
$$(6.28)$$

The foregoing analysis is only appropriate for use with flow fields which are induced by the surroundings of the vortical core. Actual vortical cores, even if they are very small, do not have radii, δ, which are equal to zero. Therefore, it is not possible to use $\bar{x}$ = 0, $\bar{r}$ = 0, and k^2 = 1, in order to solve for the induced axial flow speed, V_x, according to equation (6.24).

If one looks at Fig 6.4 (a), then, it is possible to suppose that the vertical cross sections of the vortices have equal circulations, Γ (m^2/s), and that they are a pair of circular spirals or vortices which have opposite directions. The two vortices mutually induce each other as follows:

At each place in the heart of the vortex where $\bar{r}$ = 1, the axial flow speed induced is

$$V_x' = \frac{\Gamma}{4\pi r_0}, \quad [m/s] \qquad (6.29)$$

This explains the fact that, even if one is considering gases completely at rest, if one is thinking in terms of the vortical core, there is displacement in a positive direction along the x axis (the forward, counter-current flow of the surrounding gases) at a velocity V'_x. Therefore, these vortices are not capable of being stable at a fixed position. If, however, one is concerning himself with a uniform flow field in which the counter-current flow speed along the x axis, $-V_x =$ $= (\Gamma/4\pi r_0)$, then, this condition can be maintained, stable and unmoving, in relation to the vortical core, and, in this case, stability of combustion can be main-

tained.

If one is considering the whole vortex, then, those vortical centers along the circumference also mutually induce each other, and, the result is that the speed of the forward displacment of the counter-current vortices or eddies must be considerablly faster than what is the case in equation (6.29). (Refering to Hydrodynamics, Lamb, 6th ed. 1945, p. 241) it is possible, on the basis of the equation below, to figure the speed of counter-current flow displacement in eddies:

$$V'_s = \frac{\Gamma}{2\pi r_0}\left[\ln\left(\frac{8r_0}{\delta}\right) - \frac{1}{4}\right]$$

δ = the radius of the vortical core

(6.30)

The form of Fig (6.4) (a) shows the drawing of surrounding gases into the form of an ellipsoid sphere by a stable eddy vortex. According to the reference cited, the long axis of the ellipsoid sphere = 4.18 r_c. Assume that radius of the eddy vortex is more or less equal to the average radius of the eddy devices, $\bar{r} = \frac{1}{2}(r_1 + r_2)$; if this is true, then, the interior radius of the flame tube must be at least somewhat larger than 2.09 r_c. If it is smaller than this value, then, the eddy vortex will be squeezed and elongated.

Sec 6   Spiral Vortices

The design of manufacture for the intake plates of the "fish bowl" combustion chamber of a turbine jet II may possibly be based on the principle " ten point pools of a free vortex is the same as a spiral vortex." This principle is also appropriate for use in the design of "centripetal radial flow turbines" as well as "super-sonic centrifugal compressors and diffussers." Fig (6.5) shows that, on the intake vanes, the "rubbing plate holes" or "fish scale holes" that are arranged in three rings all meet the intake flow lines along the direction n — n of the normal line N, " along the points of intersection of the spiral line and the radius. Therefore, there are dozens of spiral jets shooting into the combustion chamber from the holes in the "rubbing or friction plates" and winding around the fuel distribution plates creating violent whirlwinds. The diameter of the fuel dispersion plates, r = 70mm and is larger that the vortical core of solid rotation. When the rotation speed, n = 22,000 r.p.m, then, the tangential velocity can reach V_m = ≈160 m/s.

Chapter 4, Sec 2 talks about the fact that the flow speed direction is the normal line of the equipotential line when ϕ = a constant. In two-dimensional flow fields, the speed value ϕ = a constant and the flow function ϕ = a constant are

129

both sets of curves that meet each other at right angles, that is to say, that the two tangent lines at points where ϕ and ψ cross are perpendicular to each other; therefore, ϕ and ψ are called orthogonal functions. If we use the complex variable

$$Z = (x + iy) = re^{i\theta} = r(\cos\theta + i\sin\theta)$$

and the complex function $\quad F(Z) = F(x + iy) = F(re^{i\theta}) = \phi + i\psi$

to show the "orthogonal functions" of a two-dimensional flow field, then, it is easy to solve for the answer. Fig 6.6 illustrates the relationship between perpendicular coordinates and polar coordinates as well as the complex variable $\quad Z = x + iy = re^{i\theta}$ and the way in which they are used for display. Obviously,

$$\frac{\partial Z}{\partial x} = 1, \quad \frac{\partial Z}{\partial y} = i, \quad i = \sqrt{-1} \qquad (6.31)$$
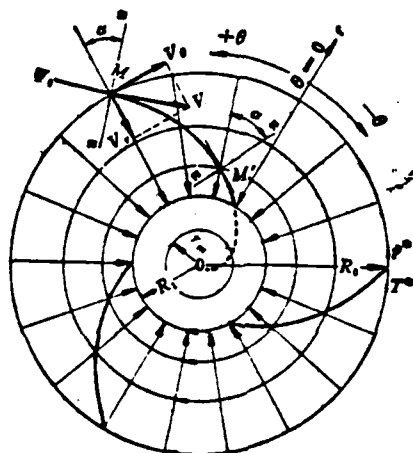

Fig 6.5

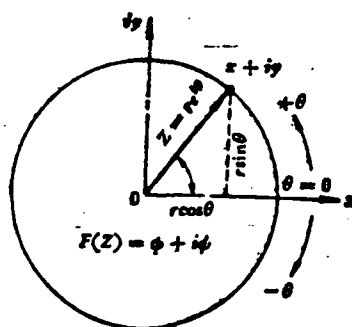"Spiral Line Vortex"= Free Vortex + Point

Fig 6.6

Complex Variables and Polar Coordinates

130

If one analyses Fig 6.6, it is possible to come to know that

$$\frac{\partial F}{\partial x} = \frac{dF}{dZ} \cdot \frac{\partial Z}{\partial x} = \frac{dF}{dZ}, \quad \frac{\partial F}{\partial y} = \frac{dF}{dZ} \cdot \frac{\partial Z}{\partial y} = i\frac{dF}{dZ};$$

Therefore

$$\frac{\partial F}{\partial y} = i\frac{\partial F}{\partial x}, \quad \text{或} \quad \frac{\partial F}{r\partial \theta} = i\frac{\partial F}{\partial r};$$

However,

$$\frac{\partial F}{\partial x} = \frac{\partial \phi}{\partial x} + i\frac{\partial \psi}{\partial x}, \quad \frac{\partial F}{\partial y} = \frac{\partial \phi}{\partial y} + i\frac{\partial \psi}{\partial y};$$

Therefore,

$$\frac{\partial \phi}{\partial y} + i\frac{\partial \psi}{\partial y} = i\frac{\partial \phi}{\partial x} - \frac{\partial \psi}{\partial x} \qquad (6.32)$$

If one separates the meaningful quantities in equation (6.32) from the meaningless quantities, one finds that they separate out into equal pairs

$$\frac{\partial \phi}{\partial x} = \frac{\partial \psi}{\partial y} = V_x \qquad \qquad \frac{\partial \phi}{\partial r} = \frac{\partial \psi}{r\partial \theta} = V_r \left.\vphantom{\begin{array}{c} \\ \\ \\ \end{array}}\right\}$$

or, in

polar

$$\frac{\partial \phi}{\partial y} = -\frac{\partial \psi}{\partial x} = V_y \qquad \qquad \text{coordin-} \qquad \frac{\partial \phi}{r\partial \theta} = -\frac{\partial \psi}{\partial r} = V_\theta \left.\vphantom{\begin{array}{c} \\ \\ \\ \end{array}}\right\}$$

ates

$$(6.33)$$

In Fig (6.6), if one assumes that there is a dimension = 1 which is perpendicular to the surface of the illustration, then, the "point sink" centripetal flow along the entire circumference, $G = 2\pi \rho r V_r =$ a constant; if one also recognizes that $\rho =$ a constant, then,

Point sources:

$$rV_r = \frac{G}{2\pi\rho}$$

= a constant C, and the already known amounts of flow, G and ρ determine C (6.34)

According to equation (6.4), free vortices:

$$rV_\theta = \frac{\Gamma}{2\pi}$$

= a constant K, and, if we already know Γ , then, it is possible to determine K   (6.35)

131

If we assume that the complex function

$$F_1(Z) = -C \ln Z = -C \ln(re^{i\theta}) = -C(\ln r + i\theta)$$
$$= (\phi_1 + i\psi_1);$$

Due to this fact, as far as the "point pool" is concerned,

its potential function is $\phi_1 = -C \ln r$

its flow function is $\psi_1 = -C\theta$ (6.36)

Therefore, the equipotential line of the "point sink", ϕ_1 = a constant, is r = a

constant in several concentric circles; the equal flow line of the "point pool",

ψ_1 = constant, is θ = a constant of several radiating lines (radii). If one assumes the complex function

$$F_2(Z) = iK \ln Z = iK \ln(re^{i\theta})$$
$$= iK \ln r - K\theta = (i\phi_2 - \phi_2);$$

Then, consequently, in the case of a free vortex,

its potential function $\phi_2 = K\theta$, and its flow function $\psi_2 = K \ln r$, (6.37)

its flow, the equipotential line of the free vortex, ϕ_2 = a constant, is r = a

constant of several concentric circles. "Point sink" + "free vortex" = the flow

of the spiral vortex.

$$\Psi = \phi_1 + \phi_2 = -C\theta + K \ln r, \qquad (6.38)$$

$$\frac{\partial \Psi}{r \partial \theta} = \frac{\partial \psi_1}{r \partial \theta} = -\frac{C}{r} = -V_r,$$

$$\frac{\partial \Psi}{\partial r} = \frac{\partial \psi_2}{\partial r} = \frac{K}{r} = V_\theta; \qquad (6.39)$$

If we assume that $\begin{cases} r = R_1 \\ \theta = 0, \end{cases} \Psi_i = K \ln R_1$ = a constant, then, from equation

then, it is possible to obtain $K \ln R_1 = -C\theta + K \ln r$

$$\frac{C\theta}{K} = \ln r - \ln R_1 = \ln\left(\frac{r}{R_1}\right),$$

Therefore, the flow line equation of the spiral vortex is

$$r = R_1 e^{\frac{C\theta}{K}} \qquad (6.40)$$

Equation (6.40) is called a "logrithmic spiral" or "isometric spiral" equation. If

one already knows R_1, C and K, then, is is possible, according to $\ln r = \ln R_1 + \frac{C}{K}\theta$

132

to consult the table of natural logarithms and, point by successive point, to plot
out the flow line. The peculiar characteristic of an "isometric flow line" is that
the normal line, n—n, of the points of intersection such as M and M' between the curve
and the radius are equal to the included angle, α, of the radius (Fig 6.5). Because of
the fact that the circumferential flow speed of a free vortex, V_θ, forms a reverse
proportion with the radius, r, for a certain radius, R_1, V_θ = the critical speed of
sound

$$a_1 = \sqrt{\frac{2}{k+1} kgRT^*},$$

According to equal circulation

$$\frac{\Gamma}{2\pi} = K = rV_\theta = R_1 a_1,$$
or velocity
coefficient
$$\lambda = \frac{V_\theta}{a_1} = \frac{R_1}{r} \leqslant 1 \qquad (6.41)$$

Under ideal conditions, when the radius is reduced to r_m, the static pressure drops
to p = 0, V_θ is at a maximum value, and $\lambda_{max} = 2.45$, then, $\left(\frac{r_m}{R_1}\right)_0 = \frac{1}{2.45} = 0.408$.

This explains the fact that, within the circumference generated when the radius, r_m,
is at its extreme minimum value, p = 0 and there is a true vacuum, in the interval
in which $r_m \rightarrow R_1$, theoretically speaking, one can see the appearance of areas of
super-sonic flow in which $1 < \lambda < 2.45$. Practically speaking, the path of the cent-
ripetal flow as a compression maneuver, and, in the case of similar sub-sonic con-
vergent jet tubes, it is not possible to produce super-sonic flow. The R_1 circle or
circumference is called the "sonic circle." Within the "sonic circle," there is
already no two-dimensional, plane centripetal flow. In actuality, this circumfer-
ence at R_1 is already covered or protected by the jet nozzle in the middle of the
eddy current device or by the horizontal cross section of the axis of rotation of
the solid body, and if this is not the case, then, it is taken over by air flow com-
ing out of the nozzle and is changed into a flow which goes along the same axis as
all the rest of the normal flow.

Concerning "point pools," if one considers the fact that density, ρ, varies with
changes in flow, then, the continuity equation (6.34) should be changed to be

$$\rho r V_r = \frac{G}{2\pi} = C', \ V_r = aM; \ a = \text{ speed of sound } (6.42)$$

The flow, G, can be taken as a control, and, on the basis of G, it is possible
to choose a constant $C' = \rho^* a^* R_1 = \frac{G}{2\pi},$; the R_1 in this expression is

the radius of the "sonic circle" when one is only considering a free vortex. ρ^* and a^* are the stagnation density and the acoustic velocity of stagnation respectively for the surrounding environment of a free vortex; M = the local Mach number. Due to the ratio between point sinks and radii

$$\left(\frac{r}{R_1}\right)_r = \left(\frac{\rho^*}{\rho}\right) \cdot \left(\frac{a^*}{a}\right) \cdot \frac{1}{M} = \frac{1}{M}$$
$$\times \left[1 + \frac{k-1}{2} M^2\right]^{\frac{k+1}{2(k-1)}} \qquad (6.43)$$

When, in equation (6.43), $k = 1$, the centripetal flow speed of the point sink $V_r = a$. If we assume that $k = 1.4$, then,

$$\frac{\text{the point pool radius of the sonic circle}}{\substack{\text{the radius of the sonic circle for a} \\ \text{free vortex}}} = \left(\frac{r_1}{R_1}\right)_r = \left[\frac{k+1}{2}\right]^{\frac{2.4}{0.8}}$$
$$= [1.2]^3 = 1.728 \qquad (6.44)$$

According to the transformation formula

$$M^2 = \frac{\frac{2}{k+1}\lambda^2}{1 - \frac{k-1}{k+1}\lambda^2}, \quad \text{one obtains} \quad \left(\frac{r}{R_1}\right)_r = \frac{1}{\lambda}\left(\frac{2}{k+1}\right)^{-\frac{1}{2}}$$
$$\times \left[1 - \frac{k-1}{k+1}\lambda^2\right]^{-\frac{1}{k-1}} \qquad (6.45)$$

the flow speed of a spiral line vortex is $V^2 = V_\theta^2 + V_r^2$;

The speed coefficient $\lambda = \frac{V}{a_1}$ $\qquad (6.46)$

However, from equation (6.46)

$$V_\theta^2 = \left(\frac{K}{r}\right)^2,$$

From equation (6.46),

$$V_r^2 = \left(\frac{C}{\rho r}\right)^2,$$

therefore,

$$V^2 = \left(\frac{K}{r}\right)^2 + \left(\frac{C}{\rho r}\right)^2 = \frac{1}{r^2}\left[K^2 + \left(\frac{C}{\rho}\right)^2\right],$$

On the basis of this one can obtain

$$r^2 = \frac{1}{V^2}\left[K^2 + \left(\frac{C}{\rho}\right)^2\right] \quad (6.47) \quad \text{, the smaller the radius is, the faster V is.}$$

134

Equation (6.47) is a spiral line equation that takes into consideration changes in ρ. If we take the square of the radius of the sonic circle for a free vortex, R_1^2, and use it to eliminate all at once the various quantities in equation (6.47), then, it is possible to obtain the square of the ratio of radii for a spiral line or skew vortex

$$\left(\frac{r}{R_1}\right)^2 = \frac{1}{V^2}\left[\frac{r^2 V_\theta^2}{R_1^2} + \frac{r^2 V_r^2}{R_1^2}\right] = \left(\frac{r}{R_1}\right)_\theta^2 + \left(\frac{r}{R_1}\right)_r^2 \quad (6.48)$$

If we substitute equations (6.11) and (6.45) into equation (6.48)

$$\left(\frac{r}{R_1}\right)^2 = \frac{1}{\lambda^2} + \frac{1}{\lambda^2}\left(\frac{2}{k+1}\right)^{-1}\left[1 - \frac{k-1}{k+1}\lambda^2\right]^{-\frac{2}{k-1}}$$

$$(6.49)$$

When $V = a$, and $\lambda = 1$, the radii ratio for a spiral line or skew vortex

$$= \sqrt{1 + 1.728^2} = \sqrt{3.986} \cong 2$$

Therefore, when one considers compressibility, the radius of the sonic circle for a spiral line or skew vortex is about twice the size of the radius of the sonic circle for a free vortex. In order to suit the tangential velocity of the fuel dispersion plates, $V_\theta = V_m$ and in order to prevent the losses from obstacles to the flow of gases from being excessively large, it is necessary for the pitch radii of the holes in the milling plates or the inner ring of the intake vanes of a turbine jet II to be $\geq 4R_1$.

If we assume that the overall temperature at the exhaust of the compressor is $T_2^* = 480$, then, the critical acoustical velocity

$$a_1 = 18.3\sqrt{T_2^*} = 18.3\sqrt{480} = 18.3 \times 21.9 = 400[m/s] = V_m.$$

When $n = 30,000$ revolutions per second, the tangential velocity to the circumference of the fuel dispenser plates is $V_\theta \cong 160$ (m/s) $= V_m$, the radius of the fuel dispenser plates is $r = 70mm$, and there is equal circulation, then, $V_\theta r = a_1 R_1$; therefore, the radius of the sonic circle is

$$R_1 = \frac{V_\theta r}{a_1}$$

$$R_1 = \frac{160 \times 70}{400} = 28mm.$$

$$4R_1 = 112mm.$$

Sec 7 Viscous Current Spirals

It is only because liquids have a viscosity, μ, and a velocity gradient $\partial u/\partial y$,

135

which produces viscous shear stresses, τ, that a rotation can be wound around to form a spiral or vortex. Because of this fact, actual vortices and spirals are all viscous spirals and vortices. An avortical potential flow free vortex + a vortical core of solid body rotation = a circular vortex; this idealized, approximate concept only ignores viscosity. Practical experience shows that the tangential velocity distribution along a radius, r, from the center of the vortex is $V_\theta = f(r)$ and that it is most certainly not similar to the one shown in Fig (6.3) (b); on the circumference, R_1, around the edge of the vortical core, there is a "sudden change" and then a moderate change along r (Fig 6.7). The distribution of vorticity in a vortical viscous flow field is a distribution of the quantity $\xi = \text{curl}\mathbf{V} = \nabla \times \mathbf{V} = 2\omega$, and it is not even; moreover, it is diffused into the outer environment over an interval of duration, t. This is due to the fact that the energy losses due to viscous friction cause the vortical strength of the rotating vortical masses (also called circulation) to gradually attenuate and it causes the vortex to be dispersed and break up into several minute pulsating vortical masses (that is to say, turbulence flow organizational structures). This is called the "vortex disipation and breakdown turbulence form." Looking at it from this point of view, the basic nature or substance of vortices and turbulence flows is the same; it is only the size of the scale and the dimensions which are different. Because of this fact, turbulence flow fields and viscous vortical flow fields cannot be equal circulation flow fields.
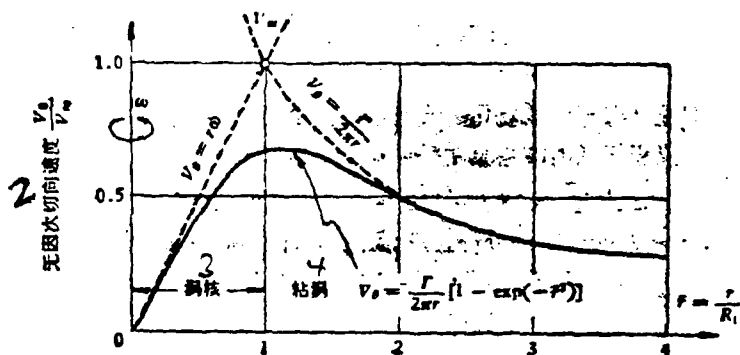

图6.7 粘流旋洞切线速度分布规律

Fig 6.7

1. Rules Governing the Tangential Velocity Distribution of Viscous Flow Vortices
2. Non-dimensional Tangential Velocity V_θ / V_m 3. Vortical Core 4. Viscous Vortex

If we use the kilogram as the unit of mass, then, the unit of force should be (Γ), and, the unit of density which we use should be (kg/m^3); due to these facts,

the unit of viscosity is μ (kg/m·s), and the unit of dynamic viscosity, v, is (m^2/s). This is the same as the unit for the coefficient of diffusion, D. Because of this fact, the curl or vorticity of a vortex, ξ, because of the effects of viscosity, is capable of diffusing out into the surrounding environment by transference, and the coefficient of this transfer $= v$. According to a method in Chapter 4, if one presumes a given volume, V_s, in a viscous vortical flow field, and one also presumes its closed surface, S, and the gradient of the vorticity, ξ, along the outside normal line of the surface, $\text{grad}\xi = \nabla\xi$, then, within a duration, dt, the vorticity put out from a surface, S, is

$$\xi = -dt \oint \mu(\nabla \cdot \xi)\, dS \qquad (6.50)$$

By the appropriate use of Gauss's integration theorem, we get

$$\xi = -dt \oint^{V_s} \nabla \cdot (\mu\nabla \cdot \xi)\, dV, \qquad (6.51)$$

In a duration, dt, the vorticity within V_s is reduced to

$$\xi = -dt \oint^{V_s} \rho\, \frac{\partial \xi}{\partial t}\, dV, \qquad (6.52)$$

The vorticity put from V_s is equal to the reduction in vorticity within V_s; equations (6.51) and (6.52) equal each other, and the integrands ought also to be equal. If we presume that μ is equal to a constant, then,

$$\rho\frac{\partial \xi}{\partial t} = \mu\nabla^2 \cdot \xi, \quad \text{or } \frac{\partial \xi}{\partial t} = v\nabla^2\xi \qquad (6.53)$$

The Laplacian operation with cylindrical coordinates

$$\nabla^2 = \frac{\partial^2}{\partial r^2} + \frac{1}{r}\frac{\partial}{\partial r} + \frac{1}{r^2}\frac{\partial^2}{\partial \theta^2} + \frac{\partial^2}{\partial z^2},$$

If one utilizes a two-dimensional axially symmetrical flow field, then,

$$\frac{\partial^2}{\partial z^2} = 0, \quad \frac{\partial^2}{\partial \theta^2} = 0$$

and, consequently, one obtains the differential equation for a viscous vortex

$$\frac{\partial \xi}{\partial t} = v\left(\frac{\partial^2 \xi}{\partial r^2} + \frac{1}{r}\frac{\partial \xi}{\partial r}\right) \qquad (6.54)$$

Given the initial conditions: $t = 0$ and circulation (vortical strength) $\Gamma = 2\pi K = 2\pi R_0^2\omega$, , then, one gets vortices appearing; given the terminal conditions: $r \to \infty$,

137

and circulation (vortical strength) $\Gamma \to 0$, then, vortices attenuate, dissipate and break up; the boundary conditions are; $\bar{r} = 0$, and the tangential velocity, $V_\theta = 0$ (Fig 6.7); when $\bar{r} = 1$, then, the tangential velocity, $V_\theta = \left(1 - \frac{1}{e}\right) V_\infty$;

and, when $\bar{r} \to \infty$, then, the tangential velocity, $V_\theta \to 0$.

According to a method employing similar parameters, when one solves for the special solution which corresponds to the conditions stated above, one finds it to be

$$\xi = \frac{K}{4\nu t} \exp\left(-\frac{r^2}{4\nu t}\right), \quad K = \frac{\Gamma}{2\pi} = R_1^2 \omega \quad (6.55)$$

Going according to what was said in Chapter 5, the circulation, Γ = the vorticity, ξ, multiplied by the circulation around the area. The amount of circulation in the round area, r. is

$$\Gamma = \int_0^r \xi 2\pi r dr = \int_0^r \frac{K}{4\nu t} \exp\left(-\frac{r^2}{4\nu t}\right) 2\pi r dr$$

$$= 2\pi K \left[1 - \exp\left(-\frac{r^2}{4\nu t}\right)\right] \quad (6.56)$$

If one assumes that the radius of the vortical core, $R_1 = 2\sqrt{\nu t}$, then, $\bar{r} = r/R_1$. This corresponds to the rules governing the occurrence, development and attenuation of vortices. That is to say that, when $t \geq 0$, the vortical core, beginning from the heart of the vortex developes and expands. Because of viscous diffusion transference, the vorticity transmitted from the interior air flow layers to the exterior rings also, simultaneously, transmits mass and momentum, inducing the surrounding gases to rotate around the vortical core. If one is dealing with an eddy, then, it is capable of attracting the gases downstream to flow upstream. If the space involved does not suffer from any limitation, then, when $r \to \infty$ 时, $R_1 \to \infty$, and the circulation, $\Gamma \to 0$. That is to say, the gases move in an avortical rotation. If we go on the basis that $\Gamma = 2\pi r V_\theta$, then, from equation (6.56) we can obtain the fact that the tangential velocity

$$V_\theta = \frac{K}{r}\left[1 - \exp\left(-\frac{r^2}{R_1^2}\right)\right]$$

$$= \frac{\Gamma}{2\pi r}\left[1 - \exp(-\bar{r}^2)\right] \quad (6.57)$$

According to the analysis that we have done in this section, the eddies in the exhaust of the vortical flow devices in Sec 5 are not stationary and unchanging; on the contrary, they are constantly being produced, developing and attenuating in a process of successive renewal and degeneration. What is referred to as "stable combustion" must necessarily depend on the careful coordination and adjustment of

138

"fuel concentration distribution" and "chemical reaction processes" with the process of development of this eddy in space and time. If the eddy or vortex is unstable, then, the combustion will be unstable.

Sec 8 Axial Turbulence Jets From Layers of Spiral Flow

The path between two layers of spiral or vortical flow can be seen as being the height of a flat jet nozzle = $2b_c$. The two-dimensional turbulence jet put out from a flat jet quickly expands. Various cross sections of axial flow speed distribution are shown in Fig 6.8.
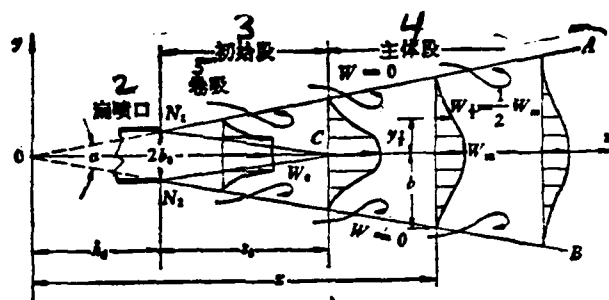

图6.8 扁喷口二元紊流射流扩展及速度分布

Fig 6.8

1. Expansion and Velocity Distribution of Two-dimensional Turbulence Jet From a Flat Jet Nozzle 2. Flat Jet Nozzle 3. Initial Section 4. Main Body Section 5. Curling Formation

N_1A and N_2B are the outer limit lines of the jet. N_1C and N_2C are the inner limit lines of the jet. The two outer limit lines, at the mouth of the jet, flow together and meet at the "origin point" O. The triangular area inside the interior boundary lines is called the "jet core." The axial flow speed within the jet core, W_0 is even and unchanging and is equal to the axial flow speed of the intake. On the basis of induction from experimental data, the distance from the origin point to the jet nozzle, $h_c = 0.41 (b_c/a)$, and the length of the core, $s_c = 1.03 (b_c/a)$; the experimental constant, $a = 0.015 \sim 0.27$. In general, $s_c \approx 4 \sim 5$ times b_c.

Sec 9 Methods For Diagraming Counter-current Areas Behind Eddy Current Apparatus

(1) If we already know the height of a flat jet, $2b_c$, and we choose the constant, $a = 0.15 \sim 0.27$, then, on the basis of equation (6.59), we can figure out h_c and s_c, and we can draw the exterior boundary lines within the two-dimensional turbulence jet in Fig 6.8. The axis of symmetry cuts the jet in half. If, along the axis line,

we cut out a certain number of sections, 1, 2, 3, ..., i, then, we can measure out from the line of the axis to the interior and exterior boundary lines the coordinates, b_0, b_1, b_2, ... as well as the thicknesses of the boundary layer of the turbulence flow, 0, y_1, y_2, ...

(2) We already know that the cone-shaped shell in the forward section of the flame tube has a maximum inner diameter of R and a hemi-pyramid angle of β. We also already know the external diameter of the vortical flow device, r_1, and the internal diameter of the vortical flow device, r_2; $b_c = (r_1-r_2)$, the number of vortical flow vanes is n; the vortical flow angle is ϕ (Fig 6.4), and both these quantities are already know as are, δ, the thickness of the vane blades, G_0, the amount of intake, the overall intake temperature and pressure and the axial flow speed coefficient, λ.

(3) If we take the jet flow speed of the ring-shaped rotation at the exhaust of the vortical flow device, q, and divide it up into the tangential component of velocity, V, forming an eddy (Fig 6.4) and the axial flow speed, W, which forms a semi-jet field (Fig 6.11) that has, for its axis of symmetry the wall surface in the forward part of the flame tube.

(4) If we take the outer circumference of the exhaust of the vortical flow device as the origin point, and if, on the basis of the same scale of measurement, we take the contour line of the inner wall of the forward section and make it the axis of symmetry, and, in the same way as before, cut it up to make a certain number of sections1, 2, 3, ...i, then, the normal lines of the various sections along the inner wall, in turn, take the inner and outer boundary coordinates of the semi-jet flow field, b_0, b_1, b_2, ... as well as 0, y_1, y_2...... and transplant or translocate them across. By connecting the end points of these y_1, y_2, ... coordinates, it amounts to the same thing as drawing out the boundary of the area of counter-current flow, $W = 0$. The reason for this is that on the external boundary line of the semi-jet flow, the axial velocity, $W = 0$ (Fig 6.11).

(5) According to the preceding analysis in Section 5 and Section 7, if the radius of a stable eddy, $r_c = 0.5a$, then, that should be precisely the maximum radius of the area of counter-current flow. The boundary line of the area of counter-current flow is the track of displacement of the heart of the eddy.

The vector, q, for the ring-shaped rotational jet flow speed at the exhaust of the vortical flow device forms a hyperbolic flow surface. On an x-y plane, this flow surface projects a curve as shown in Fig 6.10. From Fig 6.9 it can be seen that:

$$x^2 = AD^2 - BD^2$$
$$BD = AD \cos\phi$$
$$x^2 = \left(\frac{1}{\cos^2\phi} - 1\right)BD^2; \quad \text{from } \triangle DBO,$$
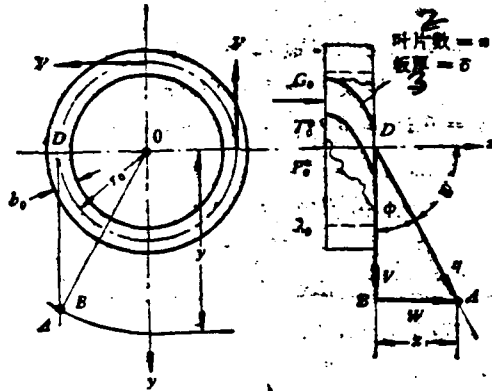$$OB = y, \quad BD^2 = OB^2 - r_0^2;$$

图6.9 涡流器迫使气流旋转

Fig 6.9

1. Air Flow Rotation Caused By Vortical Flow Device   2. Number of Vane Blades = n
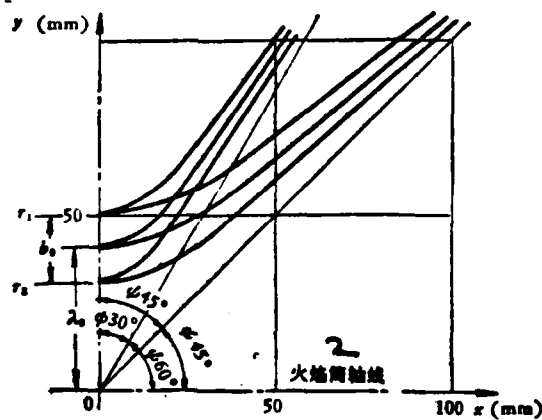
3. Plate Thickness = δ

图6.10 涡流器出口流面投影

Fig 6.10

1. Projection of the Flow Surface at the Exhaust of the Vortical Flow Device
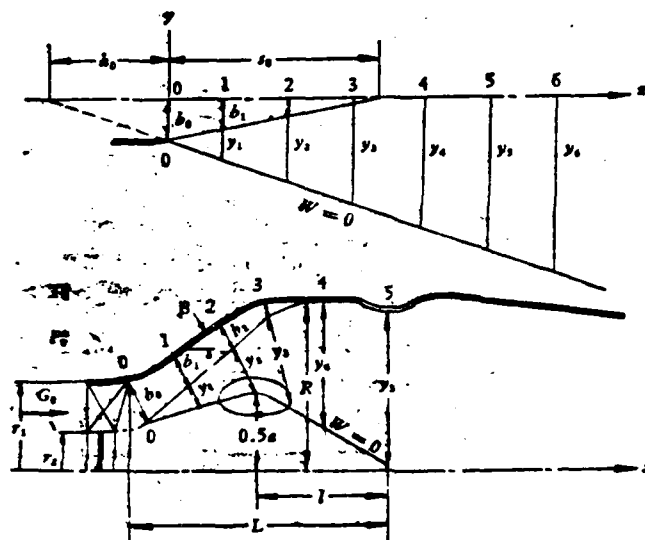
2. Flame Tube Axis Line

141

Fig 6.11

Diagramming Method for Determining the Boundaries of Areas of Counter-current Flow By the Use of the Transplantation or Transposition of a Semi-jet Flow Field

therefore

$$x^2 = (y^2 - r_0^2)\frac{1 - \cos^2\phi}{\cos^2\phi} = (y^2 - r_0^2)\text{tg}^2\phi \quad (6.59)$$

It is possible to use the hyperbolic line that goes out from r_0 in order to correct the transposition of the inner boundary line of the jet flow.

Sec 19. Air Flow Structure of the Forward Section of Flame Tubes

Fig 6.12 is an illustration of the air flow structure of the forward section of a flame tube. I = the core section of the semi-jet flow. II = the parallel flow area of a turbulence flow boundary layer and its vortical flow field. III = a counter-current flow area, an externally surrounding jet flow suction and eddy induction which produce radial and axial pressure gradients and form a central trough of low pressure. IV = flow lines which wind around and stick to the surface of the counter-current flow area and which, when they reach their tail end are twisted into vortical wakes which are also called "vortical rolls." r_1 and r_2 = the external
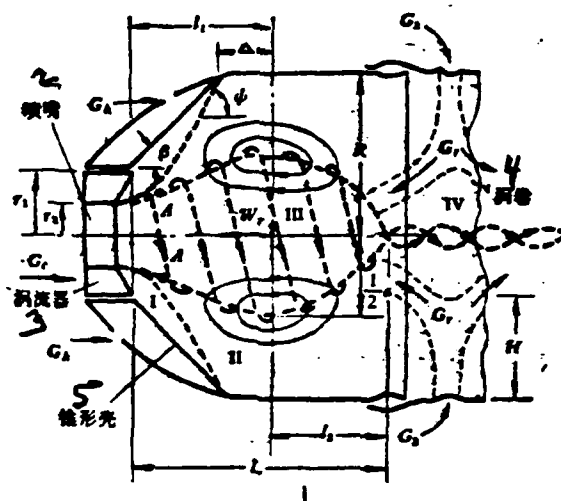
142

图6.12 火焰筒头部气流结构

Fig 6.12

1. Air Flow Structure of the Forward Section of a Flame Tube 2. Jet Nozzle
3. Vortical Flow Device 4. Vortical Roll 5. Cone-shaped Shell

and internal radii of the ring-shaped path of the vortical flow device. β = the semi-pyramid angle of the cone shaped shell. ϕ = half of the angle of expansion of the rotational jet which is approximately equal to the angle of installation of the rotational flow vanes. l_1 = to the distance from the cross section of the maximum diameter, a. of the counter-current flow area to the exhaust of the vortical flow device. Δ = the distance in which the symmetrical surface of the eddy enters the cylindrical portion; this is generally $\Delta \cong 20\,mm$. R = the internal radius of the forward section of the flame tube. l_2 = the distance from the symmetrical surface of the eddy to the end point of the area of counter-current flow. L = the length of the area of counter-current flow. G_c = the amount of supplemental intake in the forward area. G_a = the amount of intake gas of the main fuel holes. H= penetration depth of the main fuel hole intake. G_r = amount of reflux flow. The continuous or sustained ignition sources, A and A, are capable of being located in the initial stage of the boundary layer of the turbulence flow close to the vicinity of the boundary of the counter-current flow, approximately 20-30mm distant from the exhaust of the vortical flow device.

After one uses the semi-jet flow field transposition method to draw out the boundaries of the area of counter-current flow, one already knows R, r_1, β, and ϕ, and it is possible to use the experimental or empirical formula set out below

143

to compare and solve for the maximum diameter of the area of counter-current flow, a, and its length, L; comparing these quantities to each other:

$$l_1 = \frac{R - r_1}{tg\,\beta} + \Delta, \quad a = 2R\sin\psi, \quad l_2 = 2.7R\sin\psi \quad (6.60)$$

The length of the area of counter-current flow

$$L = l_1 + l_2 = (R - r_1)ctg\,\beta + \Delta + 2.7R\sin\psi \quad (6.61)$$

The semi-pyramid angle of the cone-shaped shell needs to be smaller than or equal to half the angle of expansion of the rotational jet, and, if $\beta \leq \phi$, one can choose $\beta \approx \phi - 10°$. If $\beta > \phi$, then, the core area of the half jet between the interior wall of the cone-shaped shell and the expansion surface of the jet produces a rotational vortex due to the influence of boundary layer separation, and reflex roll up in the flame tube causes the core-shaped shell to overheat. The boundary layer separation on the interior walls of the cone-shaped shell also causes the occurrence of accumulation of ash around the circumference of the jet nozzle. A possible reason for this may be that in conditions of high temperature and a shortage of oxygen fuel and air mixtures that have already been burned assure continuous combustion from III through the ring flow at I and to the 11 area. Separation vortices obstruct this normal circulation; the ignition points, A and A are displaced down the flow path, and the circumference of the jet nozzle stretches out behind itself a section of whirlwind composed of a high temperature fuel and air mixture that has already been burned. A part of the fuel vapor which is shot out from the jet, within this small whirlwind, is cracked in a coking process and congeals to become a kind of "carbon gruel" which changes the angle of the spray. In order to prevent the overheating and accumulation of carbon which is mentioned above, it is possible to change the cone-shaped shell into a hemisphere-shaped "air flow guide", open small holes in the surface of this guide and open a number of supplementary intake holes in the top end of the flame tube (for example, the forward section of a turbine jet 7 is altered in precisely this manner). These small holes not only provide a supplementary supply of fresh air, but they also blow away the accumulation of carbon at the same time.

If the total amount of intake for each flame tube equals G, then, the amount of gases passing through the vortical flow device and entering the initial level, $G_1 \approx (9 - 10\%) G$; the amount of supplementary intake at the top end, $G_4 \approx 10\%\,G$; the amount of counter-current flow in the main combustion apertures, $G_2 \approx (8 \sim 10\%)G$; if we figure that $G_2 = (0.4 \sim 0.5)\ G_2$, then, G_2 = the amount of secondary gas intake entering from the main combustion aperture. The principle is that the overall

144

amount of intake in the main combustion area of the forward end of the flame tubes, $G_c + G_k + G_r = (28 - 30\%)$ G, which causes, in the area of main combustion, the average coefficient of residual gas, α, to be slightly larger than 1.0. The counter-current flow speed on the axis line of the counter-current flow area $-W_r$ is capable of being estimated on the basis of equations that have been previously discussed. If one considers the case in which there is no amount of supplementary gas coming from the top end ($G_k = 0$) and there is also no amount of secondary intake gas in the main combustion aperture ($G_c = 0$), then, due to the effect of eddy induction, the area ...... the .... core still ......ses a portion of the "circulation", G_r, and, ... an ....rical formula, that amount of circulation is

$$ G_r^\circ = 0.118(2R)^2 \sin^3\phi \cdot \rho W. \text{ [kg/s]}, \quad (6.62) $$

$\rho = $ ... . in the main area of combustion (kg/m^3). $W_r = $ .... on .... axis line (m/s).

... . amount of circulation is

$$ G_r = G_r^\circ \left(1 + \sqrt{\frac{G_k}{G_a}}\right)\left[1.75 + 0.75 \, \text{th} 2.4 \right. $$
$$ \left. \times \left(\frac{G_i}{G_a \sin\phi} - 2.05\right)\right]. \quad (6.63) $$

.. .. $\text{th}x = \dfrac{e^x - e^{-x}}{e^x + e^{-x}}$; .. ..

.... the .... on for this by ...ulting a table of data.
.. . ., it is ...ible to raise the exothermic stre-
..., ... of combustion; however, ... high altitude flights at low indica-
ted .....s, it is ... to ..... flameout to be premature. The main combustion aper-
tures sup..ly a secondary amount of gas, $G_2 = 2 \sim 3$ times G_0; the position of the
holes ..... are opened should be at the tail end point of the counter-current flow
.... or the ....m side; their depth of penetration should be $H \approx 0.6R$.

If the angle of installation of the vortical flow vanes of the vortical flow
.... is too great, and the rotation of the ring-shaped jet is too strong, then,
... axial flow speed, W, is too low, the amount of intake, G_0, is too small, and the
counter-current flow area is too long. In this type of situation, there is an exces-
sively rich fuel mixture and a scarcity of oxygen in the forward portion of the flame
tubes; combustion is slow; flames are long, and efficiency is low; however, this
condition is useful for reignition und r conditions of high altitude and low pres-
sure. In general, ϕ should be chosen so that it is less than or equal to $60°$.

The conic angle of the jet vapor from a centrifugal jet nozzle, Θ, ought to be
somewhat larger than the angle of expansion of the area of counter-current flow, α.

$$\text{tg}\left(\frac{\alpha_v}{2}\right) = \frac{0.5\, s}{l_1}; \quad \sigma \geq 2\left(\text{arc tg}\,\frac{0.5\, s}{l_1}\right); \quad (6.64)$$

The "vortical roll" in the wake of the area of counter-current flow comes from the formation of a high temperature gas flow in the area of violent combustion (the flame peak or tip). If the jets from the main combustion apertures and other holes cannot penetrate to the axis line, then, the twisting energy or capability of the long and thin "vortical rolls" is very strong, and the turbulence diffusion is very weak; therefore, it is possible to maintain a high temperature air flow right down to the exhaust of the flame tube, forming a "hot spot" in the temperature field of the exhaust, and this is very difficult to eliminate. The reason for this can also be traced to the fact that the angle of installation, ϕ, of the vertical flow vanes of the vertical flow device is too large. If one inserts a large funnel into the main combustion apertures in order to conduct gases in a fixed direction (as, for example, in a Spey flame tube), then, it is possible to push and squeeze the eddies forward, blow apart or shorten the vortical rolls, lower the smokiness and improve the temperature field of the exhaust. The practice of using transparent flame tubes of adequate dimensions in order to make model experiments with flowing water and equal Reynolds numbers has already proven to be an effective technique. We ought to explain Fig 6.12, which is nothing but an illustration of the form of a ring-shaped turbulence jet added to an eddy; this is not the same as a photograph of actual air flow structures.

Sec 11 Vortex Strength Numbers and Tests on Rotational Jets

The ring-shaped rotational jets at the exhaust of the vertical flow devices produce eddies and areas of counter-current flow, and it is possible to use these to control the shape of flames, their dimensions, their exothermic strength, their efficiency of combustion as well as their stability. Naturally, it is only possible to achieve satisfactory combustion capabilities when there is careful adjustment and coordination of the conic angle of fuel jet vaporization, σ, the amount of supplementary gas intake at the top end of the flame tubes, G_k, the positioning of the main flow apertures, the penetration depth, H and the amount of secondary gases supplied. However, the scope and strength of these rotational jets gives rise to a basic induction effect. The ratio of the rate of flow of the tangential momentum of the rotational jet to the rate of flow of its axial momentum is called the

146

"vortical strength number", S, and it represents the vortical strength number of the vortical flow device, which is,

$$S = \frac{M_\theta}{M_x r_2} = \frac{\text{the moment of angular momentum of the rotational jet}}{\text{the axial impulse strength x the radius of the exhaust of the vortical flow device}}$$

$$= \frac{\int_{r_1}^{r_2} \rho(Vr)W \cdot 2\pi r\,dr}{r_2\left[\int_{r_1}^{r_2} \rho W^2 \cdot 2\pi r\,dr + \int_{r_1}^{r_2} \Delta p\, 2\pi r\,dr\right]} \qquad (6.65)$$

We already know the tangential velocity, V, of the ring-shaped rotational jet at the exhaust of the vortical flow device as well as the axial flow speed, W, and the static pressure differential, Δp, in terms of the principles governing their distribution along r; only when these quantities and principles are known is it possible to integrate equation (6.65) in order to solve for the vortical strength number, S. If one already has the vortical flow device, then, it is possible to experimentally determine the axial impulse force, M_x, of the ring-shaped rotational jet as well as its moment of angular momentum, M$_\theta$. Fig 6.13 is an illustration which ... possible to take a vortical flow device and install it in the exhaust of a ... ... and to install at an appropriate distance outside the exhaust sensors for measuring force (for example, a ... ... spring supported flat plate), and, with this setup, how it is possible to measure the impulse force, M_x. In Fig 6.14, the vortical flow device is installed in the exhaust of the wind tunnel in the same way. If we use a smooth round tube with a rather large diameter to adjust to the vortical flow device, he rotational jet, when it enters the round tube, possesses a tendency to make the round tube follow it in its rotational motion. If one takes the round tube and places it on a torsional balance, then, it is possible to ... ... moment of angular momentum, M$_\theta$. In order to just be able to record accurate data, one can install, inside the after portion of the round tube, a fence-like plate that "combs out" the flow, and this eliminates the momentum of rotation; this, in turn causes, at point B outside the exhaust, the absence of any types of flow except the axial flow speed, W; the tangential flow speed, V≈0.

Considering Fig 6.13, if the static pressure, p, at the exhaust of the vortical flow device is equal to the pressure, p_a, of the surrounding environmental gases, then, $\Delta p = p - p_a = 0$; when this is the case, the impulse force, M'_x, that one measures, is only the rate of change of momentum per second of the jet as it collides with

147

the blocking plate. If one assumes that ρW^2 is a quantity distributed evenly along the radius, r, then, on the basis of that fact, the axial impulse force is

$$M'_a = \int_{r_1}^{r_2} \rho W^2 \cdot 2\pi r \, dr = \pi \rho W^2 (r_2^2 - r_1^2)$$

$$= \pi \rho W^2 r_2^2 \left[1 - \left(\frac{r_1}{r_2} \right)^2 \right] \qquad (6.66)$$

If the vortical flow device uses flat blades, and the angle of installation, ϕ, of the blades along the radius, r, does not change, then, from Fig 6.9 one can see that $V = W \, \mathrm{tg} \, \phi$, ; if one recognizes the fact that ρW^2 along r does not change, then, the moment of angular momentum

$$M'_\theta = \int_{r_1}^{r_2} \rho (V r) W \cdot 2\pi r \, dr = \pi \rho W^2 \, \mathrm{tg} \, \phi \int_{r_1}^{r_2} 2\pi r^2 \, dr$$

$$= \frac{2}{3} \pi \rho W^2 \, \mathrm{tg} \, \phi (r_2^3 - r_1^3) = M'_a \, \mathrm{tg} \, \phi \cdot r_2 \frac{2}{3}$$

$$\times \left[\frac{1 - \left(\frac{r_1}{r_2} \right)^3}{1 - \left(\frac{r_1}{r_2} \right)^2} \right] \qquad (6.67)$$

The "vorticity number" of the ring-shaped vortical flow device

$$S = \frac{M'_\theta}{M'_a r_2} = \frac{2}{3} \left[\frac{1 - \left(\frac{r_1}{r_2} \right)^3}{1 - \left(\frac{r_1}{r_2} \right)^2} \right] \cdot \mathrm{tg} \, \phi \qquad (6.68)$$

On the basis of this simplified method of calculation, it is only necessary to know the interior and exterior radii of the vortical flow device, r_1 and r_2, as well as the angle of installation of the blades, ϕ, and it then becomes possible to solve for the "vorticity number" or "vortical strength number," S'. This S' is higher than the S in equation (6.65).

When the "Vortical strength number", $S \leq 0.6$, this is called a weakly rotational flow in which there is present only an extremely weak counter-current flow and no eddies.

When the "Vortical strength number", $S > 0.6$, this is called a strongly rotational flow in which one can find both eddies and areas of counter-current flow.
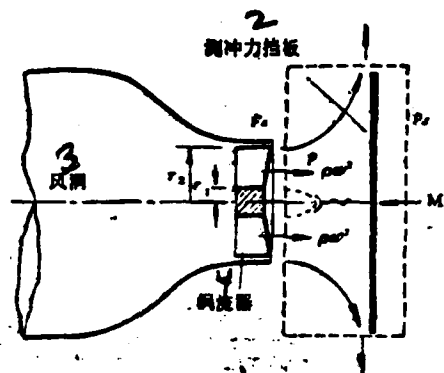
图6.13 实验测轴向冲力 M_x

Fig 6.13

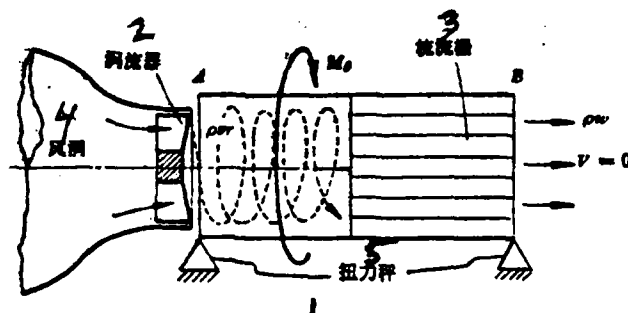1. Empirical Measurement of Axial Impulse Force, M_x. 2. Plate Measuring Impulse Force 3. Wind Tunnel

图6.14 实验测旋转射流角动量矩 M_θ

Fig 6.14

1. Experimental Measurement of the Moment of Angular Momentum of Rotational Jets, M_θ 2. Vertical Flow Device 3. Flow Comb Plate 4. Wind Tunnel 5. Torsion Balance

Sec 12 The Influence of "Vortex Strength Number" $\underline{s}$ on Aerodynamic Structures

(1) The influence of the "vortical strength number" on the efficiency of the vertical flow device, η_s.

The purpose of the vortical flow device is to produce a rotational jet; sim-

ilarly, a jet tube takes the power of lowered pressure and turns it into the kinetic energy of a jet. In the interval between the intake and the exhaust of the vortical flow device, $1\sim2$, it is appropriate to use Bernoulli's equation,

$$\int \frac{dp}{\gamma} + \frac{\overline{W}^2}{2g} + l_r = \text{a constant} \quad (6.69)$$

The kinetic energy put out by the jet every second is

$$E = \frac{G_c}{2g} \overline{W}^2 (1 + \delta S^2) \quad (6.70)$$

$l_r =$ the frictional power disipated by each kg of air as it flows past; if one assumes that γ does not change, then,

$$\int_1^2 \frac{dp}{\gamma} = \frac{-(p_1 - p_2)}{\gamma} = \text{the power of lowered pressure.}$$

δ is equal to a coefficient which is determined by the special characteristics of a vortical flow and the wheel hub ratio (r_4/r_2) in the vortical flow device; $\overline{W} =$ is the average axial flow speed at the exhaust of the vortical flow device.
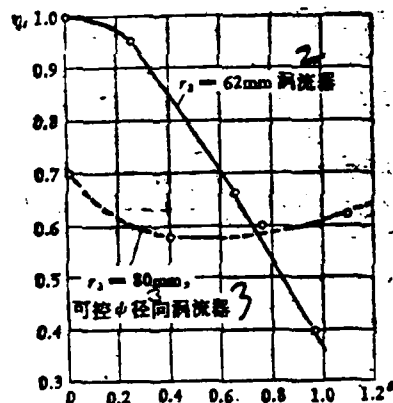

图 6.15 涡流器效率随 S 变化

Fig 6.15

1. The Efficiency of the Vortical Flow Device Varies With Changes in S 2. Vortical Flow Device 3. A Radial Vortical Flow Device Capable of Controling ψ

The efficiency of the vortical flow device is η, which is equal to the kinetic energy put out each second by the jet divided by the power of lowered pressure each second in the jet or

$$= \frac{\frac{G_0}{2g} \overline{W}^2 (1 + \delta S^2)}{\frac{G_0}{\gamma_-}(p_1 - p_2)} \quad (6.71)$$

Fig 6.15 graphically illustrates the way in which two types of vortical flow device efficiency, η_v, vary with changes in the vertical strength number, S. If one is looking from the point of view of the form of the axial blades, then, the efficiency, η_v, is very low when the vertical flow device has a high vertical strength number, $S \geqslant 1.0$. To the extent that the production of the required rotational or spiral flow speed requires a large pressure differential $(p_1 - p_2)$, then, to that extent, the hindrance to flow is very great. By the use of radial vortical flow devices which are capable of automatically controlling the angle of installation, ψ so that it is appropriate for different vertical strength numbers, S, it is possible to increase η_v.

(2) The influence of the "vertical strength number", S, on the velocity field.

The larger the vertical strength number, S, the larger the tangential component of velocity of the rotational jet will be; the smaller the axial component of velocity. That is, the larger the angle of expansion of the jet, 2ψ, will be; the stronger the eddies are, the larger the diameter of the eddies, a, will be; and, the larger the amount of gas which is induced to roll up backwards, the more violent the diffusion of the turbulent flow and the greater the amount of energy that is dissipated; because of all these facts, the various component velocities in the jet flow — radial velocity, u; tangential velocity, v; axial velocity, w— all become attenuated and reduced along the x axis very quickly. If one assumes that x/d at the exhaust of the vertical flow device is equal to 0, then, the three component velocities on the cross section are u_0, v_0 and w_0; further down the flow stream, for a different value, x/d_1, the maximum values for the three component velocities on the cross section are u_m, v_m and w_m. Fig 6.16 graphically presents the way in which experimental measurements show the attenuation and reduction of the three component velocities along x/d. The three vortical strength number curves are ① S = 0.47, ② S = 0.94, and ③ S = 1.57.

(3) The influence of the "vertical strength number", S, on the dimensions of the area of counter-current flow.

Fig 6.17 shows that the larger is the vertical strength number, S, the larger the dimensions of the area of counter-current flow will be. When the secondary amount of air, G_n, is added for the main combustion aperture, and the penetration of
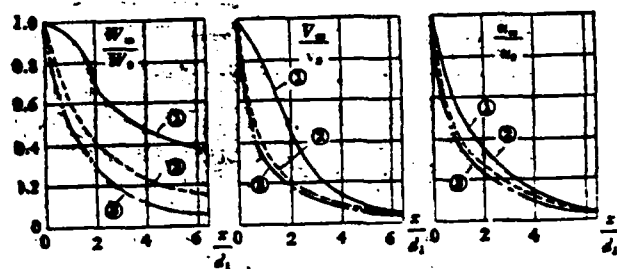
151

Fig 6.16

The Axial Attenuation and Reduction of the Three Component Velocities of a Rotational Jet

If it is relatively deep, then, it is possible to shorten the length of the area of counter-current flow, L. That guides can also shorten the area of counter-current flow.
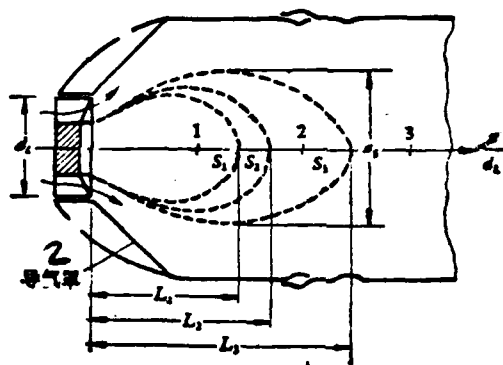

图6.17 旋强数 S 对逆流区尺寸的影响

$(S_1 = 0.78, S_2 = 1.04, S_3 = 1.43)$

Fig 6.17

1. Influence of the Vortical Strength Number, S, on the Dimensions of the Area of Counter-current Flow 2. Flow Guide

Fig 6.18 graphically shows the situation of distributions along the radius, r, of the three component vectors of velocity, u, v, and w, as well as the static pressure, p' when these quantities are measured from a cross section 10cm down the air flow from the vortical flow device; this Fig presents these distributions for the case in which, ① , there are no flow guides, and, ②, when flow guides are present; all the empirical measurements taken to construct the graphs in this figure were

152

taken assuming the same vortical flow device and the same vortical strength number, S.
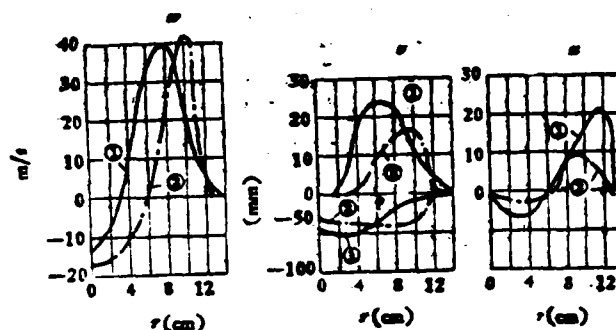

图6.18 ①无导气罩 ②有导气罩,铜流器下游 x = 10cm
截面上三个分速及静压 p 沿半径 r 分布情况

Fig 6.18

1. The Distributions Along the Radius, r, of the Three Component Velocities and the Static Pressure, p, as Measured on a Cross Section x = 10 cm Down the Flow Stream from the Vortical Flow Device for the Cases ① When There Are No Flow Guides and ② When Flow Guides Are Present

Chapter 7 Short Discussion of the Theory of Jets with Basic Equations

Sec 1 Physical Parameters of Turbulence Free Jets

Fig 7.1 shows a two-dimensional turbulent free jet form with a width = L, a height = $2b_0$, and an amount of flow put out by a narrow-crack jet = G_c. What is called a free jet is composed of homogeneous gases which are expelled into a space without being hindered or completely stopped. The uniform speed of the jet when it has just left the jet nozzle = u_0. The maximum flow speed for each of the various cross sections on the axis of symmetry, x, = u_m. The initial momentum flow rate of a stable jet at the jet nozzle = M_c. The jet induces the surrounding gases to roll back on themselves; it induces turbulence diffusion, and it induces the cross-current exchange of mass, momentum and energy. The farther out one goes from the jet nozzle, the more numerous are the surrounding gases which are pulled along by the jet, and the smaller is the amount of energy contained in each unit of mass. Therefore, the width of the jet, 2b, is quickly enlarged and expanded, so that the axial flow

speed, u, for the various cross sections are gradually reduced to lower values. On the basis of methods for the investigation and measurement of flow fields by making them visible, it has been discovered that jets can be divided into an "initial stage" and a "basic pattern stage". The area between the exterior and interior boundary lines of the jet is called a "turbulence boundary layer." Within the boundary layers, large amounts of turbulence flow cause pulsations in the masses of gas so that they rub against each other at a high frequency and a high speed causing friction: the viscous shear stress, τ_T, is much larger than the corresponding shear forces of stress, τ, for the two bound ry layers when they pass each other smoothly. Therefore, the turbulence viscosity, μ_T, as compared to the boundary layer viscosity, μ, can be 20 or 30 to as much as several hundred times larger. The rate of change of the turbulence shear stress, τ_T, in the y direction $(\partial \tau_T/\partial y)$ has a decisive influence on the nature of the distribution of the axial flow speed, u, along y.

The area from the jet nozzle to the point where the boundary layers come together is the initial stage; it is also the length of the jet core, s_0. The flow speeds at the various cross sections of the core of the jet are all equal to the uniform value, u_0. If one takes the two external boundary lines and extends them in the opposite direction to the current flow, then, they will intersect at the origin point (also called the point spring) 0. The distance from the origin point to the jet nozzle = h_0.

The peculiar characteristic of a turbulence free jet is this— the axial flow speed, u, for the gas flow in the "basic pattern stage" at various cross sections has distributions along y which are all governed by similar principles of rules; moreover, these have no relationship to the Reynolds number, Re. Looking at it from the point of view of probability theory, u is a random variable. The location of the various individual turbulence air masses changes randomly; however, when one is measuring the average values for the large-scale collective movements of turbulence air masses, then, it is possible to know the probability (that is to say, how big the chances are or what the possibility is) for the appearance of u at a certain set of coordinates. If we take ox as the axis of symmetry, $\pm$ y to be the horizontal coordinate, and the axial flow speed, u, to be the vertical coordinate, then, on the basis of measured data, it is possible to draw the distribution curves for distributions along y for the flow speed, u, for different cross sections, x, from the jet nozzle on out (Fig 7.2 (a) and Fig 7.1). These curves are all similar Gaussian normal distribution curves. The jet pulls on the surrounding gases and makes them roll up on themselves along x; it also increases the amount of common

gas flow and reduces u; therefore, the common gas flow, $G > G_o$. The jet expands and develops; however, the axial momentum flow rate, M is almost maintained unchanged.

At any given cross section, x, the coordinate, b, of the determined $u = \frac{1}{2} u_m$ represents half the width of expansion of the jet; the angle of expansion of the jet $= 2\alpha$. If one takes $(y/b) = \eta$ to be the horizonatal coordinate and takes $(u/u_m = f(\eta)$ to be the vertical coordinate, then, the flow speed distribution curves for different cross sections, x, are all induced to become a non-dimensionalized curve as shown in Fig 7.2 (b). This is precisely what is known as a wave form self-patterning curve. The black dots on the graph in the illustration are induced from experimental data; the continuous curve is figured out on the basis of Tollmien theory.

Sec 2 Expansion of Turbulence Free Jets

Within the basic or self patterning stage of a turbulence free jet, the flow speed, temperature and concentration at any given point all behave in the form of irregular pulsations. Instantaneous parameters = average time parameters + pulse parameters. If we take, as an example, a two-dimensional jet, then,

$$u = \bar{u} + u' \quad v = \bar{v} + v'$$

The average time value for the amount of pulse, $\overline{u'}$ and $\overline{v'}$ are both equal to zero. According to the Prandtl theory, on the basis of the concept of the free movement of molecules, the "free movement" or "free path of travel" of the turbulence gas bodies is equal to the cross flow mixing distance, 1. If one measures the pulse flow speed, u', and the average time flow speed gradient $(\partial \bar{u}/\partial y)$, then, it is possible to figure out the mixing distance, 1, as follows:

The pulse flow speed is approximately equal to the mixing distance times the flow speed gradient, u', which is approximately equal to $u' \cong l(\partial \bar{u}/\partial y)$ (7.1)

According to the concepts of elastic dynamics, we can imagine that the turbulence gas bodies are stretched out in the x direction due to the influence of the pulsations and shortened in the y direction for the same reason. This works both ways. Therefore, the pulse flow speed along y, v', and the pulse flow speed along x, u', are directly proportional; however, they have oppostie signs:

$$-v' \propto u', \quad -v' \cong l(\partial \bar{u}/\partial y) \qquad (7.2)$$

Inside and outside the boundary layers of turbulence free jets, there are no

755
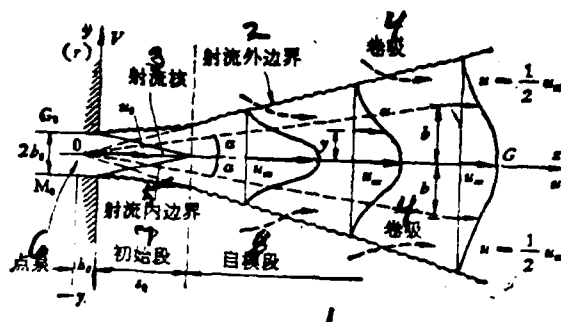
图7.1 二元紊乱自由射流几何特征示意

Fig 7.1

1. A Picture of the Geometrical Characteristics of a Disturbed Two-Dimensional Free Jet 2. Exterior Boundary of the Jet 3. Core of the Jet 4. Roll Back Attraction
5. Interior Boundary Line of the Jet 6. Point Spring of Source 7. Initial Stage
8. Basic Pattern or Self-Patterning Stage

图7.2 二元紊乱射流速u沿y分布自模化

Fig 7.2

1. Self-Patterning of Distributions Along y of Jet Speed, u, in a Two-dimensional Disturbed Jet 2. Distance From the Jet Nozzle 3. Tollmien Theory Calculations

图7.3 紊流射流流场自模段的 $(u/u_m) =$ const 直线

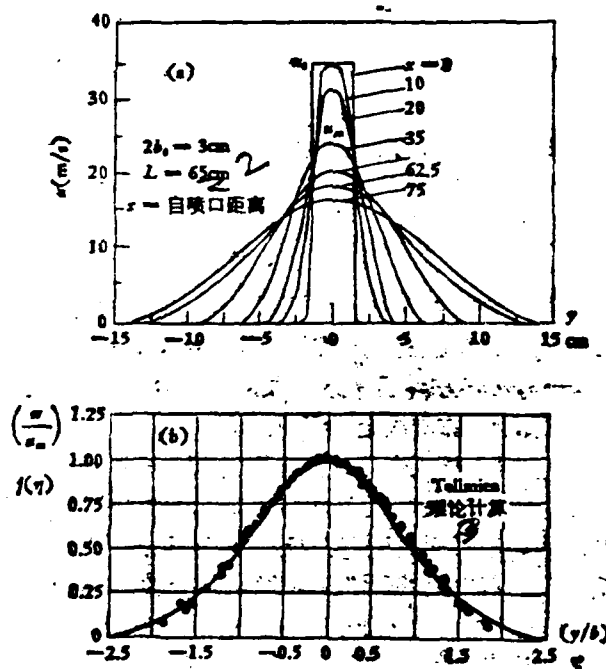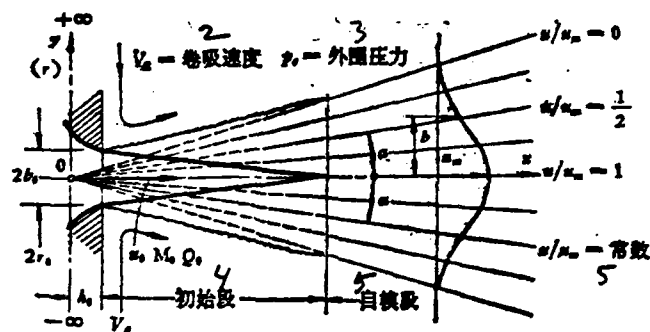solid obstacles to hinder gas flow pulsations; therefore, it is possible to con-
sider the mixing distance, l, to be constant in the y direction.

Besides this, from Fig (7.2) (b) it can be seen that the ratio of flow speeds
for various cross sections of the basic pattern or self-patterning stage (u/u_m)
follows the pattern curve of the non-dimensional coordinates, $n = (y/b)$ and is a
probability density curve for a Gaussian normal distribution. Therefore, it is
possible to recognize that fact that the mixture distance, l, for different cross
sections of a two-dimensional point spring or point source turbulence jet are in
direct proportion with the half-width, b, of these cross sections

$$l = \beta b, \quad \beta = \text{proportional constant} \quad (7.3)$$

Prandtl assumes that the rate of expansion and development of the half-width,
b, of the turbulence boundary layers is in proportion to the horizontal pulse flow
speed, v', as follows:

$$\frac{db}{dt} \propto v' \cong -l\frac{\partial \bar{u}}{\partial y}, \quad \frac{\partial \bar{u}}{\partial y} < 0; \quad (7.4)$$

The flow speed gradient of the various cross sections, $(\partial \bar{u}/\partial y)$ is proportional
to the height-to-width ration (u_m/b) of the flow speed distribution curves for these
cross sections. $u = (dx/dt), u \propto u_m$; therefore, equation (7.4) becomes

$$\left(\frac{db}{dt}\right) \cong \text{constant} \cdot b \cdot (u_m/b) = \text{constant} \cdot u_m \quad (7.5)$$

$$\left(\frac{db}{dt}\right) = \frac{db}{dx} \cdot \frac{dx}{dt} = \text{constant} \frac{db}{dx} u_m \quad (7.6)$$

If one compares equation (7.5) to equation (7.6), it is possible to determine that

$$\frac{db}{dx} = \text{a constant}$$

or $b = Cx$ (7.7)

Fig 7.3 shows that, in the basic pattern or self-patterning stage of the jet,
if one connects the constants, (u/u_m), for the various cross sections into a straight
line, then, that line is the radial line, $tg\alpha = (y/x)$, which starts at
the point source, O, and moves out at a constant angle of expansion, α .

The conclusions in this section are also appropriate for use in the self-pat-
terning stages of the axisymmetric flow fields of round jet nozzles. All that is

157

necessary to make the transition is to change $2b_o$ into $(2r_c)$ and y into (r).

Sec 3   Gaussian Normal Distribution and Probability Density

When one is doing experiments, one measures a certain physical parameter n times and obtains the data, s_1, s_2, s_3 ... s_n. The average arithmetical values for these data, $A = \frac{1}{n} \Sigma s_i \, (i = 1, 2, \cdots n.)$, have the highest probabilities and are closest to the actual values of the parameters measured. The error in measurement is $\eta_i = s_i - A$. When the distribution interval of error, $\Delta \eta$, is small enough, and measured values, s, which fall in the range between η and $\eta + \Delta \eta$ are not more numerous than 1, then, it is possible to recognize the following:

When the error is η_1, the probability of the measured value, s_1, appearing is
$$\mathscr{P}_1 = f(\eta_1)\Delta\eta,$$

When the error is η_2, the probability of the measured value, s_2, appearing is
$$\mathscr{P}_2 = f(\eta_2)\Delta\eta,$$

When the error is η_i, the probability of the measured value, s_i, appearing is
$$\mathscr{P}_i = f(\eta_i)\Delta\eta,$$

When the error is η_n, the probability of the measured value, s_n appearing is
$$\mathscr{P}_n = f(\eta_n)\Delta\eta.$$

$f(\eta)$ is called the probability density function of a normal distribution of error. What is meant by this normal distribution is that the opportunities for the appearance of small errors are greater than the opportunities for the appearance of large errors; and, at the point where $\eta = 0$, the probability density reaches its maximum value; the frequency of opportunities for the appearance of errors which are equal in magnitude but have opposite signs are the same, which leads to the fact that the probability distribution in question is the axially symmetric curve with $\eta = 0$. The probability of the appearance of an error which is of maximum value and has a positive sign is unusually small, that is to say, $f(\pm\infty) \to 0$.

Because of that fact that each of the various measurements are taken of mutually unrelated events, therefore, the total probability of the simultaneous appearance of the various types of measurement errors is the product of all the probabilities:

$$\mathscr{P} = f(\eta_1)f(\eta_2)\cdots f(\eta_i)\cdots f(\eta_n)(\Delta\eta)^n \qquad (7.8)$$

If one takes the logarithms of the two sides of the equation above, then, one obtains

$$\ln \mathscr{P} = \ln f(\eta_1) + \ln f(\eta_2) + \cdots$$
$$+ \ln f(\eta_n) + n \ln (\Delta \eta) \qquad (7.9)$$

Since the average arithmetical value, A, is the maximum probability of appearance of the measured value, then, $\ln \mathscr{P}$ should have a maximum value, and, differentiating over A, equation (7.9) ought to be equal to zero. $\Delta \eta$ is unrelated to A.

$$\frac{d(\ln \mathscr{P})}{dA} = \frac{d \ln f(\eta_1)}{d\eta_1} \frac{d\eta_1}{dA} + \frac{d \ln f(\eta_2)}{d\eta_2} \frac{d\eta_2}{dA}$$
$$+ \cdots \frac{d \ln f(\eta_n)}{d\eta_n} \frac{d\eta_n}{dA} = 0 \qquad (7.10)$$

Because of the fact that $\qquad \eta_i = s_i - A, \; d\eta_i/dA = -1 \qquad$; therefore,

$$\frac{df(\eta_1)}{d\eta_1 f(\eta_1)} + \frac{df(\eta_2)}{d\eta_2 f(\eta_2)} + \cdots + \frac{df(\eta_n)}{d\eta_n f(\eta_n)} = 0 \quad (7.11)$$

If one assumes that $\qquad \phi(\eta_i) = \frac{df(\eta_i)}{d\eta_i f(\eta_i)}, \; i = 1, 2, \cdots n \qquad (7.12)$

then, equation (7.11) can be written in the form

$$\phi(\eta_1) + \phi(\eta_2) + \cdots \phi(\eta_n) = \sum_{i=1}^{n} \phi(\eta_i) = 0 \quad (7.13)$$

According to the methods used for solving differential equations, take $\phi(\eta_i)$ and represent it in the form of an exponential series

$$\phi(\eta_1) = C_0 + C_1 \eta_1 + C_2 \eta_1^2 + C_3 \eta_1^3 + \cdots$$
$$\phi(\eta_2) = C_0 + C_1 \eta_2 + C_2 \eta_2^2 + C_3 \eta_2^3 + \cdots$$
$$\vdots$$
$$\phi(\eta_n) = C_0 + C_1 \eta_n + C_2 \eta_n^2 + C_3 \eta_n^3 + \cdots$$

From equation (7.13), we obtain

$$\sum_{i=1}^{n} \phi(\eta_i) = n C_0 + C_1 \sum_{i=1}^{n} \eta_i + C_2 \sum_{i=1}^{n} \eta_i^2$$
$$+ C_3 \sum_{i=1}^{n} \eta_i^3 + \cdots = 0 \qquad (7.14)$$

It is necessary first to satisfy equation (7.13) and then the various quantities in equation (7.14) will be equal to zero, and the constants, C_o, C_2 and so on must all be equal to zero. However, from the definition of an average arithmetical value, it should be true that

$$\sum_{i=1}^{n} \eta_i = \sum_{i=1}^{n} (s_i - A) = \sum_{i=1}^{n} s_i - nA = 0 \quad (7.15)$$

In equation (7.14), the factor of C_1, $\sum_{i=1}^{n} \eta_i$ is already equal to zero. If two numbers are multiplied together, and one of them is equal to zero, then, the other one cannot help but be equal to zero; therefore, it is not necessary for C_1 to be equal to zero. Because of this fact, from equation (7.1?), we can obtain

$$\phi(\eta) = \frac{df(\eta)}{d\eta f(\eta)} = C_1 \eta, \; \frac{df(\eta)}{f(\eta)} = C_1 \eta d\eta$$

When we solve for the integral, we obtain

$$\ln f(\eta) = \frac{1}{2} C_1 \eta^2 + \ln K, \text{ or } f(\eta) = K e^{C_1 \eta^2 / n} \quad (7.16)$$

When $\eta = 0$, $f(\eta)$ reaches its maximum value, K; when $\eta \to \pm \infty$, $f(\eta) \to 0$. Therefore, from equation (7.14), we know that C_1 must have a negative value. If we assume that $\frac{1}{2} C_1 = - h^2$, then, we obtain

$$f(\eta) = K e^{-h^2 \eta^2} = K \exp(-h^2 \eta^2) \quad (7.17)$$

According to the characteristics of a Gaussian normal distribution, the integral of the probability density, $f(\eta)$, between $\pm \infty$ ought to be equal to 1. And, if the appearance of a certain measured parameter, s_i, is considered to always be significant, then, the probability of the appearance of the parameter is equal to 1, and it will certainly appear:

$$\mathscr{P} = \int_{-\infty}^{+\infty} f(\eta) d\eta = \int_{-\infty}^{+\infty} K e^{-h^2 \eta^2} d\eta = 1 \quad (7.18)$$

If we assume that $h\eta = x$, $d\eta = dx/h$, then, because $f(\eta)$ and $\eta = 0$ are axisymmetric

$$2K \int_{0}^{\infty} e^{-x^2} \frac{dx}{h} = \frac{2K}{h} \cdot \frac{\sqrt{\pi}}{2} = 1, \qquad \text{therefore} \qquad K = \frac{h}{\sqrt{\pi}},$$

160

The probability density function

$$f(\eta) = \frac{h}{\sqrt{\pi}} e^{-h^2\eta^2}, \quad \eta = 0, \quad f(0) = \frac{h}{\sqrt{\pi}}; \quad (7.19)$$

h = the accuracy factor which determines the slope of the probability density curve.

If one assumes that $h = \frac{1}{\sigma\sqrt{2}}$, then, σ = the "standard deviation" or, as it is also called, the root-mean-square of error or deviation which determines the gentleness of the probability density curve. Another form of the Gaussian normal distribution of the probability density function is

$$f(\eta) = \frac{1}{\sigma\sqrt{2\pi}} e^{-\eta^2/2\sigma^2} = \frac{1}{\sigma\sqrt{2\pi}} \exp\left(-\frac{\eta^2}{2\sigma^2}\right) \quad (7.20)$$

If we take $x = h\eta$ and substitute it into equation (7.19), then, it is possible to reintegrate and obtain the error or deviation function:

$$\frac{2}{\sqrt{\pi}} \int_0^{h\eta} e^{-x^2} dx = \text{erf}(h\eta) \quad (7.21)$$

Sec 4   Basic Equations of Turbulence Jet Fields

Concerning the case of a jet which is viscous, compressible and composed of actual gases and is being impelled into an unlimited space, if the Reynolds number, Re, is quite low, then, it is possible to recognize that the flow of gases is divided into layers of slippage which leads to a laminar flow. If we assume that $\mathbf{V}$ = the vector of flow speed, ρ = gas density, μ = the viscosity of laminar flow, p = pressure, and we ignore gravity, then, the vector form of the n-dimensional Stokes equation is similar to equation (5.31), or,

$$\rho\frac{d\mathbf{V}}{dt} = -\nabla p + \frac{1}{3}\mu\nabla\cdot(\nabla\cdot\mathbf{V}) + \mu\nabla^2\cdot\mathbf{V} \ [\text{N/m}^3],$$

$$(7.22)$$

In actuality, turbulence jet fields are large and small vertical masses rolling over each other and pulsating. The physical parameters can be represented as:

$$u = \bar{u} + u', \quad v = \bar{v} + v', \quad w = \bar{w} + w', \quad p = \bar{p} + p',$$
$$T = \bar{T} + T', \quad \rho = \bar{\rho} + \rho', \quad \rho u = \overline{\rho u} + (\rho u)'$$

and so on.

Because of the fact that the vertical masses rub against each other producing friction and excessive "turbulence flow stress" (normal stress, $\bar{\sigma}$, and shear or tan-

gential stress), the tensor for turbulence flow stress, II, has a mutual correspond-
ance with the tensor of the average time value of the product of the pulsation vec-
tors:

$$
\Pi = \begin{Bmatrix} \sigma_x & \tau_{xy} & \tau_{xz} \\ \tau_{yx} & \sigma_y & \tau_{yz} \\ \tau_{zx} & \tau_{zy} & \sigma_z \end{Bmatrix} = \begin{Bmatrix} -\overline{(\rho u)'u'} & -\overline{(\rho u)'v'} & -\overline{(\rho u)'w'} \\ -\overline{(\rho v)'u'} & -\overline{(\rho v)'v'} & -\overline{(\rho v)'w'} \\ -\overline{(\rho w)'u'} & -\overline{(\rho w)'v'} & -\overline{(\rho w)'w'} \end{Bmatrix}
$$

In the n-dimensional equation for a turbulence jet flow field, one should in-
clude divergence, $\nabla \cdot \Pi$, of the tensor for the turbulence flow stresses (also called
Reynolds stresses), that is,

$$
\rho \frac{D\mathbf{V}}{Dt} = -\nabla p + \mu \nabla^2 \cdot \mathbf{V} + \frac{1}{3} \mu \nabla \cdot (\nabla \cdot \mathbf{V}) - \nabla \cdot \Pi
$$

$$(7.23)$$

If, in the combustion chamber, the flow speed is not high, $\mathbf{V} \leqslant 60$ (m/s), then,
to simplify manipulations, it is possible to ignore compressibility, that is to say,
$\rho = $ a constant and does not change; in such a case, in equation (7.23), the quan-
tity, $\nabla \cdot \mathbf{V}$, which stands for the "divergence" of the flow field, is equal to zero.
Due to this fact, the Reynolds equation for a turbulence jet flow field which is not
compressible and has an equivalent viscosity can be simplified to read

$$
\rho \frac{\partial \mathbf{V}}{\partial t} + \rho \mathbf{V} \cdot \nabla \mathbf{V} = -\nabla p + \mu \nabla^2 \cdot \mathbf{V} - \nabla \cdot \Pi \quad (7.24)
$$

Using a rectilinear coordinate system in x, y, and z, if we take the average
time velocity components, $\bar{u}$, $\bar{v}$, and $\bar{w}$, and add them to the pulse velocity components,
u', v', and w', and use these components to replace the instantaneous velocity com-
ponents, u, v, and w, then, assuming that the dynamic viscosity of laminar flow, ν
$= (\mu/\rho)$, and we can expand equation (7.24) into the three equations

$$
\frac{\partial \bar{u}}{\partial t} + \bar{u} \frac{\partial \bar{u}}{\partial x} + \bar{v} \frac{\partial \bar{u}}{\partial y} + \bar{w} \frac{\partial \bar{u}}{\partial z} = -\frac{1}{\rho} \frac{\partial \bar{p}}{\partial x}
$$
$$
+ \nu \left(\frac{\partial^2 \bar{u}}{\partial x^2} + \frac{\partial^2 \bar{u}}{\partial y^2} + \frac{\partial^2 \bar{u}}{\partial z^2} \right) - \left(\frac{\overline{\partial u'^2}}{\partial x} + \frac{\overline{\partial u'v'}}{\partial y} + \partial \frac{\overline{u'w'}}{\partial z} \right)
$$
$$
\frac{\partial \bar{v}}{\partial t} + \bar{u} \frac{\partial \bar{v}}{\partial x} + \bar{v} \frac{\partial \bar{v}}{\partial y} + \bar{w} \frac{\partial \bar{v}}{\partial z} = -\frac{1}{\rho} \frac{\partial \bar{p}}{\partial y}
$$

$$+ \nu\left(\frac{\partial^2 \bar{v}}{\partial x^2} + \frac{\partial^2 \bar{v}}{\partial y^2} + \frac{\partial^2 \bar{v}}{\partial z^2}\right) - \left(\frac{\partial \overline{v'u'}}{\partial x} + \frac{\partial \overline{v'^2}}{\partial y} + \frac{\partial \overline{v'w'}}{\partial z}\right)$$

$$\frac{\partial \bar{w}}{\partial t} + \bar{u}\frac{\partial \bar{w}}{\partial x} + \bar{v}\frac{\partial \bar{w}}{\partial y} + \bar{w}\frac{\partial \bar{w}}{\partial z} = -\frac{1}{\rho}\frac{\partial \bar{p}}{\partial z}$$

$$+ \nu\left(\frac{\partial^2 \bar{w}}{\partial x^2} + \frac{\partial^2 \bar{w}}{\partial y^2} + \frac{\partial^2 \bar{w}}{\partial z^2}\right) - \left(\frac{\partial \overline{w'u'}}{\partial x} + \frac{\partial \overline{w'v'}}{\partial y} + \frac{\partial \overline{w'^2}}{\partial z}\right)$$

$$(7.25)$$

The continuity equation of the flow field is

$$\nabla \cdot \mathbf{V} = \frac{\partial \bar{u}}{\partial x} + \frac{\partial \bar{v}}{\partial y} + \frac{\partial \bar{w}}{\partial z} = 0 \qquad (7.26)$$

Sec 5. Momentum Equations for Flat Mouth Turbulence Jets

If we assume that we are dealing with an average time quasi-steady state flow field, then, $\bar{u}$, $\bar{v}$, and $\bar{w}$ are average time flow speeds, that is to say, $(\partial \bar{u}/\partial t)=0$, $(\partial \bar{v}/\partial t)=0$. If one is dealing with a two-dimensional flow field

$$\bar{w}=0, \quad w'=0, \quad \overline{u'w'}=0, \quad \overline{v'w'}=0.$$

[several faded lines of text] According to the special case of mixing, $\bar{u} \gg \bar{v}$; the flow speed gradient of the [...] and the corresponding gradients also [...]

$$(\partial \bar{u}/\partial y) \gg (\partial \bar{u}/\partial x), \quad (\partial \tau/\partial y) \gg (\partial \tau/\partial x).$$

[faded line of text]

$$\bar{u}\frac{\partial \bar{u}}{\partial x} + \bar{v}\frac{\partial \bar{u}}{\partial y} = -\frac{1}{\rho}\frac{\partial \bar{p}}{\partial x} + \nu\frac{\partial^2 \bar{u}}{\partial y^2} - \frac{\partial \overline{u'^2}}{\partial x} - \frac{\partial \overline{u'v'}}{\partial y}$$

$$\tag{7.27}$$

$$0 = -\frac{1}{\rho}\frac{\partial \bar{p}}{\partial y} - \frac{\partial \overline{v'^2}}{\partial y} \tag{7.28}$$

$$\frac{\partial \bar{u}}{\partial x} + \frac{\partial \bar{v}}{\partial y} = 0 \tag{7.29}$$

[several faded lines of text] continuously, since the pressure is $\bar{p}_e$, and that the pressure of the environment surrounding the jet is p_e; then, if we integrate equation (7.28) from y out to the environment, we get

$$\bar{p} = p_e - \rho\overline{v'^2}$$

If we differentiate the equation above by x, we obtain

$$(d\bar{p}/dx) = (dp_e/dx) - \rho\frac{\partial}{\partial x}(\overline{v'^2})$$

162b

If we take the equation above, and substitute it into equation (7.?); then, we obtain:

$$\bar{u}\frac{\partial \bar{u}}{\partial x} + \bar{v}\frac{\partial \bar{u}}{\partial y} = -\frac{1}{\rho}\frac{dp_e}{dx} + \nu\frac{\partial^2 \bar{u}}{\partial y^2} - \frac{\partial \overline{u'v'}}{\partial y}$$

$$- \frac{\partial}{\partial x}(\overline{u'^2} - \overline{v'^2}) \qquad (7.27)\,(a)$$

In the flow field approximating similar turbulence flow characteristics in various directions, then: $\overline{u'^2} \cong \overline{v'^2}$. If one is constructing a jet which is projecting into a stationary gas in an unlimited space, then, the pressure, p_e, in the environment around the jet is a constant, that is to say, $(dp_e/dx) = 0$. Therefore, equation (7.27) (a) can be simplified as such:

$$\bar{u}\frac{\partial \bar{u}}{\partial x} + \bar{v}\frac{\partial \bar{u}}{\partial y} = \frac{1}{\rho}\frac{\partial}{\partial y}\left(\mu\frac{\partial \bar{u}}{\partial y}\right) + \frac{1}{\rho}\frac{\partial}{\partial y}(-\rho\overline{u'v'})$$

$$= \frac{1}{\rho}\frac{\partial}{\partial y}(\tau_L + \tau_T)$$

In the equations above, τ_L = the laminar flow shear force, and $\tau_T = \tau_{xy} = -\rho\overline{u'v'}$ is the turbulence flow shear force. The turbulence flow shear force, τ_T, is equal to several hundred times the laminar flow shear force, τ_L. That is to say that the motion and turbling exchange and motion of the vertical masses is much more violent than the exchange of momentum which takes place in the free collisions of molecules. Therefore, it is possible to ignore the laminar flow shear force, τ_L. Later, in our discussion of turbulence flow fields, we will use μ_m to represent the turbulence flow viscosity and τ_T to represent turbulence flow shear force. This means that the symbols, u and v, for average time flow speeds, will no longer be dealt with.

Finally, we can obtain the basic equations for a point source, non-compressible, two-dimensional turbulence flow field:

$$u\frac{\partial u}{\partial x} + v\frac{\partial u}{\partial y} = \frac{1}{\rho}\frac{\partial \tau_T}{\partial y} \qquad (7.30)$$

$$\frac{\partial u}{\partial x} + \frac{\partial v}{\partial y} = 0, \qquad (7.31)$$

162c

Sec 6 Integrals of Momentum Equations and Force Net Analysis

Take a look at Fig 7.3 to see what happens when a point source disturbed jet is impelled into an unlimited space filled with gases at rest. According to the previous section's analysis, we will simplify our equations and take the pressure gradient $(\partial p_e/\partial u)$ to be equal to zero along the direction of the main flow, x. If we ignore gravity, then, the jet expands freely into surroundings of equal pressure, induces the gases around itself to roll up along the path of the flow, and this induction has a velocity, u_e. Because there are no obstacles in the form of external forces, it is possible to predict the momentum flow rate, M, of the jet along the x axis, and the fact that it will be equal to M_c and will be conserved and unchanging. From the axis line of the jet, $y = 0$, to $y = \infty$, if we integrate equation (7.30), then,

$$\rho \int_0^\infty u \frac{\partial u}{\partial x}\,dy + \rho \int_0^\infty v \frac{\partial u}{\partial y}\,dy = \int_0^\infty \frac{\partial \tau_T}{\partial y}\,dy \quad (7.32)$$

If we separately solve the three integrals in equation (7.32), then, we get

$$\rho \int_0^\infty u \frac{\partial u}{\partial x}\,dy = \frac{1}{2}\int_0^\infty \frac{\partial}{\partial x}(\rho u^2)\,dy = \frac{1}{2}\frac{d}{dx}\int_0^\infty \rho u^2\,dy$$

By utilizing equation (7.31), we can get

$$\rho \int_0^\infty v \frac{\partial u}{\partial y}\, dy = \rho \left| uv \right|_0^\infty - \rho \int_0^\infty u \frac{\partial v}{\partial y}\, dy$$

$$= 0 + \rho \int_0^\infty u \frac{\partial u}{\partial x}\, dy$$

The boundary conditions are

when $y = 0$, $u = u_m$, $v = 0$; when $y = \infty$, $u = 0$,

$v = v_e$, therefore $\left| uv \right|_0^\infty = 0$;

Therefore, the two quantities on the left side of equation (7.32) are

$$\rho \int_0^\infty u \frac{\partial u}{\partial x}\, dy + \rho \int_0^\infty v \frac{\partial u}{\partial y}\, dy = 2\rho \int_0^\infty u \frac{\partial u}{\partial x}\, dy$$

$$= \frac{d}{dx} \int_0^\infty \rho u^2 dy.$$

The turbulence shear force, $\tau_T = -\rho \overline{u'v'}$, when $y = 0$ and $v' = 0$; when $y = \infty$, and $u' = 0$, the right side of equation (7.32) is

$$\int_0^\infty \frac{\partial \tau_T}{\partial y}\, dy = \left| \tau_T \right|_0^\infty = \tau_T(\infty) - \tau_T(0) = 0.$$

Because of this fact, equation (7.32) is

$$\frac{d}{dx} \int_0^\infty \rho u^2 dy = 0,$$

$$2 \int_0^\infty \rho u^2 dy = M = M_0 = \text{constant} = 2\rho b_0 u_0^2 \qquad (7.33)$$

Concerning an explanation of equation (7.33), the following conditions apply: a flat jet nozzle with a height of $2b_0$, a width of 1 perpendicular to the surface of the illustration, a jet nozzle flow speed of u_0, and an initial momentum flow rate, $M_0 = 2b_0 \rho u_0^2$. Because of the fact that the surrounding gases are induced to roll back up on themselves and add to the amount of flow, on the axis line, the flow speed, u_m, along x is reduced; however, the momentum flow rate of the jet is still maintained in a constant state, so that $M = M_0$.

Sec 1 of this chapter talks about the fact that the patterned function of flow speed distribution in the self-patterning stage of a jet, f, only varies with changes in η and does not vary with changes in x, that is to say,

164

$$\frac{u}{u_m} = f(\eta), \quad \eta = \frac{y}{b}, \quad u = u_m f(\eta) = u_m f;$$

If one assumes that the rule according to which the flow speed, u_m, or the axis line, reduces to lower values with changes in x can be written as $u_m \propto x^p$ (7.34), then, the rule according to which the half-width of a jet, b, expands with changes in x will be $b \propto x^q$ (7.35).

$$\frac{d}{dx} \int_0^\infty \rho u^2 dy = \frac{d}{dx} \int_0^\infty \rho u_m^2 b f^2 d\eta = 0, \quad dy = bd\eta,$$

u_m and b do not vary with changes in η, and

$$\frac{d}{dx} \rho b u_m^2 \int_0^\infty f^2 d\eta = 0,$$

According to equation (7.37),

$$\int_0^\infty f^2 d\eta = \text{a constant}$$

Therefore, it is necessary that $\quad \frac{d}{dx}(bu_m^2) = 0 \quad$, that is to say,

(bu_m^2) has a product which is unrelated to x.

According to vector net analysis, it should be true that $(bu_m^2) \propto x^0$; according to equation (7.34) and equation (7.35), that means that $x^{q+2p} \propto x^0$, and this also leads to the conclusion that

$$q + 2p = 0 \qquad\qquad (7.36)$$

According to empirical analysis and vector net analysis, it is possible to to write the non-dimensional ratio of values:

$$\frac{\tau_T}{\rho u_m^2} = g(\eta) = g, \quad \text{or } \tau_T = \rho u_m^2 g(\eta) = \rho u_m^2 g \quad (7.37)$$

Substituting the last quantity into equation (7.30) we get

$$\frac{1}{\rho}\frac{\partial \tau_T}{\partial y} = \frac{1}{\rho}\frac{\partial}{\partial y}(\rho u_m^2 g) = u_m^2 \frac{\partial g}{\partial \eta} \cdot \frac{\partial \eta}{\partial y} = \frac{u_m^2}{b} g' \quad (7.38)$$

165

If we take the patterned function $u = u_m f$ and substitute it into equation (7.38), then, the two quantities on the left side are

$$\frac{\partial u}{\partial x} = \frac{\partial}{\partial x}(u_m f) = u_m \frac{df}{d\eta}\frac{\partial \eta}{\partial b}\frac{db}{dx} + f\frac{du_m}{dx},$$

$$\frac{\partial \eta}{\partial b} = -\frac{y}{b^2} = -\frac{\eta}{b};$$

In the equations above

$$f' = \frac{df}{d\eta}, \quad b' = \frac{db}{dx}, \quad u_m' = \frac{du_m}{dx},$$

Then this is true

$$\frac{\partial u}{\partial x} = f u_m' - u_m f'\frac{\eta}{b}b';$$

Because this is true

$$u\frac{\partial u}{\partial x} = u_m u_m' f^2 - \frac{u_m^2 b'}{b}\eta f f' \qquad (7.39)$$

$$v = \int_0^y \frac{\partial v}{\partial y}\,dy = -\int_0^y \frac{\partial u}{\partial x}\,dy = \int_0^y \left(\frac{b'}{b}u_m \eta f' - u_m' f\right)dy,$$

$$= u_m b' \int_0^\eta \eta f' d\eta - u_m' b \int_0^\eta f d\eta,$$

$$v = u_m b'\left(\eta f - \int_0^\eta f d\eta\right) - u_m' b \int_0^\eta f d\eta.$$

$$\frac{\partial u}{\partial y} = \frac{\partial}{\partial y}(u_m f) = u_m f'\frac{\partial \eta}{\partial y} = \frac{u_m}{b}f',$$

Therefore,

$$v\frac{\partial u}{\partial y} = \frac{u_m^2 b'}{b}\left(\eta f f' - f'\int_0^\eta f d\eta\right) - u_m u_m' f'\int_0^\eta f d\eta \quad (7.40)$$

If we take equations (7.39), (7.39), and (7.40) and substitute them into equation (7.38), then,

$$u_m u_m' f^2 - \frac{u_m^2 b'}{b}\eta f f' + \frac{u_m^2 b'}{b}\left(\eta f f' - f'\int_0^\eta f d\eta\right)$$

$$- u_m u_m' f'\int_0^\eta f d\eta = \frac{u_m^2}{b}f'$$

166

$$\frac{bu_m'}{u_m}\left(p - f'\int_0^\eta f d\eta\right) - b'f'\int_0^\eta f d\eta = g' \qquad (7.41)$$

In equation (7.41), g' on the right side of the equal sign is nothing but a function of η; therefore, the various quantities on the left side of the equal sign must also simply be functions of η. If these conditions are to be satisfied, then, it is necessary that b' and $\left(\frac{bu_m'}{u_m}\right)$ both do not vary with changes in x, that is to say, $x^{q+p-1+p} = x^{q-1} = x^0$, , so $q = 1$.

If we substitute this into equation (7.36), then, we obtain

$$p = -\frac{1}{2};$$

Therefore:

$$u_m \propto \frac{1}{\sqrt{x}} \text{ and } b \propto x \qquad (7.42)$$

Sec 7 Curl Intake Gas Volume Theory

If we assume a dimension of 1 perpendicular to the surface of the illustration, then, the initial jet m volume of the flat jet in Fig 7.7 is $Q_c = 2b_0 u_c \ (m^2/s)$. Because of the fact that the surrounding gases are induced to roll up, the gas flow volume for a given cross section of the jet somewhere down the flow is $Q > Q_c$:

$$Q = 2\int_0^\infty u \, dy, \ \frac{dQ}{dx} = 2\frac{d}{dx}\int_0^\infty u \, dy = 2v_e$$

which is equal to the rate of increase of the gas volume along x $(m^2/m \cdot s)$. (7.43)

On the axis line, the faster the flow speed is, the stronger is the strength of the force inducing the surrounding gases to roll up; the gathering of the flow of the surrounding gases along the axis line adds to the jet flow, and the stronger the inducing force, the stronger this tendency is; therefore, v_e and u_m are in direct proportion with each other.

If we assume that a_e = the coefficient of roll induction, then, $v_e = a_e u_m$, a_e

which does not vary with changes in x; because of this fact,

$$\frac{d}{dx}\int_0^\infty u\,dy = a_1 u_m, \text{ or } \frac{d}{dx}(u_m b)\int_0^\infty f\,d\eta = a_1 u_m.$$

Because of the fact that

$$\int_0^\infty f\,d\eta = \text{a constant} \qquad\qquad ;$$

therefore,

$$\frac{\dfrac{d}{dx}(u_m b)}{u_m} \propto x^c,$$

, and, on the basis of equation

(7.14) and equation (7.15), it should also be true that

$$\frac{u'_m b + u_m b'}{u_m} = x^{q-1} + x^{q-1} = 2\,x^{q-1} \propto x^0,$$

therefore, the exponent $q = 1$.

According to equation (7.16), the exponent $p = -1$; this is the same as the conclusion reached in Sec 6.

From the straight line radiating out from the point source 0 in Fig 7.1 and Fig 7.3, it can be seen that half the width of the jet, b, forms a direct proportion with x. By experimentation, it can be induced that

$$b = \lg \alpha \cdot x \cong 0.1x, \quad a_1 \cong 0.053.$$

Chapter 8   Turbulence Jet Flow Speed Distribution

Sec 1   Use of Mixing Distance, l, to Obtain a Typical Flow Speed Curve

The objective of research into jets is to make it possible, on the basis of the dimensions of the jet nozzle mouth, $l \times 2b_0$ or πr_0 and assuming one already knows certain initial conditions, such as, original flow volume, G_0, (or the volume of gas flow, Q_0), the original flow speed, u_0, the temperature, T_0, the concentration, c_c, the density, ρ_0, the original momentum flow rate, M_0, and the original pressure, p_0, and further as uming that one already knows certain boundary conditions, such as, the velocity of surrounding gases, u_e, pressure, p_e, density, ρ_e, as well as T_e, and so on, to coordinate or adjust physical parameters which are already known or are selected for use, such as, constant pressure specific heat, c_p, rate of thermal conductivity in turbulence flow, k, turbulence flow viscosity, μ_T, the coefficient of turbulence flow diffusion, D_T, and so on, so as to lay out a set of partial differential equations, on the basis of the theory of turbulence flow boundary layers, and to solve these equations for the velocities of jet flow fields, the rules governing temperature and concentration distributions, the rate of width expansion of jets, (db/dx) or the angle of expansion, α, and the gas volume ratio of induced pull up. $(G/G_0) > 1$.   These data and material have reference value for the designing of combustion chambers.

If, in Chapter 7, one refers to equations (7.1), (7.2), (7.3) and (7.7), it is possible to obtain the turbulence flow shear force

$$\tau_T^- = -\rho\overline{u'v'} = \rho l^2 \left|\frac{\partial u}{\partial y}\right|^2 = \rho(\beta C x)^2 \left|\frac{\partial u}{\partial y}\right|^2 \quad (8.1)$$

The right side of equation (7.30) is

$$\frac{1}{\rho}\frac{\partial \tau_T}{\partial y} = \frac{1}{\rho}\frac{\partial}{\partial y}\left[\rho\beta^2 C^2 x^2 \left|\frac{\partial u}{\partial y}\right|^2\right] = 2(\beta C)^2 x^2 \left|\frac{\partial u}{\partial y}\right|\frac{\partial^2 u}{\partial y^2}$$
$$(8.2)$$

β and C are both constants, and it is possible to determine values for them by experimentation.   If one assumes that $2(\beta C)^2 = a^3 =$ a constant, then, equation (8.2) can be written as

$$\frac{1}{\rho}\frac{\partial \tau_T}{\partial y} = a^3 x^2 \frac{\partial u}{\partial y}\frac{\partial^2 u}{\partial y^2} \quad (8.3)$$

In order to make solution easier, first, separately deal with the two quantities

on the left side of equation (7.30).

From equation (7.42), we know that $u_\infty \propto x^{-\frac{1}{2}}$, and, if we assume that the ratio constant is n, then, $u_\infty = n/\sqrt{x}$ (8.4).

If we use $\phi = (y/ax)$ as the horizontal coordinate, then,

$$(u/u_\infty) = f(y/ax) = f(\phi) \quad (8.5)$$

If we utilize the average time flow function

$$\psi = \int u \, dy, \text{ then } u = \frac{\partial \psi}{\partial y}, \quad v = -\frac{\partial \psi}{\partial x}; \quad (8.6)$$

If we assume that the integral function of the rational curve

$$F = \int f(\phi) \, d\phi, \quad f(\phi) = \frac{dF}{d\phi} = F' \quad (8.7)$$

then, it is possible to obtain

$$\psi = \int u \, dy = \int u_\infty f(\phi) \cdot ax \, d\phi$$

$$= \int \frac{n}{\sqrt{x}} \cdot ax \cdot f(\phi) d\phi = an\sqrt{x} \cdot F \quad (8.8)$$

$$v = -\frac{\partial \psi}{\partial x} = -\frac{\partial}{\partial x}(an\sqrt{x} \cdot F)$$

$$= -an\left(\frac{F}{2\sqrt{x}} - \sqrt{x}\, F' \frac{\phi}{x}\right)$$

$$= \frac{an}{\sqrt{x}}\left(\phi F' - \frac{1}{2} F\right) \quad (8.9)$$

$$\frac{\partial u}{\partial x} = \frac{\partial}{\partial x}\left(\frac{n}{\sqrt{x}} f\right) = \frac{\partial}{\partial x}\left(\frac{n}{\sqrt{x}} \cdot F'\right)$$

$$= -\frac{1}{2}\frac{nF'}{x\sqrt{x}} - \frac{n}{\sqrt{x}} F'' \frac{\phi}{x}$$

$$= -\frac{n}{x\sqrt{x}}\left(\frac{F'}{2} + \phi F''\right),$$

$$u = u_\infty f = \frac{n}{\sqrt{x}} F' \quad (8.10)$$

Therefore,

$$u\frac{\partial u}{\partial x} = -\frac{n^2}{x^2}\left(\frac{1}{2} F'^2 + \phi F' F''\right) \quad (8.11)$$

$$\frac{\partial u}{\partial y} = \frac{\partial}{\partial y}\left(\frac{n}{\sqrt{x}} F'\right) = \frac{n}{\sqrt{x}} F'' \frac{1}{ax},$$

170

$$\frac{\partial^2 u}{\partial y^2} = \frac{n}{ax\sqrt{x}} \frac{\partial F''}{\partial \phi} \cdot \frac{\partial \phi}{\partial y} = \frac{n}{a^2 x^2 \sqrt{x}} F''';$$

And, because of this fact, it is also true that

$$v \frac{\partial u}{\partial y} = \frac{n^2}{x^2}\left(\phi F' F'' - \frac{FF''}{2}\right) \qquad (8.12)$$

$$\frac{1}{\rho} \frac{\partial \tau_T}{\partial y} = a^3 x^2 \frac{\partial u}{\partial y} \frac{\partial^2 u}{\partial y^2} = \frac{n^2}{x^2} F'' F''' \qquad (8.13)$$

If we take equations (8.11), (8.12), and (8.13) and substitute them into equation (7.30), eliminating the common factor, n^2/x^2, then, it is possible to obtain

$$-\left(\frac{1}{2} F'^2 + \phi F' F''\right) + \left(\phi F' F'' - \frac{1}{2} FF''\right) = F'' F'''$$

and from this it can be inferred that

$$2 F'' F''' + FF'' + F'^2 = 0.$$

or

$$2 F'' F''' + \frac{d}{d\phi}(FF') = 0 \qquad (8.14)$$

If we refer to Fig 7.4 (b) and Fig (7.3), and lay out the boundary conditions of the jet, then, when

$$y = 0, \quad \eta = 0, \quad \phi = 0;$$
$$(u/u_m) = f(\phi) = F'(\phi) = 1;$$
$$v = 0, \quad v = \frac{an}{\sqrt{x}}\left(\phi F' - \frac{1}{2} F\right), \quad \text{therefore} \quad F(\phi) = 0;$$
$$\tau_T = 0, \quad (\partial \tau_T/\partial y) = 0, \quad (\partial u/\partial y) = 0, \quad \text{therefore} \quad F''(\phi) = 0;$$

and, when

$$y = \infty, \quad \eta = \infty, \quad \phi = \infty;$$
$$(u/u_m) = f(\infty) = F'(\infty) = 0;$$
$$\tau_T = 0, \quad F''(\infty) = 0.$$

171

If we integrate equation (8.14), we obtain

$$F''' + FF' = C \qquad (8.15)$$

If we utilize the boundary condition, $\phi = 0$, then, $F'' = 0$, and $F = 0$; if we set the integral constant, C, so that it is equal to zero, then, in the final analysis, we obtain the non-linear, second degree ordinary differential equation for the patterned curve of the integral function, $F(\phi)$, and, this equation is

$$F''' + FF' = 0 \qquad (8.16)$$

ϕ	η	$F(\phi)$
0	0	1
0.1	0.105	0.979
0.2	0.209	0.940
0.3	0.314	0.879
0.4	0.419	0.842
0.5	0.524	0.782
0.6	0.628	0.721
0.7	0.733	0.660
0.8	0.838	0.604
0.9	0.942	0.538
1.0	1.048	0.474
1.1	1.150	0.411
1.2	1.255	0.357
1.3	1.360	0.300
1.4	1.465	0.249
1.5	1.570	0.200
1.6	1.675	0.165
1.7	1.780	0.125
1.8	1.880	0.095
1.9	1.990	0.067
2.0	2.100	0.046

Table 8.1

Tollmien utilized the numerical calculation method of successive approximations to solve equation (8.16), and he obtained $F'(\phi) = f(\phi) = (u/u_m)$ the data for which is contained in Table 8.1. $\phi = (y/ax)$, $\eta = (y/b)$. When $\eta = 1.0$, then, $\phi = 0.955$, and $f(\eta) = (u/u_m) = 0.5$.

Sec 2 Using Turbulence Dynamic Viscosity to Obtain a Typical Flow Speed Curve

The level of violence of the exchange of momentum which occurs when turbulence flow air masses rub against each other, pulsate and diffuse is called the "turbulence flow dynamic viscostiy", $\varepsilon = \mu_T/\rho\,[m^2/sec]$. The turbulence flow equivalence viscosity, $\mu_T = \rho\varepsilon$, therefore, the turbulence shear forces are equal to the turbulence flow equivalence viscosity times the average time flow speed gradient,

$$\tau_T = \rho\varepsilon \left|\frac{\partial u}{\partial y}\right| = -\rho\overline{u'v'}, \qquad (8.17)$$

According to Prandtl's theory of mixing distance, the turbulence flow shear forces

$$\tau_T = \rho l^2 \frac{\partial u}{\partial y}\left|\frac{\partial u}{\partial y}\right|; \qquad (8.18)$$

If one compares equation (8.17) and equation (8.18), then, it can be seen that "turbulence flow dynamic viscosity", $\varepsilon = l^2(\partial u/\partial y)$. From equation (7.5), one can obtain the fact that $l = \beta b$, and, from looking at Fig (7.2) (a), one can see that the slope $(\partial u/\partial y)$ of the distribution curve for flow speed, u, also for different cross sections is in direct proportion with the height-to-width ratio, (u_m/b), of the curves; therefore,

$$\varepsilon = \text{a constant} \qquad \beta^2(u_m/b) = kbu_m, \quad \tau_T = \rho kbu_m(\partial u/\partial y).$$
$$(8.19)$$

Let us consider the differentiated control layers, $dx \cdot 1$, (Fig 8.1), (a thickness of 1 perpendicular to the surface of the illustration) which are contained within the boundary layers of the self-patterning stage of two-dimensional, point source, disturbed free jets. If we ignore gravity and suppose that there is an even expansion of pressure, then, 1) the momentum flow rate of entrance flow for the control layer, $dx \cdot 1 = \rho uv dx \cdot 1$, 2) the momentum flow rate of exit for the control layer, $dx \cdot 1$, is equal to dM, and, 3) the turbulence flow friction applied against the boundary layer $= \tau_T \cdot dx \cdot 1$

$$-dM = d\int_y^\infty \rho u^2 dy$$

therefore, the impulse force equilibrium of the boundary layer is

173

$$\rho u v dx + d \int_{-\infty}^{y} \rho u^2 dy - \rho \varepsilon \left| \frac{\partial u}{\partial y} \right| dx = 0$$

$$uv + \frac{\partial}{\partial x} \int_{-\infty}^{y} u^2 dy - \varepsilon \left| \frac{\partial u}{\partial y} \right| = 0 \qquad (8.20)$$
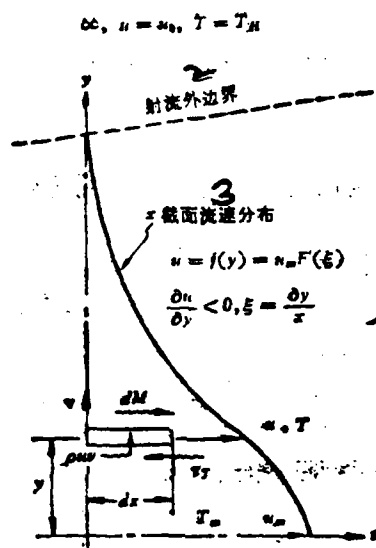

图8.1 二元点泉紊乱射流自模段内控制层冲力平衡

Fig 8.1

1. Impulse Force Equilibrium of Control Layer in Self-patterning Stage of Two-dimensional Point Source Disturbed Free Jet 2. External Boundary of Jet Flow 3. Flow Speed Distribution for a Cross Section, x

If one assumes that the flow speed ratio

$$\frac{u}{u_m} = F'\left(\frac{\sigma y}{x}\right) = F'(\xi) = F' = \frac{dF}{d\xi}, \quad u = u_m F' = \frac{a}{\sqrt{x}} F'. \qquad (8.21)$$

$\sigma =$ a constant $\quad \xi = \left(\frac{\sigma y}{x}\right), \quad \frac{\partial \xi}{\partial x} = -\frac{\sigma y}{x^2} = -\frac{\xi}{x}, \quad \frac{\partial \xi}{\partial y} = \frac{\sigma}{x};$

$$\qquad (8.22)$$

The average time flow function

174

$$\phi = \int u \, dy = \int \frac{n}{\sqrt{x}} F' \frac{x}{\sigma} \, d\xi$$

$$= \frac{n\sqrt{x}}{\sigma} \int F' d\xi = \frac{n\sqrt{x}}{\sigma} F \qquad (8.23)$$

The cross flow speed is

$$v = -\frac{\partial \psi}{\partial x} = -\frac{\partial}{\partial x}\left[\frac{n\sqrt{x}}{\sigma} F\right]$$

$$= -\frac{n}{\sigma}\left[\frac{F}{2\sqrt{x}} - \frac{\xi F'}{\sqrt{x}}\right] = \frac{n}{\sigma\sqrt{x}}\left[\xi F' - \frac{1}{2} F\right] \quad (8.24)$$

The parallel flow speed (with the current) is

$$u = \frac{\partial \psi}{\partial y} = \frac{\partial}{\partial y}\left[\frac{n\sqrt{x}}{\sigma} F\right] = \frac{n\sqrt{x}}{\sigma} F' \frac{\partial \xi}{\partial y} = \frac{n}{\sqrt{x}} F'$$
$$(8.25)$$

$$\left|\frac{\partial u}{\partial y}\right| = \frac{\partial}{\partial y}\left[\frac{n}{\sqrt{x}} F'\right] = \frac{n}{\sqrt{x}} F'' \frac{\partial \xi}{\partial y} = \frac{n\sigma}{x\sqrt{x}} F''$$
$$(8.26)$$

The turbulence flow shear forces are

$$\tau_T = \rho \varepsilon \left|\frac{\partial u}{\partial y}\right| = \rho k b u_m \frac{\partial}{\partial y}\left[\frac{n}{\sqrt{x}} F'\right],$$

Because of the fact that $b = Cx$, $C = $ a constant

$$u_m = \frac{n}{\sqrt{x}},$$

therefore,

$$\tau_T = \rho k (Cx) \frac{n}{\sqrt{x}} \cdot \frac{n}{\sqrt{x}} F'' \frac{\partial \xi}{\partial y} = \rho k C \sigma \frac{n^2}{x} F'' \quad (8.27)$$

If we take equations (8.24), (8.25), (8.26) and (8.27) and substitute them into equation (8.20), then, it is possible to obtain

175

$$\frac{1}{2} FF' + kC\sigma^2 F'' = 0 \qquad . \quad \text{If one selects} \quad \sigma = \frac{1}{2\sqrt{kC}},$$

then, $\quad 2FF' + F'' = 0,$ $\qquad\qquad\qquad$. If we then integrate this equation, we

obtain $\quad F^2 + F' = K \qquad (8.28)$.

If we consider the boundary conditions as they apply in Fig 8.1, then, when

$$y = 0, \ \xi = 0, \ u = u_m, \ \frac{u}{u_m} = 1, \quad \text{then} \quad F'(0) = 1$$
$$\tau_T = 0, \quad \text{then} \quad F''(0) = 0$$
$$v = 0, \quad \text{then} \quad F(0) = 0$$

$$y = \infty, \ \xi = \infty, \ u = 0, \ F'(\infty) = 0$$
$$\tau = 0, \ F''(\infty) = 0$$

By employing the boundary conditions, it is possible to obtain $\quad F^2 + F' = 1 \quad (8.29)$.

The solution function of the differential equation (8.28) is:

$$F = \text{th}(\xi) = \frac{e^{\xi} - e^{-\xi}}{e^{\xi} + e^{-\xi}} = \frac{1 - e^{-2\xi}}{1 + e^{-2\xi}} \qquad (8.30)$$

The equation for the patterned curve of flow speed distribution is:

$$F' = \frac{u}{u_m} = 1 - \text{th}^2(\xi) \qquad (8.31)$$

Applying equation (8.31),

$$\frac{v}{u_m} = \frac{1}{\sigma}\left[\xi - \xi\text{th}^2(\xi) - \frac{1}{2}\text{th}(\xi)\right] \qquad (8.32)$$

In Table 8.2 one can see the solution data which Goertler compiled on the patterned curve of flow speed, $F'(\xi) = (u/u_m)$.

On the basis of experimentation, the constant $\sigma = 7.67$. We already know u_c and b_c and, when this is true, we can solve for precise values of $\quad n = 3.5u_0\sqrt{b_0};$

$$u_m = \frac{n}{\sqrt{x}} \simeq \frac{3.5u_0\sqrt{b_0}}{\sqrt{x}}.$$

176

$\xi = \sigma \dfrac{y}{x}$	$\eta = \dfrac{y}{b}$	$F(\xi) = \dfrac{u}{u_m}$
0	0	1
0.1	0.114	0.990
0.2	0.227	0.961
0.3	0.341	0.915
0.4	0.455	0.855
0.5	0.568	0.786
0.6	0.682	0.711
0.7	0.795	0.635
0.8	0.909	0.558
0.9	1.022	0.486
1.0	1.136	0.420
1.2	1.362	0.302
1.4	1.590	0.218
1.6	1.820	0.149
1.8	2.045	0.102
2.0	2.270	0.070
2.2	2.500	0.048
2.5	2.840	0.021

Table 9.2

Sec 7 Use of Momentum Diffusion Distance to Obtain a Typical Flow Speed Curve

The previous chapter talked about the rubbing together and pulsating which is done by the turbulence flow vortical masses of a turbulence flow jet flow field and the subsequent diffusion and transmission of momentum, energy and mass. The pulsations of vortical masses change randomly; therefore, it is only necessary to use the methods of probability and statistics in order to solve for the average time flow speeds, u, and v, the average time temperature $\bar{T}$, and the average time momentum density flow, ρu^2 ; the average time turbulence shear force, $s_T = -\rho \overline{u'v'}$, and so on, and so on.

Reichardt, on the basis of experimentation, has precisely measured, in turbulence jet flow fields, the distribution of momentum density flow in the x direction along the cross-flow direction, y, and these measurements are similar to a Gaussian normal distribution (Chapter 7, Sec 5).

In the boundary layers of non-compressible, average time equivalents of stable states in two-dimensional disturbed jets, the momentum of jet flow in the axial dir-

177

ection, x, is conserved so that $M = M_0 = 2b_0\rho u_\infty^2$. Concerning the expansion, y, of jet boundary layers in the x direction, there is a change in width, b. Due to this fact, the reduction of impulse force along x is equal to the momentum density flow of diffusion, that is to say,

$$-\frac{\partial}{\partial x}(\bar{p} + \rho\bar{u}^2) = \frac{\partial}{\partial y}(\rho\overline{uv}),$$

$$\frac{\partial}{\partial x}\left(\frac{\bar{p}}{\rho} + \bar{u}^2\right) + \frac{\partial\overline{uv}}{\partial y} = 0$$

Because of the fact that the violence of the turbulence flow pulsations is much greater than the agitation momentum that is transferred by molecular motion diffusion, and, because it is also true that the turbulence flow is several times larger than the shear or tangential forces of the boundary layers, so that $\tau_T \gg \tau_L$, it is possible to ignore the dynamic viscosity of laminar flow, $\nu \cong 0$.

If one is considering the expansion of a jet in an environment of constant pressure, then, $\bar{p}$ is equal to a constant, and, because of this fact, $\partial\bar{p}/\partial x = 0$.

Due to this fact,

$$\frac{\partial\bar{u}^2}{\partial x} + \frac{\partial\overline{uv}}{\partial y} = 0, \quad \text{or} \quad \frac{\partial\bar{u}^2}{\partial x} = -\frac{\partial}{\partial y}(\overline{uv}) \quad (8.33)$$

Reinhardt postulates that the momentum density flow of cross-current diffusion, $\rho\overline{uv}$, is in direct proportion with the negative gradient of axial momentum density flow along y $\frac{-\partial}{\partial y}(\rho\bar{u}^2)$. If we assume that Λ is equal to a ratio constant or proportional constant which is also called the momentum diffusion distance, then,

$$\rho\overline{uv} = -\Lambda\rho\frac{\partial\bar{u}^2}{\partial y}, \quad \text{or} \quad \overline{uv} = -\Lambda\frac{\partial\bar{u}^2}{\partial y} \quad (8.34)$$

If we merge equation (8.33) with equation (8.34), then we obtain

$$\frac{\partial\bar{u}^2}{\partial x} = \Lambda\frac{\partial^2\bar{u}^2}{\partial y^2}. \qquad \text{(the dimension of } \Lambda \text{ is length)}$$
$$(8.35)$$

If the momentum diffusion distance, Λ, is actually a constant, then, equation (8.35) is linear, is a second degree partial differential equation with a parabolic shape, and has the same form as an equation for thermal conductance. The standard solution is a "deviation function." However, due to the fact that $\Lambda = \Lambda(x)$, this will be a good deal more complicated than solving the thermal conductance equation.

The standard or normal function we have been talking about in this section (equivalent to a probability density function) is not a flow speed ratio (u/u_m), but, it is a momentum density flow (or dynamic pressure) ratio $(\rho\bar{u}^2/\rho\bar{u}_m^2)$. Assume that the non-dimensional coordinate, $\eta = (y/b)$.

According to the conservation of axial momentum and self-patterning or normalizing conditions, it is possible to know that the momentum density flow on the axis-line and the half-width, b, of the boundary layer of a point source jet are inversely proportional to each other. That is to say that, as the width of the jet is increased, $\rho\bar{u}_m^2$ is decreased in value ... (see Fig. 7.6 (a)):

$$\overline{u_m^2} = \frac{n^2}{b};\qquad (8.36)$$

; n = an experimentally determined constant

The standard or proper function for momentum density flow

$$f(\eta) = \frac{\rho\bar{u}^2}{\rho\bar{u}_m^2},\qquad \text{therefore } \overline{u^2} = \frac{n^2}{b}f(\eta) \quad (8.37)$$

$$\left.\begin{array}{l}
\dfrac{\partial \overline{u^2}}{\partial x} = -\dfrac{n^2}{b^2}\dfrac{db}{dx}\left[f(\eta) + \eta f'(\eta)\right] \\[2mm]
\dfrac{\partial \overline{u^2}}{\partial y} = \dfrac{n^2}{b^2}f'(\eta) \\[2mm]
\dfrac{\partial^2 \overline{u^2}}{\partial y^2} = \dfrac{n^2}{b^3}f''(\eta)
\end{array}\right\} \qquad (8.38)$$

If we take equation (8.37) and equation (8.38) and substitute them into equation (8.39), then,

$$-[f(\eta) + \eta f'(\eta)]b\frac{db}{dx} = \Lambda f''(\eta) \qquad (8.39)$$

According to the concept of Prandtl's mixing distance, L, (see equation 7.1 and equation 7.5), $\Lambda = Cb, \; b = Cx, \; (db/dx) = C$; on this basis, it is possible to postulate that $\Lambda = b\dfrac{db}{dx} = Cb = C^2x,$ that is to say that the diffusion distance of momentum density flow, Λ, varies with linear changes in x. Because of this fact, equation (8.39) can be simplified to read

$$f''(\eta) + \eta f'(\eta) + f(\eta) = 0 \qquad (8.40)$$

By integrating equation (8.40), it is possible to obtain

$$f(\eta) = C_1 e^{-\eta^{1/2}} \pm C_2 = C_1 \exp\left(-\frac{\eta^2}{2}\right) + C_2 \quad (8.41)$$

According to the boundary conditions for a point source, two-dimensional free jet (See Figure 7.1 and Figure 8.1), when $y = 0$, $\eta = 0$, $f(\eta) = 1$.　　　　　　　　　　　　　　. When $y = \pm\infty$, $\eta = \pm\infty$, $f(\eta) = 0$.

Because of all this, one can precisely fix the integration constants $C_2 = 0$, $C_1 = 1$. And, on the basis of this, it is possible to obtain

$$f(\eta) = \exp\left(-\frac{\eta^2}{2}\right), \text{ or } \overline{u^2} = \overline{u_m^2}\exp\left(-\frac{\eta^2}{2}\right). \quad (8.42)$$

180
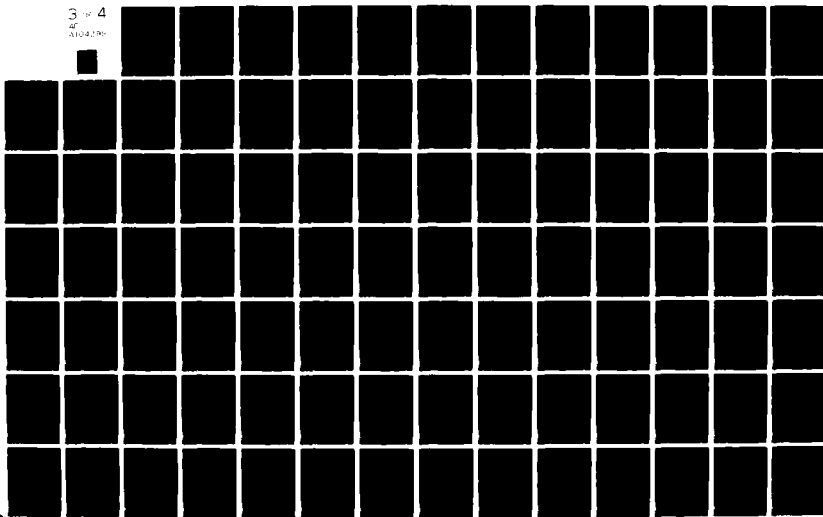
Section 4. Initial Phase Flow Speed Distribution
for Flat Mouth Jets

Let us assume that the height of a flat mouth jet $= 2b_0$. The
initial impelling jet flow speed is distributed evenly along y, and is
equal to U_0. The initial volume of flow is $Q_0 = 2b_0U_0$. The length
of the jet core $= x_0$, and, within the core, the axial flow speeds at
various cross sections are all equal to U_0. After the gas flow leaves
the rim of the flat jet, 0, there is a sudden change in flow speed due
to the fact that the gases in the jet make contact with the stationary
gases in the surrounding environment, producing vortical turbulence,
inducing the surrounding gases to roll up on themselves and form a turbulent
boundary layer which is also called a "mixture layer". OA is the interior
boundary of the mixture layer, and A is the end point of the core of
the jet. OB is the exterior boundary of the mixture layer (Figure 8.2).
On the external boundary line, the axial flow speed, u = 0. The angle
of expansion of the interior boundary line $= \alpha_1$. The angle of expansion
of the exterior boundary line $= \alpha_2$ and, the width of the mixture
layer at a cross section $x = b = C_x$. The turbulent flow dynamic
viscosity $= \varepsilon = kbU_0 = kCxU_0$.

According to Equation (8.19) one can assume that the turbulence
shear force

$$\tau_J = \rho k C x U_0 \left(\frac{\partial u}{\partial y} \right) \tag{8.43}$$

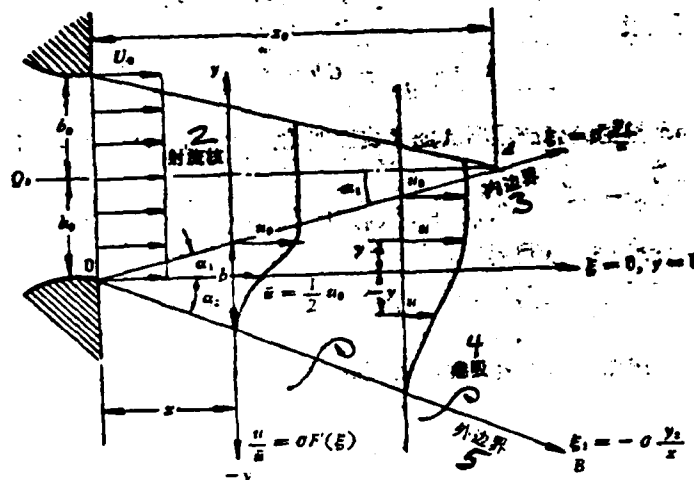At a cross section, x, let us assume $\xi = \sigma \frac{y}{x}$ is the independent variable. Then

181

Fig. 8.8

1. Illustration of Flow and Distribution of Mixture Layer in the Initial Stage of a Flat Mouth Jet 2. Jet Core 3. Interior Boundary Line 4. Main Stream Induction 5. Exterior Boundary Line

$$\bar{u} = \frac{1}{2} U$$

$$\frac{\partial \xi}{\partial x} = -\frac{\sigma y}{x^2} = -\frac{\xi}{x}, \quad \frac{\partial \xi}{\partial y} = \frac{\sigma}{x}, \quad \text{a constant} \ \sigma = \text{II} \qquad (8.44)$$

Assume that there is no pressure gradient. Then formation

$$\psi = \bar{u}xF(\xi) = \bar{u}xF = \int u\,dy \qquad (8.45)$$

$$u = \frac{\partial \psi}{\partial y} = \bar{u}xF'(\xi)\frac{\sigma}{x} = \sigma\bar{u}F', \quad \text{or} \ \frac{u}{\bar{u}} = \sigma F' \qquad (8.46)$$

$$v = -\frac{\partial \psi}{\partial x} = -\frac{\partial}{\partial x}(\bar{u}xF) = -\bar{u}\left[F - xF'\frac{\xi}{x}\right],$$

or

$$\frac{v}{\bar{u}} = (\xi F' - F), \qquad (8.47)$$

$$\frac{\partial u}{\partial x} = \frac{\partial}{\partial x}(\sigma\bar{u}F') = -\bar{u}\sigma F''\frac{\xi}{x},$$

$$\frac{u}{\bar{u}} = \sigma F'(\xi) = \sigma F';$$

181 A

$$u\frac{\partial u}{\partial x} = (\bar{u}\sigma F')\left(-\bar{u}\sigma F''\frac{\xi}{x}\right) = -\frac{\sigma^2\bar{u}^2}{x}\xi F'F'', \quad (8.48)$$

$$\frac{\partial u}{\partial y} = \frac{\partial}{\partial y}(\sigma\bar{u}F') = \sigma\bar{u}F''\frac{\partial\xi}{\partial y} = \frac{\sigma^2\bar{u}}{x}F'',$$

$$v\frac{\partial u}{\partial y} = \bar{u}(\xi F' - F)\frac{\sigma^2\bar{u}}{x}F'' = \frac{\sigma^2\bar{u}^2}{x}(\xi F'F'' - FF''),$$

$$\quad (8.49)$$

$$\frac{1}{\rho}\frac{\partial \tau_I}{\partial y} = \frac{\partial}{\partial y}\left(kC x u_0\frac{\partial u}{\partial y}\right)$$

$$= kC x u_0\frac{\partial}{\partial y}\left(\bar{u}\sigma^2\frac{F''}{x}\right) = 2kC\bar{u}^2\sigma^3\frac{F'''}{x} \quad . \quad (8.50)$$

The basic equations for a flat mouth jet are still

$$u\frac{\partial u}{\partial x} + v\frac{\partial u}{\partial y} = \frac{1}{\rho}\frac{\partial \tau_I}{\partial y} \quad\quad (7.30)$$

$$\frac{\partial v}{\partial y} = -\frac{\partial u}{\partial x} \quad . \quad\quad (7.31)$$

If we take the equations from (8.48) to (8.50) and substitute them into equation (7.30), then,

$$-\frac{\sigma^2\bar{u}^2}{x}\xi F'F'' + \frac{\sigma^2\bar{u}^2}{x}(\xi F'F'' - FF'')$$

$$- 2kC\frac{\sigma^3\bar{u}^2}{x}F''' = 0 \quad .$$

This can be simplified to read $2kC\sigma F''' + FF'' = 0$. $\quad (8.51)$

If we assume that the relationship of the constants is $4kC = \frac{1}{\sigma^2}$ (this can

be checked by experimentation), then, $F''' + 2\sigma FF'' = 0$. $\quad (8.52)$

The boundary conditions are as follows (See Fig 8.2): when

$$\left.\begin{array}{l} y \to -\infty, \ \xi \to -\infty, \ F'(-\infty) = \dfrac{u}{\bar{u}} = 0 \\[2mm] y \to \infty, \ \xi \to +\infty, \ F'(+\infty) = \dfrac{u_0}{\bar{u}\sigma} = \dfrac{2}{\sigma} \end{array}\right\} (8.53)$$

In order to solve equation (8.52), Goertler utilizes the infinite series below

182

$$\sigma F(\xi) = \xi + F_1(\xi) + F_2(\xi) + \cdots = \sum_{i=0}^{\infty} F_i(\xi),$$

$$\sigma F_0(\xi) = \xi \qquad\qquad (8.54)$$

If, on the basis of equation (8.54), we solve for the second degree and third degree derivative functions and substitute them into equation (8.52), then, it is possible to obtain a series of closely similar solutions

$$\frac{u}{\bar{u}} = \sigma F' = 1 + \frac{2}{\sqrt{\pi}} \int_0^{\xi} \exp(-z^2)\,dz = 1 + \mathrm{erf}(\xi)$$

or

$$\frac{u}{u_0} = 0.5 + \frac{1}{\sqrt{\pi}} \int_0^{\xi} \exp(-z^2)\,dz = \frac{1}{2}[1 + \mathrm{erf}(\xi)] \qquad (8.55)$$

The deviation or error function, erf (ξ), in equation (8.55), can be determined by consulting tables of data which are already available. These can be graphed out in the form of a curve as shown in Fig 8.3. If we already know F', then, we can integrate to solve for F, and, on the basis of equation (8.47), it is possible to solve for v.
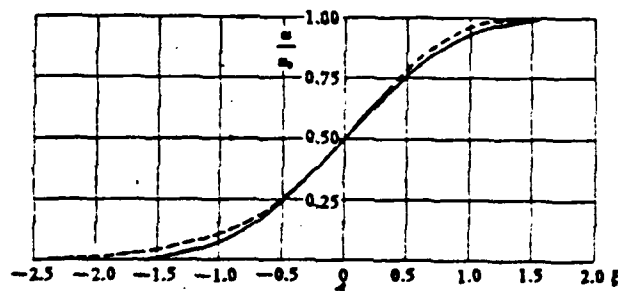

图8.3 扁喷口射流初始段参混层中流速分布曲线
（实线表示一级近似，虚线表示二级近似）

Fig 8.3

1. Flow Speed Distribution Curve Within the Mixture Layer of the Initial Stage of a Flat Mouth Jet (The Solid Line Represents a One-dimensional Approximation, The Broken Line Represents a Two-dimensional Approximation)

According to experimental observations and measurements, the constant, ⁻ = 11.0, the interior boundary expansion angle is equal to the half-wedge angle of the

183

jet core, $a_1 \cong 4.8°$, the exterior boundary expansion angle $a_2 \cong 9.5°$, and the width

of the mixture layer $b = Cx \cong 0.176x$. The induction roll up gas vol-

ume ratio (Q/Q_0), in the initial stage, is approximately equal to $1+0.035$ (x/b_0).

The length of the jet core is $x_0 \cong 12 b_0$. . Therefore, at the end point of

the initial stage of a flat mouth jet, the induction roll up gas volume ratio (Q/Q_0)

already reaches an approximate value of 1.42.

Sec 5 Round Aperture Jet Boundary Level Equations

The shape of axisymmetrical disturbed free jets put out by a round aperture

with a radius, r_0, is completely similar to that of jets put out by crack apertures

or flat mouth jet nozzles (See Fig 7.1, Fig 7.2 (a), (b)), and they can be divided in⁻

initial stages and normal or patterned stages. In the normal or patterned stage, the

distribution of axial average time flow speed, $\bar{u}$, in the cross-current direction, y,

is also described by a Gaussian normal distribution. The jet expands in width along

the x direction. On the axis line, the maximum average time flow speed, $\bar{u}_m$, atten-

uates and drops in value along x. The half-width of the jet boundary layer $b = Cx$,

C = an experimentally determined constant. When a jet enters a gas at rest with

a uniform pressure, p_e, there is a roll up induction flow speed, v_e. If we ignore

gravity, then, the axial momentum flow rate $M = M_0 = \pi r_0^2 \rho u_0^2 = $ a constant.

If we recognize these jet fields to be average time quasi-stable state

flow fields, then, local acceleration = 0. Concerning the fact that the turbulence

shear forces are much larger than the laminar flow shear forces, $(\tau_T \gg \tau_L)$, it is

possible to ignore the laminar flow dynamic viscosity, v. Because of this fact, the

Reynolds equation, (7.24), for a non-compressible disturbed jet flow field can be

simplified to read $\rho V \cdot \nabla V = -\nabla \bar{p} - \nabla \cdot \Pi$ $[N/m^3]$.

(8.56)

If we make use of cylindrical coordinates in x, r, and 0, then, the average time

velocity in an axial direction, $\bar{u}$, in a radial direction, $\bar{v}$, in a circumferential dir

ection, $\bar{w}$, as well as the component velocities of pulsation, u', v', and w' can all

be expressed as cylindrical coordinate values. The form corresponding to the average

time product of turbulence flow stress tensor, Π , and component velocities of pulse

is

$$\Pi = \begin{Bmatrix} \sigma_{xx} & \tau_{xr} & \tau_{x\theta} \\ \tau_{rx} & \sigma_{rr} & \tau_{r\theta} \\ \tau_{\theta x} & \tau_{\theta r} & \sigma_{\theta\theta} \end{Bmatrix} = \begin{Bmatrix} -\rho \overline{u'u'} & -\rho \overline{u'v'} & -\rho \overline{u'w'} \\ -\rho \overline{v'u'} & -\rho \overline{v'v'} & -\rho \overline{v'w'} \\ -\rho \overline{w'u'} & -\rho \overline{w'v'} & -\rho \overline{w'w'} \end{Bmatrix}$$

(8.57)

If we take the average time values and add them to the pulse values, for example,

184

$(\bar{u} + u')$ and so on, and use these new quantities to replace the instantaneous values or u, etc., then, we can take equation (8.56) and expand it into three momentum equations for an axisymmetric jet:

In the direction of the axis, x,

$$\bar{u}\frac{\partial \bar{u}}{\partial x} + \bar{v}\frac{\partial \bar{u}}{\partial r} = -\frac{1}{\rho}\frac{\partial \bar{p}}{\partial x} - \left(\frac{\partial \overline{u'u'}}{\partial x}\right.$$
$$\left. + \frac{\partial \overline{u'v'}}{\partial r} + \frac{1}{r}\overline{u'v'}\right) \tag{8.58}$$

Along the radius, r,

$$\bar{u}\frac{\partial \bar{v}}{\partial x} + \bar{v}\frac{\partial \bar{v}}{\partial r} - \frac{\bar{w}^2}{r} = -\frac{1}{\rho}\frac{\partial \bar{p}}{\partial r}$$
$$- \left(\frac{\partial \overline{v'u'}}{\partial x} + \frac{\partial \overline{v'v'}}{\partial r} + \frac{\overline{v'v'}}{r} - \frac{\overline{w'w'}}{r}\right) \tag{8.59}$$

Along the circumference, θ,

$$\bar{u}\frac{\partial \bar{w}}{\partial x} + \bar{v}\frac{\partial \bar{w}}{\partial r} + \frac{\bar{w}\bar{v}}{r}$$
$$= -\left(\frac{\partial \overline{w'u'}}{\partial x} + \frac{\partial \overline{w'v'}}{\partial r} + 2\frac{\overline{w'v'}}{r}\right) \tag{8.60}$$

If one is considering non-rotational jets, then, the circumferential component of velocity, $\bar{w} = 0$, and its derivative functions are all equal to zero. According to the special characteristics of boundary layers

$$\bar{u} \gg \bar{v}, \quad \frac{\partial}{\partial r} \gg \frac{\partial}{\partial x}.$$

Besides this, from experimental observations and measurements, the radial and circumferential normal stresses of turbulence flow are generally equal, that is to say that,

$$\rho\overline{v'v'} \approx \rho\overline{w'w'}.$$

On the basis of these postulated conditions, equations (8.58) to (8.60) can be simplified yet another step to be:

In the axial direction, x,

$$\bar{u}\frac{\partial \bar{u}}{\partial x} + \bar{v}\frac{\partial \bar{u}}{\partial r} = -\frac{1}{\rho}\frac{\partial \bar{p}}{\partial x}$$
$$- \left[\frac{\partial \overline{u'u'}}{\partial x} + \frac{1}{r}\frac{\partial}{\partial r}(r\overline{u'v'})\right] \tag{8.61}$$

In the radial direction, r,

$$\frac{1}{\rho}\frac{\partial \bar{p}}{\partial r} = -\frac{\partial}{\partial r}\overline{v'v'}, \qquad d\bar{p} = -\rho d(\overline{v'v'}) \qquad (8.62)$$

By integrating equation (8.62), one can obtain

$$\bar{p} = p_e - \rho\overline{v'v'}, \quad \frac{\partial \bar{p}}{\partial x} = \frac{\partial p_e}{\partial x} - \rho\frac{\partial \overline{v'v'}}{\partial x}, \qquad (8.63)$$

If we take equation (8.63) and substitute it into equation (8.61), then, p_e is equal to the stationary pressure of the environmental gases surrounding a jet:

$$\bar{u}\frac{\partial \bar{u}}{\partial x} + \bar{v}\frac{\partial \bar{u}}{\partial r} = -\frac{1}{\rho}\frac{\partial p_e}{\partial x} - \frac{1}{r}\frac{\partial}{\partial r}(r\overline{u'v'})$$

$$-\left(\frac{\partial \overline{u'u'}}{\partial x} - \frac{\partial \overline{v'v'}}{\partial x}\right), \qquad (8.64)$$

The mean square of the pulsation velocity component, $\overline{u'u'} = \overline{u'^2}$ represents the axial turbulence flow strength. According to the theory of measurement of similar turbulence flows in various different directions, $\overline{u'u'} \approx \overline{v'v'}$. The static pressure of the environmental gases surrounding the jet, p_e= a constant, and the turbulence flow shear force, $\tau_{rx} = \tau_{xr} = -\rho\overline{u'v'}$. Therefore, equation (8.64) can be simplified to be the turbulence flow boundary layer momentum equation

$$\bar{u}\frac{\partial \bar{u}}{\partial x} + \bar{v}\frac{\partial \bar{u}}{\partial r} = \frac{1}{\rho r}\frac{\partial(r\tau_{xr})}{\partial r} \qquad (8.65)$$

The turbulence flow boundary layer continuity equation is

$$\frac{\partial(r\bar{u})}{\partial x} + \frac{\partial(r\bar{v})}{\partial r} = 0, \quad \frac{\partial(r\bar{v})}{\partial r} = -\frac{\partial(r\bar{u})}{\partial x}. \qquad (8.66)$$

Sec 6 Integral of Momentum Equations for Round Aperture Jets

If we take ρr and, by successive multiplications of the various quantities in equation (8.65), reintegrate from $r = 0$ to $r = \infty$, and, if we declare this to be the average time velocity vector, u, without any additional force from v, then, we can simply write $\tau_{xr} = \tau$:

$$\int_0^\infty \rho u r \frac{\partial u}{\partial x}\, dr + \int_0^\infty \rho v r \frac{\partial u}{\partial r}\, dr = \int_0^\infty \frac{\partial(r\tau)}{\partial r}\, dr \qquad (8.67)$$

186

$$\int_0^\infty \rho u r \, \frac{\partial u}{\partial x} \, dr = \frac{1}{4\pi} \frac{d}{dx} \int_0^\infty 2\pi r \, dr \, \rho u^2,$$

$$\int_0^\infty \rho v r \, \frac{\partial u}{\partial r} \, dr = \left| \rho u v r \right|_0^\infty - \int_0^\infty \rho u \, \frac{\partial (rv)}{\partial r} \, dr$$

$$= \int_0^\infty \rho u \, \frac{\partial (ru)}{\partial x} \, dr = \frac{1}{4\pi} \frac{d}{dx} \int_0^\infty 2\pi r \, dr \, \rho u^2,$$

$$\int_0^\infty \frac{\partial (r\tau)}{\partial r} \, dr = \left| r\tau \right|_0^\infty = 0,$$

The axial momentum flow rate

$$M = \int_0^\infty 2\pi r \, dr \, \rho u^2.$$

If we substitute this into equation (8.67), then it is possible to obtain

$$\frac{d}{dx} \int_0^\infty 2\pi r \, dr \, \rho u^2 = \frac{d}{dx} M = 0.$$

Therefore, M = a constant. (8.68)

This proves that the momentum flow rate of a jet, along the axial direction, x, is conserved, that is to say,

$$M = M_0 = \pi r_0^2 \rho u_0^2.$$

If we assume that $(u/u_m) = f(\eta) = f$, $\quad \eta = \frac{r}{b}$; $\quad u_m \propto x^p$, $\quad b \propto x^q$. $\qquad$ (8.69)

If we take equations (8.69) and substitute them into equation (8.68), then, we obtain

$$\frac{d}{dx} \rho u_m^2 b^2 \int_0^\infty 2\pi \eta f^2 \, d\eta = 0 \ . \qquad (8.70)$$

In equation (8.70), the non-dimensional momentum flow rate of an axially symmetrical jet

$$\int_0^\infty 2\pi \eta f^2 \, d\eta = \text{a constant}$$

Therefore, the preceding coefficient, $u_m^2 b^2$, is necessarily unrelated to x, that is to say that $u_m^2 b^2 \propto x^t$, or the exponents that are written out are equal:

$$x^{2p} \cdot x^{2q} = x^0, \quad 2p + 2q = 0, \quad p = -q.$$

Previously, we have already made use of the fact that the jet half-width, b, is in a direct proportion with x, so that $b = Cx$, that is to say that q = 1, and, therefore, p = -1.

On the basis of dimensional analysis or the theory of gas volume induction roll up, it is possible to prove the similar rules that govern the expansion of jets, i.e., $b = Cx$, as well as the rule governing the attenuation and reduction U_m, $u_m = n \cdot x$, n = an experimentally determined constant.

Sec 7 Employing ε to Obtain a Typical Curve

Assume that

$$\xi = \sigma \frac{r}{x}, \quad \frac{\partial \xi}{\partial x} = -\sigma \frac{r}{x^2} = -\sigma \frac{\xi}{x},$$

$$\frac{\partial \xi}{\partial r} = \frac{\sigma}{x}; \quad dr = \frac{x}{\sigma} d\xi;$$

$$\frac{u}{u_m} = f(\xi) = f, \quad u = u_m f = \frac{n}{x} f, \qquad (8.71)$$

n and σ are experimentally determined constants. $\qquad (8.72)$

Let us assume that there is an average time flow function:

$$\psi = \int_0^r r u \, dr = \int_0^\xi \frac{x}{\sigma} \xi \cdot \frac{n}{x} f \cdot \frac{x}{\sigma} d\xi = \frac{nx}{\sigma^2} \int_0^\xi \xi f \, d\xi \qquad (8.73)$$

Make

$$\int_0^\xi \xi f \, d\xi = F(\xi) = F, \quad f = \frac{1}{\xi} \frac{dF}{d\xi} = \frac{1}{\xi} F' \qquad (8.74)$$

If one is considering a non-compressible axially symmetrical jet, then,

$$rv = -\frac{\partial \psi}{\partial x} = -\frac{\partial}{\partial x} \left(\frac{nx}{\sigma^2} F \right)$$

$$= -\frac{n}{\sigma^2} \left(x F' \frac{\xi}{x} - F \right) = -\frac{n}{\sigma^2} (\xi F' - F), \qquad (8.75)$$

Because of this it is also true that

188

$$v = \frac{\sigma}{\xi x} \cdot \frac{n}{\sigma^2}(\xi F' - F) = \frac{n}{\sigma x}\left(F' - \frac{F}{\xi}\right) \qquad (8.76)$$

$$u = \frac{n}{x} f = \frac{nF'}{x\xi} \qquad (8.77)$$

According to equation (8.19), the turbulence flow dynamic viscosity

$$\varepsilon = kbu_m = kCx \cdot \frac{n}{x} = kC\bar{n} = \text{a constant}$$

Because of these relationships, it is also true that the quantity, ε, for a round aperture jet, does not vary with changes in x. Due to this fact, the turbulence flow shear force

$$\tau = \rho\varepsilon\left|\frac{\partial u}{\partial r}\right| = \rho k C n \left|\frac{\partial u}{\partial r}\right| = (\rho k C n)\frac{\partial}{\partial r}\left(\frac{nF'}{x\xi}\right)$$

$$= k \cdot \frac{n}{x} \frac{\partial}{\partial r}\left(\frac{F'}{\xi}\right);$$

Let us assume that the constant $(\rho k n C) = k$, then, it will also be true that

$$\tau = \frac{kn\sigma}{x^2}\left(\frac{F''}{\xi} - \frac{F'}{\xi^2}\right) \qquad (8.78)$$

If we take equation (8.76), equation (8.77) and equation (8.78) and substitute them into equation (8.65), and, moreover, if we determine that

$$\sigma = \frac{1}{\sqrt{kC}},$$

then it is possible to obtain the relationship

$$FF' = F' - \xi F'' \qquad (8.79)$$

The boundary conditions for a round aperture axially symmetrical disturbed free jet are as follows:

189

$$\left.\begin{array}{l}
\text{when} \quad r = 0,\ \xi = 0, \\[4pt]
\quad u = u_m,\ (F'/\xi) = 1, \qquad F'(\xi) = F'(0) = 1; \\[4pt]
\quad v = 0,\ \left(F' - \dfrac{F}{\xi}\right) = 0, \quad F(\xi) = F(0) = 0, \\[4pt]
\text{when} \quad r \to \infty,\ \xi \to \infty, \\[4pt]
\quad u = 0,\ (F'/\xi) = 0, \qquad F(\xi) = F(\infty) = 0.
\end{array}\right\} \tag{8.80}$$

If we conform to the boundary conditions in (8.80), then, the solution for (8.79) is

$$F = \frac{0.5\,\xi^2}{1 + 0.125\,\xi^2},$$

or

$$\left(\frac{u}{u_m}\right) = f = \frac{F'}{\xi} = \frac{1}{(1 + 0.125\,\xi^2)^2} \tag{8.81}$$

By employing equation (8.76), it is possible to obtain

$$\sigma\left(\frac{v}{u_m}\right) = \frac{\xi - 0.125\,\xi^3}{2(1 + 0.125\xi^2)^2} \tag{8.82}$$

Because of the fact the turbulence flow dynamic viscosity, ϵ, (also called the turbulence flow momentum exchange coefficient) does not vary with changes in x, therefore, the form of the solutions for the flow speed distribution standard or pattern function equations (8.81) and (8.82) as well as for the boundary layers of laminar flow is the same. The difference is simply ϵ which is several times larger than the laminar flow dynamic viscosity, v.

In Table 8.3, b is the radius of a jet where $u = 0.5\ u_m$ and $\xi = \sigma\dfrac{b}{x} = 1.81$ when $r = b, \eta = 1$.

The axial momentum flow rate is conserved as follows:

$$\int_0^\infty 2\pi r\,dr\,\rho u^2 = M_0 = \pi r_0^2 \rho u_0^2,$$

If we utilize the relationships $r = \dfrac{\xi x}{\sigma}$, $dr = \dfrac{x}{\sigma}d\xi$, $u = u_m\dfrac{1}{\xi}F'$

and substitute them into the equation above in order to simplify it, then,

表8.3 圆喷口射流规化曲线数据表

$\xi = \sigma \frac{r}{x}$	0	0.5	1.0	1.5	2.0	2.5	3.0
$\eta = \frac{r}{b}$	0	0.276	0.552	0.829	1.105	1.383	1.659
$\frac{u}{u_m} = \frac{1}{\xi} F'$	1.0	0.94	0.79	0.608	0.445	0.316	0.221
$\sigma \frac{v}{u_m} = F' - \frac{1}{\xi} F$	0	0.228	0.346	0.328	0.221	0.087	−0.047

$\xi = \sigma \frac{r}{x}$	3.5	4.0	4.5	5.0	5.5	6.0	∞
$\eta = \frac{r}{b}$	1.94	2.21	2.49	2.762	3.04	3.315	∞
$\frac{u}{u_m} = \frac{1}{\xi} F'$	0.156	0.111	0.08	0.059	0.044	0.033	0
$\sigma \frac{v}{u_m} = F' - \frac{1}{\xi} F$	−0.144	−0.222	−0.276	−0.314	−0.334	−0.347	−0.4

Table 8.3

1. Round Aperture Jet Standard Curve Data Table

$$2\pi\rho \frac{u_m^2 x^2}{\sigma^2} \left[\int_0^\infty \frac{(F')^2}{\xi} d\xi \right] = \pi r_0^2 \rho u_0^2,$$

or

$$\frac{u_m}{u_0} = \frac{\sigma}{\sqrt{2}} \cdot \left[\int_0^\infty \frac{(F')^2}{\xi} d\xi \right]^{-\frac{1}{2}} \cdot \frac{r_0}{x}; \qquad (8.83)$$

We already know $\frac{1}{\xi} F'$, r_0, u_0 and σ for the standard curve, and, in such a case, it is possible to arrive at the fact that, on the axis line, the pattern that governs the attenuation and reduction of the maximum flow speed, u_m, along x, is a parabolic curve defined by the relationship $u_m \cdot x = $ a constant; this curve starts from the end point of the core of the jet, and $x > x_0$, where x_0 is equal to the length of the jet core. If, on the basis of Goertler's standard curve, we solve for the integral of equation (8.83), then

$$\frac{u_m}{u_0} = \frac{\sigma}{1.61} \frac{r_0}{x}, \quad d_0 = 2r_0,$$

By measurement we can obtain the value $\sigma = 18.5$, and then,

$$\frac{u_=}{u_0} = 5.75 \frac{d_0}{x} \qquad\qquad (8.84)$$

Based on experimental observations and measurements, the ratio constant of the jet half-width, b, as it varies with expansion, x, is $C \approx 0.1$, $b = 0.1x$. The coefficient of induction roll up $a_r = v_r/u_m \approx 0.026$.

The induction roll up gas volume ratio $(Q/Q_0) = 0.32 \frac{x}{d_0}$, the initial flow volume $Q_3 = \pi r_0^2 u_0 \ [m^3/s]$.

Sec 8   Initial Phase Flow Speed Distribution for Circular Aperture Jets
Flowing With the Current

Let us assume that we are dealing with a jet in which a round aperture with a diameter $d = 2r_0$ puts out an even flow speed, U_0, and in which there is an initial momentum flow rate, M_0, (Fig 8.4). Point n is a point on the edge of the jet nozzle. n1 is the interior boundary; the angle of expansion $= a_1$. n2 is the exterior boundary with an angle of expansion $= a_2$. The area between the interior and exterior boundaries is the turbulence mixture layer. Ox is the jet aperture axis line. The core length of the round cone-shaped jet $= x_0$. The radius from the axis line to the interior boundary $= r_1$; the radius from the axis line to the exterior boundary $= r_2$. r= the radius at a certain point in the mixture layer. The area surrounding a round aperture jet includes gases which flow along with the current at a flow speed $= U_1 < U_0$, $(U_1/U_0) = \lambda$. On the axis line, the maximum corresponding flow speed $u_m = U_0 - U_1$. The corresponding flow speed at a place with a certain radius, r, is $u = U - U_1$. At a place where

$U = \frac{1}{2} U_0$, the width of the mixture layer $= b$, and it expands along x, forming a sharply delineated type of mixture layer. At a fixed point, x, the total width of the mixture layer is $\delta = (r_2 - r_1)$.

Let us assume that the corresponding flow speed ratio is

$$\left(\frac{u}{u_m}\right) = \frac{U - U_1}{U_0 - U_1},$$

The non-dimensional coordinates

192

$$\xi = \frac{r_2 - r}{r_2 - r_1}; \quad \left(\frac{u}{u_m}\right) = f(\xi)$$

Let us adjust the flow speed ratio between the surroundings and the jet so that λ is equal to a constant and $0 \leqslant \lambda < 1$; on the basis of a great deal of data obtained from experimental observations and measurements, it is possible to utilize the smallest square to induce the non-dimensional flow distribution function $f(\xi)$ for different cross sections, x, and draw out similar curves to the one shown in Fig 8.5.
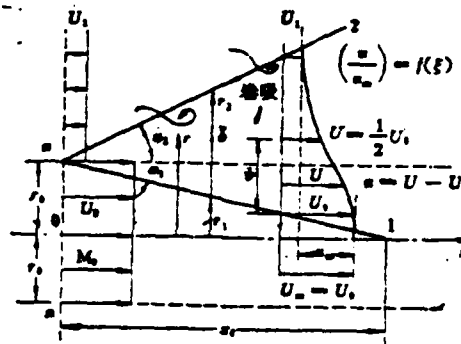

Fig. 8.4. Round aperture jet initial stage mixture layer.

Key: 1. Induced roll up.

$$f(\xi) = \frac{1}{2}(1 - \cos \pi \xi)$$

(8.85)

If we consider the case in which the jet flow speed, U_o, is already fixed, then, the magnitude of the parallel flow speed of the surrounding gases, U_1, that is to say, the magnitude of λ, influences the total width of the mixture layer, $\overline{b}$, as well as the length of the jet core, x_o. If one is considering the case in which U_1 is increased in size, and λ is increased in size, then, even though λ is still smaller than one, the mixture layer is made narrower (Fig 8.6), and the angles of expansion, α_1 and α_2, are both reduced in size (Fig 8.7); the core of the jet flow, x_0, is elongated. When $\lambda = 1$, then, there are formed two evenly parallel flows, the mixture layer is narrowed to nothing, and the jet core is lengthened to infinity. After $\lambda > 1, U_1 > U_o$, the nozzle jet becomes a weakly induced flow. Because of the effects of the fact that the surrounding gas flow is violently induced to roll up on itself, the mixture layer is narrowed, and the length of the jet core
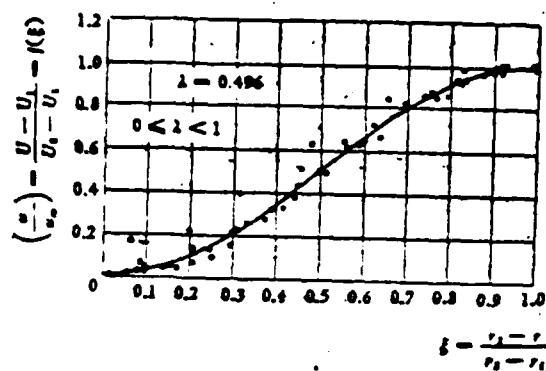
193

Fig. 8.5. Similar flow speed distribution curves.

is shortened. The surrounding gas flow interacts with the turbulence flow by transferring momentum to the weaker of the two flows, and, thereby, raising the static pressure along the axis line of the jet, x; this process can continue even to the point where it creates a positive pressure gradient $(\partial \bar{p}/\partial x)$. In situations where the dynamic pressure of the weak flow, $1/2 \, \rho U_1^2$, cannot overcome this positive pressure gradient, one can see the production of points of impedance, with the appearance of counter-current flows and localized reflux areas. If one is not dealing with a mixture layer in an environment of constant pressure, then it is not possible to simply use the axial conservation of momentum method in order to deal with the problem. If $\lambda = 0$, that is to say, if a round aperture jet flow, U_0 is entering a gaseous environment which is at rest, $U_1 = 0$; then, in the mixture layer, the flow speed distribution is still similar to the curve found in Fig 8.5. If one is dealing with a round aperture free jet flow, so that $\lambda = 0$, then the expansion of the interior and exterior boundaries of the mixture layer can be represented by the radius test formula below:

$$\frac{r_1}{r_0} = 0.95 - 0.097 \frac{x}{r_0}$$
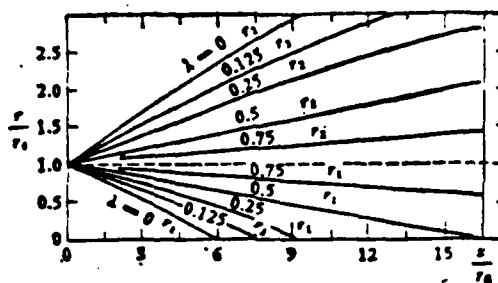
(8.86)

194

Fig 8.6

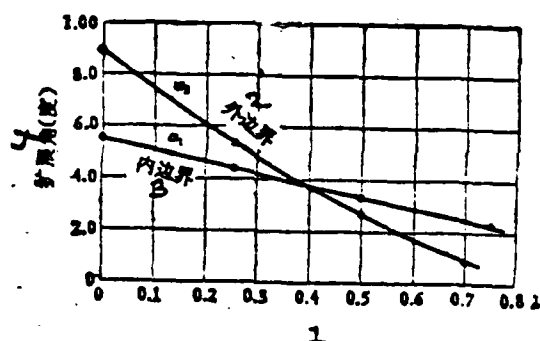1. The Expansion of Round Aperture Jet Mixture Layers for Different Values of

图 8.7 顺流射流初始区，内外扩展角变化

Fig 8.7

1. Changes in the Interior and Exterior Angles of Expansion in the Initial Stage of a Parallel Flow Jet 2. Exterior Boundary 3. Interior Boundary 4. Expansion Angle (in degrees)

$$\frac{r_2}{r_0} = 1.07 + 0.158 \frac{x}{r_0}$$

(8.87)

The induction roll up gas volume ratio is

$$\frac{Q}{Q_0} = 1 + 0.083 \left(\frac{x}{d}\right) + 0.013 \left(\frac{x}{d}\right)^2$$

(8.88)

Chapter 9 Distribution of Temperature and Concentration in Jets

Sec 1 Potential Energy Equations for Boundary Level Laminar Flow Jets

Let us make use of the following assumptions about boundary layers:

$$(1)\ v \ll u;\ (2)\ (\partial u/\partial x) \ll (\partial u'/\partial y),\ (\partial T/\partial x) \ll (\partial T/\partial y).$$

Let us also assume that x is the primary direction of flow. Diffusion of momentum, thermal energy and mass takes place primarily in the y direction. Let us separate minute control bodies from the boundary layers of laminar flow (or boundary layers), $dx \cdot dy \cdot 1$, (assume that there is a dimension = 1 which is perpendicular to the surface of the illustration). Let us check into the entry and exit energy flow rates of the control bodies as shown in Fig 9.1 (a), (b) and (c). Let us talk for a moment about these minute control bodies, $dx \cdot dy \cdot 1$.

The differential of added kinetic energy due to enthalpy in the control bodies between the time of their entry and exit is equal to the differential of cross-current thermal conductance plus the differential of friction energy. Let us assume that

$$q^2 = u^2 + v^2,\ i = c_p T,\ di = c_p dT,$$
$$(\partial i/\partial x) = c_p(\partial T/\partial x);$$

The differential of the density flow of the additional kinetic energy due to enthalpy is equal to

$$\approx \frac{\partial}{\partial x}(\rho u)\left(i + \frac{q^2}{2}\right)$$
$$+ \frac{\partial}{\partial y}(\rho v)\left(i + \frac{q^2}{2}\right) = \left(i + \frac{q^2}{2}\right)\left[\frac{\partial}{\partial x}(\rho u)\right.$$
$$+ \frac{\partial}{\partial y}(\rho v)\Big] + \rho u \frac{\partial}{\partial x}\left(i + \frac{q^2}{2}\right) + \rho v \frac{\partial}{\partial y}\left(i + \frac{q^2}{2}\right),$$

According to the continuity equation

$$\frac{\partial}{\partial x}(\rho u) + \frac{\partial}{\partial y}(\rho v) = 0,$$

Therefore, the energy equilibrium equation is

196

$$\rho u\left[c_p\frac{\partial T}{\partial x} + \frac{\partial}{\partial x}\left(\frac{q^2}{2}\right)\right] + \rho v\left[c_p\frac{\partial T}{\partial y} + \frac{\partial}{\partial y}\left(\frac{q^2}{2}\right)\right] \qquad (9.1)$$

$$= \frac{\partial}{\partial y}\left(\lambda\frac{\partial T}{\partial y}\right) + \frac{\partial}{\partial y}\left(\mu u\frac{\partial u}{\partial y}\right),$$

$$\rho v dx\left(i + \frac{q^2}{2}\right) + \frac{\partial}{\partial y}\left[\rho v dx\left(i + \frac{q^2}{2}\right)\right]dy$$

$$\rho u dy\left(i + \frac{q^2}{2}\right) \quad \rho u dy\left(i + \frac{q^2}{2}\right) + \frac{\partial}{\partial x}\left[\rho u dy\left(i + \frac{q^2}{2}\right)\right]dx$$

$$dy \qquad dx \qquad \rho v dx\left(i + \frac{q^2}{2}\right)$$

(a) 进出焓及动能

$$-\lambda\frac{\partial T}{\partial y}dx + \frac{\partial}{\partial y}\left(-\lambda\frac{\partial T}{\partial y}dx\right)dy \qquad u\mu\frac{\partial u}{\partial y}dx + \frac{\partial}{\partial y}\left[u\mu\frac{\partial u}{\partial y}dx\right]dy$$

$$dy \qquad dy \qquad dx$$

$$-\lambda\frac{\partial T}{\partial y}dx \qquad u\mu\frac{\partial u}{\partial y}dx$$

(b) 进出传导热   (c) 进出摩擦热

Fig 9.1

1. Entrance and Exit Enthalpy and Kinetic Energy   2.   Entrance and Exit Heat
Transference   3.   Entrance and Exit Heat of Friction

Due to the fact that we have assumed that the boundary layers are formed so that
$v \ll u$, therefore, the total temperature

$$T^* = T + \frac{q^2}{2c_p} \cong T + \frac{u^2}{2c_p}; \qquad (9.2)$$

197

If the isobaric specific heat, c_p = a constant, then, from equation (9.2), it is possible to obtain

$$u \frac{\partial u}{\partial y} = \frac{\partial}{\partial y}\left(\frac{u^2}{2}\right) = c_p\left(\frac{\partial T^*}{\partial y} - \frac{\partial T}{\partial y}\right) \approx \frac{\partial}{\partial y}\left(\frac{q^2}{2}\right)$$

and, by the same reasoning,   (9.3)

$$\frac{\partial}{\partial x}\left(\frac{q^2}{2}\right) \approx c_p\left(\frac{\partial T^*}{\partial x} - \frac{\partial T}{\partial x}\right) \approx \frac{\partial}{\partial x}\left(\frac{u^2}{2}\right) = u\frac{\partial u}{\partial x};$$

The Prandtl number

$$Pr = \frac{\mu c_p}{\lambda} = \frac{\nu}{a},$$

The coefficient of temperature conductivity is

$$a = \frac{\lambda}{c_p \rho};$$

If we take the relationships at (9.3) and substitute them into equation (9.1), then, it is possible to obtain

$$\rho u \frac{\partial T^*}{\partial x} + \rho v \frac{\partial T^*}{\partial y} = \frac{\partial}{\partial y}\left(\mu \frac{\partial T^*}{\partial y}\right)$$
$$+ \frac{\partial}{\partial y}\left[\left(\frac{1}{Pr} - 1\right)\mu \frac{\partial T}{\partial y}\right] \qquad (9.4)$$

Concerning the momentum equations of boundary layers of laminar flow, if we compare them to equation (7.27) (in which there is no pulsation velocity component u' or v'), it should be true that

$$\rho u \frac{\partial u}{\partial x} + \rho v \frac{\partial u}{\partial y} = -\frac{\partial p}{\partial x} + \frac{\partial}{\partial y}\left(\mu \frac{\partial u}{\partial y}\right) \qquad (9.5)$$

If one takes u and performs successive multiplications on the various quantities of the equation above, then, after the manipulations are finished, one can obtain

$$\rho u \frac{\partial}{\partial x}\left(\frac{u^2}{2}\right) + \rho v \frac{\partial}{\partial y}\left(\frac{u^2}{2}\right) = -u\frac{\partial p}{\partial x} + u\frac{\partial}{\partial y}\left(\mu \frac{\partial u}{\partial y}\right)$$
$$= -u\frac{\partial p}{\partial x} + \frac{\partial}{\partial y}\left(\mu u \frac{\partial u}{\partial y}\right) - \mu\left(\frac{\partial u}{\partial y}\right)^2; \qquad (9.6)$$

Because of the boundary layers, let us assume that

$$\frac{\partial p}{\partial y} \approx 0, \quad \frac{\partial v}{\partial y} \approx 0,$$

Therefore,

$$u \frac{\partial}{\partial x}\left(\frac{v^2}{2}\right) \quad \text{and} \quad v \frac{\partial}{\partial y}\left(\frac{v^2}{2}\right) \quad \text{can be ignored in any computations.}$$

If we subtract equation (9.6) from equation (9.1), then it is possible to obtain

$$\rho u c_p \frac{\partial T}{\partial x} + \rho v c_p \frac{\partial T}{\partial y} = u \frac{\partial p}{\partial x}$$

$$+ \frac{\partial}{\partial y}\left(\lambda \frac{\partial T}{\partial y}\right) + \mu \left(\frac{\partial u}{\partial y}\right)^2 \qquad (9.7)$$

If we take ρc_p and use it to perform successive multiplications on the various quantities in the equation above, and, if we assume that ρ, c_p, λ and μ are all constants, then, it is possible to obtain

$$u \frac{\partial T}{\partial x} + v \frac{\partial T}{\partial y} = \frac{u}{\rho c_p} \frac{\partial p}{\partial x} + \left(\frac{\lambda}{c_p \rho}\right) \frac{\partial^2 T}{\partial y^2}$$

$$+ \frac{\mu}{427 \rho c_p}\left(\frac{\partial u}{\partial y}\right)^2$$

If one assumes that the static pressure, p, along x is invariable, then, $(\partial p/\partial x) = 0$. Because of the fact that the power of viscose friction which is turned into a quantity of heat is much smaller than the cross flow which is turned into thermal conductance, therefore, it is possible to ignore the quantity $\mu(\partial u/\partial y)^2$, and, due to this fact, the thermal energy diffusion equation for a boundary layer of laminar flow is

$$u \frac{\partial T}{\partial x} + v \frac{\partial T}{\partial y} = a \frac{\partial^2 T}{\partial y^2}. \qquad (9.8)$$

Sec 2 Equations for Heat Energy Dissipation in Boundary Layers of Turbulent Flow

Let us consider the case of an average time quasi-stable state two-dimensional turbulence flow field. The turbulence flow shear force $\tau_o = \tau_T$; the turbulence flow thermal density flow $= q_T$, and, let us take the average time parameters

199

plus the pulsation parameters and substitute that quantity for the instantaneous parameters, as we see below,

$$\left.\begin{array}{lll}
u = \bar{u} + u' & \rho u = \overline{\rho u} + (\rho u)' & T = \bar{T} + T' \\
v = \bar{v} + v' & \rho v = \overline{\rho v} + (\rho v)' & \tau_T = -\rho \overline{u'v'} = \mu_T \dfrac{\partial \bar{u}}{\partial y} \\
\rho = \bar{\rho} + \rho' & p = \bar{p} + p' & q_T = -c_p \overline{(\rho v)'T'} = k \dfrac{\partial \bar{T}}{\partial y}
\end{array}\right\} \qquad (9.9)$$

Let us take the relationships at (9.9) and substitute them into equation (9.7); then, if we are considering a case in which compressibility is not a factor, and $\bar{\rho}=$ a constant, it is possible to obtain

$$
\begin{aligned}
c_p \rho \bar{u} \frac{\partial \bar{T}}{\partial x} + c_p \rho \bar{v} \frac{\partial \bar{T}}{\partial y} &= \bar{u} \frac{\partial \bar{p}}{\partial x} + \frac{\partial}{\partial y} \left(\lambda \frac{\partial \bar{T}}{\partial y} \right) \\
&+ \mu \left(\frac{\partial \bar{u}}{\partial y} \right)^2 + \frac{\partial}{\partial y} [-c_p \overline{(\rho v)'T'}] - \rho \overline{v'u'} \frac{\partial \bar{u}}{\partial y},
\end{aligned} \qquad (9.10)
$$

Let us further assume that c_p, λ, μ are all constants, that the static pressure, $\bar{p}$, along x, is invariable, and that $(\partial \bar{p}/\partial x) = 0$; if we assume all these things, then,

$$
\begin{aligned}
c_p \rho \left[\bar{u} \frac{\partial \bar{T}}{\partial x} + \bar{v} \frac{\partial \bar{T}}{\partial y} \right] &= (\lambda + k) \frac{\partial^2 \bar{T}}{\partial y^2} \\
&+ (\mu + \mu_T) \left(\frac{\partial \bar{u}}{\partial y} \right)^2,
\end{aligned} \qquad (9.11)
$$

In a laminar flow, the transference of heat through molecular motion is much smaller than the transference of heat which is due to the motion of the masses of gas in a turbulence flow, $k \gg \lambda$; therefore, it is possible to ignore λ. Concerning the final quantity in equation (9.11), this is the power dissipation due to friction in a laminar flow plus a turbulence flow, and, after this is converted into heat energy, this can also be ignored. Due to this fact, equation (9.11) can be simplified to read

$$
\bar{u} \frac{\partial \bar{T}}{\partial x} + \bar{v} \frac{\partial \bar{T}}{\partial y} = \left(\frac{k}{c_p \rho} \right) \frac{\partial^2 \bar{T}}{\partial y^2} = \varepsilon_T \frac{\partial^2 \bar{T}}{\partial y^2} \qquad (9.12)
$$

The quantity $\varepsilon_T = \dfrac{k}{c_p \rho}$, is called the "turbulence flow coefficient of temp-

erature conductivity," and it is measured in units of (m^2/s).

If we assume that $\varepsilon = \dfrac{\mu_T}{\rho}$, which is called the "turbulence flow dynamic

200

viscosity," then the turbulence flow shear force $\tau_T = \rho \varepsilon \dfrac{\partial \bar{u}}{\partial y}$; from equation (7.30), we can derive

$$\bar{u}\,\frac{\partial \bar{u}}{\partial x} + \bar{v}\,\frac{\partial \bar{u}}{\partial y} = \frac{1}{\rho}\,\frac{\partial}{\partial y}\left(\rho \varepsilon \,\frac{\partial \bar{u}}{\partial y}\right) = \varepsilon\,\frac{\partial^2 \bar{u}}{\partial y^2} \qquad (9.13)$$

If one makes a careful mutual comparison between equation (9.12) and equation (9.13), and, if the "turbulence flow coefficient of temperature conductivity," ε_T , is completely equal to the "turbulence flow dynamic viscosity," ε , then, the two differential equations are completely similar, and their solutions are identical; therefore, velocity distribution is nothing more than temperature distribution. This corresponds to a state in which the turbulence flow Prandtl number, Pr'=1.

The laminar flow Prandtl number is

$$Pr = \frac{\nu}{a} = \frac{\mu c_p}{\lambda},$$

and the turbulence flow Prandtl number is

$$Pr' = \frac{\varepsilon}{\varepsilon_T} = \frac{\mu_T c_p}{k};$$

However, different gases at different temperatures have different Prandtl numbers (Fig 9.2). The viscosity, μ , is also different (Fig 9.3). If the multiple of turbulence flow and laminar flow viscosity is approximately equal to the multiple of the rate of thermal conductance of turbulence flow and laminar flow, that is to say, $(\mu_T/\mu) \approx (k/\lambda)$, then, it is possible to consider $Pr' \cong Pr$, and it is also possible to borrow the Prandtl number for laminar flow.
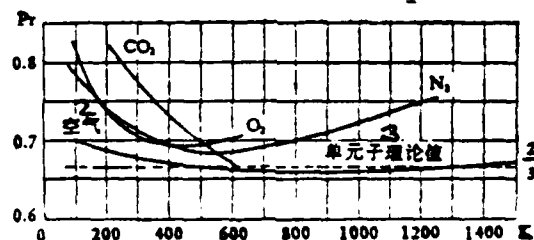

Fig 9.2

1. Prandtl Numbers, $Pr = \frac{\mu c_p}{\lambda}$ Follow changes in temperature, T (K)

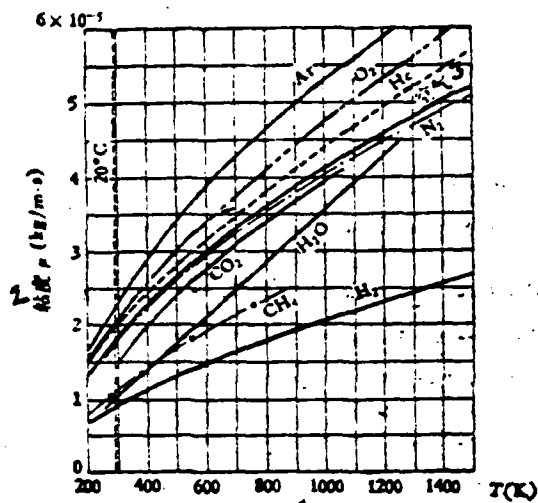2. Air 3. A Theoretical Value for Unity

図9:3 气体粘度 $\frac{1}{\mu}$ 随温度变化

Fig 9.3

1. Gas Viscosity, μ , As It Varies With Changes in Temperature 2. Viscosity
3. Air

Sec 3   Initial Phase Temperature Distribution for Flat Mouth Jets

Let us make a consideration of this subject on the basis of what we have already said in Chapter 8, Sec 4 and a look at Fig 8.2. Let us continue to select as the base line $\xi_T = 0$ where $u = \frac{1}{2} U_0$. Let us assume that σ_T is an experimentally

determined constant and that

$$\xi_T = \sigma_T \frac{y}{x}, \quad \frac{\partial \xi_T}{\partial x} = -\frac{\sigma_T y}{x^2} = -\frac{\xi_T}{x}, \quad \frac{\partial \xi_T}{\partial y} = \frac{\sigma_T}{x};$$

(9.14)

T — the temperature at a certain point y in a boundary layer

$$\frac{u}{u} = \sigma F'(\xi) = \sigma F',$$

$T_\bullet$ — the maximum temperature inside a boundary layer

$$F'' = \frac{d^2 F}{d \xi^2}, \quad F = \int_0^\xi F' d\xi;$$

T_H — the ambient temperature outside a boundary layer

$$F''' = \frac{d^3 F}{d \xi^3},$$

202

T_e — the initial temperature of the jet

$$\theta' = \frac{d\theta}{d\xi}, \quad \theta'' = \frac{d^2\theta}{d\xi^2}.$$

Let us assume that $T_e = \frac{1}{2}(T_a + T_H)$; then, the ratio of temperature

differentials is

$$2\frac{\Delta T}{\Delta T_e} = \frac{T - T_H}{T_e - T_H} = \sigma_T \theta(\xi_T) \qquad (9.15)$$

On the basis of Chapter 8, Sec 4, the rules governing the expansion of the width of
a boundary layer are

$$b_T = C_T x, \quad C_T = \text{ a constant}$$

$$K_T = \text{ a constant, and the turbulence flow coefficient of}$$
$$\text{temperature conductivity is}$$

$$\epsilon_T = K_T b_T U_e = K_T C_T x U_e,$$
$$\sigma_T = \frac{1}{2\sqrt{K_T C_T}}, \qquad (9.16)$$

If one states that he is dealing with an average time quasi-stable state, in the
thermal energy dissipation equation for a boundary layer, the symbols do not
reappear:

$$u\frac{\partial T}{\partial x} + v\frac{\partial T}{\partial y} = \epsilon_T \frac{\partial^2 T}{\partial y^2}$$

If we take equation (9.14), (9.15) and (9.16) and substitute them into equation
(9.12), after the manipulations are over, it is possible to obtain

$$\theta'' + 2\sigma_T \theta' F = 0, \quad \frac{1}{\sigma_T}\frac{\theta''}{\theta'} = -2F \qquad (9.17)$$

From equation (8.52)

$$F''' + 2\sigma F F'' = 0, \quad \frac{1}{\sigma}\frac{F'''}{F''} = -2F \qquad (9.18)$$

If we make a comparison of equations (9.17) and (9.18), and then assume that
$\delta = \frac{\sigma_T}{\sigma}$, it will follow that $\frac{\theta''}{\theta'} = \frac{F'''}{F''}\frac{\sigma_T}{\sigma} = \frac{F'''}{F''}\delta$ $\qquad (9.19)$

Integrating once

203

$$\ln C_1 \theta' = \ln(F'')^s, \quad C_1 \theta' = (F'')^s \tag{9.20}$$

Integrating again

$$C_1 \theta = \int_0^\xi [F''(\xi)]^s d\xi + C_2 \tag{9.21}$$

According to the Goertler solution method in Chapter 8, Sec 4

$$F''(\xi) \cong \frac{1}{\delta} F_1''(\xi) = \frac{2}{\sigma \sqrt{x}} e^{-\xi^2}.$$

If we take this equation and substitute it into equation (9.21), then,

$$C_1 \theta = \int_0^\xi \left[\frac{2}{\sigma \sqrt{x}} e^{-z^2} \right]^s dz + C_2 \tag{9.22}$$

If we utilize the following boundary conditions

when $\xi = 0$, $\Delta T = 0.5\Delta T_0$, that is, $\sigma_T \theta = 1$;

when $\xi \to \infty$, $\Delta T = \Delta T_0$, that is, $\sigma_T \theta = 2$;

then, after we solve for C_1 and C_2, it is possible to obtain

$$\frac{\Delta T}{\Delta T_0} = \frac{1}{2} \sigma_T \theta = 0.5 + \frac{1}{\sqrt{x}} \int_0^{\xi_T} e^{-z^2} dz, \quad \xi_T = \xi \sqrt{\delta}; \tag{9.23}$$

The form of this equation and the form of equation (8.55) are the same; therefore, the temperature differential distribution and the flow speed distribution both have similar curves (Fig 8.3). However, due to the fact that $\delta \ne 1$, the horizontal coordinate should be changed into ξ_T ; this value differs from the coordinate ξ in Fig 8.3 by $\sqrt{\delta}$ times. If we assume that $\delta = 2$, then, experimental data and theoretical computations agree with each other.

Sec 4   Distribution of Normal Phase Temperature Differences for Narrow Crack and Round Aperture Jets

According to Chapter 8, Sec 2 (Fig 8.1), let us take a look at the thermal energy equilibrium of the integrated control layer, dx·1, in the normal or pattern stage of a jet (assume that there is a thickness = 1 which is perpendicular to the surface of the illustration). Let us assume that the temperature differential is $\Delta T = T - T_H$.

The amount of increase in enthalpy which flows toward the control layer, dx·1,

$= \rho v c_r \Delta T \cdot dx \cdot 1$ [kcal/s],

The amount of increase in enthalpy which flows out of the control layer, dx·1,

$$= dQ = -d \int_y^\infty (\rho u c_p \Delta T) dy \quad [\text{kcal/s}],$$

The thermal energy which is dissipated in a turbulence flow across a control layer =

$$q_T dx \cdot 1 = k \frac{\partial \Delta T}{\partial y} \cdot dx \cdot 1 \quad [\text{kcal/s}];$$

The thermal energy equilibrium of a control layer is

$$\rho v c_p \Delta T dx + d \int_{-\infty}^y (\rho u c_p \Delta T) dy - k \frac{\partial \Delta T}{\partial y} = 0,$$

The turbulence flow coefficient of temperature conductivity is

$$\varepsilon_T = \frac{k}{c_p \rho},$$

Therefore,

$$v \Delta T + \frac{\partial}{\partial x} \int_{-\infty}^y u \Delta T dy - \varepsilon_T \frac{\partial \Delta T}{\partial y} = 0 \tag{9.24}$$

In the pattern or normal stage, let us assume that the turbulence flow coefficient of temperature conductivity is

$$\varepsilon_T = K_T C_T x u_m, \quad [\text{m}^2/\text{s}] \tag{9.25}$$

Along the x axis line, the rule governing the attenuation and reduction of the maximum temperature differential is

$$(T_\infty - T_H) = \Delta T_\infty = \text{a constant} \frac{r}{\sqrt{x}} \tag{9.26}$$

Let us assume that the non-dimensional temperature differential distribution function is

$$\theta(\xi_T) = \frac{\Delta T}{\Delta T_\infty}, \quad \xi_T = \sigma_T \frac{y}{x}; \tag{9.27}$$

$$\Delta T = \frac{r}{\sqrt{x}} \theta(\xi_T) = \frac{r}{\sqrt{x}} \theta, \quad \xi_T = \frac{\sigma_T}{\sigma} \xi,$$

$$\xi = \sigma \frac{y}{x}, \quad \frac{\partial \xi_T}{\partial y} = \frac{\sigma_T}{x};$$

$$\frac{\partial \Delta T}{\partial y} = \frac{r}{\sqrt{x}} \theta' \frac{\partial \xi_T}{\partial y} = \frac{r \sigma_T}{x \sqrt{x}} \theta' \tag{9.28}$$

If we take the equations from (9.35) to (9.38) and substitute them into equation (9.34), then we can obtain

205

$$F\theta + 2K_T C_T \sigma_T \sigma \theta' = 0 \qquad (9.29)$$

If we assume yet again that

$$\sigma_T = \frac{1}{2\sqrt{K_T C_T}}, \quad \sigma = \frac{1}{2\sqrt{kc}},$$

$$2K_T C_T \sigma_T \sigma = \frac{2K_T C_T}{4\sqrt{kc} \cdot \sqrt{K_T C_T}} = \frac{1}{2}\sqrt{\frac{K_T C_T}{kc}};$$

k, c, σ have precise values determined for them by experimental measurements of *flow speed distribution*, and, if we assume that

$$\delta = \sqrt{\frac{K_T C_T}{kc}} = \frac{\varepsilon_T}{\varepsilon} = \frac{1}{Pr};$$

K_T, C_T, σ_T have precise values determined for them by experimental measurements of temperature distribution. Equation (9.29) can be simplified to read

$$2F\theta + \delta\theta' = 0, \quad \delta\frac{\theta'}{\theta} = -2F \qquad (9.30)$$

If we utilize equation (8.28), then,

$$2FF' + F'' = 0, \quad \frac{F''}{F'} = -2F \qquad (9.31)$$

Therefore, the relationship between the temperature differential and the standardized flow speed function is

$$\delta\frac{\theta'}{\theta} = \frac{F''}{F'} \qquad (9.32)$$

If we employ the boundary conditions which follow, i.e.,

$$\xi = 0, \ u = u_m, \ F' = 1, \ \Delta T = \Delta T_m, \ \theta = 1,$$

and then integrate the equation above, it is possible to obtain

$$\theta^\delta = F', \quad \text{or} \quad \left(\frac{\Delta T}{\Delta T_m}\right) = \left(\frac{u}{u_m}\right)^{1/\delta} = \left(\frac{u}{u_m}\right)^{Pr} \qquad (9.33)$$

Experimentation proves that, if $\delta = 2$, or Pr=0.5, then, there is agreement with the relationships at (9.33).

When one is considering the case of the patterned or normal stage of an axially symmetrical turbulence flow jet, which is put out from a round aperture, the rela-

206

tionship between the temperature differential distribution and the flow speed distribution is the same as equation (9.33). Therefore, we already know Pr and the flow speed distribution, that is to say, it is possible to obtain the temperature differential distribution.

Sec 5   Experiments on Concentration Distributions in Boundary Layers of Turbulence
Jets

In gases which mix at rest, if the gas consists of two types of gas, A and B, then the distributions of concentration, c_A and c_B, are uneven. Because of molecular motion, both A and B diffuse from areas in which they are highly concentrated toward areas in which their concentrations are low. It is only necessary to have enough time, and it is possible to reach an even mixing, that is to say, at various points in the space, c_A and c_B are evenly distributed. This is called "free molecular diffusion." Taking gas A as the basis, at any given instant there is a distributional lay-out for the concentration, c_A. This form or lay-out can be drawn out in the form of a concentration distribution curve.

Concerning a flat mouth or round aperture jet, when gas A is propelled into a stationary gas B, it is obvious that the concentration of gas A will be highest (c_m) on the axis line of the jet. Because of the fact that the masses of gas in the turbulence flow tumble over each other and pulsate, the movement of gas A in a circumferential direction toward the surrounding environment and across the flow of the jet produces the situation that the farther one goes from the axis line of the jet, the lower is the concentration, c_A. It is also true that the farther down the flow one goes from the jet nozzle the lower becomes the value of c_m on the axis line. If the original flow speed of the jet, u_o, and the initial concentration of the jet, c_o, do not change, and the flow speed distribution of the average time stable state does not change either, then, in both the cross-current direction and the parallel flow direction it is possible to attain a stable concentration distribution. This is called "turbulence flow pulse diffusion."

Figure 9.4 represents a comparison between the distribution of the concentration ratio, c/c_m, which measures the burden of carbon dioxide (CO_2) at various cross sections such that $\bar{x} = x/b_o = 10, 20, 30, 40$ as it pertains to a flat moutn jet with $2 b_o = 3$ [mm] and a width of $2 h_o = 300$ [mm] which is propelling carbon dioxide (CO_2) into stationary air at an initial flow speed $u_o = 55.9$ (m/s) and the distributions of temperature differential and flow speed. $y_{0.5}$ is the vertical co-

ordinate for a place where the flow speed $u=0.5u_m$. The weight concentration ratio
is the ratio between the weight of the CO_2 contained in each unit of volume and the
weight of the air contained in it. It is possible to withdraw a sample of gas from
the jet and use a chromatograph to determine the concentration, c, of the CO_2 which
it contains. Or, it is also possible to use pulse lasers to illuminate and measure
flow fields, take integrated information photography for the analysis of interfer-
ence pattern spectra, and to measure the concentration distribution of CO_2. The
error in this measurement of concentration is less than or equal to 3%. From look-
ing at Fig 9.4, it is possible to see that the corresponding concentration (c/c_m)
datum points for different cross sections $\bar{x} = (x/b_0)$ which are used to obtain measure
ments of the pattern or normal stage of a jet almost all fall on the normal curve
for temperature differential distribution. This explains the fact that the process
of turbulence flow concentration diffusion (mass exchange) and the process of
turbulence flow thermal energy dissipation are similar; however, they are very
different from the flow speed distribution (momentum exchange).

If it happens that the environment surrounding the jet itself contains carbon
dioxide in a concentration c_H, then, it is possible to utilize the concentration
differential $\Delta c = c - c_H$. On the axis line, the maximum concentration dif-
ferential $\Delta c_m = c_m - c_H$. As far as an average time quasi-stable state
jet is concerned, the amount of a certain substance (for example, CO_2), which is
put out by each unit of width of a jet nozzle each second is $M_0 = 2 b_0 u_0 \cdot 1 \cdot \rho_0 \Delta c_0$
and this is a constant. If we assume that the area of a jet cross section $= F$,
then,

$$M = \int_0^F \rho \Delta c u \, dF = M_0 = \text{a constant} \quad (9.34)$$

Concerning a flat mouth two dimensional jet, half the height $= b$, $dF = dy \cdot 1$,
and, if we use non-dimensional parameters like (u/u_m), $(\Delta c/\Delta c_m)$, (y/x),
in a non-compressible flow where $p =$ a constant, and, if we only consider half the
jet, and recognize that the attenuation and reduction of Δc_m and u_m along x are the
same, then,

$$\Delta c_m u_m x \int_0^{b/x} \frac{\Delta c}{\Delta c_m} \cdot \frac{u \, dy}{u_m \, x}$$

$$= (\Delta c_m)^2 x \int_0^{b/x} \frac{\Delta c}{\Delta c_m} \cdot \frac{u}{u_m} \cdot \frac{dy}{x} = \text{a constant} \quad (9.35)$$

Because of the fact that the flow speed ratio u/u_m and the ratio of concentration
differentials $\Delta c/\Delta c_m$ are both normal functions, they are unrelated to x; there-
fore, the integral of equation (9.35) should be a constant. On the basis of the

conservation of mass equation (9.34), it should be true that

$$(\Delta c_m)^2 x = \text{ a constant, or } \Delta c_m = \frac{\text{a constant}}{\sqrt{x}} \qquad (9.36)$$

As far as a round aperture axially symmetrical jet is concerned, if half the height
of the boundary layers is $=r$, and the integrated cross section $dF = 2\pi y\,dy$,
then,

$$2\pi x^2 u_m \Delta c_m \int_0^{r/x} \frac{\Delta c}{\Delta c_m} \cdot \frac{u}{u_m} \cdot \frac{y}{x} \cdot \frac{dy}{x} = \text{ a constant}$$

By the same reasoning, it is possible to obtain the relationship

$$\Delta c_m = \frac{\text{a constant}}{x}. \qquad (9.37)$$
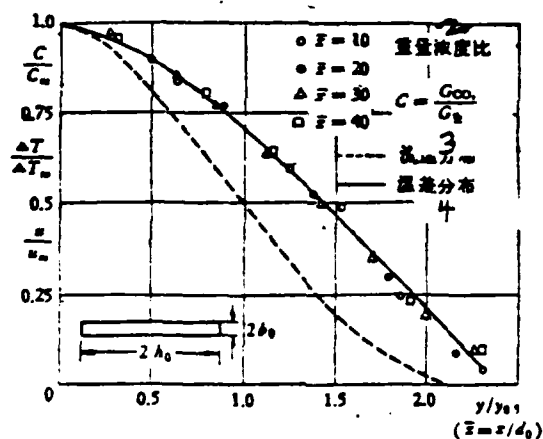
Fig 9.4

1. Flow Speed, Temperature Differential and Concentration Distributions in the
Self-patterning or Normal Stage of a Flat Mouth Turbulence Flow Jet 2. Weight
Concentration Ratio 3. Flow Speed Distribtution 4. Temperature Differential
Distribution

From a two-dimensional laminar flow field, let us separate and remove a minute control body $dx \cdot dy \cdot 1$ (there is a thickness = 1 and perpendicular to the surface of the illustration). Let us take a look at the situation concerning the non-dimensional concentration, c, of a certain substance as it occurs in the parallel flow and cross-current flow of the entry and exit of control bodies (Fig 9.5).

The differential between rates of flow of a certain substance during its entrance and exit along x

$$- \frac{\partial}{\partial x} (\rho u c \cdot dy) dx,$$
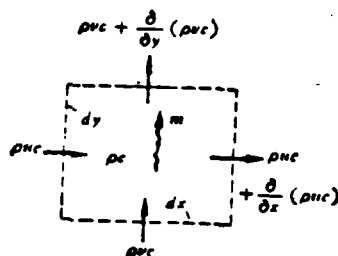
Fig 9.5

1. The Situation Concerning Concentration Diffusion

The differential between rates of flow of a certain substance during its entrance and exit along y

$$- \frac{\partial}{\partial y} (\rho v c \cdot dx) dy,$$

The cross-current diffusion density flow

$$m = - D \rho \frac{\partial c}{\partial y}, \quad D = \text{ the molecular diffusion coefficient } (\text{m}^2/\text{s}).$$

Because of the fact that the input and output are not in equilibrium, there are initiated within the control bodies changes in concentration over time

$$= - \frac{\partial}{\partial t} (\rho c\, dx\, dy);$$

According to the conservation of mass, it is possible to write (if one assumes that the density, ρ, does not change)

$$\frac{\partial(uc)}{\partial x} + \frac{\partial(vc)}{\partial y} = \frac{1}{\rho} \frac{\partial m}{\partial y} - \frac{\partial c}{\partial t} = D \frac{\partial^2 c}{\partial y^2} - \frac{\partial c}{\partial t} \quad (9.38)$$

The incompressible, two-dimensional continuity equation is

$$\frac{\partial u}{\partial x} + \frac{\partial v}{\partial y} = 0 \qquad (9.39)$$

The left side of equation (9.38) can be expanded into

$$\frac{\partial(uc)}{\partial x} + \frac{\partial(vc)}{\partial y} = u \frac{\partial c}{\partial x} + v \frac{\partial c}{\partial y} + c \left(\frac{\partial u}{\partial x} + \frac{\partial v}{\partial y} \right), \quad (9.40)$$

If one is dealing with a stable laminar flow, then,

$$\frac{\partial c}{\partial t} = 0,$$

If we take equation (9.40) and substitute it into equation (9.38), then, it is possible to obtain

$$u \frac{\partial c}{\partial x} + v \frac{\partial c}{\partial y} = D \frac{\partial^2 c}{\partial y^2}. \qquad (9.41)$$

Sec 7 Concentration Diffusion Equations for Flat Mouth Turbulence Jets

Let us look at the case in which one is considering an average time quasi-stable state non-compressible turbulence flow field. In such a case it is possible to use the average time parameters plus the pulse parameters to replace the instantaneous parameters as follows:

211

$$c = \bar{c} + c', \quad u = \bar{u} + u', \quad v = \bar{v} + v', \cdots,$$
$$\overline{cu} = \bar{c}\bar{u} + \overline{c'u'}.$$

If we substitute these parameters into equation (9.41), then, it is possible to obtain

$$\frac{\partial(\bar{c}\bar{u})}{\partial x} + \frac{\partial(\bar{c}\bar{v})}{\partial y} + \frac{\partial(\overline{c'u'})}{\partial x} + \frac{\partial(\overline{c'v'})}{\partial y} = D\frac{\partial^2\bar{c}}{\partial y^2} \qquad (9.42)$$

In the equation above, $\dfrac{\partial(\overline{c'u'})}{\partial x}$ and $\dfrac{\partial(\overline{c'v'})}{\partial y}$ represent the energy

with which a certain type substance is transported by parallel flow and cross-current pulsations of turbulence flow air masses; this quantity is several times larger and stronger than the molecular motion diffusion of such a substance. Therefore, it is possible to ignore the quantity $D\dfrac{\partial^2\bar{c}}{\partial y^2}$.

The average time quasi-stable state continuity equation is

$$\frac{\partial \bar{u}}{\partial x} + \frac{\partial \bar{v}}{\partial y} = 0, \quad \text{or} \quad \left[\bar{c}\frac{\partial \bar{u}}{\partial x} + \bar{c}\frac{\partial \bar{v}}{\partial y}\right] = 0 \qquad (9.43)$$

If we take the first two quantities on the left side of equation (9.42) and expand them, then,

$$\frac{\partial(\bar{c}\bar{u})}{\partial x} + \frac{\partial(\bar{c}\bar{v})}{\partial y} = \bar{u}\frac{\partial \bar{c}}{\partial x} + \bar{v}\frac{\partial \bar{c}}{\partial y}$$
$$+ \left[\bar{c}\frac{\partial \bar{u}}{\partial x} + \bar{c}\frac{\partial \bar{v}}{\partial y}\right] = \bar{u}\frac{\partial \bar{c}}{\partial x} + \bar{v}\frac{\partial \bar{c}}{\partial y}.$$

Besides this, according to the assumptions about boundary layers, the flow speed change gradient along x is much smaller than the corresponding gradient along y. Therefore, it is possible to ignore the quantity $\dfrac{\partial(\overline{c'u'})}{\partial x}$. Due to this fact, equation (9.42) can be simplified to read

$$\bar{u}\frac{\partial \bar{c}}{\partial x} + \bar{v}\frac{\partial \bar{c}}{\partial y} + \frac{\partial(\overline{c'v'})}{\partial y} = 0 \qquad (9.44)$$

212

On the basis of the Taylor theory of turbulence flow, pulse concentration is

$$c' \propto l_T \frac{\partial \bar{c}}{\partial y},$$

l_T= the Taylor mixing distance. $v' \propto -u'$, the cross-current pulse component of velocity is

$$v' \propto - l_T \left| \frac{\partial \bar{u}}{\partial y} \right|, \quad l_T = kx\sqrt{2}, \quad k = \text{ a constant}$$

If we substitute these relationships into equation (9.44), then, we can obtain

$$\bar{u} \frac{\partial \bar{c}}{\partial x} + \bar{v} \frac{\partial \bar{c}}{\partial y} = 2k^2x^2 \frac{\partial}{\partial y}\left(\frac{\partial \bar{u}}{\partial y} \cdot \frac{\partial \bar{c}}{\partial y} \right) = D_T \frac{\partial^2 \bar{c}}{\partial y^2}. \qquad (9.45)$$

In the equations above, the turbulence flow diffusion coefficient is

$$D_T = 2k^2x^2 \frac{\partial \bar{u}}{\partial y} \ [\text{m}^2/\text{s}], \qquad (9.46)$$

The turbulence flow dynamic viscosity $= \frac{\mu_T}{\rho} = \varepsilon \ [\text{m}^2/\text{s}]$, and the Schmitt number $= \frac{\varepsilon}{D_T}$ \qquad (9.47).

If we take the three equations for the diffusion of momentum, thermal energy and mass in the self-patterning or normal stage of a noncompressible, average time quasi-stable state flat mouth turbulence flow jet and study them in comparison to each other, then, they will appear as below

$$\bar{u} \frac{\partial \bar{u}}{\partial x} + \bar{v} \frac{\partial \bar{u}}{\partial y} = \varepsilon \frac{\partial^2 \bar{u}}{\partial y^2}, \qquad (9.13)$$

, turbulence flow dynamic visosity, ε (9.13)

$$\bar{u} \frac{\partial \bar{T}}{\partial x} + \bar{v} \frac{\partial \bar{T}}{\partial y} = \varepsilon_T \frac{\partial^2 \bar{T}}{\partial y^2}, \qquad (9.12)$$

, turbulence flow coefficient of temperature conductivity, ε_T (9.12)

$$\bar{u} \frac{\partial \bar{c}}{\partial x} + \bar{v} \frac{\partial \bar{c}}{\partial y} = D_T \frac{\partial^2 \bar{c}}{\partial y^2}, \qquad (9.45)$$

, turbulence flow diffusion coefficient, D_T \qquad (9.45)

213

It can be seen that, if ε, ε_{η} and D_{η} are all constants, then the forms of the three differential equations above are completely similar, and the methods for solving them are all similar. Because of this fact, the solutions for them are completely similar. On the basis of equation (9.33), *it is possible to deduce that*

$$\left(\frac{\Delta T}{\Delta T_m}\right) = \left(\frac{\Delta c}{\Delta c_m}\right) = \left(\frac{u}{u_m}\right)^{\nu\sigma} = \left(\frac{u}{u_m}\right)^{\nu\sigma},$$

$$\delta = \frac{\varepsilon_T}{\varepsilon} = \frac{1}{Pr}; \tag{9.48}$$

Therefore, if we already know δ or the Prandtl number, Pr, then, it is possible, by utilizing the normal functions that have already been derived in Sec 2 and Sec 7 of Chapter 8, i.e.

$$(u/u_m) = F'(\xi) = 1 - \text{th}^2(\xi), \quad \xi = \sigma\frac{y}{x}; \tag{8.3_}$$

$$\left(\frac{u}{u_m}\right) = f = \frac{1}{(1 + 0.125\xi^2)^2}, \quad \xi = \sigma\frac{r}{x}; \tag{8.8_}$$

to directly derive the temperature differential distribution and the concentration differential distribution in the boundary layers of flat mouth and round aperture jets. Δc = the concentration differential between a certain coordinate, y, in a boundary layer, and the environment. Δc_m = the concentration differential between values on the axis line of a boundary layer and those in the external environment.

Chapter 10 Rotational Jets

Sec 1 Integral Equations for Rotational Jets and Vortex Strength Numbers S

The various kinds of vortical flow devices are all designed so that, before a jet flow leaves the jet nozzle, the vortical flow device forces the jet to rotate so that it has a tangential component of velocity, w. The particular characteristic about rotational jets is that their cross-current diffusion as well as their attenuation and reduction are both particularly fast. If the component of rotational velocity, w, is sufficiently strong, and, along x, there is a positive pressure gradient, then not long after the jet leaves the nozzle one can see the production of counter-current flow and the formation of areas of reflux. This can shorten flames and stabilize combustion. If we use cylindrical coordinates in x, r, and θ; average time components of velocity, u, v, and w, pulse components of velocity, u', v', and w', and, if we use normal stresses $\sigma_x, \sigma_r, \sigma_\theta$, and shear stresses of $\tau_{xr}, \tau_{\theta r}$ (See Chapter 8, Sec 5), then, the basic jet equations are as follows:

$$u\frac{\partial u}{\partial x} + v\frac{\partial u}{\partial r} = -\frac{1}{\rho}\frac{\partial p}{\partial x}$$
$$-\frac{\partial \overline{u'v'}}{\partial r} - \frac{\overline{u'v'}}{r} - \frac{\partial \overline{u'u'}}{\partial x} \quad (10.1)$$

$$u\frac{\partial v}{\partial x} + v\frac{\partial v}{\partial r} - \frac{w^2}{r} = -\frac{1}{\rho}\frac{\partial p}{\partial r}$$
$$-\frac{\partial \overline{v'v'}}{\partial r} - \frac{\overline{v'v'}}{r} + \frac{\overline{w'w'}}{r} - \frac{\partial \overline{u'w'}}{\partial x} \quad (10.2)$$

$$u\frac{\partial w}{\partial x} + v\frac{\partial w}{\partial r} + \frac{vw}{r} = -\frac{\partial \overline{v'w'}}{\partial r} - 2\frac{\overline{v'w'}}{r} - \frac{\partial \overline{u'w'}}{\partial x}$$
$$(10.3)$$

$$\frac{\partial ru}{\partial x} + \frac{\partial rv}{\partial r} = 0 \quad (10.4)$$

If one is considering a non-compressible flow, then, it is possible to ignore the turbulence flow normal stresses $\sigma_x = -\rho\overline{u'u'}, \sigma_r = -\rho\overline{v'v'}, \sigma_\theta = -\rho\overline{w'w'}$ as well as their derivatives. If we employ the assumptions which relate to axisymmetric boundary layers, that is to say,

$$u \gg v, \quad \frac{\partial}{\partial r} \gg \frac{\partial}{\partial x}, \quad (10.1)'$$

215

Equation (10.3) can be simplified to be

$$u \frac{\partial u}{\partial x} + v \frac{\partial u}{\partial r} = - \frac{1}{\rho} \frac{\partial p}{\partial x} + \frac{1}{\rho r} \frac{\partial}{\partial r} (r \tau_{xr}) \quad (10.5)$$

$$\rho \frac{w^2}{r} = \frac{\partial p}{\partial r} \quad (10.6)$$

$$u \frac{\partial w}{\partial x} + v \frac{\partial w}{\partial r} + \frac{vw}{r} = - \frac{1}{\rho} \frac{\partial}{\partial r} (\tau_{\theta r}) + \frac{2}{\rho} \frac{\tau_{\theta r}}{r} \quad (10.7)$$

If we take ρr and use it to perform successive multiplications on equation (10.5) and then integrate by r (when r=0, v=0, when $r \to \infty$, U=0):

$$\int_0^\infty \rho u \frac{\partial u}{\partial x} r \, dr + \int_0^\infty \rho v r \frac{\partial u}{\partial r} \, dr$$

$$= - \int_0^\infty \frac{\partial p}{\partial x} r \, dr + \int_0^\infty \frac{\partial r \tau_{rr}}{\partial r} \, dr \quad (10.8)$$

$$\int_0^\infty \rho u \frac{\partial u}{\partial x} r \, dr = \frac{1}{2} \frac{d}{dx} \int_0^\infty \rho u^2 r \, dr$$

$$\int_0^\infty \rho v r \frac{\partial u}{\partial r} \, dr = \left| \rho u v r \right|_0^\infty - \int_0^\infty \rho u \frac{\partial (r v)}{\partial r} \, dr$$

$$= - \frac{1}{2} \frac{d}{dx} \int_0^\infty \rho u^2 r \, dr$$

$$\int_0^\infty \frac{\partial p}{\partial x} r \, dr = \frac{d}{dx} \int_0^\infty p r \, dr$$

$$\int_0^\infty \frac{\partial (r \tau_{rr})}{\partial r} \, dr = \left| r \tau_{rr} \right|_0^\infty = 0$$

If we then substitute into equation (10.8), it is possible to obtain

$$\frac{d}{dx} \int_0^\infty (p + \rho u^2) r \, dr = 0, \quad (10.9)$$

That is to say, along the axial direction, x, the impulse force does not vary. Along the axial direction, x, and the radial direction, r, the static pressure, p, is variable. It is possible to take the pressure gradient along x, divide it up for purposes of integration and write it in the form

$$\int_0^\infty \frac{\partial p}{\partial x} r \, dr = \left| \frac{r^2}{2} \frac{\partial p}{\partial x} \right|_0^\infty - \int_0^\infty \frac{r^2}{2} \frac{\partial}{\partial r} \left(\frac{\partial p}{\partial x} \right) \, dr$$

or

$$= - \int_0^\infty \frac{r^2}{2} \frac{\partial}{\partial x} \left(\frac{\partial p}{\partial r} \right) \, dr$$

216

$$\frac{d}{dx}\int_0^\infty prdr = -\int_0^\infty \frac{r^2}{2}\frac{\partial}{\partial x}\left(\frac{\rho w^2}{r}\right)dr$$

$$= -\frac{1}{2}\frac{d}{dx}\int_0^\infty \rho w^2 rdr,$$

Substituting into equation (10.9), we get

$$\frac{d}{dx}\int_0^\infty \rho\left(u^2 - \frac{w^2}{2}\right)rdr = 0 \qquad (10.10)$$

If we take ρr^2 and use it to perform successive multiplications of the various quantities in equation (10.7), and, then, integrate by r we get

$$\int_0^\infty r^2\rho u\frac{\partial w}{\partial x}dr + \int_0^\infty r^2\rho v\frac{\partial w}{\partial r}dr + \int_0^\infty r\rho vwdr$$

$$= \int_0^\infty r^3\frac{\partial \tau_{\theta r}}{\partial r}dr + 2\int_0^\infty r\tau_\theta dr, \qquad (10.11)$$

(a) $\displaystyle\int_0^\infty r^2\rho u\frac{\partial w}{\partial x}dr = \int_0^\infty \rho rdr\left(u\frac{\partial wr}{\partial x}\right)$

$$= \int_0^\infty \rho rdr\left[\frac{\partial(uwr)}{\partial x} - wr\frac{\partial u}{\partial x}\right]$$

$$= \frac{d}{dx}\int_0^\infty r^2\rho uwdr + \int_0^\infty \rho rw\frac{\partial(rv)}{\partial r}dr$$

In the equations above, use was made of

$$\frac{\partial}{\partial x}(uwr) = \frac{\partial u}{\partial x}(wr) + u\frac{\partial(wr)}{\partial x},$$

as well as the continuity equations

$$\frac{\partial(ru)}{\partial x} = -\frac{\partial(rv)}{\partial r};$$

(b) $\displaystyle\int_0^\infty r^2\rho v\frac{\partial w}{\partial r}dr = \left|r^2\rho vw\right|_0^\infty - \int_0^\infty w\frac{\partial}{\partial r}(\rho vr^2)dr$

$$= 0 - \int_0^\infty w\frac{\partial}{\partial r}(\rho vr^2)dr$$

$$= -\int_0^\infty \rho wr\frac{\partial(vr)}{\partial r}dr - \int_0^\infty \rho vwrdr$$

(c) $\displaystyle\int_0^\infty r^2 \frac{\partial \tau_{\theta r}}{\partial r}\,dr + 2\int_0^\infty r\tau_{\theta r}dr$

$$= \int_0^\infty \frac{\partial}{\partial r}(r^2\tau_{\theta r})dr = \left| r^2\tau_{\theta r}\right|_0^\infty = 0.$$

If we take (a), (b) and (c) and substitute them into equation (10.11), then we can obtain

$$\frac{d}{dx}\int_0^\infty r^2\rho uw\,dr = \frac{1}{2\pi}\frac{dT}{dx} = 0 \qquad (10.12)$$

The physical significance of equation (10.12) is as follows: if we assume that we are dealing with a place on a certain cross section, x, of a rotational jet at which the radius of the cross section is r, and there is a density flow ρu; if we assume that it is also true that the mass flow rate when the jet passes through a minute, ring-shaped cross section $2\pi r dr$ is equal to $2\pi r dr \cdot \rho u$, and that the momentum flow rate in a circumferential direction θ (or tangential impulse force) $= 2\pi r dr \cdot \rho u \cdot w$, and if we further assume that the equivalent impulse force distance around x or angular momentum $= 2\pi r dr \cdot \rho u \cdot w \cdot r$; then, on the basis of these assumptions, it follows that the moment of torsional force in the air flow around x is

$$T = 2\pi\int_0^\infty r^2\rho uw\,dr,$$

and that it is conserved around x and does not vary.

From equation (10.9), we know that the impulse force along the direction of the axis, x, is invariable and is

$$M = 2\pi\int_0^\infty (p + \rho u^2)r\,dr.$$

If we assume that the jet nozzle has a radius=r_0, then, it is possible to obtain a vortex strength number to represent the strength of a rotational jet, so that

$$S = \frac{T}{Mr_0} \qquad (10.13)$$

Sec 2 Theoretical Estimates of Flow Speed Distribution of Rotational Jets

If we assume that, on a certain cross section, x, the maximum axial flow speed

218

$=u_m$, that, for $u = \frac{1}{2} u_m$ which has a radius $r_1 = b$, the non-dimensional vertical coordinate $(r/b) = \eta$; and, if we further assume that the maximum tangential component of velocity $= w_m$, then, when the vortical strength number $S \leqslant$ 0.6, the principles which govern the distribution of axial components of velocity (u/u_m) and tangential components of velocity (w/w_m) are similar.

$$\left(\frac{u}{u_m}\right) = f\left(\frac{r}{b}\right) = f(\eta) = f, \quad u = u_m f, \quad dr = bd\eta,$$

$$\left(\frac{w}{w_m}\right) = g\left(\frac{r}{b}\right) = g(\eta) = g, \quad w = w_m g, \quad r = b\eta;$$

If we assume that b follows the principles of expansion of x, $b \propto x^q$, and that the rules governing the attenuation and reduction of components of velocity are

$$u_m \propto x^p, \quad w_m \propto x^s \qquad (10.14)$$

then, equation (10.10) can be changed to read

$$\frac{d}{dx}\int_0^\infty \left(u_m^2 f^2 - \frac{1}{2} w_m^2 g^2\right) b^2 \eta d\eta = 0 \qquad (10.15)$$

It follows that

$$F_1 = \int_0^\infty \eta f^2 d\eta, \quad F_2 = \int_0^\infty \eta g^2 d\eta;$$

$$\frac{d}{dx}\left\{u_m^2 b^2 \left[F_1 - \frac{1}{2}\left(\frac{w_m}{u_m}\right)^2 F_2\right]\right\} = 0 \qquad (10.16)$$

We can divide this into three cases, that is to say

(1) $u_m \gg w_m$, then $\frac{d}{dx}(u_m^2 b^2 F_1) \cong 0$ (10.17)

(2) $u_m \ll w_m$, then $\frac{d}{dx}\frac{1}{2}(b^2 w_m^2 F_2) \cong 0$ (10.18)

(3) $u_m \cong w_m$, then, we still have equation (4.16).

From case (1):

$(u_m^2 b^2 F_1)$ = a constant, and, from equation (10.14) we know that it is necessarily true that $2p + 2q = 0, p = -q,$ (10.19)

From case (2):

$(b^2 w_m^2 F_2)$ = a constant, and, from equation (10.14), we know that it is necessarily true that $2q + 2s = 0, q = -s,$ (10.20)

From case (3):

219

$$\left[\frac{d(b^2 u_m^2)}{dx} \Big/ \frac{d}{dx} (b^2 w_m^2) \right] = \frac{F_2}{F_1} \propto x^0$$

$$\left[\frac{x^{2p} \cdot x^{2q}}{x^1} \Big/ \frac{x^{2s} \cdot x^{2q}}{x^1} \right] \propto x^0$$

that is to say, $(2q + 2p - 1) - (2q + 2s - 1) = 0;$ therefore, p=s. (10.21)
Equation (10.12) can be rewritten in the form

$$\frac{d}{dx} u_m w_m b^3 \int_0^\infty \eta^2 f g \, d\eta = 0, \text{ or } \frac{d}{dx} (u_m w_m b^3) = 0;$$

$$(u_m w_m b^3) = \text{ a constant } = x^0, \text{ or } p + s + 3q = 0. \quad (10.22)$$

Concerning utilization of the theory of induction roll up, if we assume
$u_m \gg w_m$, that the flow speed of induction roll up = v_e, and that half the
boundary width of a jet at a place where the axial component of velocity u $\cong$ 0,
is equal to $\bar{b}$, then, the rate of increase in the amount of gas involved in
induction roll up along x is

$$\frac{d}{dx} \int_0^\infty 2\pi r dr \cdot u = 2\pi \bar{b} v_e = \frac{dQ}{dx}. \quad (10.23)$$

If the gas volume ratio of induction roll up = α_e , then, on this basis, $v_e = \alpha_e u_m$,
therefore $\bar{b} v_e \propto b u_m \propto x^{p+q}$; and

$$\frac{d}{dx} u_m b^2 \int_0^\infty \eta f d\eta \propto x^{p+q},$$

or

$$p + 2q - 1 = p + q, \text{ therefore } q = 1; \quad (10.24)$$

From equation (10.19) and equation (10.22), we can figure out $p = -1, s = -2.$
Therefore, the rules governing the expansion of a weak rotation jet and the
attenuation and reduction of such a jet are

$$b \propto x, \quad u_m \propto \frac{1}{x}, \quad w_m \propto \frac{1}{x^2} \quad (10.25)$$

Sec 3 Similarities of Movement Equations in Strength Net Analysis (Limited to Middle Range Vortex Strengths)

Let us consider the third case mentioned in the previous section in which

$u_m \cong w_m$. In simplified notation, this is

$$u'_m = \frac{du_m}{dx}, \quad b' = \frac{db}{dx}, \quad f' = \frac{df}{d\eta}, \quad u = u_m f,$$

$$\left. \frac{u}{u_m} = f(\eta) = f, \quad \eta = \frac{r}{b}; \right\} \quad (10.26)$$

$$\frac{d\eta}{dx} = \frac{d\eta}{db} \cdot \frac{db}{dx} = -\frac{rb'}{b^2} = -\frac{\eta b'}{b}, \quad dr = b \, d\eta;$$

We can take the various quantities in equation (10.5) and write them as functions of η as follows

(a) $\quad u \dfrac{\partial u}{\partial x} = u_m f \dfrac{\partial}{\partial x}(u_m f) = u_m f \left[f \dfrac{\partial u_m}{\partial x} + u_m \dfrac{\partial f}{\partial x} \right]$

$$= u_m f^2 u'_m + u_m^2 f \frac{\partial f}{\partial \eta} \cdot \frac{d\eta}{dx}$$

$$= u_m u'_m f^2 - \frac{u_m^2 b'}{b} \eta f f'$$

If we utilize continuity equation (10.4), then, it is possible to obtain

$$v = \frac{1}{r} \int_0^\eta (u_m b b' \eta^2 f' - u_m b^2 \eta f) \, d\eta$$

(b) $\quad v \dfrac{\partial u}{\partial r} = \dfrac{u_m^2 b' f'}{b\eta} \int_0^\eta \eta^2 f' \, d\eta - u_m u'_m \dfrac{f}{\eta} \int_0^\eta \eta f \, d\eta.$

If we consider the integral equation (10.6), then,

$$p = p_\infty - \int_0^\infty \frac{\rho w^2}{r} \, dr, \quad p_\infty$$

, and this is equal to the pressure of the environment of the jet

If we differentiate the equation above by x, then,

$$-\frac{1}{\rho} \frac{\partial p}{\partial x} = \frac{\partial}{\partial x} \left[w_m^2 \int_0^\infty \frac{g}{\eta} \, d\eta \right] = \frac{\partial}{\partial x} [w_m^2 G],$$

$$G = \int_0^\infty \frac{g}{\eta} \, d\eta;$$

(c) By differentiating the equation above, we can obtain

$$-\frac{1}{\rho} \frac{\partial p}{\partial x} = 2 w_m w'_m G - \frac{w_m^2 b'}{b} \eta G',$$

$$G' = \frac{dG}{d\eta};$$

221

If we assume that $\frac{\tau_{rr}}{\rho u_m^2} = h(\eta)$, then it is possible to obtain

$$\frac{1}{\rho r}\frac{\partial(r\tau_{rr})}{\partial r} = \frac{u_m^2}{b}\left(h' + \frac{h}{\eta}\right), \quad h' = \frac{dh}{d\eta};$$

If we take (a), (b), (c) and (d) and substitute them into equation (10.5), then, we can obtain

$$u_m u_m' f^2 - \frac{u_m^2 b'}{b}\eta f f' + \frac{u_m^2 b'}{b}\frac{f}{\eta}\int_0^\eta \eta^2 f' d\eta$$

$$- u_m u_m' \frac{f}{\eta}\int_0^\eta \eta f d\eta = 2 w_m w_m' G$$

$$- \frac{w_m^2 b'}{b}\eta G' + \frac{u_m^2}{b}\left(h' + \frac{h}{\eta}\right),$$

or

$$\left(h' + \frac{h}{\eta}\right) = \frac{b u_m'}{u_m}\left[f^2 - \frac{f}{\eta}\int_0^\eta \eta f d\eta\right]$$

$$- b'\left[\eta f f' - \frac{f}{\eta}\int \eta^2 f' d\eta\right]$$

$$+ b'\left(\frac{w_m}{u_m}\right)^2 \eta G' - \frac{b w_m'}{w_m}\left(\frac{w_m}{u_m}\right)^2 \cdot 2G \quad (10.27)$$

In the equation above, the functions of η, f, g, G, h as well as their derived functions are all non-dimensional; therefore, equation (10.27) ought to be a non-dimensional equation. It should still also be in accordance with the rules governing the attenuation and reduction of the flow speed of jets as well as with the rules governing the expansion of jets as these rules are presented in equation (10.14), that is to say, $u_m \propto x^p$, $b \propto x^q$, $w_m \propto x^s$. Let us check out the coefficients of the various quantities involved,

$$\frac{b u_m'}{u_m}, \quad x^q \cdot x^{p-1} \cdot x^{-p} = x^{q-1} = x^0,$$

$$b', \quad x^{q-1} = x^0$$

$$\frac{b w_m'}{w_m}, \quad x^q \cdot x^{s-1} \cdot x^{-s} = x^{q-1} = x^0; \quad \text{Therefore, the exponent } q = 1.$$

If we utilize the conditions: $p = s$, $p + s + 3q = 0$; then we can solve for the following relationships

$$q = 1, \; b \propto x, \; p = -\frac{3}{2}, \; u_m \propto \frac{1}{x\sqrt{x}},$$

$$s = -\frac{3}{2}, \; w_m \propto \frac{1}{x\sqrt{x}}.$$

Sec 4   Experimental Data on Rotational Jets

Concerning the case in which there is a continuous source of gas, if, in front of the jet nozzle, there are placed tangential holes which supply two currents of air, then, the presence of these currents will force the engine to put out a rotational jet. If one changes the pressure and the amount of gas involved in the two currents of air, then, it is possible to change the vortex strength number, S, of the rotational jet. If we utilize a five hole spherical pitot tube (or a laser doppler flow speed meter) then, it is possible to investigate and make measurements of the distributions along x and r of the flow speeds u and w as well as the static pressure, p, in a rotational jet flow field. On the basis of the data obtained in these investigations and measurements, it is possible to sketch out the boundary lines of the jet (Fig 10.1). $\overline{b}=$ the half-width of the exterior boundary of the jet; d=the diameter of the jet nozzle, assuming that the distance of the point source inside the jet nozzle = a. It can be seen from all this that, if one raises the vortex strength number, S, then, the rotational jet diffuses rapidly and becomes wider. If we are dealing with a situation in which the vortex strength number, $S \leqslant$ 0.5, the pressure gradient along x is still insufficient to produce counter-current flow. The flow speed in the normal stage is

$$\frac{u}{u_m} = \exp(-K_1 \lambda^2) \qquad (10.28)$$

This is still a Gaussian normal distribution (Fig 10.2). However, when the vortex strength number, S = 0.6, then, the point at which (u/u_m) has its highest value is no longer on the axis line, and it is moved out along the radius, r, to form a "ring-shaped mountain." After it travels down the flow to the point where $(x/d)=$ 15, then and only then does the "ring-shaped mountain" draw close to the axis line

22_3

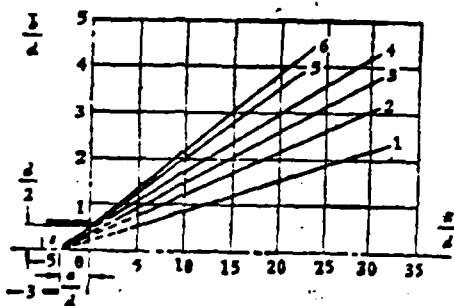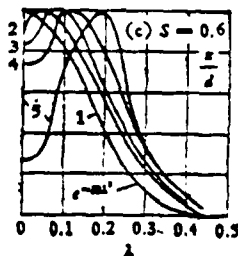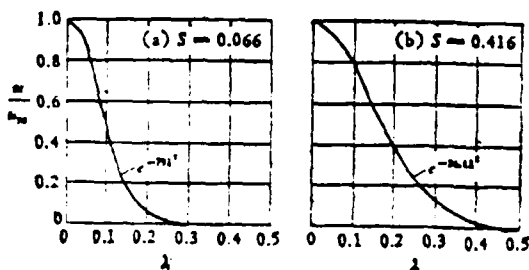to form a single peak (Fig 10.2 (c)). It is only necessary for the vortex strengths

图 10.1 圆喷口旋转射流边界扩展
(1. 无旋转 $S=0$; 2. 有旋转 $S=0.13$; 3. 有旋转
$S=0.23$; 4. 有旋转 $S=0.27$; 5. 有旋转 $S=0.35$;
6. 有旋转 $S=0.63$)

Fig 10.1

1. Boundary Diffusion of a Round Nozzle Rotational Jet 2. No Rotation 3. With Rotation

$\frac{x}{d}$: $1=15$, $2=8.3$, $3=6.2$,
$4=4.1$, $5=2.0$.

Fig 10.2

1. Distribution Curves for the Axial Flow Speed Ratio u/u_m Along the Radial Direction $\lambda = \frac{r}{x+a}$ for Different Vortical Strength Numbers, S

S, to be equal, and the curves plotting out the changes in the tangential component of velocity (w/w_m) for the different cross sections $x/d = 2, 4.1, 6.2, 8.3, 10$ as they vary with changes in λ are all similar (Fig 10.3). When the vortex strength number, $S \leqslant 0.5$, it is possible to deduce, from experimental data, an empirical formula to represent the distribution of the tangential component of velocity along r:

$$\left(\frac{w}{w_m}\right) = C\lambda + D\lambda^2 + E\lambda^3, \quad \lambda = \frac{r}{x+a}. \quad (10.29)$$

In the equation above, one can obtain values for the coefficients C, D, E by consulting Table 10.1. After the vortex strength number, $S \geqslant 0.6$, one begins to see the appearance of areas of reflux (Fig 10.3(c)). The area corresponding to the highest peak of (w/w_m) is the vortical core where the boundary radius is r_0. In the case where $r \leqslant r_0$ is a tangential flow speed distribution with a solid rotational form. The case in which $r \geqslant r_0$ is a tangential flow speed distribution with a free spiral form. This corresponds to the Rankine spiral or vortex or viscous flow. If we assume that
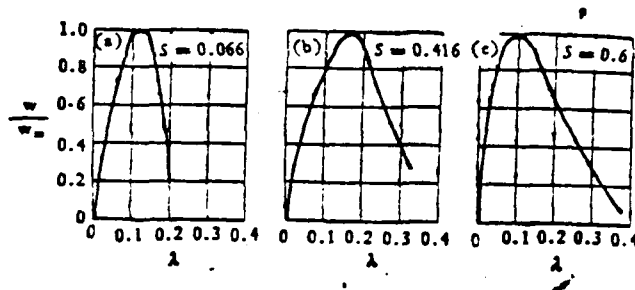
$$\bar{r} = \frac{r}{r_0},$$

Fig 10.3

The Distribution of the Tangential Velocity Component Ratio w/w_m Along r For a Rotational Jet

then, the maximum tangential speed of the boundary of a non-viscous vortical core is

225

$w_0 = r_0\omega$, and ω = the rotational speed of the vortical core; the maximum tangential boundary velocity or a vortical core which has viscosity is

$$w_m = \left(1 - \frac{1}{e}\right)r_0\omega, \quad \text{circulation } \Gamma = 2\pi r_0^2\omega;$$

$$w = \frac{\Gamma}{2\pi r}[1 - \exp(-\bar{r}^2)] = \frac{r_0\omega}{\bar{r}}[1 - \exp(-\bar{r}^2)]$$

$$= \frac{w_m}{\left(1 - \frac{1}{e}\right)\bar{r}}[1 - \exp(-\bar{r}^2)];$$

If we take $\bar{r}$ to be the horizontal coordinate, then,

$$\left(\frac{w}{w_m}\right) = \frac{1}{\bar{r}(1 - e^{-1})}[1 - e^{-\lambda}] \qquad (10.30)$$

Therefore, when

$$\bar{r} = 0, \ \lambda = 0, \ \left(\frac{w}{w_m}\right) = 0;$$

$$\bar{r} = 1, \ \lambda = 0.1, \ \left(\frac{w}{w_m}\right) = 1;$$

$$\bar{r} \to \infty, \ \lambda \to \infty, \ \left(\frac{w}{w_m}\right) \to 0.$$

Let us assume that p_∞ = the static pressure of the environment around a rotational jet, that p = the static pressure at a place where there is a given radius r, that p_m = the static pressure on the center line of a rotational jet, and that $(p_\infty - p)/(p_\infty - p_m)$ = the pressure differential ratio $\bar{p}$.

On the basis of the dimensional analysis of the self-patterning or normal stage characteristics of a rotational jet as it appeared in the preceding section, it is only necessary that the vortex strength numbers S, be equal, and the distribution of the pressure differential $\bar{p}$ for different cross sections (x/d) should also be similar (Fig 10.4). The rule which can be induced from experimental data to describe how the pressure differential ratio, $\bar{p}$, varies with changes in λ is also a Gaussian normal distribution:

$$\bar{p} = \frac{p_\infty - p}{p_\infty - p_m} = \exp(-k_1\lambda^2) \qquad (10.31)$$

The coefficients K_1 and k_2 of the exponential functions both decrease in value along with the vortex strength number, S.
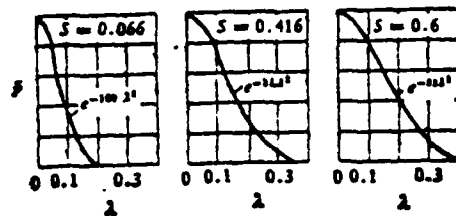
Fig 10.4

Curves of the Distribution of the Pressure Differential Ratio, $\bar{p}$, Along r

At a specified cross section (x/d) = a constant, the total gas flow volume of a jet, Q and the ratio it forms with the initial jet gas volume, Q_o, reflects the induction roll up energy of the jet. The higher the vortex strength goes, the stronger does the induction roll up energy become. Experimentation produces the following relationship: the total amount of gas flow/the initial amount of jet gas is

$$\frac{Q}{Q_o} = (0.32 + 0.8S)\frac{x}{d} \quad (10.32)$$

The rule which governs the way in which the flow speed is attenuated and reduced along with x is

$$\frac{u_m}{u_{m0}} \propto \frac{d}{x}, \quad \frac{w_m}{w_{m0}} \propto \frac{d^2}{x^2}, \quad (p_m - p_\infty) \propto \frac{d^4}{x^4}. \quad (10.33)$$

次数	原始 u_{m0}[m/s]	原始 w_{m0}[m/s]	旋涡数 S	系数 c	系数 D	系数 E
1	12.5	1.46	0.066	7.7	71.5	−542
2	13.5	5.4	0.234	18.1	−98.8	138
3	15.1	7.94	0.416	15.1	−67.2	75
4	16.0	10.86	0.608	22.8	−155	275
5	17.7	12.8	0.640	25.2	−186	359

Table 10.1

Principal Experimental Data on Rotational Jets (See equation 10.29)
2. Sequence Number 3. Initial 4. Vortex Strength Number 5. Coefficient

227

Sec 1 Curvature Deformations of Main Horizontal Cross Flows of Round Aperture Jets

Let us assume that there is, on the wall of a flame tube, a round hole with a diameter equal to d and with a center line perpendicular to the surface of the wall $\theta_0 = 90°$ (Fig 11.1). Because of the pressure differential between the inside and the outside of the flame tube, the air from the exterior ring cavity passes through the round aperture and is propelled as a jet into the flame tube. The initial flow speed $= U_0$. The initial volume of flow is equal to Q_0. The jet which penetrates horizontally into the main flow, V_0, faces into the wind and receives a blast of dynamic pressure equal to $1/2\,\rho V_0^2$. The leeward face of the jet feels the influence of the vortical curling caused by the drop in pressure in the wake of the jet. Concerning the sides of the jet, because of the previous collision, the flow speed, u, is already basically very low, and because of the fact that, on top of this initial slowness, the jet is also influenced by the impact of the shear forces from the main flow, V_0, the sides of the jet are very easily deformed. The result of this is that the jet is gradually curved to conform to the direction of flow of the main current. A typical cross section of the jet (See Fig 11.1, A-A) is squeezed, flattened and rolled to become a kidney shape. On the concave surface of the kidney shape, there later appear a pair of counter-rotational vortices $+\Gamma$, $-\Gamma$. This pair of vortices develops and expands as they flow downstream and they are weakened and dissipate only after they have flowed far down the stream. In the area between the curvilinearly deformed jet and the main flow, due to the fact that the effect of the turbulence flow vortical masses producing friction by rubbing together is very strong, the induced roll up and mixing are particularly violent. Beginning with the center of the round aperture, the curved jet can be generally divided into three sections; I is the core of the jet, 0_{s_0}, . This is shorter than the core of a free jet and is slanted downstream; II is the obviously curved section. The cross section of the jet is rapidly deformed; III is the vortical expansion section. This is turned downstream in the direction of the main flow.

On Fig 11.1, 0_s = the axial line of the jet. This line is the maximum flow speed, U_m, for the various cross sections connected together into a line; the vertical coordinate = y. 0_c = the center line of the jet; the vertical coordinate = Y_c. From the edge of the round aperture to b is the exterior boundary of the jet; the vertical coordinate is y_b. From the center of the aperture, 0,

228

the length of the arc along the axis line = s. The included angle between the jet and the x axis = θ , and the included angle between the jet and the y axis = $\bar{\theta}$. The width of the cross section of the jet along the axis, z = Δz. The area of the cross section of the jet = S_n. If we assume that the flow speed ratio $\sigma = (U_\bullet/V_\bullet) > 1$, or that $\lambda = (V_\bullet/U_\bullet) < 1$, then it is possible to use the empirical formulae presented below to represent the penetration depth

$$\left. \begin{aligned} \frac{y_\lambda}{\sigma d} &= 2.63 \left(\frac{x}{\sigma d}\right)^{0.2}, \qquad 5 < \sigma < 35 \\ \frac{y_\epsilon}{d} &= 1.59\, \sigma^{0.8} \left(\frac{x}{d}\right)^{0.3}, \; 2 < \sigma < 10 \end{aligned} \right\} \quad (11.1)$$

Sec 2 Experimental Measurements Describing Jet Curvature Forms

Let us consider the case in which we use a transparent flame tube model on a test bed to carry out cold air flow experiments. If we first raise the temperature of the horizontally penetrating jet approximately 50°C, creating a sufficient density differential between the penetrating jet and the main jet flow, or, if we add to the penetrating jet a tracer agent, then, by borrowing from the techniques of schlieren photography or from measurements obtained by the use of a laser thermal line wind speed aparatus, it is possible to draw out the axis lines of the curved jet flow as they appear in Fig 11.2 and Fig 11.3.

Fig 11.2 is the result of measurements from a low speed continuous wind tunnel using a round aperture jet with d = 6.5mm. The range of the flow speed ratio is $0 < \lambda < 0.152$. Due to the fact that the exterior ring cavity density $\rho_\bullet$ is larger than the density of the main flow inside the flame tube ρ_0, $\beta = (\rho_0/\rho_\bullet) < 1$, therefore, let us use the ratio of momentum flow rates of the main flow and the jet to solve for λ_c .

$$\lambda^2 = \left(\frac{\rho_0}{\rho_\bullet}\right)\frac{V_0^2}{U_\bullet^2} = \beta \frac{V_0^2}{U_\bullet^2}.$$

If one considers Fig 11.2, then it is possible to deduce the fact that the empirical formula for penetration depth is

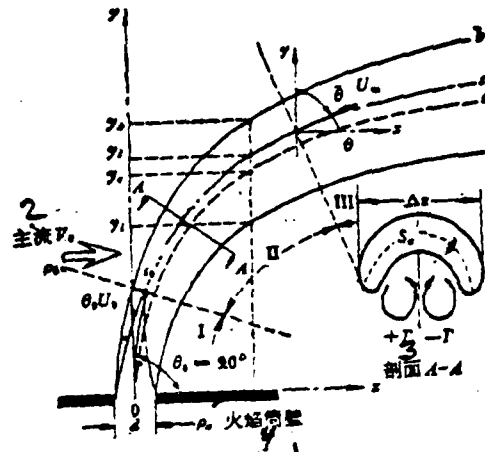$$\left(\frac{y}{d}\right) = \lambda^{-1.85}\left(\frac{x}{d}\right)^{0.3}. \qquad (11.2)$$

229

图 11.1 横穿主流圆孔射流弯曲变形示意

Fig 11.1

1. An Illustration of the Curvature Deformation of a Horizontally Penetrating Jet
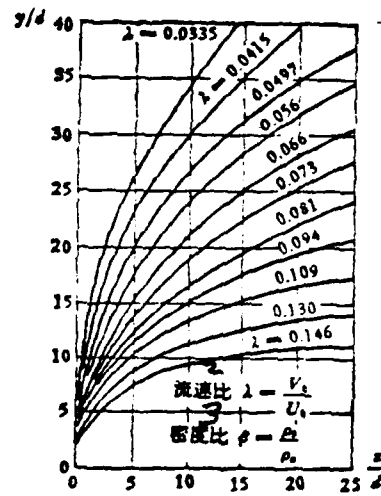As It Enters a Main Jet Stream 2. Main Flow 3. Cross Section 4. Flame Tube Wall

图 11.2 射流穿透深度

Fig 11.2

1. Penetration Depth of Jet 2. Flow Speed Ratio 3. Density Ratio

Figure 11.3 is the result of the influence of the corrections of inequalities
between the density of the jet and the density of the main flow $\rho = (\rho_s, \rho_h)$, as
well as the influence of the flow coefficient, C_d, on the penetration distance
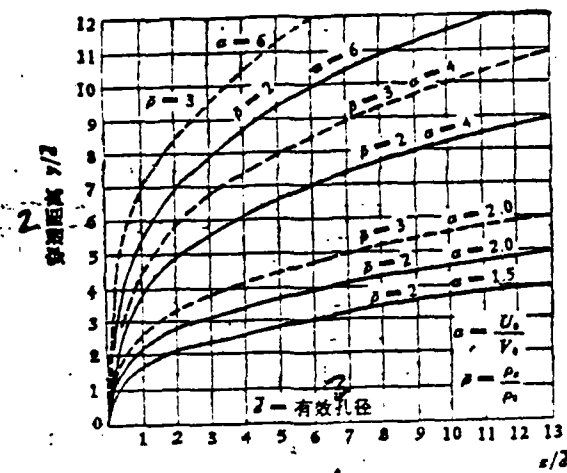$(y/\overline{d})$. If one assumes that $\overline{d}$ = the effective diameter of the aperture, then

230

图11.3 射流穿透距离(虚线表示考虑密度差)

Fig 11.3

1. Penetration Distance of the Jet (The Broken Line Represents the Case in Which We Consider Differences in Density) 2. Penetration Distance 3. Effective Diameter of Aperture
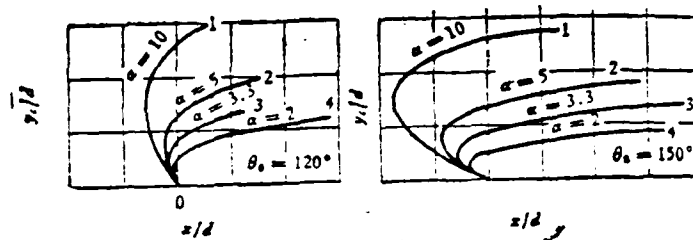

图11.4 射流轴线形状

Fig 11.4

1. Axis Line Configuration of Jets

the flow coefficient, C_d, is equal to the effective cross section of the jet gases/ the geometrical area of the round aperture which is

$$\pi = \frac{\bar{d}^2}{d^2} < 1,$$
$$\bar{d} = \sqrt{C_d} \cdot d$$

The empirical formula for the penetration distance is

231

$$\frac{y}{d} = 0.87\beta^{0.47}\alpha^{0.85} \qquad \times \left(\frac{x}{d}\right)^{0.32}\sin\theta_\bullet \qquad (11.3)$$
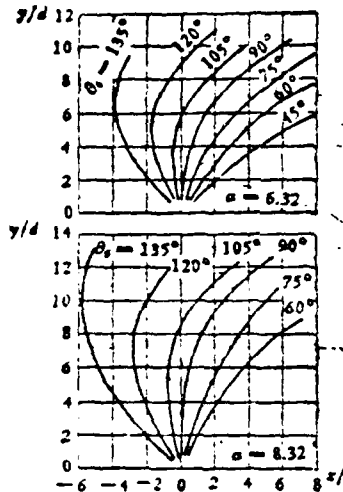

图 11.5 射流中心线形状

Fig 11.5

1. Configuration of the Center Lines of Jets

In order to control the structure of the flow fields in the flame tubes, (for example, the forward slant of the main combustion aperture of a Spey flame tube), we intentionally used baffles inserted into the sides in order to guide the air flow and make the jet penetrate the main flow at a slant $\theta_\bullet \gtrless 90°$ Fig. 11.4 and Fig. 11.5 draw out the curved axis lines of jets with different $\theta_\bullet$ and different α as well as the configurations of their center lines.

Sec 3 Analysis of the Curvature of Main Skew Cross Currents in Narrow Slit Jets

Let us assume that there is, on the surface of a smooth wall, a narrow slit with a width, b_0, through which a jet with an initial density of $\rho_\bullet$, a flow speed of U_0, and an angle of slant of $\theta_\bullet$ is entering a parallel flow main flow V_0 with a density of ρ_0.   The axis line of the jet flow receives an influence from the pressure differential of the gas flow and is deformed in the form of a curve. Let us take a differential section of the jet and analyze the balance of forces acting on it (Fig 11.6). it is equal to the differential length along the axis line. A = the width of the jet. Δz = the thickness of the cross section perpendicular to the differential section of the surface x-y. The area of the cross section of the differentiated section, $S_\bullet = A\Delta z$; the volume of the differential section $= S_\bullet ds$. The lateral area of the differential section $= \Delta z ds$.

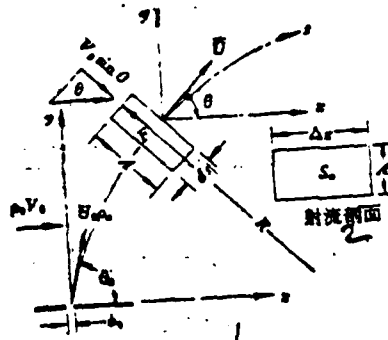The impulse force received from the dynamic pressure of the main flow

232

図 11.6 . 射流微元動力平衡

Fig 11.6

1. The Equilibrium of Forces Acting on the Differential Section of Jet Flow
2. Jet Flow Cross Section

on the windward surface of the differential section $-C_n\Delta z ds \cdot \frac{1}{2}\rho_0(V_0\sin\theta)^2$,

the centrifugal force produced by the curvilinear flow of the differential section

$-\rho_g S_g ds\frac{\bar{U}^2}{R}$, moreover, C_n = the gas flow resistance force coefficient, and R = the radius of the rate of curvature of the axis line of the differentiated section. The equilibrium of forces acting along R in the differential section is

$$C_n\Delta z ds\frac{1}{2}\rho_0 V_0^2\sin^2\theta = -\rho_g S_g ds\frac{\bar{U}^2}{R} \qquad (11.4)$$

From Fig 11.6, we can see that

$$y' = \frac{dy}{dx} = \mathrm{tg}\theta, \quad \sin\theta = \frac{\mathrm{tg}\theta}{\sqrt{1+\mathrm{tg}^2\theta}} = \frac{y'}{(1+y'^2)^{0.5}};$$
$$(11.5)$$

The rate of curvature radius is

$$R = \frac{(1+y'^2)^{1.5}}{y''}, \quad y'' = \frac{d^2y}{dx^2}. \qquad (11.6)$$

Let us assume that the area of the initial cross section of the jet is $S_{g0} = \Delta z\delta_0$, where δ_0 = to the width of the jet when it has just left the narrow slit. Let us assume that, in the direction y, the momentum flow rate of the jet (that is to say, the impulse force) is conserved and invariable, which means that

$$\rho_g\bar{U}^2 S_g \sin\theta = \rho_g U_0^2 S_{g0}\sin\theta_0 = \text{a constant} \qquad (11.7)$$

Equation (11.4) can be written in the form of

233

$$RC_n \Delta z \rho_0 V_0^2 \sin^2\theta = -2\rho_e S_e \bar{U}^2 \qquad (11.8)$$

The conditions which apply to equation (11.7) should be applied to equation (11.8)

$$C_n \Delta z \rho_0 V_0^2 R \sin^2\theta = -2\rho_e U_e^2 S_{e0} \sin \theta_0$$

Utilizing equation (11.5) and equation (11.6), we can obtain

$$R \sin^3\theta = \frac{(1 + y'^2)^{1.5}}{y''} \cdot \frac{-y'^3}{(1 + y'^2)^{1.5}}$$

or

$$= -\frac{2\rho_e U_0^2 \, S_{e0}}{\rho_0 V_0^2 \, C_n \Delta z} \sin \theta_0$$

If we say that

$$\frac{y'^3}{y''} = -\frac{2\rho_e U_0^2 \, \delta_0}{\rho_0 V_n^2 \, C_n} \sin \theta_0 \qquad (11.9)$$

$$\xi = y' = \frac{dy}{dx}, \quad \frac{d\xi}{dx} = y'',$$

Then, equation (11.9) can be rewritten to be

$$\frac{d\xi}{\xi^3} = -\frac{C_n \rho_0 V_0^2 \, dx}{2\delta_0 \rho_e U_0^2 \sin \theta_0} \qquad (11.10)$$

We already know θ_0, δ_0, $\rho_e U_0$ and $\rho_0 V_0$; if we consider that a precise value for C_n can be determined by experimentation, then,

$$\frac{C_n \rho_0 V_0^2}{\delta_0 \rho_e U_0^2 \sin \theta_0} = k = \text{a constant}$$

Because of this fact

$$-2\,\xi^{-3}d\xi = k\,dx,$$

By integration, we can obtain $\quad \xi^{-2} = kx + C_1 \qquad (11.11)$

If one is considering Fig 11.6, then, when

$$x = 0, \ y = 0, \ \xi_0^{-2} = \left(\frac{dx}{dy}\right)_0^2 = \text{ctg}^2\theta_0, \qquad \text{it follows that} \qquad C_1 = \text{ctg}^2\theta_0;$$

and, because of this fact,

$$\frac{1}{\xi} = \frac{dx}{dy} = \pm\sqrt{kx + \text{ctg}^2\theta_0} \qquad (11.12)$$

If we integrate equation (11.12), it is possible to obtain the equation for the curved axis line of the jet from a narrow slit, which is

$$y = \frac{2}{k}\left(\pm\sqrt{kx + ctg^2\theta_0} - ctg\theta_0\right) \qquad (11.13)$$

If the initial angle of slant is $\theta_0 > \frac{\pi}{2}$, then, we use a negative sign in front of the square root sign. By experimentation, $C_n \simeq$ 1-3.

Sec 4 Analysis of the Curvature of Main Skew Cross Currents in Round Aperture Jets

At the same time that jets are being curved, they are also expanding, so that their cross sections become kidney-shaped (Fig 11.1 A-A). The width of the cross section, Δz, varies with changes in the arc length of the axis line, s. Of course, Δz and the diameter of the round aperture, d, are in direct proprortion to each other. On the basis of experiments made in a smoke-equipped wind tunnel[1], it is possible to determine an empirical equation to describe Δz as it changes along the axis line O_s, that is,

$$\frac{\Delta z}{d} = 1 + N\left(\frac{y}{d}\right), \quad N = 5.2\left(\frac{U_0}{V_0}\right)^{-0.2} = 5.2\,a^{-0.2},$$

$$d = \text{the diameter of the round aperture} \qquad (11.14)$$

Let us select a differential section, ds, from the curved jet. Let us assume that the kidney-shaped cross section has an area equal to S_n. Along ds, in a tangential direction, the average flow speed $= \bar{U}$ (Fig 11.6). If we assume that $\tilde{\rho}_0 = \rho_e = \rho$, then, on the basis of equation (11.4), it is possible to set out the equilibrium equation for the centrifugal forces and the aerodynamic forces along the direction R of the radius of the rate of curvature of the differential section, that is,

$$C_n \cdot \frac{1}{2}\rho V_0^2 \sin^2\theta \cdot \Delta z \cdot ds = -\frac{1}{R}\rho S_n ds \bar{U}^2 \qquad (11.15)$$

If we assume that along the flow line O_s the gas flow rate of the jet (the impulse force) remains invariable and is conserved, then, that means that,

1) Crowe and Riesebieter, 1967 AGARD Reprint.

$$\rho S_* \bar{U}^2 = \frac{\pi}{4} d^2 \rho U_0^2 = \text{a constant} \qquad (11.16)$$

If we substitute this into equation (11.15), we can obtain

$$- C_* V_0^2 R \sin^2\theta \left(\frac{\Delta z}{d}\right) = \frac{\pi d}{2} U_0^2 \qquad (11.17)$$

Also, according to what was said in the previous section

$$\left.\begin{array}{l} y' = \dfrac{dy}{dx} = \mathrm{tg}\,\theta, \quad \sin\theta = \dfrac{y'}{(1+y'^2)^{0.5}} \\[2mm] y'' = \dfrac{d^2y}{dx^2}, \quad \text{radius at curvature } R = \dfrac{(1+y'^2)^{1.5}}{y''} \\[2mm] \text{curved axis line arc } s = \displaystyle\int_0^y \left[1 + \left(\dfrac{dx}{dy}\right)^2\right]^{\frac{1}{2}} dy \end{array}\right\} \quad (11.18)$$

If we utilize equation (11.18) and equation (11.14) for the purpose of manipulating equation (11.17), and, if, moreover, we stipulate that $\eta = y/d$, $d\eta = dy/d$, then, we can integrate and obtain the curved axis line equation

$$\frac{x}{d} = \int_0^{y/d} \mathrm{sh}\left[\frac{\eta + 2.6\alpha^{-0.8}\eta^2}{\frac{\pi}{2C_*}\alpha^2}\right] d\eta \qquad (11.19)$$

The aerodynamic obstruction coefficient in equation (11.19) is $C_* \approx 1.5$. Fig 11.7 draws out the curved axis lines for round aperture jets on the basis of computations made with equation (11.19) and on the basis of experiments which were done with a smoke-equipped wind tunnel; Fig 11.7 also makes a comparison of these axis lines. ① $\alpha^2 = 4.75$, the small circles represent $d = 20$ [mm], the black dots represent $d = 14$ [mm]. ② $\alpha^2 = 7.8$. ③ $\alpha^2 = 16.35$, the empty white triangles represent $d = 20$ [mm], and the black triangles represent $d = 14$ [mm]. If, on the wall of a flame tube, there is opened a crack or a hole in order to supplement combustion or to lower the temperature, then, of course, it is to be hoped that the penetration depth (y/d) will be as deep as possible; however, the basic principle in this matter is that if two holes are opened across from each other then the jets from them cannot be allowed to mutually collide or the main flow will be obstructed and losses will be increased.
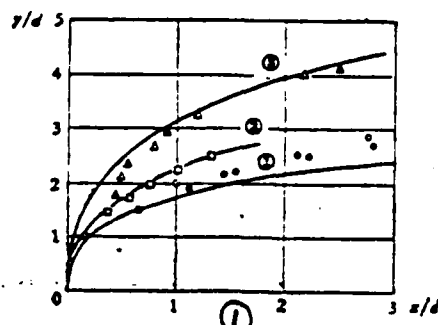
图 11.7 圆孔射流弯曲计算及实验比较

Fig 11.7

1. Comparison of Computations and Experimental Data Determining the Curves of Round
Aperture Jets

Sec 5 Coefficients of Flow As Determined by Experimentation For Round Aperture Jets

The flow coefficient, C_d, in the preceding Sec 2 determined the effective aper-
ture radius, $\bar{d}$, and influenced the depth of penetration, the flow distribution and
losses in pressure differential. It is possible to simulate in the laboratory the
opening of a hole in the wall of a flame tube in order to carry out cold air cir-
culation experiments to determine the *flow coefficient*, C_d, as is shown in Fig
11.8. The gas supply tube diameter, D_1, the cross section S_1, and the flow speed
U_1, simulate the intake and exhaust of the combustion chamber or the configuration
of the interior ring cavity as well as the Reynolds number, Re. Let us make pre-
cise measurements of the round aperture diameter d_o, the cross section s_o and the
static pressures, P_1 and P_2, for the beginning and end of the process. The contract-
ion ratio of the tube $m = (S_o/S_1) = (d_o^2/D_1^2) < 1$. At the round aperture,
the flow lines come together and squeeze the flow which passes through the round
aperture and is gradually turned in a curved direction; not only are the flow
speeds in this type of situation uneven, they are not parallel either. Only after
one has gone somewhat downstream from the round aperture does the jet flow become
one in which the flow speeds U_2 are even and parallel, the cross sections of the
jet are such that $S_2 < S_o$,   and the radius $d_2 < d_o$.   The contraction
ratio of the jet is $C_c = (S_2/S_o) = (d_2^2/d_o^2) < 1$. If we assume that the weight
of the gases supplied in the ring cavity (kg/m^3) $= \gamma$, then, according to Bernoulli's
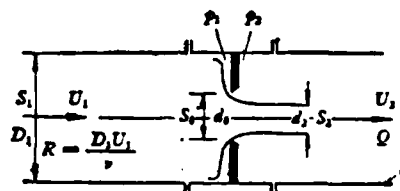equation, the round aperture volume flow

237

Figure 11.8

Determination of the flow coefficient C_d

$$Q = C_d S_0 U_2 = C_d S_0 \left[\frac{2g}{\gamma} (p_1 - p_2) \right]^{\frac{1}{2}} \quad [\mathrm{m^3/s}] \quad (11.20)$$

The round aperture weight of flow is

$$G = \gamma Q = C_d S_0 [2g\gamma(p_1 - p_2)]^{\frac{1}{2}} \quad [\mathrm{kg/s}] \quad (11.21)$$

On the basis of flow continuity

$$Q = S_1 U_1 = S_2 U_2 = C_c S_0 U_2 = m C_c S_1 U_2, \quad U_1 = m C_c U_2,$$
$$(11.22)$$

If we are considering a case in which there are no friction losses, then,

$$p_1 - p_2 = \frac{\gamma}{2g} (U_2^2 - U_1^2) = \frac{\gamma}{2g} (1 - m^2 C_c^2) U_2^2$$

Therefore,

$$U_2 = \left[\frac{2g(p_1 - p_2)}{\gamma(1 - m^2 C_c^2)} \right]^{\frac{1}{2}}, \qquad (11.23)$$

Because of losses due to friction, the actual jet flow speed $U_2' < U_2$; if we assume that the flow speed loss coefficient is

$$\xi = \frac{U_2'}{U_2} < 1,$$

then, the round aperture volume of flow is

$$Q = C_c S_0 U_2' = C_c \xi S_0 U_2 \qquad (11.24)$$

By using U_2 from equation (11.23), we can obtain

$$Q = \frac{C_c \xi}{\sqrt{(1 - m^2 C_c^2)}} S_0 \left[\frac{2g}{\gamma} (p_1 - p_2) \right]^{\frac{1}{2}} \quad [\mathrm{m^3/s}],$$
$$(11.25)$$

If we make a comparison of equations (11.20) and (11.25), the coefficient of flow is

$$C_d = \frac{C_c \xi}{\sqrt{(1 - m^2 C_c^2)}}, \quad \text{and, in general} \quad \xi = 0.96 \sim 0.98 \quad (11.26)$$

The coefficient of flow, C_d, is a function of the Reynolds number of the supplied gas and the contraction ratio of the tube, m. Above a certain Reynolds number, C_d

238

is almost maintained as a constant. Fig 11.9 is the set of standard curves put out by the ISA (the international standardization association) for the flow coefficients of round apertures as they vary with changes in Re and m. The error involved in consulting this illustration is approximately $\pm$ 1%.
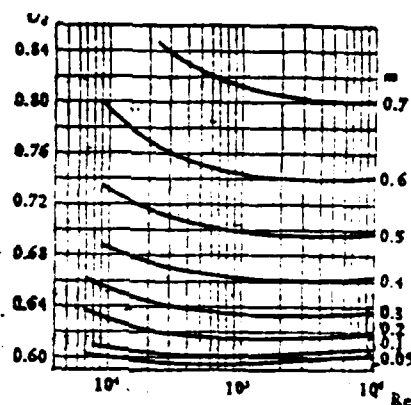

图 11.9 ISA 标准圆孔流量系数

Fig 11.9

1. ISA Standard Round Aperture Flow Coefficients

The round aperture pressure loss differential is

$$\Delta p = \frac{\gamma}{2g}(U_2 - U_1)^2 = \frac{\gamma}{2g}U_2^2(1 - mC_c)^2$$

$$= (p_1 - p_2)\frac{1 - mC_c}{1 + mC_c}. \qquad (11.27)$$

m	0.05	0.10	0.15	0.20	0.25	0.30
C_d	0.598	0.602	0.608	0.615	0.624	0.63
m	0.35	0.40	0.45	0.50	0.55	0.60
C_d	0.646	0.66	0.676	0.695	0.716	0.74

Table 11.1

1. When the Air Supply Reynolds Number is $Re \geqslant 4 \times 10^4$, Then, C_d Is Maintained as a Constant in a Fashion Shown Below

Sec 6   Complex Variable Functions and Conformal Transformations as Used to Obtain Coefficients of Contraction

If one is considering the case of a non-compressible, non-viscous two-dimensional stationary flow field, then, it is possible to utilize complex variables, complex functions and conformal transformations to solve flow line equations; because of this fact, one can draw out flow line spectra. If we choose a coordinate x, y, on a physical surface, then, it is possible to use a complex variable $z = x + iy$, to represent the location of a certain point on a flow field. If we assume that r = the modulus of the complex variable z, and we also assume that θ = the amplitude angle (the angle contained between r and x), then,

$$z = x + iy = r(\cos\theta + i\sin\theta) = re^{i\theta},$$
$$r = \sqrt{x^2 + y^2}$$

The conjugate complex variable

$$\bar{z} = x - iy = r(\cos\theta - i\sin\theta) = re^{-i\theta},$$
$$\text{tg}\,\theta = \frac{y}{x}$$

(11.28)

On the surface of an object z, the equal flow speed position ϕ = a constant and the flow line ψ = constant form orthogonal curve net, that is to say that the minute mesh of curve intersections $\phi = k_1$ and $\psi = k_2$ are rectangles or squares as shown in the narrow wall aperture flow field shown in Fig. 11.10.

If we assume that the complex velocity value

$$F = \phi + i\psi, \quad \frac{\partial\phi}{\partial x} = u, \quad \frac{\partial\psi}{\partial x} = v; \qquad (11.29)$$

$$\frac{\partial\phi}{\partial x} + i\frac{\partial\psi}{\partial x} = \frac{\partial F}{\partial x} = \frac{dF}{dz} \cdot \frac{\partial z}{\partial x}$$

$$= \frac{dF}{dz} = u - iv = w; \qquad (11.30)$$

then, the complex flow speed is

$$w = \frac{dF}{dz} = u - iv = q(\cos\theta - i\sin\theta) = qe^{-i\theta}$$

and the conjugate complex flow speed is

$$\bar{w} = \frac{d\bar{F}}{d\bar{z}} = u + iv = q(\cos\theta + i\sin\theta) = qe^{i\theta} \qquad (11.31)$$

240

If we take ϕ to be the real number amplitude and $i\psi$ to be the imaginary number amplitude, then, on the complex velocity value plane, a certain point $F = \phi + i\psi$ corresponds to a certain point on the physical surface $z = (x + iy)$, an example would be a certain intersection point $\phi\bar{\psi}$ in the curve grid net. If it is possible to find an appropriate complex function $F = f(z)$, then it is possible to take various points on the surface z and successively transfer them to surface F; this is done in order to maintain the similarity of the minute forms of the grid network as well as maintaining the equality of the angles of refraction or bending. This is called a "conformal transformation." Obviously, when the curves representing equal values of ϕ, and equal values of ψ on the surface, z, are conformally transformed onto the surface F, they become mutually perpendicular lines. What were originally straight lines on the surface, z, are transformed into curves on the surface F.
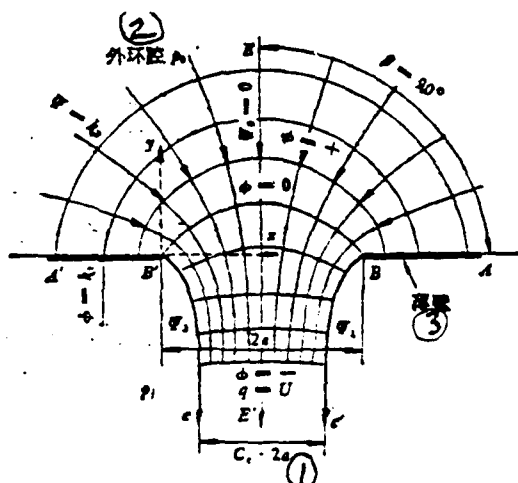

图 11.10　薄壁矩孔射流收缩器流线谱

Fig 11.10

1. A Narrow Wall Aperture Jet Field Contraction Flow Line Spectrum. 2. Exterior Ring Cavity 3. Narrow Wall

Fig 11.10 represents the flow line spectrum of a narrow wall aperture jet in which the flow lines are concentrated and approach each other. Let us assume that there is a dimension perpendicular to the surface of the illustration and equal to 1, that the area of the aperture $BB' = 2a$, that the contraction ratio $= C_c$, and that the jet contraction reaches an effective cross section area $= 2aC_c$ in which there is an even parallel flow speed $q = U$. The narrow walls AB and A'B' are extensions of the boundary flow lines. BC and B'C' are "boundary flow lines." The flow function along the boundary flow lines is $\psi = $ a constant; the modulus, q, of

241

flow speed vector, W = a constant; p_i = the static pressure of the external environment. EE' is the center line of the jet; $\psi_0 = 0$, and the vertical to the narrow wall, $\beta = 90°$. If we select BB' to open a hole, then, the velocity value on the edge, $\phi = 0$; the front of the hole is $+\phi$, and the back of the hole is $-\phi$. The flow function along the boundary flow line A'B'C', $\psi_2 = C_c a U$, the flow function along the boundary flow line ABC, $\psi_1 = -C_c a U$, the effective amount of flow $\psi_2 - \psi_1 = 2 a C_c U [m^3/s]$. One can solve the boundary flow line equations in order to draw out the flow lines, that is to say that it is possible to precisely fix the ratio of contraction $C_c < 1$.

Sec 7 Complex Variable Function Transfer Formulae

According to the theories of Schwarz and Christoffel, if one assumes that there is a complex variable $F = \phi + i\psi$ and that $\zeta = \xi + i\eta$. If one is considering the case in which there is a polygon on a surface F, let one assume that the various vertical angles are $\alpha_1, \alpha_2 \cdots \alpha_n$, and n = the number of its sides. In such a case, the sum of all its angles is $\alpha_1 + \alpha_2 + \cdots \alpha_n = (n - 2)\pi$. On a surface ζ, on the real number axis ξ there are coordinate points $\xi_1, \xi_2 \cdots \xi_n$ for a total of n separate points. In such a case, if one utilizes the formula below, then, it is possible to take the n apex points of the angles in the polygon on surface F and transfer them into n separate coordinate points on the real number axis ξ of the surface ζ :

$$\frac{dF}{d\zeta} = K(\zeta - \xi_1)^{\frac{\alpha_1}{\pi} - 1}(\zeta - \xi_2)^{\frac{\alpha_2}{\pi} - 1} \cdots (\zeta - \xi_n)^{\frac{\alpha_n}{\pi} - 1}$$

(11.32)

From Fig 11.10 it can be seen that all lines defined by equal values of ψ originate in the $+\phi$, of the exterior ring cavity, concentrate themselves in the open hole BB', which is $\phi = 0$, and tend toward a $-\phi$ at which point they become an even, parallel jet. At the point C'C, the magnitude and directions of flow speeds are entirely the same, i.e., q = U. The boundary lines ψ_1, and ψ_2 form themselves into a long thin area ACA'C', as shown in Fig 11.11 (a). In order to later solve the flow line equations, it is necessary to first utilize the formula (11.32) to take the long thin area and transform it into an unlimited plane above the real number axis ξ of the plane ζ. The intersection point C'C is a point $\xi_1 = 0$. The vertical angle along A'C' $\alpha_1 = 0$. On the basis of this fact, let us compare Fig 11.11 (a) and (b)
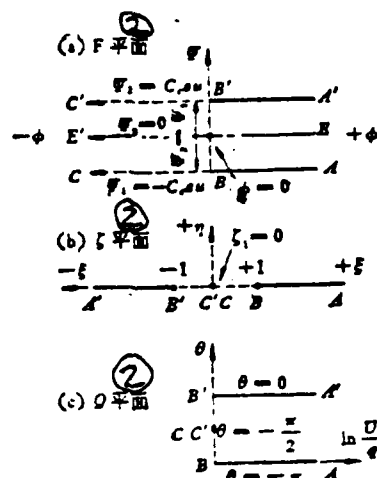
242

图11.11 复变函数变换平面
Fig 11.11

1. Complex Function Transformation Planes. 2. Plane

$$\frac{dF}{d\zeta} = K(\zeta - 0)^{-1}, \quad \text{or} \quad F = K\ln\zeta + L \quad (11.33)$$

At point B, $F_1 = 0 - i\phi_1 = -iC_\ell aU$. If we take point B and transform it into $\xi = 1, \eta = 0$, of plane ζ, that is to say, $\zeta = 1$, then, it is possible to precisely determine the integration constant $L = -iC_\ell aU$. If we take point B' and transform it into $\zeta = -1$, then,

$$iC_\ell aU = K\ln(-1) - iC_\ell aU, \quad \ln(-1) = \frac{i2C_\ell aU}{K},$$

$$-1 = e^{i(2C_\ell aU/K)} = \cos\left(\frac{2C_\ell aU}{K}\right) + i\sin\left(\frac{2C_\ell aU}{K}\right),$$

Therefore,

$$\left(\frac{2C_\ell aU}{K}\right) = \pi, \quad K = \frac{2C_\ell aU}{\pi};$$

If we substitute in equation (11.33), then, we can obtain the transformation formula for the planes F and ζ

$$F = \frac{2C_{,a}U}{\pi} \ln \frac{\cdot}{\cdot} - iC_{,a}U \qquad (11.34)$$

Sec 8   Terminal Velocity Loci for Boundary Lines of Flow

Let us assume that the amount of flow is a constant; if we assume this, then, the even, parallel jet flow speed U is a constant. According to equation (11.31), the complex flow speed is

$$W = \frac{dF}{dz} = u - iv = qe^{-\theta},$$

Therefore,

$$\frac{U}{W} = U\frac{dz}{dF} = \frac{U}{q}e^{i\theta} \qquad (11.35)$$

If we consult Fig 11.10, we can see that the farther down the flow one goes from the aperture BB',-the lower is the modulus of complex flow speed, q. Along the narrow wall A'B' and AB, the direction of the flow lines, θ , is already determined; however, the modulus increases from 0 to q. Along the boundary flow lines B'C' and BC, the modulae of W are all equal to q; however, the amplitude angle, θ , changes continuously. On the physical plane, z, when the boundary flow line B'C'BC is sketched out, on the U/W plane, the modulus (U/q) = 1 describes a semi-circle as shown in Fig 11.12(a). The amplitude angle indicating the wall surface A'B' is

θ = 0. Therefore, from B' to C' the amplitude angle decreases from 0 to $-\pi/2$, and, from C to B, it decreases again to $-\pi$. This is called the "terminal velocity trajectory or 1 locus" of U/W. If we assume a conformal transformation function

$$Q = \ln\left(\frac{U}{W}\right) = \ln\frac{U}{q} + i\theta \qquad (11.36)$$

If we take $\ln\frac{U}{q}$ and θ to be the coordinates, then, it is possible to take the semi-circle on the plane $\frac{U}{W}$ and transform it into a straight line on the surface, Q, as shown in Fig 11.12(b). At the point A', which is fairly well upstream from the opening $W \cong 0, q \cong 0, U/q \cong \infty$. At the point B' $U = q, \ln\frac{U}{q} = 0$.   The boundary flow line B'C' gradually turns from $\theta = 0 \rightarrow \theta = -\pi/2$. . The flow line CB gradually turns from $\theta = -\frac{\pi}{2} \rightarrow \theta = -\pi$. The polygon on plane Q is an open rectangle, and it only leaves two vertical angles $\alpha_1 = \alpha_1 = \frac{\pi}{2}$.
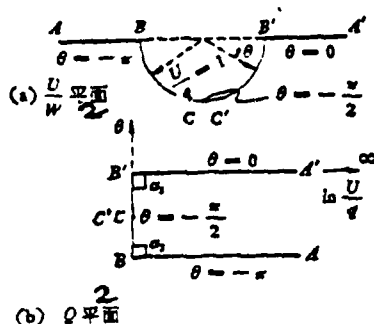
244

Fig 11.12

The Terminal Velocity Locus Transformation Plane 2. Plane

If we utilize the transormation formula (11.32), and we compare the real number axis, ζ , of Fig 11.11(b), then, it is possible to write

$$\frac{dQ}{d\zeta} = K(\zeta + 1)^{-\frac{1}{2}}(\zeta - 1)^{-\frac{1}{2}} = K(\zeta^2 - 1)^{-\frac{1}{2}} \quad (11.37)$$

By integrating equation (11.37), it is possible to obtain

$$Q = K\text{Arch}\zeta + L, \quad L = \text{ integration constant} \quad (11.38)$$

In the equation above, the cosine of the inverse hyperbola is

$$\text{Arch}\zeta = \ln(\zeta + \sqrt{\zeta^2 - 1})$$

On the boundary flow line BCC'B', q = U; therefore, $Q = \ln\frac{U}{q} + i\theta = i\theta$. (11.39)

In Fig 11.12(b), the indicated point B is the origin point of the plane Q, and, due to this fact, $Q = -i\pi$, corresponding to $\zeta = +1$, on the ζ plane in Fig 11.11(b); if we make a substitution in equation (11.38), then, $-i\pi = K\ln(1 + 0) + L$, giving a precise value for the integration

$$\text{constant } L = -i\pi.$$

Q, at point B', = 0. which corresponds to $\zeta = -1$ on the ζ plane; due to this fact, one can obtain from the equation (11.38) the fact that

245

$$0 = K\text{Arch}(-1) - ix,$$

Because of the fact that

$$\text{ch}\theta = \cos(i\theta), \quad \text{Arch}(-1) = ix;$$
$$Kix - ix = 0,$$

; therefore, $K = 1$.

Let us take plane Q and transform it into the formula for the semi-limitless plane above the real number axis of plane ζ, that is,

$$Q = \text{Arch}\,\bar{\zeta} - ix = \ln\left(\frac{U}{W}\right) = \ln\left(U\,\frac{dz}{dF}\right)$$

(Refer to Fig 11.11 (c))   (11.40)

Sec 9   Boundary Flow Line Equations and Ratios of Contraction

The complex velocity value, F, in equation (11.34) is a function of ζ, $F = f(\zeta)$. The complex flow speed in equation (11.40) $W = \frac{dF}{dz}$, is also a function of ζ, $\frac{dF}{dz} = g(\zeta)$. By means of the complex variable $\zeta = \xi + i\eta$ let us make a connection and link together the corresponding points on plane F and plane Q (Fig 11.11). If we eliminate the parameter ζ from the two equations (11.34) and (11.40), then it is possible to obtain the complex function $F = f(z)$, which is necessary for a conformal transformation. It is only necessary to draw out the boundary flow lines B'C' and BC, and it is then possible to determine a precise value for the ratio of contraction, C_c; therefore, in this problem, it is not necessary to first solve the complex function $F = f(z)$, ; it is only necessary to solve boundary flow line equations, and that will suffice.

In Fig 11.10, the B' indicated is the x, y coordinate origin point $z = 0$. On the boundary flow line B'C', the included angle between the x axis and the tangents at the various points $= \theta$. If we assume that the minute or differentiated are length of the boundary flow line $= ds$, then,

$$\left.\begin{array}{l} \dfrac{dx}{ds} = \cos\theta, \quad \dfrac{dy}{ds} = \sin\theta; \\[2mm] dz = dx + idy = ds(\cos\theta + i\sin\theta) = ds\,e^{i\theta}; \end{array}\right\} \quad (11.41)$$

246

On the boundary flow line, the modulus of $\frac{U}{W}$ is $\frac{U}{q}$ $q=1$; if one takes a look at equations (11.40) and (11.39), he can see that

$$\left| U \frac{dz}{dF} \right| = \left| e^Q \right| = \left| e^{i\theta} \right| = 1,$$

$$\left| U \frac{dz}{dF} \right| = \left| \frac{dz}{d\zeta} \cdot \frac{U d\zeta}{dF} \right| = \left| \frac{ds e^{i\theta}}{d\zeta} \cdot \frac{U d\zeta}{dF} \right|$$

$$= \frac{ds}{d\zeta} \left| U \frac{d\zeta}{dF} \right| = 1; \qquad (11.42)$$

On the physical plane, z, the transition B' $\rightarrow$ C' corresponds to a similar transition form −1 to 0 by ζ on the ζ plane.

If we differentiate equation (11.34) by ζ , then, we can obtain

$$\frac{dF}{d\zeta} = \frac{2 C_r a U}{\pi \zeta}, \qquad \text{therefore} \qquad U \frac{d\zeta}{dF} = \frac{\pi \zeta}{2 C_r a};$$

If we substitute this into equation (11.42), we can obtain

$$\frac{\pi \zeta}{2 C_r a} \frac{ds}{d\zeta} = 1, \quad \frac{ds}{d\zeta} = \frac{2 C_r a}{\pi \zeta};$$

Also, from equation (11.40):

$$Q = i\theta = \text{Arch}\zeta - i\pi, \quad \text{Arch}\zeta = i(\theta + \pi),$$
$$\zeta = \text{ch} i(\theta + \pi) = \cos(\theta + \pi) = -\cos\theta,$$
$$d\zeta = \sin\theta\, d\theta;$$

Because of these facts

$$\frac{ds}{d\theta} = \frac{ds}{d\zeta} \cdot \frac{d\zeta}{d\theta} = \frac{2 C_r a}{\pi} \frac{\sin\theta}{\cos\theta} = \frac{2 C_r a}{\pi} \text{tg}\theta \quad (11.44)$$

If we utilize equation (11.41) for integration:

$$x = \frac{2 C_r a}{\pi} \int_0^\theta \cos\theta \,\text{tg}\theta \, d\theta = \frac{2 C_r a}{\pi} (1 - \cos\theta) \quad (11.45)$$

$$y = \frac{2 C_r a}{\pi} \int^\theta \sin\theta \,\text{tg}\theta \, d\theta = \frac{2 C_r a}{\pi} [\ln(\text{tg}\theta + \sec\theta) - \sin\theta]$$
$$(11.46)$$

At point C, $\theta = -\frac{\pi}{2}$; therefore, $x = \frac{2 C_r a}{\pi}$, this is the length of the projection of the boundary flow line BC' on the axis, x. Fig 11.10 is an axially symmetric

flow line spectrum; therefore, the area of the aperture is

$$2a = 2C_c a + 2\left(\frac{2C_c a}{\pi}\right);$$

Because of this fact, the ratio of contraction is

$$C_c = \frac{\pi}{2 + \pi} = 0.611. \qquad (11.47)$$

If the included angle between the center line of the jet and the narrow wall is $\beta < 90°$, then it follows that the aperture is turned into a sort of funnel, and, on the basis of the theoretical calculations discussed above, the coefficient of contraction, C_c, must be a good deal larger than 0.611; if $\beta > 90°$, then, C_c must be smaller than 0.611. The theoretically calculated values for the ratio of contraction, C_c. in the funnel shaped aperture jets for different values of β can be found in Table 11.2 along with the experimentally determined values for the same quantities.

		22.5°	45°	67.5°	90°	112.5°	135°	157.5°	180°
1	漏斗半张角 β	22.5°	45°	67.5°	90°	112.5°	135°	157.5°	180°
2	理论收缩比 C_c	0.855	0.745	0.666	0.611	0.568	0.537	0.516	0.500
3	实验收缩比 C'_c	0.882	0.753	0.684	0.632	0.608	0.577	0.546	0.541

Table 11.2

1. The Half-Arc Angle β of the Funnels 2. The Theoretical Ratio of Contraction, C_c 3. The Experimentally Determined Ratio of Contraction, C'_c

The opening of gas mixture apertures in the walls of flame tubes and the forming of the impulse pressure into the shape of the mouth of a trumpet or the concentration of flow lines to form a baffle inserted into the mouth of the aperture are all things done in order to increase the ratio of contraction, C_c, and, by so doing, to increase the coefficient of flow, C_d, (see formula (11.26) and Table 11.1).

The theoretically calculated values for C_c are generally smaller than the experimentally determined values for C'_c. This is due to the fact that the theoretical calculations ignore changes in gaseous density. If one assumes that the value for the specific heat ratio of air is k = 1.4, on the basis of the approximate calculations done by the theory of jets held by Chaplygin, the ratio of contraction of

a narrow wall aperture compressible jet is $C_c \approx 0.714$ (Refer to The Fluid
Dynamics of Jets, by Bo Shi Yi).

Chapter 12 Wall Jets

Sec 1 Wall Jet Gas Film Cooling

In order to maintain the temperature of the walls of the flame tube and the temperature of the blade surfaces of the directional vanes so that they do not exceed the permissible limits, gas film cooling is often employed. That is to say that one can utilize the low temperature air of the outer ring cavity to be propelled through small apertures or narrow cracks and follow the inner walls of the flame tube (or the surface of the blades of the directional vanes) to form a gas film. Cut off by a metal surface, there is no contact made with high temperature air flow. Actually, this gas or air film is a half-jet added to the boundary layer along the walls; therefore, it is possible to distinguish between turbulence boundary layers and parallel flow jets in order to solve for the components of velocity and, then, merge them back together. If we assume that we are dealing with a non-compressible, two-dimensional flow field with isobaric mixing, then, the flow speed components for the initial stage of a narrow crack jet gas film are as shown in Fig 12.1. b_0 = the height of the narrow crack. The original jet flow speed = U_0. The speed of the main flow in the interior of the flame tube = U_H. The flow speed ratio $m_0 = (U_H/U_0) > 1$.

01 is the boundary line of the boundary layer. 0'1 is the interior boundary line of the mixing boundary layer, coordinate y_1. 0'2 is the exterior boundary line of the mixing boundary layer, coordinate y_2. 00'1 corresponds to the jet core; the length = x_H. The width of the mixture boundary layer $-b = y_1' + y_2' = y_2 - y_1$.

The thickness of the boundary layer = ε . In this initial stage, the jet core and the boundary layers are separated by the main flow and the walls flow within the gas film is small, and thermal transference is slow, consequently, the amount of heat flow which travels from the main flow across the gas film to the surface of the walls is also small; because of this fact, the heat shielding or insulating effects are comparatively good. If one is dealing with boundary layers of laminar flow, then, the heat shielding or insulating effects are even better. Once one reaches the lower part of the jet flow core, the boundary layers merge together, turbulence flow mixing is violent, and the effectiveness of the heat shielding declines. Because of this fact, it is common to employ several ordered states of narrow crack jet gas films which overlap and transfer energy from one to the other; this is done in order to prevent parallel flows at wall temperature from rising.

The curve defining the distribution along y of the flow speed in the initial phase of a gas film can be divided into three parts or sections:

① Within a turbulence flow boundary layer $0 < y < \delta$, the distribution is governed according to a rule of the exponent 1/7, that is,

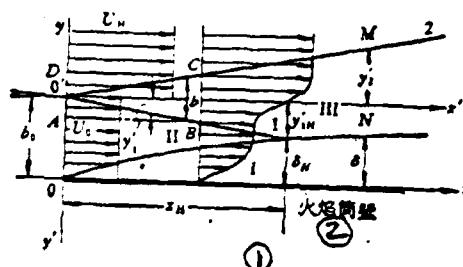$$\frac{U}{U_0} = \left[\frac{y}{\delta}\right]^{\frac{1}{7}} \qquad (12.1)$$

图 12.1 贴壁射流起始段流速分布

Fig 12.1

1. Flow Speed Distribution in the Initial Stage of a Wall Jet   2.   Flame Tube Wall

② Within the jet core $\delta < y < y_1$, the flow speed $U = U_0$ is evenly distributed.

③ Within a mixing boundary layer $y_1 < y < y_2$, the mixing of two-dimensional parallel jets is governed by the rule:

$$\frac{U}{U_0} = 1 - (1 - m_0)\left[1 - \left(\frac{y - y_2}{b}\right)^{1.5}\right]^2 \qquad (12.2)$$

The assumption that we made previously of isobaric mixing along x is also appropriate in connection with a flow speed ratio $m_0 \leqslant 3$.   If $m_0 > 3$, this leads to the narrow crack jet flow speed being too low, and, when this is true, the exterior boundary lines of a jet curl in toward the wall surfaces, consequently, it is not possible to assume isobaric mixing. If we take O'x' and O'y' to be the coordinate axises, then, on the basis of the equations below, it is possible to precisely determine the locations of the interior and exterior boundary lines of a jet O'1 and O'2:

$$\frac{y_1'}{b} = 0.416 + 0.134 m_0, \quad \frac{y_2'}{b} = -0.584 + 0.134 m_0. \qquad (12.3)$$

251

$$\frac{db}{dx} = \mp 0.27 \frac{1-m_0}{1+m_0}, \quad m_0 > 1,$$

, using a negative sign

(12.4)

From Fig 12.1, the height of the narrow crack is

$$b_0 = \delta_H + y'_{sa}$$

(12.5)

From the three equations above, it is possible to obtain a formula for calculating the jet core length, x_H, which is

$$\frac{x_H}{b_0} = \left[\frac{\delta_H}{x_H} \mp 0.27(0.416 + 0.134 m_0) \frac{1-m_0}{1+m_0} \right]^{-1}$$

(12.6)

Let us assume that the Reynolds number is

$$\dot{R}_x = \frac{\rho_0 U_0 x_H}{\mu},$$

According to the formula for the increase in thickness along a flat surface of a turbulence flow boundary layer

$$\frac{\delta_H}{x_H} = \frac{0.37}{R_x^{0.2}}.$$

(12.7)

We already know or can select a value for m_0; let us assume at the outset that $\delta_H = 0$, and let us try to figure out a first approximation value for (x_H, b_0).

We can then take this approximate value of x_H and substitute it back into equation (12.6), then, we can calculate a second approximate value. In engineering, one generally takes calculations to a second approximation as being adequately precise.

From equation (12.7), it can be seen that, if δ_H is generally maintained invariable, and the Reynolds number, R_x, is raised, then, the jet core, x_H, is extended in length as is the length of the gas film which is effective in thermal isolation or insulation. In such a case, it is possible to use several less sections of gas film and, in this way, to economize on the amount of gas used in gas film cooling. This intensified pressure is higher than the pressure in the exterior ring cavity of the combustion chamber of a jet engine And, there is a possibility of raising the narrow crack jet velocity $U_0 > U_H$, this will lead to a flow speed ratio $m_0 < 1$ (use a positive sign in formula 12.4). This can raise the effectiveness of

252

using gas films for thermal isolation or insulation.

Sec 2 Flow Speed Distribution For Auto-modeling Phase of Wall Jets

The distribution curves along y for flow speed U, as they are measured at
different cross sections (x/b_O) of a self-patterning or typical section after the
boundary layers have come together are as illustrated in Fig 12.2(a). If we use the
non-dimensional coordinates (U/U_m) and $(y/y_{\frac{1}{2}})$, then, the flow speed distributions
for different jet velocities, U_O, and different cross sections (x/b_O) can all be
reduced to a standard curve as shown in Fig 12.2(b). The broken lines on the illus-
tration are all theoretical calculations for laminar flow in wall jets. The solid
lines show calculations based on turbulence flow.

Let us assume that U_H = an even, parallel main flow speed, U_O = an original
jet velocity $> U_H$, that U_m = the maximum flow speed at any given cross section, x,
in the self-patterning or normal stage; let us further assume that $(U_H/U_o)=m_o<1$,
that U = the flow speed at a point with coordinate y on any given cross section, x,
in the normal stage, that $(U-U_H)$ = u which equals the flow speed differential at
a point with coordinate y on any given cross section, x, in the normal stage, and
let us further assume that (U_m-U_H) = u_m which equals the maximum flow speed
differential on any given cross section, x, in the normal stage;
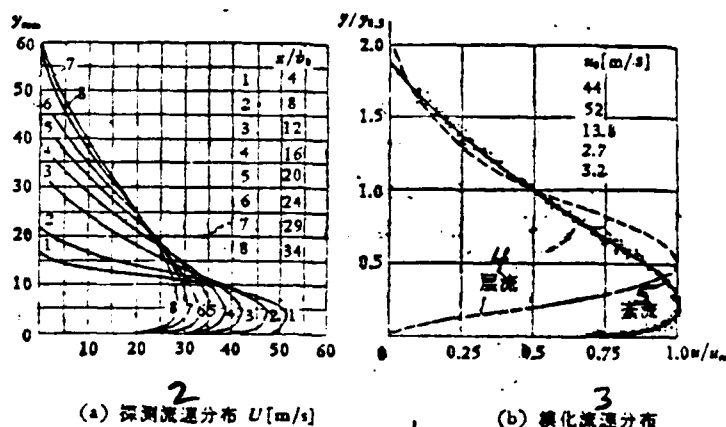

(a) 探测流速分布 $U[\text{m/s}]$ (b) 模化流速分布

图12.2 贴壁射流自模段

Fig 12.2

1. The Normal Stage of a Wall Jet 2. Investigation of Distribution of Flow Speed
U (m/s) 3. The Normalized Distribution of Flow Speed 4. Laminar Flow 5. Tur-
bulence Flow

$y_{\frac{1}{2}}$ = the vertical coordinate of a point where $\mu = 0.5u_m$ on any given cross section, x, in the normal phase. If we consider the gas film of wall jets to be similar non-compressible, viscous laminar boundary layers, and assume that $\nu = \mu/\rho$, then, the set of motion equations is as presented below:

The boundary conditions are:

$$u \frac{\partial u}{\partial x} + v \frac{\partial u}{\partial y} = \nu \frac{\partial^2 u}{\partial y^2}; \text{ (a)}$$

when $y = 0,\ u = v = 0;$ (12.8)

$$\frac{\partial u}{\partial x} + \frac{\partial v}{\partial y} = 0, \text{ (b)}$$

when $y \to \infty,\ u = 0;$

If we employ normalized variables, then,

$$(u/u_m) = F'(\phi) = F',\ u_m = Ax^\alpha,\ \phi = Byx^\beta,$$

(12.9)

A and B are constants, and α and β are treated as specific exponents; if we substitute them into equation (12.8), then, it is possible to obtain an ordinary differential equation like the one below

$$F''' + \frac{A}{2\nu B^2}[(\alpha+1)FF'' - 2\alpha F'^2] = 0,$$

$$F = \int_0^\phi F'd\phi; \qquad (12.10)$$

The equation for the relationships when the exponents or indices are treated as fixed is $2\beta = \alpha - 1$ (12.11); the flow velocity of induced roll-up is

$$v = -\frac{A}{2B}x^{\frac{\alpha-1}{2}}[(\alpha-1)\phi F' + (\alpha+1)F] \quad (12.12)$$

In equation (12.8), if we take u and perform successive multiplications on the continuity equation (b) and then add it to the motion equation (a), we can obtain

$$\frac{\partial}{\partial x}(u^2) + \frac{\partial}{\partial y}(uv) = \nu \frac{\partial^2 u}{\partial y^2},$$

If we integrate the equation above along y, and employ the boundary conditions, then, it is possible to obtain

$$\frac{\partial}{\partial x}\int_0^y u^2 dy + uv = \nu \frac{\partial u}{\partial y} - \nu\left(\frac{\partial u}{\partial y}\right)_{y=0} \quad (12.13)$$

$$y \to \infty,\quad u = 0,\quad \frac{\partial u}{\partial y} = 0,$$

254

Therefore,

$$\frac{d}{dx} \int_0^\infty u^2 dy = - \nu \left(\frac{\partial u}{\partial y} \right)_{y=0} \qquad (12.14)$$

If we take u and perform successive multiplications of equation (12.13) and then integrate along y from 0 to infinity, then,

$$\int_0^\infty u \frac{\partial}{\partial x} \left(\int_0^y u^2 dy \right) dy + \int_0^\infty u^2 v \, dy$$

$$= 0 - \nu \left(\frac{\partial u}{\partial y} \right)_{y=0} \int_0^\infty u \, dy \qquad (12.15)$$

The first quantity in the left side of the equation above can be broken down into

$$\int_0^\infty u \frac{\partial}{\partial x} \left(\int_0^y u^2 dy \right) dy = \frac{d}{dx} \int_0^\infty u \left(\int_0^y u^2 dy \right) dy$$

$$- \int_0^\infty \frac{\partial u}{\partial x} \left(\int_0^y u^2 dy \right) dy ,$$

If we use continuity equations and then divide them up for purposes of integration, the second quantity on the left side of the equation above can be changed to be

$$\int_0^\infty \frac{\partial u}{\partial x} \left(\int_0^y u^2 dy \right) dy = - \int_0^\infty \frac{\partial v}{\partial y} \left(\int_0^y u^2 dy \right) dy$$

$$= - v_\infty \int_0^\infty u^2 dy + \int_0^\infty u^2 v \, dy .$$

If we substitute into equation (12.15), then,

$$\frac{d}{dx} \int_0^\infty u \left(\int_0^y u^2 dy \right) dy + v_\infty \int_0^\infty u^2 dy$$

$$= - \nu \left(\frac{\partial u}{\partial y} \right)_{y=0} \int_0^\infty u \, dy \qquad (12.16)$$

From the continuity equation, the flow speed of induced roll-up is

$$v_\infty = - \frac{d}{dx} \int_0^\infty u \, dy ,$$

If we utilize equation (6.14), then, equation (6.16) can be rewritten to be

255

$$\frac{d}{dx}\int_{0}^{\infty}u\left(\int_{0}^{y}u^2dy\right)dy - \frac{d}{dx}\int_{0}^{\infty}udy\left(\int_{0}^{\infty}u^2dy\right)$$

$$-\left(\frac{d}{dx}\int_{0}^{\infty}u^2dy\right)\left(\int_{0}^{\infty}udy\right)$$

This can be manipulated to be

$$\frac{d}{dx}\left\{\int_{0}^{\infty}u\left(\int_{0}^{y}u^2dy\right)dy - \left(\int_{0}^{\infty}udy\right)\left(\int_{0}^{\infty}u^2dy\right)\right\} = 0,$$

In the equation above, if we integrate various parts of the first quantity, then,

$$\frac{d}{dx}\int_{0}^{\infty}u^2\left(\int_{0}^{y}udy\right)dy = 0,$$

Within each integration symbol there is a factor of the constant p, so that we obtain

$$\int_{0}^{\infty}\rho u^2\left(\int_{0}^{y}\rho udy\right)dy = K,$$

That is to say that the product of the impulse force J_x and the amount of flow G is invariable along x. (12.17)

If we take the relationships $u = u_m F' = Ax^\alpha F'$ (12.17) and substitute them into the equation above, then,

$$\frac{A^3}{B^2}x^{3\alpha-2\beta}\int_{0}^{\infty}FF''d\phi = \frac{K}{\rho^2} = \text{ a constant}$$

and this does not vary with changes in x. Therefore, it is necessary that $3\alpha - 2\beta = 0$. When we compare the expression $2\beta = \alpha - 1$, in equation (12.11), then, we can figure out that

$$\alpha = -\frac{1}{2}, \quad \beta = -\frac{3}{4}; \qquad (12.18)$$

Let us assume that

$$J_1 = \int_{0}^{\infty}FF''d\phi, \quad \frac{A^3}{B^2} = \frac{K}{\rho^2 J_1}, \quad \frac{A}{B^2} = 4\nu; \quad (12.19)$$

If we use equations (12.18) and (12.19), then, the differential equation for the normalized flow speed distribution (12.10) can be simplified to be

256

$$F''' + FF'' + 2F'^2 = 0 \qquad (12.20)$$

The boundary conditions are: when $\phi = 0$, $F = F' = 0$; and when $\phi \to \infty$, $F' = 0$. $\quad (12.21)$

(12.21)

If we take F and multiply the various quantities in equation (12.20) and integrate one time, then,

$$FF'' + F^2F' - \frac{1}{2}F'^2 = C_1, \quad \text{, from equation (12.21), } C_1 = 0.$$

If we take $F^{-\frac{1}{2}}$ and multiply the various quantities of the equation above, then, we obtain

$$F^{-\frac{1}{2}}F'' + F^{\frac{1}{2}}F' - \frac{1}{2}F^{-\frac{1}{2}}F'^2 = 0$$

If we integrate the equation above, we obtain

$$F^{-\frac{1}{2}}F' + \frac{2}{3}F^{\frac{1}{2}} = C_2 \text{ , because of the fact that } \phi \to \infty, \ F' = 0,$$

Therefore, $\qquad\qquad\qquad\qquad C_2 = \frac{2}{3}F_\infty^{\frac{1}{2}},$

Because of this fact

$$F^{-\frac{1}{2}}F' + \frac{2}{3}(F^{\frac{1}{2}} - F_\infty^{\frac{1}{2}}) = 0 \qquad (12.22)$$

If we substitute new variables, then,

$$f(\phi) = \sqrt{F(\phi)}, \quad f = F^{\frac{1}{2}}, \quad f' = \frac{df}{d\phi}; \quad (12.23)$$

Equation (12.22) changes to become $\qquad f' + \frac{1}{3}(f^2 - f_\infty^2) = 0 \quad (12.24)$

By direct integration, we obtain the solution for equation (12.24), which is,

$$\phi + C_3 = \frac{1}{2f_\infty}\ln\left[\frac{f^2 + ff_\infty + f_\infty^2}{(f_\infty - f)^2}\right]$$
$$+ \frac{\sqrt{3}}{f_\infty}\text{arctg}\left[\frac{2f + f_\infty}{f_\infty\sqrt{3}}\right] \qquad (12.25)$$

If we utilize the boundary conditions

$$\phi = 0, \ F = F' = 0, \ f = 0, \ F_\infty \neq 0, \ f_\infty \neq 0;$$

257

we can precisely determine the integration constant

$$C_1 = \frac{\sqrt{3}}{F_\infty} \text{arc tg} \left(\frac{1}{\sqrt{3}} \right) \quad \text{(12.26)}$$

On the basis of equation (12.23), we can utimately reduce everything to $F = f^2$;

$$\phi = \frac{1}{2F_\infty} \ln \left[\frac{F + \sqrt{FF_\infty} + F_\infty}{(\sqrt{F_\infty} - \sqrt{F})^2} \right]$$
$$+ \frac{\sqrt{3}}{F_\infty} \left[\text{arctg} \frac{2\sqrt{F} + \sqrt{F_\infty}}{\sqrt{3F_\infty}} - \text{arctg} \frac{1}{\sqrt{3}} \right] \quad \text{(12.27)}$$

As far as equations (12.22) and (12.27) are concerned, we can connect them by the use of F, F' and ϕ. If we designate a set of values for F, we then get a set of corresponding set of values for F' and ϕ ; all these sets of values are numerical. Because of this fact, it is possible to draw out a normalized non-dimensional flow speed distribution curve as shown in Fig 12.3.

$$\left(\frac{u}{u} \right) = F'(\phi).$$

From equation (12.19), it is possible to solve for the values

$$A = \left[\frac{K}{4\rho^2 \nu J_1} \right]^{\frac{1}{4}}, \quad B = \frac{1}{2} \left[\frac{K}{4\rho^2 \nu^3 J_1} \right]^{\frac{1}{4}} \quad \text{(12.28)}$$

After we precisely determine the normalized flow speed function $F'(\phi)$, then, the three integrals below are all constants.
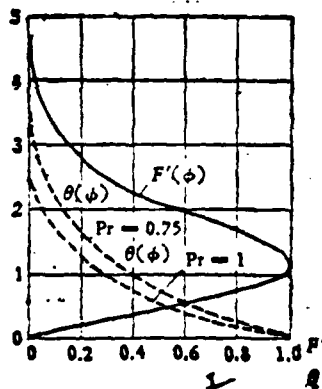

图12.3 层流气膜汽化流速分布

Fig 12.3

1. Laminar Flow Gas Film Normalized Flow Speed Distribution

$$F_\infty = \int_0^\infty F' d\phi \ , \quad J_1 = \int_0^\infty F F''^2 d\phi, \quad J_2 = \int_0^\infty F''^2 d\phi.$$

The amount of flow is

$$G = \int_0^\infty \rho u \, dy = F_\infty \left[\frac{4 K \rho^2 \nu x}{J_1}\right]^{\frac{1}{4}},$$

The impulse force is

$$J_s = \int_{a_0}^\infty \rho u^2 dy = J_2 \left[\frac{K^3}{4 \rho^2 \nu J_1^3 x}\right]^{\frac{1}{4}};$$

Therefore, the amount of flow x the impulse force $= J_s G$

$$= F_\infty \frac{J_2}{J_1} K \ [4 \ \rho^2 \nu x]^{\frac{1}{4}} [4 \ \rho^2 \nu x]^{-\frac{1}{4}}$$

$$= F_\infty \frac{J_2}{J_1} K = 常数.$$

Sec 3   Temperature Difference Distribution for Wall Jet Layer Gas Films

According to the energy equation for boundary layers of laminar flow (9.8) which is found in Chapter 9, Sec 1, if we consider that the pressure is equally distributed along x, $(\partial p / \partial x) = 0$ and, if we ignore losses from the production of heat by friction, then, the thermal energy dispersion equation is similar in form to the motion equation (12.8)(a), that is,

$$u \frac{\partial T}{\partial x} + v \frac{\partial T}{\partial y} = a \frac{\partial^2 T}{\partial y^2} r$$

The rate of thermal conductivity/the isobaric specific heat x the density $= \dfrac{\lambda}{C_p \rho}$

which is, in turn, equal to the coefficient of thermal conductivity $a \ [m^2/s]$ (12.29) .
If we assume even parallel heating, then, the temperature of the gas flow, $= T_\infty$, $T_\infty - T = \Delta T$, $y \to \infty$, $T = T_\infty$; the temperature of the jet gas flow at coordinate $y = T$, $T_\infty - T_\omega = \Delta T_{\omega, \prime}$ $\quad \theta(\phi) = \dfrac{\Delta T}{\Delta T_\omega} = \theta;$ } (12.30)
If the temperature of the wall surface of the flame tube is fixed as equal to T_ω, and $y = 0$, $T = T_\omega$, then, the function for the normalized distribution of flow speed is $\quad \dfrac{u}{u_\infty} = \dfrac{U - U_H}{U_\infty - U_H} = F'(\phi) = F', \quad F = \int_0^\infty F' d\phi.$ (12.31)

259

If the indicated temperature of the wall, T_w, and the temperature of the heated gases T_∞ are invariable, and, if we utilize the non-dimensional functions of θ and F, then, it is possible to take equation (12.29) and turn it into

$$\theta'' + Pr \cdot F \cdot \theta' = 0, \quad \theta' = \frac{d\theta}{d\phi}; \quad (12.32)$$

In the equation above, the "Prandtl" number is

$$Pr = \frac{\mu C_p}{\lambda} = \frac{\nu}{a}$$

This reflects the fact that the levels of momentum transference across boundary layers and the transference of thermal energy are similar. If the $Pr = 1$, then the distributions of flow speed and temperature are similar.

We can also use the rules governing diffusion of a jet along x and the attenuation and reduction of flow speed, that is, $u_m = U_m - U_H = Ax^r$, $\phi = Byx^s$, ΔT_m does not vary with changes in x; the boundary conditions are

$$\phi = 0, \quad y = 0, \quad \theta = 1; \quad \phi \to \infty,$$
$$y \to \infty, \quad \theta = 0; \quad (12.33)$$

If we integrate equation (12.32) two times, then, we can obtain

$$\theta = 1 - \left[\int_0^\phi \exp\left(-Pr \int_0^\phi F d\phi \right) d\phi \right]$$
$$\times \left[\int_0^\infty \exp\left(-Pr \int_0^\phi F d\phi \right)^{-1} d\phi \right]; \quad (12.34)$$

On the basis of equation (12.34), if one draws out $(\Delta T / \Delta T_w) = \theta$ for $Pr = 1$ and $Pr = 0.75$ as it varies with changes in ϕ, then, it would appear as it is illustrated with the broken lines in Fig 12.3.

Chapter 13 The Wakes of Blunt Bodies

Sec 1 The Configuration of the Wakes of Blunt Bodies

In thrust augmentation combustion chambers, the various forms of flame stabiliza-
tion devices are all blunt obstacles. The forward edge of a blunt body is a point
at which the flow of the gases is directly impeded ("watersheds"). The gas flow
divides itself up into sections and follows the surface of the blunt object until it
reaches the rear edge of the object. At this point, the speed of the wake, u, is
lower than the flow speed, U, of the surrounding gases, and the sudden change in flow
speed upon contact with the surface causes boundary layer separation. Because of
the fact that viscosity produces vortices, there is an exchange of mass, momentum and
energy between the surrounding flow and the flow of the wake and a mixing layer or
boundary layer which is similar to that of parallel flow jets. In the vortical reflu:
areas immediately behind blunt bodies, there is a wake flow core similar to a jet cor(
however, the flow speed distribution and the size of the jet core are not the same
(for counter-current even distributions see Sec 7 of this chapter). The cross-cur-
rent diffusion of the wake mixing layer gradually increases in width (see Fig 13.1).
On the external boundary of the mixing layer, y=b, the flow speed differential
$U - u = u_1 = 0$; on the axis line behind a blunt object, the flow speed differential
U-u=u_{1m} is at a maximum. The distribution of the flow speed differential, u_1,
along y is governed by the rules of a Gaussian normal distribution. If we assume
that the height of the cross flow of a blunt object $= d_0 = 2b_0$, then, the dynamic
viscosity of the gas $= \nu$. If it so happens that the Reynolds number of the flow is
high enough $R_0 = (U d_0/\nu) \geq 10^4$., then, the flow speed distribution is normalized if
one goes sufficiently far down the flow from the blunt object. That is to say that
the distribution of the non-dimensional velocity differential ratio (u_1/u_{1m}) along
the non-dimensional coordinates $(y/y_{0.5})$, then, it is possible to deduce a
normalized curve $\dfrac{u_1}{u_{1m}} = f\left(\dfrac{y}{y_{0.5}}\right)$, $y_{0.5}$, and $u_1 = 0.5 u_{1m}$ (13.1)

where $y_{0.5}$ (13.1)
Fig 13.2 is a comparison between the normalized curve of theoretical calculations
and the experimental data from the situation in which, in a wind tunnel generated
even flow field, there is a cylindrical body with $d_0 = 10$ [mm]   , $U \approx 50$ [m/s],
$R_0 \approx 2.38 \times 10^4$, and the coefficient of aerodynamic blockage of the cylinder

is $C_* \cong 1.32$ (the black spots on the illustration represent data for different cross sections, x).

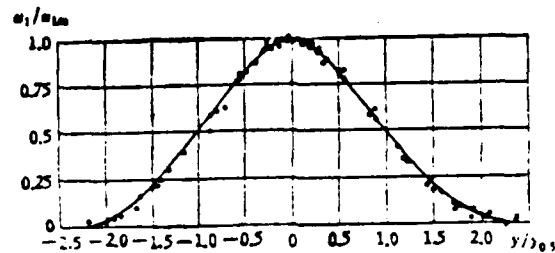
Fig 13.2

The Normalized Curve for the Velocity Differential Distribution in the Wake of a Cylindrical Body, $d_* = 10mm$

Sec 2 Theoretical Analysis of the Normalized Velocity Differentials in the Wakes of Cylindrical Objects

Let us consider the principles governing the cross-current diffusion of wakes; let us assume that the width, b, the rate of increase in thickness, $\frac{db}{dt}$, and the component velocity of cross-current pulsation, v', are all directly proportional to each other, so that,

$$\frac{db}{dt} = \frac{db}{dx} \cdot \frac{dx}{dt} \infty v', \quad \frac{dx}{dt} = u,$$

therefore,

$$\frac{db}{dx} \infty \frac{v'}{u},$$

If one is considering an area sufficiently far behind a blunt object, then,

$$u \cong U: \qquad \text{therefore} \qquad \frac{db}{dx} \infty \frac{v'}{U}.$$

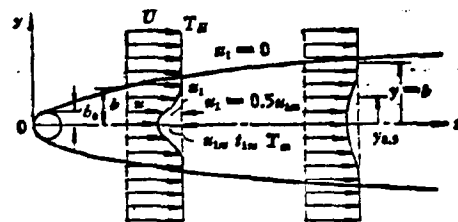The component velocity of cross-current pulsation, v', is in direct propor-

262

Fig. 13.1 The cross-current diffusion of the
wake mixing layer gradually increases in width.

tion to u_{1m}; because of this fact, $\dfrac{db}{dx} \propto \dfrac{u_{1m}}{U}$.   (13.2). If we assume that the
pressure along x is invariable, that there is a dimension of one unit perpendicular
to the surface of the illustration, and that, for a non-compressible flow, ρ = a
constant, then, in the wake flow, the rate of flow of matter through the
differentiated cross section $dy \cdot 1$ is $dm = \rho u_1 dy \cdot 1 = \rho(U - u_1)dy$. The loss rate
for momentum in a normalized wake flow is

$$ -\int_{-\infty}^{+\infty} u_1 dm = \rho \int_{-\infty}^{+\infty} u_1(U - u_1)dy = \text{a constant} \quad (13.3) $$

If one goes sufficiently far down the flow from the back of a blunt object, then,
$U - u_1 \cong U$; because of this fact, it is possible to write

$$ \rho U \int_{-\infty}^{+\infty} u_1 dy = \text{a constant} $$

or

$$ \rho u_{1m} U b \int_0^1 \left(\frac{u_1}{u_{1m}}\right) d\left(\frac{y}{b}\right) = \text{a constant} \quad (13.4) $$

Because of the fact that the integrated area of a velocity differential distribution
curve for a normalized wake flow

$$ -\int_0^1 \left(\frac{u_1}{u_{1m}}\right) d\left(\frac{y}{b}\right) = \text{a constant,} $$

therefore, it is necessary that $\rho u_{1m} U b =$ a constant; because of the fact
that we already assumed that the flow speed of the environment, U = a constant;
therefore, one can obtain

$$ u_{1m} = \frac{\text{a constant}}{b} $$, and, if we substitute in equation (13.2), then,

one can see that $b\,db =$ a constant , or, $b = K\sqrt{x}$ (13.5) .

In the equation above, K is a constant a precise value for which is determined
by experimentation. Because of the fact that the maximum flow speed differential,
u_{1m}, is directly proportional to the flow speed of the environment, therefore,

$$ u_{1m} = \text{a constant} \qquad \frac{U}{b} = \text{a constant} \qquad \frac{U}{K\sqrt{x}} = \frac{n\,U}{\sqrt{x}}, \; n = \text{a constant} \; (13.6) $$

263

According to equation (8.18), if we use the Prandtl mixture distance, 1, to represent turbulence flow shear forces:

$$\tau_T = \rho l^2 \left(\frac{\partial u}{\partial y} \right)^2,$$

then, in the wake of a cylindrical object, in order to draw out the minute or differentiated control layer, it is necessary to refer to the equilibrium of impulse forces in the control layer:

$$\rho u v + \rho \frac{\partial}{\partial x} \int_{-}^{y} \overline{u^2} dy + \rho l^2 \left(\frac{\partial u}{\partial y} \right)^2 = 0 \qquad (8.20)$$

If one goes sufficiently far downstream behind a blunt object, then,

$$u_1 \ll U, \quad u \cong U, \quad u^2 = (U - u_1)^2 \cong U^2 - 2 U u_1, \quad v \ll u_1;$$

and again, because of the fact that the flow speed of the environment, $U = a$ constant, therefore $(\partial U / \partial x) = 0$, $\cdot (\partial U / \partial y) = 0$; on the basis of this, it is possible to make the following simplification

$$2 \frac{\partial}{\partial x} \int_{-}^{y} U u_1 dy + l^2 \left(\frac{\partial u_1}{\partial y} \right)^2 = 0 \qquad (13.7)$$

If we use non-dimensional coordinates, so that, $\eta = \frac{y}{b}$, then, the normalized function

$$\left(\frac{u_1}{u_{1m}} \right) = f(\eta) = f; \quad \frac{df}{d\eta} = f'; \qquad (13.8)$$

The Prandtl mixture distance is

$$l = \beta b = \beta K \sqrt{x}, \quad \beta = \text{ a constant} \quad (13.9)$$

From equation (13.5) and equation (13.8), it is possible to obtain

$$\left. \begin{array}{l} \eta = \dfrac{y}{K \sqrt{x}}, \quad \dfrac{\partial \eta}{\partial x} = -\dfrac{\eta}{2x}, \quad \dfrac{\partial \eta}{\partial y} = \dfrac{1}{K \sqrt{x}}, \\[2ex] \dfrac{\partial u_1}{\partial y} = u_{1m} \dfrac{\partial f}{\partial \eta} \dfrac{\partial \eta}{\partial y} = \dfrac{nU}{Kx} f', \quad \alpha = \dfrac{2 \beta^2 \eta}{K}, \end{array} \right\} \quad (13.10)$$

If we take equation (13.10) and substitute it into equation (13.7), then, it is possible to obtain the differential equation for the function, f, of the normalized velocity differential ratio

$$\eta f = \alpha (f')^2, \quad \alpha \text{ can be treated as a constant} \quad (13.11)$$

264

The boundary conditions are as follows: on the boundary of wake flows, $\eta = 1$,

$$u_1 = 0, \quad \frac{\partial u_1}{\partial y} = 0, \quad f = 0, \quad f' = 0; \quad (13.12)$$

On the axes of wake flows,

$$\eta = 0, \quad u_1 = u_{1m}, \quad \frac{\partial u_1}{\partial y} = 0, \quad f = 1, \quad f' = 0. \quad (13.13)$$

In equation (13.11), with separate variables, $\alpha^{\frac{1}{2}} f^{-\frac{1}{2}} df = \eta^{\frac{1}{2}} d\eta$; by integration, it is possible to obtain

$$2\alpha^{\frac{1}{2}} f^{\frac{1}{2}} = \frac{2}{3} \eta^{\frac{3}{2}} + C,$$

If we employ the boundary conditions, then, equation (13.12) allows us to obtain

$$C = -\frac{2}{3},$$

Because of this fact, we can also obtain the normalized function

$$\left(\frac{u_1}{u_{1m}}\right) = f = \left(\frac{-1}{3\sqrt{\alpha}}\right)^2 \left(1 - \eta^{\frac{3}{2}}\right)^2 = \frac{1}{9\alpha}\left(1 - \eta^{\frac{3}{2}}\right)^2$$

$$(13.14)$$

By employing the boundary conditions in (13.13), we can obtain precise values for the constants $9\alpha = 1$, $f(\eta) = (1 - \eta^{\frac{3}{2}})^2$ $\quad (13.15)$

By the use of experimentation, it is difficult to measure values for $u_1 = 0, y = b$, because of this fact, we can use $y_{0.5}$ where $u_1 = 0.5 u_{1m}$

in order to draw Fig (13.2). From equation (13.15, we can deduce that

$$\eta_{0.5} = \frac{y_{0.5}}{b} = 0.441 \quad (13.16)$$

Schlichting and Reichardt have induced an empirical formula for the radii of diffusion of flow wakes which is

$$\frac{y_{0.5}}{\sqrt{x}} = 0.35 \sqrt{C_x b_0} = \frac{0.441 b}{\sqrt{x}}.$$

It is possible to obtain values for the half-width of wake flows by using the relationship $b = 0.8 \sqrt{C_x b_0 x}$, on the basis of this relationship, it can also be said that, in equation (13.5), $K = 0.8 \sqrt{C_x b_0}$. $\quad (13.17)$

265

The wake from a blunt object (Fig 13.1) is vertically symmetrical along the x axis. Vertical to the x-y plane, every unit of length of a cylindrical body receives an aerodynamic drag or resistance equal to

$$D = C_x b_0 \rho \frac{U^2}{2} \cdot 1 \qquad (13.18)$$

The aerodynamic drag or resistance which is felt by each unit of length or a cylindrical body = the rate of momentum loss in the wake flow; because of this fact, equation (13.4) should be equal to equation (13.18), that is,

$$C_x b_0 \rho \frac{U^2}{2} = \rho u_{1m} U b \int_0^1 \left(\frac{u_1}{u_{1m}}\right) d\left(\frac{y}{b}\right) \qquad (13.19)$$

By using (13.15), we can solve for the integral of the right side of (13.19), that is to say,

$$\int_0^1 \left(\frac{u_1}{u_{1m}}\right) d\left(\frac{y}{b}\right) = \int_0^1 (1 - \eta^{\frac{3}{2}})^2 d\eta = 0.45 \qquad (13.20)$$

From equation (13.19), we can obtain

$$\frac{1}{2} C_x b_0 U = 0.45 u_{1m} b, \quad u_{1m} = U \frac{C_x b_0}{0.9 b}, \qquad (13.21)$$

If we take the b from equation (13.17) and substitute it into (13.21), then, we can obtain

$$u_{1m} = U \frac{C_x b_0}{0.9 \times 0.8 \sqrt{C_x b_0 x}} = \frac{1.4 \sqrt{C_x b_0}}{\sqrt{x}} U \qquad (13.22)$$
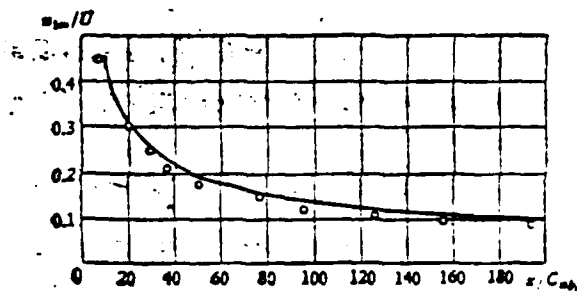

Fig 13.3

The Normalized Curve for the Attenuation and Reduction of the Velocity

266

(Fig 13.3 cont'd) Differential Ratio Along x in the Wake Flow From a Cylindrical
Object 2. °   Schlichting Experimental Data ------Drawn Out on the Basis of
Formula (13.22)

If we make a comparison with (13.6), then, we can see that the experimental constant
$n = 1.4 \sqrt{C_r b_o}$ (13.23). And now, it is possible to obtain precise values for the
constants in equation (13.9) and (13.10), that is

$$\beta = \frac{l}{b} = \sqrt{\frac{\alpha K}{2n}} = \left[\frac{0.8 \sqrt{C_r b_o}}{18 \times 1.4 \sqrt{C_r b_o}} \right]^{\frac{1}{4}} = 0.18 \quad (13.24)$$

Sec 4   The Temperature Distribution in the Wakes of Heated Cylindrical Objects

   If we assume that, in the wake of a cylindrical object, the temperature at a
given coordinate y = T, and that the temperature differential $t_1 = T - T_H$;
and, if we further assume that the temperature where y = 0 on the axis line of the
wake from a cylindrical object = T_m, and that the temperature differential in this
case is $t_{1m} = T_m - T_H$;   and, if we finally assume that the temperature of the
environment around the wake flow from a cylindrical object = T_H, and that
the non-dimensional coordinate $\eta = y/b$; then, the non-dimensional temperature
differential distribution function

$$\frac{t_1}{t_{1m}} = \theta(\eta) = \theta_s \qquad (13.25)$$

According to the Prandtl theory, the turbulence flow coefficient of thermal
conductivity, $\varepsilon_T = l_T^2 \frac{\partial u_1}{\partial y}$, l_T = the mixing distance. In a wake flow, if one wants to
draw out the minute or differentiated control layer, then, it can be done on the
basis of thermal energy equilibrium equations for control layers as they are
presented in Chapter 7, Sec 4; an example would be equation (9.34)

$$\overline{v t_1} + \frac{\partial}{\partial x} \int_{-\infty}^{y} t_1 u \, dy = \varepsilon_T \frac{\partial t_1}{\partial y}, \quad \frac{\partial t_1}{\partial y} < 0 \quad (13.26)$$

Because of the fact that $v \ll U$, $u_1 = (U - u)$ if one goes sufficiently far downstream
from a blunt body, then $u \approx U$; because of this fact, the equation above can be
simplified to be

267

$$\frac{\partial}{\partial x} \int_{-\infty}^{\prime} t_1 U dy + l_f^2 \frac{\partial u_1}{\partial y} \frac{\partial t_1}{\partial y} = 0 \qquad (13.27)$$

The rate of added enthalpy for an average-time quasi-stable state wake flow as compared with the surrounding flow is

$$\rho U C_p \int_{-\infty}^{+\infty} t_1 dy = \text{a constant } [kcal/s] \qquad (13.28)$$

If we change this into non-dimensional form, we get

$$\rho U C_p t_{1m} b \int_0^1 \left(\frac{t_1}{t_{1m}}\right) d\left(\frac{y}{b}\right) = \text{a constant} \qquad \eta = \frac{y}{b}; \qquad (13.29)$$

In the normal stage of the wake flow

$$\int_0^1 \left(\frac{t_1}{t_{1m}}\right) d\left(\frac{y}{b}\right) = \int_0^1 \overline{\theta(\eta)} d\eta = \text{a constant} \qquad (13.30)$$

The equation above represents half the integrated area under the normalized distribution curve for temperature differential. In a non-compressible flow, $\dot{\rho} = $ a constant; we already know that the even environmental flow speed, $U = $ a constant, and from (13.29), we can obtain the relationship

$$t_{1m} b = \text{a constant } (T_o - T_H) = \text{a constant } t_{01} \qquad (13.31)$$

T_o = the stable and unchanging temperature on the surface of a cylindrical object, and t_{01} = the original stable temperature differential.

If we can assume that the rule governing the attenuation and reduction of the maximum temperature differential, t_m, along the axis line is similar to the rule governing the attenuation and reduction of the maximum velocity differential, then, according to equation (13.6)

$$t_{1m} = \frac{m}{\sqrt{x}} t_{01}, \quad m = \qquad \text{an as yet unfixed constant} \qquad (13.32)$$

From equation (13.10) and (13.25)

$$\tau_1 = \tau_{1\infty}\theta(\eta), \quad \frac{\partial t_1}{\partial y} = \frac{mt_{01}}{\sqrt{x}} \cdot \frac{\partial \theta}{\partial \eta} \cdot \frac{\partial \eta}{\partial y} = \frac{mt_{01}}{Kx} \cdot \theta',$$

$$\left[\frac{\partial \eta}{\partial y} = \frac{1}{K\sqrt{x}},\right] \qquad (13.33)$$

If we employ the Taylor mixing distance from Chapter 9, Sec 7, then,

$$l_T = Kx\sqrt{2}, \qquad (13.34)$$

If we take the equations (13.34), (13.33), (13.31) and (13.10) and substitute them into the thermal energy equilibrium equation (13.27), then, after simplification, we can obtain

$$\eta\theta = 2\alpha f'\theta', \quad \frac{\theta'}{\theta} = \frac{\eta}{2\alpha f'}; \qquad (13.35)$$

If we refer to equation (13.11), then,

$$\eta f = \alpha(f')^2, \quad \frac{f'}{f} = \frac{\eta}{\alpha f'};$$

and, if we make a comparison with equation (13.35), then, we can obtain

$$\frac{\theta'}{\theta} = \frac{1}{2}\frac{f'}{f},$$

By integration, we can obtain

$$\ln\theta = \frac{1}{2}\ln f + \ln C,$$

and, because of this fact $\theta = C\sqrt{f}$. On the axis line, $\theta = f = 1$, therefore,
$C = 1;$ (13.36) ; therefore, since we already know that the distribution function
for the normalized velocity differentials, $f(\eta)$, has a certain value, the normalized
distribution for temperature differential is

$$\theta = \theta(\eta) = \frac{t_1}{t_{1\infty}} = \frac{T - T_H}{T_\infty - T_H} = \left[\frac{U - a}{U - u_\infty}\right]^{\frac{1}{2}} =$$

$$= \left(\frac{u_1}{u_{1\infty}}\right)^{\frac{1}{2}} = [f(\eta)]^{\frac{1}{2}} = (1 - \eta^{\frac{3}{2}}); \qquad (13.37)$$

Sec 5   Laws Governing the Reduction of Maximum Temperature Differentials in
Wakes Along Axis Lines

Let us consider for a moment half the thermal energy dissipated every second

269

from the surface of a cylindrical body for each unit of its length; if we assume that α = the coefficient of thermal dissipation $[kcal/m^2 \cdot s \cdot K]$, then,

$$q = \alpha(T_\bullet - T_H)\pi\delta_\bullet \cdot 1 = \alpha t_m \pi b_\bullet \quad [kcal/s] \quad (13.38)$$

This heat flow should be equal to the rate of increase in enthalpy of the surrounding flow, that is,

$$\rho U C_p t_{1m} b \int_0^1 \left(\frac{t_1}{t_{1m}}\right) d\left(\frac{y}{b}\right) = \alpha t_m \pi b_\bullet \quad (13.39)$$

$$\int_0^1 \left(\frac{t_1}{t_{1m}}\right) d\left(\frac{y}{b}\right) = \int_0^1 \theta d\eta = \int_0^1 (1 - \eta^{\frac{3}{2}}) d\eta = 0.6 \quad (13.40)$$

If we take the expression from equation (13.17), $b = 0.8\sqrt{C_x b_\bullet x}$, and substitute it into equation (13.39) and we also utilize equation (13.40), then, it is possible to obtain

$$t_{1m} = t_{01}\frac{\alpha \pi b_\bullet}{0.6 C_p \rho U \times 0.8\sqrt{C_x b_\bullet x}}$$

$$= t_{01}\frac{6.55\alpha}{C_p \rho U}\left(\frac{b_\bullet}{C_x x}\right)^{\frac{1}{2}} \quad (13.41)$$

It is first necessary to pick precise values for the quantities: α, the coefficient of thermal diffusion from the surface of a cylindrical body; the environmental flow speed, U; the coefficient of aerodynamic drag or resistance of a cylindrical body, C_x; the isobaric specific heat of gases, C_p; the radius of the cylindrical body, and the initial temperature differential, $t_{01} = T_\bullet - T_H$; only after this is done is it possible to draw out the curve for the attenuation and reduction of the maximum temperature differential along x in accordance with equation (13.41).

Sec 6 Distributions of Typical Temperature Differentials and Speed Differentials of Axially Symmetrical Wakes

If we assume that the blunt object in Fig (13.1) is a sphere with a diameter $d_\bullet = 2r_\bullet$, then, the wake behind the sphere expands symmetrically until it reaches the limiting radius $r > r_\bullet$. If we still follow the method put forward in the previous section, then, where $r_{0.5}$, $u_1 = 0.5 u_{1m}$, and, if we assume that

$$u_1 = U - u, \quad u_{1m} = U - u_m, \quad t_1 = T - T_H, \quad t_{1m} = T_m - T_H, \quad \eta = \frac{y}{r};$$

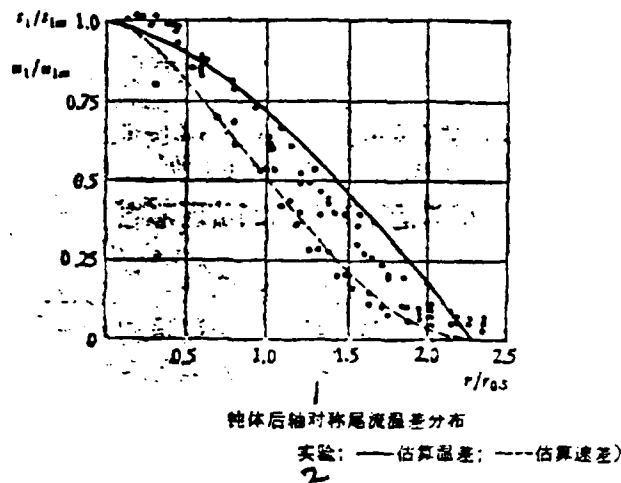then, on the basis of the equilibrium of the impulse forces, we can obtain

270

转体后轴对称尾流温差分布

（实验: ——估算温差; ----估算速差）

Fig 13.4

1. Temperature Distribution in the Axisymmetric Wake Behind a Blunt Object

2. $\bullet x/d_o = 17.1$ Halt and Hislop Experiments; —————— Calculated Temperature Differential, ——————— Calculated Velocity Differential

$$\eta f = a^2 (f')^2, \quad f' = \frac{df}{d\eta}; \qquad (13.42)$$

$$a^2 = 3n\beta^2, \quad a = \frac{1}{3};$$

Using the boundary conditions $\eta = 0$, $f = 1$, $\eta = 1$, $f = 0$, $f' = 0$, if we integrate equation (13.42), then, we can obtain

$$\frac{u_1}{u_{1\infty}} = f(\eta) = (1 - \eta^{\frac{1}{2}})^2, \qquad (13.43)$$

Let us assume that

$$\theta = \frac{t_1}{t_{1\infty}} = \theta(\eta),$$

Using the method put forward in the previous section, we can obtain $\eta\theta = 2a^2 f' \theta'$ (13.44) and, if we make a comparison between this and equation (13.42), then, we can obtain

$$\theta = \frac{t_1}{t_{1\infty}} = \sqrt{f(\eta)} = (1 - \eta^{\frac{1}{2}}) \qquad (13.45)$$

The normalized distributions of temperature differentials and velocity differentials in axisymmetric wakes are as shown in Fig 13.4.

Sec 7 Shapes of Back-Flow Areas Behind Blunt Objects in Conduits

In combustion chambers, one often uses the vortical reflux areas behind blunt objects for the purpose of providing a source of continuous ignition in order to maintain the stability of combustion. If we assume that the interior diameter of the round tube is $= R$, that the radius of the blunt object is $= B$, we can then assume that the blockage ratio, $\beta = (B/R)^2$. We will also assume that the even axial flow speed for a round conduit is $= u_1$, that the even counter-current flow speed in the core of a wake flow is $= u_2$, and that the flow speed ratio is $m = (u_2/u_1)$. The surrounding flow, at point 0 on the after edge of the blunt object, divides up to become the mixing boundary layers 0-1-2, as shown in Fig 13.5. The width of expansion of a parallel flow mixing layer $= b$, and the width ratio is $\bar{b} = (b/B)$. Because the pressure behind the blunt object is low, the surrounding flow rolls up on itself in an axisymmetrical fashion and forms an elongated and flattened vortical ring. MM' is the plane of the vortical ring. 0-1 = the exterior boundary line of the mixing layer, 0-2 = the interior boundary line of the mixing layer, 0-3-N is the boundary line of the area of reflux flow, 0-4-N is the dividing line between the parallel flow and the counter-current flow; on this line the axial flow speed is u=0; however, the tangential and radial flow speeds v and w are not both equal to zero. Within mixing layers, the flow speed decreases from u_1 on the exterior boundary line to zero and then changes again to be $-u_2$ in the core of the wake flow core. If we take 0-x to be the coordinate axis, then, along the line MM', the vertical coordinate, y_1, is positive on the exterior boundary line of the mixture layer; the coordinates y_3 for the boundary of the area of reflux flow, y_4 for the boundary which marks off the counter current flow, and y_2 for the interior boundary are all negative values.

If we assume that the non-dimensional vertical coordinate is

$$\eta = \frac{y - y_2}{y_1 - y_2} = \frac{y - y_2}{b},$$

, if we follow the analytical methods put forward in Sec 2, then, it is possible to obtain the non-dimensional velocity differential distribution

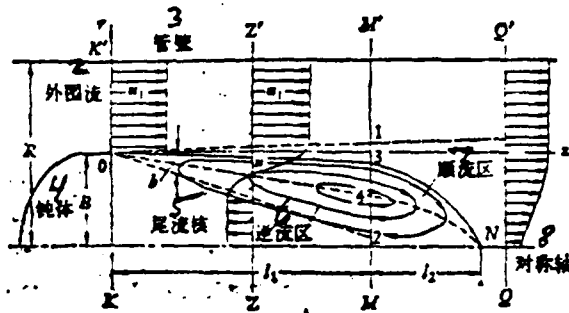$$\frac{u_1 - u}{u_1 - u_2} = f(\eta) = (1 - \eta^{1.5})^2 \qquad (13\cdot6)$$

图13.5 圆管内钝体 B 后轴对称回流区示意

Fig 13.5

1. An Illustration of the Axially Symmetrical Reflux Flow Area Behind the Blunt
Object B in a Round Tube 2. Surrounding Flow 3. Wall of the Tube 4. Blunt
Object 5. Wake Flow Core 6. *Counter-current Flow Area* 7. Parallel Flow
Area 8. Axis of Symmetry

Sec 8 Estimated Measurements of the Back-Flow Areas Behind Blunt Objects in Conduits

If we refer to Fig 13.5, then, the area of reflux flow can be divided into a
forward and aft section: on the plane MM', let us take a look at l_1 for the forward
section and l_2 for the after section. In the l_1 section, due to the fact that there
is induced roll up in the surrounding gas flow and because of turbulence flow trans-
fer, gases pass from the area of counter-current flow, across the boundary line 0-4-
N and enter into the area of parallel flow. In the l_2 area, because of the fact
that there is a positive axial pressure gradient $+(\partial p/\partial x)$, gases are forced from
the area of parallel flow across the boundary line 0-4-N and into the area of
counter-current flow. In average time quasi-stable state flow fields, the amount of
gas that flows out from the l_1 area and out of the area of counter-current slow
should be equal to the amount of gas that flows from the l_2 area and into the area
of counter-current flow. This portion of recycled gases most certainly is not
entirely from the area of counter-current flow and its gases; it is continuously
renewed in the cycle of the gases entering, being burned and being brought back in
the reflux flow. The length of the area of reflux flow is $l_c = l_1 + l_2$. If
we take B as the basis, then, the non-dimensional length of the area of reflux
flow is $l_c = (l_c'/B) = (l_1/B) + (l_2/B) = l_1 + l_2$ (13.47). The non-dimensional

vertical coordinate is

$$\bar{y}_1 = \frac{y_1}{B}, \quad \bar{y}_2 = \frac{y_2}{B}, \quad \bar{y}_3 = \frac{y_3}{B}, \quad \bar{y}_4 = \frac{y_4}{B};$$

The non-dimensional horizontal coordinates are

$$l = \frac{l}{B}$$

, l is figured from the back edge of the blunt $l = 0$ object KK',

If we assume that there is isobaric mixing in the l_1 section, then, we can check out the impulse force equilibrium in the intake and exhaust of the control area KK'ZZ' and get

$$\rho u_1^2 \pi (R^2 - B^2) = \rho u_1^2 \pi [R^2 - (B + y_1)^2]$$
$$+ 2\pi\rho \int_{y_2}^{y_1} u^2 (B + y) dy + \rho u_1^2 \pi (B + y_2)^2 \quad (13.48)$$

For the equilibrium of gas flow in the intake and exhaust we get

$$\rho u_1 \pi (R^2 - B^2) = \rho u_1 \pi [R^2 - (B + y_1)^2]$$
$$+ 2\pi\rho \int_{y_2}^{y_1} u (B + y) dy + \rho u_1 \pi (B + y_3)^2 \quad (13.49)$$

The amount of recycled gas flow in the area of reflux flow is

$$2\pi\rho \int_{y_2}^{y_3} u (B + y) dy \quad (13.50)$$

In the plane MM', if we assume that the average flow speeds of the area of parallel flow $3 \rightarrow 4$ and the area of counter-current flow $2 \rightarrow 4$ both have equal values $\bar{u}$, or that the ring-shaped cross section $3 \rightarrow 4$ = the ring-shaped cross section $2 \rightarrow 4$, that is to say that, then, $\pi(B + y_3)^2 - \pi(B + y_4)^2 = \pi(B + y_4)^2$ (13.51). If we now take the three equations from equation (13.48) to equation (13.50) and, one at a time, simplify them by eliminating u_1^2, B^2 and $u_1 B^2$, change them to non-dimensional equations, take l to be the independent variable, and solve by the use of graphs (see G.N. Abramovich, Theory of Turbulent Streams , 1960, pp 466-473.) then, it is possible to solve for the flow speed ratio $m = (u_2/u_1) = f(l)$ (Fig 13.6) and the vertical coordinates for the area of reflux flow $\bar{y}_2, \bar{y}_3, \bar{y}_4$ as they are distributed in terms of changes in l (Fig 13.7); it then becomes possible to draw out the shape of the area of reflux flow.

According to the conditions which pertain to equation (13.51), it is possible to solve for the flow speed ratio $m = -0.51$, $l_1 = 3.1$ in the plane MM'.
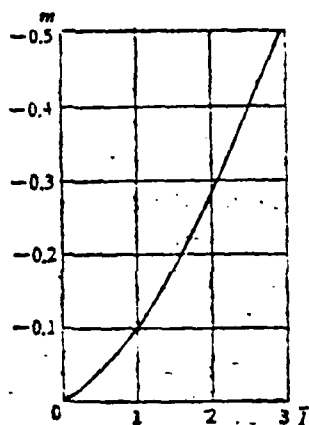
273

图 13.6 流速比 m 在 l_1 段变化

Fig 13.6

1. Changes in the Flow Speed Ratio
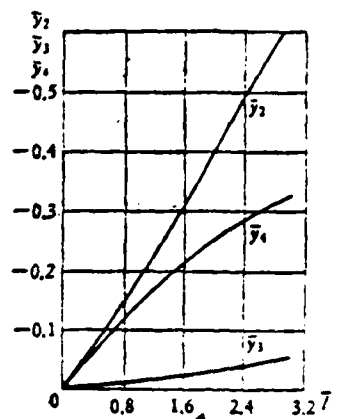m in the l_1 Section

图 13.7 无量纲坐标在 l_1 段分布

Fig 13.7

1. Distribution of Non-dimensional
Coordinates in the l_1 Section

Because this is so, in the tube or conduit, the overall length, l_c, of the area of
reflux flow behind a blunt object is approximately equal to $l_1 = 0.85$, or a value
four times the height B of the blunt object, that is, $l_c = l_1 + l_2 \cong 4$ (13.52).

The equation above is appropriate for use with the flow speed ratio $m \cong 0.5$,
as well as a blockage ratio $\beta \cong 0.75$, $B = 0.866\,R$ (where R is the radius of the
tube or conduit). This method assumes that there is isobaric mixing, and it does
not take into consideration the influence of boundary layers along the walls of
the tube; because of these facts it is not adequately accurate.

274

Chapter 14   Jet Diffusion Plumes

Sec 1   Forms of Jet Diffusion Plumes

Combustion is the result of the violent collision and compounding of molecules of a gaseous fuel and oxygen. If the number of molecules of oxygen and gaseous fuel is large enough (that is to say, if the environmental or ambient pressure is high enough), moreover, if there is even mixing according to the appropriate ratio Ω for chemical reactions, and the speed of molecular motion is adequately high (that is to say that the ambient temperature is adequately high) and, therefore, the energy of collision is adequately large, then, combustion will be very fast. The time occupied by combustion does not even reach one millisecond. Because of this fact, when one is considering the case of even pre-mixing before combustion it is very important to maintain control by means of the mechanism of the chemical reaction, that is to say, by means of the Arhenius formula that relates the rate of chemical reaction to the ratio of concentrations and temperatures.

In turbine jet combustion chambers, general or multi-purpose liquid-type fuel is vaporized and mixed with air. This does lead to vaporization of fuel prior to its reaching the jet nozzle or the vaporization tube; however, it is still not evenly pre-mixed fuel. This type of vaporized fuel jet is diffused into and interacts with the surrounding air in the form of combustion, and this is called a jet diffusion plume. It is important that the speed of combustion be decided on the basis of the speed of turbulence diffusion mixing. Fig 14.1 is an illustration of the diffusion plume of a round-aperture jet. Fig 1.2 shows the jet plume used in a combustion chamber. The length of the plume is = L.
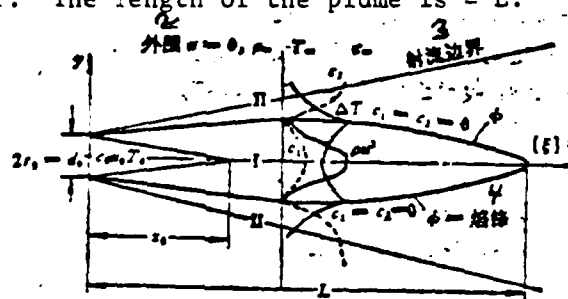

图 14.1   圆口射流扩散火焰示意图
Fig 14.1

1. Illustration of the Diffusion Plume of a Round Aperture Jet   2. In the Environment   3. Boundary of the Jet   4. Flame Tip

275

Let us assume that the diameter of the jet nozzle is $d_o = 2r_o$, that
the uniform jet flow speed in the nozzle is $= u_0$, that the original concentration of
the gaseous fuel is c_0, and that the original temperature is T_0. The length of the
jet core is x_0. An axisymmetric disturbed jet flow field can be divided into two
areas or regions; I is an area which only has fuel and fuel that has already been
burned in it. II is an area that only has oxygen and already burned fuel in it.
The layer that divides the two areas is called the "flame tip or peak", that is to
say, the surface of the flame; this surface is called φ . On the flame tip, φ ,
$T = T_\varphi$, which is the maximum temperature of combustion. The concentration, c_1,
of the fuel within in the surface of the flame tip diffuses in the direction of the
surrounding environment. The concentration of oxygen which is contained in the
surrounding environment diffuses toward the flame tip and is called c_2. Because the
chemical reaction is very fast, in fact occupying almost no time at all, c_1 and c_2
combine according to the appropriate chemical ratio, $\varOmega$, and, when they diffuse
toward and reach the surface, φ , they are immediately burned up and become gases
which have already undergone combustion. Because of this, on the flame tip,
$c_1 = 0, c_2 = 0$. Besides this, because of the fact that turbulence flow masses of
gas pulsate and tumble over each other, there is an exchange as heat and kinetic
energy across the surface of the flame tip. Within the flame tip and outside it,
along the direction y, the distributions of the concentrations c_1 and c_2, of the
temperature differential, $T - T_\bullet = \Delta T$ and the kinetic pressure ρu^2 are as
shown in Fig 14.1. Given an equal temperature, on the surface T_φ , $c_\varphi = 0$.

Sec 2   Unstable Heat Conduction Equations

From the midst of an axisymmetrical disturbed jet flow field, we can separate
out six fan-shaped, differentiated areas $y d\theta dy dx = dV$. Let us assume that
there is only a thermal conductance flow along the radial direction y. If this is
so, then, the thermal flow which enters the control area has a differential, dV, $=$
the rate of change of thermal energy within the control area (Fig 14.2). Let us
assume that the rate of thermal conductance for the turbulence flow $= k$, then, the
density flow of thermal conductance is

$$q = -k \frac{\partial T}{\partial y}, \; [\text{kcal}/\text{m}^2 \cdot s] \qquad (14.1)$$

276

$$\left(q + \frac{\partial q}{\partial y}\,dy\right)(y + dy)d\theta dx - qyd\theta dx$$

$$= \frac{\partial}{\partial \tau}(\rho c, T) \cdot yd\theta dy dx$$

$$\rho c_p \frac{\partial T}{\partial \tau} = k\left[\frac{\partial^2 T}{\partial y^2} + \frac{1}{y}\frac{\partial T}{\partial y}\right].$$
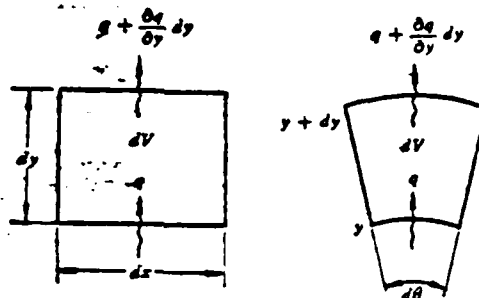

Fig 14.2

Let us assume that the coefficient of thermal conductivity is

$$\frac{k}{\rho c_p} = \varepsilon_T [m^2/s].$$

If this is true, then,

$$\frac{\partial T}{\partial \tau} = \varepsilon_T\left[\frac{\partial^2 T}{\partial y^2} + \frac{1}{y}\frac{\partial T}{\partial y}\right] \qquad \text{, and } \quad \tau \text{ represents time} \qquad (14.2)$$

The standard solution for the equation of unstable thermal conductivity (14.2) is to take T and y to be the coordinates and to take τ, to be the "error function" parameter.

Sec 3   Analogical Generalization of Unstable Heat Conduction Equations

According to the previous sections, it is possible to put forward the definition that momentum density flow $= \rho u^2 = z_1$; $\Delta T = T - T_*$; the enthalpy differential density flow $= \rho u c_p \Delta T = z_2$, $\Delta c = c_1 - 0,$, or $c_2 = 0$; the concentration density flow $= \rho u \Delta c_1 = z_3$. (14.3).

The mechanisms of the diffusion of temperature and concentration are the same, that is to say that the normalized functions for the distributions of temperature

277

and concentration are same (see Chapter 9). However, the mechanisms for the diffusion of momentum and temperature as well as concentration are not the same. This phenomenon is a reflection of the Prandtl number, Pr and the special vortical number, Sc; that is to say that the turbulence flow Prandtl number is

$$Pr = \frac{\varepsilon}{\varepsilon_T} < 1,$$

The special vortical number is

$$Sc = \frac{\varepsilon}{D_T} < 1. \qquad (14.4)$$

Concerning the question of the mixing of gases in combustion, it is possible to use the values Pr = Sc = 0.75, that is to say that the turbulence flow kinetic viscosity, $\varepsilon = 0.75\varepsilon_T = 0.75D_T$. D_T = the turbulence flow coefficient of diffusion (m^2/s) the turbulence flow coefficient of thermal conductivity, ε_T . The significance of the Prandtl number $Pr < 1$ is that, within the same interval of time, $\Delta\tau$, the diffusion of thermal energy and concentration is faster than the diffusion of momentum by quite a bit, it extends considerably farther, and it has an area of diffusion ξ , which is considerably larger. There is a turbulent transference between the section of flow which has a high temperature and a low velocity and the section of flow which has a low temperature and a high velocity; because of this fact, the overall enthalpy quotient for the section of flow with the high velocity is supplemented from the outside. On a cross section of the jet, the distribution of overall temperature is uneven, and, in places where the flow speed is high, the overall temperature is also high. Let us assume that $\xi_1 = \varepsilon\Delta\tau, \xi_2 = \varepsilon_T\Delta\tau, \xi_3 = D_T\Delta\tau$.

Let us use the new variables $\xi_i = \xi_i(x)$ to replace the duration symbol, τ, in equation (14.2), and let us take z_1, z_2, and z_3 in equation (14.3) to be dependent variables; if we do this, then, it is possible to write three differential equations similar to equation (14.2), as follows,

$$\frac{\partial(\rho u^2)}{\varepsilon\partial\tau} = \frac{\partial(\rho u^2)}{\partial\xi_1} = \frac{\partial^2(\rho u^2)}{\partial y^2} + \frac{1}{y}\frac{\partial(\rho u^2)}{\partial y}, \qquad (14.5)$$

$$\frac{\partial(\rho u c_p\Delta T)}{\varepsilon_T\partial\tau} = \frac{\partial(\rho u c_p\Delta T)}{\partial\xi_2} = \frac{\partial^2(\rho u c_p\Delta T)}{\partial y^2}$$

$$+ \frac{1}{y}\frac{\partial(\rho u c_p\Delta T)}{\partial y}, \qquad (14.6)$$

278

$$\frac{\partial(\rho u \Delta c)}{D_T \partial \tau} = \frac{\partial(\rho u \Delta c)}{\partial \xi_3} = \frac{\partial^2(\rho u \Delta c)}{\partial y^2}$$

$$+ \frac{1}{y}\frac{\partial(\rho u \Delta c)}{\partial y}, \qquad (14.7)$$

ξ_1, ξ_2, ξ_3 respectively represent momentum, thermal energy, and concentration in terms of the dimensions of their respective areas of diffusion. If we make a deduction from the relationship between ϵ, ϵ_T and D_T, then, it is possible for us to acknowledge that $\xi_1 \approx 0.75\ \xi_2 \cong 0.75\ \xi_3 = \xi_1(x) = Kx^2$ (14.8). Equations (14.5), (14.6) and (14.7) can all be deduced to be partial, linear differential equations of the second degree with a parabolic form and using the dependent variable z_i, that is to say that this is a description of the equations for jet diffusion plumes:

$$\frac{\partial z_i}{\partial \xi_i} = \frac{1}{y}\frac{\partial}{\partial y}\left(y\frac{\partial z_i}{\partial y}\right), \quad i = 1, 2, 3. \qquad (14.9)$$

Sec 4   Boundary Conditions for Jet Diffusion Plumes

The I area inside of the flame tip ϕ only contains fuel and gases that have already been burned. When $x = 0, \xi_i = 0, 0 \leqslant y < r_0$,

$$z_i = z_{0i}, \quad \frac{\rho u^2}{\rho_0 u_0^2} = 1, \quad \frac{\rho u c_p (T - T_\phi)}{\rho_0 u_0 c_{p0}(T_0 - T_\phi)} = 1,$$

$$\frac{\rho u(c_1 - c_\phi)}{\rho_0 u_0 (c_0 - c_\phi)} = 1. \qquad (14.10)$$

When

$$\xi = \xi_\phi, \quad y = y_\phi, \quad \frac{\rho u c_p (T - T_\phi)}{\rho_0 u_0 c_{p0}(T - T_\phi)} = 0,$$

$$\frac{\rho u(c_1 - c_\phi)}{\rho_0 u_0 (c_0 - c_\phi)} = 0. \qquad (14.11)$$

In the II area outside of the flame tip ϕ, there is nothing but oxygen and gases which have already been burned. When $\xi_i = 0, r_0 < y \leqslant \infty$, and

$$0 < \xi < \infty, \quad y \to \infty; \quad \frac{\rho u'}{\rho_\phi u_\phi'} \to 0.$$

$$\frac{\rho u c_p (T - T_\infty)}{\rho_\phi u_\phi c_{p\phi}(T_\phi - T_\infty)} \to 0; \quad \frac{\rho u (c_2 - c_\infty)}{\rho_\phi u_\phi (c_\phi - c_\infty)} \to 0; \quad (14.12)$$

When
$$\xi = \xi_\phi, \quad y = y_\phi, \quad \frac{\rho u c_p (T - T_\infty)}{\rho_\phi u_\phi c_{p\phi}(T_\phi - T_\infty)} = 1,$$

$$\frac{\rho u (c_2 - c_\infty)}{\rho_\phi u_c (c_\phi - c_\infty)} = 1; \quad (14.13)$$

Right on the flame tip, $\xi = \xi_\phi$, $y = y_\phi$, $z_2 = z_1 = 0$; let us now assume that the diffusion coefficient for fuel in turbulence flow = D_1, that the turbulence flow diffusion coefficient of oxygen = D_2, and that, along the normal line, n, of the surface $\rightleftharpoons$, the diffusion density flow from the inside toward the outside and from the outside toward the inside are both distributed in precisely the correct way, then,

$$- D_1 \frac{\partial c_1}{\partial n} = Q D_2 \frac{\partial c_2}{\partial n} \quad (14.14)$$

Because of the fact that we are dealing with a symmetrical flow fields, on the axis line,

$$y = 0, \quad \frac{\partial z_i}{\partial y} = 0; \quad (14.15)$$

Sec 5 Solution Methods for Jet Diffusion Plume Equations

If we employ the similar variable method as well as using the "Chuan Id Ye Integration" method as well as the boundary conditions from (14.10) to (14.15), then it is possible to solve the differential equation (14.9) and obtain the functional equation $z_i = a_i + b_i \Psi(\xi, y)$ (a_i, b_i = a constant (14.16). According to Fig 7.3, if one uses the extreme coordinates r and a of a jet line from a point source, then, $x = r \cos a$, $y = r \sin a$, and the function for the equation above is

$$\Psi(\xi, y) = \frac{1}{2 \pi \xi_i} \int_0^r \int_{-\frac{\pi}{2}}^{+\frac{\pi}{2}} \exp\left[- \frac{y^2 + r^2 - 2 y r \sin a}{4 \xi_i}\right] r \, dr \, da$$

$$(14.17)$$

280

At the very tip of the plume

$$\Psi(\xi_{\phi m}, 0) = 1 - \exp\left[-\frac{r_0^2}{4\xi_{\phi m}}\right], \quad (\xi_{\phi m} = KL^2)$$
(14.18)

If the initial flow speed, u_0, from a round aperture jet is evenly distributed along the radius, r_0, then, in the case of equation (14.17), it is possible to consult the "probability error function table," and to utilize the numerical integration method to obtain the solution $\Psi(\xi, y)$.

Let us assume that the isobaric specific heat is c_p, that the rate of thermal conductivity in turbulence flow is k, that the coefficient of diffusion in turbulence flow is $D_1 = D_2 = D_T$ and that all of them are constants; if we assume all these things, then, if we follow the boundary conditions, we can obtain the solution shown below:

$$\frac{\rho u^2}{\rho_0 u_0^2} = \Psi(\xi, y),$$

on the axis line,

$$y = 0, \quad \frac{\rho u_m^2}{\rho_0 u_0^2} = 1 - e^{\frac{-r_0^2}{4\xi_1}};$$
(14.19)

If we are concerned with the I area, then,

$$\left.\begin{array}{l}
\dfrac{T - T_0}{T_\bullet - T_\bullet} = 1 - \left(\dfrac{\rho_0}{\rho}\right)^{\frac{1}{2}} F(\xi_3, y) \\[2mm]
\dfrac{c}{c_\bullet} = \left(\dfrac{\rho_0}{\rho}\right)^{\frac{1}{2}} F(\xi_3, y) \\[2mm]
\left(\dfrac{\rho_0}{\rho}\right)^{\frac{1}{2}} = \dfrac{1}{2}\left\{\left[\left(\dfrac{\rho_0}{\rho_\phi} - 1\right)^2 F^2(\xi_3, y) + 4\left(\dfrac{\rho_0}{\rho_\phi}\right)\right]^{\frac{1}{2}}\right. \\[2mm]
\left. - \left(\dfrac{\rho_0}{\rho_\phi} - 1\right) F(\xi_3, y)\right\} \\[2mm]
F(\xi_3, y) = [\Psi(\xi_1, y)]^{-\frac{1}{2}} \\[2mm]
\qquad \times\left[1 - \dfrac{1 - \Psi(\xi_3, y)}{1 - \Psi(\xi_{4\phi}, y_\phi)}\right]
\end{array}\right\}
$$
(14.20)

If we are concerned with the II area, then,

281

$$\frac{T - T_\infty}{T_\bullet - T_\infty} = \left(\frac{\rho_\bullet}{\rho_\infty}\right)^{\dagger} \cdot F_1(\xi_1, y)$$

$$\frac{c}{c_\infty} = 1 - \left(\frac{\rho_\bullet}{\rho_\infty}\right)^{\dagger} F_1(\xi_1, y)$$

$$\left(\frac{\rho_\bullet}{\rho_\infty}\right)^{\dagger} = \left[\left(1 - \frac{\rho_\bullet}{\rho_\infty}\right)^3 F_1^2(\xi_1, y)\right.$$

$$\left. + 4\left(\frac{\rho_\bullet}{\rho_\infty}\right)\right]^{\dagger} - \left(1 - \frac{\rho_\bullet}{\rho_\infty}\right) F_1(\xi_1, y) \qquad (14.21)$$

$$F_1(\xi_1, y) = \frac{\Psi(\xi_1, y)}{\Psi(\xi_{1\bullet}, y_\bullet)}\left[\frac{\Psi(\xi_{1\bullet}, y_\bullet)}{\Psi(\xi_1, y)}\right]$$

Sec 6   Experimentally Determined Data

If we use a shadowgraph, a sclieren instrument or a laser interference meter in order to take some photos, then, it is possible to photograph the shape of the flame plume turbine gallery; because of this fact, it is possible to measure the coordinates, x_ϕ , y_ϕ , of the surface of the flame tip ϕ .

An analysis of the dimension of the new variable, ξ , should be an area (m^2); because of this fact, the function defining the relationship between ξ and x is $\xi_1(x) = Kx^2$. This K is a constant which is determined by experimentation by the use of the method presented below.

We already know the original kinetic pressure of the jet $\rho_0 u_0^2$, and, if we measure the kinetic pressure, ρu_m^2 , on different cross sections along the axis line, x, then, it is possible to obtain the equation for the relationship of the distribution of the kinetic pressures along the axis line, that is,

$$\frac{\rho u_m^2}{\rho_0 u_0^2} = f\left(\frac{x}{d_0}\right) = f(\bar{x}), \quad \bar{x} = \frac{x}{d_0}; \qquad (14.22)$$

According to the formula (14.9), $y = 0$, $u = u_m$; it is possible to consult the probability function table and figure out ρu_m^2 as it increases with changes in ξ_1 as well as the equation which governs the relationship that controls its attenuation and weakening, that is,

$$\frac{\rho u_m^2}{\rho_0 u_0^2} = F\left(\frac{\sqrt{\xi_1}}{d_0}\right), \quad \xi = \frac{\xi_1}{d_0^2}; \qquad (14.23)$$

From the functions, $f(\bar{x})$ and $F(\sqrt{\xi_1})$, for the attenuation and weakening

282

of the kinetic pressure which can be figured from consulting tables and by the use of empirical measurements, it is possible to draw out the relationship between $\bar{z}$ and $\sqrt{\xi_1}$. We can take $\sqrt{\xi_1}$ and $\bar{x}$ and let them be the vertical and horizontal coordinates and, in this way, draw out the curve for them, as shown in Fig 14.3. A method of the same type makes it possible to solve the relationship between $\sqrt{\xi_1}$ and $\bar{x}$. Because of this fact, it is possible to deduce the fact that $(\xi_1/\xi_1) = Pr$.
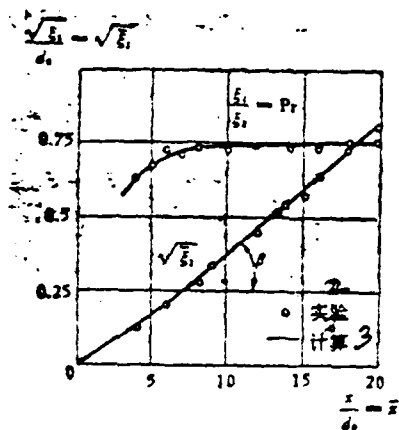

Fig 14.3

The Curve for the Relationship Between $\sqrt{\xi_1}$ and $\bar{x}$ 2. Experiment 3. Calculation

From Fig 14.3, it is possible to see that curve which represents the changes in $\sqrt{\xi_1}$ as it varies with changes in $\bar{x}$ is almost a straight line. The rate of slope of the straight line, $\mathrm{tg}\,\beta$, can be measured out. Because of this fact,

$$\sqrt{\xi_1} = \mathrm{tg}\,\beta\bar{x}, \quad \mathrm{tg}\,\beta \cong 0.04, \quad \text{or,} \quad \xi_1 = \mathrm{tg}^2\beta x^2 = Kx^2 \quad (14.24)$$

Due to this fact, if we determine a precise value for the constant, K, and choose a value of Pr = 0.75, then, from equation (14.8) $\xi_1 = Pr\xi_2 = Pr\xi_3$, and we can determine precise values for ξ_2 and ξ_3. On the basis of the solutions for the equations (14.19), (14.20) and (14.21), it is possible to figure out the distributions for concentration, temperature differential and kinetic pressure along y.

Sec 7 Estimating the Length of Jet Diffusion Plumes

The formula for the mutual diffusion along the interior and exterior normal lines of the surface of the flame tip, as shown in equation (14.14) are also

283

suitable for use on the apex point of the flame plume where $y = 0, \xi_1 = \xi_{\infty} = KL^2$. On the flame tip, the fuel concentration, c_1, and the concentration of contained oxygen, c_2, are both equal to zero, and the turbulence flow diffusion coefficient $D_1 = D_2$. At the apex point of the flame plume, the normal line, n, is nothing else than the direction of the coordinate ξ . Because of this fact, on the basis of equation (14.14)

$$\frac{\partial c_1}{\partial n} = -\Omega \frac{\partial c_2}{\partial n},$$

or

$$-\frac{\partial c_1}{\partial \xi_1} = \Omega \frac{\partial c_2}{\partial \xi_1}, \quad y = 0, \quad \xi_1 = \xi_{\infty}, \quad (14.25)$$

From equation (14.20), we get

$$\frac{c_1}{z_0 c} = \left(\frac{\rho_0}{\rho}\right)^{\frac{1}{2}} F(\xi_1, y),$$

and, from equation (14.21), we get

$$\frac{c_2}{c_{\infty}} = 1 - \left(\frac{\rho_0}{\rho_{\infty}}\right)^{\frac{1}{2}} F_1(\xi_1, y);$$

If we first separately differentiate (c_1/c_0) and (c_2/c_{∞}) in terms of ξ_1 , and then, substitute into equation (14.25), we can obtain

$$\frac{\exp\left(-\frac{r_0^2}{4\xi_{\infty}}\right)}{\left[1 - \exp\left(-\frac{r_0^2}{4\xi_{\infty}}\right)\right]^{\frac{1}{2}}} \cdot \left\{\frac{\exp\left(\frac{-r_0^2}{4\xi_{\infty}}\right) - 1}{\exp\left(-\frac{r_0^2}{4\xi_{\infty}} Pr\right) - 1} - \frac{1}{2Pr^2}\right\}$$

$$= \frac{1}{2c_{\infty}}\left\{\Omega c_0 \left(\frac{\rho_1}{\rho_0}\right)^{\frac{1}{2}}\left(1 + \frac{\rho_0}{\rho_{\infty}}\right)\right\} \quad (14.26)$$

From equation (14.26) it can be seen that the appropriate value for the chemical ratio, Ω , is already fixed, and that the original fuel concentration, c_0, is already fixed, and so it is also true that the length of the diffusion plume L of a jet is determined by the jet nozzle d_0. That is to say,

$$\frac{\sqrt{\xi_{em}}}{r_0} = \frac{2\sqrt{\xi_{em}}}{d_0} = \frac{2\sqrt{KL^3}}{d_0}$$
$$= 2\sqrt{K}\,\frac{L}{d_0} =$$

a constant, d_O is somewhat larger, and
L is somewhat longer.

Fig 1.2 employs the two rings of quite numerous small jet nozzles which are arranged in an interior ring and an exterior ring in the forward section of a double ring cavity, and, although the diameter of these apertures, d_O, is small, their number is large. The object of doing this is to shorten the length of the flame plume, L, and, because of this, to shorten the length of the combustion chamber.

In Fig 14.5(a), (b) and Fig (14.6)(a) and (b) we see a comparison between the data obtained experimentally and the values calculated on the basis of the methods put forward in this chapter for the calculation of the distributions of the temperature ratio and the kinetic pressure ratio for a jet diffusion plume in two different cross sections, $\bar{z}$, along $\bar{y} = \frac{y}{r_0}$. Fig 14.4 is a comparison between the distributions of kinetic pressure ratios along the axial direction as these distributions were obtained on the basis of theoretical calculations and empirical measurements. $u_0 = 40 \sim 70$ [m/s], $c_0 = 0.053 \sim 0.12$ [kg/kg], $T_0 = 1100 \sim 1300$ [K]. The fuel is propane and butane.
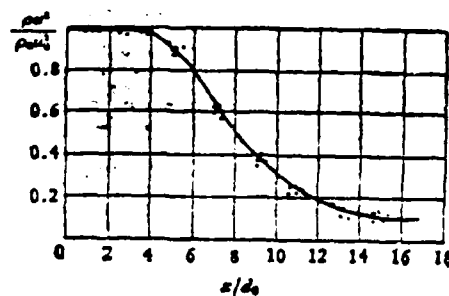

图 14.4 动压比在 x/d_0 分布

Fig 14.4

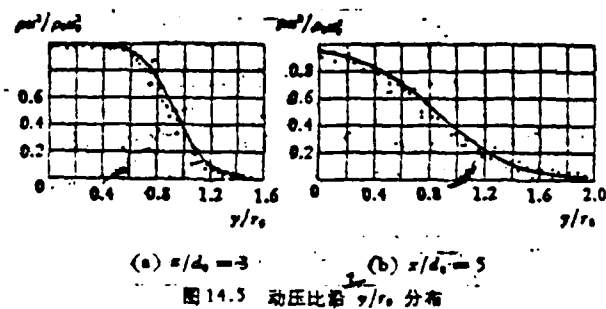1. Distribution of Kinetic Pressure Ratio Along x/d_O

285

(a) $x/d_o = 3$ (b) $x/d_o = 5$

图14.5 动压比沿 y/r_o 分布

Fig 14.5

1. Distribution of Kinetic Pressure Ratio Along y/r_o

(a) $x/d_o = 3$
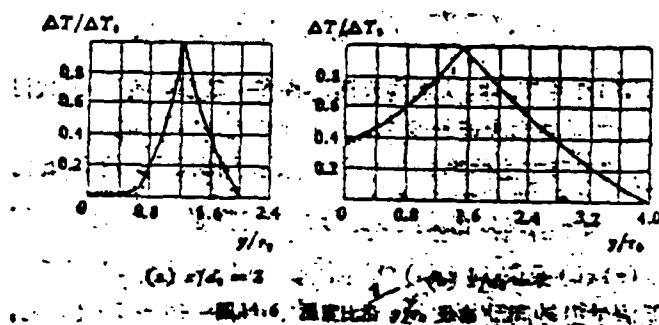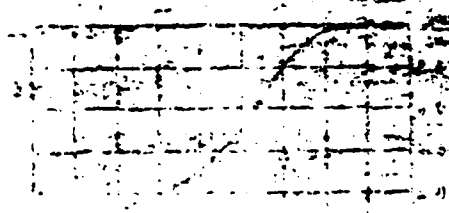
图14.6 温度比沿 y/r_o 分布

Fig 14.6

1. Distribution of the Temperature Ratio Along y/r_o

Chapter 15 Turbulence Diffusion and Combustion

Sec 1 Strength of Turbulence

If one observes the boiler rooms in great storms or the black smoke which comes
out of the smoke stacks on the front of locomotives as that smoke rolls over and
over itself, as it is turned over and drawn into itself without ceasing, then one
can observe that this smoke and dust diffuses in a lateral flow and gradually
thins out to nothing. This is nothing other than the phenomenon of turbulence
flow diffusion. In the flame tubes of combustion chambers, the globules of vapor-
ized fuel, the fuel vapor, the oxygen, the kinetic energy, the thermal energy and
all the rest take on the vortical turbulence and are diffused over a wide area,
increase their speed of mixing and augment the combustion. When the time comes,
then, the velocity field, the concentration field, and the temperature field
all tend toward a uniform distribution. Sec 7 of Chapter 9 talks about how,
because of the influence of viscous friction, vortices can attenuate and change so
that they are split up into turbulence flows. Turbulence flow is nothing else
than an uncertain number of large and small vortical masses of gas which pulsate
and roll over and over each other. It is also possible to say that vortices are
large scale turbulence flows and that turbulence flows are vortices of small
dimensions. At a specific point in space, the vector components of flow speed,
U, V, W , the pressure, p, the concentration, c, the temperature, T, and the
energy, E, all vary irregularly with changes in the time, t. The numerical values
which are measured by contact-type sensors are "average time" flow speed $\bar{U}, \bar{V}, \bar{W}$;
and pressure, $\bar{p}$, and concentration, $\bar{c}$, and temperature, $\bar{T}$, and so on. Adding an
apostrophe to the angles above represents their pulsation values u', v', w', p', c', T' ,
and, given this, then, the instantaneous value = the average time value + the
pulsation value, i.e., $U = \bar{U} + u'$, and other similar cases can be treated in the
same way (15.1).

If we use photoelectric methods or small inertia sensors, then, it is possible
to record instantaneous flow speeds U or pressures, p, in the form of pulsation
wave forms (Fig 15.1). According to the "mean value limit theory" of statistical
physics, if we take the mean value $\bar{U}$ as the basis, then, the chances for the
pulsation value, u', to deviate to the positive or negative direction are equal.
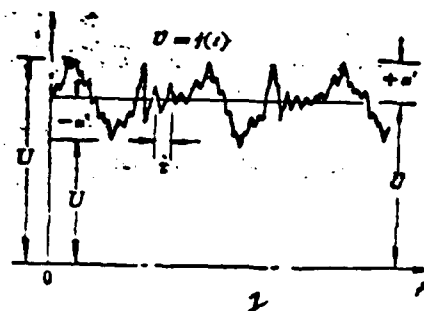Because of this fact, the average statistical instantaneous value for the amount of
pulsation is

287

图15.1 紊流脉动波形

Fig 15.1

1. Turbulence Flow Pulsation Waveform

$$\bar{u}' = \frac{1}{t} \int_0^t u' dt = 0, \quad \bar{c}' = \frac{1}{t} \int_0^t c' dt = 0, \qquad (15.2)$$

and similar cases can be figured in a similar fashion. One can see from Fig 15.1 that the positive and negative areas between the turbulence flow pulsation wave and the horizontal line, $\bar{U}$ cancel each other out. When the area between the pulsation wave and the axis   is eliminated by the time of investigation, t, then, one can obtain an average time flow speed, $\bar{U}$. Let us assume that τ = the period of pulsation; if we can assume that $t \gg \tau$, then,

$$\bar{U} = \frac{1}{t} \int_0^t U dt \qquad (15.3)$$

The "mean square" of the pulsation value $\overline{u'^2}$, the "mean product" $\overline{u'v'}$ and the "mean square" $\bar{u} = \sqrt{\overline{u'^2}}$, can all be figured in similar ways and are all not equal to zero. The ratio of the pulsation flow speed "mean square root" $\bar{u}$ to the average time flow speed $\bar{U}$ is called the "turbulence flow strength", ε. A case in which the turbulence flow strength, ε, is equal along all three coordinate directions is called a "turbulence flow field which has the same nature in differing directions."

$$\varepsilon = \frac{\sqrt{\overline{u'^2}}}{\bar{U}} = \frac{\bar{u}'}{\bar{U}} = \frac{\sqrt{\overline{v'^2}}}{\bar{v}} = \frac{\bar{v}'}{\bar{v}} = \frac{\sqrt{\overline{w'^2}}}{\bar{w}} = \frac{\bar{w}'}{\bar{w}} \% \qquad (15.4)$$

The mean square root of the pulsation flow speed is

$$\bar{u} = \sqrt{\overline{u'^2}} = \left\{ \frac{1}{t} \int_0^t (U - \bar{U})^2 dt \right\}^{\frac{1}{2}} \qquad (15.5)$$

288

The distance, $l = u'\tau$, which is swept out during one period, τ , of pulsaticn in which the turbulence flow air masses tumble over each other and pulsate is called the "turbulence flow scale." However, when one is dealing with a very large number of turbulence air flow masses of sizes ranging from quite large to very small, then, the period of pulsation, τ , or the frequency, f, are not the same; the direction of the pulsations are not the same, and the dimension, l, of the air mass as well as the turbulence flow strength, ι , both attenuate, dissipate and change in response to changes in the space (that is to say, the time) involved. When the frequency of pulsation of large turbulence flow air masses is low, then, the distance which is swept out by each period of pulsation is long. When the frequency of pulsation of small turbulence flow air masses is high, then, the distance which is swept out by each period of pulsation is short. If one is considering the interval between large and small turbulence flow air masses, then, it is possible to see a mutual influence between the two kinds of air mass on the basis of a diffusion transference of momentum, mass and energy. Because of this fact, the behavior of each individual turbulence flow air mass is composed of random changes, and is disorderly and unpredictable; however, it is possible, on the basis of methods involving statistical theory, to measure the "average space" occupied collectively by turbulence flows or the characteristic of "average duration" as is shown in the form of equations (15.4) and (15.5).

The pulsation energy for each unit of mass along the direction, x, for turbulence flow air masses is $E = \frac{1}{2}u'^2$; obviously, there is a relationship between this quantity and the pulsation frequency, f. The chances for the occurrence of the conditions when l is large, f is low, and E is small, or when l is small, f is high, and E is large are very small in both cases. Let us assume that the "probability amplitude" for the distribution of energy in turbulence flow air masses, that is to say, the rate of change of the amount of kinetic energy, E, in a turbulence flow for each unit of mass, as it varies with changes in f, is

$$E(f) = \frac{1}{2}\, d\overline{u'^2}/df$$; if we take f to be the horizontal coordinate, then, it is

possible to draw out the curve defining the probability distribution as shown in Fig 15.2. If one takes a type of sensor in which a piece of $\phi = 5\mu$ pure platinum or tungsten wire is strung across the gap between two sharp rods with a distance of 1mm between them in order to form a "heat sensitive resistor," and this is mated to an electrical bridge in delicate equilibrium, then, this is what is called

a "hot-wire wind speed meter." When the gas flow involved in pulsation is perpendic-
ular to the heat sensitive resistor when it passes over it, the electrical resistance
varies as a function of the cooling from the pulsation flow speed, u'. With an
oscilliscope, it is possible to record the type of pulsation *flow speed waveforms*
which appear in Fig 15.1. A frequency spectrum analyzer can take non-periodic
pulsation waves, $u' = f(t)$, and, according to the Chaun Li-ye integration trans-
form method, form a frequency spectrum (Fig 15.3). Fig 15.2 is a representation of
the "envelope" of the frequency spectra of Fig 15.3. From these envelope lines it
is very easy to determine the following: the frequency during pulsation, $\bar{f}$,
of most turbulence flow air masses which are of a representative type, The turbu-
lence flow scale, l , between frequencies, which corresponds to this interval, is
equal to or corresponds to the wavelength involved; because of this fact, the
interstical turbulence flow scale x the interstical frequency = the average time flow
speed, that is, $\bar{l}\bar{f} = \bar{U}$ [cm/s] (15.6). If, by measurement, we obtain $\bar{U}$
and $\bar{f}$, then, it is possible to deduce the interval turbulence flow scale l .
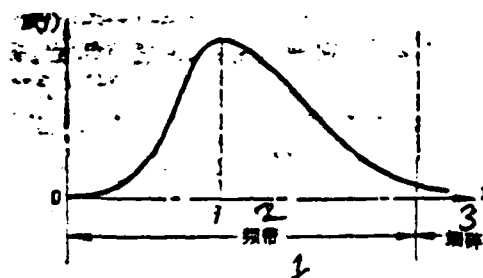The root mean square of the pulsation flow speed, $\bar{u}'$, times the interstical or

图15.2 表流能量概率分形曲线

Fig 15.2

1. Turbulence Flow Energy Probability Distribution Curve   2.   Frequency Band
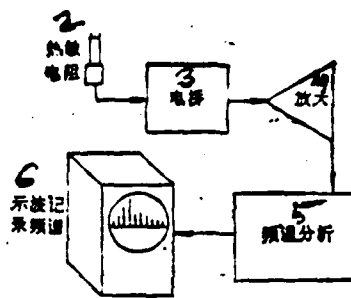3. Broken Static

图15.3 频谱分析方块示意

Fig 15.3

1. A Block Diagram of a Spectrum Analyser 2. Heat Sensitive Resistor 3. Electric
Bridge 4. Amplifier 5. Frequency Spectrum Analyser 6. Oscilloscope
Recording Frequency Spectrum

290

interval turbulence scale = turbulence diffusion coefficient $D_T = \bar{u}l$ [cm²/s]. (15.7).

Sec 3 Mixture Distances

Prandtl theory recognizes the fact that the cross-flow displacements of turbulence flow air masses have a fixed mixing distance, 1, and that this gives rise to the root mean square of pulsation flow speed, $\hat{u}$ in the direction of parallel flow as well as the root mean square of the pulsation temperature, $\hat{T}$, and so on. In the process of this displacement, these turbulence flow gas masses approximately maintain their original characteristics. According to theory, the values of the mean roots of turbulence flow pulsation, $\hat{u}, \hat{T}$, and so on, for the new positions is the differential between the average time coefficients for the new and the old positions (Fig 15.4). Let us assume that the old position was - point A and that the new position is at point B; if the turbulence flow gas masses move from A to B, then, the root mean square of the pulsation flow speed is

$$\hat{u} \cong l\frac{d\overline{U}}{dy} = \overline{U}_\mathrm{B} - \overline{U}_\mathrm{A} \qquad (15.8)$$

The root mean square of pulsation temperature is

$$\hat{T} \cong l\,\frac{d\overline{T}}{dy} = \overline{T}_\mathrm{B} - \overline{T}_\mathrm{A} \qquad (15.9)$$
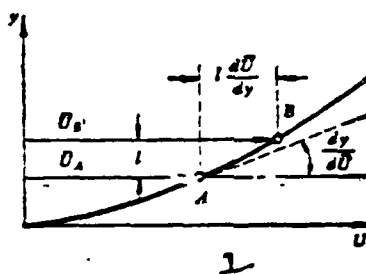

图15.4 渗混距离示意图

Fig 15.4

1. Illustration of Mixing Distance

Because of the fact that the processes involved in the turbulence flow transference of momentum and thermal energy, one can consider the mixing distances involved

291

to be the same. The methods for measuring precise values for the mixing distance, 1, and the interval or interstical turbulence flow scale, $\bar{1}$, are different and their definitions are different; however, both represent the scale of the size involved in the turbulence flow. In order to solve for 1, it is necessary first to measure the distributions of the average time flow speed and the temperature.

Sec 4   Turbulence Stress

When one is washing clothes with soap, why is it necessary to scrub them: Or, if one is using a brush, why is it necessary to brush repeatedly? Without question, it is because these methods make possible the use of the friction involved in going back and forth in order to take dirty clothes and scrub them out. The tumbling over each other and the pulsation of large and small turbulence flow gas masses is a form of scrubbing by friction. It is possible tc deduce from this the fact that, in turbulence flow fields, the frictional forces which are exerted on the surface of the pulsating masses of gas, also called "turbulence stress", τ_τ , is much larger than the viscosity stress or force which is exerted against the surface of the smoothly sliding masses of gas in a laminar flow field; these stresses τ or forces are also called "shear forces or stresses." Because of the fact that the pulsation of turbulence flows is erratic, confused and unpredictable, it is not possible to draw out the type of undisturbed flow lines which one can draw in a laminar flow field. It is only possible to have a direction of flow and flow lines which are decided on the basis of average time values and their statistical averages. On the basis of the mean square, $\overline{u'^2}$, and the mean product $\overline{u'v'}$, and so on, it is also possible to say that there are "quasi-stable state" or average time turbulence flow fields.

The average value of the product = the product of the average values; the average values of the average values are still = the average value and do not change. For example, the average time density flow = the mean product $\overline{\rho U}$ of the instantaneous density flow and the flow speed. However, the average time pulsation values $\overline{u'}, \overline{\rho'}, \overline{v'}\ldots$ are all equal to zero. Because of this fact, $\overline{\rho u'} = \rho \overline{u'}$, are all equal to zero.

292

$$\overline{\rho U} = \overline{(\bar{\rho} + \rho')(\bar{U} + u')} = \overline{\bar{\rho}\bar{U}} + \overline{\bar{\rho}u'} + \overline{\rho'\bar{U}}$$
$$+ \overline{\rho'u'} = \bar{\rho}\bar{U} + \overline{\rho'u'}$$
$$\overline{\rho V} = \overline{(\bar{\rho} + \rho')(\bar{V} + v')} = \overline{\bar{\rho}\bar{V}} + \overline{\bar{\rho}v'} + \overline{\rho'\bar{V}}$$
$$+ \overline{\rho'v'} = \bar{\rho}\bar{V} + \overline{\rho'v'} \qquad (15.10)$$

On the basis of the same principles,

$$\overline{\rho U^2} = \overline{(\bar{\rho} + \rho')(\bar{U} + u')^2}$$
$$= \overline{(\bar{\rho} + \rho')(\bar{U}^2 + 2\bar{U}u' + u'^2)}$$
$$= \overline{\rho\bar{U}\bar{U}} + \overline{(\rho u)'u'}$$
$$\overline{\rho U V} = \overline{(\bar{\rho} + \rho')(\bar{U} + u')(\bar{V} + v')}$$
$$= \overline{(\bar{\rho} + \rho')(\bar{U}\bar{V} + \bar{U}v' + u'\bar{V} + u'v')}$$
$$= \overline{\rho\bar{V}\bar{U}} + \overline{(\rho v)'u'} \qquad (15.11)$$
$$\rho = \bar{\rho} + \rho', \quad \tau_{xy} = \bar{\tau}_{xy} + \tau'_{xy},$$
$$\overline{\rho'} = 0, \quad \overline{\tau'_{xy}} = 0$$

On the basis of the principle of the conservation of momentum and mass as well as
equations (15.10) and (15.11) it is possible to write continuity equations and
momentum equations of "average time turbulence flow fields"; however, it is
necessary to include the topic of the "influence of turbulence flow pulsation", for
example, $\overline{\rho'u'}$, $\overline{(\rho v)'u'}$, and so on. Fig 15.5 shows a separating out of the differenti-
ated control body $dxdy \cdot 1$, from the two-dimensional stable compressible viscous
flow field; it assumes that there is a dimension = 1 perpendicular to the surface
of the illustration. (a) represents the changes which occur when the density flow
enters and leaves the control body; (b) represents the pressure and shear stresses
which are exerted on the control body along x; (c) represents the changes which
occur in the momentum flow rate when it enters and leaves the control body along
x. The differential between the amounts of flow that enter and leave the control
bodies in stable flow fields = 0; because of this fact, we can obtain the
continuity equation

$$\frac{\partial}{\partial x}(\rho U) + \frac{\partial}{\partial y}(\rho V) = 0 \qquad (15.12)$$

If we take equation (15.10) and substitute into equation (15.12), then, it
is possible to obtain the average time stable state continuity equation

$$\frac{\partial(\overline{\rho U})}{\partial x} + \frac{\partial(\overline{\rho V})}{\partial y} = \frac{\partial(\overline{\rho}\overline{U})}{\partial x} + \frac{\partial(\overline{\rho}\overline{V})}{\partial y}$$

$$+ \frac{\partial(\overline{\rho' u'})}{\partial x} + \frac{\partial(\overline{\rho' v'})}{\partial y} = 0 \qquad (15.13)$$

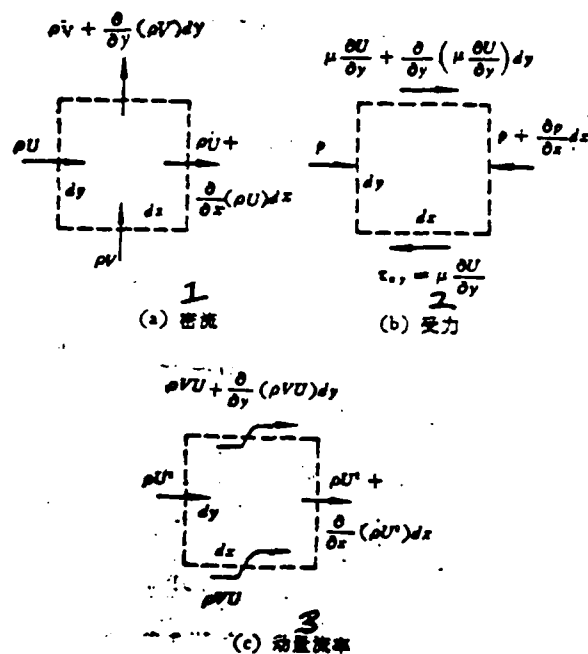(a) 密流　　　　　　　(b) 受力

(c) 动量流率
图 15.5

Fig 15.5

1. Density Flow　2. Forces Exerted　3. Momentum Flow Rate

When the two first quantities in equation (15.13) added together = 0, this represents the continuity equation for the stable state of an "undisturbed flow pulsation." When the partial differentials of the turbulence flow density flow for the last two quantities, $\overline{\rho' u'}$ and $\overline{\rho' v'}$, added together, make zero, this represents the average time continuity equation of a "pulsation in a flow which does have turbulence."

If we ignore gravity, stable flow fields, then, can be assumed to be so set up that the surface forces which are exerted on control bodies in the direction, x, (Fig 15.5(b)) = the rate of change of momentum entering and leaving (Fig 15.5(c)). The momentum equations are

$$-\frac{\partial p}{\partial x} + \frac{\partial}{\partial y}\left(\mu\,\frac{\partial U}{\partial y}\right) = \frac{\partial}{\partial x}(\rho UU) + \frac{\partial}{\partial y}(\rho UV),$$

$$\tau_{xy} = \mu\,\frac{\partial U}{\partial y}; \qquad (15.14)$$

If we take equation (15.11) and substitute it into equation (15.14), then, it is possible to obtain the momentum equation of an "average time turbulence flow field", that is,

$$\frac{\partial}{\partial x}\left[\overline{\rho U U} + \overline{(\rho u)'u'}\right] + \frac{\partial}{\partial y}\left[\overline{\rho V U} + \overline{(\rho v)'u'}\right]$$

$$= -\frac{\partial \overline{p}}{\partial x} + \frac{\partial \overline{\tau}_{xy}}{\partial y}$$

$$\overline{U}\frac{\partial}{\partial x}(\overline{\rho U}) + \overline{\rho U}\frac{\partial \overline{U}}{\partial x} + \frac{\partial}{\partial x}\overline{(\rho u)'u'} + \overline{U}\frac{\partial}{\partial y}(\overline{\rho V})$$

$$+ \overline{\rho V}\frac{\partial \overline{U}}{\partial y} + \frac{\partial}{\partial y}\overline{(\rho v)'u'} = -\frac{\partial \overline{p}}{\partial x} + \frac{\partial \overline{\tau}_{xy}}{\partial y}$$

If we employ equation (15.12), then it is possible to remove from the equation above

$$\overline{U}\left[\frac{\partial}{\partial x}\overline{(\rho U)} + \frac{\partial}{\partial y}\overline{(\rho V)}\right]$$

If these two quantities are eliminated, then, it follows that

$$\overline{\rho U}\frac{\partial \overline{U}}{\partial x} + \overline{\rho V}\frac{\partial \overline{U}}{\partial y} = -\frac{\partial \overline{p}}{\partial x} + \frac{\partial \overline{\tau}_{xy}}{\partial y}$$

$$-\frac{\partial}{\partial x}\overline{(\rho u)'u'} - \frac{\partial}{\partial y}\overline{(\rho v)'u'} \qquad (15.15)$$

In equation (15.15)

$$\frac{\partial \overline{\tau}_{xy}}{\partial y} = \frac{\partial}{\partial y}\left(\mu\frac{\partial \overline{U}}{\partial y}\right)$$

This is the viscous shear force, $\overline{\tau}_{xy}$, as a gradient of change along the direction y; μ — laminar flow viscosity.

$$-\overline{(\rho u)'u'} \quad \text{and} \quad -\overline{(\rho v)'u'}$$

These two quantities both have units of "average time pulsation momentum flow rates" which are similar to those for the friction stresses produced by turbulence flows, (N/m^2) and those of the average time viscous shear forces, $\overline{\tau}_{xy}$; these are simply called "turbulence flow stresses or forces", $\overline{\tau}_T$. If one is considering "turbulence flow forces", according to their functional directions, they can be divided into the positive stresses or forces which are perpendicular to the surface, $(\sigma_{xy})_T$, and the tangential or shear forces which hug the surface, $(\overline{\tau}_{xy})_T$. According to

the Newtonian formula for viscous shear forces, the turbulence flow positive force is

$$(\sigma_{xx})_T = \mu_T \frac{\partial \bar{U}}{\partial x} = -\overline{(\rho u)' u'}$$

and the turbulence flow shear force is   (15.16)

$$(\bar{\tau}_{xy})_T = \mu_T \frac{\partial \bar{U}}{\partial y} = -\overline{(\rho v)' u'}$$

μ_T is called the "turbulence flow viscosity;" the unit is (kg/s.m). $\mu_T/\rho = \nu_T$, is called the turbulence flow kinetic viscosity, and the unit for it is (m²/s). If we compare equations (15.14) and (15.15), then, it is possible to see that, if one only considers the average time values and ignores the pulsation values, then, the momentum equations for stable laminar flow and average time turbulence flow are completely similar. Equation (15.16) represents the forces which are exerted on the surface of the turbulence flow masses of gas due to abrasion from friction. On an actual material surface, the quantities $-\overline{(\rho u)' u'} \ldots$, and so on, represent "rate of momentum exchange" for the pulsation in a turbulence flow; because of this fact, μ_T is actually the "coefficient of momentum exchange". If the Reynolds number, Re, is quite high, then, the turbulence flow stress $(\bar{\tau}_{xy})_T$ will be larger than the viscosity shear force, $\bar{\tau}_{xy}$, by quite a few times. Because of this fact, if one is considering the average time turbulence flow field, then, it is possible to ignore, $\bar{\tau}_{xy}$. For example, let us assume that the root mean square of the amount of pulsation is $\bar{\rho} = 0.1\rho$, $\bar{v} = \bar{u} = 0.1\bar{U}$, and that D = the diameter of the round tube. If we make these assumptions, then, the turbulence flow shear force or stress is $(\bar{\tau}_{xy})_T = -\overline{(\rho v)' u'} = 0.1\rho \times 0.1\bar{U} \times 0.1\bar{U} = 10^{-3}\rho\bar{U}^2$. Working with similar assumptions, the viscosity shear force or stress is

$$\bar{\tau}_{xy} = \mu \frac{\partial \bar{U}}{\partial y} \cong \mu \frac{\bar{U}}{D}; \quad \rho\nu = \mu;$$

$$\frac{(\bar{\tau}_{xy})_T}{\bar{\tau}_{xy}} = \frac{10^{-3}\rho\bar{U}^2 \cdot D}{\mu\bar{U}} = 10^{-3} \frac{\bar{U}D}{\nu} = 10^{-3}Re,$$

If $\frac{\partial \bar{U}}{\partial y}$ is the same, then, $\frac{\mu_T}{\mu} = 10^{-3}Re$.

If the Reynolds number Re $\geq 10^5$, then, $(\bar{\tau}_{xy})_T \geq 100\bar{\tau}_{xy}$, or $\mu_T \geq 100\mu$.

295a

The turbulence flow shear force represents the level of violence of the continuous mixing of masses of gas. Because of this feet, the turbulence flow has a speed of propagation which more than or equal to 100 times that of combustion flames in combustion in laminar flows.

Sec 5 Turbulence Heat Transfer

If one is dealing with viscous laminar flow with flow lines which come from a flow field which obeys stable principles, then, as far as cutting across the flow lines is concerned, one can only rely on the transfer of heat by the diffusion of molecular motion. If we are only considering the heat flow along one direction, then, according to equation (4.2), the laminar flow stable heat flow is

$$q = -\lambda \frac{\partial T}{\partial y} = -\rho V c_p T \quad [\text{kcal}/\text{m}^2 \cdot \text{s}] \quad (15.17)$$

The unit which is used to measure the coefficient of thermal conductivity, λ, is (kcal/m.s.K); the density flow is $\rho = [\text{kg}/\text{m}^3]$, the isobaric specific heat is $c_p = [\text{kcal}/\text{kg} \cdot \text{K}]$; the "coefficient of temperature conductivity" is $a = \lambda/\rho c_p = [\text{m}^2/\text{s}]$, because of these facts, equation (15.17) can be written in the form of $VT = a \frac{\partial T}{\partial y}$.

In turbulence flow fields, there are no regular flow lines. In the interval between large and small pulsating masses of gas, there are temperature gradients; if one is involved with the transfer of heat by diffusion in turbulence flows, then, one should use the average time coefficient $\overline{VT}$, that is to say, the average time turbulence flow heat flow, which is

$$q = -k \frac{\partial \overline{T}}{\partial y} = -\rho \bar{c}_p \overline{VT} \quad [\text{kcal}/\text{m}^2 \cdot \text{s}] \quad (15.18)$$

According to equation (15.10), $\overline{VT} = \overline{(\bar{V} + v')(\bar{T} + T')} = (\bar{V}\bar{T} + \bar{V}\overline{T'} + \overline{v'}\bar{T} + \overline{v'T'})$, as presented in Sec 1 of this chapter, the average time values $\overline{v'}$ and $\overline{T'}$ which pertain to the amount of pulsation, are both equal to zero. Let us assume that $T = \bar{T}$, on the basis of this assumption, equation (15.18) becomes

$$q = -\rho \bar{c}_p \overline{\bar{V}\bar{T}} - \rho \bar{c}_p \overline{v'T'} = q + \bar{q}$$
$$= -\lambda \frac{\partial \bar{T}}{\partial y} - k \frac{\partial \bar{T}}{\partial y} \quad (15.19)$$

Equation (15.19) explains that fact that heat flow of turbulence flow fields

296

includes two quantities; the first of these is a quantity which corresponds to the stable heat transfer of molecular diffusion in equation (15.17); the second of these quantities is the average time transfer of heat from pulsating masses of gas. What has been presented up to now explains that fact that the viscosity of turbulence flow is 100 times or more larger than the viscosity of laminar flow. Because of the fact that the processes involved in the diffusion of heat and the diffusion of momentum are similar, it is also true that it is only required that Re be greater than or equal to 10^5, and the turbulence flow coefficient of thermal conductivity, k, will also be larger than the λ of laminar flow by 100 times or more; because of this, it is possible to ignore, λ , and only use the value of turbulence flow heat transfer

$$\bar{q} = - k \frac{\partial \bar{T}}{\partial y} = - \bar{\rho}\bar{c}_p \overline{v'T'} = - \Gamma_\lambda \frac{\partial i}{\partial y} \quad [\text{kcal/m}^2 \cdot \text{s}]$$

$$(15.20)$$

The turbulence flow coefficient of thermal conductivity is

$$a_T = \frac{k}{\bar{\rho}\bar{c}_p} \quad [\text{m}^2/\text{s}], \quad \overline{v'T'} = a_T \frac{\partial \bar{T}}{\partial y} \quad (15.21)$$

$\rho_a_T = \Gamma_\lambda$ (is called the thermal diffusion coefficient of turbulence flow. The ratio between the levels of diffusion of momentum and thermal energy in pulsating masses of gas is a basic standard of non-dimensional similarity Pr (the Prandtl number). The Pr of a turbulence flow field = the kinetic viscosity/the coefficient of thermal conductivity $= \frac{\nu_T}{a_T} = \frac{\mu_T}{\bar{\rho}a_T} = \frac{\mu_T}{\Gamma_\lambda} = 0.7 \sim 1.0 \quad (15.22)$

If the ratio between the viscosity of turbulence flow and the viscosity of laminar flow, (μ_T/μ) and the ratio between the coefficients of thermal conductivity, (a_T/a) , are the same, then, the Prandtl numbers, Pr, for the turbulence flow and the laminar flow will be the same, and it becomes possible to use the Pr value of the laminar flow for everything.

Sec 6 Turbulence Concentration Diffusion

In the combining of gases which takes place in combustion chambers, the "partial pressure, Pj, for the type of gas j is also appropriate for use with the

297

equation of state of "perfect gases." Because of the fact that $\Sigma p_i = p_1 + p_2 + \cdots = P$, it also follows that $p_i = c_i RT$, $R = 1.985$ [kcal/mol·K] (15.23). c_j = the concentration of the jth type of gas. The molar concentration of the mixed gases = c [mol·m³]. The total density of the mixed gases = ρ [kg/m³]. The ratio between the overall density of the mixed gases and the jth type gas (for example, vaporized fuel, f, or oxygen, O_2) is $(\rho_i/\rho) = m_i$, and this is called the relative concentration. Obviously, $\Sigma m_i = m_1 + m_2 + \cdots = 1$.

Let us assume that the differentiated control body, $dV_s = dx\,dy\,dz$; if we assume this, then, the mean product, J_j, of the concentration and density flow of the jth type of gas is equal to the differential between $-\overline{\rho v' m_j'}$ as it enters and leaves dV_S; this in turn is equal to the rate of change of the concentration of the jth type of gas within dV_S.

According to equation (4.3), if one is only considering the concentration density flow of the jth type gas along the direction, y, then,

$$(J_i)_y = f = -\overline{\rho v' m_i'} = -D_T \frac{\partial \bar{c}_i}{\partial y}$$

$$= -\Gamma_i \frac{\partial m_i}{\partial y} \quad [\text{kg/m}^2 \cdot s] \quad (15.24)$$

If the Reynolds number, Re $\geq 10^5$, then, the coefficient of turbulence flow diffusion, D_T, is several hundred times larger than the D for laminar flow. The ratio between the kinetic viscosity of turbulence flow, ν_T, and D_T is called the special concentration number, Sc.

Sc = ν_T/D_T = the level of diffusion of momentum of turbulence flow/the level of diffusion of mass of turbulence flow = $\frac{\mu_T}{\rho D_T} = \frac{\mu_T}{\Gamma_i}$ (15.25)

Yet another "basic standard of similarity" is called the Liu Wei-si number, Le, that is, $Le = (a_T/D_T) = (Sc/Pr)$ (15.26). The coefficient of concentration diffusion of turbulence flow for the jth type of gas is $\Gamma_i = \rho_i D_T$ [kg/m·s] (15.27)

The turbulence flow viscosity, μ_T, the rate of thermal conductance of turbulence flow, k, and the coefficient of turbulence flow diffusion, D_t, are related to the normal equation of state for turbulence flow; they are not physical properties of a gas, and are difficult to calculate theoretically. The process of determining them by experimentation is also relatively complicated and difficult.

298

Because of the fact of the similarity of the natures of the processes of diffusion transference of momentum, mass and heat in turbulence flows, it is only necessary that $Re \geqslant 10^5$, and the ratio between the three coefficients of turbulence and laminar flow, (μ_T/μ), (k/λ) & (D_T/D) are all values with just about the same multiples. When there is a paucity of reliable experimental data, it is possible to borrow the use of the basic standards of similarity with laminar flow, Pr, Sc and Le.

The coefficient of diffusion, D, for different gases in stable, laminar flow is different. D varies with changes in the temperature, that is,

$$\frac{D}{D_0} = \left(\frac{T}{T_0}\right)^{1.75} \quad \cdots \quad (15.28)$$

At standard temperature and pressure, that is $T_0 = 273\,K$, $p_0 = 760\,mm$, the values of D_0 for different gases can be seen in Table 15.1 and Table 15.2. In Table 15.2, ϕ is the unifying value against which are represented Pr, Sc and Le, as they vary with changes in temperature, that is,

$$\phi = \phi_0 \frac{K + T_0}{K + T}\left(\frac{T}{T_0}\right)^{2.5}.$$

表15.1　不同气体扩散系数

气体 (0℃)	D_0 [cm²/s]
氢 H₂	0.611
水汽 H₂O	0.216
氧 O₂	0.178
二氧化碳 (20℃) CO₂	0.160
甲烷 CH₄	0.196
乙烷 C₂H₆	0.108
丙烷 C₃H₈	0.088
丁烷 C₄H₁₀	0.075
戊烷 C₅H₁₂	0.067
一氧化碳 CO	0.185

Table 15.1

1. The diffusion Coefficients of Different Gases 2. Gas 3. Hydrogen 4. Water Vapor 5. Oxygen 6. Carbon Monoxide 7. Mehtyl Hydride or Methane 8. Ethane 9. Propane 10. Butane 11. Pentane 12. Carbon Monoxide

表 15.2 不同气体"相似准则"

气体 (0°C)	$Pr = \dfrac{\nu}{a}$	$Sc = \dfrac{\nu}{D}$	$Le = \dfrac{Sc}{Pr}$	公式φ中常数K
空气	0.71	—	—	115
氧	0.72	0.747	1.04	138
氮	0.705	—	—	107
一氧化碳	0.74	0.72	0.98	102
氢	0.69	0.218	0.31	83(74)
水 汽	0.72	0.62	0.866	670(650)
二氧化碳	0.75	0.95	1.22	225
甲 烷	0.734	0.74	1.01	198

Table 15.2

1. The "Basic Principles or Standards of Similitude" Between Different Gases
2. Gas 3. Air 4. Oxygen 5. Nitrogen 6. Carbon Monoxide 7. Hydrogen
8. Water Vapor 9. Carbon Dioxide 10. Methyl Hydride or Methane 11. The
Constant, K, in the Formula, ϕ

Sec 7 Turbulence Field Continuities and Momentum Equations

If we base our explanation on the three analytical equations presented
previously, i.e., (15.13), (15.15) and (15.19) as well as (15.24), then, as far as
turbulence flow fields are concerned it is possible, on the basis of a comparison
with stable laminar flow fields, to make use of the average time density flow, $\overline{\rho v'}$
the average time momentum flow rate, $\overline{(\rho v)'u'}$, the average time flow of heat,

$-\rho \tilde{c}_p \overline{v'T'}$ as well as the average time concentration density flow of the
jth type of gas, $-\overline{\rho' v' c_i'}$, and write quasi-stable state, average time continuity
equations, momentum equations, thermal transference equations and concentration
diffusion equations. Because of the fact that the turbulence flow viscosity, μ_T,
the turbulence flow rate of thermal conductance, k, and the turbulence flow
diffusion coefficient, D_T, are all several hundred times larger than the correspond-
ing numerical values for stable laminar flow fields, i.e., μ, λ , and D, when one is
figuring the distributions of the turbulence flow field average time velocities

$\overline{U}, \overline{V}, \overline{W}$, the average time concentration, $\tilde{c}_i$, as well as the distribution
for the average time temperature, $\overline{T}$ for this type of flow field, then it is
possible to ignore the viscosity, μ , the rate of thermal conductivity, λ ,

300

and the coefficient of diffusion, D, as they pertain to molecular motion in a stable laminar flow.

In the three previous sections, consideration was given only to changes in momentum and density flow in one coordinate direction. When one is analysing the turbulence flow fields or ring-shaped combustion chambers or fields of this type inside flame tubes, it is best to use a cylindrical coordinate system in r, θ, and z. If one states at the outset that he is dealing with a quasi-stable state average time turbulence flow field, then, it is not necessary to add the average time symbol ($^-$) again to each of the individual parameters after the general announcement has been made. The three component vectors of the velocity vector, $\mathbf{V}$, are the radial component, u, the circumferential component, v, and the axial component, w. If we assume that we are dealing with a rotational turbulence flow field which is axisymmetric, then, it follows that the various parameters, such as ρ, v and T, are invariable in the circumferential direction, $r\theta$.

(1) Continuity Equations.

From a turbulence flow field, let us separate out a differentiated fan-shaped control body, $dV, = r d\theta dr dz$, as is shown in Fig 15.6. On the basis of the principle of the conservation of mass, the differential in the rate of flow of mass into and out of the control body = the rate of change of mass inside the control body. If the flow out is greater than the flow of mass in, then, the rate of change of mass inside the control body is negative. The differential in the rate of flow of mass in the three directions, r, $r\theta$, and z (ignoring the fourth degree differential $dr dr d\theta dz$) are as follows: the radial direction, r, is

$$\left[\rho u + \frac{\partial(\rho u)}{\partial r} dr\right](r + dr)d\theta dz - \rho u r d\theta dz$$

$$= \frac{\partial(\rho u)}{\partial r} dr r d\theta dz + \frac{(\rho u)}{r} r d\theta dr dz$$

the circumferential direction, $r\theta_i$, (axisymmetric) is $\rho v - \rho v = 0$, and the axial direction is

$$\left[\rho w + \frac{\partial(\rho w)}{\partial z} dz\right]r d\theta dr - (\rho w)r d\theta dr$$

$$= \frac{\partial(\rho w)}{\partial z} r d\theta dr dz$$

The total differential in the rate of flow of mass for all three directions = the rate of change of mass inside the control body, which is,

301

$$-\frac{\partial \rho}{\partial t}\, rd\theta dr dz$$

$$\frac{\partial(\rho u)}{\partial r}\, rd\theta dr dz + \frac{(\rho u)}{r}\, rd\theta dr dz$$

$$+\frac{\partial(\rho w)}{\partial z}\, rd\theta dr dz = -\frac{\partial \rho}{\partial t}\, rd\theta dr dz$$
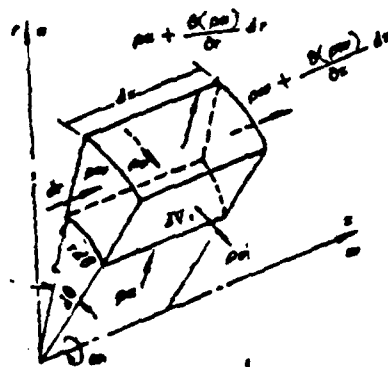

图15.6 微元扇形控制体 dV_s

Fig 15.6

1. Differentiated Fan-shaped Control Body, dV_s

If we eliminate $dV_s = rd\theta dr dz$, then, we can obtain

$$\left[\frac{\partial(\rho u)}{\partial r} + \frac{(\rho u)}{r}\right] + \frac{\partial(\rho w)}{\partial z} + \frac{\partial \rho}{\partial t} = 0 \quad (15.29)$$

The first two quantities in equation (15.29) are capable of being merged into

$$\frac{1}{r}\frac{\partial}{\partial r}(r\rho u) = \frac{1}{r}\left[r\frac{\partial(\rho u)}{\partial r} + (\rho u)\right].$$

Because of this feet, if the quasi-stable state average time turbulence flow field is what one is dealing with, and the average time density, ρ, does not vary with changes in time, and $\partial\rho/\partial t = 0$; then, it follows that the continuity equation is

$$\frac{1}{r}\frac{\partial}{\partial r}(r\rho u) + \frac{\partial}{\partial z}(\rho w) = 0 \qquad (15.30)$$

302

(2) Equation of Momentum.

Let us assume that we are still using the differentiated control body $dV_s = r d\theta dr dz$. If we ignore gravity, then, according to the second of Newton's Laws, the rate of change of momentum coming into and leaving the control body = the total of the forces exerted against the surface of the control body. Because of this fact, if one is dealing with an axisymmetrical flow field, then, it follows that it is possible to slice out a meridian surface, $dr \cdot dz$, as well as a horizontal cross section, $r d\theta \cdot dr$, and separately apply the laws mentioned above to each case. Fig 15.7 draws out the momentum flow rate (a) going into and coming out of the control body, dV_s, along the axis, z, as well as the forces exerted against the surface (b). The left and right end areas of $dV_s = r d\theta dr$; the bottom area = $r d\theta dz$; and the top area = $(r + dr) d\theta dz$. We will ignore the fourth degree differential, $dr dr d\theta dz$. The rate of change of momentum is equal to the total surface force, that is,

$$\frac{\partial(\rho w^2)}{\partial z} dV_s + \frac{\partial}{\partial r}(\rho u w) dV_s + \frac{\rho u w}{r} dV_s$$

$$= -\frac{\partial p}{\partial z} dV_s + \frac{\partial \tau_{rz}}{\partial r} dV_s + \frac{\tau_{rz}}{r} dV_s + \frac{\partial \sigma_{zz}}{\partial z} dV_s .$$

If we eliminate dV_s from each quantity, then, we can obtain

$$\frac{\partial}{\partial z}(\rho w w) + \frac{\partial}{\partial r}(\rho u w) + \frac{(\rho u w)}{r}$$

$$= -\frac{\partial p}{\partial z} + \left[\frac{\partial \tau_{rz}}{\partial r} + \frac{\tau_{rz}}{r}\right] + \frac{\partial \sigma_{zz}}{\partial z}$$

$$= -\frac{\partial p}{\partial z} + \frac{1}{r}\frac{\partial}{\partial r}(r \tau_{rz}) + \frac{\partial \sigma_{zz}}{\partial z} . \quad (15.31)$$
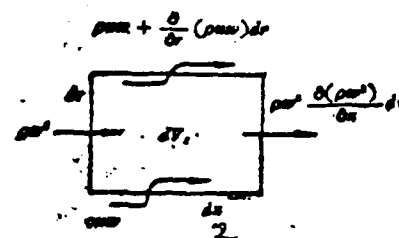
If we take the two quantities on the left side of the equal sign in equation (15.31) and, on the basis of the two function products $(\rho w)w$ 及 $(\rho u)w$, solve the differential expansion, then, we can obtain

$$w \frac{\partial(\rho w)}{\partial z} + (\rho w)\frac{\partial w}{\partial z} + w \frac{\partial(\rho u)}{\partial r} + (\rho u)\frac{\partial w}{\partial r}$$
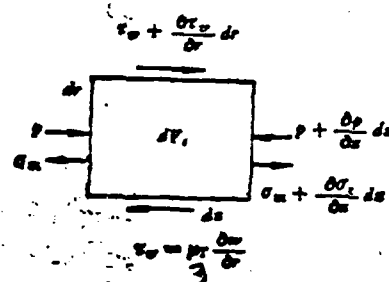
303

$$+ w \frac{(\rho u)}{r} = \left[w \frac{\partial(\rho w)}{\partial z} + w \frac{1}{r} \frac{\partial}{\partial r} (r \rho u) \right]$$
$$+ (\rho w) \frac{\partial w}{\partial z} + (\rho u) \frac{\partial w}{\partial r},$$

According to equation (15.30), the quantity inside the square parentheses in this equation = 0; it follows from this that equation (15.31) can become the axial momentum equation

$$\rho \left[w \frac{\partial w}{\partial z} + u \frac{\partial w}{\partial r} \right] = - \frac{\partial p}{\partial z}$$
$$+ \frac{1}{r} \frac{\partial}{\partial r} (r \tau_{zr}) + \frac{\partial \sigma_{zz}}{\partial z} \ [kg/m^3], \quad (15.32)$$

(a) 动量流率

(b) 表面受力

图15.7 轴向力平衡 (dV_s 子午面投影)

Fig 15.7

1. Axial Force Equilibrium (dV_s meridian plane projection) 2. Momentum Flow Rate 3. Forces Exerted on the surfaces

Fig 15.8 draws out the end plane and meridian planes of dV_s. (a) clearly points out, along the radial direction, r, the momentum flow rate into and out of the control body; (b) highlights the set up of the forces which are exerted on the surface along the radial direction, r; and, (c) divides up the circumferential positive forces, $\sigma_{\theta\theta}$, along r. If we figure that any forces added along the

coordinate axis have a positive sign, then, the division of the forces along r on the two side surfaces is

$$-2\sigma_{\theta\theta}\sin\frac{d\theta}{2}\cdot dr\,dz \approx -\sigma_{\theta\theta}d\theta\,dr\,dz$$

$$= -\frac{\sigma_{\theta\theta}}{r}r\,d\theta\,dr\,dz = -\frac{\sigma_{\theta\theta}}{r}dV_s;$$

The rate of change of momentum is equal to the total surface forces, that is,

$$\frac{\partial(\rho uu)}{\partial r}dV_s + \frac{(\rho uu)}{r}dV_s + \frac{\partial(\rho wu)}{\partial z}dV_s - \rho\frac{v^2}{r}d^{\cdot}$$

$$= -\frac{\partial p}{\partial r}dV_s + \frac{\partial\sigma_{rr}}{\partial r}dV_s + \frac{\sigma_{rr}}{r}dV_s$$

$$+ \frac{\partial\tau_{rz}}{\partial z}dV_s - \frac{\sigma_{\theta\theta}}{r}dV_s;$$

If we eliminate dV_s, then we obtain

$$\frac{\partial(\rho w)u}{\partial z} + \frac{\partial(\rho u)u}{\partial r} + (\rho u)\frac{u}{r} - \rho\frac{v^2}{r}$$

$$= -\frac{\partial p}{\partial r} + \left[\frac{\partial\sigma_{rr}}{\partial r} + \frac{\sigma_{rr}}{r}\right] + \frac{\partial\tau_{rz}}{\partial z} - \frac{\sigma_{\theta\theta}}{r}; \quad [N/m^3]$$

$$(15.33)$$

If we take the left side of equation (15.33) and, according to the product of two differentiated functions, make the expansion as follows, then,

$$(\rho w)\frac{\partial u}{\partial z} + u\frac{\partial(\rho w)}{\partial z} + (\rho u)\frac{\partial u}{\partial r} + u\frac{\partial(\rho u)}{\partial r}$$

$$+ (\rho u)\frac{u}{r} - \rho\frac{v^2}{r} = u\left[\frac{\partial(\rho w)}{\partial z} + \frac{\partial(\rho u)}{\partial r} + \frac{(\rho u)}{r}\right]$$

$$+ \rho\left[w\frac{\partial u}{\partial z} + u\frac{\partial u}{\partial r}\right] - \rho\frac{v^2}{r} = u\left[\frac{\partial(\rho w)}{\partial z}\right.$$

$$\left. + \frac{1}{r}\frac{\partial}{\partial r}(r\rho u)\right] + \rho\left[w\frac{\partial u}{\partial z} + u\frac{\partial u}{\partial r} - \frac{v^2}{r}\right],$$

If we employ the continuity equation (15.30), then, the quantity inside the square parentheses in the first quantity of this equation = 0; the momentum equation in the radial direction is

305

$$\rho\left[w\frac{\partial u}{\partial z} + u\frac{\partial u}{\partial r} - \frac{v^2}{r}\right] = \frac{\partial \tau_{rz}}{\partial z} + \frac{1}{r}\frac{\partial}{\partial r}(r\sigma_{rr})$$

$$- \frac{\sigma_{\theta\theta}}{r} - \frac{\partial p}{\partial r} \quad [N/m^3], \qquad (15.34)$$

When one is working out the force equilibrium equation for the horizontal cross section, $rd\theta dr$, along the circumferential direction, $r\theta$, in the differentiated control body, $dV_r = rd\theta drdz$, one should be careful to consider the fact there is an angular velocity, ω, as well as a rate of angular deformation (1/s), in the vortical core of rotational jets. Along the radius, r, the rate of angular deformation between any two given points should be solved for by taking ω to be the basis and then solving for the corresponding rate of angular deformation (Fig 15.9); the radial component of velocity, u, does not vary with changes in θ it follows from this that $\frac{\partial u}{r\partial \theta} = 0$.

$$\left(\frac{\partial v}{\partial r} - \omega\right) = \left(\frac{\partial v}{\partial r} - \frac{v}{r}\right), \ [1/s] \qquad \text{corresponds to the rate of angular momentum,}$$

it follows from this that the turbulence shear force or stress in the circumferential direction inside the surface, $rd\theta dz$ of the cylinder which is perpendicular to the radius, r, is

$$\tau_{\theta r} = \mu_T\left(\frac{\partial v}{\partial r} - \frac{v}{r}\right) = \mu_T r \frac{\partial}{\partial r}\left(\frac{v}{r}\right), \ [N/m^2] \quad (15.35)$$
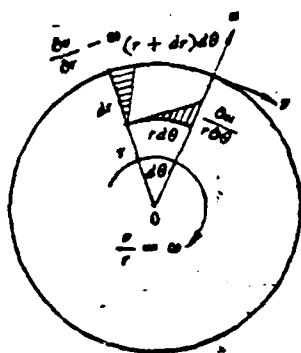

图15.9 相对角变密率

Fig 15.9

1. Rate of Deformation of Related Angles

Fig 15.10 draws out the rate of change of momentum along the circumferential direction, $r\theta$, as it enters and leaves $dV_r = rd\theta drdz$; this is (a); besides this, it also draws out the setup of the forces exerted on the six faces along $r\theta$; this is (b). If one is considering the case of axisymmetrical flow fields, then, along $r\theta$ the direction $\frac{\partial}{r\partial\theta} = 0$, that is to say, $\rho(uv), \rho(vv), \rho(wv), \sigma_{\theta\theta}$ 及 $\tau_{r\theta}$ are

306

all invariable along the circumference, $r\theta$. Because of this fact, when one is considering the case of rotational flow fields, if there is a tangential velocity, v, then, at the same time, there is a radial velocity, u; due to this fact, perpendicular to the radius, r, there is produced a Ke Shi acceleration, uv/r, and there is a Ke Shi force $(\rho uv/\ r)[N/m^3]$. In Fig 15.10(b), dV_s has two end surfaces on which there are turbulence flow shear forces, $\tau_{r\theta}$. Because of the fact that, in a case in which dV_s is in a condition of equilibrium, if one takes a given edge as the axis and solves for the total moment of force, it should be equal to zero. Due to this fact, $\tau_{r\theta} = \tau_{\theta r}$. The shear or tangential forces, $\tau_{r\theta}$, which is exerted against the two end faces of dV_s have a component of force along the direction $r\theta$ which is

$$\tau'_{r\theta} = \tau_{r\theta} \sin\frac{d\theta}{2}, \quad 2\tau'_{r\theta} = 2\tau_{r\theta}\sin\frac{d\theta}{2} \simeq \tau_{r\theta}d\theta \quad (15.36)$$

The rate of change of momentum is equal to the total surface force, that is,

$$\frac{\partial}{\partial r}(\rho uv)dV_s + \frac{\rho uv}{r}dV_s + \frac{\partial}{\partial z}(\rho wv)dV_s$$
$$+ \rho\frac{uv}{r}dV_s = \frac{\partial}{\partial z}\tau_{\theta z}dV_s + \frac{\partial}{\partial r}\tau_{\theta r}dV$$
$$+ \frac{\tau_{\theta r}}{r}dV_s + \frac{\tau_{\theta r}}{r}rd\theta dr dz,$$

If we eliminate dV_s, then, we can obtain

$$\frac{\partial}{\partial z}(\rho w)v + \left[\frac{\partial}{\partial r}(\rho u)v + \frac{(\rho u)v}{r}\right] + \rho\frac{uv}{r}$$
$$= \frac{\partial\tau_{\theta z}}{\partial z} + \left[\frac{\partial\tau_{\theta r}}{\partial r} + 2\frac{\tau_{\theta r}}{r}\right] \quad (15.37)$$
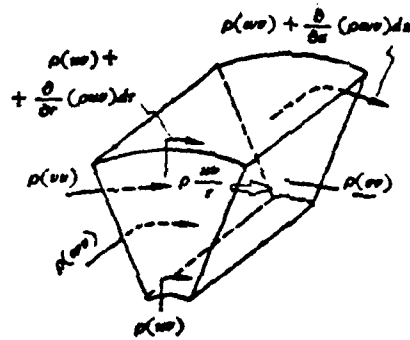
If we solve for the differential on the basis of the two function product, $(\rho w)v$; then, if we take equation (15.37) and expand the left and right side of it, we can get

$$v\left[\frac{\partial(\rho w)}{\partial z} + \frac{1}{r}\frac{\partial}{\partial r}(r\rho u)\right] + \rho\left(u\frac{\partial v}{\partial r} + w\frac{\partial v}{\partial z}\right)$$
$$+ \rho\frac{uv}{r} = \frac{\partial\tau_{\theta z}}{\partial z} + \frac{1}{r^2}\frac{\partial}{\partial r}(r^2\tau_{\theta r}), \quad (15.38)$$
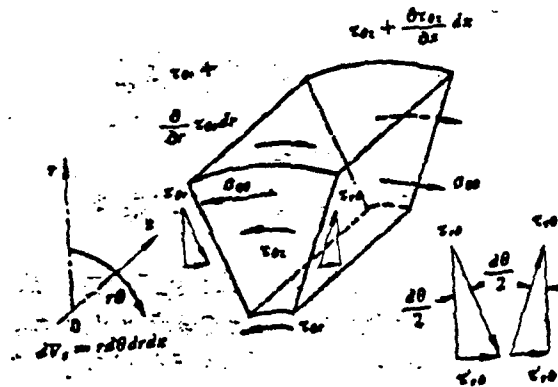
According to the continuity equation (15.30), the quantity in the square parentheses in the first quantity on the left side of equation (15.38) = 0. If we take the right side of equation (15.38) and make a differential expansion, we then obtain the last two quantities on the right side of equation (15.37), that is,

307

$$\frac{1}{r^2}\frac{\partial}{\partial r}(r^2\tau_{\theta r}) = \frac{1}{r^2}\left[r^2\frac{\partial\tau_{\theta r}}{\partial r} + 2r\tau_{\theta r}\right]$$

$$= \left[\frac{\partial\tau_{\theta r}}{\partial r} + \frac{2\tau_{\theta r}}{r}\right].$$

(a) 动量变化率

(b) 表面受力

Fig 15.10

Force Equilibrium of dV_s, Circumferential Direction $\vec{r\theta}$ 2.   Rate of Change of Momentum 3.   Surface Forces

The equation of circumferential momentum is

$$\rho\left(u\frac{\partial v}{\partial r} + w\frac{\partial v}{\partial z} + \frac{uv}{r}\right) = \frac{\partial\tau_{\theta z}}{\partial z} + \frac{1}{r^2}\frac{\partial}{\partial r}(r^2\tau_{\theta r}).$$

$$(15.39)$$

The six faces of the fan-shaped, differentiated control body, dV_s, has exerted against it normal turbulence flow stresses from three directions, that is, $\tau_{rr}, \sigma_{\theta\theta}$ and σ_{ss} ; these faces also have exerted against them turbulence flow shear forces from six directions; these are $\tau_{r\theta}, \tau_{\theta r}; \overline{\tau_{\theta s}, \tau_{s\theta}}; \tau_{sr}, \tau_{rs}$. Because of these facts, when one is dealing with a situation in which there is stable equilibrium, the turbulence flow shear forces exerted against neighboring sets of faces of dVs are equal to each other in the appropriate pairs, that is to say, $\tau_{r\theta} = \tau_{\theta r}$, $\tau_{\theta s} = \tau_{s\theta}, \tau_{sr} = \tau_{rs}$. It follows from this that, if we speak in terms of numerical quantities, then, there are only six types of different turbulence flow shear forces. On each plane of the three coordinate planes in a cylindrical coordinate system, there are three shear forces exerted, and it is possible to combine these into one vector. Three shear force vectors combine to form a "shear force tensor" II; we can make a comparison between the matrix form and the mean products of the pulsation values by writing out the following:

$$
\Pi = \begin{Bmatrix} \sigma_{rr} & \tau_{r\theta} & \tau_{rs} \\ \tau_{\theta r} & \sigma_{\theta\theta} & \tau_{\theta s} \\ \tau_{sr} & \tau_{s\theta} & \sigma_{ss} \end{Bmatrix} = \begin{Bmatrix} -\overline{(\rho u)'u'} & -\overline{(\rho u)'v'} & -\overline{(\rho u)'w'} \\ -\overline{(\rho v)'u'} & -\overline{(\rho v)'v'} & -\overline{(\rho v)'w'} \\ -\overline{(\rho w)'u'} & -\overline{(\rho w)'v'} & -\overline{(\rho w)'w'} \end{Bmatrix}
$$

$$(15.40)$$

The matrix is set out in a framework which presents, in a reasonable order, the array of numbers involved. When the number of items in the horizontal and vertical rows of the matrix are equal, then, the matrix is called a "square matrix." When one is dealing with a case in which the top right and lower left positions on each diagonal have corresponding values which are equal, as is found in the square matrix II of turbulence flow shear forces from equation (15.40), i.e., $\tau_{r\theta} = \tau_{\theta r}, \tau_{\theta s} = \tau_{s\theta}, \tau_{rs} = \tau_{sr}$; then, this is called a "symmetrical square matrix." If we were to take the rows and columns of the matrix of equation (15.40) and exchange them with each other, this would be called a "transposition matrix." The values in a "transposition matrix" are still equal to the original values of the "symmetrical matrix.

Fig 15.11 represents the set up of the distribution of the rate of linear deformation and the rate of angular deformation which are caused by the normal and shear or tangential forces of turbulence flow, σ_T and τ_T , which are exerted on the three cross sections of the differentiated control body, dV_s. According

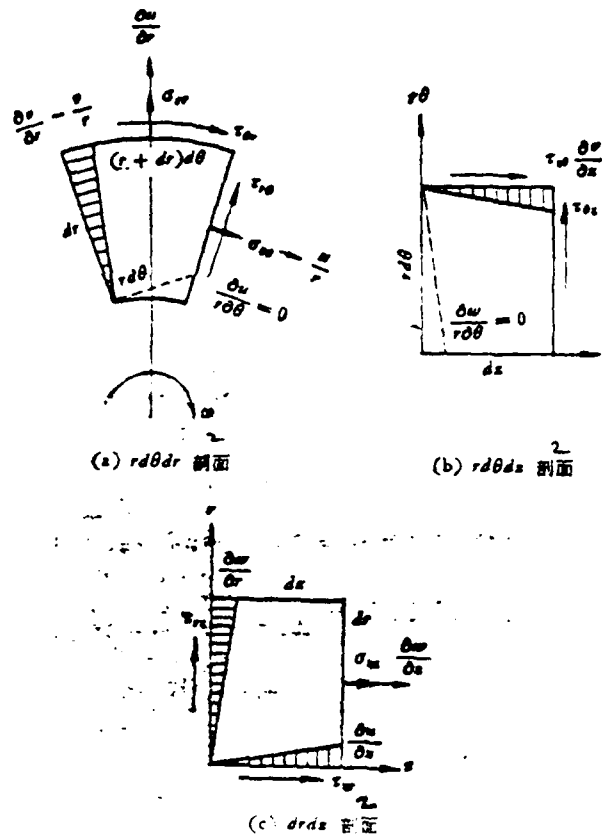(a) $rd\theta dr$ 剖面　　　　　(b) $rd\theta dz$ 剖面

(c) $drdz$ 剖面

图 15.11　dV，三剖面变形事分析

Fig 15.11

1. Distribution of Rate of Deformation of the Three Cross Sections of dV_s　2. Cross Section

to equation (15.16), the normal shear force of turbulence flow, σ_{τ}, = the turbulence flow viscosity, μ_{τ}, x the rate of linear deformation along the normal line direction; moreover, the shear force of turbulence flow, τ_{τ}, = the turbulence flow viscosity, μ_{τ}, x the rate of angular deformation of the edge. The linear deformation or strain, ε, = the distance of lengthening or shortening which results from the pull or pressure exerted along a certain selected section is eliminated by the length of the original line segment; the rate of linear deformation is $\dfrac{\partial \varepsilon}{\partial t}$ = the amount of the increase (or reduction in flow speed along the given line segment/the length of the given line segment. For example (see Chapter 5, Sec 2), the rate of linear deformation along r $= \dfrac{\Delta u}{\Delta r} = \dfrac{\partial u}{\partial r} = \dfrac{\partial \varepsilon}{\partial t}$, and the

310

turbulence flow normal force $\sigma_{rr} = 2\mu_T \left(\frac{\partial u}{\partial r}\right)$, the rate of linear deformation along

$$r\theta = \frac{(r + dr)d\theta - rd\theta}{rd\theta \cdot dt} = \frac{dr}{rdt} = \frac{u}{r};$$; the turbulence

flow normal stress $\sigma_{\theta\theta} = 2\mu_T\left(\frac{u}{r}\right)$; the rate of linear deformation along z

$= \frac{dz}{dz} = \frac{\partial w}{\partial z}$, and the turbulence flow normal stress $\sigma_{zz} = 2\mu_T\left(\frac{\partial w}{\partial z}\right)$. Because $\left.\begin{array}{c}\\ \\ \\ \\ \\ \\ \end{array}\right\}$ (15.41)

of these facts, if one is considering the case of an axisymmetric flow field, then, the edge $rd\theta$ has no rate of angular deformation, that is to say,

$$\frac{\partial u}{r\partial\theta} = \frac{\partial v}{r\partial\theta} = \frac{\partial w}{r\partial\theta} = 0;$$

It follows from this that u, v, and w are invariable along the circumferential direction $r\theta$. Because of this fact, the rate of deformation of related angles within the cross section $rd\theta dr$ $\left(\frac{\partial v}{\partial r} - \frac{v}{r}\right)$; the turbulence flow shear force $\tau_{\theta r} = \tau_{r\theta} = \mu_T r \frac{\partial}{\partial r}\left(\frac{v}{r}\right)$; the rate of deformation of related angles within the cross section $rd\theta dz = \partial v / \partial z$; the turbulence flow shear force $\tau_{\theta z} = \tau_{z\theta} = \mu_T \frac{\partial v}{\partial z}$; $\left.\begin{array}{c}\\ \\ \\ \\ \\ \end{array}\right\}$ (15.42)

the rate of deformation of related angles within the cross section $drdz$ $\frac{\partial w}{\partial r} + \frac{\partial u}{\partial z}$

and, the turbulence flow shear force $\tau_{rz} = \tau_{zr} = \mu_T\left(\frac{\partial w}{\partial r} + \frac{\partial u}{\partial z}\right)$.

The turbulence flow force matrix Π is a symmetrical square matrix. If we make a connection between it and equation (15.41) and equation (15.42), then, it is possible to form them into the matrix equations which follow

$$\Pi = \left\{\begin{array}{ccc} \sigma_{rr} & \tau_{r\theta} & \tau_{rz} \\ \tau_{\theta r} & \sigma_{\theta\theta} & \tau_{\theta z} \\ \tau_{zr} & \tau_{z\theta} & \sigma_{zz} \end{array}\right\} = \mu_T \left\{\begin{array}{ccc} \frac{\partial u}{\partial r} & r\frac{\partial}{\partial r}\left(\frac{v}{r}\right) & \frac{\partial w}{\partial r} \\ 0 & \frac{u}{r} & 0 \\ \frac{\partial u}{\partial z} & \frac{\partial v}{\partial z} & \frac{\partial w}{\partial z} \end{array}\right\}$$

311

$$+ \mu_T \left\{ \begin{matrix} \dfrac{\partial u}{\partial r} & 0 & \dfrac{\partial u}{\partial z} \\[2mm] \dfrac{\partial}{\partial r}\left(\dfrac{v}{r}\right) & \dfrac{u}{r} & \dfrac{\partial v}{\partial z} \\[2mm] \dfrac{\partial w}{\partial r} & 0 & \dfrac{\partial w}{\partial z} \end{matrix} \right\} - \left\{ \begin{matrix} p & 0 & 0 \\ 0 & p & 0 \\ 0 & 0 & p \end{matrix} \right\}$$

$$- \frac{2}{3}\mu_T \left\{ \begin{matrix} \nabla V & 0 & 0 \\ 0 & \nabla V & 0 \\ 0 & 0 & \nabla V \end{matrix} \right\} \qquad (15.43)$$

According to the various elements in corresponding positions in the matrices on the two sides of the equal sign in equation (15.43), it is possible to write out a turbulence flow force formula for each quantity, for example,

$$\sigma_{zz} = 2\mu_T \frac{\partial w}{\partial z} - p - \frac{2}{3}\mu_T \nabla V = -\overline{(\rho w)' w'},$$

$$\tau_{r\theta} = \mu_T r \frac{\partial}{\partial r}\left(\frac{v}{r}\right) = -\overline{(\rho u)' v'}, \quad \text{etc.}$$

Sec 9 Axially Symmetrical Turbulence Heat Transfer Equations

Equation (15.19) only represents the turbulence flow heat transfer density flow in the coordinate direction y. On the basis of this, it is possible to write out the turbulence flow heat transfer density flows for the three coordinate directions as follows: in the radial direction, r,

$$q_r = -\overline{\rho u' c_p T'} = -\overline{\rho u' i'} = -\Gamma_h \frac{\partial i}{\partial r} \quad [\text{kcal}/\text{m}^2 \cdot s]$$

$$(15.44)$$

in the circumferential direction $r\theta$, $q_\theta = 0$; this is due to the fact that the field in question is axisymmetrical. In the axial direction, z, we find

$$q_z = -\overline{\rho w' c_p T'} = -\overline{\rho w' i'} = -\Gamma_h \frac{\partial i}{\partial z} \quad [\text{kcal}/\text{m}^2 \cdot s]$$

$$(15.45)$$

Fig 15.12 draws out the changes in the turbulence flow heat transfer density flow within the meridian plane $dV_l = r d\theta dr dz$ of $dr dz$.
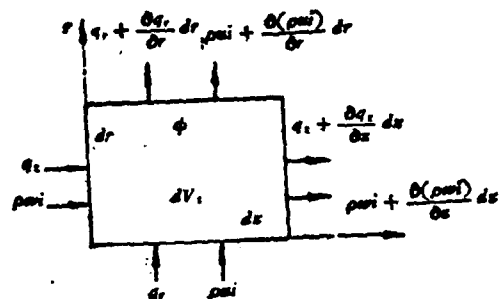
312

Fig. 15.12 Changes in the Turbulence flow
Heat Transfer Density

According to the conservation of energy, the rate of change of the flow of heat into and out of the control body is equal to the rate of change of the heat transfer density flow $(q_r + q_z)$ of the surface of the control body plus the loss function Φ (that is to say the rate of the production of heat by surface friction). According to these basic principles, we can set out the equation

$$\left[\frac{\partial(\rho u i)}{\partial r}\,dr + (\rho u i)\right](r + dr)d\theta dz - (\rho u i)r d\theta dz$$

$$+ \left[\frac{\partial(\rho w i)}{\partial z}\,dz + (\rho w i)\right]r d\theta dr - (\rho w i)r d\theta dr$$

$$= -\left[q_r + \frac{\partial q_r}{\partial r}\,dr\right](r + dr)d\theta dz + q_r r d\theta dz$$

$$- \left[q_z + \frac{\partial q_z}{\partial z}\,dz\right]r d\theta dr + q_z r d\theta dr + \phi dV,$$

$$\frac{\partial(\rho u i)}{\partial r} + \frac{(\rho u i)}{r} + \frac{\partial(\rho w i)}{\partial z} = -\left(\frac{\partial q_r}{\partial r} + \frac{q_r}{r}\right)$$

$$-\frac{\partial q_z}{\partial z} + \phi \quad [\text{kcal}/\text{m}^3\cdot\text{s}] \qquad (15.46)$$

On the basis of the two functions $(\rho u)i$ and $(\rho w)i$, if we solve for the partial derivative and then take the left side of equation (15.46) and expand it, we can obtain

$$i\,\frac{\partial(\rho u)}{\partial r} + i\,\frac{(\rho u)}{r} + i\,\frac{\partial(\rho w)}{\partial z} + \rho u\,\frac{\partial i}{\partial r}$$

$$+ \rho w\,\frac{\partial i}{\partial z} = -\frac{\partial q_z}{\partial z} - \frac{1}{r}\,\frac{\partial}{\partial r}\,(r q_r) + \phi$$

The first three quantities on the left side of the equation above can become

$$i\left[\frac{1}{r}\,\frac{\partial}{\partial r}\,(\rho r u) + \frac{\partial(\rho w)}{\partial z}\right] = 0$$

(See equation 15.30).

$$\rho\left[u\,\frac{\partial i}{\partial r} + w\,\frac{\partial i}{\partial z}\right] = -\frac{\partial q_z}{\partial z}$$

$$- \frac{1}{r}\,\frac{\partial}{\partial r}\,(r q_r) + \phi, \quad [\text{kcal}/\text{m}^3\cdot\text{s}] \qquad (15.47)$$

Heat is produced by the pulling and pushing pressure on the normal lines along the

313

surface, that is to say, the normal stress multiples the rate of linear deformation

$$\sigma_{rr} \frac{\partial u}{\partial r} \quad [\text{N} \cdot \text{m}/\text{m}^3 \cdot \text{s}];$$

The tangent lines along the surface out across each other and produce heat, which is to say that the tangential stresses multiply the rate of angular deformation

$$\tau_{r\theta} \frac{\partial \tau}{\partial z} \quad [\text{N} \cdot \text{m}/\text{m}^3 \cdot \text{s}].$$

The loss function ϕ = the overall rate of heat production caused by the rubbing of friction in turbulence flow as it occurs on the surface of the control body, that is,

$$\phi = \sigma_{rr} \frac{\partial u}{\partial r} + \sigma_{\theta\theta} \frac{u}{r} + \sigma_{zz} \frac{\partial w}{\partial z} + \tau_{r\theta} \left(\frac{\partial \tau}{\partial r} - \frac{\tau}{r} \right)$$
$$+ \tau_{\theta z} \left(\frac{\partial \tau}{\partial z} \right) + \tau_{zr} \left(\frac{\partial w}{\partial r} + \frac{\partial u}{\partial z} \right), \quad (15.48)$$

Sec 10 Axially Symmetrical Concentration Diffusion Equations

Let us generalize the use of equation (15.24) in axisymmetrical turbulence flow fields. If we are considering the density flow of the concentration of the jth type of gas, then, in the radial direction, r,

$$(J_i)_r = - \overline{\rho u' m_i'} = -D_T \frac{\partial \bar{c}_i}{\partial r} = -\Gamma_i \frac{\partial m_i}{\partial r}, \quad [\text{kg}/\text{m}^2 \cdot \text{s}]$$
$$(15.49)$$

in the circumferential direction, $r\theta$, $(J_i)_{r\theta} = 0$, and, because of the fact that $\bar{c}_i$ is invariable along $r\theta$, $(\partial \bar{c}_i / r \partial \theta) = 0$; along the axial direction, z,

$$(J_i)_z = - \overline{\rho w' m_i'} = -D_T \frac{\partial \bar{c}_i}{\partial z}$$
$$= -\Gamma_i \frac{\partial m_i}{\partial z} \quad [\text{kg}/\text{m}^2 \cdot \text{s}], \quad (15.50)$$

According to the conservation of mass, the differential between the concentration

314

of the jth type of gas as it enters and leaves dV_s ought to be equal to the rate of change of the density flow of concentration on the surface of dV_s+ the rate of formation of the jth type of gas within dV_s, R_j. According to this principle, if we take a look at Fig 15.12, then, it is possible to set out the concentration diffusion equation for the jth type of gas, that is,

$$\left[\frac{\partial(\rho u m_i)}{\partial r} dr + (\rho u m_i)\right](r + dr)d\theta dz - (\rho u m_i)r d\theta dz$$

$$+ \left[\frac{\partial(\rho w m_i)}{\partial z} dz + (\rho w m_i)\right]r d\theta dr - (\rho w m_i)r d\theta dr$$

$$= -\left[\frac{\partial(J_i)_r}{\partial r} dr + (J_i)_r\right](r + dr)d\theta dz$$

$$+ (J_i)_r r d\theta dz - \left[\frac{\partial(J_i)_z}{\partial z} dz + (J_i)_z\right]r d\theta dr$$

$$+ (J_i)_z r d\theta dr + R_j dV, \frac{\partial(\rho u m_i)}{\partial r} + \frac{(\rho u m_i)}{r}$$

$$+ \frac{\partial(\rho w m_i)}{\partial z} = -\left[\frac{\partial(J_i)_r}{\partial r} + \frac{(J_i)_r}{r}\right]$$

$$- \frac{\partial(J_i)_z}{\partial z} + R_i \qquad (15.51)$$

And, continuing in this vein, if we expand the left side of equation (15.51) on the basis of the previous solution by using the partial derivative of the products $(\rho u)m_j$ and $(\rho w)m_j$ then, we can obtain

$$m_i\left[\frac{\partial(\rho u)}{\partial r} + \frac{\rho u}{r} + \frac{\partial(\rho w)}{\partial z}\right] + \rho\left[u\frac{\partial m_i}{\partial r} + w\frac{\partial m_i}{\partial z}\right]$$

$$= -\frac{\partial(J_i)_z}{\partial z} - \frac{1}{r}\frac{\partial}{\partial r}[r(J_i)_r] + R_i$$

According to (15.30), the three quantities in the equation above

$$\left[\frac{\partial(\rho u)}{\partial r} + \frac{(\rho u)}{r} + \frac{\partial(\rho w)}{\partial z}\right]$$

$$= \left[\frac{1}{r}\frac{\partial}{\partial r}(r\rho u) + \frac{\partial(\rho w)}{\partial z}\right] = 0,$$

Because of this fact, it is also true that

$$\rho\left[u\frac{\partial m_i}{\partial r} + w\frac{\partial m_i}{\partial z}\right] = -\frac{\partial(J_i)_z}{\partial z}$$

$$- \frac{1}{r}\frac{\partial}{\partial r}[r(J_i)_r] + R_i \quad [kg/m^3 \cdot s] \qquad (15.52)$$

315

In flame tubes, right in the combustion area, it is possible for there to be n type of gases coexisting at the same time. According to the preceding Sec 6, it is necessary to symbolize this as

$$\sum_i \dot{m}_i = \dot{m}_1 + \dot{m}_2 + \dot{m}_3 + \cdots = \dot{V}$$

$$j = 1, 2, 3, \cdots n$$

Combustion areas are different; the pressure and concentrations of dV_s are different; because of these facts, there are n types of gas concentration diffusions and n equations with a form similar to that of equation (15.52). Fuel and gases which have not yet been burned react with substances and and undergo a chemical reaction to become products of already burned fuel and gases. If we pick the concentration, $\bar{c}_i$, of a certain reacting substance to be the basis (for example c_{CH_4}), then, the rate of dissolution and reduction of concentration is nothing else than the rate of the chemical reaction, that is, the rate of the dissolution and reduction of the amount of CH_4 or, in other words,

$$R_j = -\frac{d(\bar{c}_{CH_4})}{dt}.$$

Or, the rate of the formation of CO_2 is

$$R_i = \frac{d(\bar{c}_{CO_2})}{dt}. \qquad (15.53)$$

Sec 11 Combustion Reaction Rate W

In the previous section, the rate of loss of reacting substances or the rate of formation of the products of reaction, $R_i [kg/m^3 \cdot s]$, is nothing else than the rate of combustion reaction, W, which represents the speed of burning. In the main combustion area, fuel is continuously supplied and vaporized and then mixed with air to form "unburned fuel and gases or unburned fuel and air mixture." It is only necessary for the ratio of composition or blending, s, to be appropriate in the mixture of unburned fuel and air in terms of the content of oxygen concentration (c_{ox}) and the concentration of fuel (c_f), and for the environmental temperature, T, and pressure, p, to be adequately high, as well as for the flow

316

speed, V, to be not too fast, and then, the atoms of oxygen and the molecules of fuel can violently collide, breaking up the molecular structure of the fuel and forming into a new molecule with the attendant production of heat in the quantity, Q.

Kerosene is a mixture of several types of compounds of carbon and hydrogen. This mixture must first be vaporized to form a hydro-carbon compound in a gaseous state, such as, CH_4, C_3H_6, and so on, and, only when it has been reduced to the form of these types of simple molecules can it be introduced to the combustion. During combustion, there is also no immediate, one-step reaction to form CO_2 and H_2O. Individual molecules must first break down to become atoms. The atoms and molecules must collide with each other to produce a series of transitional products such as CO, OH, and so on; this chain reaction takes place in stages and, finally, results in the formation of CO_2 and H_2O. During the process of all this, the stage of the reaction which happens most slowly determines the overall rate of reaction. If one is dealing with a case in which there is a rich mixture of fuel and a shortage of air, then, because of the agitation or liveliness of activity of the oxygen atoms, they are picked up first in the formation of H_2O. There is a certain amount of carbon left over which can only go into the formation of CO. If the shortage of oxygen is too severe, then, there will be an excess amount of compounds of hydrogen and oxygen.

(1) The Breakdown of Individual Molecules, Stage One Reaction

Let us assume that $\cdot [AB] \rightarrow A + B$. Let us take c to represent the instantaneous concentration of (AB) $(kmol/m^3)$; according to the "laws for the behavior of matter", the rate of reaction and the instantaneous concentration, c, form a ratio; if we assume that k = the coefficient of reaction, then, the stage one or level one reaction is

$$\frac{-dc}{dt} = kc = W_1 \quad [kmol/m^3 \cdot s] \qquad (15.54)$$

$$-\frac{dc}{c} = k dt, \quad \ln c = -kt + const.$$

When t = 0, the original molecular concentration of (AB) in moles = c_0, and $const = \ln c_0$, then, it follows from these conditions that the function of the change over time of the molar concentration ratio is

$$\frac{c}{c_0} = e^{-kt}, \quad t \rightarrow \infty, c \rightarrow 0. \qquad (15.55)$$

(2) Two Molecules Collide With One Another, Stage Two Reaction

Let us take the parentheses to represent the molecular weight of various

317

different types of gases, (A), (B), ...; let us also take c_A, c_B to represent the instantaneous molar concentration $(kmol/m^3)$; let us further take a, b ... to represent the appropriate coefficients of distribution or mixing of the various types of materials or gases in the equations for the reactions; if we assume all these values, (Q) = the amount of heat generated in the reaction, and the equation of the reaction is $a[A] + b[B] \rightarrow f[F] + g[G] + (Q)$ (15.56). The rate of combustion reaction is

$$W_A = -\frac{dc_A}{dt} = k c_A^a c_B^b \quad [kmol/m^3 \cdot s] \quad (15.57)$$

For example: $OH + H_2 \longrightarrow H + H_2O + 14.2\,kcal$ (15.58). Equation (15.58) represents the collision of two molecules with each other and their coefficients of composition or mixing $a = 1$, $b = 1$, $(a + b) = 2$; because of this fact, this is called a "class two or level two reaction." k is called the "coefficient of reaction." If the units of concentration of c_A, and c_B are different, then, the unit for k is also different. If H_2 and OH have concentrations measured in units expressed in $(kmol/m^3)$, then, the unit used to express the coefficient of reaction, k, is $(m^3/kmol.s)$.

(3) If we are dealing with a case in which three molecules or atoms simultaneously collide with each other and combine to form a new molecule, then, this is called a "third level or class three reaction." According to the theory of molecular motion, the chances of this type of collision occuring are very small; if we are considering the reactions of combustion, then, it is possible to not consider it at all. In the main combustion area, in the combustion gases, there are many types present; the chances of collision are very large, and it is possible to simultaneously have the existence of class one and class two reactions. Because of this fact, if one looks from the point of view of the results, then, if one considers the combustion reaction as a whole, the number of occurrences of each class of reaction may possibly not be a whole number 2 (for example, 1.75, ... 1.95).

Sec 12 Collision Frequency of Two Molecules

The rate of class two reactions, W_2, is obviously related to the frequency of collision of the contents of each cm^3 during each second as this refers to two types of molecules, A and B (or atoms, for that matter). The higher is the frequency of collision, z, the more numerous are the instances of collision during

318

each second; of course, the chances of combining are then also higher, and the combustion is faster.

According to the theory of molecular motion, if, by using the distribution curve for velocity probability of molecular as it has been developed by Boltzmann and others, we solve for the root-mean-square of molecular velocity, $\bar{u}$, when the temperature is T, then,

$$\bar{u} = \sqrt{\frac{8RT}{\pi M}} = 14500\sqrt{\frac{T}{M}} \ [cm/s] = 145\sqrt{\frac{T}{M}} \ [m/s]$$

(15.59)

If we assume that $1cal = 4.18 \ Joule = 4.18 \times 10^7$ ergs, then, in the equation universal gas constant $R = 1.986 [cal/mol \cdot K] = 8.314 \times 10^7 [gr \cdot cm^2/mol \cdot s^2 \cdot K]$; T = the absolute temperature (K); and, M = the molecular weight (gr/mol). $\bar{u}$ is directly proportional to $\sqrt{T}$ and inversely proportional to $\sqrt{M}$.

The volume for each gram of molecular weight is $V = 22.4 \times 10^3 \ [cm^3/mol]$. When $T_0 = 273 \ K, \ p_0 = 760 \ mmHg$, it makes no difference whether the molecules are large or small, whether they are light or heavy; the number of molecules contained in $22.4 \times 10^3 [cm^3]$ is $N = 6.023 \times 10^{23}$. Because of this fact, the concentration of molecules (the number of molecules contained in each cm3) is

$$n = n_0 \frac{p}{p_0} \frac{T_0}{T}, \quad n_0 = \frac{6.023 \times 10^{23}}{22.4 \times 10^3}$$
$$\simeq 2.68 \times 10^{19} \ [1/cm^3]$$

(15.60)

Let us assume that, in a reaction volume, there are two types of molecules, A and B. The molecular weight of A = M_A; the molecular weight of B = M_B; the diameter of A = d_A; the diameter of B = d_B; the molecular velocity of A = $\bar{u}_A$, and the molecular velocity of B = $\bar{u}_B$. The molecular concentrations of A and B are, respectively, n_A and n_B, and $n_A + n_B = n$. The effective distance of molecular collisions is

$$\bar{d} = \frac{1}{2}(d_A + d_B).$$

The velocity of combustion when two molecules collide is $\bar{u} = \sqrt{\bar{u}_A^2 + \bar{u}_B^2}$. The effective space of collision for molecules during each second involved $= \pi \bar{d}^2 \bar{u}$. According to experimentation, $\bar{d} \simeq (4 \sim 5) \times 10^{-8} [cm]$. The number of occurrences of collisions between one molecule A and n_B molecules B is $z_A = \pi \bar{d}^2 \bar{u} n_B$. The number of instances of collision between n_A molecules A and n_B molecules B is $z_{AB} = \pi \bar{d}^2 \bar{u} n_A n_B \ [1/cm^3 \cdot s]$ If we make use of equation (15.59), then, the frequency of collision between the two types of

molecules, A and B, within each cm^3 is

$$z_{AB} = n_A n_B \pi^2 \sqrt{\frac{8\pi RT}{M'}} \quad [1/cm^3 \cdot s] \qquad (15.61)$$

The effective molecular weight that all this amounts to is

$$M' = \frac{M_A M_B}{M_A + M_B},$$

The kinetic energy of collision totals up to

$$E' = \frac{1}{2} M' \bar{u}^2 \qquad (15.62)$$

Sec 13   Reaction Coefficient k

When two molecules, A and B, collide with each other, it is most certainly not true that there is a new molecule formed in every case. It is only in cases in which the velocity of combination, $\bar{u}$, is adequately high, and the kinetic energy of collision, E', is large enough to make it possible to break up the molecular structures involved that we find the causation of a chemical reaction; this happens only when these conditions are met. The energy which is required for the breaking up of these molecular structures is called the "energy of activation". Because of this fact, it is only necessary that there be a collision of molecules such that E' $\geqslant$ E, and there will be an effective combining; this combining will only take place, however, if this condition is met. Let us assume that z'_{AB} = the number of occurrences of effective collisions in each cm^3 during each second; if we assume this, then, the activation factor = z'_{AB}/z_{AB} = the frequency of effective collisions/the frequency of theoretical collisions = the coefficient of effective reaction/the coefficient of theoretical reaction =

$$\frac{k}{k_0} = e^{-\frac{E}{RT}} \ll 1; \qquad (15.63)$$

From equation (15.63), it is possible to explain why, when the molecules of fuel are large (this requires that the energy of activation, E, be large) and, during periods when the temperature is low, that $k \ll k_0$, that is to say that combustion

320

is difficult to achieve. If we take the molecular concentrations n_A and n_B to represent the rate of combustion reaction, i.e.,

$$W_A = -\frac{dn_A}{dt} = k n_A n_B = k_0 e^{\frac{-E}{RT}} n_A n_B \quad [1/cm^3 \cdot s] \quad (15.64)$$

And, if we further take the molar concentrations (c_A) and (c_B) (kmol/m3) for representation, then, due to the fact that each kmol of volume contains, in 22.4 m^3, the number of molecules

$$N = 6.023 \times 10^{26}, \ 1m^3 = 10^6 cm^3,$$
$$n_A = 6.023 \times 10^{26} \times 10^{-6}[c_A]; \quad (15.65)$$
$$W_A = -\frac{d[c_A]}{dt} = 6.023 \times 10^{20} n_{AB} e^{\frac{-E}{RT}}$$

$$= 6.023 \times 10^{20} \times \sqrt{8\pi R} \ [c_A][c_B] \sqrt{\frac{T}{M'}} \ e^{\frac{-E}{RT}} d^2,$$

Because of these facts,

$$W_A = -\frac{d[c_A]}{dt} = 6.023 \times 10^{20}$$

$$\times \sqrt{8\pi \times 8.315 \times 10^3} \ [c_A][c_B] \sqrt{\frac{T}{M'}} \ e^{\frac{-E}{RT}} d^2$$

$$= 6.023 \times 10^{20} \times 4.57$$

$$\times 10^4 \ [c_A][c_B] \sqrt{\frac{T}{M'}} e^{\frac{-E}{RT}} d^2$$

$$W_A = k[c_A][c_B] = 2.75$$

$$\times 10^{25} d^2 \ [c_A][c_B] e^{\frac{-E}{RT}} \sqrt{\frac{T}{M'}} \quad [kmol/m^3 \cdot s] \quad (15.66)$$

If we make a comparison with equation (15.66), the coefficient of effective reaction is

$$k = 2.75 \times 10^{25} d^2 \ e^{\frac{-E}{RT}} \sqrt{\frac{T}{M'}} = k_0 e^{\frac{-E}{RT}} \quad [m^3/kmol \cdot s]$$

$$(15.67)$$

It follows from this that the coefficient of effective reaction, k, is a function of the total molecular weight, M', the effective distance of molecular collision, d, the energy of activation, E, and the temperature, T.

We already know the molecular weight M_A or the A type gas, and its rate of loss is $-R_A = M_A W_A \,[kg/m^3 \cdot s]$ (15.68) .

If we first make experimental measurements of the rate of combustion reaction, W_A, the instantaneous concentration (c_A and (c_B), and the temperature, T, then, on the basis of equation (15.66), it is possible to calculate the energy of activation, E, of these combustion reactions, or the coefficient of reaction, k. If we calculate the coefficients of reaction, k, for different temperatures, T, then, it is possible on the basis of equation (15.67), to draw out the logarithmic subordinate straight line, as is seen in Fig 15.13, in order to represent changes in lnk as it varies with changes in the inverse of the temperature (1/T), that is,

$$k = k_0 e^{\frac{-E}{RT}},$$
$$\ln k = \ln k_0 - \frac{E}{R}\left(\frac{1}{T}\right) \qquad (15.69)$$

The slope of this straight line should be equal to $E/R = \text{tg}\,\alpha$; it then follows from this that it is possible to estimate the energy of activation, E.

If we experimentally determine the energy of activation of the combustion of heptane (C_7H_{16}) and oxygen (O_2) to be $E = 3.6 \times 10^4\,[cal/mol]$, then, the coefficient of reaction is $k_0 \approx 4 \times 10^{10}\,[cm^3/gr \cdot s] = 4 \times 10^7\,[m^3/kg \cdot s]$.
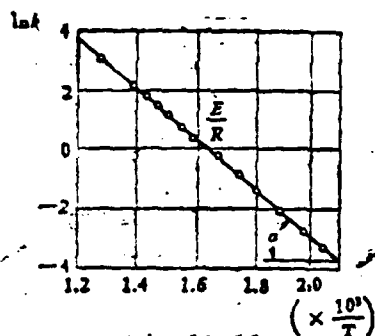

Fig 15.13

1. lnk As It Varies with Changes in (1/T), (HI)

Sec 14   Combustion Mass Equilibrium

It is possible to use C_8H_{16} for the formula of a stable molecule of kerosene.

322

The components of the weight include Carbon, $C \approx 0.856$, hydrogen, $H \approx 0.144$ and in the appropriate gas combination ratio with air, $L_0 = 14.7$. The combustion characteristics of octane are very close to those of kerosene; when one does quantitative tests, one always uses octane (C_8H_{18}) to take the place of kerosene. One may consider that each mole of air contains oxygen 0.21 and 0.79 of nitrogen and that each mole of oxygen will combine itself with 3.76 moles of nitrogen. The equation for combustion reactions in which the coefficient of excess air, $a = 1$, is

$$C_8H_{18} + 12.5\ O_2 + 12.5 \times 3.76 N_2 \longrightarrow 8 CO_2$$
$$+ 9 H_2O + 47 N_2 + Q \qquad (15.70)$$
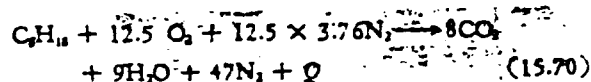
The molecular weights are $C = 12$, $H = 1$, $O = 16$, $N = 14$. The molecular weights are

$$O_2 = 32,\ N_2 = 28,\ CO_2 = 44,\ H_2O = 18.$$
$$C_8H_{18} = 8 \times 12 + 18 = 114,\ 12.5\ O_2 = 12.5 \times 32 = 400,$$
$$47 N_2 = 47 \times 28 = 1316,\ 8 CO_2 = 8 \times 44 = 352,\ 9 H_2O =$$
$$9 \times 18 = 162.$$

114kg (octane) + 400kg (oxygen) = 1316kg (nitrogen) $\rightarrow$ 352kg (carbon dioxide) + 162kg (water vapor) + 1316kg (nitrogen) + (114x10400) kcal. The masses of the mixtures of unburned gases and gases which have already been burned are equal, that is 1830kg (unburned gas mixture) $\rightarrow$ 1830kg (gas mixture which has already been burned) + 1.186×10^6 kcal. From the equation for the combustion reaction, (15.70), is possible to calculate that the appropriate ratio of gases is

$$L_0 = \frac{400 + 1316}{114} = \frac{1716}{114} = 15,\ [\text{kg air/kg octane}$$

that the appropriate ratio of fuel to oxygen is

$$S_0 = \frac{400}{114} = 3.51,\ [\text{kg air/kg octane}$$

and that each mole of gases that have already been burned comes out to have carbon dioxide in it so that

$$r_{CO_2} = \frac{8}{8 + 47} = 14.54\%,$$

If we take samples from the gases and perform quantitative analysis on them, and if one finds that, in the gases which have already been burned, $CO_2 < 14.54\%$. then, this explains the incompleteness of the combustion, $\eta = (1 - \phi) < 1$.

Equation (15.70) is an equation which describes a case in which one assumes that the time of combustion is adequately long, that the space is adequately large, that the environmental or ambient temperature of combustion and the pressure in the combustion are invariable, and that the supply of fuel being mixed with the air is maintained at the appropriate ratio, L_o, and does not vary, and this equation also assumes that there is ideally even mixing in an ideally stable and continuous combustion reaction. In actuality, the volume of the main combustion area, V, is limited, the stop-over time of the mixed gases, τ_s, will not be very long, because of the presence of counter-current flow diffusion mixing cannot be one-hundred-percent even, and the distributions of temperature and pressure are not set up evenly; it follows from all of this that, even if there is an appropriate mixture of ingredients, there will still be a great deal of left over oxygen, and the fuel may also not necessarily be completely consumed. Because of the fact that the chemical reactiveness of hydrogen atoms is strong, if there is first a sudden influx of oxygen into the composition of the mixture and $\alpha > 1$, and combustion takes place when the fuel mixture is lean, then, there will again be, in the gases that have already been burned, an appearance of carbon monoxide (CO). when $\alpha < 1$, and combustion takes place when the fuel mixture is rich, then, one can get the appearance of unburned fuel, but this only happens under these conditions and no others; this unburned fuel is (c_f).

Whether one considers the situation before combustion or after combustion, the numbers of the same types of atoms should be equal. For example, concerning equation (15.70), in the unburned gases, there are 12.5x2 = 25 atoms of oxygen, and, in the gases that have already been burned, there are 8x2+9 = 25 atoms of oxygen.
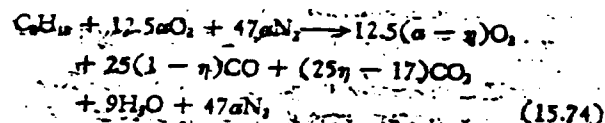
If we take the oxygen to be the index or reference coordinate, and then take the amount of oxygen in the mixture during perfect combustion as the base value or standard, then, when there is a lean mixture or a rich mixture, in the mixture of gases, the corresponding ratio between fuel and air is $\phi = \frac{1}{\alpha} \leq 1$.

Let us assume that β = the appropriate or optimum amount of oxygen to be mixed in / the actual oxygen content ≤ 1, and let us also assume that a lean mixture is $\alpha > 1$, or 或 $\phi < 1$, $\beta = \frac{1}{\alpha}$ let us further assume that a rich mixture is $\alpha < 1$, or $\phi > 1$, $\beta = 1$, (15.71)

The instantaneous localized combustion efficiency is η = the actual amount of oxygen lost/the appropriate or optimum amount of oxygen in the combination = 1 - the concentration of oxygen which has not been dissipated or lost/the concentration of oxygen which is appropriate or optimum to enter into the combustion = $1 - r/r_0$ (15.72). Let us assume that T = the actual temperature of gases that have already been burned, that T_0 = the original temperature of the gases that have not already been burned, and that T_m = the maximum temperature of gases that have already been burned if the combustion is ideally complete ψ = 0. If we assume that ψ = r/r_0 = the oxygen consumption ratio, then, the instantaneous local combustion efficiency is

$$\eta = \frac{T - T_0}{T_m - T_0} = 1 - \frac{r}{r_0} = 1 - \psi. \qquad (15.73)$$

If we are considering the case of a lean mixture, $a \geq 1$, then, due to the fact that the mixing is uneven, and the time is inadequate, the combustion reaction for $\eta < 1$ is

$$C_9H_{18} + 12.5aO_2 + 47aN_2 \rightarrow 12.5(a - \eta)O_2$$
$$+ 25(1 - \eta)CO + (25\eta - 17)CO_2$$
$$+ 9H_2O + 47aN_2 \qquad (15.74)$$

On the basis of the fact that, in the gases that have already been burned and in the gases that have not already been burned, the numbers of atoms of the same types are equal, if one checks out the number of moles of CO_2, x, then,

$$25a = 25(a - \eta) + 25(1 - \eta) + 2x + 9,$$
$$= 25a - 52\eta + 25 - 25\eta + 2x + 9,$$
$$0 = -50\eta + 34 + 2x;$$

It follows from this that,

$$x = \frac{1}{2}(50\eta - 34) = (25\eta - 17).$$

If one is considering a case in which $\eta < 1$, then, it must be that $x < 8$, and that there is imperfect combustion with a lean mixture; it follows from this that there would be evidence of the appearance of CO. From equation (15.74), it is possible to calculate, in the gases that have already been burned, the molar

concentration ratio for the CO and excess O_2 contained in them; this ratio is r. The total number of moles in the gases which have already been burned =

$$12.5\alpha - 12.5\eta + 25$$
$$- 25\eta + 25\eta - 17 + 9 + 47\alpha = 59.5\alpha$$
$$- 12.5\eta + 17 = 12.5(4.76\alpha - \eta + 1.36),$$

The molar concentration ratio is

$$
\begin{aligned}
r_{CO} &= \frac{25(1 - \eta)}{12.5(4.76\alpha - \eta + 1.36)} \\
&= \frac{2(1 - \eta)}{(4.76\alpha - \eta + 1.36)}; \\
r_{O_2} &= \frac{12.5(\alpha - \eta)}{12.5(4.76\alpha - \eta + 1.36)} \\
&= \frac{(\alpha - \eta)}{(4.76\alpha - \eta + 1.36)}.
\end{aligned}
\qquad (15.75)
$$

We already know α and η for the main combustion chamber; on the basis of the equation (15.75), it is possible to calculate the molar concentration for the excess oxygen, r_{O_2}. If one is calculating the actual excess oxygen coefficient α_* , for an augmenter combustion chamber, then, one ought to use this concentration of excess oxygen.

Sec 15   Overall Reaction Rate of Octane and Experimentation

The combustion of complicated compounds of hydrogen and oxygen like octane (C_8H_{18}) and kerosene are reactions that proceed in several stages. If we first fix the overall class of reaction, m, and the class of the fuel reaction, n, then, we can, on the basis of equation (15.57) and assuming that (c_f) = the molar concentration of the fuel, and that (c_{cx}) = the molar concentration of oxygen, write out the consumption rate of oxygen (that is the reaction rate) which is

$$W_{ox} = -\frac{d[c_{ox}]}{dt} = k[c_{ox}]^{m-n}[c_f]^n$$

If we assume that the molar concentration of the mixture $= [c_M] [\text{mol/l}]$, then, $p = [c_M] RT$. On the basis of equation (15.75), let us use the molar

326

concentration ratio $r_0[c_{ox}] = [c_{ox}]$, $r_f[c_f] = [c_f]$; the coefficient of reaction, k, according to equation (15.67), can be written as

$$k = k_1\sqrt{T}\cdot e^{\frac{-E}{RT}}, \quad k_1\sqrt{T} = k_{ox}$$
$$[c_{ox}]^{m-n}[c_f]^n = [c_M]^m \cdot r_{0_2}^{m-n} \cdot r_f^n$$

It follows from this that the rate of oxygen reaction is

$$W_{ox} = k_1\sqrt{T}\left(\frac{p}{RT}\right)^m r_{0_2}^{m-n} r_f^n \cdot e^{\frac{-E}{RT}} \; [\text{mol}/1\cdot\text{s}] \tag{15.75a}$$

Let us assume that V = the volume of the combustion chamber (1), that G_0 = the gas supply circulation (mol/s), and that G_{ox} = the rate of consumption of oxygen (mol/s); in such a case, [mol/s], $r_f = r_{CO}$, $m = 1.8 \rightarrow 2.0$, $n = 0.8 \rightarrow 1$, $G_{ox} = 0.21\beta\eta G_0 = VW_{ox}$, in a lean mixture $\beta = \frac{1}{\alpha}$, and a rich mixture means $\beta = 1$; in a lean mixture, the gas supply circulation is

$$G_0 = 4.67\,\alpha V \frac{k_1\sqrt{T}}{\eta}\left(\frac{p}{RT}\right)^m e^{\frac{-E}{RT}}$$
$$\times \frac{[2(1-\eta)]^n(\alpha-\eta)^{m-n}}{(4.76\alpha - \eta + 1.36)^m}, \;\text{設}\; m = 1.8, \; n = 0.8$$

In a lean mixture where $\alpha > 1$, the circulation load is

$$\xi = \frac{G_0}{V\cdot(p)^{1.8}} = 4.76\frac{\alpha}{\eta}\frac{k_1 T^{1-1.8}}{R^{1.8}}e^{\frac{-E}{RT}}$$
$$\times \frac{2(1-\eta)^{0.8}(\alpha-\eta)}{(4.76\alpha - \eta + 1.36)^{1.8}} \tag{15.76}$$

In a rich mixture, the gas supply circulation is

$$G_0 = 4.67V\frac{k_1}{\eta}\left(\frac{p}{R}\right)^{1.8} T^{1-1.8}e^{\frac{-E}{RT}}\left(\frac{0.08}{\alpha}\right)^{0.8}$$
$$\times \left[\frac{(1-\eta)\alpha}{(4.76-\eta)\alpha + 0.08(1+16\eta)}\right]^{1.8}$$

In a rich mixture, where $\alpha < 1$, the gas flow or circulation load is

$$\xi = \frac{G_0}{V(p)^{1.8}} = 4.76\frac{k_1}{\eta R^{1.8}} T^{1-1.8}e^{\frac{-E}{RT}}\left(\frac{0.08}{\alpha}\right)^{0.8}$$

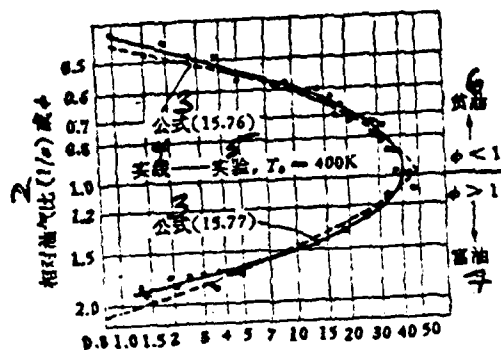$$\times \left[\frac{(1-\eta)\alpha}{(4.76-\eta)\alpha + 0.08(1+16\eta)}\right]^{1.4} . \quad (15.77)$$

图15.14 通气负荷

Fig 15.14

1. Circulation or Gas Flow Load $\xi = 4.76\frac{W_{0x}}{p^{1.4}V}\left[\frac{mol}{s\cdot l(atm)^{1.8}}\right]$ 2. Corresponding Fuel-to-Air Ratios (1/ α) or ϕ, 3. Formula 4. Solid Line 5. Experimental Tests
6. Lean Mixture of Fuel 7. Rich Mixture of Fuel

表15.3 瞬时局部燃烧温度 T 是 α 及 η 的函数（燃料 C_8H_{18}）

η	$\phi = \frac{1}{\alpha}$, $T_0[K]$	0.3	0.4	0.5	0.6	0.7	0.8	0.9	1.0	1.1	1.2
1.0	300	1084	1307	1515	1712	1899	2077	2225	2315	2285	2215
	400	1170	1389	1595	1791	1976	2155	2275	2355	2345	2285
	500	1256	1473	1677	1771	2055	2210	2330	2390	2400	2350
0.9	300	987	1178	1360	1533	1699	1855	2004	2145	2053	1957
	400	1073	1269	1440	1616	1779	1933	2079	2215	2129	2035
	500	1159	1348	1527	1698	1860	2013	2155	2270	2195	2120
0.8	300	882	1046	1203	1351	1492	1627	1757	1879	1783	—
	400	970	1133	1288	1435	1575	1709	1837	1958	1864	—
	500	1057	1218	1371	1517	1656	1789	1905	2030	1943	—
0.7	300	775	913	1042	1173	1279	1395	1502	1600	—	—
	400	863	999	1127	1249	1360	1475	1584	1650	—	—
	500	952	1087	1214	1335	1450	1560	1665	1767	—	—

Table 15.3

1. The Instananeous Local Combustion Temperature, T, As a Function of α and η
(Fuel C_8H_{18})

Let us assume that the original temperature of the gases which have not yet been burned is $T_o = 400[K]$, $\rho = 0.2 \sim 1.0[atm]$, $E = 4.2 \times 10^4[cal/mol]$, $R = 1.986[cal/mol \cdot K]$, let us further assume that, if we are dealing with a lean mixture, when $\alpha > 1$, then, $k_o = k_1\sqrt{T} = 1.67 \times 10^{10}$ and, if we are dealing with a rich mixture, when $\alpha < 1$, then, $k_o = k_1\sqrt{T} = 11.1 \times 10^{10}$ On the basis of the data which have been postulated above, if we substitute into equations (15.76) and (15.77), then, we can figure out the curve which represents the changes of air current load, ξ, for the combustion of octane and oxygen as it varies with corresponding changes in the fuel-to-air ratio, $1/\alpha$; this curve is represented by the broken line in Fig 15.14. If one grants the basic assumptions of a sherical, ventilated combustion chamber in which the temperature is maintained and the mixing is even, then, the results of experimentation with the combustion of octane and air are represented by the solid line in Fig 15.14. If one arranges to increase the air current load, ξ, that is to say, if one arranges to increase the air supply to the combustion chamber, then, one will also succeed in increasing the speed of the rate of oxygen consumption. Sooner or later, because of the fact that, within the combustion chamber, the stop-over time, τ_c, is too short, the flame will be blown out.

Sec 16   Combustion Heat Balance

From Table 15.3 it is possible to find out the fact that, for perfect combustion, $\eta = 1$, as well as the ideal maximum temperatures, T_m, for different original temperatures, T_o, and different corresponding fuel-to-air ratios, ϕ ; besides this it is also possible to find out the temperatures, T, to which the gases which have already been burned can attain assuming that we already know ϕ and we are considering different values of T_o and different rates of combustion, η . Fig 15.15 (a) represents the main combustion area in the midst of stable continuous combustion. Let us assume that the coefficient of excess oxygen, $\alpha = 1$, and that the combustion reaction generates the following amount of heat for each mole of oxygen, that is,

$$H_o = \frac{1.186 \times 10^6}{12.5} \quad [kcal/mol],$$

If we assume these things, then, the rate of the release of heat for the main combustion area is $Q_1 = H_o G_{ox} = H_o V W_{ox} = 0.21 \eta G_o H_o$ [kcal/s] (15.78). V = the volume of the main combustion area (m^3 or 1); W_{ox} = the rate of reaction of oxygen (equation 15.75 a). The amount of heat which comes along with the gases which have already
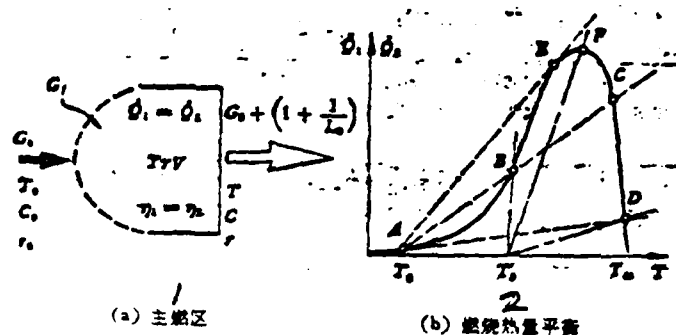
329

Fig 15.15

1. Main Combustion Area 2. Combustion Heat Equilibrium

been burned as they come out of the main area of combustion = the heat output rate, which is,

$$Q_1 = G_0 \left(1 + \frac{1}{L_0}\right) \bar{c}_p (T - T_0).$$

Let us consider that the main area of combustion has absolutely even mixing, and let us not take into consideration the problem of the dissipation of heat by the walls of the flame tubes. If we take the mole to be the unit, then, $L_0 = 12.5 + 47 = 59.5$. When there is thermal equilibrium, then, $Q_1 = Q_2$; it follows from this that

$$H_0 V k_0 \left(\frac{p}{RT}\right)^{1.8} r_{O_2} r_{CO} e^{\frac{-E}{RT}}$$

$$= G_0 \left(1 + \frac{1}{L_0}\right) \bar{c}_p (T - T_0) \quad [\text{kcal/s}] \quad (15.79)$$

The left side of the equation above is the curve ABEFCD in Fig 15.15 (b) the right side is AE, AB and other such straight lines. Point A represents the low temperature point at which ignition has just taken place; point B represents the end of the period of pre-combustion, and BF is the period of stable combustion. Point C represents the a region of the maximum temperature of combustion, T_m, with an attendant rapid reduction and slowing in the rate of reaction, W_{ox}. If the gas or air supply, G_0, is very small (the straight line AD), then, it is only possible to have combustion when one has temperature T_D; no other condition will do. If one

330

increases G_o, then, the straight line and the curve will cross at point E, and there will be blow out; if one increases T_o', then, there will be stability

Chapter 16 An Outline of the Computation of Combustion Flow Fields

Sec 1   Standardization of Combustion Flow Fields

If one is going to consider the case in which he is going to make theoretical calculations and analyses of combustion flow fields, then, he ought to consider all the physical and chemical processes. For example, concerning turbulence flow strength, ε , and scale, 1, are vortices attenuated, weakened and broken up? Is turbulence flow homogeneous in various different directions? If one is considering the case of the kinetic frequency spectra of turbulence flow, then, what about the idea of mapping out a "turbulence flow model" or "normal turbulence flow?"

Are there or are there not areas of vortical counter-current flow? What is the influence of the counter- current flow on the size of the scale involved? What is the voricity number S equal to? And what about the location of the vaporized fuel jet, the angle of dispersion of the vapor, the rules governing the distribution of the fuel droplets, and the speed or slowness of the rate of evaporation? What about the distribution of the fuel-to-air ratio (concentration), and the speed or slowness of the turbulence flow diffusion mixing? What about the length or shortness of the stop-over time of the gas mixture in the combustion area, τ_s , the diffusion time, τ_D , and the reaction time, τ_k ? The rate of disappearance or formation of different types of gases, R_j = the rate of the combustion reaction, W; what about the mechanisms of reaction in the various steps of combustion, the overall class of the reaction and the presence or absence of thermal decomposition? What about the scope and speed or slowness of heat flow diffusion and radiant transfer of heat? What about the geometrical dimensions of the form of the combustion chamber, its boundary conditions and its operational configurations? And what about the initial conditions which still must be known if one is considering non-stable flow fields?

If one were to consider all of the ten conditions discussed above with their influences on each other, then, the set of differential equations for a turbulence flow diffusion three-dimensional combustion flow field would be very difficult to solve. It follows from this that one should first, before setting out the equations, look toward the operational configurations of actual combustion chambers and draw up a set of standardized or normalized methods of numerical solution which are simple and can be used on physical and chemical problems.

If we are considering the problem of figuring the average time velocity, V, of
a rotational jet combustion flow field as well as its concentration, c_j (or m_t), its
distribution of temperature, $\overline{T}$, and its thermal flow, q, through the interior walls,
then, it is necessary to know the turbulence diffusion (transfer) coefficients of
momentum, heat, and mass, $\mu_T, \Gamma_h \& \Gamma_l$. These coefficients should represent the
functions of the localized parameters of gas flow for density, flow speed and
temperature. It is only when empirical measurements and theoretical analysis combine
that it is possible to precisely determine the "effective viscosity of turbulence
flow", μ_T . By the use of a hot-wire wind speed meter or a laser scan of the flow
field, it is possible to make a precise determination of the distribution of the
turbulence flow strength, ε . If we make a precise determination of the frequency
spectrum of density flow momentum, then, it is possible to determine the distribu-
tion of the turbulence flow scale or dimension, 1; it also becomes possible to
determine a calculated value for the coefficient of turbulence flow diffusion, D_T.
If we are considering a case in which the vortical strength number $S \geqslant 0.6$, in a
rotational jet, then, due to eddy induction (see Chapter 6), the strong pressure gra-
dient $+\partial p / \partial z$, $+ \partial p / \partial r$, which is produced in the parallel flow direction and in the
radial direction goes to form areas of counter-current flow and areas of reflux
flow. If we are dealing with a case in which the turbulence flow strength $\varepsilon \geqslant 50\%$,
then, the turbulence flow shear stress or force, τ_T , is quite large. If we can
arrange for the diffusion mixing to be violent and fast, then, it is possible to
raise the strength of the heat produced as well as the efficiency of combustion;
it is also possible to shorten the flame and raise the level of stability of the
combustion. One might even be able to say that the ease or hardness of ignition,
the speed or slowness of flame propagation as well as the stability of combustion
are all dependent on the diffusion coefficients of momentum, heat and mass,
$\mu_T, \Gamma_h \& \Gamma_l$. The influence of the speed or slowness of the mixing on the jet
nozzle vaporization and the "diffusion flame" of the combustion of fuel evaporation
is even greater than that of the evaporation-tube-type "pre-mix flame." If we
are considering the case in which we are doing measurements of the distributions of
the flow speed and turbulence flow strength of the flow fields in cold air testing,
then, it is possible to extrapolate the distributions of concentration and tempera-
ture of the "diffusion flame."

(1) When the vortical strength number $S < 0.6$, counter-current flow is exremely

weak. Let us assume theat the root-mean-square of the turbulence flow speed is homogeneous in different directions, so that, $\tilde{u} = \tilde{v} = \tilde{w}$; if we assume this, then, because of the fact that there is a similarity between the diffusion phenomena for momentum, heat and mass, and, consequently, between $\mu_T, \Gamma_h, \Gamma_i$, it is possible to presume that these quantities are also homogeneous in different directions. Let us make use of the concept of the "prandtl" mixing distance, 1, and use a set of cylindrical coordinates in r, θ and z, as well as the component vectors of velocity, $\overline{U}, \overline{V}$ and $\overline{W}$. Let us first assume that we are dealing with a non-rotational turbulence flow field, then, according to equation (15.8), the root-mean-square of the pulsation flow speed is

$$\tilde{w} = l\,\frac{\partial \overline{W}}{\partial r},\ \tilde{w} \cdot \tilde{w} = l^2\left(\frac{\partial \overline{W}}{\partial r}\right)^2 \qquad (16.1)$$

From equation (15.42), we can consider it to be true that, within the rz meridian plane, the gradients of the shear force velocities along r and z are equal, that is to say $\dfrac{\partial \overline{W}}{\partial r} \cong \dfrac{\partial \overline{U}}{\partial z}$; in such a case, the turbulence flow shear or

tangential force is $\tau_{rz} = \tau_{zr} \cong 2\mu_T\left(\dfrac{\partial \overline{W}}{\partial r}\right) = -\rho\overline{u'w'} = -\rho\tilde{w} \cdot \tilde{w}$ (16.2). If we compare equations (16.1) and (16.2), then,

$$2\rho\nu_T\left(\frac{\partial \overline{W}}{\partial r}\right) = -\rho\tilde{w} \cdot \tilde{w} = -\rho l^2\left(\frac{\partial \overline{W}}{\partial r}\right)^2,$$

It follows from this that

$$\nu_T \cong \frac{1}{2}\,l^2\left(\frac{\partial \overline{W}}{\partial r}\right) \qquad (16.3)$$

The kinetic energy of turbulence flow is $E = \dfrac{1}{2}\rho\tilde{w}^2$ [N $\cdot$ m/m^3], or $\dfrac{E}{\rho} = \dfrac{1}{2}\tilde{w}^2$ [m^2/s^2], $\dfrac{E}{\rho} = \dfrac{1}{2}l^2$; [m^2/s^2] (16.4). The stronger the pulsation is, the larger is the viscosity of turbulence flow: $\nu_T^2 \cong \dfrac{1}{4}l^2 \cdot l^2\left(\dfrac{\partial \overline{W}}{\partial r}\right)^2 = \dfrac{1}{4}l^2\tilde{w}^2$ [m^4/s^2] (16.5)

$$\frac{1}{\rho}\left(\frac{\rho\overline{V}^2}{r}\right)\ [\text{m}/\text{s}^2] \qquad (16.6)$$

In a rotational turbulence flow field, each unit of mass has exerted on it the centrifugal force $\dfrac{\partial p}{\partial r} = \rho\,\dfrac{\overline{V}^2}{r}$, [N/m^3] (16.7). If we assume that the micro-masses of a gas diffuse through the mixing distance, 1, then, the mechanical energy produced and exerted against the micro-masses of that gas in the flow field = (the centrifugal force x the mixing distance) divided by the mass density, that is to say,

334

$$\frac{1}{\rho}\left(\frac{\partial p}{\partial r}\right) = \frac{1}{\rho}\left[\frac{\rho\bar{V}^2}{r}\right] = \frac{E}{\rho} = \frac{1}{2}\bar{q}^2\ [m^2/s^2],\ \bar{q} = l\left(\frac{\partial\bar{V}}{\partial r}\right);$$

$$(16.8)$$

Within the $r\theta$ cross section, if we assume that axisymmetrical flow only takes into consideration the absolute rate of angular deformation $\left(\dfrac{\partial\bar{V}}{\partial r}\right)$, then, from equation (15.42), we can say that the turbulence flow shear or tangential force is

$$\tau_{r\theta} = \tau_{\theta r} = \mu_T\left(\frac{\partial\bar{V}}{\partial r}\right) = -\overline{\rho u'v'}$$

$$= -\rho\tilde{v}\cdot\bar{q} = -\rho l^2\left(\frac{\partial\bar{V}}{\partial r}\right)^2 \qquad (16.9)$$

And, according to equation (16.3),

$$\rho\nu_T\left(\frac{\partial\bar{V}}{\partial r}\right) = -\rho\tilde{v}\cdot\bar{q} = -\rho l^2\left(\frac{\partial\bar{V}}{\partial r}\right)^2,$$

It follows from this that,

$$\nu_T = l^2\left(\frac{\partial\bar{V}}{\partial r}\right) \qquad (16.10)$$

Concerning rotation,

$$\nu_T^2 = l^2\cdot l^2\left(\frac{\partial\bar{V}}{\partial r}\right)^2 = l^2\bar{q}^2 = l^2\cdot\frac{2l}{\rho}\left[\frac{\rho\bar{V}^2}{r}\right]$$

$$= l^2\cdot\frac{2l^2 c}{\rho r}\cdot\frac{\Delta(\rho\bar{V}^2)}{l} = \frac{2l^4 c}{\rho r}\cdot\frac{\partial(\rho\bar{V}^2)}{\partial r} \qquad (16.11)$$

Fig 16.1 represents a flow field in which a vortex is being deformed as it weakens and is breaking up (consult Sec 7 of Chapter 6). Let us assume that, on the circumference described by a radius, r, there is diffusion movement toward the outside in the case of the gas mass ① and toward the inside in the case of gas mass ②. If one is dealing with the same circumference, the operating forces, F_1 and F_2, which are exerted on the two rotating masses of gas in their opposite inward and outward movements should, respectively, form a direct proportion with the differential of centrifugal forces, that is,

$$F_1 = C_1\frac{\rho_1\bar{V}_1^2 - \rho\bar{V}^2}{r},\ F_2 = C_2\frac{\rho_2\bar{V}_2^2 - \rho\bar{V}^2}{r}, \qquad (16.12)$$

If we assume that the two proportional constants of equation (16.12) are the same, so that, $C_1 = C_2 = C$, then, the corresponding velocities of the two masses

335

= the radial direction root-mean-square of pulsation velocity, $(\bar{U}_1 - \bar{U}_2) = \bar{u}$, the radial distances after diffusion for the two masses of gas are $(r_2 - r_1) = l = \Delta r$, and the radial direction turbulence flow kinetic energy is

$$E = \frac{1}{2}\rho\bar{u}^2 = l\Delta F = l(F_1 - F_2)$$

$$= l_c \left[\frac{\rho_1 \bar{V}_1^2 - \rho_2 \bar{V}_2^2}{r}\right] = \frac{l^2 c}{r}\left[\frac{\rho_1 \bar{V}_1^2 - \rho_2 \bar{V}_2^2}{(r_2 - r_1)}\right]$$

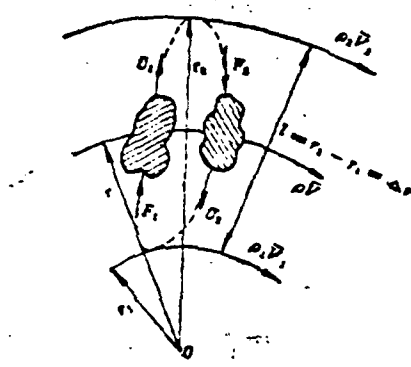$$\cong \frac{l^2 c}{r}\frac{\Delta(\rho\bar{V}^2)}{\Delta r};$$

图16.1 旋涡衰变流场示意

Fig 16.1

1. An Illustration of a Flow Field in Which a Vortex is Decreasing in Strength

From the equation above, it is possible for us to obtain the radial direction root-mean-square of the velocity of pulsation, that is,

$$\bar{u}^2 \cong \frac{2l^2 c}{\rho r} \cdot \frac{\Delta(\rho\bar{V}^2)}{\Delta r} = \frac{2l^2 c}{\rho r}\frac{\partial(\rho\bar{V}^2)}{\partial r} = \bar{u}^2; \quad (16.13)$$

Equation (16.13) confirms the last quantity of equation (16.11). If we are considering the overall influence which turbulence flow and rotation have on kinetic viscosity, from equations (16.5) and (16.11), we know that the turbulence

flow $4\mathbf{v}_T^2$ + the rotation $\mathbf{v}_T^2$ =

$$= r^2 \left[\left(\frac{\partial \overline{W}}{\partial r} \right)^2 + \frac{2c}{\rho r} \frac{\partial}{\partial r} (\rho \overline{V}^2) \right];$$

$$\mathbf{v}_T = \frac{l^2}{\sqrt{5}} \left[\left(\frac{\partial \overline{W}}{\partial r} \right)^2 + \frac{2c}{\rho r} \frac{\partial (\rho \overline{V}^2)}{\partial r} \right]^{\frac{1}{2}}, \quad (16.14)$$

$$\mu_T = \rho \mathbf{v}_T = \frac{\rho l}{\sqrt{5}} \left[l^2 \frac{(\Delta \overline{W})^2}{(\Delta r)^2} + \frac{2cl^2}{\rho r} \frac{\Delta(\rho \overline{V}^2)}{\Delta r} \right]^{\frac{1}{2}},$$

If the average radius of a ring-shaped jet nozzle = L, and the mixing distance $l = \xi L$, then,

$$\mu_T = \frac{\rho \xi L}{\sqrt{5}} \left[(\Delta \overline{W})^2 + \frac{2c\xi L}{\rho r} \Delta (\rho \overline{V}^2) \right]^{\frac{1}{2}}, \quad \xi = \text{ a constant}$$

$$(16.15)$$

$$\mu_T = \frac{\xi \rho L (\Delta \overline{W})}{\sqrt{5}} \left\{ 1 + \frac{2c\xi L \Delta(\rho \overline{V}^2)}{r\rho (\Delta \overline{W})^2} \right\}^{\frac{1}{2}}, \quad (16.16)$$

The larger is the Reynolds number, Re = $\dfrac{\rho L (\Delta \overline{W})}{\mu_T}$, which represents the turbulence flow viscosity, the stronger is the turbulence flow; the smaller is the screw pitch ratio, $N = \dfrac{W_0}{V_0} = \dfrac{\overline{W}}{\overline{V}}$, which represents the strength or weakness

characteristic of a vortex, the stronger will be the rotation; and, the larger is the vortical strength number $S \propto \dfrac{L \Delta(\rho \overline{V}^2)}{r\rho (\Delta \overline{W})^2}$ which represents the strength or

weakness of a vortex, the stronger the vortex will be.

Let us assume that

$$\frac{1}{N^2} \propto \frac{L \Delta(\rho \overline{V}^2)}{r\rho (\Delta \overline{W})^2},$$

In such a case,

$$Re^{-1} = K_1 \left[1 + \frac{K_2}{N^2} \right]^{\frac{1}{2}}; \quad (16.17)$$

It is necessary, on the basis of the shape and dimensions of the combustion chamber as well as the experimental conditions, to determine values for the constants, K_1 and K_2 in the equation above.

If we are dealing with a cold air rotational free jet, then,

337

$$Re^{-1} = 0.00294\left[1 + \frac{91.1}{N^2}\right]^{\frac{1}{4}} \qquad (16.18)$$

If we are dealing with a combustion rotational jet flame, them,

$$Re^{-1} = 0.0078\,\bar{\rho}^{\frac{1}{4}}\left[1 + \frac{91.1}{N^2}\right]^{\frac{1}{4}} \qquad (16.19)$$

In the equation above, the density ratio $\bar{\rho}$ = the lowest density in the center of a rotational flame jet/the density of the environment around the rotational jet flame · 1; we already know Re, so we can calculate μ_T .

(2) If we are dealing with a case in which the vortical strength number $S \geqslant$ 0.6, then, it is obvious that, as far as counter-current flow is concerned, it is not possible to assume that the turbulence flow is homogeneous in different directions, and, it would also be true in such a case that the turbulence flow density, μ_T, would be different in different directions. Let us continue to use a cylindrical coordinate system in r, θ, and z as well as the component vectors of flow speed, $\widehat{U}$, $\widehat{V}$ and $\widehat{W}$. Let us assume that we have already determined by experimentation values for the mixing distance, l, or the scale involved with the turbulence flow (see Sec 2 of Chapter 15). In such a case, it would follow that, within the meridian plane rz, the total or overall viscosity μ_{rz} = the viscosity of the turbulence flow μ_T + the viscosity of laminar flow μ , that is,

$$\mu_{rz} = \rho l^2 \sqrt{2}\left\{\left(\frac{\partial\overline{W}}{\partial z}\right)^2 + \left(\frac{\partial\overline{U}}{\partial r}\right)^2 + \left(\frac{\overline{U}}{r}\right)^2\right.$$
$$\left. + \frac{1}{2}\left(\frac{\partial\overline{W}}{\partial r}\right)^2 + \frac{1}{2}\left[r\,\frac{\partial}{\partial r}\left(\frac{\overline{V}}{r}\right)\right]^2 + \frac{1}{2}\left(\frac{\partial\overline{V}}{\partial z}\right)^2\right\}^{\frac{1}{2}} + \mu$$

$$(16.20)$$

The total or overall viscosity on the horizontal cross section $_r\theta$ is $\mu_{r\theta} = \frac{\mu_{rz}}{\sigma}$, where σ is a constant > 1; it follows from this that $\mu_{r\theta} < \mu_{rz}$. In the equation above, the constant $\sigma = 1 + 5S^{\frac{1}{2}}$, and S = the vortical strength number which is $\geqslant 0.6$ (see Sec 11 of Chapter 6).

If we are dealing with a case in which there are no experimentally determined values, then, it is possible, on the basis of the empirical formula presented below, to calculate the mixing distance, l. Let us assume that the radius between the center line of the flame or the center line of the ring-shaped cavity and the main axis line of the combustion chamber is r_0; if we assume this, then, the mixing

distance, 1, varies symmetrically with respect to this r_o center line. On the line, r_o, the axial flow speed, $\overline{W}_m$, is the largest; on other lines such that $r \leqslant r_o$, the axial flow speed $= \overline{W}$. $\overline{W} = 0.05\overline{W}_m$ is the boundary of a ring-shaped rotational jet. If we already know the distribution of $\overline{W}$ along r, then, it is possible to determine the ratio of radii (r/r_o) for the boundary of the jet.

$$\frac{l}{r_o} = \lambda\left(\frac{r}{r_o}\right) \overline{W} = 0.05\overline{W}_m, \quad \lambda = 0.08(1 + 0.6S) \quad (16.21)$$

(3) A rough calculation of μ_T.

If we are dealing with a case in which we already know the viscosity of laminar flow, μ , as well as the root-mean-square of the speed of pulsation, $\tilde{u}$, and we accurately calculate the Reynolds number Re for a vortical flame, then, it is possible, on the basis of Sec 4 of Chapter 15, to calculate $\mu_T \cong 10^{-3} \text{Re}\, \mu$. If we already possess the frequency spectrum analysis of the turbulence flow field and we obtain the root-mean-square of the speed of pulsation, $\tilde{w}$, as well as the scale or magnitude, $\overline{l}$, involved with the central turbulence flow, then, on the basis of equation (15.7), it is possible to calculate the coefficient of diffusion of the turbulence flow $D_T = \tilde{w}l$; from Table 15.2, if we borrow the analogous standard "Prandtl" number Pr for laminar flow as well as the "Schmitt" number Sc, then, it is possible to calculate the following (see equations (15.22) and (15.25)): the turbulence flow viscosity is $\mu_T = \rho\nu_T = \text{Sc} \cdot \rho D_T = \text{Sc} \cdot \Gamma_l$, or $\mu_T = \text{Pr} \cdot \rho a_T = \text{Pr} \cdot \Gamma_\lambda$ (16.22). Because of this fact, it is possible to determine precise values for all the quantities $\mu_T, \Gamma, \not \boxtimes \Gamma_\lambda$, which determine the scale and the level of the diffusion of turbulence flow. In Chapter 15, μ_T, in equation (15.41) to (15.42) Γ_λ, in equations (15.44) to (15.45), and Γ_l in equations (15.49) to (15.50) all have precisely determinable numerical values, and these can be used in making preparations for doing difference calculations. If we use the vector differentiation symbol ∇ , then, the degree of divergence of turbulence flow forces = $\nabla \cdot \Pi$ (see equation (15.43)). The degree of divergence of the heat flow is $-\nabla \cdot q = \nabla(\Gamma_\lambda \nabla l)$, and the degree of divergence of the concentration is $-\nabla \cdot J_i = \nabla(\Gamma_l \nabla m_i)$ (16.23) .

Sec 3   Standard Types of Fuel Vapor Atomization

Different types or shapes of jet nozzles spray out vaporized fuel from different

positions; the size of the value of ϕ for the jet aperture, the fuel pressure P and the angle of spread or divergence, $_3$, of the vapor jet all go together to determine the vaporized mass. The amount of jet fuel $G_i[kg_i s]$ or $\cdot Q_i$ $[m^3/s]$ is composed of fuel droplets of various diameters, a_i, which distribute themselves in terms of size in accordance with a probability distribution. The accelerating or decelerating movements of the droplets of fuel, the elimination of heat through evaporization or the release of heat by combustion all have very large influences on the capabilities of a combustion chamber. A yellow-colored flame represents diffusion combustion in the wakes of fuel droplets. Blue-colored flames represent gaseous combustion of evaporated vapors which have already left the fuel droplets. The concentration of oxygen contained in the gases surrounding the fuel droplets, $c_{ox} = (\rho_{ox}/\rho)$ as well as the corresponding velocity, V_r, of the fuel droplets to the gas flow determine the color of the flames. When one is dealing with a situation in which the diffusion mixing in the main combustion area is violent, the amount of reflux flow of high temperature gases which have already been burned is large, the concentration of oxygen contained, c_{ox}, is dilute, and the corresponding velocity, V_r, is very high, then, because of these factors, one sees the appearance of. the phenomenon of blue flames which are due to the combustion of "pre-mix gases", and this represents combustion which is especially rapid.

If one makes large-scale tests of jet fuel vaporization, and one measures the jet fuel pressure $P[N/cm^2]$, the amount of jet fuel $Q_i[cc/s]$ or $G_i = a_i Q_i [gr/s]$ as well as the percentage, $y_i\%$, of an amount of jet fuel which is occupied by large and small fuel droplets, then, it is possible to draw out the curve for the probability distribution of fuel droplet vaporization, as is shown in Fig 16.2 and Fig 16.3. If one assumes that $\bar{a}$ = the median diameter (that is to say, the fuel droplets with diameters which are larger that $\bar{a}$ and the fuel droplets that have diameters smaller than $\bar{a}$ both occupy 50% of the amount of the jet fuel) and that this represents the degree of fineness of the vaporization, and, if one further assumes that n = the uniformity or evenness index of vaporization = 1.5 2, then, the integral function of probability, F(a) is

$$F(a) = 1 - \exp\left[-0.693\left(\frac{a}{\bar{a}}\right)^n\right] \qquad (16.24)$$

The distribution function of probability is
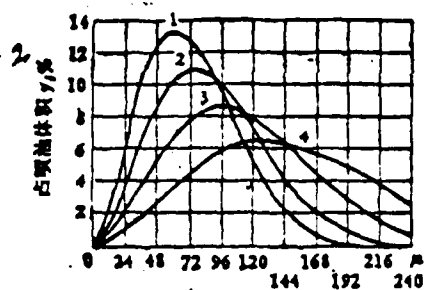
$$y_i\% = \frac{dF(a)}{da} \times 100\%$$

340

图 16.2 油压对油珠直径 a 分布的影响
喷嘴流量 $G_f = 4 [gr/s]$. 喷油压力 $P [kg/cm^2]$: 1:33.7;
2:17.6; 3:8.42; 4:3.52.

Fig 16.2

1. The Influence Which Fuel Pressure Has on the Distribution of Fuel Droplet
Diameter, a 2. The Volume of Jet Fuel Occupied by $y_i\%$ 3. The Amount of Jet
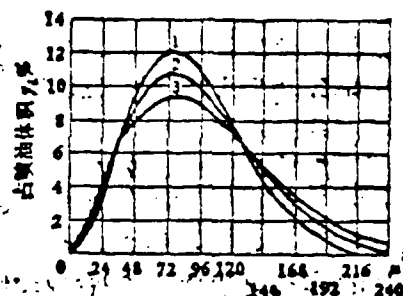Nozzle Flow 4. Jet Fuel Pressure

图 16.3 喷孔对油珠直径 a 分布的影响
油压 $P = 17.6 [kg/cm^2]$. 喷孔口径 $\phi [mm]$ 及喷油量
$G_f [gr/s]$ 1:0.425, 2.8; 2:0.56, 4; 3:0.73, 6.

Fig 16.3

1. The Influence Which the Jet Aperture Has on the Distribution of Fuel Droplet
Diameter, a 2. Fuel Pressure 3. The Gauge of the Jet Aperture 4. Jet Fuel
Amount, 5. The Volume of Jet Fuel Occupied by $y_i\%$

The conditions of high fuel pressure and small jet aperture make it possible to
raise the "degree of fineness" of the vaporization of the jet fuel as well as the
"degree of evenness or uniformity." The traces or trajectories of large and small

341

fuel droplets in their various motions are not the same; their corresponding velocities, V_r, are not the same; the resistance to the "brushing clean" effect of the air flow is different in different cases, and, the speeds of convection heat transmission, diffusion and evaporization are not the same; for all these reasons, the sequence or order of combustion can be different. Each fuel droplet, from the jet to the end of combustion, has its own course of transformation. The relatively smaller droplets of fuel evaporate quickly, and their combustion is almost immediate. It follows from this that a group of fuel droplets with an average diameter of $\bar{a}$ would, in the time period, t, after the jet, gradually increase in size as is shown by the broken line in Fig 16.4. If we use the instrumentation of the study of optics to observe and measure the order or sequence of combustion as it is broken down for a group of fuel droplets with a diameter, a_i, then, it is possible to record the probability distribution curves for large and small fuel droplets at each instant (Fig 16.4). We already know the amount of jet fuel, Q_f which corresponds to the integrated area under the probability curve for a jet time of t = 0.0. If we solve for the integrated area under the probability curve corresponding to t = 3.35 (ms), then, this should represent the volume of fuel droplets which are left after 3.35 (ms) of combustion. In still air, the rate of evaporation for each fuel droplet, M_i, is

$$M_i = \frac{d}{dt}\left(\rho_f \cdot \frac{4}{3}\pi r_i^3\right) = \rho_f \cdot 4\pi r_i^2 \left(\frac{dr_i}{dt}\right) \ [kg/s],$$

(16.25)

$$M_i = \frac{4\pi r_i k}{c_f} \ln\left[1 + \frac{c_f}{L}\Delta T + \frac{c_{ox}H_u}{S_0 L}\right] \ [kg/s], \quad (16.26)$$

ρ_f = fuel density (kg/m^3); r_i = the radius (m) of a fuel droplet i; c_f = the specific heat of the fuel (kcal/kg.K); k = the rate of thermal conductivity of the fuel (kcal/m.s.K); ΔT = the differential of temperatures between the surface of the fuel droplet and the surroundings (K); $c_{ox} = (\rho_{ox}/\rho)$ the concentration ratio of included oxygen; H_u = the heat value of the fuel (kcal/kg); S_o = the chemically appropriate fuel-to-oxygen ratio = 0.232 × L_o = 0.232 × 14.7 ; and L = the latent heat of evaporization in the fuel (kcal/kg).

The momentum or inertia of large fuel droplets is large, and the corresponding velocities, V_r, are large; if there is forced convection transfer of heat, then,

the rate of evaporization, M_i, must be multiplied by a correction factor; only if this is done can one obtain the rate of evaporation, M_i', for convection, that is,

$$M_i' = [1 + 0.276 Re^{\frac{1}{2}} \cdot Pr^{\frac{1}{3}}] M, \quad [kg/s],$$

$$Re = \frac{V_r a_i}{\nu_T}, \quad Pr = \frac{\mu_T}{\Gamma_s}; \qquad (16.27)$$

The number of fuel droplets is extremely large. In order to reduce the number of differential equations and economize on the amount of measuring to be done and on the calculation time, let us take the fuel droplets and divide them up into n groups on the basis of size (for example 5 ~ 10 groups); let us assume the fact that, within each of the groups, the diameters of the fuel droplets, $a_i (i = 1, 2, \cdots n)$, are all the same; if we do this, then, it is possible to set out n equations.

Let us assume that the concentration ratio of the fuel droplets = the concentration of fuel droplets of a diameter a_i which are contained in each m^3 of gas mixture/the concentration of each m^3 of gas mixture which is equal to

$$= f_i = \frac{\rho_i}{\rho} y_i \% \qquad (16.28)$$

Obviously,

$$\sum_1^{\cdot} y_i = 1, \quad \sum_1^{\cdot} f_i = \text{fuel/air ratio} = \frac{1}{a L_0} = \frac{1}{14.7 a} \quad (16.29)$$

Let us assume that R_i = the weight of fuel droplets of the ith group which appear in each m^3 of the combustion chamber volume every second; we may simply call this quantity the appearance rate for i fuel droplets; Γ_s = the turbulence flow diffusion coefficient for the fuel droplets (kg/s.m); on the basis of the gaseous concentration diffusion equation (15.52), it is possible to obtain a liquid-state concentration diffusion equation for a quasi-stable state average time turbulence flow axisymmetrical combustion flow field as it appears below:

$$\rho \left[u \frac{\partial f_i}{\partial r} + w \frac{\partial f_i}{\partial z} \right] = \frac{\partial}{\partial z} \left(\Gamma_i \frac{\partial f_i}{\partial z} \right)$$
$$+ \frac{1}{r} \frac{\partial}{\partial r} \left[r \left(\Gamma_i \frac{\partial f_i}{\partial r} \right) \right] + R_i \ [kg/m^3 \cdot s] \quad (16.30)$$

If one knows the boundary conditions of the combustion chamber and the appearance rate for i fuel droplets, R_i, then, it is possible to solve equation (16.30) and obtain the liquid-state concentration distribution of the combustion flow field.
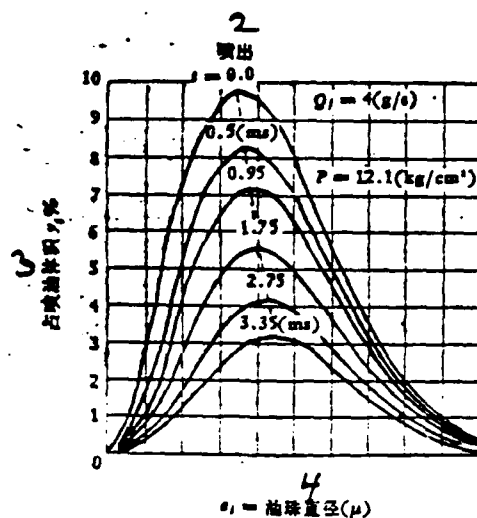
343

図 16.4 油珠密率分布沿时间变化

Fig 16.4

1. Probability Distributions of Fuel Droplets As They Vary with Changes in Time
2. Passage Through the Jet 3. Volume Occupied by the Jet Fuel $y_i\%$
4. Diameter of fuel droplets

This is only possible under these conditions and no others. The gradients of the parameters for each direction of the normal lines of the solid wall surfaces should correspond appropriately to the principle of non-permenability, for example $\frac{\partial f_i}{\partial a} = 0$.

The quantity $\partial f_i/\partial z$ on the center line of a flame tube or ring cavity as well as of the even parallel flow of the exhaust is very small, $\partial^2 f_i/\partial z^2 = 0$. At the jet nozzle, f_i = a constant; at the intake, f_i = 0. When we solve for R_i, we ought to consider the fact that, due to evaporation and combustion, the radii of fuel droplets are quickly shortened. This corresponds to and is appropriate to the diffusion of the fuel and gases into the gas flow and the simultaneous movement of the concentration ratio of the fuel droplets, f_i, into a lower group, f_{i-1}, (Fig 16.5).

The range of the distribution of probability for the fuel droplets is

$$m_i = \rho \frac{df_i}{dr} \; [\text{kg/m}^4]$$

The concentration of the fuel droplets in the ith group is $\rho_i = \rho f_i = \int_{r_i}^{r_b} m_i dr \; [\text{kg/m}^3]$ Let us assume the fact that the mixture of gases has a density, ρ, which is temporarily invariable; if we assume this, then, the rate of change of the liquid state density, from $r > r_h$ through the change to $r < r_h$ is

344

$$\rho \frac{df_i}{dt} = \rho \frac{df_i}{dr} \cdot \frac{dr}{dt} = \left(m_i \frac{dr}{dt} \right)_k \quad [kg/m^3 \cdot s];$$

from $r = r_1$ through the change to $r < r_1$ is

$$\rho \frac{df_i}{dt} = \rho \frac{df_i}{dr} \cdot \frac{dr}{dt} = \left(m_i \frac{dr}{dt} \right)_t \quad [kg/m^3 \cdot s];$$

Fig 16.5
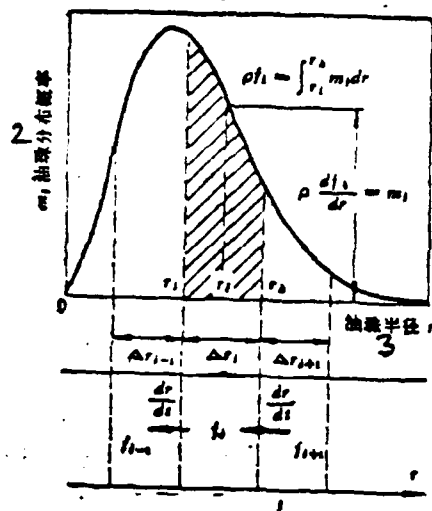
1. An Illustration of the Evaporization, Shortening Up and Exchange Between Groups of Fuel Droplets 2. The Probability Distribution of Fuel Droplets m_i 3. Fuel Droplet Radius, r

Along the three directions, the diffusion rate for the gases formed by the evaporation of the fuel droplets is

$$= 3 \int_{r_1}^{r_k} \frac{m_i}{r} \left(\frac{dr}{dt} \right) dr \quad [kg/m^3 \cdot s];$$

Within the combustion chamber, the rate of appearance of i group fuel droplets for each m^3 of volume each second (or the rate of occurrence of liquid state concentration) is

$$R_i = - m_i \left(\frac{dr}{dt} \right)_i + m_{i+1} \left(\frac{dr}{dt} \right)_{i+1}$$

$$- 3 \int_{r_i}^{r_{i+1}} \frac{m_i}{r} \left(\frac{dr}{dt} \right) dr \quad [kg/m^3 \cdot s] \quad (16.31)$$

If we use a straight line to take the place of the curved section of the

345

probability distribution of the fuel droplets, then, as a function of the shortening up of the fuel droplets, the range of the probability distribution of the fuel droplets has an average value of $\overline{\overline{m}}_i$ which is

$$\overline{\overline{m}}_i = \frac{\rho f_i}{r_{i+1} - r_i} \quad [\text{kg/m}^4];$$

In such a case, then, $\quad m_i = \frac{\overline{\overline{m}}_{i-1}(r_{i+1} - r_i) + \overline{\overline{m}}_i(r_i - r_{i-1})}{r_{i+1} - r_{i-1}} \quad [\text{kg/m}^4] \quad (16.32)$

If we employ equation (16.25) and (16.26) to solve for the rate of shortening up or shrinking $\left(\frac{dr}{dt}\right)$, then equation (16.31) changes to be

$$R_i = \rho f_i \left\{ -M_i \left[\frac{1}{\rho_i 4\pi r_i^2(r_{i+1} - r_i)} + \frac{3}{\rho_i 4\pi r_i} \right] \right.$$
$$+ M_{i+1} \left[\frac{r_{i+2} - r_{i+1}}{\rho_i 4\pi r_{i+1}^2(r_{i+1} - r_i)(r_{i+2} - r_i)} \right] \right\}$$
$$+ \rho f_{i+1} \left\{ \left[\frac{M_{i+1}}{\rho_i 4\pi r_{i+1}^2} \right] \left[\frac{r_{i+1} - r_i}{(r_{i+2} - r_{i+1})(r_{i+2} - r_i)} \right] \right\}$$
$$(16.33)$$

Sec 4 Combustion Reaction Types

In combustion chambers, the chemical reactions which take place at the same time are very numerous. The types of gases which participate in these reactions are also very numerous. However, if we take an overall view of everything, then, we can take the view that there are only three types of components into which the mixture of gases can be divided, that is oxygen, m_{ox}, gaseous fuel, m_f, and gases which have already been burned, m_b. The concentration ratio of their masses is

$$m_{ox} = \frac{\rho_{ox}}{\rho}, \quad m_f = \frac{\rho_f}{\rho}, \quad m_b = \frac{\rho_b}{\rho};$$

moreover, $\quad m_{ox} + m_f + m_b = 1 \quad\quad (16.34)$

Let us assume that the reaction time of combustion, τ_k, is very short, that is, smaller than 1 millisecond; let us also assume that the time of mixing diffusion is $\tau_D \approx 3 \sim 4$ milliseconds; if we make these assumptions, then, at a certain single coordinate in the space of the combustion chamber, there cannot exist both m_{ox} and m_f at the same time. Let us assume that we have the chemically appropriate ratio

346

between the masses of oxygen and fuel $S_O = 0.232L_O$, and that $L_O =$ the appropriate mixture ratio between air and fuel. When one is dealing with a situation in which the combustion of a lean mixture is taking place, then, the oxygen left over $= (m_{oz} - m_f S_0)$. If one is dealing with a situation in which the combustion of a rich mixture is taking place, then, the fuel left over $= (m_f - m_{oz}/S_0)$. If we assume that the overall class of the reaction is m = 2 and that the class of the fuel reaction is n = 1, then, on the basis of the rate of the disappearance of oxygen which is written down as (15.75a) of Chapter 15 = the reaction rate of combustion, which is

$$\rho \frac{dm_{oz}}{dt} = R_{oz} = -W_{oz} = K_0 m_{oz} \cdot m_f \cdot e^{\frac{-E}{RT}} \quad [\text{kg/m}^3 \cdot \text{s}],$$

$$K_O = \text{the reaction constant} \qquad (16.35)$$

Sec 5 Basic Equation System for Combustion Flow Fields

Let us take the basic differential equations for the axisymmetrical average-time turbulence flow gaseous fuel combustion flow fields in Sections 7, 9 and 10 of Chapter 15 and let us put them together below, as follows:

Continuity Equation

$$\frac{1}{r} \frac{\partial}{\partial r}(r\rho u) + \frac{\partial}{\partial z}(\rho w) = 0 \quad [\text{kg/m}^3 \cdot \text{s}] \quad (15.30)$$

Axial Momentum

$$\rho \left(w \frac{\partial w}{\partial z} + u \frac{\partial w}{\partial r} \right) = -\frac{\partial p}{\partial z}$$
$$+ \frac{1}{r} \frac{\partial}{\partial r}(r\tau_{wr}) + \frac{\partial \sigma_{zz}}{\partial z} \quad [\text{N/m}^3] \qquad (15.32)$$

Radial Momentum

$$\rho \left(w \frac{\partial u}{\partial z} + u \frac{\partial u}{\partial r} - \frac{v^2}{r} \right) = \frac{\partial \tau_{rz}}{\partial z} + \frac{1}{r} \frac{\partial}{\partial r}(r\sigma_{rr})$$
$$- \frac{\sigma_{\theta\theta}}{r} - \frac{\partial p}{\partial r} \quad [\text{N/m}^3] \qquad (15.34)$$

Circumferential Momentum

347

$$\rho\left(u\,\frac{\partial v}{\partial r} + w\,\frac{\partial v}{\partial z} + \frac{uv}{r}\right) = \frac{\partial \tau_{\theta z}}{\partial z}$$

$$+ \frac{1}{r^2}\frac{\partial}{\partial r}(r^2\tau_{\theta r}) \quad [\text{N/m}^3] \qquad (15.39)$$

Coefficient of Heat Flow

$$\rho\left(u\,\frac{\partial I}{\partial r} + w\,\frac{\partial I}{\partial z}\right) = -\frac{\partial q_z}{\partial z}$$

$$- \frac{1}{r}\frac{\partial}{\partial r}(rq_r) + \phi \quad [\text{kcal/m}^3\cdot s] \qquad (15.47)$$

Concentration Diffusion

$$\rho\left(u\,\frac{\partial m_i}{\partial r} + w\,\frac{\partial m_i}{\partial z}\right) = -\frac{\partial}{\partial z}(J_i)_z$$

$$- \frac{1}{r}\frac{\partial}{\partial r}r(J_i)_r - R_i \quad [\text{kg/m}^3\cdot s] \qquad (15.52)$$

On the basis of Chapter 4 and Chapter 5, it is possible to take the set of equations from (15.30) to (15.52) and put them together to write the equations in vector and tensor form. The parameters of average time turbulence flow fields, such as density, ρ, and so on, do not vary with changes in time, that is, $(\partial/\partial t) = 0$, and for the axisymmetrical flow fields, $(\partial/r\partial\theta) = 0$. Let us assume that Π represents a turbulence flow stress or force tensor. Let us take the vectors and tensors and use them to write out the basic set of equations for a flow field as they appear below:

Continuity equation $\qquad\qquad \nabla \cdot (\rho V) = 0 \qquad (16.36)$

Energy equation $\qquad \rho(V \cdot \nabla)I = -\nabla \cdot q + \phi - p(\nabla V) \ (16.37)$

Momentum equation $\qquad \rho(V \cdot \nabla)V = -\nabla p + \nabla \cdot \Pi \qquad (16.38)$

Concentration Diffusion $\qquad \rho(V \cdot \nabla)m_i = -\nabla \cdot J_i + R_i \qquad (16.39)$

If we take the four equations above, we still are not able to solve for the pressure field $p = p(r,\theta,z)$; neither can we solve for the velocity field $V = V(r,\theta,z)$; or the temperature field $T = T(r,\theta,z)$ or the concentration field $m_i = m_i(r,\theta,z)$; this is due to the fact that ρ, I, R_i, Π, q and J_i are still not determined with precise values. It follows from this that it is still necessary to find six more equations, that is,

The status equation $\quad p = \rho\dfrac{R}{M}T$, where M = the average molecular weight of the mixture of gases. (16.40)

The total enthalpy equation $\quad I = c_p T^* + m_i H_u$, where H_u = the heat value of the fuel (kcal/kg) (16.41).

The reaction equation $-R_{ss} = K_0 m_{ss} m_f e^{\frac{-E}{RT}}$, where the reaction constant is K_0 (kg/m³.s) (16.42).

The stress or force tensors are

$$\Pi = \mu_T \begin{Bmatrix} \dfrac{\partial u}{\partial r} & r\dfrac{\partial}{\partial r}\left(\dfrac{v}{r}\right) & \dfrac{\partial w}{\partial r} \\ 0 & \dfrac{u}{r} & 0 \\ \dfrac{\partial u}{\partial z} & \dfrac{\partial v}{\partial z} & \dfrac{\partial w}{\partial z} \end{Bmatrix} + \mu_T \begin{Bmatrix} \dfrac{\partial u}{\partial r} & 0 & \dfrac{\partial u}{\partial z} \\ r\dfrac{\partial}{\partial r}\left(\dfrac{v}{r}\right) & \dfrac{u}{r} & \dfrac{\partial v}{\partial z} \\ \dfrac{\partial w}{\partial r} & 0 & \dfrac{\partial w}{\partial z} \end{Bmatrix}$$

$$ - \begin{Bmatrix} p & 0 & 0 \\ 0 & p & 0 \\ 0 & 0 & p \end{Bmatrix} - \frac{2}{3}\mu_T \begin{Bmatrix} \nabla V & 0 & 0 \\ 0 & \nabla V & 0 \\ 0 & 0 & \nabla V \end{Bmatrix},$$

Or $\Pi = \mu_T(\nabla V + V\nabla) - p - \dfrac{2}{3}\mu_T \nabla V$, see equation (5.28) (16.43).

The heat flow equation $q = -\Gamma_h \nabla I$, see equation (15.45) (kcal/m².s) (16.44).

The concentration density is $J_i = -\Gamma_i \nabla m_i$, see equation (15.49) (kg/m².s) (16.45).

After we get values for μ_T, T_h, T_i and R_i, and we map out the form of the turbulence flow and the form of the reaction, then, it is possible to set our sights on the problem of operational configurations and boundary conditions for actual missions or projects and the consideration of how solve for these.

Sec 6 Proper Logical Order for Calculations of Combustion Flow Fields

(1) What is included in Task Analysis? Choice of structural form, main engine combustion capability requirements the effects of new technologies and new materials, capital, labor, equipment, deadlines, and so on.

(2) What is included in theoretical principles? To distinguish from each other and analyze out the scope of a flow field as well the laws of the conservation of mass, momentum and energy which pertain to it, the turbulence flow viscosity, the turbulence flow stresses or forces, the diffusion of heat flow, as well as the principle governing the diffusion of concentration, one must also deal with the selection of independent variables, dependent variables and a coordinate system; all of this is aimed at the simplification of the set of equations involved in an actual project.

(3) Dependent variables of transformation. If we are considering the case of a vortical combustion flow field which has a vortical strength number $S \geq 0.6$, then,

349

任务分析　　　　　　　理论原则

偏微分方程组

紊流模式
反应模式
雾化模式
辐射模式

改换变量
差分方程

形状尺寸
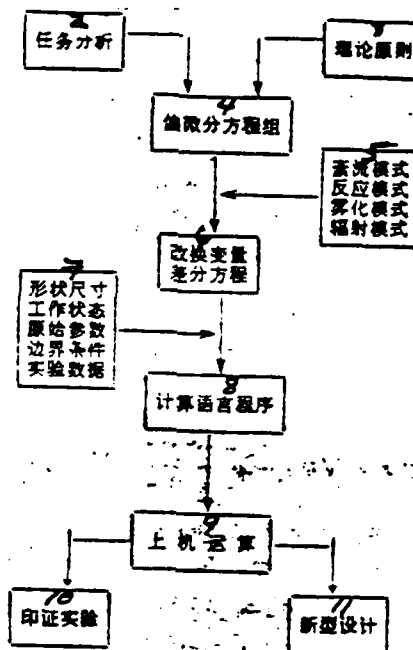工作状态
原始参数
边界条件
实验数据

计算语言程序

上机运算

印证实验　　　　　　新型设计

图16.6　流场计算逻辑顺序

Fig 16.6

1.　The Logical Order or Sequence for the Calculation of a Flow Field　2.　Task Analysis　3.　Theoretical Principles　4.　Set of Partial Differential Equations 5.　Form of Turbulence Flow, Form of Reaction, Form of Vaporization, Form of Radiation　6. Transformation Variable Difference Equations　7.　Dimensions of the Shape, Operational Configurations, Original Parameters, Boundary Conditions, experimental Data　8.　Computational Language Program　9.　Machine Entry Operations　10.　Verifying Experimentation　11.　New Design Form

due to the fact that counter-current flow is present, changes in pressure as one goes down the flow have an influence on the upper reaches of the flow.　It follows from this that it is not possible to use the "parallel flow scanning method" and, on the basis of the numerical values for some nodal points, to deduce the numerical values for others.　In order to overcome this difficulty, it is possible to take the dependent variables u, w and p from the set of differential equations for an axisymmetrical average time turbulence flow field and change them into the flow function ψ and curl or degree of vorticity ω (see Sections 8 and 6 of Chapter 4).　From the continuity equation in the Section 5 of this chapter, because of the fact that there is no relationship between r and z, it is possible to take equation (15.30) and change it into

$$\frac{\partial}{\partial r}(r\rho u) = -\frac{\partial}{\partial z}(r\rho w) \qquad (16.46)$$

Let us assume that we have an average time flow function ϕ to satisfy equation (16.46); if this is the case, then, it should also be true that

$$\rho u = -\frac{1}{r}\frac{\partial \psi}{\partial z}, \quad \rho w = \frac{1}{r}\frac{\partial \psi}{\partial r},$$

$$\frac{\partial}{\partial r}\left(\frac{\partial \psi}{\partial z}\right) = \frac{\partial}{\partial z}\left(\frac{\partial \psi}{\partial r}\right); \qquad (16.47)$$

Let us further assume that the curl or degree of vorticity within the meridian plane of the flow field is $\omega = \frac{\partial u}{\partial z} - \frac{\partial w}{\partial r}$; if this is the case, then the new variable is $\xi = \frac{\omega}{r}$; $\qquad (16.48)$. In order to simplify calculations let us assume that μ_T, Γ_k and Γ_l in various different directions are all equal to each other, and let us also assume that the normal stresses or forces produced by turbulence flow friction, $\sigma_{rr}, \sigma_{\theta\theta}, \sigma_{zz}$ are also all equal to each other. If we take ϕ to represent a certain dependent variable such as ϕ, ξ, the excess of left-over fuel concentration ratio, m_f, the total enthalpy I, and so on (Sec 4 of this chapter), then, the five equations from (15.30 to (15.52) can all be subsumed under the all-purpose equation set out below, that is,

$$a_\phi\left[\frac{\partial}{\partial z}\left(\phi\frac{\partial \psi}{\partial r}\right) - \frac{\partial}{\partial r}\left(\phi\frac{\partial \psi}{\partial z}\right)\right] - \frac{\partial}{\partial z}\left[b_\phi r\frac{\partial}{\partial z}(c_\phi\phi)\right]$$

$$-\frac{\partial}{\partial r}\left[b_\phi r\frac{\partial}{\partial r}(c_\phi\phi)\right] = rd_\phi \qquad (16.49)$$

The parameters a_ϕ, b_ϕ, c_ϕ and d_ϕ in the equation above are all functions, which are already known, of other independent variables.

For example, if we utilize $\phi = \phi$, then, $a_\phi = 0, b_\phi = \frac{1}{r^2\rho}, c_\phi = 1, d_\phi = \frac{\omega}{r}$; if we use $\xi = \frac{\omega}{r} = \omega$, then, $a_\phi = r^2, b_\phi = r^2, c_\phi = \mu_T,$ and

$$d_\phi = \frac{\partial}{\partial z}(\rho V^2) + r\left[\frac{\partial}{\partial z}\left(\frac{u^2 + w^2}{2}\right)\frac{\partial \rho}{\partial r}\right.$$

$$\left. - \frac{\partial}{\partial r}\left(\frac{u^2 + w^2}{2}\right)\frac{\partial \rho}{\partial z}\right];$$

351

If we utilize the fuel concentration ratio $m_f = \phi$, then, $a_\phi = 1$, $b_\phi = \frac{\mu_T}{Sc} = \Gamma_1$, $c_\phi = 1$, $d_\phi = R_{1,\cdot}$.

If we use the total enthalpy $I = \phi$, then $a_\phi = \Gamma$, $b_\phi = \Gamma_h$, $c_\phi = 1$, $d_\phi = \Phi /$ $_{427}$.

Sec 7 Difference Equations and Solution Methods

Equation (16.49) is a second-degree, non-linear, non-homogeneous partial differential equation with an ellipsoid shape. If there are N dependent variables ϕ , then, combustion flow field, it is first necessary to take this type of differential equation and change it into a difference equation. Take the rz plane of the flow field and divide it up into several grid nodal points, then, use the "implicit, full-field relaxation, successive approximation method" to solve for the numerical values of the nodal points. The flow function ϕ and the vorticity or curl ω ought to be solved for simultaneously, and then one should utilize equations (16.47) and (16.48) to solve for u and w; after this is done, then, it is possible to use a momentum equation to solve for p. What is known as "full field relaxation"; that is, in the repeated application of the successive approximation method, causes the reduction of all the computational remainders (errors) $\cdot s$ at each of the nodal points in the flow field. This type of successive approximation leads directly to the minimization of the errors, e , for each nodal point. What is known as "implicity," that is, the computation of data for the nodal points in the lower reaches of the flow, is entirely contained in the equations, and it is not possible to directly utilize the earlier repeated substitution of values, and it becomes necessary to solve three or five simultaneous algebraic equations. If we assume that n is the indicator for the number of times approximations are done (not an exponent), then, i and j are the indicators for the rows and columns of the nodal points. Fig 16.7(a) has an implicit unifilar 3 point computational formula which is

$$a_1 \phi^{n+1}_{i+1,j} + a_2 \phi^{n+1}_{ii} + a_3 \phi^{n+1}_{i-1,j} = s^n_{ii}$$

$$+ \text{(other n class quantities)} \quad (16.50)$$

The formula for the five point computation of the stability function full field method for Fig 16.7(b) is

$$a_1\phi_{i+1,j}^{n+1} + a_2\phi_{i,j}^{n+1} + a_3\phi_{i-1,j}^{n+1} + a_4\phi_{i,j+1}^{n+1} + a_5\phi_{i,j-1}^{n+1} = \varepsilon_{i,j}^{0} + \text{(other n class quantities)} \quad (16.51)$$

The length of the interval between nodal points in the grid is
$$\Delta z_1 = z_{i,j} - z_{i-1,j} \quad \Delta z_2 = z_{i+1,j} - z_{i,j}; \quad \Delta r_1 = r_{i,j} - r_{i,j-1} \quad \Delta r_2 = r_{i,j+1} - r_{i,j}.$$

The implicit full field relaxation method difference equation for equation (16.49) is

$$-C_{i+1,j}\phi_{i+1,j} - C_{i-1,j}\phi_{i-1,j} - C_{i,j+1}\phi_{i,j+1}$$
$$- C_{i,j-1}\phi_{i,j-1} - C_{i,j}\phi_{i,j} + \frac{d_\phi}{b_\phi} = 0 \quad (16.52)$$

The non-linear parameters of the equation above are

$$C_{i+1,j} = \left\{ C_{z3}(1) + \left[\frac{C_{z1}(1)}{rb_\phi}\right]\frac{\partial b_\phi r}{\partial z} \right\}_{ij} C_{\phi,i+1,j}$$
$$- \left[\frac{a_\phi C_{z1}(1)}{rb_\phi}\right]_{ij}\left(\frac{\partial \psi}{\partial r}\right)_{ij} \quad (16.53)$$

$$C_{i-1,j} = \left\{ C_{z3}(3) - \left[\frac{C_{z1}(3)}{rb_\phi}\right]\frac{\partial b_\phi r}{\partial z} \right\}_{ij} C_{\phi,i-1,j}$$
$$+ \left[\frac{a_\phi C_{z1}(3)}{rb_\phi}\right]_{ij}\left(\frac{\partial \psi}{\partial r}\right)_{ij} \quad (16.54)$$

$$C_{i,j+1} = \left\{ C_{r3}(1) + \left[\frac{C_{r1}(1)}{rb_\phi}\right]\frac{\partial b_\phi r}{\partial r} \right\}_{ij} C_{\phi,i,j+1}$$
$$+ \left[\frac{a_\phi C_{r1}(1)}{rb_\phi}\right]_{ij}\left(\frac{\partial \psi}{\partial z}\right)_{ij} \quad (16.55)$$

$$C_{i,j-1} = \left\{ C_{r3}(3) - \left[\frac{C_{r1}(3)}{rb_\phi}\right]\frac{\partial b_\phi r}{\partial r} \right\}_{ij} C_{\phi,i,j-1}$$
$$- \left[\frac{a_\phi C_{r1}(3)}{rb_\phi}\right]_{ij}\left(\frac{\partial \psi}{\partial z}\right)_{ij} \quad (16.56)$$

$$C_{ij} = C_{zij} + C_{rij}$$
$$= \left\{ C_{z3}(2) - \left[\frac{C_{z1}(2)}{rb_\phi}\right]\frac{\partial b_\phi r}{\partial z} \right\}_{ij} C_{\phi ij}$$
$$+ \left[\frac{a_\phi C_{r1}(2)}{rb_\phi}\right]_{ij}\left(\frac{\partial \phi}{\partial r}\right)_{ij} + \left\{ C_{r3}(2) \right.$$
$$\left. - \left[\frac{C_{r1}(2)}{rb_\phi}\right]\frac{\partial b_\phi r}{\partial r} \right\}_{ij} C_{\phi ij}$$
$$- \left[\frac{a_\phi C_{r1}(2)}{rb_\phi}\right]_{ij}\left(\frac{\partial \psi}{\partial z}\right)_{ij} \quad (16.57)$$

In order to improve the degree of precision or accuracy, we can make particularly fine divisions in the interval of the grid in those areas close to the boundaries. If we proceed in this way, then, the length of the intervals Δr and Δz are not uniformly equal. After drawing out a grid network which is not uniformly even in the density with which its divisions are laid out, then, it is possible to make

353

all-purpose use of the row and column indicators C_n, C_{n}, C_{n}, C_n (see Fig 16.7b).
If we already know the interval lengths $\Delta r_1, \Delta r_2, \Delta z_1, \Delta z_2$, then

$$
\begin{aligned}
C_{n}(1) &= \frac{\Delta r_1}{\Delta r_3}(\Delta r_1 + \Delta r_2) \\
C_{n}(2) &= \frac{(\Delta r_1 - \Delta r_2)}{\Delta r_1 \Delta r_3} \\
C_{n}(3) &= \frac{\Delta r_2}{\Delta r_1}(\Delta r_1 + \Delta r_2) \\
C_{n}(1) &= \frac{2}{\Delta r_3}(\Delta r_1 + \Delta r_2) \\
C_{n}(2) &= \frac{2}{\Delta r_1}(\Delta r_2) \\
C_{n}(3) &= \frac{2}{\Delta r_1}(\Delta r_1 + \Delta r_2)
\end{aligned}
\qquad (16.58)
$$

$$
\begin{aligned}
C_{z1}(1) &= \frac{\Delta z_1}{\Delta z_2}(\Delta z_1 + \Delta z_2) \\
C_{z1}(2) &= \frac{(\Delta z_2 - \Delta z_1)}{\Delta z_1 \Delta z_2} \\
C_{z1}(3) &= \frac{\Delta z_2}{\Delta z_1}(\Delta z_1 + \Delta z_2) \\
C_{z1}(1) &= \frac{2}{\Delta z_2}(\Delta z_1 + \Delta z_2) \\
C_{z1}(2) &= \frac{2}{\Delta z_1}(\Delta z_2) \\
C_{z2}(3) &= \frac{2}{\Delta z_1}(\Delta z_1 + \Delta z_2)
\end{aligned}
\qquad (16.59)
$$

The procedure for the solution of (16.52) for numerical values is as follows: on the basis of the materials at hand and the task, first make an initial guess at the distribution of ϕ. Write out the equations for the remaining error ε for each of the nodal points in the entire field. Then, use a "reversing implicit" computational language to simultaneously solve this entire set of remaining error equations. If we proceed in this way, then, each time we make an approximation, the remaining errors, ε, for the entire field are all reduced one more time.

354

At the nodal point, ij, the equation for the remaining error $\varepsilon_{\phi_{ii}}^n$ left after the nth approximation is as follows $\varepsilon_{\phi_{ii}}^n = -C_{i+1,j}^n \phi_{i+1,j}^n - C_{i-1,j}^n \phi_{i-1,j}^n - C_{i,j+1}^n \phi_{i,j+1}^n$

$$- C_{i,j-1}^n \phi_{i,j-1}^n + C_{ij}^n \phi_{ii}^n + \left(\frac{d_\phi}{b_\phi}\right)_{ij}^n \quad (16.60)$$

For the limiting case,

$$d\varepsilon_{\phi_{ii}}^n = \left[\frac{\partial \varepsilon_{\phi_{ii}}}{\partial \phi_{i-1,j}}\right]^n d\phi_{i-1,j}^n + \left[\frac{\partial \varepsilon_{\phi_{ii}}}{\partial \phi_{i+1,j}}\right]^n d\phi_{i+1,j}^n$$

$$+ \left[\frac{\partial \varepsilon_{\phi_{ii}}}{\partial \phi_{i,j+1}}\right]^n d\phi_{i,j+1}^n + \left[\frac{\partial \varepsilon_{\phi_{ii}}}{\partial \phi_{i,j-1}}\right]^n d\phi_{i,j-1}^n$$

$$+ \left[\frac{\partial \varepsilon_{\phi_{ii}}}{\partial \phi_{ii}}\right]^n d\phi_{ij} + \Phi_{ii}^n \quad (16.61)$$

If we partially differentiate equation (16.60) against ϕ, then we can obtain the various parámeters

$$- C_{i+1,j}^n = \left[\frac{\partial \varepsilon_{\phi_{ii}}}{\partial \phi_{i+1,j}}\right]^n, \quad - C_{i-1,j}^n = \left[\frac{\partial \varepsilon_{\phi_{ii}}}{\partial \phi_{i-1,j}}\right]^n,$$

$$- C_{i,j+1}^n = \left[\frac{\partial \varepsilon_{\phi_{ij}}}{\partial \phi_{i,j+1}}\right]^n, \quad - C_{i,j-1}^n = \left[\frac{\partial \varepsilon_{\phi_{ii}}}{\partial \phi_{i,j-1}}\right]^n,$$

$$C_{ij}^n = \left[\frac{\partial \varepsilon_{\phi_{ij}}}{\partial \phi_{ii}}\right]^n; \quad (16.62)$$
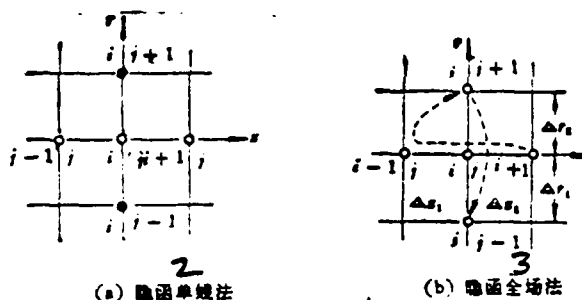

图16.7 松弛步骤

(a) 隐函单线法   (b) 电函全场法

Fig 16.7

1. Relaxation Procedure   2. Implicit Unifilar Method   3. Implicit Full Field Method

Because of the fact that the various parameters C_{ij}^n are all implicit functions, besides which it is also true that other variables also influence the remaining error, ε, it follows that we should use Φ_{ij}^n to represent the influence on ε of the total of several quantities.

If we once solve the chain formula (16.61) to represent a set of full field relaxation equations, then, it is possible to undertake the (n+1)the approximation. If, when we start, we already know Φ_{ij}^n, then it is possible, on the basis of the

355

algebraic equations of Newton and others for the extraction of roots, to solve
equation (16.61).

The first step is to make an attempt at solving the equation in question; to
do this, first assume $\Phi_{ij}^* = 0$. From equation (16.61), figure out an
intermediate value, ϕ_{ij}^*. From the results of this calculation and on the basis
of the "outward stretch" method, select a value for Φ_{ij}. We can then use this
value for ϕ_{ij}^* in the second step determination of a precise value for the (n+1)th
approximation to the value of ϕ; on the basis of this, we can then figure out
that $d\phi_{ij}^* = \phi_{ij}^* - \phi_{ij}^-$. If we make use of equation (16.52), then, the relaxation
approximation formula in the tentative try at a solution in step one becomes

$$-C_{i+1,j}^-\phi_{i+1,j}^* - C_{i-1,j}^-\phi_{i-1,j}^* - C_{i,j+1}^-\phi_{i,j+1}^*$$
$$- C_{i,j-1}^-\phi_{i,j-1}^* + C_{i,j}^-\phi_{ij}^* = -\left(\frac{d_q}{\phi_q}\right)_{ij}^* \quad \dots \quad (16.63)$$

If, around each nodal point (ij) in a flow field grid network we write an
equation of the form of equation (16.63), then, we obtain a set of linear algebraic
equations. We then solve this set of linear algebraic equations on the basis of
the "alternating or reversing direction implicit" method of solution.

Form solving equation (16.63), we obtain the dependent variable intermediate
value ϕ_{ij}^*; after this is done, then on the basis of equations (16.53) to (16.57),
we figure out all the parameters C_{ij}, and use equation (16.52) to figure out the
remaining error $\varepsilon_{\phi ij}^*$.

On the basis of the data which have already been figured out, we then extend
the process to the nth approximation and the intermediate value (*), and deduce
Φ_{ij}^* for the (n+1)th approximation.

Let us assume that, when we are figuring the nth approximation, the error ϕ_{ij}^-
or deviation = 0; on the basis of this assumption, we can say that $d\phi_{ij}^* = 0$; in
this case, from equation (16.52), the remaining error or deviation that we
calculated should be $\varepsilon_{\phi ij}^*$; it follows from this that, from equation (16.60), it is
possible to obtain the relationship $\Phi_{ij}^* = \varepsilon_{\phi ij}^*$.

If we are considering the fact that, from the nth to the *th approximations,
there are two instances of error or deviation, because of the fact that, in the
case of the first step in which we made a tentative attempt at a solution, we
already knew that the remaining error or deviation was $\varepsilon_{\phi ij}^*$, and we also knew
that, in this situation, $\Phi_{ij}^* = 0$, we can utilize the secant method (Fig 16.8), and,
in the second step, select for use a Φ_{ij}^* which should be

$$\Phi_{ij}^* = \frac{\varepsilon_{\phi ij}^*}{1 - \frac{\varepsilon_{\phi ij}^*}{\varepsilon_{\phi ij}^*}} \qquad (16.64)$$
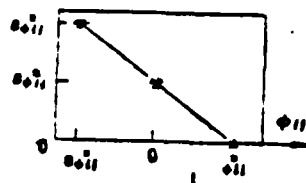
356

图 16.8 射域外插法

Fig 16.8

1. The Secant Extrapolation Method

If we take the intermediate value * between the two approximations, and push them to the (n+1)th approximation, then, it is possible to take equation (16.63) and expand it; after this is done, then, if we substitute the value for Φ_{ij}^{*}, which we obtained, into equation (16.64), we can solve for ϕ_{ij}^{*+1}. , as follows,

$$- C_{i+1,j}^{*}\phi_{i+1,j}^{*+1} - C_{i-1,j}^{*}\phi_{i-1,j}^{*+1} - C_{i,j+1}^{*}\phi_{i,j+1}^{*+1}$$
$$- C_{i,j-1}^{*}\phi_{i,j-1}^{*+1} + C_{ij}^{*}\phi_{ij}^{*+1} = -\left(\frac{d_{\phi}}{b_{\phi}}\right)^{*} - \Phi_{ij}^{*} \quad (16.65)$$

The two-step "implicit function relaxation approximation method" certainly appears to be a lot of trouble; actually, it is very helpful and effective. For example, if we assume that all the parameters C_{ij} are unrelated to ϕ_{ij} , then, $\Phi_{ij}^{*} = 0$; on the basis of this, we can simply approximate one time, and we can then obtain an accurate solution. The strong point of this method is that, when one is carrying out an approximation, the remaining errors or deviations for the whole field all tend toward zero, and the mutually related non-linear influences can be represented by Φ_{ij}^{*} .

Let us consider the Alternating Direction Implicit computational language, ADI. Equation (16.63) or (16.65) is the numerical standard or normal equation for the remaining error or deviation from the ellipsoid partial differential equation for a combustion flow field; it can be written in an all-purpose form as follows:

(Let us assume that $C_{ij}^{*} = Cz_{ij}^{*} + Cr_{ij}^{*}$, then, $f_{ij}^{*} = -\left(\frac{d_{\phi}}{b_{\phi}}\right)^{*} - \Phi_{ij}^{*}$)

$$- C_{i-1,j}^{*}\phi_{i-1,j}^{*+1} + Cz_{ij}^{*}\phi_{ij}^{*+1} - C_{i+1,j}^{*}\phi_{i+1,j}^{*+1}$$
$$- C_{i,j+1}^{*}\phi_{i,j+1}^{*+1} + Cr_{ij}^{*}\phi_{ij}^{*+1} - C_{i,j-1}^{*}\phi_{i,j-1}^{*+1} = f_{ij}^{*}$$

$$(16.66)$$

The solution of equation (16.66) requires the use of a five-line diagonal matrix. The ADI method takes the five lines and turns them into a three-line diagonal matrix, and, finally, uses the "Gaussian block elimination method" to achieve a solution.

In order to utilize the ADI method, it is first necessary to take the difference quantities for the horizontal (j not changing) and the vertical (i not changing) out of equation (16.66) and separate them, that is,

$$
\begin{aligned}
- C_{i-1j}^{*}\phi_{i-1j}^{*+1} + C z_{ij}^{*}\phi_{ij}^{*+1} - C_{i+1j}^{*}\phi_{i+1j}^{*+1} + \rho\phi_{ij}^{*+1} \\
= \rho\phi_{ij}^{*+1} + C_{ij-1}^{*}\phi_{ij-1}^{*+1} - C r_{ij}^{*}\phi_{ij}^{*+1} \\
+ C_{ij+1}^{*}\phi_{ij+1}^{*+1} + f_{ij}^{*} \qquad (16.67)
\end{aligned}
$$

$$
\begin{aligned}
C_{ij-1}^{*}\phi_{ij-1}^{*+1} + C r_{ij}^{*}\phi_{ij}^{*+1} - C_{ij+1}^{*}\phi_{ij+1}^{*+1} \\
+ \rho\phi_{ij}^{*+1} = \rho\phi_{ij}^{*+1} + C_{i-1j}^{*}\phi_{i-1j}^{*+1} \\
- C z_{ij}^{*}\phi_{ij}^{*+1} + C_{i+1j}^{*}\phi_{i+1j}^{*+1} + f_{ij}. \qquad (16.68)
\end{aligned}
$$

The ρ in the two equations above is called the "acceleration approximation coefficient." Let us assume that m = the numerical value for the first acceleration coefficient or parameter ρ_i which was used. If we are considering a case in which the three-line diagonal matrix involved has a maximum value = b and a minimum value = a, then,

$$
\rho_i = b\left(\frac{a}{b}\right)^{\frac{(2i-1)}{2m-2}}, \ i = 1, 2, \ldots, m. \qquad (16.69)
$$

If we use the equation below to figure out the smallest whole value for m, then, it is possible to decide how best to use several different values of ρ_i, that is,

$$
(b)^{\frac{a}{m}} \leq \frac{a}{b}, \ b = \sqrt{2} - 1 = 2.414 \qquad (16.70)
$$

The ADI method utilizes equations (16.67) and (16.68) by switching their calculations back and forth. If one reaches the point at which the corresponding errors or deviations for two successive approximations are

$$
\frac{\phi_{ij}^{*} - \phi_{ij}^{*+1}}{\phi_{ij}} \leq 0.001 \qquad (16.71)
$$

then, it is possible to end the calculation.

Sec 8   Sample Results of Combustion Flow Field Calculations

(1)   Flame tube-type combustion flow fields.   If we take the flow function ψ and the curl or vorticity ω and use them to replace the flow speeds u and w as well as the pressure gradient $(\partial p/\partial z)$, then, on the basis of the difference equations employed in previous sections on axisymmetric flow fields as well as on the basis of numerical calculations, it is possible to obtain an average time quasi-stable flow line spectrum for the forward part of a flame tube. We already know the internal ring and external ring diameters, d and D, of the intake vortical flow devices, the amount of intake gas flow G_O (kg/s) as well as the temperature T_O and the pressure p_O. According to Sec 11 of Chapter 6, the vortical strength number figures out to be S = 1.57. Large and strong rotational jets, in the forward part of flame tubes, create radial and axial pressure gradients which cause the formation of areas of counter-current flow ($\psi/\psi_\bullet$ = a negative value) as well as vortical rings. If we take as a basis the facts that the counter-current boundary line is w = 0, and that $\dfrac{\psi}{\psi_0} =$ 0, then, along inward-tending and outward-tending radii, one sees represented flow lines for different amounts of flow (Fig 16.9). According to equation (16.47) $\phi = \int_0^r r\rho w \, dr$, $\phi_\bullet$ is the flow line which hugs the inside wall of the outer ring of a vortical flow device.

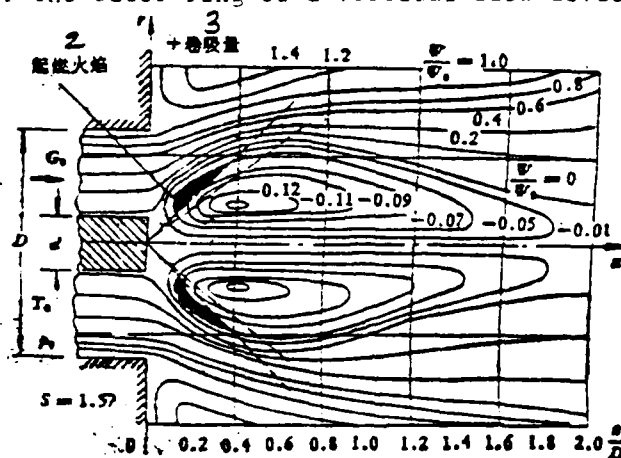图16.9. 火焰筒式燃烧流场的流线谱

Fig 16.9

1.   The Flow Line Spectrum for a Flame Tube-type Combustion Flow Field 2.   Ignition Flame 3.   The Amount of + Roll Up

(2)   A comparison between experimentation and calculations concerning the combustion of round tube combustion chamber rotational jets.   Natural gases are

supplied from a jet nozzle in the center of one end of a round tube combustion
chamber with an internal diameter of 200 (mm) (the most important of these is
methane or methyl hydride). Around the jet nozzle, there·is the presence of an
axial gas supply G_o and a tangential gas input volume G_ϕ ; this situation forms
a rotational jet. It is possible to adjust (G_ϕ/G_o) so that it will be equal to S'
and represent the vortical strength number. We did experimental measurements of
the gas temperatures T (K) along the axis of symmetry (Fig 16.10). Besides this,
on the basis of the set of average time quasi-stable state differential equations
set out in previous sections for axisymmetric combustion flow fields and on the
basis of the associated difference equations, we figured out a comparison between
the calculated distribution of gas temperatures along the axis line and the
experimental values obtained for this distribution. It can be seen that, if one
raises the tangential and axial gas supply ratio, S', (as well as the vortical
strength number, S), then, it is possible to shorten the flame and raise the
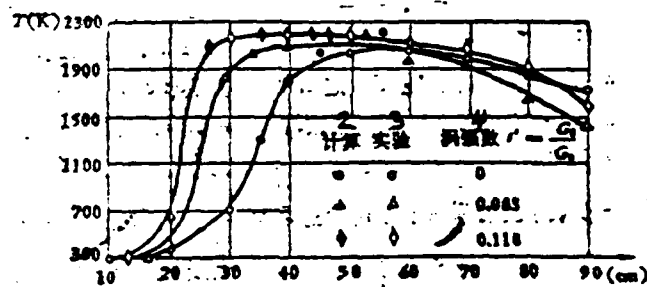temperature of combustion. Combustion efficiency and stability are also raised
along with S'.

图 16.10 旋涡影响沿对称轴线上温度分布对比

Fig 16.10
1. A Comparison of the Influence of Vortices on the Temperature Distribution
Along the Axis of Symmetry 2. Calculation 3. Experimentation 4. Vortical
Strength Number